

2
mix

~~77~~

CR-128735



VOUGHT MISSILES
AND SPACE COMPANY
TEXAS DIVISION

P. O. Box 6267

Dallas, Texas 75222

(NASA-CR-128735) EC/LSS THERMAL CONTROL
SYSTEM STUDY FOR THE SPACE SHUTTLE
Interim Report (LTV Aerospace Corp.)
292 p HC \$16.75

CSCL 22B

N73-17884

Unclass

G3/31 62305

Interim Report
Contract NAS9-11166

EC/LSS THERMAL CONTROL SYSTEM
STUDY FOR THE SPACE SHUTTLE

Report No. T201-RP-20001

6 December 1972

Submitted by

LTV AEROSPACE CORPORATION

To

THE NATIONAL AERONAUTICS AND SPACE ADMINISTRATION
MANNED SPACECRAFT CENTER
Houston, Texas

Prepared by:

Approved by:

H. R. Howell
H. R. Howell

R. J. French
R. J. French, Supervisor
Environmental Control/
Life Support Systems

PRECEDING PAGE BLANK NOT FILMED

FOREWORD

This interim report is submitted as fulfillment of Task 3.1 of the Statement of Work of Contract NAS9-11166, EC/LSS Thermal Control System for The Space Shuttle. The majority of the work reported herein was performed in the July 1970 to September 1970 time period during the formulative stages of the Shuttle. At that time the parametric weight analyses were completed and it was realized that more definitive mission design conditions were required for the heat rejection system selection. The results of the parametric weight analysis were given to NASA-MSC in an oral presentation in March 1971. The program work was stopped from that time until May 1972 when documentation and updates to the previous work to reflect the latest Shuttle configuration were initiated.

Mr. D. W. Morris of the NASA-MSC Crew Systems Division is the contact Technical Monitor. Mr. H. R. Howell served as the Technical Project Engineer. Principal investigators and contributing authors include Messrs. T. D. Blount, J. B. Dietz, M. L. Fleming, J. E. Pearce, D. D. Worley and Dr. R. L. Cox.

TABLE OF CONTENTS

	<u>PAGE</u>
1.0 SUMMARY	1
2.0 INTRODUCTION	2
3.0 PARAMETRIC ANALYSES	4
3.1 Vapor Cycle Refrigeration	4
3.1.1 Vapor Compression Cycle	5
3.1.2 Working Fluids	5
3.1.3 System Performance	8
3.1.4 Component Weight Data	9
3.1.5 Parametric Weight Analyses	14
3.2 Gas Cycle Refrigeration	15
3.2.1 Gas Cycle	16
3.2.2 Working Fluids	18
3.2.3 System Performance	19
3.2.4 Component Weight Data	20
3.2.5 Parametric Weight Analysis	25
3.3 Space Radiator	25
3.3.1 Radiator Area Requirements	26
3.4 Expendable Fluid Cooling System	33
3.4.1 Candidate Fluids	33
3.4.2 Expendables System Weight Analysis	35
3.5 Ram Air	42
3.5.1 Ram Air System Weights	42
4.0 WEIGHT PENALTY EVALUATION	46
4.1 Power Penalty	46
4.1.1 Weight Estimates	47
4.2 Radiator Weight Penalty	53
4.2.1 Deployed Radiator Concepts	55
4.2.2 Skin Mounted Concept	56
4.2.3 Radiator Penalty Summary	60
5.0 OVERALL EC/LSS HEAT REJECTION SYSTEM SELECTION	62

TABLE OF CONTENTS (CONT)

5.1	Design Requirements	62
5.1.1	Prelaunch	62
5.1.2	Launch	62
5.1.3	Orbit	62
5.1.4	Reentry	65
5.1.5	Atmospheric Flyback	65
5.1.6	Post Landing	65
5.1.7	General Design Criteria	66
5.2	System Weight Analysis	67
5.3	System Selection	71
6.0	RECOMMENDATIONS	73
	REFERENCES	74

APPENDICES

APPENDIX A	Refrigeration System Plotting and Generalized Analysis Technique (RSPLAT) Parametric Weight Analyses
APPENDIX B	Determination of Orbiter Space Radiator Steady State Design Environments
APPENDIX C	Space Radiator Design

LIST OF TABLES

		PAGE
1	Theoretical Refrigerant Performance	7
2	Aircraft Vapor Compression System Weights	13
3	Parameters Used In Refrigeration System Parametric Analysis .	16
4	Gas Cycle Fluid Properties	19
5	Gas Cycle Operating Conditions	21
6	Summary of Radiator Steady-State Design Sink Temperature . .	29
7	Radiator Area Requirements	31
8	Expendable Fluids Heat Absorption	34
9	Relative Safety of Expendable Fluids	36
10	Orbiter Subsonic Aerodynamic Characteristics	44
11	Power System Specific Weights	48
12	State-of-the-Art Fuel Cells	49
13	Fuel Cell Radiator System Weight Summary	50
14	Hydrogen and Oxygen Tank Weights	52
15	APU Weight Data	54
16	Deployed Radiator Design Summary	57
17	Single Door Deployed Radiator Weight Estimate	58
18	Double Door Deployed Radiator Weight Estimate	59
19	Skin Mounted Radiator Weight Estimate	61
20	Orbiter EC/LSS Heat Rejection System Design Requirements . .	63
21	Typical Reference Mission Timelines	64
22	Overall EC/LSS Heat Rejection System Weight Summary	70

LIST OF FIGURES

	PAGE
1 Simple Vapor Compression System	77
2 Refrigerant Theoretical Performance Data	78
3 Refrigerant Theoretical Performance Data	79
4 Refrigerant Theoretical Performance Data	80
5 System Performance With A Secondary Coolant Loop	81
6a Vapor Compression System Configuration For Parametric Weight Analyses	82
6b Vapor Compression System Configuration For Parametric Weight Analyses	82
7 Compressor Weights	83
8 Electric Motor Weight Data	84
9 Typical Speeds For Pumps	85
10 Pump Weights (Excluding Motor)	86
11 Orbital Mechanical Refrigeration System Weights	87
12 Atmospheric Flight Mechanical Refrigeration System Weights	88
13 Vapor Compression Orbital Heat Rejection System Weights - Direct Cond. Rad. Wt. Penalty = 0.5 lb/ft^2	89
14 Vapor Compression Orbital Heat Rejection System Weights - Direct Cond. Rad. Wt. Penalty = 1.0 lb/ft^2	90
15 Vapor Compression Orbital Heat Rejection System Weights - Direct Cond. Rad. Wt. Penalty = 1.5 lb/ft^2	91
16 Vapor Compression Orbital Heat Rejection System Weights - Direct Cond. Rad. Wt. Penalty = 2.0 lb/ft^2	92
17 Vapor Compression Orbital Heat Rejection System Weights - With HX loop, Rad Penalty = 0.5 lb/ft^2	93
18 Vapor Compression Orbital Heat Rejection System Weights - With HX loop, Rad. Penalty = 1.0 lb/ft^2	94
19 Vapor Compression Orbital Heat Rejection System Weights - With HX loop, Rad. Penalty = 1.5 lb/ft^2	95
20 Vapor Compression Orbital Heat Rejection System Weights - With HX loop, Rad. Penalty = 2.0 lb/ft^2	96
21 Vapor Compression Atmospheric Flight Heat Rejection System Weights	97
22 Vapor Compression Atmospheric Flight Heat Rejection System Weights - With Direct Condensing ATM Convactor Wt. Penalty = $.05 \text{ lb/ft}^2$	98

LIST OF FIGURES (CONTD)

	PAGE
23 Vapor Compression Atmospheric Flight Heat Rejection System Weights - With HX loop, Rad Penalty = 0.5 lb/ft ²	99
24 Vapor Compression Atmospheric Flight Heat Rejection System Weights - With Direct Condensing ATM. Convect. Weight Penalty = 1.0 lb/ft ²	100
25 Vapor Compression Atmospheric Flight Heat Rejection System Weights - With HX loop, Rad Penalty = 1.0 lb/ft ²	101
26 Vapor Compression Atmospheric Flight Heat Rejection System Weights - With Direct Condensing ATM. Convect. Weight Penalty = 1.5 lb/ft ²	102
27 Vapor Compression Atmospheric Flight Heat Rejection System Weights - With HX loop, Rad Penalty = 1.5 lb/ft ²	103
28 Vapor Compression Atmospheric Flight Heat Rejection System Weights - With Direct Condensing ATM. Convect. Weight Penalty = 2.0 lb/ft ²	104
29 Vapor Compression Atmospheric Flight Heat Rejection System Weights - With HX loop, Rad Penalty = 2.0 lb/ft ²	105
30 An Ideal Closed Gas Cycle For Refrigeration	106
31 Effect Of Ratio Of Specific Heats On Gas Cycle Performance . .	107
32 Gas Cycle System Performance	108
33 Orbiter Gas Cycle Schematics	109
34 Operational Aircraft Aircycle System Weights	110
35 Gas Cycle Orbital Heat Rejection System Weight - Rad Wt. Penalty = 0.5 lb/ft ²	111
36 Gas Cycle Orbital Heat Rejection System Weights - Rad Wt. Penalty = 1.0 lb/ft ²	112
37 Gas Cycle Orbital Heat Rejection System Weights - Rad Wt. Penalty = 1.5 lb/ft ²	113
38 Gas Cycle Orbital Heat Rejection System Weights - Rad Wt. Penalty = 2.0 lb/ft ²	114
39 Gas Cycle Atmospheric Flight Heat Rejection System Weights . . .	115
40 Shuttle Boost/Reentry Temperatures	116
41 Orbiter Radiator Concepts.	117
42 Space Radiator Heat Rejection	118
43 Condensing Radiator Temperature Profile	119
44 Condenser Heat Rejection	120

LIST OF FIGURES (CONTD)

	PAGE
45 Transient Radiator Analysis Steady State Design Conditions . . .	121
46 Determination of Average Q/A	122
47 Radiator System Schematic For Transient Performance Analysis . .	123
48 Transient Performance of Orbiter Radiator	124
49 Radiator Cooldown Transient After Reentry	125
50 Integral Radiator Atmospheric Flight Heat Rejection	126
51 Integral Radiator Atmospheric Flight Heat Rejection	127
52 Expendable Fluids Latent Heat	128
53 Vapor Pressure of Expendable Fluids	129
54 Schematic of the Direct Expendable System	130
55 Schematic of the Baseline Cryogenic Coolant System	131
56 Schematic of the Cryogenic Hydrogen System with Expansion Turbine	132
57 Expendable Cryogenic H ₂ System Weight For A 10KW Heat Load . . .	133
58 Expendable Cryogenic H ₂ & Gas Cycle System Weight For A 10KW Heat Load	134
59 Expendable Water System Weight For A 10KW Heat Load	135
60 Comparison of Orbital Expendable Cooling Systems	136
61 Suborbit Heat Rejection System Orbital Boil-Off Penalty	137
62 Atmospheric Flight Expendable Fluid Heat Rejection System Weights	138
63 Ram Air Temperature	139
64 Ram Air System Schematic	140
65 Ram Air Inlet Requirements	141
66 Ram Air System Weights For A 10KW Heat Load	142
67 Single Door Deployed Radiator	143
68 Double Door Deployed Radiator	144
69 Modular Deployed Panel Design	145
70 Integral Radiator Panel Installation	146
71 Radiator Panel Mounting Configurations	147
72 Integral Panel Design	148
73 Typical Orbiter Power Profile	149
74 Baseline EC/LSS Heat Rejection System	150

LIST OF FIGURES (CONTD)

	PAGE
75 EC/LSS Heat Rejection System - Configuration 1	151
76 EC/LSS Heat Rejection System - Configuration 2	152
77 EC/LSS Heat Rejection System - Configuration 3	153
78 EC/LSS Heat Rejection System - Configuration 4	154
79 EC/LSS Heat Rejection System - Configuration 5	155
80 EC/LSS Heat Rejection System - Configuration 6	156
81 EC/LSS Heat Rejection System - Configuration 7	157
82 EC/LSS Heat Rejection System - Configuration 8	158
83 EC/LSS Heat Rejection System - Configuration 9	159
84 EC/LSS Heat Rejection System - Configuration 10	160
85 EC/LSS Heat Rejection System - Configuration 11	161

1.0

SUMMARY

This report presents the results of a parametric weight analysis of heat rejection systems for the Space Shuttle Orbiter. The objective of this investigation is to select two candidate heat rejection systems for the sub-orbit mission phases for preliminary design analysis. A design goal of integrating the suborbital heat rejection system with the overall heat rejection system design and the possible use of a common system for both on-orbit and suborbital operations requires that an overall system be selected and the parametric analyses be applicable to all mission phases. The concept of equivalent weights, with weight penalties assigned for power, induced aircraft drag and radiator area is used to determine weight estimates for the following candidate systems in all mission phases:

- (1) vapor cycle refrigeration
- (2) gas cycle refrigeration
- (3) radiators (space and atmospheric convectors)
- (4) expendable heat sinks
- (5) ram air

Analyses have been conducted to determine the Orbiter power penalty and ram air penalty. Extensive analyses and preliminary design of a space radiator system have also been conducted to determine the radiator weight penalty. A baseline mission has been established which details the heat rejection requirements, timelines and operating conditions.

The parametric analyses are then used with the specific penalties and design conditions to select the optimum overall heat rejection system. Various combinations of different systems are examined with non-optimum systems used in some mission phases in order to examine the concept of commonality. The vapor compression system and an expendable fluid system which utilizes a multi-fluid spraying flash evaporator are selected as the two most promising suborbital heat rejection systems. These systems are used for maximum on-orbit heat rejection in combination with or as a supplement to a space radiator.

Since NASA-MSC is pursuing the development of vapor compression systems and flash evaporators under separate contracts, it is recommended that the remainder of this contractual effort be directed toward additional system optimization and integration studies. The selected systems need to be examined under a range of mission timelines and design conditions to determine the extent of their applicability. Further areas of investigation should include integration of the orbital heat rejection system with the payload cooling requirements and integration of the suborbital heat rejection system with the hydraulic system cooling.

The Space Shuttle Orbiter which is currently under development by the National Aeronautics and Space Administration (NASA) will require a heat rejection system that can operate effectively over a wide range of environment conditions. These conditions include pre-launch, boost, earth orbit, reentry, atmospheric flight and post landing. The uniqueness of each of these environments suggest that a different heat rejection system be used for each mission phase. However, the use of a common system for all or a majority of the mission phases would reduce system complexity, increase reliability and possibly reduce overall system weight.

This report summarizes the work accomplished to date by LTV under Contract NAS 9-11166. The objectives of the work being performed under this contract are to (1) perform trade studies of various heat rejection systems for all mission phases of the Shuttle Orbiter Environmental Control/Life Support Systems (EC/LSS), (2) determine the Orbiter EC/LSS thermal control concepts which optimally satisfy heat rejection requirements for all mission phases, (3) perform preliminary design analyses of the two most promising suborbital heat rejection systems, and (4) determine the capability of existing hardware to fulfill the performance requirements of the selected suborbital heat rejection systems. This interim report describes the trade studies and the selection of the two most promising sub-orbital heat rejection systems.

The following candidate systems have been established for consideration in the selection of the overall heat rejection system.

- (1) vapor cycle refrigeration
- (2) gas cycle refrigeration
- (3) radiators (space and atmospheric convector)
- (4) expendable heat sinks
- (5) ram air

The approach taken in the selection of the overall heat rejection system is as follows: First, parametric weight analyses were conducted for the above systems in all mission phases (prelaunch, boost, orbit, reentry, atmospheric flight and post landing). The concept of equivalent weights was utilized with weight penalties assigned for power required, radiator areas required, and aircraft drag.

Next, the specific design requirements for each mission phase were estimated. With the known design requirements, such as radiator weight and power penalty, the parametric weight data can be used to select the best system for each mission phase. Combinations of systems, with non-optimum systems used in some mission phases, have been examined to determine the lowest overall system weight.

3.0

PARAMETRIC ANALYSES

At the time that this investigation was initiated, the Orbiter was in a preliminary design phase and the heat rejection system design requirements and operating conditions were just beginning to be defined. In order to account for the natural evolution of the design requirements and insure that the system selection is based on the most recent requirements, the weight estimates were conducted on a parametric basis. This will also allow the data to be used for future system selection if the design requirements are further changed. The fixed weight of each candidate system was determined for an assumed heat load and converted to a lb per kilowatt of cooling basis for application to any heat load. The total equivalent system weight was determined for a range of operating conditions and penalties. The parameters included:

- (1) Power Penalty
- (2) Heat sink temperature
- (3) Radiator weight penalty
- (4) Mission Time

The subsequent paragraphs of this section present a discussion of each candidate system, describes the weight analysis, and gives the results.

3.1 Vapor Cycle Refrigeration

The results of a comprehensive evaluation of various heat rejection systems which could be used to provide spacecraft cooling is presented in reference 1. This study uses an effectiveness function to select the heat rejection system on the basis of cost. The effectiveness function considers not only the optimum system weight, but also system volume penalty, maintenance requirements, redundancy requirements, technical risks and development and fabrication costs. For the Space Shuttle earth orbit mission the study showed that for a radiator sink temperature of 20°F, a mechanical vapor compression system ranks above the conventional space radiator system. Based on the results of this study, a vapor cycle refrigeration system was selected as a candidate EC/LSS cooling system for use in both orbit and suborbit mission phases.

For suborbital operations some means of obtaining a low heat sink temperature must be made for effective EC/LSS heat rejection. Ambient air can be used at altitudes above approximately 17,000 feet. For altitudes below this mechanical refrigeration or expendable heat sinks must be used. Gas cycle mechanical refrigeration is considered in paragraph 3.2 and expendable heat sinks are considered in paragraph 3.4.

The advantage in the use of a refrigeration system is due to the fact that the heat rejection temperature is increased above that normally available from the EC/LSS. Condenser temperatures of 120 to 150°F can be used with reasonable operating efficiency thus allowing ambient air to be used for cooling during suborbit operations and allowing the system to operate at higher radiator sink temperatures during orbit operations. For example, as discussed in paragraph 4.2, the steady-state earth orbit, design sink temperature of the orbiter radiator will be approximately 26°F. Since it is desired to have a maximum radiator outlet temperature of approximately 40°F, it is evident that extremely large radiators will be required. Although the total heat rejection requirements are increased by the use of a refrigeration system, the radiator area is reduced due to a higher radiating temperature. For example, consider a radiator inlet of 120°F and an outlet of 40°F. The radiator area requirement for this condition (see paragraph 3.3.1) is: $Q/A_{re} = 29.65 \text{ BTU/hr-ft}^2$.

For the vapor cycle system the condenser heat rejection is given by:

$$Q_c = Q \left(1 + \frac{1}{\text{COP}} \right) \quad (1)$$

where COP is the ratio of the refrigeration capacity to the work required to achieve it. The heat rejection requirements of the system are further increased due to the additional power source waste heat generated by the vapor cycle system power used. For a fuel cell power supply with an efficiency of 0.60, the additional heat rejection is

$$Q_{\text{add}} = Q \left(\frac{.6}{\text{COP}} \right) \quad (2)$$

Assuming that the fuel cell waste heat is rejected at the same temperature as the condenser, the total heat rejection of the system is

$$Q_c = Q \left(1 + \frac{1.6}{\text{COP}} \right) \quad (3)$$

Cycle thermodynamic analyses indicate that a COP of 2.7 is reasonable for a system with a 40°F evaporator and a 120°F condenser. With a direct condensing radiator the average radiator temperature will be very close to the condensing temperature. For the vapor cycle system

$$Q/A\eta_e = \frac{.1713 \times 10^{-8} (580^4 - 490^4)}{1 + \frac{1.6}{2.7}} = 59.6 \text{ BTU/hr ft}^2$$

The above example illustrates that the use of a vapor cycle system can reduce the radiator area requirements by a factor of 1.43. Reduction of the radiator area for the Orbiter is of prime importance since the radiator may have to be deployable in order to protect it from boost and reentry heating, or the radiator coatings may have to be refurbished between flights if the radiator is an integral part of the Orbiter skin. For either concept, a minimum radiator area is desirable for a weight savings and reduction of maintenance problems.

The method used to evaluate the refrigeration systems involves the concept of total equivalent weight. First, system fixed weights are determined. Weight penalties are then assigned to the power used by the system, the radiator area required for orbital operations and the radiator/convector required for suborbital operations or the drag induced by the ram air heat exchanger. The penalty factors for these items are normally the largest contributors to the total equivalent weight of the system. Since the utilization of power and the radiator area requirements are highly dependent on the individual system characteristics as well as the operating conditions, the optimum radiator or heat rejection temperature must be evaluated for the particular Orbiter design conditions. However, the design conditions have not been definitized at this time. Therefore, the refrigeration systems are optimized parametrically for various power penalties, radiator weight penalties, radiation sink temperatures and operating altitudes.

The following sections describe the selection of the refrigeration systems operating characteristics, and the determination of the system fixed weight. A description of the computer routine used to optimize the systems is presented along with detailed results in Appendix A.

3.1.1 Vapor Compression Cycle

In an ideal vapor compression cycle, the refrigerant changes phase at a constant pressure from liquid to vapor as it absorbs heat in the evaporator. A compressor withdraws the vapor generated in the evaporator at a low pressure, isentropically compresses the vapor to a high temperature and pressure condition, and discharges it to the condenser. The refrigerant changes phase from vapor to liquid at a constant pressure in the condenser as heat is rejected to the sink. High pressure liquid refrigerant is then expanded irreversibly in the expansion valve and fed to the evaporator to complete the refrigeration cycle. Figure 1 shows the basic vapor cycle component arrangement.

An actual cycle differs from the ideal in several ways. First, the system is not frictionless; pressure drops do occur in the evaporator, condenser and connecting lines. Second, the compression is not isentropic due to heat transfer between the vapor and compressor walls, fluid friction within the compressor, and mechanical friction losses. Third, any heat gain to the system between the expansion valve and evaporator inlet represents a net loss in the amount of heat that can be removed in the evaporator.

Another actual cycle operating characteristic is that it is desired to insure that the refrigerant is entirely in the vapor phase at the compressor inlet. A mixture of liquid and vapor causes compressor mechanical problems and increases the inefficiency. Some sort of refrigerant flow control is required to insure that all refrigerant is evaporated in the evaporator. This is usually accomplished in the expansion valve since the control system for a variable speed motor increases the system complexity. To insure that pipe friction losses do not cause the condensation of any vapor between the evaporator and compressor, a few degrees of superheat is desirable. The super heat can be accomplished in the evaporator or by a regenerative heat exchanger which heats the evaporator outlet by subcooling the liquid out of the condenser. The regenerative heat exchanger method is lighter than the additional evaporator weight if the temperature difference between the condenser and evaporator is greater than the difference between the heat source and the evaporator.

3.1.2 Working Fluids

Sixty-nine different refrigerants have been assigned standard designations or refrigerant numbers by the American Society of Heating, Refrigerating and Air Conditioning Engineers (reference 3). While all of these refrigerants have been used or can be advantageously employed under certain conditions, only a few are used commercially at the present time. The Freon family of halocarbons or halogenated hydrocarbons are most widely

used commercially and appear best suited for the Orbiter. They are characteristically non-toxic, non-irritating and non-flammable. Halocarbons are synthetically produced by the substitution of the halogen (fluorine, chlorine or bromine) for one or more of the hydrogen atoms in methane, ethane or propane (CH_4 , C_2H_6 , C_3H_8). A two or three digit number is used for the halocarbon designations. The 200 series numbers indicate a basic propane structure, the 100 series indicates an ethane structure, and the two digit series (a blank and two digits) indicates a methane structure. The last digit in the designation (the one on the right) indicates the number of fluorine atoms in the molecule of the compound formed. The second digit from the right is one more than the number of hydrogen atoms remaining. The bromine atoms in the compound are indicated by the letter B and the number of atoms following the numerical designation. Thus R-13B1 has the chemical formula CBrF_3 . Azeotropes which are mixtures of two halocarbons are designated by the 500 series numbers.

Table 1 presents some refrigerant property data and theoretical operating characteristics of various refrigerants which are important for refrigerant selection for the Orbiter. General property data to be considered include the freezing point for quiescent orbital operation and the vapor pressure at 200°F (design temperature for inside of cargo bay door during reentry). These properties are important; however, refrigerants with high freezing points or vapor pressures cannot be ruled out completely since special designs such as storing the refrigerant in a more favorable environment (orbiter interior) could be accomplished if the refrigerant had other superior properties. The most important criteria for the orbiter is the power required to run the vapor cycle system. Table 1 indicates that R-11, R-21, R-113, R-12, R-22 and R-500 have the lowest theoretical power requirements of the refrigerants considered. The actual power requirement is primarily determined by the compressor efficiency which in turn is influenced by the refrigerant. Compressor discharge temperature, displacement, flow rate and compression ratio all have an effect on the type of compressor selected and the adiabatic efficiency. For example, R-21 has a high compressor discharge temperature (Table 1) which increases heat transfer to the compressor walls; R-11 requires a high compressor displacement indicating a centrifugal or high speed rotary type of compressor, but also has a high compression ratio. Centrifugal compressors are usually used for low pressure ratios; normally from 2.5 to 4.5 per stage when using one or two stages (reference 3). Other considerations in the selection of a refrigerant include the evaporator and condenser pressures. Low pressures allow the design of lighter weight equipment.

Final selection of a refrigerant and compressor for the orbiter vapor compression refrigeration system is a complex problem requiring the consideration of many variables. Previous aircraft vapor compression systems appear to have put a premium on component weight and volume requirements. For the orbiter, the power penalty is the major contributor to the system weight and the system design should be tailored for maximum power utilization. Within the scope of the parametric analyses conducted herein, it appears that R-11, R-21, R-113, R-12, R-22 and R-500. All have possible applications to the orbiter vapor compression system.

TABLE 1 THEORETICAL REFRIGERANT PERFORMANCE

BASED ON ONE TON OF REFRIGERATION
+40°F EVAPORATING; 130°F CONDENSING

	"R-11"	"R-12"	"R-13B1"	"R-21"	"R-22"	"R-113"	"R-114"	"R-115"	"R-C318"	"R-502"	"R-500"
Comp. Suction Gas Temp., °F	40	40	40	40	40	54.1***	63.0***	53.6***	72.4***	40	40
Evap. Pressure, psia	7.02	51.67	138.6	12.32	83.72	2.66	15.08	73.65	22.13	94.90	60.75
Cond. Pressure, psia	38.67	195.71	448.9	65.15	314.0	18.45	72.66	268.77	106.66	332.7	231.9
Comp. Ratio	5.51	3.79	3.24	5.29	3.74	6.95	4.82	3.67	4.82	3.51	3.81
Net Refrig. Effects **, Btu/lb	61.77	42.88	19.98	82.06	59.08	48.90	36.39	19.90	24.08	35.71	51.24
Refrig. Circ. lb/min	3.238	4.664	10.010	2.437	3.385	4.090	5.497	10.049	8.305	5.601	3.9
Sp. Volume of Vapor, cuft/lb	5.430	0.774	0.213	4.130	0.658	11.001	2.100	0.426	1.223	0.447	.792
Comp. Displacement, cuft/min	17.58	3.61	2.13	10.07	2.23	44.99	11.54	4.28	10.15	2.50	3.09
Power, kw	0.738	0.835	1.125	.746	.85	.797	.91	1.78	1.13	.961	.841
COP	4.745	4.214	3.132	4.729	4.144	4.397	3.870	1.978	3.097	3.643	4.16
Comp. Discharge Temp., °F	145.9	141.3	153.1	175.0	168.7	130.0	130.0	130.0	130.0	147.0	145.5
Freezing Temp., °F	-168	-252	-270 *****	-211	-256	-31	-137	-159 *****	-42.5	<-80 *****	-254
Vapor Press @ 200°F, psia	105.5	430.9	574.9	180	686.36	54.66	178.4	458	260	619	511.1

** Saturated vapor and liquid

*** Superheat required to prevent condensation in comp.

**** At critical press.

3.1.3 System Performance

When evaluating the thermodynamic suitability of a refrigeration cycle, it is useful to consider the coefficient of performance. The coefficient of performance (COP) of a refrigeration cycle is equal to the ratio of the refrigerating effect produced to the energy of compression. Expressed in equation form, with nomenclature of Figure 1 this becomes:

$$\text{COP} = \frac{h_2 - h_1}{h_3 - h_2} \quad (4)$$

where; h = enthalpy, BTU/lb

This is a measure of the cycle's performance, but is useful only if there is some absolute standard of performance to compare it against. It is therefore convenient to define the refrigerant efficiency as:

$$\text{Refrigerant Efficiency} = 100 \times \frac{\text{Actual COP Value}}{\text{Carnot Cycle COP}} \quad (5)$$

The carnot COP is defined as:

$$\text{COP} = \frac{T_2}{T_4 - T_2} \quad (6)$$

The Carnot COP depends only on the values of T_2 and T_4 which are the evaporator and condenser temperatures respectively.² The simple vapor compression cycle is never as efficient as the optimum Carnot cycle operated at the same temperature levels.

The operating temperatures of a vapor compression cycle have a strong influence on the magnitude of the coefficient of performance. Decreasing the evaporating temperature or increasing the condensing temperature both result in a reduction of the C.O.P.. The work required to increase the pressure of the working fluid in the compressor increases, and the amount of heat that can be transferred in the evaporator is decreased.

Cycle thermodynamic analyses have been performed for the six refrigerants selected in paragraph 3.1.2. Figures 2 through 4 present the refrigerant efficiency of the candidate refrigerants for a system which utilizes a direct condensing radiator (Figure 6a). A 10°F sub-cooling and superheat were assumed for this analysis and values were obtained for compressor adiabatic efficiencies (η) of 0.6, 0.7 and 0.8 with an electric motor efficiency of 0.85. As indicated, R-11 and R-21 have the highest refrigerant efficiency especially for differences in condenser and evaporator temperatures greater than 100°F.

Figure 5 presents the results of cycle thermodynamic analyses for a system which utilizes a secondary cooling loop between the condenser and the radiator. R-21 is used as both the refrigerant and the coolant in the secondary loop. The COP for this system is calculated based on the power required to operate the refrigeration system and the pumping power for the

secondary loop. A pump efficiency of 0.6 and a secondary loop pressure drop of 10 psi was used to calculate the pump power. The secondary loop flow rate was determined from the condenser heat rejection requirements for radiator inlet-outlet temperature differences of 20, 30 and 40°F. The Carnot COP for this system is calculated on the basis of the radiator temperature which is computed from the average of the inlet and outlet with 5°F allowed for the fluid to tube temperature difference. The radiator inlet temperature is taken as 5°F less than the condenser temperature and the outlet temperature depends on the inlet-outlet temperature difference used.

3.1.4 Component Weight Data

Two vapor compression system configurations were chosen for the parametric weight analyses. One configuration (see Figure 6a) used a direct condensing radiator or atmospheric convector, which rejected its heat directly to the environment. The other configuration (Figure 6b) utilized a conventional condensing heat exchanger and a secondary fluid loop which flowed to a surface radiator or atmospheric convector. The Refrigeration Systems Plotting and Linearized Analysis Technique (RSPLAT) computer routine used to evaluate the systems computes the radiator weight or the ram air condenser weight, so the system fixed weight should not include these components.

The approach used to determine the fixed weight associated with the vapor compression refrigeration system was to perform a cycle analysis with typical operating conditions postulated for the orbiter EC/LSS. The performance requirements of the various components can then be determined and weight estimates made for each component. Weights were estimated for the following components:

- Evaporator
- Condenser
- Subcooler
- Compressor
- Pump
- Electric Motor

and the total system fixed weight determined by summing the appropriate components for each configuration. The weight of the system controls, valves, lines, ducts, mounting frames, etc. were estimated by applying a factor of 0.5 to the sum of the component weights as recommended by reference 4.

Heat Exchangers

The procedure used to evaluate the heat exchangers (evaporator, condenser and subcooler) weight was taken from reference 5.

The weight of the heat exchanger is estimated from

$$W = 1.34 P_c V_c^{.882} \quad (7)$$

Where, P_c is the core weight density taken as 19.2 lb/ft³ for a finned tube type exchanger and 34.1 lb/ft³ for a shell and tube type exchanger. The core volume, V_c is given by

$$V_c = \frac{Q}{U A \Delta T} \quad (8)$$

Where:

- Q = required heat transfer rate, BTU/hr
 ΔT = the temperature difference between the hot and cold fluids
 (assumed to be 10°F)
 UA = overall heat transfer coefficient, BTU/hr °F ft³

$$\frac{1}{UA} = \frac{1}{\epsilon h_1 A_1} + \frac{1}{\epsilon h_2 A_2} \quad (9)$$

Where:

- ϵ = the heat exchanger effectiveness (assumed to be 0.85, except for the subcooler)
 h = the heat-transfer coefficient BTU/hr ft² °F
 A = the heat exchanger surface area per unit volume of the exchanger core

Typical heat transfer coefficients were taken from reference 5 as follows:

<u>h - BTU/hr ft² °F</u>	<u>Conditions</u>
10	Flowing gas
200	Flowing liquid
1000	Boiling liquid
750	Condensing liquid

The surface area density was also taken from reference 5 as follows:

<u>Applications</u>	<u>A-ft²/ft³ of core volume</u>	
	<u>Side 1</u>	<u>Side 2</u>
Liquid to gas	46.7	597
Liquid to liquid	280	313

Compressors

Reference 5 gives an estimation curve for piston and centrifugal compressors. This data is presented as Figure 7 which also shows actual manufacturer's data. It is not clear whether the compressor weights include the electric motor or not; however, the manufacturer's data indicates that the curve includes the motor. The manufacturer's data also indicates that the motor weights are probably not aerospace type motors which are lighter than non-aerospace motors. The data presented in Figure 7 was therefore used in the following manner: The weight value read from the curve for the required horsepower was multiplied by 0.5 and this value is used as the compressor only weight. Weight estimates of the motor are then made from aerospace motor data.

Electric Motors

Figure 8 presents weight data for aerospace electric motors. As indicated, there is considerable scatter of data and a wide discrepancy in weights, particularly for motors above 10 horsepower. The line drawn through the data computed by reference 4 was used in the parametric weight analysis. This data appears to be conservative and is for motors used to drive compressors, turbines and fans.

Pumps

The pump weight was estimated from the data presented in reference 6. This data is presented in Figures 9 and 10. Figure 9 presents typical values of pump speed and displacement volume per revolution. This curve was used to insure that the displacement volume used to read the pump weight from Figure 10 yielded reasonable pump speeds. The upper line of Figure 10 will be more typical of a piston pump while the lower line is more typical of a light weight vane pump. At displacements below 0.2 in³/rev the gear pump weight compares with a vane pump; above this value it compares more to a light weight piston pump.

System Specific Weight

The above weight estimates for the vapor compression system components were used to determine the weight of a typical system that could be used on the Orbiter. The system parameters used are:

$$Q_{\text{LOAD}} = 30,000 \text{ BTU/hr}$$

$$\eta_{\text{COMP}} = .70$$

$$T_{\text{EVAP}} = 40^{\circ}\text{F}$$

$$T_{\text{COND}} = 140^{\circ}\text{F}$$

$$\text{Refrigerant: R-21}$$

$$\text{Superheat} = 10^{\circ}\text{F}$$

For the above conditions the system performance is:

$$\begin{aligned} \text{COP} &= 2.47 \text{ with direct condenser} \\ &= 2.09 \text{ with secondary cooling loop and pump} \end{aligned}$$

$$\text{Compression Ratio} = 6.14:1$$

$$\text{Superheater heat load} = 480 \text{ BTU/hr}$$

$$\text{Compressor power} = 4.08 \text{ hp}$$

$$\text{Motor power} = 4.77 \text{ hp}$$

$$\text{Pump motor power} = 0.174 \text{ hp}$$

$$\text{Compressor outlet temperature} = 250^{\circ}\text{F}$$

$$\text{Refrigerant flow} = 368 \text{ lb/hr}$$

$$\text{Secondary coolant flow} = 128 \text{ lb/min}$$

The component weights for this system are:

(a) Configuration 1, direct condenser

Evaporator	19
Subcooler	1
Compressor	11.5
Electric Motor	9
Freon charge	4
Controls, lines, valves, mounts, etc.	22

Total 66.5 lb.

or 7.6 lb per kilowatt cooling

(b) Configuration 2, secondary cooling loop

Evaporator	19
Subcooler	1
Compressor	11.5
Electric motor	9
Condenser	26
Pump	5
Pump motor	3
Coolant charge	4
Freon charge	4
Controls, lines, valves, mounts, etc.	22

Total 104.5



or 11.9 lb per kilowatt cooling

Table 2 presents component and system specific weights for aircraft Freon 11 vapor compression systems designed by the computer routine described in reference 4. This routine includes a ram air condenser and a pump or fan to provide coolant flow on the hot side of the evaporator. These components are not included in the specific weight of the orbiter Configuration 1 system and have been subtracted from the total weight in order to obtain comparable specific weights. As indicated by Table 2, the specific weight obtained by the computer routine ranges from 4.4 to 24.6 lb/kw and it appears that a value of 7.6 lb/kw would be representative. References 7 and 8 give weight data for the XB-70 and Constellation Aircraft vapor compression cooling systems of 8.04 lb/kw and 13.3 lb/kw, respectively.

The application of a vapor compression system to the orbiter must consider the reliability requirements. Using the fail-operational, fail-safe requirements for mechanical equipment and fail-safe requirements for structure, the following system weights are obtained:

TABLE 2 AIRCRAFT VAPOR COMPRESSION SYSTEM WEIGHTS

Specific Weights From AIRSCOPE Computer Routine

DESIGN CONDITIONS FOR 9.5 kw COOLING LOAD				
MACH NO.	ALTITUDE FT.	EVAP. TEMP. °F	CONDENSER TEMP. °F	SPECIFIC WEIGHT* lb/kw
.2	0	12.85	119.1	13.0
.2		29.15	130.	6.4
.2		43.32	126.1	7.2
.2		86.6	128.2	7.1
.4		19.52	129.1	14.5
.4		29.15	139.4	5.7
.4		43.32	139.2	6.0
.4		86.6	143.0	4.7
.6		32.9	144.4	24.6
.6		42.5	159.5	5.8
.6		43.3	155.9	6.6
.6		86.6	155.6	5.3
.8		55.8	184.9	8.3
.8		86.6	185.7	5.3
1.0		82.5	227.1	13.4
1.0		86.6	228.0	5.1
.2	10,000	-7.2	89.4	8.9
.2		29.15	92.3	8.6
.2		43.3	101.2	7.3
.4		-0.5	99.2	7.7
.4		29.15	100.0	7.3
.4		43.3	101.2	7.6
.4		86.6	128.2	5.3
.6		12.9	119.1	7.8
.6		29.15	119.3	6.0
.6		43.3	118.6	6.5
.6		86.6	128.2	5.8
.8		26.2	139.2	19.1
.8		29.15	143.7	6.9
.8		43.3	145.1	6.5
.8		86.6	143.0	6.2
1.0		55.8	184.9	6.6
1.0		86.6	185.7	4.4

* Does not include ram air condenser and pump or fan for evaporator hot side coolant flow.

(a) Configuration 1, direct condenser

Evaporator (2)	38
Subcooler (2)	2
Compressor (3)	34.5
Electric motor (3)	27
Refrigerant charge (2)	8
Controls, lines, valves, mounts, etc.	<u>44</u>
Total	153.5 lb

or 17.5 lb per kilowatt cooling

(b) Configuration 2, secondary loop

Evaporator (2)	38
Subcooler (2)	2
Compressor (3)	34.5
Electric Motor (3)	27
Pump (3)	15
Pump motor (3)	9
Coolant Charge (2)	8
Refrigerant Charge (2)	8
Controls, lines, valves, mounts, etc.	<u>44</u>
Total	185.5 lb

or 21.1 lb per kilowatt cooling

The specific weight of the system will vary with the size of the system, component operating efficiencies and operating temperatures. For example, the compressor and electric motor weights would not double for a system designed for twice the evaporator load and the heat exchanger weights are seen to be a function of the heat load to the 0.882 power. However, the two systems analyzed above are felt to be representative of systems that could be used on the orbiter and system specific weights of 17.5 lb/kw_C and 21.1 lb/kw_C will be used in the parametric weight analyses.

3.1.5 Parametric Weight Analyses

The Refrigeration System Plotting and Linearized Analyses Technique (RSPLAT) computer routine described in Reference 1, was used to conduct parametric weight analyses of a vapor compression refrigeration system for the orbit and atmospheric flight mission phase. To do this analysis, RSPLAT was modified to include a ram air condenser and an external convecting radiator to be used in the atmospheric flight phase. A description of the modified routine is presented in Appendix A. Three simple vapor compression systems were analyzed. Each of these systems utilized a different condenser. The first system uses a direct condensing radiator, which rejects heat directly into the environment, (either space or the atmosphere). The second type utilizes a conventional condensing heat exchanger to transfer the heat load

to a secondary fluid loop. This secondary loop flows to a radiator which dissipates the system heat load. The last condenser system is a ram air heat exchanger which is applicable only to the atmospheric flight portion since it rejects heat by forced convection to the captured air. This system requires a ram air inlet, which must be protected during reentry, and interior air ducts to the heat exchanger.

The RSPLAT routine computes and plots the total system weight as a function of heat rejection temperature (radiator, atmospheric convector, or ram air condenser). The optimum heat rejection temperature for the specified conditions is then determined from the minimum weight point. The systems were evaluated on a parametric weight basis (lb/kw_C) so the results can be utilized for any heat load. The total system weight at any particular set of conditions is the sum of three terms. These include the weight quantities contributed by the fixed weight, the electrical power penalty, and the radiator weight penalty or the ram air penalty. The system and flight parameters used to compute these weight quantities are: COP data, fixed weight, evaporator temperature, condenser temperature, heat rejection sink temperature, radiator weight penalty, altitude and external radiator heat transfer coefficient. The system operating characteristics and fixed weights developed in Paragraphs 3.1.3 and 3.1.4 were input to RSPLAT and system weights computed for a variety of power penalties, radiator weight penalties and environment conditions. Two flight regimes were examined; the orbital phase which consisted of a seven day earth orbit and the atmospheric fly back. The flight envelope for the atmospheric fly back ranged from an altitude of 50,000 ft. to sea level. A MIL STD 210A hot day atmosphere was used and the mach number was assumed to remain a constant 0.40 until prior to landing due to lack of better flight data. Table 3 shows the specific parameters for which weight computations were made.

Figures 11 and 12 are typical results for the orbital and flyback phases respectively. The complete results are given in Appendix A. As indicated by Figures 11 and 12 the system weight first decreases with heat rejection temperature, then increases. The minimum weight is obtained when the additional power required for operating the system at a higher temperature overcomes the weight savings of the smaller radiator area required. The complete parametric weight analyses are summarized in Figures 13-29. These figures show the minimum specific weight as a function of power penalty, radiator weight penalty and sink temperature, or altitude. The operating conditions at the minimum weight condition can be determined from the data presented in Appendix A.

3.2 GAS CYCLE REFRIGERATION

Refrigeration can be accomplished by the expansion of a high pressure gas, with the refrigerant remaining in the gaseous phase. Whereas the refrigeration effect per pound of fluid circulated in a vapor compression cycle is due mostly to the enthalpy of vaporization, in a gas cycle it is only the product of the temperature drop of the gas and its specific heat. Gas cycle systems are used commonly in the air conditioning of jet aircraft due to the

TABLE 3
PARAMETERS USED IN REFRIGERATION SYSTEM PARAMETRIC ANALYSIS

ORBITAL PHASE			FLYBACK PHASE		
T_{sink} °F	Power Penalty LB/KW _e	Rad Penalty lb/ft ²	Altitude ft x 10 ⁻³	Power Penalty lb/KW _e	Rad Penalty lb/ft ²
0	30.	0.5	1	10.	.5
10	60.	0.75	10	20.	.75
20	100.	1.0	20	30.	1.0
30	200.	1.25	30	40.	1.25
40	300.	1.5	40	50.	1.5
60	400.	1.75	50		1.75
80	500.	2.0			2.0
	600.				

ready availability of high pressure air from the jet engine and the light weight compact equipment which is typical of gas cycle systems. Due to the wide use of gas cycle systems in aircraft this system was chosen for parametric analyses. Consideration was given to the use of a gas cycle system in both the orbit and atmospheric flight mission phases. As discussed previously for the vapor compression cycle, the primary advantage of mechanical refrigeration is that the heat rejection temperature is increased above that normally available from the EC/LSS.

3.2.1 Gas Cycle

Figure 30 shows a schematic of an ideal closed gas cycle system and its thermodynamic states on the temperature-entropy diagram. The cycle shown is the Brayton refrigeration cycle or reversed Brayton cycle. As shown in Figure 30, the ideal cycle consists of two heat exchange units, a turbine, a compressor, and an external power source. Within the low temperature exchanger, the heat load is transferred to the flowing gas in a constant pressure process. The flow is then compressed to the high side pressure in an ideal isentropic compressor. The heat load is removed from the fluid in the high temperature exchanger again in a constant pressure process. To reduce the fluid pressure to its low side value, an isentropic turbine acts to expand the flow. Then the refrigerating fluid completes the cycle by returning to the low side heat exchanger. To partially offset the large amount of shaft work needed by the compressor, the turbine shaft is connected to the compressor shaft so that the turbine work produced during the expansion can drive the

compressor. The result is that the network required by the system is the difference in the two work quantities.

For an ideal gas and isentropic compression and expansion the coefficient of performance is given by:

$$\text{COP} = \left[\frac{T_4}{T_1} - 1 \right]^{-1} \quad (\text{Ref. 2}) \quad (10)$$

or

$$\text{COP} = \left[\text{CR}^{\frac{\gamma-1}{\gamma}} - 1 \right]^{-1} \quad (11)$$

Where CR is the compression or pressure ratio and γ is the ratio of specific heats.

Equation (10) indicates that as the temperature difference $T_4 - T_1$ becomes small the COP increases, approaching infinity as the temperature difference goes to zero. It would seem that the choice of a low pressure ratio would be desirable for high COP (Equation (11)). The minimum pressure ratio for an ideal cycle operating between a source temperature T_2 and a sink temperature T_4 is given by (Reference 2).

$$\text{CR} = \left(\frac{T_4}{T_2} \right)^{\gamma/\gamma-1} \quad (12)$$

However, the refrigeration per pound of fluid circulated would be zero at this pressure ratio. As the pressure ratio is increased beyond the minimum value, the required rate of fluid circulation is reduced. Losses and therefore deviation from the ideal COP will increase as the compression ratio rises, offsetting the improved efficiency of the lower flowrate. Therefore, a compromise must be made between cycle efficiency and rate of circulation of fluid.

The actual gas cycle COP varies considerably from that of the ideal cycle, primarily because of inefficiencies in gas compression and expansion, fluid friction losses within the heat exchangers and mechanical losses. Neglecting the fluid pressure drop in the heat exchangers and lines, and assuming a constant specific heat, the COP of the actual system is given by:

$$\text{COP} = \frac{T_2 - T_4 \left[1 - \eta_t + \frac{\eta_t}{\text{CR}^{\gamma-1/\gamma}} \right]}{T_2 \left[\frac{\text{CR}^{\gamma-1/\gamma} - 1}{\eta_c} \right] - T_4 \left[\eta_t - \frac{\eta_t}{\text{CR}^{\gamma-1/\gamma}} \right]} \quad (13)$$

Where

$$\eta_t = \frac{T_4 - T_1}{T_4 - T_{1s}} = \text{turbine efficiency}$$

and

$$\eta_c = \frac{T_{3s} - T_2}{T_3 - T_2} = \text{compressor efficiency}$$

where the subscript s refers to isentropic conditions.

An examination of equation (13) indicates that for a given η_t , η_c and γ a small CR is desirable to obtain the maximum COP. However, for an actual cycle to operate:

$$T_1 \leq T_2 \quad \text{and} \quad T_3 \geq T_4 \quad (14)$$

or

$$CR_{MIN} \geq \left[\frac{T_4 \eta_T}{T_2 - T_4 (1 - \eta_T)} \right]^{\gamma/\gamma-1} \quad (15)$$

and

$$CR_{MIN} \geq \left[\frac{\eta_c}{T_2} \left(T_4 + \frac{T_2}{\eta_c} - T_2 \right) \right]^{\gamma/\gamma-1} \quad (16)$$

As in the ideal cycle, the refrigeration per pound of fluid circulated would be zero if the minimum CR is determined by equations (15) and (16). For a CR greater than the minimum, a lower flow rate is required. The turbine and compressor efficiency is a function of flow rate as well as CR. Therefore, a trade-off must be made between the system flow rate and CR to obtain the optimum COP.

3.2.2 Working Fluids

The first consideration in the selection of a fluid for a gas cycle system is of course that the fluid must remain in the gaseous phase in the desired pressure-temperature range of the cycle. Other considerations are toxicity and combustibility.

Equation (13) indicates that the only thermo-physical property of the fluid that affects the cycle performance is the ratio of specific heats, γ .

The fluid specific heat determines the required flow rate and although this does not influence the cycle COP it would be generally desirable to have a lower flow rate. Reference 2 reports that a high γ improves the cycle COP, whereas reference 9 indicates a higher COP for a lower γ . The analyses conducted herein assumed a compressor and turbine efficiency and it was determined that the maximum COP was independent of γ . The γ did influence the pressure ratio for which the maximum COP was obtained. Figure 31 presents COP as a function of pressure ratio for various values of γ . As indicated the larger γ 's yield the maximum COP at small pressure ratios. This data is in agreement with reference 9 for pressure ratios greater than the optimum. It is concluded that a fluid with a high γ is desirable since the compressor and turbine efficiency decrease for high pressure ratios.

Table 4 presents average values of γ and C_p for fluids that could be used in a gas cycle system. Helium appears to have the most desirable properties. Hydrogen has the highest C_p , but is highly combustible.

Fluid	γ	C_p
Air	1.4	.24
Hydrogen	1.4	3.4
Helium	1.66	1.25
Freon 12	1.17	.14
CO ₂	1.3	.20
Nitrogen	1.4	.25
Methane	1.3	.54

TABLE 4 GAS CYCLE FLUID PROPERTIES

3.2.3 System Performance

Figure 32 presents the gas cycle COP for various compressor and turbine efficiencies as a function of the difference between the average heat rejection temperature and the heat source temperature. This data was obtained from a computer routine which systematically increments the pressure ratio to obtain the maximum COP for the particular set of conditions. The compressor inlet temperature (T_2), the expansion turbine inlet temperature (T_4) and the

compressor and turbine adiabatic efficiency were input to the routine. The required power and operating temperatures, T_1 and T_3 , are then computed for different pressure ratios until the minimum power required is obtained. Consideration must also be given to the operating temperatures at the optimum pressure ratio. The compressor outlet temperature must be within the working limits of the compressor material and the expansion turbine outlet temperature must not be so low as to cause freezing of the orbiter coolant. Table 5 presents the operating conditions for each of the cases analyzed.

Air was chosen as the working fluid for the baseline system used in the parametric weight analysis. Air requires a relatively low pressure ratio, and has an average specific heat requiring reasonable flow rates. As previously discussed helium shows the most desirable thermal properties but an air cycle should yield representative performance.

As indicated by Figure 32 the compressor and turbine efficiency greatly influences the system performance; the turbine efficiency appears to have the predominate effect on the COP. Some investigators (reference 9 and 10) have assumed efficiencies as high as 0.85 in their analytical studies. Reference 11 presents operating data for the air cycle system used on the Boeing 747 airplane. This system has the compressor and turbine operating at the same speed on a common shaft similar to the baseline system in this study. Data presented for ground operation of the unit on a hot day indicates a compressor efficiency of 0.645 and a turbine efficiency of 0.496. Based on this data of an actual system and the expected difficulty of optimizing both compressor and turbine efficiency turning at the same speed, compromise values of $\eta_c = 0.7$ and $\eta_t = 0.80$ were chosen for the system parametric weight analyses.

3.2.4 Component Weight Data

The gas cycle system fixed weight was determined by estimating the weight of each component. A cycle thermodynamic analysis with expected operating conditions was performed to determine the performance requirements of each component. Weight estimates were made for the following components.

- Compressor
- Turbine
- High Temperature Heat Exchanger
- Low Temperature Heat Exchanger
- Electric Motor

The weight of the system controls, valves, ducts, mounting frames, etc. was estimated by applying a factor of 0.5 to the sum of the component weights as recommended by reference 4.

Figure 33 shows the schematic arrangement of the above components. Figure 33A depicts the type of systems that could be used for orbital operations. The high temperature side of the gas cycle system is cooled by a coolant loop and space radiator. Preliminary analyses have indicated that direct cooling of the hot gas in a space radiator is not practical due to the low gas to tube

TABLE 5 GAS CYCLE OPERATING CONDITIONS

$$T_2 = 500^{\circ}\text{R}$$

η_c	η_t	T_1 ($^{\circ}\text{R}$)	T_3 ($^{\circ}\text{R}$)	T_4 ($^{\circ}\text{R}$)	CR	COP	EFF
.7	.6	438.8	824.5	540	3.7	.233	.019
.7	.6	428.5	1004.1	570	6.5	.168	.023
.7	.6	421.8	1255.8	610	12.5	.117	.026
.7	.6	443.2	1364.2	660	16.0	.075	.024
.7	.6	463.2	1483.7	710	20.7	.042	.018
.7	.7	435.4	773.4	540	3.1	.326	.026
.7	.7	423.2	915.8	570	5.0	.243	.034
.7	.7	413.1	1111.2	610	8.7	.178	.039
.7	.7	413.9	1314.5	660	14.3	.129	.041
.7	.7	434.9	1385.5	710	16.8	.091	.038
.7	.8	433.0	735.3	540	2.7	.444	.036
.7	.8	419.1	853.3	570	4.1	.340	.048
.7	.8	406.5	1010.7	610	6.6	.259	.057
.7	.8	397.8	1204.4	660	11.0	.196	.063
.7	.8	404.0	1334.5	710	15.0	.154	.065
.8	.6	442.3	769.6	540	3.5	.285	.023
.8	.6	431.2	926.8	570	6.2	.203	.028
.8	.6	423.9	1146.4	610	12.0	.140	.031
.8	.6	443.2	1256.2	660	16.0	.090	.029
.8	.6	463.2	1360.7	710	20.7	.051	.021
.8	.7	437.9	731.2	540	3.0	.409	.033
.8	.7	426.2	852.4	570	4.8	.301	.042
.8	.7	417.0	1015.4	610	8.2	.219	.048
.8	.7	413.9	1212.7	660	14.3	.157	.050
.8	.7	434.9	1274.8	710	16.8	.111	.047
.8	.8	440.1	687.9	540	2.5	.578	.046
.8	.8	425.8	789.0	570	3.8	.435	.061
.8	.8	413.0	923.0	610	6.1	.327	.072
.8	.8	403.6	1090.0	660	10.2	.246	.079
.8	.8	404.0	1230.2	710	15.0	.192	.081

heat transfer coefficient. If the tubes are made small to yield high heat transfer coefficients, large pressure drops result. For suborbital operations a ram air heat exchanger is used to cool the compressor outlet as shown in Figure 33b.

It would be possible to use an open cycle system during suborbit operation for cabin cooling, thus eliminating the low temperature heat exchanger. In this system flow from the expansion turbine would be routed directly to the cabin and dumped overboard and the compressor suction would be supplied from the atmosphere. However, a liquid cooling loop will be required during orbital operations and the additional duct weights required by the open cycle system would tend to offset the weight savings of removing the heat exchanger. Reference 12 reports that the combined weights of turbines and compressors of the type used in air cycle systems can be approximated by the empirical equation

$$W = 24 \dot{w}_a \quad (17)$$

where \dot{w}_a is the air flow rate in lb/sec and W is the weight in pounds. A minimum value for \dot{w}_a of 0.333 lb/sec should be used in equation (17). The above expression does not include the weight of the electric motor required to drive the compressor. The data presented in the discussion of the vapor compression system component weights (Figure 8) is used to estimate the motor weight.

The heat exchanger weights are estimated by the method presented in Paragraph 3.1.4.

The above relationship for the gas cycle components were used to determine the weight of typical systems (Figures 33A and 33B) that could be used on the orbiter. The system parameters used are:

$$\begin{aligned} Q_{\text{LOAD}} &= 30,000 \text{ BTU/hr} \\ \eta_{\text{COMP}} &= .7 \\ \eta_{\text{TURB}} &= .8 \\ T_2 &= 40^\circ\text{F} \\ T_4 &= 110^\circ\text{F} \\ \gamma &= 1.4 \\ C_p &= .24 \text{ BTU/lb}^\circ\text{F} \end{aligned}$$

For the above conditions the system performance is:

$$\begin{aligned} \text{COP} &= 0.34 \\ \text{CR} &= 4.1:1 \\ \dot{w} &= 1541 \text{ lb/hr} \end{aligned}$$

Power required = 34.7 hp

T_1 = -41°F

T_3 = 394°F

The component weights for the system shown in Figure 33A are given below. The RSPLAT routine used to optimize the system operating temperature computes the weight of the radiator so this is not included in the component weights.

High temperature heat exchanger	67.4
Low temperature heat exchanger	5.7
Turbine and compressor	10.3
Electric motor	43.0
Ducts and controls	<u>63.</u>
TOTAL	189.4

The component weights for a system which utilizes a ram air heat exchanger for cooling (Figure 33b) are the same as above with the exception of the high temperature heat exchanger. The RSPLAT routine computes the weight of the ram air heat exchanger so that this weight should not be included in the system fixed weight.

Figure 34 presents weight data from reference 7 for various military aircraft using the gas cycle refrigeration system for cooling. All of these systems use bleed air from the main engine(s) and some use the bootstrap concept whereby the load on the expansion turbine is used to drive a compressor to further compress the fluid before expansion in the turbine. All systems also use an air-to-air heat exchanger to cool the bleed air from the compressor and are open systems, i.e., the cooled air is routed directly to the cabin or equipment compartment, then dumped overboard. There are apparently no redundancy requirements; emergency ram-air ventilation provisions are included in the systems.

The data of Figure 34 indicate two distinct ranges of specific weights for transports and bombers and for fighter aircraft. This difference is attributed to the large duct weights associated with larger transport type aircraft where the high pressure engine bleed air must be routed to the expansion turbine and the conditioned air must be routed to the cabin and/or remote electronics. The fighters are much smaller and compact and the duct weights do not have as much influence on the overall system weight. Therefore, the fighter specific weight data appears to be more applicable to the closed cycle system envisioned for the Orbiter.

Application of the component weight estimates to an aircraft type system for the stated system parameters (heat load = 30,000 BTU/lb, etc.) yields the following weights:

Ram air heat exchanger and duct	85.5
Turbine and compressor (bootstrap)	10.3
Ducts and controls	<u>48.0</u>
TOTAL	<u>143.8</u> lb.

The ram air heat exchanger and duct weight estimates are made for a design condition of 100°F ram air at sea level using the techniques presented in Paragraph 3.5. The above analysis yields a system specific weight of 16.3 lb/kw_C. As indicated by Figure 34, this compares favorably with the actual installed weights indicating that the component weight estimates are representative.

The application of a gas cycle system to the Orbiter must consider the reliability requirements. Using the fail-operational, fail-safe requirements for mechanical equipment and fail-safe requirements for structure, the following system weights are obtained.

(a) Orbital System (Figure 33a)

High temperature heat exchanger (2)	134.8
Low temperature heat exchanger (2)	11.4
Turbine and compressor (3)	30.9
Electric Motor (3)	129.0
Ducts and Controls	<u>126.0</u>
TOTAL	<u>432.1</u>

or 49.1 lb/kw_C

(b) Atmospheric Flyback System (Figure 33b)

Low temperature heat exchanger (2)	11.4
Turbine and compressor (3)	30.9
Electric motor (3)	129.0
Ducts and Controls	<u>126.0</u>
TOTAL	<u>297.3</u>

or 33.8 lb/kw_C

The specific weight of the system will vary with the size of the system, component operating efficiencies and operating temperatures. For example, the electric motor weight would not double for a system designed for twice the heat load and the heat exchanger weights are a function of the heat load to the .882 power. However, the two systems analyzed above are felt to be representative of systems that could be used on the Orbiter and system specific weights of 49.1 lb/kw_C for the orbital phase and 33.8 lb/kw_C for the atmospheric flyback phase will be used in the parametric weight analyses.

3.2.5 Parametric Weight Analysis

The RSPLAT computer routine previously discussed in Paragraph 3.1.5 and described in Appendix A was used to conduct parametric weight analyses of a gas cycle refrigeration system for the orbit and atmospheric flight mission phases. The systems were evaluated on a parametric weight basis (lb/kw_C) so the results can be utilized for any heat load. The total system weight at any particular set of conditions is the sum of three terms; the fixed weight, the electrical power penalty weight and the radiator or ram air weight penalty. The system performance characteristics and fixed weight developed in Paragraphs 3.2.3 and 3.2.4 were input to the RSPLAT routine and system weights computed as a function of the average heat rejection temperature. Analyses were conducted for the power penalties, radiator weight penalties, and altitudes presented in Table 3. These are the same parameters used for the vapor compression refrigeration system analyses.

Figures 11 and 12 present typical results of the gas cycle parametric analyses for the orbital and flyback phases respectively. The complete results are given in Appendix A. Figures 35 through 39 summarize the data presented in Appendix A. For the gas cycle system the power penalty has the most significant effect on system weight. This is evident from the orbit phase results which indicate relatively high system weights and show the strong dependence on power penalties.

3.3 SPACE RADIATOR

Two types of space radiators are considered for use on the Orbiter; a conventional single phase radiator used with a pumped fluid loop, and a condensing radiator used with a vapor compression refrigeration system. The use of the radiator as an atmospheric convector after reentry is also considered.

The design of the space radiator for the Orbiter is unique in that the Orbiter will be subjected to aerodynamic heating during launch and reentry and the spacecraft will have a multiple mission capability. Previous spacecraft radiators (notably on Apollo) have been integral with the spacecraft skin, protected during launch, and not required to survive reentry. Figure 40 presents an estimate of the maximum Orbiter temperatures for the low cross range and high cross range vehicles taken from references 13 and 14. These temperatures indicate that the Orbiter radiator design will require new considerations of the radiator fluid, fin material and mounting technique.

Two basic radiator/Orbiter integration concepts have been established for consideration in this investigation. The first concept is the integral radiator in which the radiator is mounted on the external skin. Figure 41 shows three possible radiator locations for the integral concept. Location 1 has the radiators in the area of minimum boost and reentry heating, location 2 puts the radiators on opposite sides of the vehicle to reduce the environments and location 3 also reduces the environments by putting the radiators around three sides of the vehicle and also reduces the problem of radiant interchange with the cargo bay doors.

The second integration concept is to store the radiators internal to the vehicle for boost and reentry protection and to use some sort of deployment method for operation in orbit. Four possible deployment techniques are illustrated in Figure 41. One deployment scheme is to mount the radiators on the inside of the cargo bay doors, (double or single door). The double door configuration requires that the doors be left open, and the single door allows the door to be shut after deployment. A second deployment technique is to mount the radiator in a folded position on the outside of the cargo bay doors. This configuration allows radiator operation with the cargo bay doors open or closed. The door in full open position is limited in this concept to minimize radiant interchange with the Orbiter wing. The third deployment technique locates the radiators on the end of a boom which is deployed from the cargo bay and also allows the doors to be closed after deployment.

The following paragraphs discuss the methods used to determine the radiator area requirements for each of the above configurations.

3.3.1 Radiator Area Requirements

A simplified steady state analysis technique described in reference 15 is used to estimate the conventional radiator area requirements. The heat rejection per unit area is given by:

$$Q/A = \frac{\sigma \epsilon \eta T_s^3 (T_{in} - T_{out})}{\zeta(\gamma_2) - \zeta(\gamma_1)} \quad (18)$$

Where

- Q = heat rejection, BTU/hr
- A = radiator area, ft²
- T_s = effective environment radiation sink temperature, °R
- σ = Stephan Boltzmann constant, BTU/hr-ft²-°R⁴
- ε = Radiator emissivity, dimensionless
- η = Overall effectiveness, assumed equal to radiation fin effectiveness, dimensionless
- $\zeta(\gamma) = 1/4 \ln \left[\frac{\gamma + 1}{\gamma - 1} \right] + 1/2 \tan^{-1} \gamma$
- $\gamma = \frac{T_r}{T_s}$
- T_r = Tube temperature (fin root temperature), °R
- T_{in} = Fluid inlet temperature, °R
- T_{out} = Fluid outlet temperature, °R

The subscript 1 refers to the radiator inlet; 2 refers to the outlet. The tube temperature, T_r, is estimated from the fluid temperature and the fluid to tube temperature difference (ΔT_{ft}).

Figure 42 presents the radiator heat rejection per unit area as a function of sink temperature for various inlet temperatures. A radiator emissivity of 0.9, a fin effectiveness of 0.9, and an outlet temperature of 40°F was assumed in this analysis.

The condensing space radiator area requirements are estimated from:

$$Q/A = \epsilon \sigma (T_{avg}^4 - T_s^4) \quad (19)$$

where T_{avg} is the effective condenser radiating temperature. In a condensing space radiator the refrigerant enters the condenser in the super heated vapor phase, is cooled to the saturation temperature, condenses at a constant temperature and the liquid is then subcooled. The vapor and liquid phases are characterized by relatively low heat transfer coefficients and high fluid to tube temperature differences. The condensing region has high heat transfer coefficients and the tube temperature remains very close to the fluid condensing temperature. Figure 43 shows a typical temperature profile down the length of a condensing radiator. This data was obtained from a computer analysis of a steady state condensing radiator. As indicated by Figure 43, the tube temperature drops rapidly at the inlet due to the low heat transfer coefficients in the vapor phase and then is increased in the condensing region. The tube temperature profile will depend on the refrigerant flow rate, sink temperature, tube diameter, the degree of super heat and subcooling and the saturation temperature. From a review of the computer analysis it appears that an average radiating temperature approximately 5°F below the condensing temperature is obtainable with proper condenser design. The condensing space radiator area is therefore estimated from equation (19) with T_{avg} taken as 5°F less than the condensing temperature. Figure 44 presents radiator heat rejection per unit area as a function of sink temperature for various condensing temperatures. A radiator emissivity of 0.9 and a fin effectiveness of 0.9 was assumed in this analysis.

The radiation sink temperature is now required for radiator area determination. The approach used to determine the effective environment was to utilize results of transient adiabatic surface temperature predictions for an 0.040 inch aluminum plate in earth orbit. Surface coating properties of solar absorptivity (α) = 0.3 and ϵ = 0.9 were used. Cyclical repeating temperatures were obtained for flat plates located at 15° increments around the periphery of a cylinder in earth orbit. The Midwest Research Institute (MRI) computer routine (reference 16) was used for this analysis. The adiabatic surface temperatures provide an estimate of the thermal lag of the radiator in a constantly changing environment. The use of the maximum adiabatic surface temperature in orbit as the effective radiation sink temperature in the steady state method of analysis will provide a realistic radiator design. This technique has been verified by comparison of steady state performance predictions to transient earth orbit radiator performance predictions (Reference 17). Appendix B presents plots of the adiabatic surface temperatures for orbit inclinations from zero to 90 degrees for planet and solar oriented attitudes. Analyses were conducted for both the Orbiter longitudinal axis perpendicular to the orbit plane (X-POP) and the longitudinal axis parallel to the orbit plane (Y-POP).

Effective radiation environments for use with the steady state method of analysis for the integral and deployed radiator concepts presented in Figure 41 have been determined from the data presented in Appendix B. The plots of Appendix B were surveyed to determine the position in orbit which gives the maximum combination of sink temperatures for each radiator configuration. The details of this analysis are also presented in Appendix B. Table 6 summarizes the maximum sink temperature for each configuration and defines the orbit and conditions for which it occurs.

The use of a proportioning valve in the system influences the conventional radiator design conditions when the radiator is made up of multiple panels plumbed in parallel and portions of the radiator have different environments. The proportioning valve routes more flow to the panel with the best environment for heat rejection; thus optimizing the total heat rejection. The condition of maximum total absorbed heat will not be the design condition if a proportioning valve is used to distribute flow between two portions of the radiator and the environment of one portion is such that that portion can meet the heat rejection requirements. This criteria has been included in the sink temperature analysis and conditions with and without the proportioning valve are noted in Table 6.

As indicated by Table 6, only configurations 2, 3 and 4 have design sink temperatures and conditions compatible with the desired 40°F radiator outlet temperature. The other configurations would require orientation constraints to lower the sink temperature below 40°F or could only be used with mechanical refrigeration systems which increase the heat rejection temperature.

The final selection of the design sink temperature requires a determination of whether a low or high inclination orbit represents a "worst case" condition. For low inclination orbits with alternate hot and cold environments, the conventional radiator outlet could be allowed to peak for short periods of time at values above the desired outlet control point. For orbit inclinations above 68.5° (270 n.m. circular orbit), the shadow time is zero and the radiator control point must always be maintained. Therefore, although a higher design sink temperature results from a low inclination orbit, this is not necessarily the radiator design point since higher radiator temperatures are allowed for this condition. The concept of peaking has been used successfully on the Apollo ECS radiator where the outlet temperature peaks above the 45°F control point for as much as 50 percent of the time in lunar orbit. Maximum outlet temperatures of 85°F have been recorded with no detrimental effect on the ECS. The average heat rejection during the orbit must match the radiator load when the outlet temperature is allowed to peak.

The concept of peaking also applies to the condensing radiator. During periods of high sink temperatures, full condensation may not occur and the evaporator temperature may exceed its control point. However, during low sink temperature periods, subcooling occurs in the condenser increasing the system heat rejection capability. Therefore, the average orbital heat rejection should match the evaporator load.

TABLE 6
SUMMARY OF RADIATOR STEADY-STATE
DESIGN SINK TEMPERATURES

<u>CONFIGURATION</u>	<u>T_{SINK} - °F</u>	<u>ORBIT AND CONDITIONS</u>
Integral Location 1, External Double Door (door closed)	63	90° inclination, solar oriented, No peaking above control point
Integral Location 2, Single Door, Boom De- ployed and External Double Door (Door Open)	26	68.5° inclination, solar oriented, No peaking above control point, No proportioning valve
	40	0° inclination, planet oriented, Peaking above control point, with proportioning valve
Integral Location 3	24-29	Sun Oriented: 32°, 68.5° & 90° Planet Oriented: 90° & 0° Peaking above control point allowed only for inclinations less than 68.5°. No proportion- ing valve.
Double Door Deployed	34	68.5° inclination, solar oriented No peaking above control point, no proportioning valve

An analysis has been conducted to determine whether the conventional radiator design conditions are for the 68.5° inclination orbit or the 0° inclination orbit. At the time this analysis was conducted, two radiator design concepts were under consideration; one concept includes the fuel cell waste heat in the design load and the other concept includes only the EC/LSS heat load. Figure 45 shows a schematic arrangement of the radiator loop interface with the Orbiter ECS loop and the assumed operating temperatures and flow rates for the two design concepts. The primary difference in the two concepts is the radiator inlet temperature. For ease of comparison the total radiator load for each concept is maintained at 34,000 BTU/hr.

The radiator heat rejection per unit area for the two design concepts is given in Table 7 for the 0° inclination orbit and the 68.5° inclination orbit. This data is obtained from equation (18). A design to a sink temperature of 40°F (0° inclination orbit) is obviously not feasible with a radiator outlet of 40.3°F. However, if peaking is allowed then the radiator is designed to reject the average heat load with a variation in outlet temperature with orbit position. This is accomplished by determining the average Q/A as indicated by Figure 46. If the radiator outlet temperature is allowed to peak at 60°F then the average Q/A from Table 7 and Figure 46 is determined to be 30.3 BTU/hr-ft² and 46.91 BTU/hr-ft² for concept 1 (T_{in} = 82.1°F) and concept 2 (T_{in} = 141.8°F) respectively. This indicates that significantly less radiator area is required for the 0° inclination orbit when peaking is allowed than with the 68.5° inclination orbit with no peaking. However, the steady state method of analysis for this condition may not be valid due to the assumed linear change in the environment, changes in fin effectiveness due to temperature changes and changes in the temperature difference between the fluid and tube. In order to validate the steady state analysis a transient computer analysis was conducted. The average Q/A of 30.3 BTU/hr-ft² for concept 1 (T_{in} = 82.1°F) yields a total radiator area of 1122 ft² for the 0° inclination orbit. For ease of analysis the actual radiator area used in the transient analysis was 1150 ft². The radiator system is composed of 8 modular panels each of 144 ft². Figure 47 shows a schematic of the radiator system analyzed. Each panel in the bank of 4 panels will have equal flow. Therefore, only one panel in each bank is required for analysis as indicated by Figure 47. The transient analysis used environment data obtained from the MRI routine for the 0° inclination orbit with the panels located on opposite sides of the Orbiter (or back to back deployed panels). The results of this analysis are presented in Figure 48. As indicated, the radiator outlet peaked at a maximum of 62.5°F and was above the control point of 40.3°F for 0.425 hours of each orbit. This agrees well with the steady state analysis and is judged to be acceptable for the Orbiter; a radiator area of 1150 ft² is adequate for an 0° orbit. Since the 68.5° orbit requires a radiator area of 2040 ft² (Q/A = 16.6 BTU/hr-ft²), it is concluded that the radiator sizing criteria occur at this condition.

Use of the radiator as an atmospheric convector during the atmospheric flight phase (after reentry) is also being considered for the mechanical refrigeration systems which increase the heat rejection temperature above the ambient air temperature. This method of heat rejection could eliminate

TABLE 7 RADIATOR AREA REQUIREMENTS

T_{out}	$T_{sink} = 26^{\circ}F$		$T_{sink} = 40^{\circ}F$	
	Concept 1 $T_{in} = 82.1^{\circ}F$	Concept 2 $T_{in} = 141.8^{\circ}F$	Concept 1 $T_{in} = 82.1^{\circ}F$	Concept 2 $T_{in} = 141.8^{\circ}F$
40.3	16.62	29.13	00	00
55	-	-	15.06	29.70
60	-	-	17.99	34.75
65	-	-	20.45	39.10

the ram air scoop and heat exchanger but is applicable only to the integral radiator concepts (Figure 41). It is first necessary to determine whether the radiator can be effectively used after reentry. As previously discussed (refer to Figure 41) the radiation equilibrium temperature due to reentry heating in the assumed area of the radiator ranges up to 680°F, depending on whether a low or high cross range Orbiter is used. The radiator must therefore be cooled to its operational temperature before heat can be rejected. Figure 49 shows the results of a simplified transient cool down analysis. As indicated, less than 3 minutes are required for the radiator to cool from 600°F to 150°F. Thus, effective use of the radiator can be made shortly after reentry. This analysis assumed a constant inner structure temperature of 400°F.

The area requirements of the atmospheric convectors are given by:

$$Q/A = h\eta(T_W - T_a) + \epsilon\sigma(T_W^4 - T_{\text{sink}}) - Q_{\text{struct}} \quad (20)$$

T_a = the atmospheric temperature, °R

T_W = the wall temperature, °R

h = the heat transfer coefficient, BTU/hr-ft²-°R

T_{sink} = the effective radiation sink temperature, °R

Q_{struct} = heat leak from the structure to the radiator, BTU/hr-ft²

ϵ = radiator emissivity = 0.90

σ = Stefan-Boltzmann constant, 0.1713×10^{-8} BTU/hr-ft²-R⁴

η = radiation and convection fin effectiveness, both assumed = .9 for this analysis

The heat transfer coefficient was determined from reference 19, for a velocity of 400 ft/sec and a distance of 60 ft from the leading edge. The free convection h (for 0 altitude) was computed by the method presented in reference 19 for a flat vertical plate with the warm side facing upward. The values of T_a were obtained from MIL STANDARD 210A for hot day temperatures. The radiation sink temperature, T_{sink} , was computed for the atmospheric flight analysis as a function of altitude. The radiator/convector is assumed to cover a 120° circular arc looking directly into the sun. Radiation sink temperatures were calculated at zero and 50,000 ft to be 46°F and 64°F respectively. A linear interpolation is used for intermediate altitudes.

Figures 50 and 51 present the heat rejection capability of the atmospheric convector for heat rejection temperatures of 125°F and 150°F respectively. This data indicates that for a 150°F heat rejection temperature the atmospheric convector Q/A will be comparable to or greater than the space radiator Q/A . Thus, use of the space radiator as an atmospheric convector is feasible unless the flyback heat loads are significantly greater than the on-orbit loads. A 125°F heat rejection temperature will not provide heat rejection at low altitudes unless the panel thermal isolation is improved or the

structure temperature remains below approximately 300°F. Preliminary analyses also indicate that the use of the radiator as a free convector for post landing operations is restricted to heat rejection temperatures of 150°F or greater with a 200°F structure temperature.

3.4 EXPENDABLE FLUID COOLING SYSTEMS

Expendable fluid cooling systems have found wide use on spacecraft for applications such as cooling during boost, reentry, relatively short mission times and emergency back up systems. Aircraft have also used expendable cooling systems for emergency and for short high speed flight conditions (the XB-70 and F-111). Several operating characteristics of the Orbiter are postulated or are being considered that suggested that expendable cooling systems could be used. Among these are:

- 1) fuel cells used for power generation will produce excess water, which could be used for cooling
- 2) Boil-off from cryogenic hydrogen tanks which may be required for orbit operations could be used for cooling
- 3) Although the orbiter mission may be 7 to 30 days the maximum on-orbit heat rejection requirements could occur in a relatively short period.
- 4) The variable mission concept of the Orbiter requires different heat rejection rates for each mission, suggesting the simple addition or deletion of the amount of expendables according to the mission requirement and
- 5) The relatively short mission times for boost, re-entry and atmospheric flyback

3.4.1 Candidate Fluids

Although water and hydrogen could be available on board the Orbiter, other fluids have been included in the parametric weight analysis. Two basic types of fluids were considered. The first are evaporative fluids whose heat absorption capacity depends on the latent heat of vaporization. The second type are cryogenic fluids which absorb heat by vaporization at a low temperature and utilize the sensible heat capacity of the cold vapor as it is heated to the desired ECS temperature. Figure 52 presents the latent heat of several fluids of the first category. Table 8 compares the total heat absorption capability of fluids of both categories. Selection of a fluid, of course, requires more than a consideration of the heat absorption per pound of fluid. The hardware and fluid storage requirements among others must also be considered. The vapor pressure-temperature characteristics are another consideration in the selection of a suitable fluid. Figure 53 presents the vapor pressure-temperature relationships of several fluids. The expendable fluid should have

TABLE 8 EXPENDABLE FLUIDS HEAT ABSORPTION

FLUID	LIQUID DENSITY LB/FT ³	BOILING POINT °F	HEAT OF VAPORIZATION BTU/LB	TOTAL HEAT ABSORPTION-B.P. TO 100°F, BTU/LB
H ₂ (Hydrogen)	4.37	-423	194	1993
H ₂ O (Water)	62.4	212	1037	1037
He (Helium)	7.62	-452	11	697
NH ₃ (Ammonia)	40.6	- 28.0	589	655
CH ₄ (Methane)	25.9	-258.9	248	428
C ₃ H ₈ (Propane)	6.8	- 44.2	182	240
CH ₃ Cl (Methyl Chloride)	62.58	- 10.8	185	204
C ₄ H ₁₀ (Butane)	5.9	31.3	165	192
CHClF ₂ (R-22)	88.3	- 41.44	101	120
CH ₂ ClF (R-21)	87.7	48.0	104	112
CCl ₂ F ₂ (R-12)	92.7	- 21.62	71	91

NOTE: All values at 14.7 psia except water (Boiling at 0.45 psia and 100°F)

a vapor pressure greater than the ambient pressure at the desired operating temperature. For example, if a 40°F temperature is required for sea level operations then R-21 and water cannot be used. Also, the fluid should not have excessively high vapor pressures to prevent storage problems. Ammonia, for example, would have to be stored at 500 psia to prevent boiling at a maximum design temperatures above 160°F. Other properties such as chemical behavior and toxicity must also be considered in the selection of a coolant. Some fluids that would be relatively good coolants are highly toxic, or highly corrosive. Undesirable chemical properties may therefore exclude many fluids from further consideration. Table 9 presents some corrosion and relative safety properties of the candidate fluids.

Four expendable fluids with relatively high heat absorption characteristics were considered for the on-orbit mission phase. These were: hydrogen, helium, water and ammonia. For the atmospheric flight mission phase the following fluids were considered: R-22, N-butane, propane, methyl chloride, water, ammonia, helium, and hydrogen. The two flight regimes were analyzed separately because the atmospheric flight phase requires the selection of a fluid that can yield temperatures in the 40°F range at sea level pressures, whereas in the orbit phase the operating temperature (pressure) can be controlled. Also due to the short duration of the atmospheric flight phase the system hardware weights become more important and the fluid with the highest heat absorption rate does not necessarily yield the lightest system.

3.4.2 Expendables System Weight Analysis

The basic system considered for the non-cryogenic fluids consists of a storage tank and expulsion system, lines, valves, controls and a heat exchange device to transfer heat from the ECS coolant loop (Figure 54). The heat exchanger could be an evaporative heat exchanger, a wick fed boiler, a flash evaporator, or a porous plate sublimator. The flash evaporator has the advantage of being able to use multiple fluids - a single unit could be used with different fluids used in different mission phases. Evaporative heat exchanger designs are complicated by the requirement of zero and high gravity operation and are difficult to control. Wick fed boilers have difficulties for repeated start-up and shut down operations and the backpressure control which is needed to regulate the heat transfer rate is felt to be an item of reduced reliability. The sublimator has the disadvantage that repeated start-ups result in a waste of evaporant each time, the load range is limited and the porous plate both deteriorates and may support bacteria growth. For all non-cryogenic fluids the flash evaporator was assumed to be used. The weight estimate for the unit was taken as 35 lb. for a 10 KW system, including all valves, controls and redundancy. This estimate is based on work done by VMSC in reference 20 and the flight prototype development program currently in progress.

The cryogenic hydrogen system used on Dyna-soar (Reference 21) was used as a baseline system for the cryogenic fluids, hydrogen and helium. This package removes heat from, and regulates the temperature of the ECS coolant loop. Also, it regulates the temperature and pressure of the cryogenic tanks. In the case of hydrogen, it could possibly be used to supply the fuel cell and/or the RCS engines (if H₂ fueled). However, the fuel cell usually

TABLE 9 RELATIVE SAFETY OF EXPENDABLE FLUIDS

FLUID	ASA-B9 SAFETY CODE GROUP	UNDERWRITER'S LABORATORIES GROUP CLASSIFICATION	EXPLOSIVE LIMITS IN AIR % BY VOL.	COMMENTS ON CORROSION
Hydrogen	-	6	4.0 - 75.	Non corrosive to aluminum, copper, monel, inconel, austenitic stainless steels, brass, bronze, teflon & silver solder
Water	-	-	Nonflammable	
Helium	-	6	Nonflammable	
Ammonia	2	2	16.0 - 25.0	Highly corrosive to copper, brass or other alloys containing copper
Methane	3	5b	4.9 - 15.0	
Propane	3	5b	2.3 - 7.3	
Methyl Chloride	2	4	8.1 - 17.2	Forms highly flammable gas with aluminum
Butane	3	5b	1.6 - 6.5	
R-22	1	5a	Nonflammable	Not recommended for use with magnesium, zinc and aluminum alloys containing more than 2% magnesium.
R-21	1	4-S	Nonflammable	
R-12	1	6	Nonflammable	

NOTE: ASA-B9 Group Classification 1 is least toxic, 3 is most toxic.
Underwriter's Laboratories Classification 6 least toxic, 1 is most toxic

requires high quality hydrogen stored supercritically at high pressure with tank weights on the order of two times the hydrogen weight and the RCS demand schedule may not match the expendable supply. It is therefore, assumed for this study that the hydrogen used for cooling is dumped overboard and the entire amount used is charged to the weight penalty. A schematic of this system is shown in Figure 55 with typical operating conditions. It includes a fan or compressor to recirculate the heated hydrogen back to the storage tank to vaporize more hydrogen and also controls the hydrogen temperature at the inlet to the heat exchanger to -100°F . The -100°F was arbitrarily chosen and can be varied to match the requirements of the ECS loop fluid with no change in heat rejection capabilities of the system.

The use of the hydrogen in a gas cycle refrigeration system before dumping overboard could result in a considerable increase in heat rejection. This can be accomplished by adding an expanding turbine and low pressure heat exchanger into the loop (Figure 56). This modification in the loop causes a significant increase in the fixed weight, but in view of the extra heat rejection obtained, the system could be beneficial especially during the orbital phase. The expansion turbine can also be used to produce power for the hydrogen circulation system, and auxiliary power for the main power supply.

ORBITAL SYSTEM WEIGHTS

For both the non-cryogenic and cryogenic expendable cooling systems a fail-safe mode of operation was placed on the hardware and expendables. The hardware safety restriction requires a redundant backup system. The expendables safety restriction requires that enough coolant be stored separately from the main supply to enable an aborted mission to safely return. It is anticipated that this auxiliary supply will be required for from 8 to 48 hours. For the parametric analyses conducted herein the redundant supply was determined for a 48 hour abort mission. Different abort mission times will not affect the comparative results of the different fluids. The following paragraphs discuss the general aspects of the analysis of each fluid.

Hydrogen:

As indicated by Table 8, cryogenic hydrogen has the largest heat absorption capacity of the expendable fluids considered. The hydrogen tank weight was taken as 0.5 lb/lb of H_2 for low pressure subcritical storage. This weight considers the insulation required to maintain the low temperatures, the low H_2 liquid density and the zero-g acquisition device. If the Orbiter Maneuvering System (OMS) uses liquid H_2 , then the OMS tank boil-off which would normally be dumped overboard can be used to supply the cooling package. For example, Reference 22 estimates that 253 lbs of H_2 will be vented from OMS tank during a seven day orbital mission. Figure 57 presents the results of an expendable hydrogen cooling system weight analysis. Total system weights for a 10kw heat load are shown as a function of mission time. The system fixed weight includes the additional fuel cell fixed weight required to supply the H_2 compressor power and the expendables required for the 48 hour abort phase in addition to the H_2 system hardware weight. A fuel cell consumption power penalty is included in the expendable weights as a function of time.

Results are shown for various OMS boil-off rates for both the 12 hours and 48 hour emergency expendable supply. Figure 58 shows the results of a similar analysis with the expansion turbine included in the system. The use of the expansion turbine increases the heat capacity of the H₂ from 1560 to 1980 BTU/lb and eliminates the power penalty. This system produces 0.865 kw excess power which must be used.

Helium:

The cryogenic helium expendable cooling system has the same basic design as the H₂ system. Based on the differences in the liquid densities, the Helium tank weight was taken as 70 percent of the hydrogen tank weight or 0.35 lb/lb of helium. The addition of the expansion turbine increases the Helium heat capacity from 675 to 848 BTU/lb and provides 0.0725 kw electrical power for each KW of cooling.

Ammonia:

The ammonia is stored as a liquid at 70°F and 129 psia. A tank weight of 0.25 lb/lb of ammonia is used. The theoretical heat capacity of ammonia evaporated from 70°F and 129 psia to 40°F at 73 psia is approximately 500 BTU/lb. Recent tests of an ammonia flash evaporator conducted by VMSC indicate that approximately 420 BTU/lb can actually be obtained. The use of an expansion turbine with the ammonia system was also considered; it was determined that the system complexity and increased hardware weight offset the gain in heat capacity.

Water:

The expendable water cooling system also utilizes the flash evaporator. A heat absorption of 1000 BTU/lb of water was used based on operational experience by VMSC. The excess water produced by the fuel cells can be used by this system. Approximately 0.85 lb of water per kilowatt hour are produced by the fuel cells. Roughly 1.0 lb/hr of this will be required for crew consumption. For an average electrical load of 4 kw, approximately 400 lb of excess water (2.4 lb/hr) could be available from the fuel cells for heat rejection use. A tank weight of 0.15 lb/lb of water was used (the Lunar Module Ascent Stage Water tank weight is 0.125 lb/lb of water). Figure 59 shows the results of the expendable water cooling system weight analysis as a function of mission time for various rates of excess fuel cell water.

Figure 60 presents the weight estimates of the expendable cooling systems for the four candidate fluids as a function of mission time in earth orbit. The expendable H₂ with expansion turbine is the lightest weight system. The H₂ system without the turbine and the water system have comparable weights especially for the short mission times. The H₂ system weight is slightly lower based on the assumed water availability from the fuel cells (2 lb/hr). The water system weighs approximately 90 lb more than the H₂ system for the 48 hour abort phase, but the H₂ system will require power. As previously mentioned, the H₂ with expansion turbine system produces excess power which must be used.

No penalty was assigned this excess power, although the controls and distribution for such a system may offset or exceed the fuel cell expendables weight savings. The actual integration of the H₂ with turbine cooling system with the power system would require detail design considerations beyond the scope of this parametric study.

ATMOSPHERIC FLYBACK

The atmospheric flyback expendable cooling system hardware is designed to the fail-safe criteria. It is assumed that this requirement does not apply to the expendable fluid. The fuel cells can be operated in the self cooling, open cycle mode and ram air or open window operation can be used for the cabin and electronics cooling during an emergency condition. This assumption does not compromise the parametric weight analysis since only comparative weights are used and redundant expendables will double the weight of each fluid. The redundant hardware weight is added to the fixed weight of each system.

Cryogenic tank boil-off must be considered in the atmospheric flight phase analysis. The boil-off was unimportant for the orbital mission phase analysis because it could be used for cooling purposes. However, for this portion of the mission, assuming some other type of cooling is used for the orbital portion, the boil-off occurring during the seven days in orbit is lost. The amount of boil-off is inversely proportional to the fluid heat of vaporization and directly proportional to the two thirds power of the fluid volume (spherical tank). The heat leak of the tank is assumed to be .15 BTU/ft²-hr. The Apollo hydrogen storage tank has a heat leak of 0.2 BTU/hr-ft²-°F and the NASA presently has under development a large cryogenic storage system with a design goal of 0.1 BTU/hr-ft²-°F heat leak for hydrogen (Reference 22). The amount of boil-off for a seven day mission is given by:

$$W_{B.O.} = \frac{122(W/\rho)^{2/3}}{h_v} \quad \text{lb/kw} \quad (21)$$

where:

- ρ = the density of the expendable fluid (lbm/ft³)
- h_v = the heat of vaporization of the expendable fluid (BTU/lbm)
- W = the amount of expendable fluid used, qt/h(lbm)
- q = heat load (BTU/hr)
- t = duration of the flyback mission phase (hr)
- h = heat rejection capacity of the expendable fluid (BTU/lbm)

The total expendable fluid required at launch is the sum of the boil-off and that required for the atmospheric phase heat rejection. Figure 61 presents the required launch weights as a function of the weight of fluid actually used. The hydrogen systems weights are not greatly influenced by the boil-off penalty. The helium systems have large boil-off penalties due to their low heat of vaporization (11 BTU/lbm). This penalty is greater than

the total amount of fluid used during the atmospheric flight.

The following paragraphs discuss the general aspects of the analysis of each fluid. A fixed weight penalty is shown for each fluid; however, if the fluid is used for on-orbit heat rejection or for the abort system then there would be no fixed weight penalty.

Hydrogen:

Use of hydrogen as an expendable heat sink during atmospheric flight must consider the high flammability (4-74% volume) in air and the low detonation energy (one-tenth that of gasoline-air mixtures). Special considerations will have to be given to the vent design to prevent detonation by lightning and static electricity. Temperatures of about 1000°F are usually required for the ignition of hydrogen and air mixtures. However, at pressures of 3-7 psia ignition can occur at 650°F (Reference 24). This would seem to preclude the use of hydrogen during reentry, but as previously discussed, the Dynasoar reentry vehicle used expendable hydrogen. Venting hydrogen during pre-launch or post-landing operations should not prove hazardous to support personnel since hydrogen diffuses rapidly; a spill on the ground of 500 gallons of liquid hydrogen will have diffused to a non-explosive mixture after about one minute (Reference 24).

Also, special vacuum jacketed tank insulation or a nitrogen purge system will be required to prevent condensation and ice formation in the super-insulation. Nitrogen purge can be supplied by ground support equipment with a small weight penalty for pre-launch and boost, but the weight penalty could be significant after reentry. A hydrogen tank weight of 0.60 lb/lb of hydrogen was used for the atmospheric weight analysis. The use of an expansion turbine is not as efficient as for the orbital phase because the hydrogen cannot be expanded below atmospheric pressure. A total heat capacity of 1630 BTU/lb is obtainable at sea level operations.

If a hydrogen fueled Auxilliary Power Unit (APU) is used to provide hydraulic power during the atmospheric flight phase, then it may be possible to use the hydrogen for cooling purposes prior to use by the APU. The use of hydrogen with no expendable weight penalty has therefore been included in the parametric weight analysis.

The H₂ system fixed weight includes the system hardware weight only. The power penalty is evaluated on the basis of additional fuel cell expendables only. If additional power capacity is required just for the atmospheric flight phase, then it would be more efficient to use the APU's than the fuel cells.

Helium:

Helium is non-toxic and nonflammable and should present no safety hazards. The storage problem discussed above for hydrogen also applies to helium. A tank weight of 0.45 lb/lb of helium was used.

Ammonia:

Ammonia is less flammable than hydrogen but still presents a fire hazard. It is highly toxic and exposure even to small concentrations should be prevented. Ammonia is also corrosive to copper and contact with electrical wiring should be avoided.

R-22:

Refrigerant 22 is non-toxic and nonflammable. R-22 is used rather than R-21 to provide better control in the flash evaporator. Recent tests by VMSC indicate that approximately 70 BTU/lb is absorbed by the R-22 flash evaporator operating at atmospheric pressure.

Butane:

Butane is less toxic (Underwriter's Laboratory Group Classification 5b) than R-22, but is flammable. The ignition temperature of Butane is 890-1020°F. Butane can be stored at relative low pressures; the vapor pressure at 70°F is 32 psia. A tank weight of 0.20 lb/lb of Butane was assumed. The latent heat of vaporization of Butane is 157 BTU/lb. Assuming the Butane flash evaporator has the same efficiency as the R-22 system, a heat capacity of 110 BTU/lb is obtained.

Propane:

Propane is also non-toxic and flammable. It has an ignition temperature of 950-1080°F. Propane has a vapor pressure comparable to ammonia (125 psia at 70°F). A tank weight of 0.25 lb/lb of propane was assumed. Propane has a latent heat of 174 BTU/lb. The efficiency of a propane flash evaporator should be close to that of ammonia. A heat capacity of 146 BTU/lb was used in the parametric weight analysis.

Methyl Chloride:

Methyl Chloride is slightly toxic (Underwriter's Laboratories Group Classification 4) and is flammable. It has the disadvantage that it cannot be used with aluminum in any form. A highly flammable gas is formed and the explosion hazard is great. Methyl Chloride has a moderate storage pressure (73 psia at 70°F). However, special consideration must be given to the storage tank, vent and flash evaporator since aluminum cannot be used. A tank weight of 0.30 lb/lb of methyl chloride was assumed and the flash evaporator weight was taken as 70 lb for a 10 kw cooling system.

Figure 62 presents the weight estimates of the expendable cooling systems for the seven candidate fluids. System weights for a 10 kw heat load are shown as a function of mission time. The hydrogen and ammonia systems are the lightest weight. For mission times greater than 55 minutes the hydrogen system which uses the APU fuel with no weight penalty is the lightest system. Even if the APU fuel is not used the hydrogen system appears attractive. Refrigerant 22 represents the highest weight system, but has the

best safety properties (except for helium which is complicated by the requirement of cryogenic storage). Final selection of the expendable fluid requires a trade-off between the qualitative properties of safety and reliability and the quantitative properties of system weight. Ground support operations and safety criteria will have to be established before a qualitative evaluation can be made. Based on preliminary groundrules, it appears that no toxic, flammable or corrosive materials will be allowed to be dumped overboard. Therefore, the use of R-22 is dictated. It should be noted that the APU exhaust could be hydrogen rich (if hydrogen fueled) or contain ammonia (if hydrazine fueled).

3.5 RAM AIR

The ram air cooling system is inherently the simplest, lightest weight system. The use of cool ambient air during subsonic flight is attractive for use both as the primary and as the secondary or redundant system. Figure 63 shows the ram air temperature as a function of altitude for a MIL STD 210A hot day atmosphere. As indicated, sink temperatures below 40°F are available for altitudes above about 17,000 ft. For altitudes below 17,000 ft the ram air appears to only be applicable to mechanical refrigeration heat rejection or to high temperature component (fuel cells, hydraulics, high temperature electronics) heat rejection or as a back-up system for emergency survival cooling.

3.5.1 Ram Air System Weights

The basic ram air system is shown in Figure 64. It consists of a hydraulic actuated door for protection during reentry, a duct for routing the air to the heat exchanger, the heat exchanger and a discharge duct and door. The system weight includes the sum of the weights of these components plus a weight penalty for the drag induced by the system. The evaluation of the ram air penalty is made on the basis of no jet engines during the atmospheric flyback. A widely used method of determining the ram air penalty for aircraft is to determine the additional weight of fuel required for the propulsion system to overcome the ram air system drag. Since the Orbiter will not have a propulsion system during the atmospheric flyback, the following method was used: It was assumed that the vehicle design lift to drag (L/D) ratio would have to be maintained and could not be changed by the EC/LSS heat rejection system. Therefore, the ram air penalty was taken as the weight of additional lifting surfaces required to maintain the same L/D ratio. The drag is computed from the momentum change of the ram air by:

$$D = \frac{\dot{w}_a}{g_c} (V_1 - V_2) \quad (22)$$

where:

D = the drag, lb

\dot{w}_a = the required ram air flow, lb/hr

V_1 = free stream velocity, ft/hr
 V_2 = exit velocity (assumed to be 1/6 of free stream), ft/hr
 g_c = gravitational constant, lbm-ft/lbf-hr²

The ram air flow requirements are determined by:

$$\dot{w}_a = \frac{Q}{C_p(T_{out} - T_R)} \quad (23)$$

Where:

Q = heat load, BTU/hr
 C_p = air specific heat, BTU/lb°F
 T_R = ram air temperature, °F

and T_{out} is computed from

$$T_{out} = T_R - \epsilon (T_R - T_{REJ}) \quad (24)$$

Where:

ϵ = heat exchanger effectiveness
 T_{REJ} = heat rejection temperature, °F

Reference 25 reports that during subsonic flight, 90% of the low cross range (stubby wing) Orbiter lift is provided by the wing. All of the additional required lift was assumed to be provided by additional wing area. Table 10 presents the Orbiter design L/D, wing loading and wing weights taken from several Phase A Shuttle reports. For this analysis a constant L/D of 6.0, a wing loading of 90 lb/ft² and a wing weight of 8.5 lb/ft² was used. From the known drag, and above parameters, the weight of the additional wing can be determined.

The ram air heat exchanger weight was computed by the method presented in Reference 5 and previously discussed in paragraph 3.1.4. Redundant heat exchangers are used to meet the reliability requirements. The ram air duct weights were determined by computing the required flow area, based on the ambient density and flow rate. The duct length was assumed to be 10 feet and a circular cross section with an aluminum gage thickness of .1 was used to account for clamps, supports, etc. Figure 65 presents the required flow area for a 10KW cooling load as a function of altitude and Mach number for heat rejection temperatures of 120°F and 150°F. The exact Orbiter flight profile is not known, however, it is expected that the higher Mach numbers will occur at the higher altitudes and that the landing speed will be in the $M = .2$ range. As indicated by Figure 65, the required area for the 120°F heat rejection temperature increases rapidly below altitudes of approximately 10,000 ft and 5000 ft for $M = .6$ and

TABLE 10

ORBITER SUBSONIC AERODYNAMIC CHARACTERISTICS

SOURCE	SUBSONIC L/D	WING LOADING LB_f/ft^2	WING WEIGHT LBM/ft^2	COMMENTS
Reference 22	6.5	102	8.4	L/D @ 7.5° angle of attack, flap angle = 25° (Gear down)
Reference 26	6.0	146	10.45	
Reference 13	7.3 (max)	90	7.0 8.2	12,500 lb payload configuration 50,000 lb payload configuration

$M = .4$ respectively. If the Orbiter flight profile is such that these Mach numbers do occur at the lower altitudes, then a 150°F heat rejection temperature may be dictated. It is anticipated that a flow area of less than 1 ft^2 will be required for a 10KW ram air cooling load. A weight of 10 lb was estimated for the hydraulic actuated doors for a 10KW (1 ft^2) ram air system.

It should be noted that no ram air controls, such as variable scoop area or heat exchanger bypass, are anticipated. Additional cooling above design conditions will result in subcooling in the condenser of a vapor compression system and reduce the power consumption of the system.

Figure 66 shows the total ram air system weights as a function of altitude for a 10KW cooling load. A constant Mach number of 0.4 was assumed for this analysis. This data indicates that a 150°F heat rejection temperature is much more weight effective than the 120°F heat rejection temperature. However, the total heat rejection system weight includes the power penalty and fixed system weight, and the optimum system design must consider the additional power penalty resulting from operating the system at higher temperatures. Figure 66 also shows the influence of heat exchanger effectiveness. A high heat exchanger effectiveness reduces the drag penalty and duct weight, but increases the heat exchanger weight. The heat exchanger effectiveness has not been optimized; however, as indicated by Figure 66, an effectiveness of 0.5 results in a significant weight savings over the effectiveness of 0.85.

4.0

WEIGHT PENALTY EVALUATION

The use of the parametric weight analyses described in paragraph 3.0 to select the EC/LSS heat rejection system requires an estimate of the weight penalties and the Orbiter design requirements. This section presents the determination of the power penalty for orbital and suborbital operations and the radiator weight penalty. Section 5.0 presents a discussion of the mission design requirements for each mission phase. A discussion of the application of the candidate systems is then presented and examples of overall system selection are given based on postulated design conditions.

4.1

POWER PENALTY

The evaluation of the candidate Orbiter EC/LSS heat rejection systems requires that the weight required to produce power be known so that a power weight penalty can be assigned to the various systems. Weight estimates have therefore been made for the power systems expected to be used on the Orbiter. For the orbital phase, it is assumed that a hydrogen-oxygen fuel cell will be used; and for the suborbital phase, it is assumed that a hydrogen-oxygen combustion turbine driving an alternator (referred to as an APU) will be used.

The EC/LSS heat rejection power system redundancy will be required to meet the fail-operational, fail-safe requirements of mechanical equipment. Two possible operating configurations have been considered to meet this requirement depending on whether or not the primary heat rejection system is operated during abort conditions. Since the EC/LSS heat rejection system power supply will be integral with the main power supply, it is assumed that the second failure in the power system will result in an abort mode of operation. During the abort mode, heat rejection could be provided by an emergency system such as water boiling that requires no power. The weight estimates, therefore, do not require provisions for additional fuel cell or APU capacity or an emergency battery system after two power system failures. The fuel cell and APU could be designed on the basis of two equal output units to provide for two failures before an abort mode is required. This requires that the system fixed weight be doubled. It should be noted that three equal output units would require the total power system capability be only 1.5 times the nominal amount and four equal output units would require the capability to be only 1.33 times the nominal amount. Thus, doubling the weight for redundancy is conservative for this operating configuration. If the primary heat rejection system is operating during the abort mode, then at least 3 equal output power units would be required and the system fixed weight would be tripled. The use of 4 equal output units would require that the system fixed weights be doubled; five units require 1.67 times the fixed weight, and 6 units require 1.5 times the fixed weight. For either operating configuration the fail-operational, fail-safe criteria can be met by doubling the power system fixed weight. This criteria will be used to estimate the power penalty.

The power system expendables, storage tanks and plumbing are sized only on the basis of the fail-safe criterion considered to apply to structural equipment. The fuel is assumed to be stored in two tanks with the total amount

equal only to the nominal design requirements.

4.1.1 Weight Estimates

The power system weight data presented in the Shuttle Phase A reports were used to determine the power penalty. A review of the Phase A reports indicated wide discrepancies in the power system designs and system weights. The weight data from each report was therefore converted to a specific weight in lb/kw. Engineering judgement was then used to select representative values. The selected values are considered to be conservative although the highest weight values were not necessarily used.

Orbit Phase. - Table 11 presents fuel cell and power distribution weight data taken from the Phase A reports. None of the weight data shown in Table 11 includes the waste heat rejection system weights or the reactants weight. Plumbing and hardware weights are included. As indicated, the specific weights range from 25 to 125 lb/kw. Most of this variation is due to the inclusion of the power distribution system weights in some of the data. The EC/LSS heat rejection system will require a power distribution system, therefore a value of 75 lb/kw was selected for the specific weight. This value is considered conservative and represents a basic fuel cell module weight of 50 lb/kw and a power distribution system weight of 25 lb/kw. Table 12 presents weight data from Reference 28 for three fuel cell manufacturers. This data shows a specific weight range from 27.5 to 145 lb/kw and indicates that 50 lb/kw is representative.

The power penalty must also include the weight of the system to reject the power system waste heat. As previously discussed the primary advantage of a mechanical refrigeration system is the increased heat rejection temperature. However, in the case of fuel cell waste heat rejection, the temperature is in the range of 150-200°F and no advantage can be shown in using additional power to raise the heat rejection temperature. It is therefore assumed that the fuel cell waste heat rejection will be by a space radiator and the radiator weight will be included in the power penalty.

The fuel cell radiator weight estimate was based on the data presented in Reference 22. The radiator was sized on the basis of two fuel cells supplying 2.5 kw each with a total heat rejection requirement of 11,200 BTU/hr. The design sink temperature of 40°F was used based on the analysis conducted in paragraph 3.3. A radiator inlet of 200°F and a return of 144°F was used, and the area requirement was determined to be 92.6 ft². A radiator panel weight of 1.35 lb/ft² including redundant tubes was used. Table 13 presents a detailed weight estimate of the radiator system taken from Reference 22.

Based on a fuel cell weight of 75 lb/kw and a radiator weight of 43 lb/kw, the power system fixed weight was determined as follows:

TABLE 11
POWER SYSTEM SPECIFIC WEIGHTS

SOURCE	SYSTEM DESCRIPTION	POWER SOURCE WEIGHT lb.	POWER DISTRIBUTION SYSTEM WEIGHT lb.	SPECIFIC WEIGHT lb./kw.
Reference 14	4 H ₂ -O ₂ matrix type fuel cells. Each module rated at 2.0-2.5 kw.	550	700	125
Reference 26	2 H ₂ -O ₂ fuel cells. Each cell rated at 4.5 kw.	394	154	61
Reference 13	3 five kw fuel cells. Either low temperature asbestos matrix units or the solid polymer (R-membrane) unit.	750	365	74.4
Reference 27	3 five kw fuel cells. Capillary matrix, liquid cooled.	480	--	32
Reference 22	2 five kw fuel cells.	250	--	25

TABLE 12 STATE-OF-THE-ART FUEL CELLS

FUEL CELL MFG.	CELL DESIGN	RATING (KW)	WEIGHT (LBS)	SPECIFIC WEIGHT (LB/KW)	SFC (LB/KW- HR)	OPER. TEMP. °F	WASTE HEAT REJECTION (BTU/KWH)
P&W (Apollo & AAP)	Alkaline-Free Electrolyte	1.7	246	145	.86	360 to 450	2240
P&W (New)	Alkaline-Low Temp. Matrix	2.6	160	61.5	.84	180	2100
A-C (New)	"	2.5	169	67.6	.83	190	2500
G.E. (Gemini)	Ion Exchange Membrane	3.0	90	30	.98	140 to 180	2400
" (Gemini)	"	1.0	70	70	.98	"	
" (Biosatellite)	"	0.35	35	100	.98	"	2400
" (New)	New Ion Ex- change Membrane	2.0	55	27.5	.80	"	2400
" (New)	"	1.0	41	41	"	"	2400
" (New)	"	0.5	25	50	"	"	2400
A-C	Alkaline-Low	5.0	150	30	"	"	

TABLE 13
FUEL CELL RADIATOR SYSTEM WEIGHT SUMMARY

<u>COMPONENT</u>	<u>WEIGHT-POUNDS</u>
Radiator Panels	125.6
Transfer Tubing	17.0
Coolant	9.2
Mounts, Hangers, Fasteners	15.2
Water Boiler (with controls, sensors, etc.)	24.0
Water Reservoir	10.0
Water Inventory*	6.0
Transfer Plumbing and Valves (Water System)	4.0
Radiator By-Pass Valves (2)	1.7
Disconnects (Coolant) (4)	1.6
<hr/>	
Total	214.3
Specific Weight	42.86 lb/kw

* Initial supply. Excess fuel cell water used to fill tank during early part of mission.

Redundant Fuel Cells	150
Radiator System	43
Subtotal	<u>193</u>

Inverter efficiency = .80

$$\frac{193}{.8} = 241$$

Inverter weight, including redundancy	<u>84</u>
---------------------------------------	-----------

Total fixed weight = 325 lb/kw

The fuel cell expendable weights are based on a specific fuel consumption 0.9 lb/kw-hr and an oxygen-to-hydrogen ratio of 8:1. Supercritical storage of the reactants are assumed. Table 14 presents the tank weights taken from the Phase A shuttle reports. The hydrogen tank weight was taken as 1.9 lb/lb H₂ and 0.23 lb/lb O₂ was used for the oxygen tank weight. The expendables weight is therefore given by:

$$W = .9[(.111)(1 + 1.9) + .889(1 + .23)] \quad (25)$$

$$W = 1.275 \text{ lb/kw-hr}$$

The power system total specific weight for the orbital phase can now be found from:

$$W = 325 + 1.275 (\tau) \quad (26)$$

where W is the weight in lb/kw and τ is the mission time in hours. For a 168 hour (seven day) mission, the above equation yields a power penalty of 539 lb/kw for the EC/LSS heat rejection system.

The previous discussion of redundancy requirements for the heat rejection system power supply also applies to the main power supply. Thus if the main power supply is designed to the fail operational, fail safe criteria and four equal output modules are used, twice the power capacity will be available under nominal operating conditions and 1.5 times the power capacity will be available after one failure. The use of this reserve capacity for the heat rejection system power would greatly reduce the power penalty and still provide nominal operating conditions until two main power supply system failures occur. This concept is especially attractive for the heat rejection systems which would require power only a relatively short time during the nominal 168 hour orbital mission. The use of this concept would reduce the power penalty to expendables only as given by equation (25). For a 168 hour mission the resulting power penalty would be 214 lb/kw.

TABLE 14
HYDROGEN AND OXYGEN TANK WEIGHTS

SOURCE	HYDROGEN			OXYGEN		
	H ₂ Weight lb.	Tank Wt. lb.	Tank Specific Wt. lb/lb H ₂	O ₂ Weight lb.	Tank Wt. lb.	Tank Specific Wt. lb/lb O ₂
Reference 14	90	59	1.525	471	98	0.208
Reference 26	144	274	1.90	1160	272	0.234
Reference 13	27	62	2.30	291	70	0.24
Reference 27	137	329	2.39	1096.7	1471.2	1.345

Atmospheric Flight Phase. - Table 15 presents weight data for the APU's taken from the Phase A reports. The Phase A reports considered only hydrogen-oxygen turbines; however, hydrazine turbines are being considered on later Orbiter configurations. Some difficulty was encountered in obtaining the APU weights since the primary function of the hydrogen-oxygen turbine is to provide hydraulic power with the electrical power being only a small percentage of the total power output. For example, Reference 22 baselines a 102 horsepower APU with a 5-kw electrical output. The weight data given by Reference 26 appears to not include hydraulic equipment and the combined turbine-alternator weight of 10.49 lb/kw was used.

Only two Phase A reports (References 14 and 26) reported an APU specific fuel consumption. Reference 14 gives 7.36 lb/kw-hr and reference 26 recommends 7.23 lb/kw-hr. An average value of 7.3 lb/kw-hr was used for this study. The fuel was assumed to be stored subcritically with tank weights of 0.5 lb/lb H₂ and 0.23 lb/lb O₂. A hydrogen-oxygen ratio of 1.2:1 (Reference 26) was used to obtain the following expression for the expendables weight:

$$W = 7.3 [.545 (1 + .5) + .455 (1 + .23)] \quad (27)$$

$$W = 10.10 \text{ lb/kw-hr}$$

The power system total specific weight for the atmospheric flight phase can now be found from:

$$W = 21 + 10.1 (\tau) \quad (28)$$

For a 1-hour flyback mission a power penalty of 31.1 lb/kw is obtained.

4.2 RADIATOR WEIGHT PENALTY

In order to assess the radiator weight penalty it is necessary to establish a radiator design to meet the Orbiter objectives and requirements. This study concentrated on the design of a conventional single phase radiator on the assumption that a condensing radiator will require many of the same design considerations and the panel weights per unit area will be approximately the same. Three conventional radiator subsystems have been conceptually defined and evaluated; two deployed subsystems and a skin mounted radiator panel concept. One deployed subsystem consists of the single door deployment technique described in paragraph 3.3, and the other deployed subsystem consists of the double door deployment technique. The alternate concept consists of panels mounted to the vehicle skin which do not interface with vehicle structure.

The design criteria used in this study is presented in paragraph 5.1.7. Common to all concepts are the evaluation and design considerations of reliability and replacement, the panel materials, the coolant fluid, the heat load control method and the radiator coatings. These general considerations are discussed in detail in Appendix C which presents a discussion of the radiator design. Based on the information of Appendix C, the subsystem

TABLE 15
APU WEIGHT DATA

SOURCE	SYSTEM DESCRIPTION	APU WEIGHT lb.	SPECIFIC WEIGHT lb/kw	SPECIFIC FUEL CONSUMPTION lb/kw-hr	ALTERNATOR SPECIFIC WEIGHT lb/kw
Reference 14	91 hp unit for aerodynamic surface controls and hydraulics.	91	4.11	7.36	--
Reference 26	Two units to supply a total of 190 hp to hydraulic system. Weight does not include any hydraulic equipment.	318	2.24	7.23	8.25
Reference 13	Four 150 hp units for the hydraulic system. 37 hp is used to supply electrical power.	740	1.65	--	--
Reference 22	Three 102 hp units producing 85 hp hydraulic power and 5 kw electrical power. Weight includes gas generator, exhaust scroll, turbine wheel, bearings, gearbox, hydraulic pump, lube pump, and lines on the APU.	1230	5.39	--	4.34

configurations were selected and weight estimates made for the deployed and integral panel concepts. These results are reported in paragraphs 4.2.1 through 4.2.3.

4.2.1 Deployed Radiator Concepts

The radiator panels are stowed in the cargo bay compartment for protection from the severe launch/reentry thermal environments and are deployed for orbital operation.

The single door deployment sequence consists of opening the cargo bay door, deploying the radiators, and closing the door. The deployment mechanism is a 2 position drive assembly located in the cargo bay (Figure 67) which rotates the panels to the deployed position. In the event of mechanical failure, manual operation of the radiator deployment mechanism could be performed by an EV astronaut.

The panel area which can be deployed by this method is limited by the size of the cargo bay doors; the maximum area available is approximately 1800 ft² (15' x 60', with radiation from both sides of the panel).

The double door deployment technique requires that the cargo bay doors remain open while the radiators are operating. In order to reduce the thermal environment the panels are stowed in a double fold configuration and folded down over the edge of the door (see Figure 68) when deployed. This requires that the door open only to the 180° position as shown on Figure 68. A 2 position drive assembly located on the cargo bay door rotates the panels to the required position. As in the case of the single door deployment, an EV astronaut could manually deploy the radiators in the event of a failure.

The maximum area available with the double door deployed technique is 1800 ft². The deployed area is obtained by using the inside of the cargo doors and one side of the fold down panel.

Heat load control is accomplished for the deployed subsystems utilizing a bypass-stagnation concept with the two-dimensional tube pattern on the panel. This control technique allows a much wider heat load range than is currently anticipated thus permitting operation under adverse contingency conditions. If more detailed vehicle integration studies show that Freon 21 radiator control range requirements can be satisfied with simple bypass control, then the stagnation valve, flow restrictors, and two dimensional tube pattern can be eliminated with a corresponding improvement in cost and reliability.

Panel Design

The single and double door deployed radiator panels are sized for an assumed heat load of 30,000 BTU/hr and a radiator inlet temperature of 140°F and an outlet of 40°F. From Table 6 it is determined that the single

and double door design sink temperatures are 26°F and 34°F respectively. The required radiator area is read from Figure 45:

Single Door Deployed - 1051 ft²

Double Door Deployed - 1665

A modular panel size of 14.5 x 7.25 ft has been selected for both concepts. Therefore, 5 modular panels radiating from both sides are required for the single door concept and 16 modular panels radiating from one side only are required for the double door concept.

Figure 69 shows the basic panel construction of dual tube flanged extrusions welded to a thin sheet in a two dimensional tube pattern. The panel shown is door mounted; however, the folddown and single door panels have the same basic design. Structural stiffness is provided by the over/under tube arrangement on 6.21 inch centers and a frame around the edges. Additional structural support for the single door deployed panels is provided by two diagonal hat sections. Two concepts for panel mounting to accommodate differential thermal expansion between the panel and the door are also illustrated in Figure 69. Each utilizes fixed hard mounting at the center of the panel and expansion accommodation mounts at other locations as appropriate. The exact panel thickness will require a detailed structural analysis of the panels. It is anticipated that a fin thickness of approximately 0.030 inch will be required for the single door deployed panel and the fold down portion of the double door deployed panel. The panel attached to the inside of the door is expected to be approximately 0.016 inch thick. Table 16 summarizes the two deployed panel designs.

Weight estimates of the deployed panel concept are presented in Tables 17 and 18.

4.2.2 Skin Mounted Concept

The design concepts selected for skin mounted panels are shown in Figures 70 and 71. Three concepts for mounting radiator panels to the vehicle skin have been generated and consist of: unfolding (butterfly) panels which are imbedded in the vehicle skin (Figure 71a), clip-on folding panels (Figure 71b), and the clip-on non folding panels (Figure 71c). Panels which are imbedded into the vehicle skin impact the structural design of the vehicle and are, therefore, not as desirable as the clip-on panels. The non-folding clip-on panels require no deployment/folding either after launch or prior to reentry operations and are baselined for the design and weight analyses conducted herein.

The component and subsystem design are very similar to the deployed concept except for the details of radiator panels design and the addition of an overboard dump valve to vent the radiator fluid overboard for reentry. The critical design constraint for this system is the combined structural loads and high temperatures imposed on the system during ascent and reentry. For

TABLE 16
DEPLOYED RADIATOR DESIGN SUMMARY

	SINGLE DOOR	DOUBLE DOOR
Design Sink Temp - °F	26	34
Required Area - ft ²	1051	1665
Modular Panel Size	14.5 x 7.25	14.5 x 7.25
Tube Spacing - in.	6.21	6.21
Fin Thickness - in.	.030	.030(fold down panel) .016(door mounted)
Number of Panels	5	16
Total Area Available - ft ²	1051	1682

TABLE 17
SINGLE DOOR DEPLOYED RADIATOR WEIGHT ESTIMATE

Radiator Panels (0.030 inch skin) - 5 @ 80 lb each	400
Deployment Mechanism	35
Temperature Controller - 2 @ 8 lb each	16
Isolation Valve	1.5
Check Valve	0.5
Stagnation Valve - 2 @ 4 lb each	8
Bypass Valve - 2 @ 4 lb each	8
Flex Hose	<u>2</u>
Dry Weight	471.0
R-21 - 6.6 lb/panel	<u>33.0</u>
Total Weight	504.0 lb
Weight Density	0.48 lb/ft ²

TABLE 18
DOUBLE DOOR DEPLOYED RADIATOR WEIGHT ESTIMATE

Radiator Panels - 8 (.030 in skin) @ 80 lb each	640
8 (.016 in skin) @ 56 lb each	448
Deployment Mechanism	40
Temperature Controller - 2 @ 8 lb each	16
Isolation Valves - 4 @ 1.5 lb each	6
Check Valves - 4 @ .5 lb each	2
Stagnation/Proportioning Valve - 2 @ 4 lb each	8
Bypass Valve - 2 @ 4 lb each	8
Flex Hose	<u>8</u>
Dry Weight	1176
R-21 - 6.6 lb/panel	<u>105.6</u>
Total Weight	1311.6
Weight Density	0.79 lb/ft ²

maximum design flexibility and highest design confidence a modular titanium panel attached to the Orbiter skin is selected. The basic Orbiter skin could be used as the fin material if structural design integration permits. For concept comparisons it is assumed, however, that the addition of tubes, fluid and multiple fluid connections would make this integrated design unfeasible even though it could provide weight savings.

2.2 Panel Design

The design sink temperature for the skin mounted panels is the same as the single door deployed concept (26°F). Therefore the same area is required assuming that a high effectiveness radiator can be obtained. From a thermal design consideration titanium is a very poor choice of material for a radiator fin because of its low thermal conductivity. The radiator design for titanium panels will require thicker panels and additional fluid and tubes in order to maintain high radiating fin effectiveness. This will result in higher radiator panel weights than for the deployed subsystems. The computer analyses conducted in Reference 29 indicated that in order to obtain a high radiator effectiveness, a 0.06 inch titanium fin with approximately 3.0 inch tube spacing is required. Figure 72 shows the basic panel construction of 0.125 in. I.D. diameter tubes brazed to the titanium fin at 3.1 inch intervals. The secondary system tubes are located between the primary tubes. The over/under tube arrangement used for the deployed panels is not used to minimize the radiator stand-off from the Orbiter skin. Sixteen modular panels (8 on each side) each 14.5 x 7.25 ft. are required to give a total area of 1051 ft². A weight estimate of the skin mounted panel is presented in Table 19.

4.2.3 Radiator Penalty Summary

Radiator weight penalties have been determined for four different radiator design concepts as follows:

<u>CONCEPT</u>	<u>WEIGHT PENALTY</u>
Single Door Deployed	0.48 lb/ft ²
Double Door Deployed	0.79
Skin Mounted - Clip On	2.20
Skin Mounted - Integral	0.84

Final selection of a radiator design will require detailed studies of the thermal performance, operational procedures, structural performance and vehicle integration. Based on the preliminary design analyses conducted herein the single door deployed system will be the lightest weight.

TABLE 19
SKIN MOUNTED RADIATOR WEIGHT ESTIMATE

Radiator Panels - 10 @ 222 lb each	2220
Temperature Controller - 2 @ 8 lb each	16
Isolation Valve - 2 @ 1.5 lb each	3
Check Valve - 2 @ 0.5 lb each	1
Stagnation/Proportioning Valve - 2 @ 4 lb each	8
Bypass Valve - 2 @ 4 lb each	8
Pressure Relief Valve 4 @ 4 lb each	<u>16</u>
Dry Weight	2272
R-21 - 6.6 lb/panel	<u>66</u>
Total Weight	2338
Weight Density	2.2 lb/ft ²

Note: If Orbiter skin is used for fin material a weight savings of 1450 lb is realized. The resulting weight density would be 0.835 lb/ft².

5.0 OVERALL EC/LSS HEAT REJECTION SYSTEM SELECTION

5.1 DESIGN REQUIREMENTS

This section presents estimates of the heat rejection system design requirements and general groundrules. A primary consideration in the selection of a heat rejection system is the heat load-time profile for each mission phase. A survey of the Shuttle prime contractor's Phase A and Phase B reports has been made to estimate the heat load-time profiles. The results of this survey have been used to postulate a design mission profile which can be used for preliminary heat rejection system selection. Table 20 summarizes the postulated design mission. The following paragraphs present a brief discussion of the requirements for each mission phase.

5.1.1 Prelaunch

Heat rejection during the pre-launch mission phase is baselined by the prime contractors to be by the Ground Support Equipment (GSE). The weight penalty for this technique is only the GSE heat exchanger and necessary controls. However, if the primary heat rejection system could be used during pre-launch, the GSE design and requirements would be greatly simplified. For example, the use of an on-board vapor compression system would require only power to be supplied by the GSE. A pre-launch design mission time of 2.0 hours has been selected for this mission phase.

5.1.2 Launch

The actual boost (lift off to orbit) portion of the launch mission phase is relatively short and no heat rejection is required. The vehicle thermal capacity is used to absorb excess waste heat. However, supplementary heat rejection may be required prior to radiator deployment. Table 21, taken from Reference 30, presents mission timelines for three reference missions which are typical of all prime contractors. This data indicates that separation from the booster occurs approximately 3 minutes after launch at an altitude above 200,000 feet, and insertion in a 50 x 100 N.M. orbit is complete in a maximum of 8 minutes 44 seconds. It is anticipated that the radiator can be deployed at this time and the primary orbit heat rejection system utilized. However, operational constraints such as excessive crew activity, excessive power requirements or structural design requirements for having the radiators deployed during engine burn could prevent the radiators from being deployed until circularization is complete. A radiator deployment time of 28 minutes (before circularization) is given by Reference 31. A design mission requirement of one hour (from orbit insertion to radiator deployment) has been selected for the launch phase to allow for any operational constraints against early radiator deployment. The design altitude will be 50 N.M. or greater for this period.

5.1.3 Orbit

The early Shuttle concepts in which the baseline Orbiter mission was a logistic resupply of an orbiting space station resulted in a mission profile

TABLE 20
ORBITER EC/LSS HEAT REJECTION SYSTEM DESIGN REQUIREMENTS

MISSION PHASE	DURATION HOURS	HEAT LOAD (BTU/HR)	ALTITUDE (FT)
Pre-Launch	2.0	44,000	0
Launch			
Ascend	0.15	32,000	0 - 300,000
Pre- RadOrbit	0.85	40,000	> 300,000
Orbit			
Power Up	24	40,000	> 300,000
Power Down	141	20,000	> 300,000
Reentry			
Deorbit	1.12	34,000	150,000-300,000
Transition	.13	34,000	48,000-150,000
Flyback	0.5	45,000	0-48,000
Post Landing	1.0	45,000	0

TABLE 21 TYPICAL REFERENCE MISSION TIMELINES

EVENT	EASTERLY MISSION		SOUTH POLAR MISSION		RESUPPLY MISSION	
	TIME OF INITIATION	ALTITUDE	TIME OF INITIATION	ALTITUDE	TIME OF INITIATION	ALTITUDE
Lift-Off	00:00:00:00	0	00:00:00:00	0	00:00:00:00	0
Booster Engine Cut-Off	00:00:03:14.9	209,427ft	00:00:03:16	213,445ft	00:00:03:15.4	211,356ft
Separation Initiation	00:00:03:14.9	209,427	00:00:03:16	213,445	00:00:03:15.4	211,356
Orbiter Engine Ignition	00:00:03:17.4	213,190	-	-	00:00:03:17.9	215,080
Orbiter Engine & OMS Ignition	-	-	00:00:03:18.5	217,147	-	-
Orbiter Engine Shut-down/Insert	00:00:06:32.5	50x100N.M.	-	-	00:00:06:34.5	100x50N.M.
Orbiter Engine Shut-down	-	-	00:00:06:37	303,536	-	-
OMS Engine Shut-down/Insert	-	-	00:00:08:44.2	50x100N.M.	-	-
Circularize	00:00:50:13	100x100	00:00:52:24	100x100	-	-
Phase Burn 1	-	-	-	-	00:00:50:15	123x100
2	-	-	-	-	00:01:35:15	241x123
3	-	-	-	-	00:03:51:29	250x251
Corrective Combination	-	-	-	-	00:04:36:27	260x250
Coelliptic	-	-	-	-	00:05:21:27	260x260
TPI	-	-	-	-	00:06:06:27	270x260
Braking	-	-	-	-	00:06:42:26	270x270
Initiate De-orbit Burn	06:20:04:03	100x100N.M.	06:20:04:30	100x100	06:20:40:28	270x270
Entry	06:20:19:29	400,000ft	06:20:17:29	400,000ft	06:24:13:36	400,000ft
Initiate Transition Maneuver	06:20:49:24	155,00	06:20:49:19	153,000	06:21:39:01	159,000
Complete Transition	06:20:57:14	48,000	06:20:57:09	48,000	06:21:46:51	48,000
Land (Straight-In-Approach)	06:21:02:59	0	06:21:02:54	0	06:21:58:31	0

in which the maximum heat load occurred in a relative short time (rendezvous, docking and cargo transfer) and was significantly higher than the nominal heat load. Figure 73 shows a typical Orbiter power profile, which is directly related to the heat load profile, taken from Reference 32. This data indicates that during the majority of the mission (approximately 130 out of 168 hours) the nominal heat load will be less than 2.5 times the maximum heat load. Initial system selection analyses have indicated the importance of the orbital design mission profile. The key to optimum system selection lies in the duration and magnitude of the maximum orbital heat load and the feasibility of using the pre-launch, launch, reentry, flyback or post landing heat rejection system to supplement the space radiator heat rejection during the maximum orbital heat load conditions.

More recent shuttle concepts have baselined the Orbiter mission as delivery and return of a payload from orbit or retrieving or servicing a previously launched payload. This type of mission could also result in the same type of heat load profile. The high heat load would occur during payload checkout prior to the deployment or during rendezvous and checkout of an existing payload and during payload loading for return from orbit.

As indicated by Table 20, the basic postulated mission assumed that the maximum heat load occurs for 24 hours out of the nominal seven day mission and is two times the nominal heat load.

5.1.4 Reentry

The reentry mission phase is defined for purposes of this study as the time from radiator stowage until subsonic atmospheric flight is obtained. Subsonic flight occurs shortly after the transition maneuver is completed. It is assumed that the radiators will remain deployed until just prior to the deorbit burn. From Table 21 it is observed that the maximum reentry time of 66 minutes occurs for the resupply mission from a 270 N.M. circular orbit. To allow for operational procedures such as switch over from the on-orbit to reentry heat rejection system and stowage of the radiators, a design reentry mission time of 75 minutes has been estimated. All but the last eight minutes of this period are at altitudes above 150,000 feet. During the last eight minutes the operating altitude is between 150,000 and 48,000 feet.

5.1.5 Atmospheric Flyback

This mission phase is defined as the time from subsonic atmospheric flight to touchdown. Table 21 indicates the maximum mission time for a straight-in landing is 11 minutes and 44 seconds. Reference 31 gives a typical mission timeline showing less than 10 minutes, and Reference 33 gives 20 minutes. In order to allow for fly-around capability a design mission time of 30 minutes has been selected for the atmospheric flyback mission phase. The altitude range for this mission phase is from 48,000 feet to sea level.

5.1.6 Post Landing

A design mission time of one hour has been selected for this mission phase. This time allows for delays in the use of GSE cooling for missions

without the air breathing engines (no taxi capability) and allows for post flight system checkout by the crew.

5.1.7 General Design Criteria

The following general design criteria shall be considered in the design of the heat rejection systems:

- . Mission duration (lift-off to landing) of 7 days of self-sustaining lifetime shall be provided. For missions in excess of 7 days, the weight of the expendables shall be charged against the payload.
- . The shuttle shall have minimal assembly and checkout requirements at the launch pad.
- . Use of specialized facilities during around operations (e.g., clean room, altitude chambers, etc.) shall be minimized.
- . Service lines at the launch pad shall be minimal, preferably only for the main propulsion system propellants.
- . Total shuttle turn around time from landing to launch should be less than two weeks. The removal and replacement time shall be minimized with onboard checkout and module accessibility.
- . Abort condition heat rejection shall be provided for 48 hours.
- . First horizontal flight is June 1976. First manned orbital flight is April 1978. The shuttle will be operational in mid 1979.
- . All subsystems except primary structure, pressure vessels and fluid lines shall be designed to fail-operational after the failure of the most critical component, and to fail-safe for crew survival after the second failure. Electronic systems shall be designed to fail-operational after failure of the two most critical components, and to fail-safe for crew survival after the third failure. Individual subsystems reliability requirements may be revised where improvements in cost and effectiveness would result.
- . In systems where redundancy is needed, the shuttle systems shall be developed to provide redundant full mission capability, and shall avoid minimum requirement, minimum performance backup system concepts.
- . Redundant fluid lines shall be located to insure that an event which damages one line is not likely to damage the other.

- . The intended combined storage and operational service life is 10 years after becoming operational. An orbiter life of 100 missions will be provided with a cost effective level of refurbishment and maintenance.
- . Systems that are intended to operate in zero or multiple-g environment must be capable of test and verification in a one g environment during ground maintenance.
- . In general, there shall be no requirement for inflight maintenance.
- . Vehicle trajectory load factors shall not exceed 3g, and entry trajectories shall not exceed 3g for the Orbiter.

5.2 SYSTEM WEIGHT ANALYSIS

In order to assess the relative weights of the overall EC/LSS heat rejection system a baseline system has been established. This baseline was obtained by using the parametric weight data developed in Paragraph 3.0 to select the minimum weight system for each mission phase without regard to the use of a common system in two or more phases. Figure 74 shows the baseline overall heat rejection system and a tabulation of the total system weight. The operating conditions shown on the schematic of Figure 74 are for the powered up on orbit phase.

An abort phase expendable system is included in the baseline system since the radiators may not be deployable in an abort condition and the use of power will probably be limited. The baseline system assumes that cryogenic hydrogen can be used for orbital operations even though the most recent Orbiter configurations do not have subcritical storage of hydrogen (only supercritical high pressure, high purity fuel cell H_2 is presently anticipated). The baseline system further assumes that the use of H_2 or ammonia during the flyback and post landing phases is not allowed due to safety and corrosion considerations. The weight penalty associated with this restriction will be evaluated in subsequent paragraphs.

The single door deployed radiator concept is used in the baseline system for the on-orbit heat rejection. The integral skin mounted radiator concepts are not baselined due to the development status of suitable radiator materials. For the maximum on-orbit design load of 40,000 BTU/hr, the double door deployed radiator has an area requirement of 2285 ft^2 . Since the maximum area available is 1800 ft^2 , the double door concept cannot be used unless the orientation is restricted. It will be required to use expendable cooling or mechanical refrigeration to reduce the required radiator area if the double door concept is used. It should also be noted that the single door deployed concept results in the lightest weight radiator due to reduced area requirements as well as lower weights per unit area. The techniques for reducing radiator area and weight discussed in the subsequent paragraphs will therefore show a minimum impact on the overall system weight. If the double door deployed concept is used, the area reduction techniques will have a different effect on the system weight.

Other factors to be considered in the overall system selection, in addition to total system weight, include the operational simplicity of the system, the use of common systems in one or more mission phase, the dumping of expendables near experiments for on-orbit operations, the reduction of radiator area and the use of high radiator temperatures to reduce coating degradation sensitivity and allow operation under high sink-temperature conditions. All of these factors are inter-related. For example, a high temperature radiator could reduce the radiator size which in turn could simplify the deployment operation.

The operational procedures could be improved by using water as the expendable for on-orbit heat rejection. This would simplify the pre-launch and post landing operations of loading the expendables and preventing condensation in the tank insulation during atmospheric mission phases. The expendable water system is inherently simpler since it does not require as many control valves, sensors or a fan. Figure 75 shows the total system weight estimate for the configuration which uses water instead of cryogenic H₂. The fuel cells produce excess water, but the initial expendable requirement occurs during the first hour of the mission, before a reserve capacity can be built up. Excess fuel cell water with no weight penalty is shown for the deorbit phase. Total expendables must also be carried for the abort condition since the fuel cells may be operated at partial or no load.

A reduction in radiator area can be realized by extending the use of the expendables to include the 24 hour powered up phase. The space radiator is sized for the 141 hour powered down phase and the expendable system is used to top-off the radiator during the powered up phase. Figures 76 and 77 show the weight estimate for these configurations using H₂ and water respectively as the expendable. A radiator area savings of 738 ft² results from this technique.

The use of a vapor compression mechanical refrigeration system for orbital cooling reduces the radiator area, allows the use of a common system for prelaunch, on-orbit, flyback and post-landing, increases the radiator temperature and eliminates expendables dumping. Several applications of a vapor compression system have been considered. The system shown in Figure 78 refrigerates the water loop heat load by replacing the intercooler with an evaporator and direct condensing radiator. The fuel cell is cooled by a separate R-21 loop and space radiator. The fuel cell radiators operate at a high temperature such that refrigeration of the waste heat load shows no weight advantage or area reduction. The fuel cell loop heat rejection control is accomplished by a simple radiator bypass system. The vapor compression system heat rejection control is maintained by on/off system operation. The weight estimates shown in Figure 78 show the range of values for the vapor compression system that results from different power penalties. The lower value is based on the use of the excess fuel cell capacity already planned for the Orbiter. The higher value includes the fixed weight of additional fuel cell capacity. The vapor compression system application shown in Figure 79 is identical to the above system except that a dual mode orbital refrigeration system is used. This system operates as a conventional pumped, single phase

fluid radiators for nominal and low loads. During high loads the system operates as a vapor compression system with the interface heat exchanger becoming the evaporator and the radiator becoming the condenser. The dual mode system reduces the total power requirements since during nominal and low load conditions the vapor compression system is not required. Figure 79 presents the weight estimate for the dual mode system.

A third application (Figure 80) incorporates the vapor compression system with the fuel cell R-21 loop. The condenser and fuel cell are cooled by the R-21 loop and space radiator. A high temperature radiator results from this system and a single radiator system is used. The design complexity and development of a condensing radiator are also eliminated. The vapor compression system can be either an on/off type or a dual mode system so that for nominal or low load operation an intermediate cooling loop is used in place of the intercooler on the baseline system. This arrangement suffers the temperature inefficiency of an extra heat exchanger and a larger radiator area to meet the nominal load requirements. However, the total system weight as indicated by Figure 81 is reduced due to lower power usage by the dual mode system.

The partial load vapor compression system shown in Figure 82 takes advantage of the fact that not all components in the EC/LSS fluid loops require a low (40-50°F) inlet temperature. The low temperature is required to condense moisture from the cabin atmosphere. Therefore, a high radiator outlet can be allowed if a partial load vapor compression system is used to cool the cabin. For nominal load operations the vapor compression system is turned off and the water loop routed to the cabin heat exchanger. For suborbit operation the vapor compression system is on (no water flow to the cabin H/X) and the interface heat exchanger is bypassed by flowing the fuel cell and condenser in series. This allows the R-21 loop to be cooled by ram air and the water loop to be cooled by expendable R-22.

Figures 83 and 84 show weight estimates of modifications to the baseline system which use cryogenic H₂ and ammonia respectively for the expendable cooling fluid for the flyback and post landing mission phases. As previously discussed there are drawbacks to the use of these fluids and this data is presented only to evaluate whether special design considerations to allow their use may be worthwhile. The use of H₂ throughout the Orbiter mission results in a weight savings of 645 lbs over the baseline system and 64 lbs over the lightest system considered, the partial load vapor compression system. The use of ammonia during the flyback and post landing phase reduces the baseline system weight by 468 lbs and is 113 lbs heavier than the partial load vapor compression system. All of these comparisons are made with the weight estimates which use the minimum power penalty. Figure 85 presents a weight estimate of a system that uses expendable R-22 for the flyback and post landing heat rejection system. This system has a high weight, but as previously discussed, is the safest expendable fluid for these mission phases.

Table 22 presents a summary of the weight estimates for the baseline system and the 11 configurations considered. The minimum weight system is

TABLE 22
OVERALL EC/LSS HEAT REJECTION SYSTEM WEIGHT SUMMARY

<u>SYSTEM</u>	<u>TOTAL WEIGHT - LB.</u>	<u>TOTAL RADIATOR AREA FT²</u>
Baseline	3656	1475
Configuration 1	3760	1475
Configuration 2	3770	738
Configuration 3	3957	738
Configuration 4	3301-4373	704
Configuration 5	3180-4159	986
Configuration 6	3333-4415	771
Configuration 7	3230-4209	1092
Configuration 8	3075-3741	929
Configuration 9	3011	1475
Configuration 10	3188	1475
Configuration 11	4142	1475

configuration 9 which uses expendable H₂ for the flyback and post-landing mission phases. Configuration 9 weighs 64 to 645 lbs (depending on the power penalty) less than the next lightest system, Configuration 8 or the baseline system. If the lower power penalty is used then, the risks involved in dumping H₂ overboard during the suborbit mission phases are not justified. For the higher power penalty, significant weight savings result and the choice of systems is not so clear. The ammonia system, Figure 84, weighs 113 lbs more to 468 lbs less depending on the power penalty used. The use of ammonia probably does not present as many operational problems, is less hazardous than H₂ and still results in a significant weight savings if the maximum power penalty is used. The ammonia system shown in Figure 84 is used in conjunction with the expendable H₂ abort system for weight comparison to the baseline system. However, if an expendable water system is used for the abort phase, then a common water/ammonia flash evaporator could be used for system commonality.

All of the vapor compression systems (Configurations 4 through 8) show significant weight savings over the baseline system for the low power penalty and have comparable weights for the high power penalty. In addition these systems provide for significantly lower radiator areas and higher radiator temperatures. The lowest radiator area results from Configuration 4.

5.3 SYSTEM SELECTION

The vapor compression system and the expendable fluid system are selected as the suborbital heat rejection systems for further analysis and preliminary design. Both systems are potentially the weight optimum system, can be easily integrated with the orbital heat rejection system and can be used for both orbital and suborbital operations.

The vapor compression system is weight competitive with other systems and in fact shows a definite weight advantage if reserve fuel cell capacity can be used for the maximum on-orbit design condition (Figures 78 through 82). This system has the advantage of reducing the radiator area, thus simplifying deployment operations and providing growth potential for higher loads and additional area for payload heat rejection. The higher radiator temperature reduces the heat rejection sensitivity to coating degradation which implies less coating refurbishment between flights, reduced pre-flight measurement of reflectance, less constraints on handling, less ground handling protective equipment and fewer constraints on adjacent EV/IV activity on-orbit. Expendables dumping which is undesirable and restricted for some payloads is not required for the vapor compression system. The pre-launch and post landing heat rejection requirements can also be met by the vapor compression system. The pre-launch umbilical would require only electrical power and would eliminate the GSE heat exchanger. Post landing GSE would also be simplified since only electrical power would be required.

The expendable fluid suborbital heat rejection system offers a simplified, highly reliable system that requires no power. The use of R-22 as the expendable fluid results in a higher weight system (Figure 85) but is the least hazardous. The use of ammonia as the expendable fluid results

in a light weight system (Figure 84) but its use may be limited due to safety and corrosion problems. The multi-fluid flash evaporator is used for on-orbit heat rejection with water a top-off to the space radiator. This reduces the radiator area requirements with the benefits previously discussed. The water expendable system can be integrated with the excess fuel cell water system and the life support requirements with a minimum vehicle design impact. The abort phase heat rejection system will be required to be an expendable system, thus a common system can be used for the abort, on-orbit and sub-orbital phases resulting in less overall system complexity.

RECOMMENDATIONS

It is recommended that the vapor compression system and the multi-fluid spraying flash evaporator system be considered for further analysis and preliminary design. However, since the NASA-MSC is funding the development of these systems under separate contracts, it is recommended that during the remainder of this contract additional analyses and integration studies be performed on the subject systems rather than the preliminary design and development status determination tasks.

The selection of the two above systems for further consideration is based on an estimated power penalty and a postulated mission profile extracted from the prime contractor's Phase A and B reports of the 1969-71 time period. During the course of the overall system weight analysis it became apparent that the power penalty and the on-orbit powered-up heat load and duration were a key consideration in the overall heat rejection system selection. The flyback and postlanding mission phases also have an important influence on system selection. The natural evolution of the Orbiter and the recent award of the Orbiter contract to North American Rockwell Corp. should allow more specific power penalties and design mission timelines to be used. It is requested that the NASA-MSC furnish LTV with the latest power system design data and mission timelines including the expected range or deviations from the nominal. The parametric weight analyses can then be utilized with the revised data (if different) to insure that the selected systems are optimum over the expected range of design conditions.

At the outset of this investigation it was established that the payload heat rejection system weight would be charged to the payload and therefore would not be included in the Orbiter weight optimization studies. Payload heat loads can be a significant part of the overall vehicle heat rejection. Weight optimization of the total heat rejection system could result in increased payloads and/or reduced launch weights. It is therefore recommended that system integration studies be performed to optimize the total heat rejection requirements on the Orbiter system.

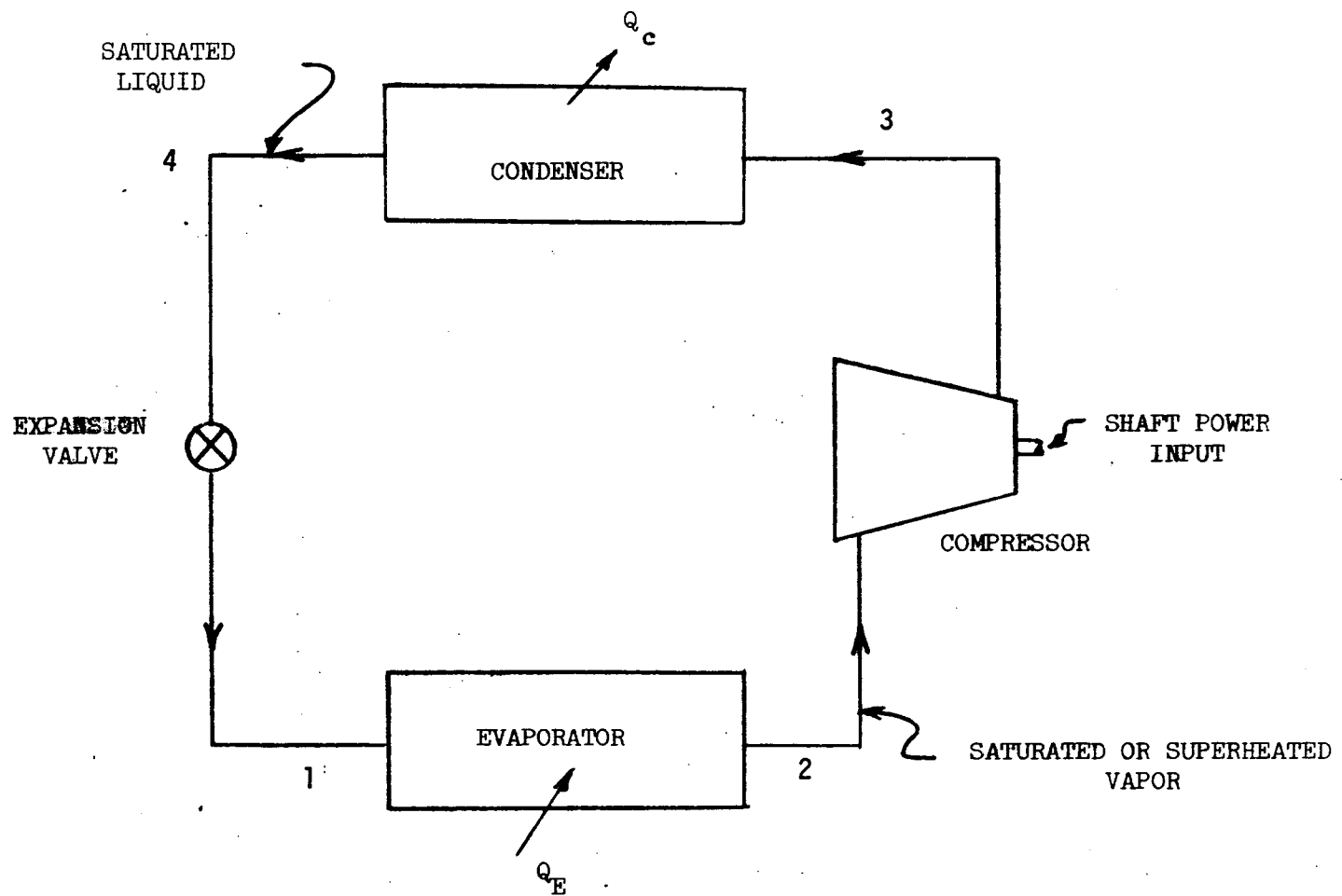
The hydraulics system heat rejection temperature is much higher (250°F) than the EC/LSS heat rejection temperature and separate heat rejection systems will probably be used. However, it is recommended that integration studies also be performed for this system. The possible use of common systems especially during the deorbit phase when atmospheric cooling cannot be used should be considered.

REFERENCES

1. Copeland, R. J., et.al., "Evaluation and Selection of Refrigeration Systems For Lunar Surface and Spacecraft Applications", Vought Missiles and Space Company Report No. T122RP04, 31 October 1971.
2. Wood, B. D., Applications of Thermodynamics, Reading Mass.: Addison-Wesley Publishing Company, 1969.
3. ASHRAE Guide and Data Book 1961 Fundamentals and Equipment, New York: American Society of Heating, Refrigerating and Air-Conditioning Engineers, Inc., 1961.
4. Rosenberg, H. N., et.al., "Thermal Control of Pod-Mounted Electronic Systems, Volume I and II", Air Force Flight Dynamics Laboratory Air Force Systems Command Wright Patterson Air Force Base, Ohio, AFFDL-TR-70-19, March 1970.
5. Blutt, J. R. and Sadek, S. E.; "A Gravity Independent Vapor Absorption Refrigerator", NASA CR-836, July 1967.
6. SAE Aerospace Applied Thermodynamics Manual. New York: Society of Automotive Engineers, Inc., SAE Committee AC-9, Aircraft Environmental Systems. 1969.
7. Krantweiss, Gerald, "Survey of Aircraft Thermal Control Systems", AFFDL-TR-66-44, November 1966.
8. Jordan, R.C., and Priester, G. B., Refrigeration and Air Conditioning, Prentice-Hall, Inc., Englewood Cliffs, N.J., 1956.
9. Honea, F. I. and Watanabe, D., "Temperature Control Systems for Space Vehicles", ASD-TDR-62-493, Part I, May 1963.
10. Mosely, T. D., "Gas Cycle Cooling Systems For Space Vehicles", WADD Technical Note 60-66, June 1960.
11. Rannenber, George C., "Simple/Bootstrap Cooling Systems for A New Transport Plane", AIAA Paper No. 69-787, July 1969.
12. Larson, V. H., "Equipment Cooling Systems for Aircraft", WADC Technical Report 56-353, January 1958.
13. North American Rockwell Space Division, "Study of Integral Launch and Reentry Vehicle System, Vol. IX, Technical Report - Second Phase Design and Subsystems Analysis", SD69-573-4, December 1969.

14. McDonnell Douglas Astronautics Co., "Integral Launch and Reentry Vehicle System, Vol. I, Book I, Configuration Design and Subsystems", NASA CR-66863-1, November 1969.
15. Radiator Design For Space Vehicles, Airesearch Manufacturing Company, Los Angeles, California, MS-AP0069, 1963.
16. Finch, H. L., "Orbiting Satellite Surface Temperature Prediction and Analysis", Midwest Research Institute Project No. 2669-E, Contract No. NAS9-1059, February 1964.
17. Dietz, J. B., et.al., "Space Station Prototype ETC/LSS Radiator and Solar Absorber Subsystems Final Preliminary Design Report", Vought Missiles and Space Company Report No. 00.1380, December 1970.
18. Harms, R. J., "A Manual For Determining Aerodynamic Heating of High Speed Aircraft, Volume I, " Bell Aircraft Corp. Report No. 7006-3352-001, June 1959.
19. Brown, A. I. and Marco, S. M., Introduction to Heat Transfer, McGraw-Hill Book Company, Inc., 1958.
20. Gaddis, J. L., "Feasibility Demonstration of a Spraying Flash Evaporator", Vought Missiles and Space Company Report No. 00.1427, 7 May 1971.
21. Forman, R. G., Gillen, R. J. and Szacik, R. S., "Description and Evaluation of Environmental Control and Cryogenic Supply Subsystems For X-20 (Dyna-Soar)", SEG-TR-65-5, April 1965.
22. "DC-3 Space Shuttle Study" NASA, April 1970.
23. "Analytical Methods For Space Vehicle Atmospheric Control Processes", ASD-TR-61-162 Part II, November 1962.
24. Hydrogen Safety Manual, Advisory Panel on Experimental Fluids and Gases, Lewis Research Center, NASA Technical Memorandum, NASA TMX-52454, 1968.
25. North American Rockwell Space Division, "Study of Integral Launch and Reentry Vehicle System Final Report, Volume III Technical Report - Second Phase Environment and Performance", SD-69-573-3, MSC00192, December 1969.
26. General Dynamics Convair Division, "Space Shuttle Final Technical Report, Volume IV, Technical Analysis and Performance", Report No. GDC-DCB69-046, 31 October 1969.
27. Lockheed Missiles and Space Co., "Integral Launch and Reentry Vehicle, Vol. I, Configuration Definition and Planning - Part B", LMSC A959837, 22 December 1969.

28. Space Division North American Rockwell, "SLA Mini-Base Concept For Extended Lunar Missions, Vol. II Crew Considerations and Systems Analysis", Report No. SD70-516, September 1970.
29. Gaddis, J. L., "Report On Preliminary Study of Crew and Equipment Thermal Control Systems For The Space Shuttle", Vought Missiles and Space Division Report No. 00.1323, 19 July 1970.
30. McDonnell Douglas Astronautics Co., "Space Shuttle System Phase B Study Final Report, Part II-1, Technical Summary Shuttle System," Report No. MDC E0308, 30 June 1971.
31. Grumman Aerospace Corp., "Alternate Space Shuttle Concepts Study Part II Technical Summary, Volume I, Shuttle Definition", Report No. MSC-03810, 6 July 1971.
32. North American Rockwell Space Division, "Phase B Final Report, Volume II Technical Summary, Book 2. Orbiter Vehicle Definition (Part 2 of 2)", Report No. MSC-03307, 25 June 1971.
33. North American Rockwell Space Division, "Phase B Final Report, Volume II Technical Summary, Book 2. Orbiter Vehicle Definition (Part 1 of 2)", Report No. MSC-03307, 25 June 1971, pp. 536.



SIMPLE VAPOR COMPRESSION SYSTEM

FIGURE 1

FIGURE 2
REFRIGERANT THEORETICAL PERFORMANCE DATA

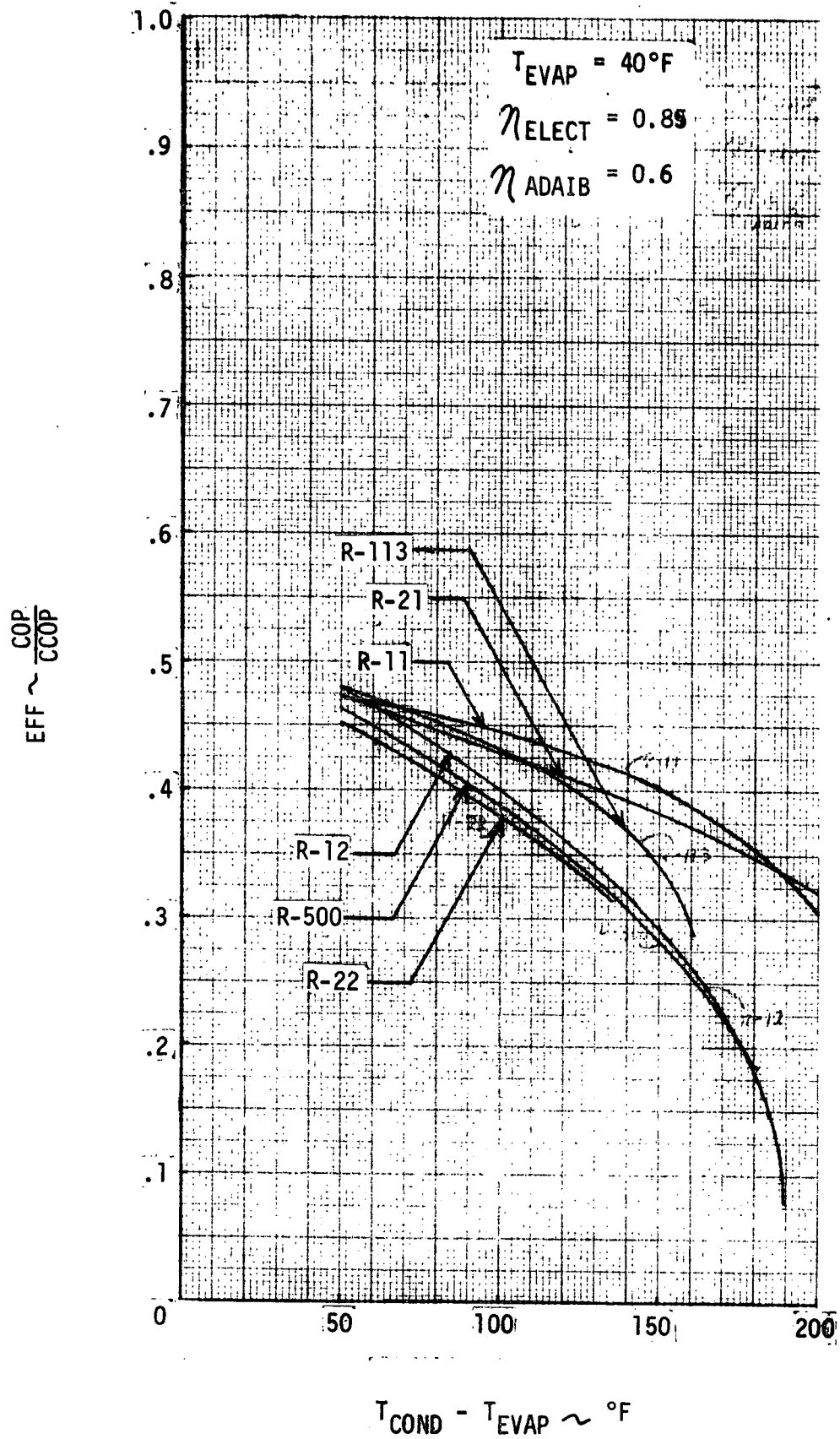


FIGURE 3
REFRIGERANT THEORETICAL PERFORMANCE DATA

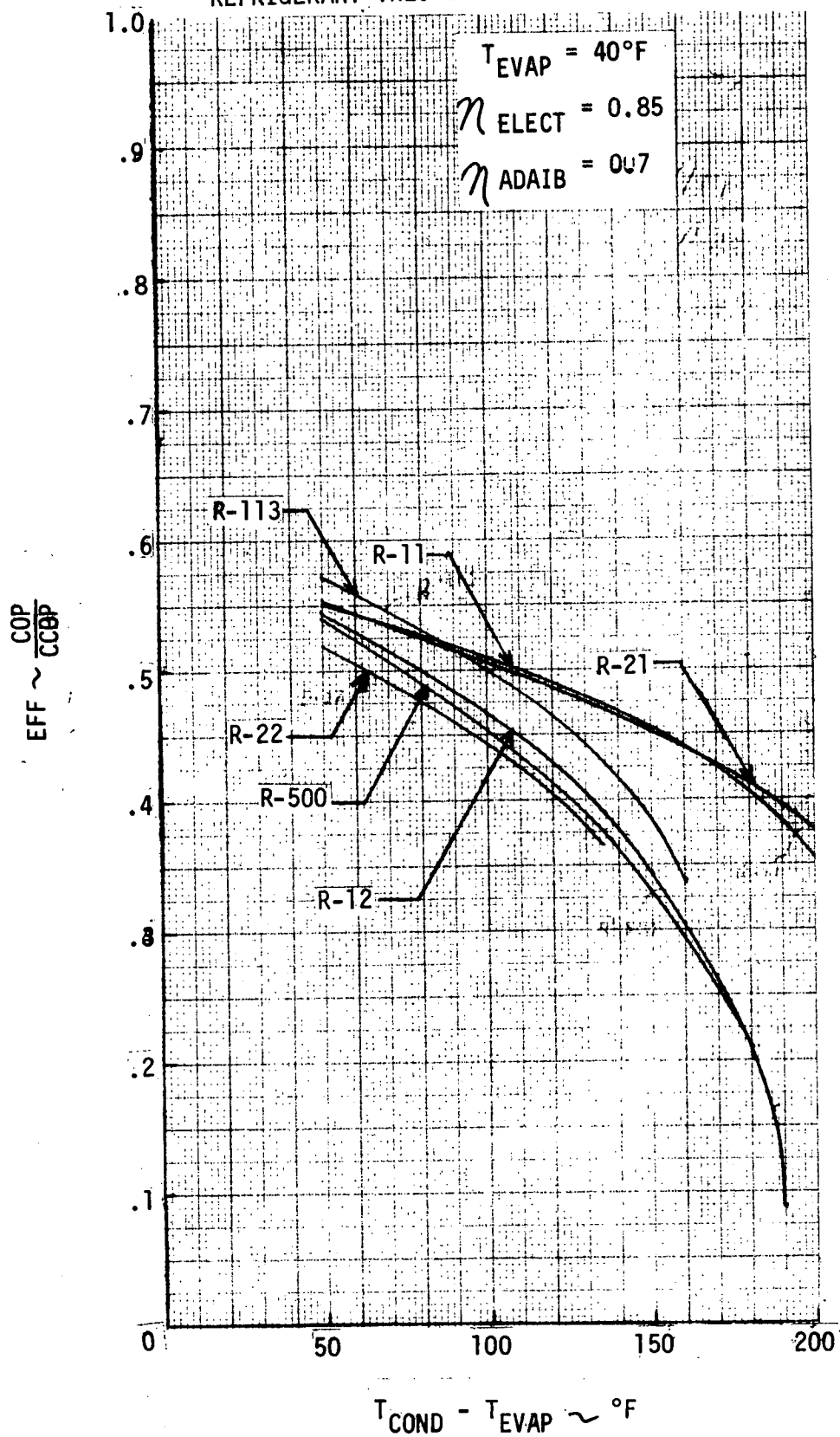


FIGURE 4

REFRIGERANT THEORETICAL PERFORMANCE DATA

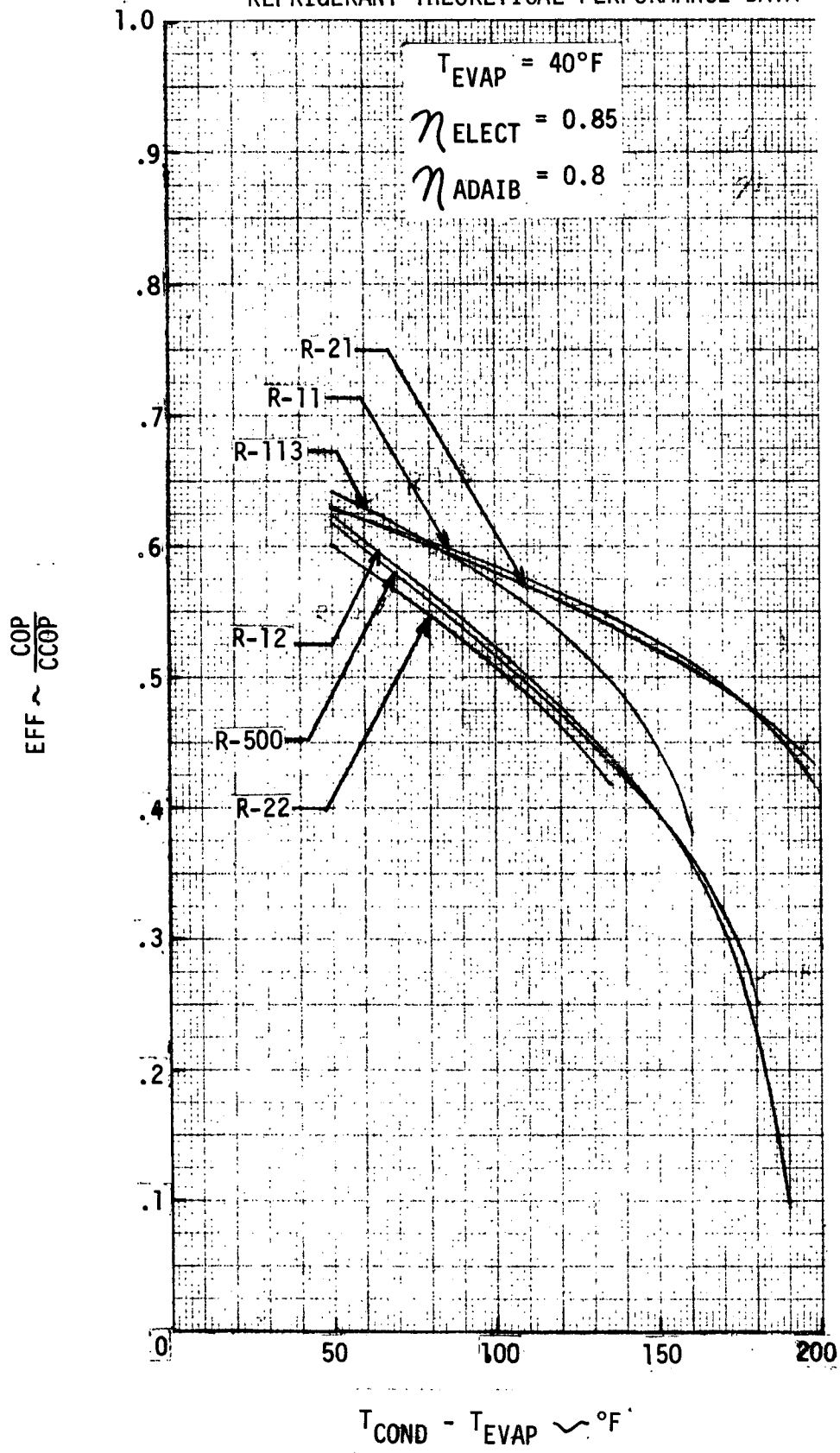
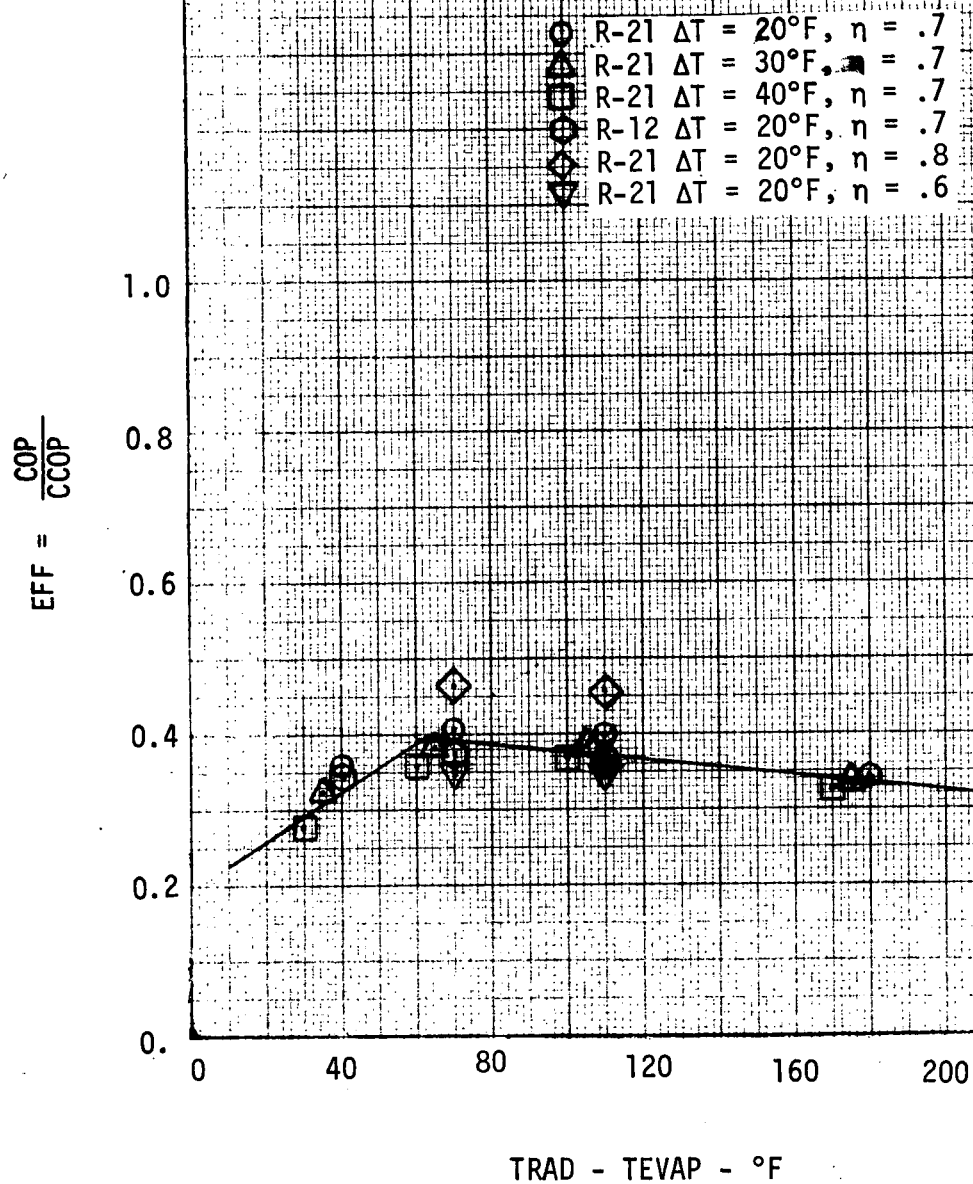


FIGURE 5
SYSTEM PERFORMANCE WITH A SECONDARY COOLANT LOOP



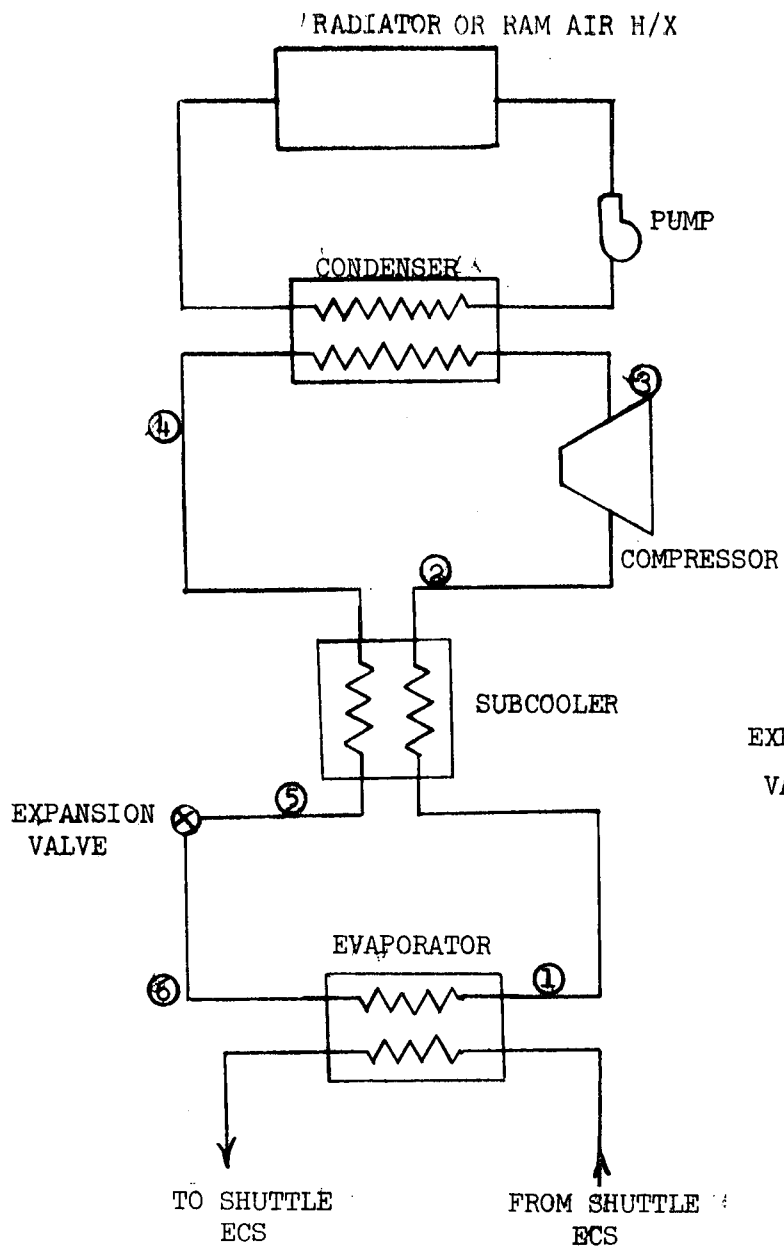


FIGURE 6a

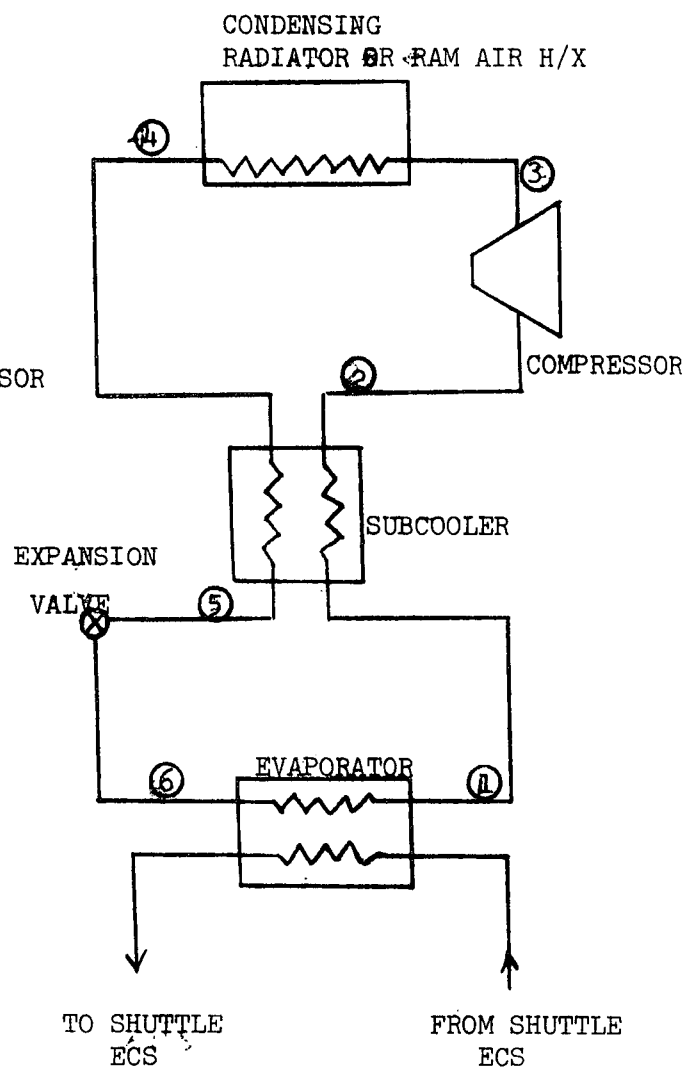


FIGURE 6b

VAPOR COMPRESSION SYSTEM CONFIGURATIONS FOR PARAMETRIC WEIGHT ANALYSES

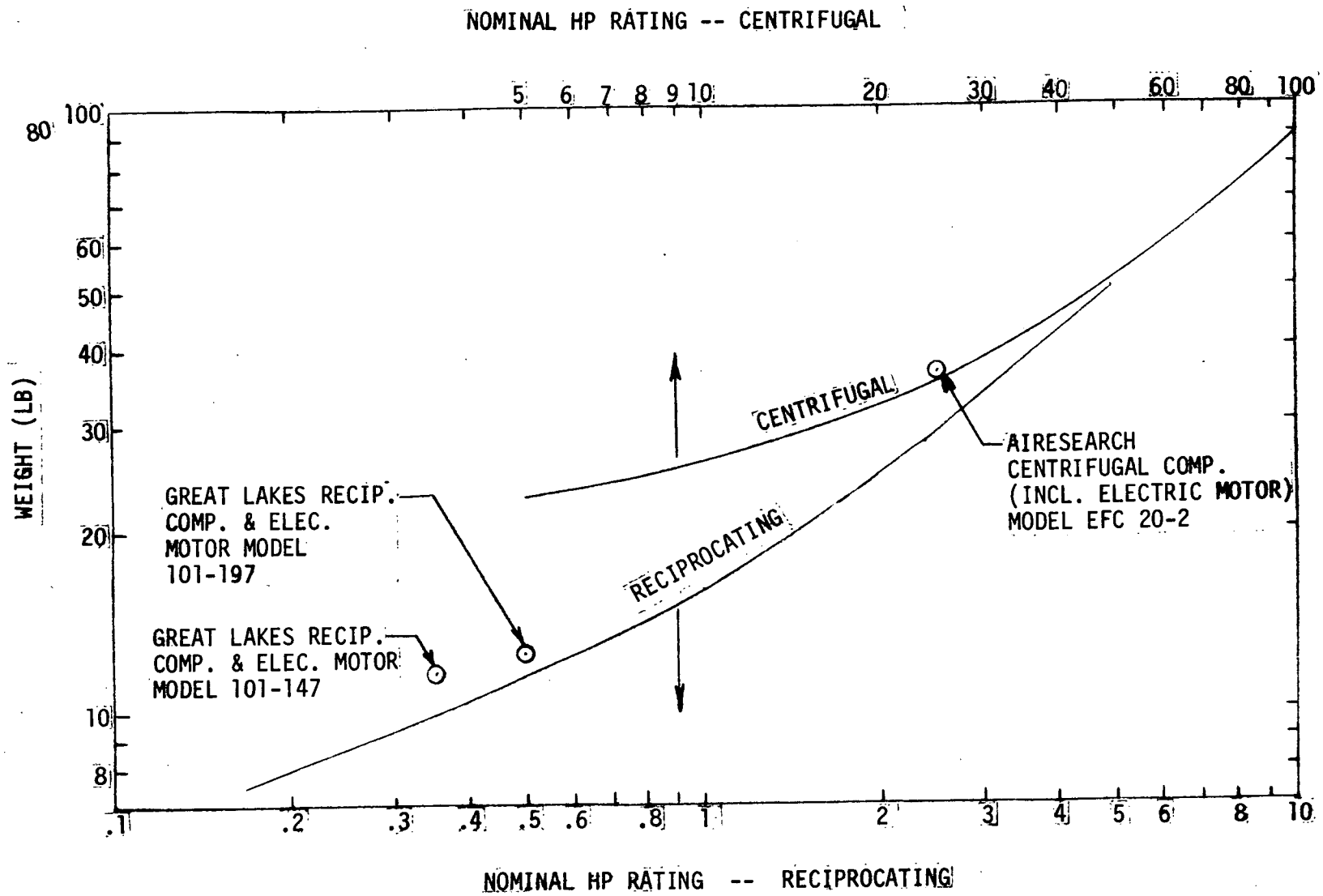


FIGURE 7 - COMPRESSOR WEIGHTS

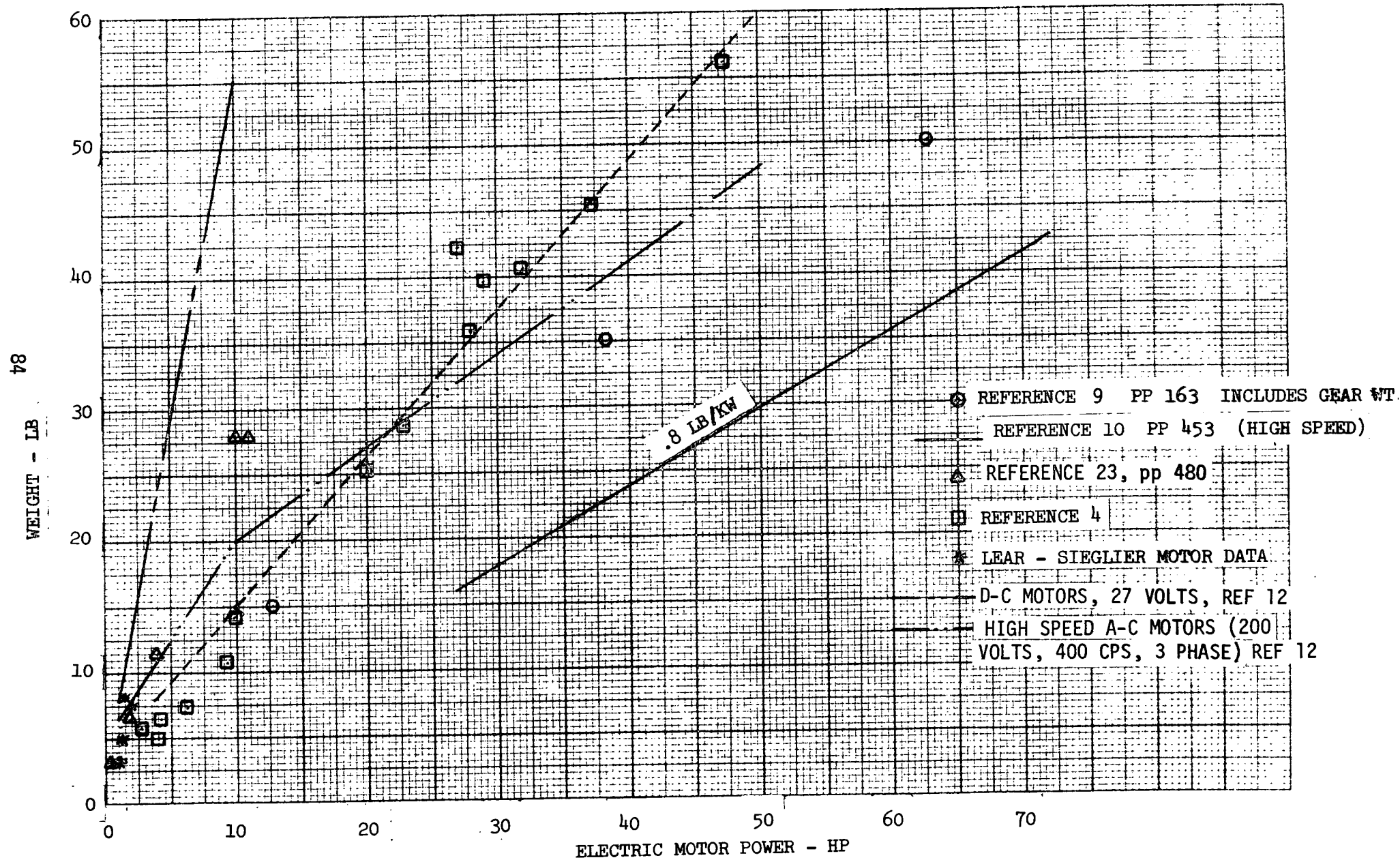


FIGURE 8 ELECTRIC MOTOR WEIGHT DATA

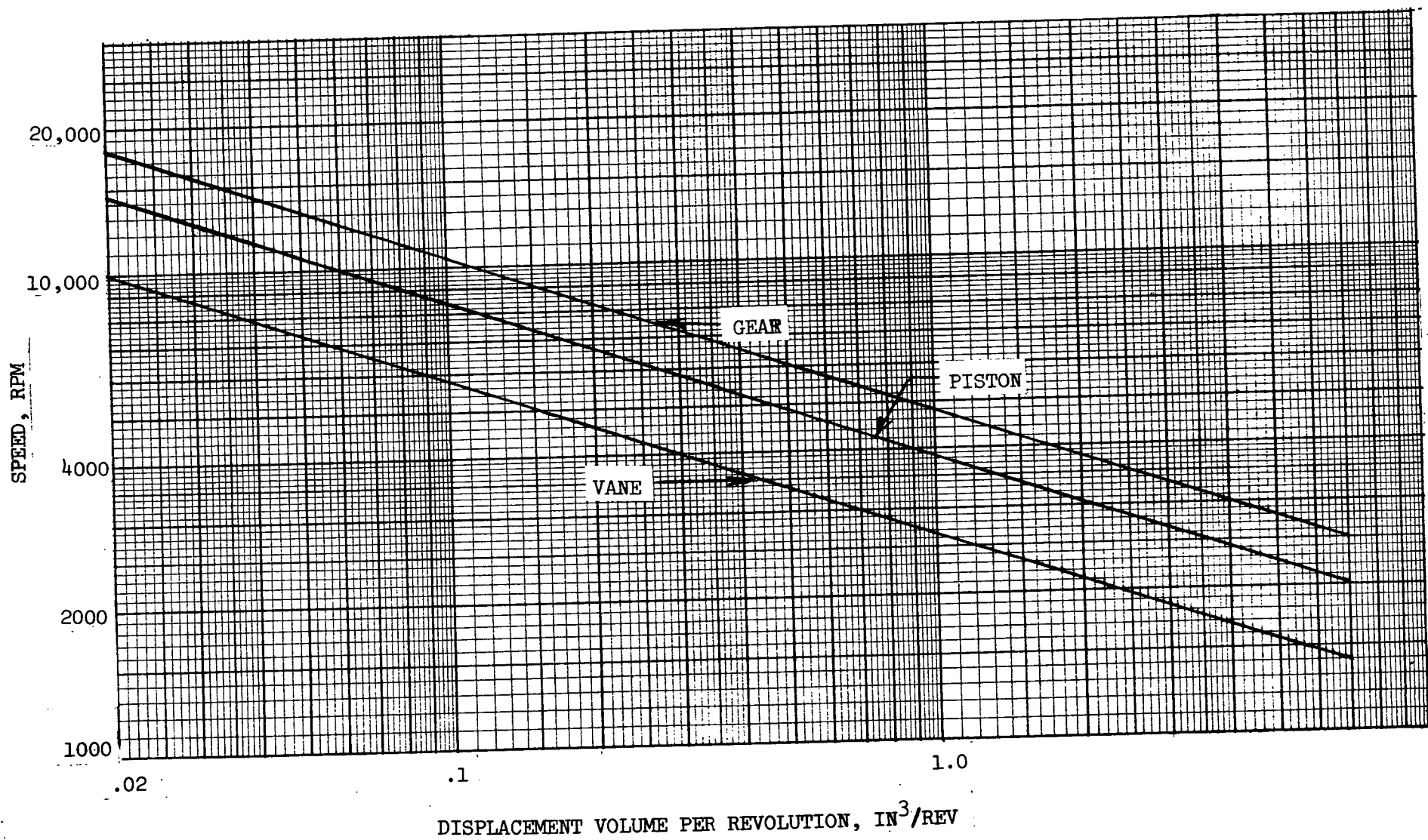
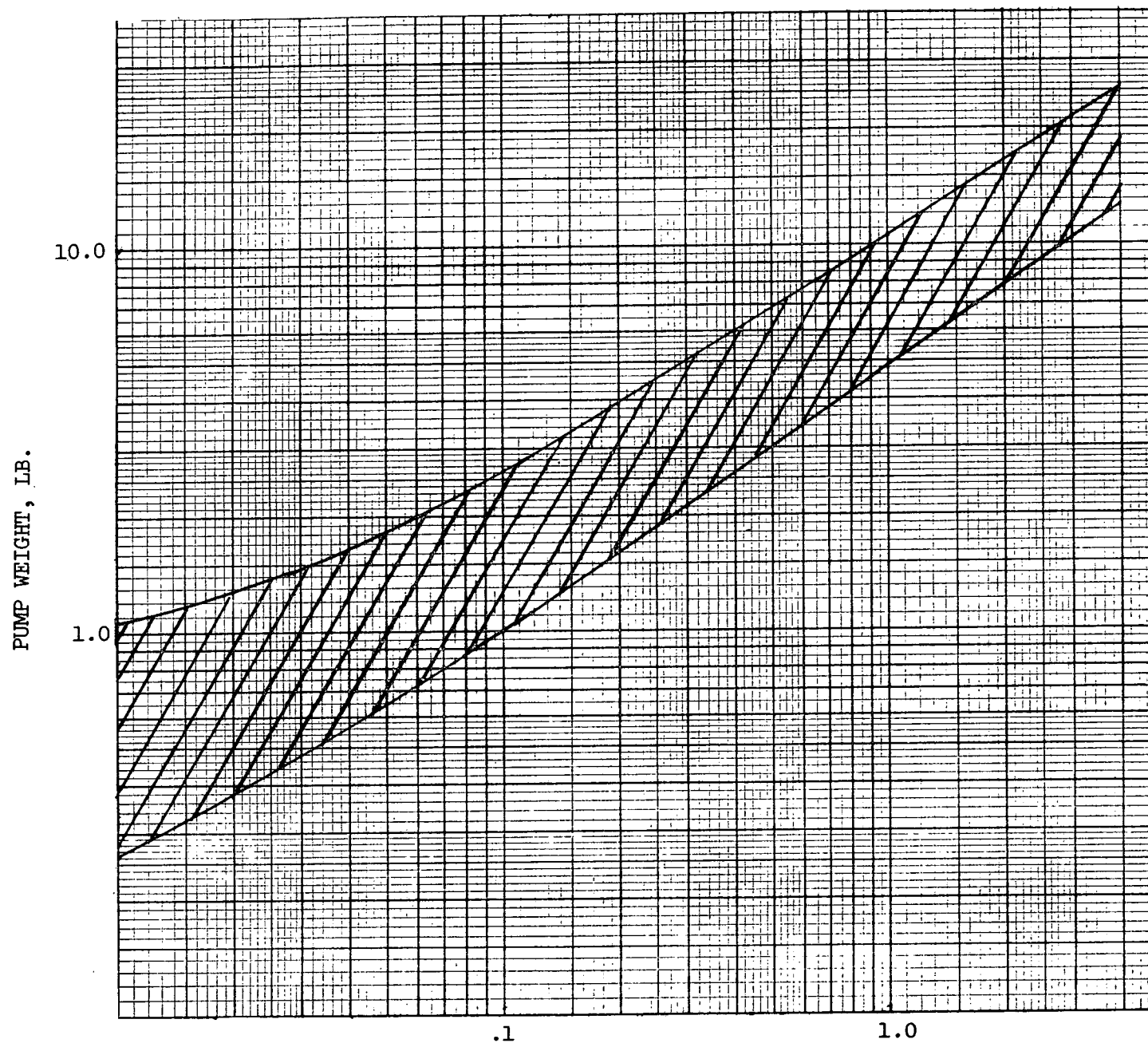


FIGURE 9 TYPICAL SPEEDS FOR PUMPS

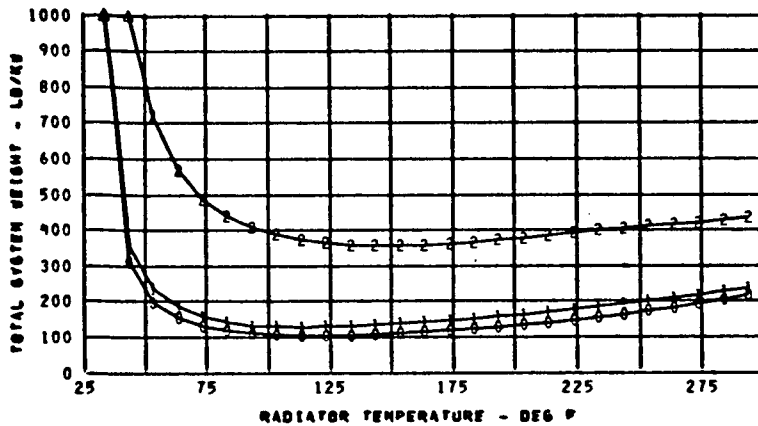


DISPLACEMENT VOLUME PER REVOLUTION, IN³/REV

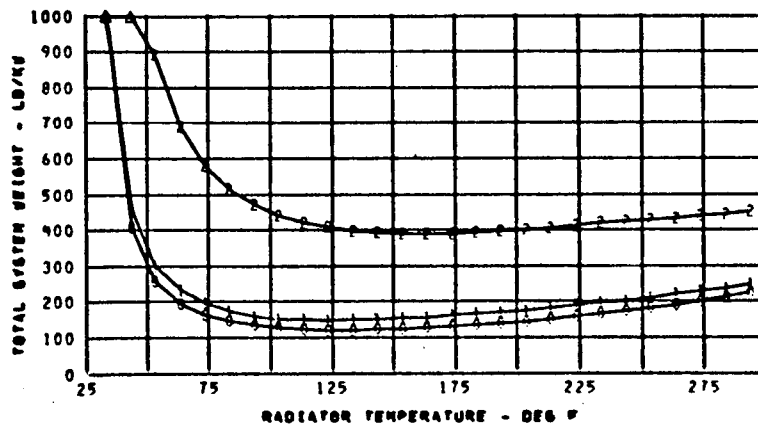
FIGURE 10 PUMP WEIGHTS (EXCLUDING MOTOR)

FIGURE 11
ORBITAL MECHANICAL REFRIGERATION SYSTEM WEIGHTS

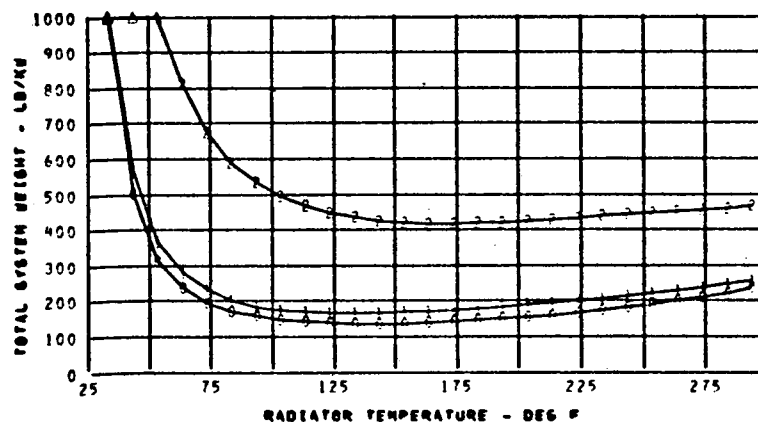
- 0 VAPOR COMPRESSION SYSTEM WITH DIRECT CONDENSING RADIATOR
- 1 VAPOR COMPRESSION SYSTEM WITH HX LOOP TO RADIATOR
- 2 GAS CYCLE SYSTEM WITH HX LOOP TO RADIATOR



TEVAP = 34.0 F
TSINK = 30.0 F
EPP = 100.0 LB/KW
RADP = .75 LB/FT²



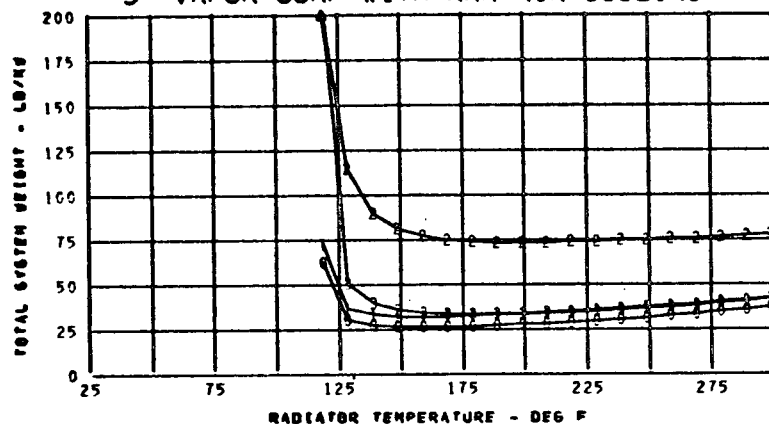
TEVAP = 34.0 F
TSINK = 30.0 F
EPP = 100.0 LB/KW
RADP = 1.0 LB/FT²



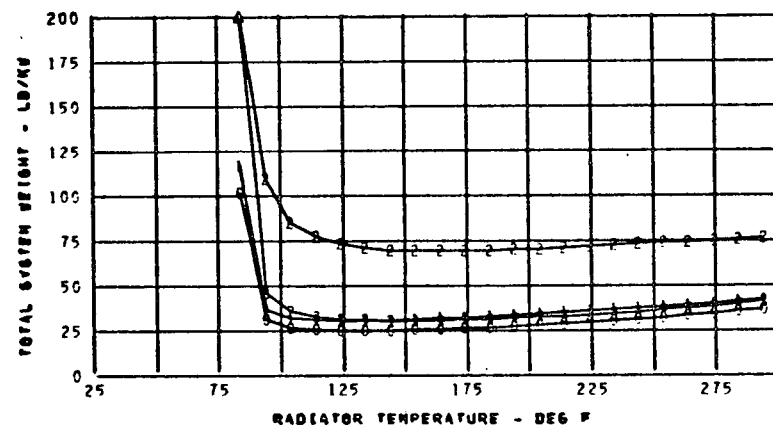
TEVAP = 34.0 F
TSINK = 30.0 F
EPP = 100.0 LB/KW
RADP = 1.2 LB/FT²

FIGURE 12
ATMOSPHERIC FLIGHT MECHANICAL REFRIGERATION SYSTEM WEIGHTS

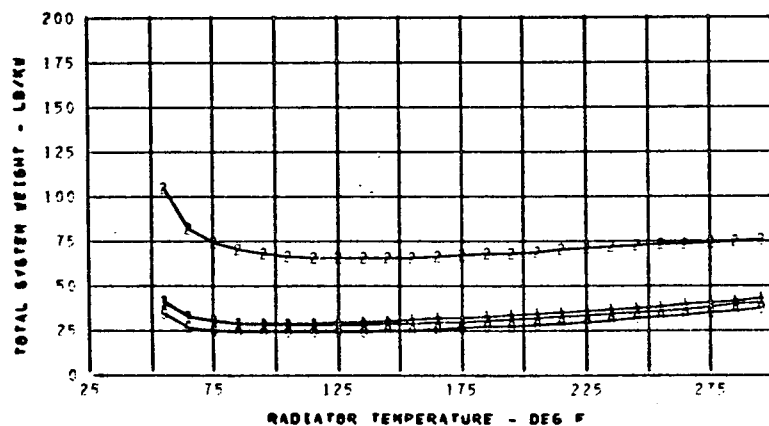
- 0 VAPOR COMP WITH DIRECT COND ATM CONVECTOR
- 1 VAPOR COMP WITH HX LOOP TO ATM CONVECTOR
- 2 GAS CYCLE WITH RAM AIR COOLING
- 3 VAPOR COMP WITH RAM AIR COOLING



ALT = 1000.0 FT
TEVAP = 34.0 F
TSINK = 46.4 F
EPP = 10.0LB/KW
RADP = .50LB/FT²



ALT = 10000.0 FT
TEVAP = 34.0 F
TSINK = 50.8 F
EPP = 10.0LB/KW
RADP = .50LB/FT²



ALT = 20000.0 FT
TEVAP = 34.0 F
TSINK = 55.6 F
EPP = 10.0LB/KW
RADP = .50LB/FT²

C2

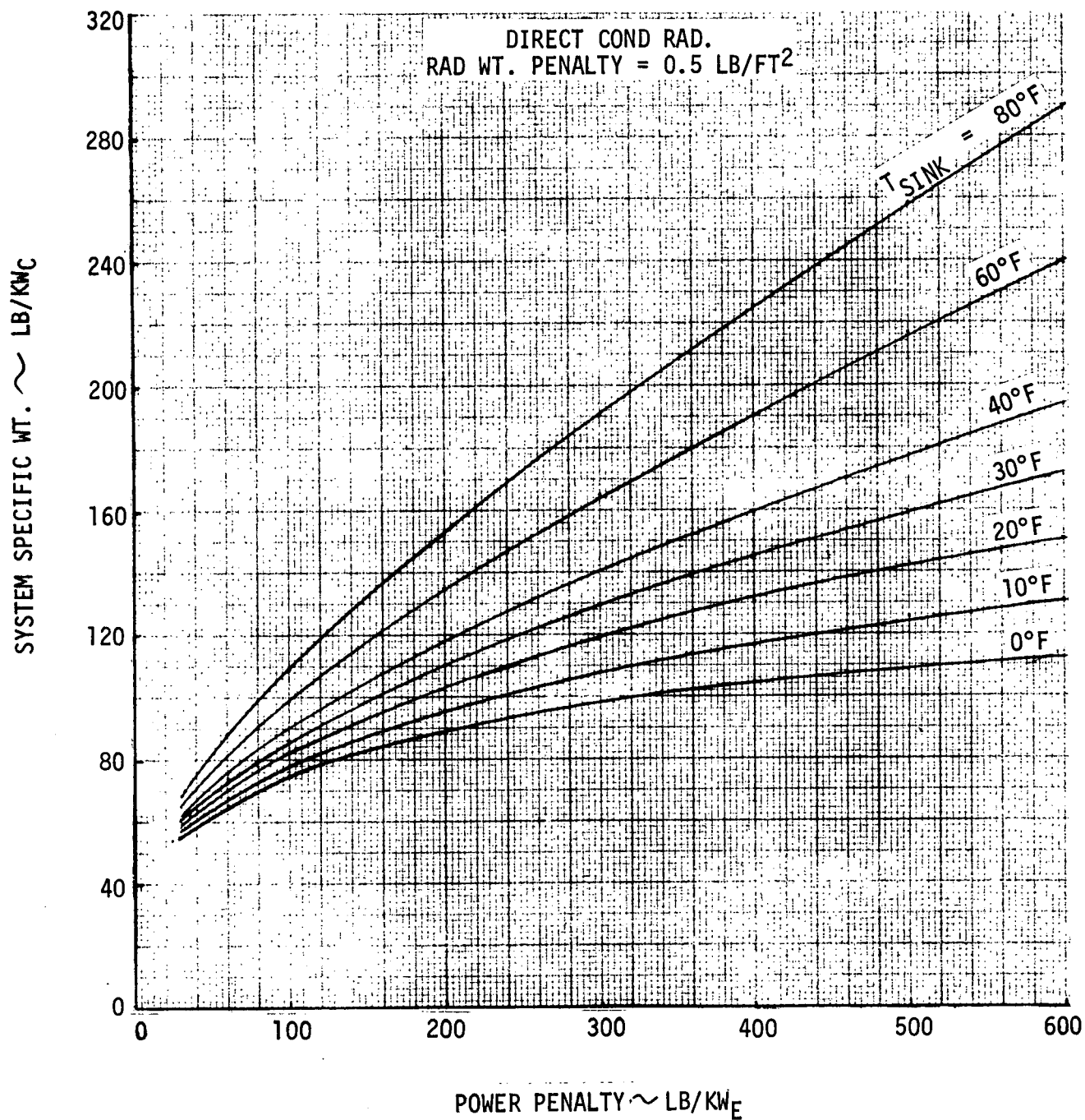


FIGURE 13 VAPOR COMPRESSION ORBITAL HEAT REJECTION SYSTEM WEIGHTS

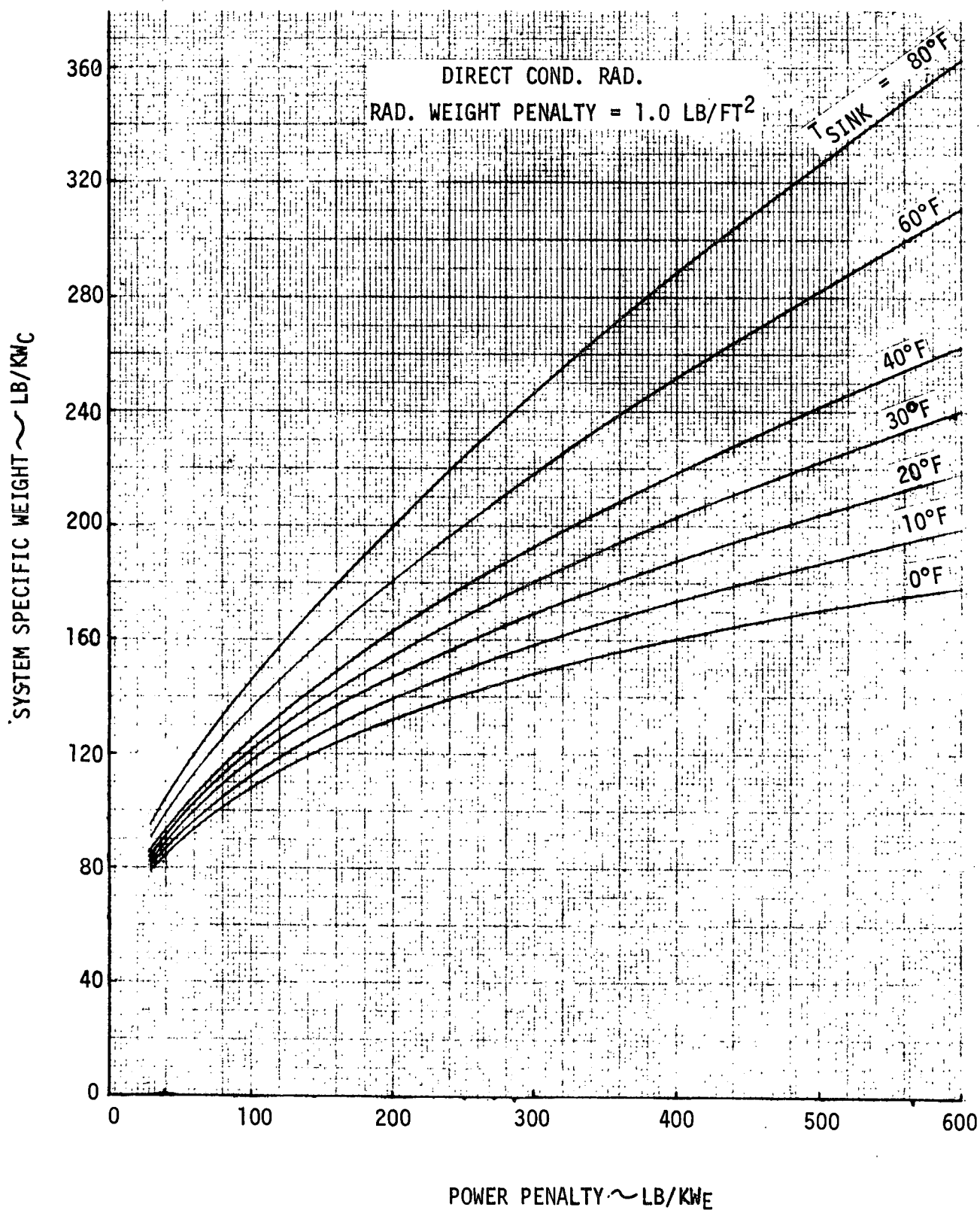


FIGURE 14 VAPOR COMPRESSION ORBITAL HEAT REJECTION SYSTEM WEIGHTS

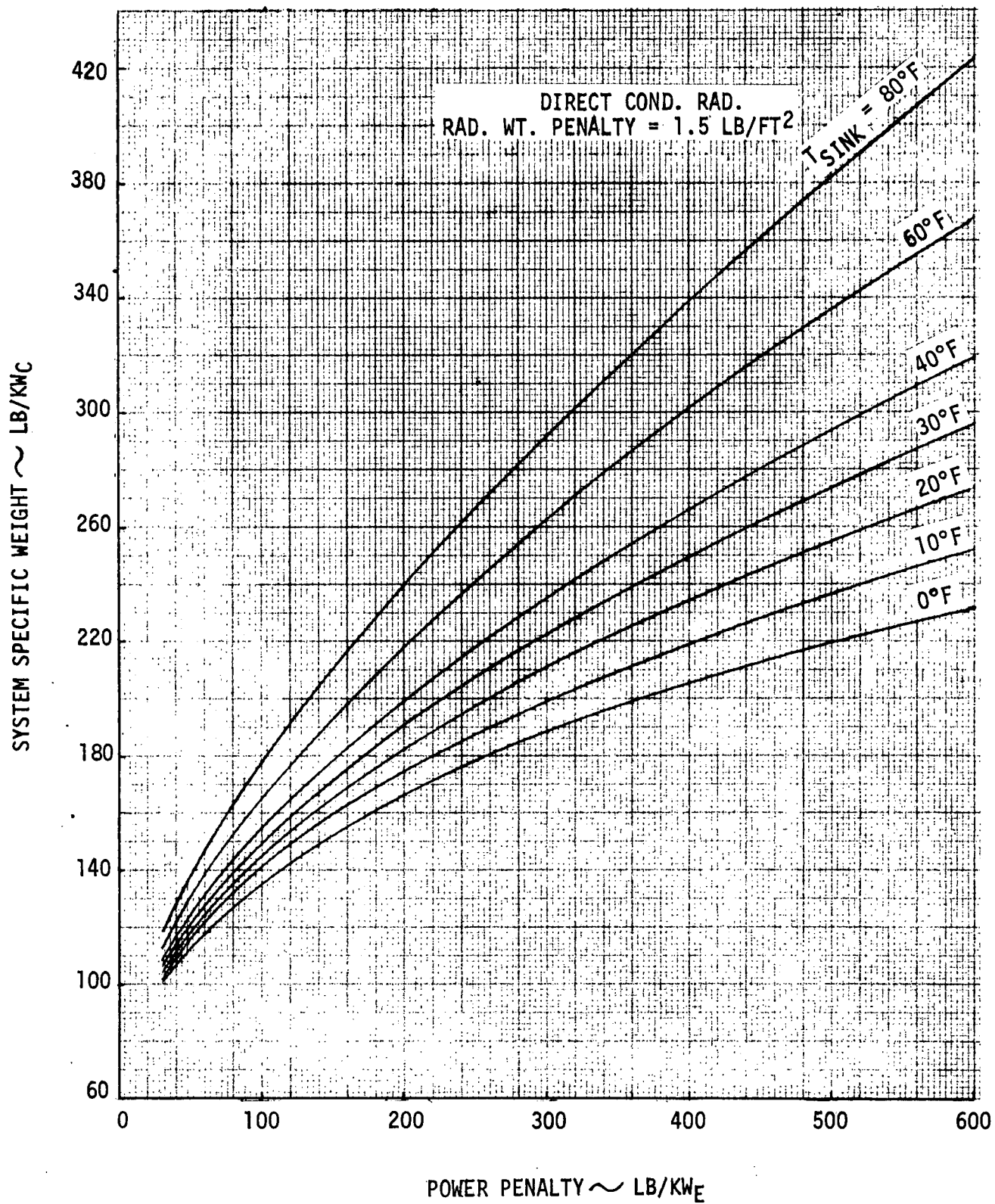


FIGURE 15 VAPOR COMPRESSION ORBITAL HEAT REJECTION SYSTEM WEIGHTS

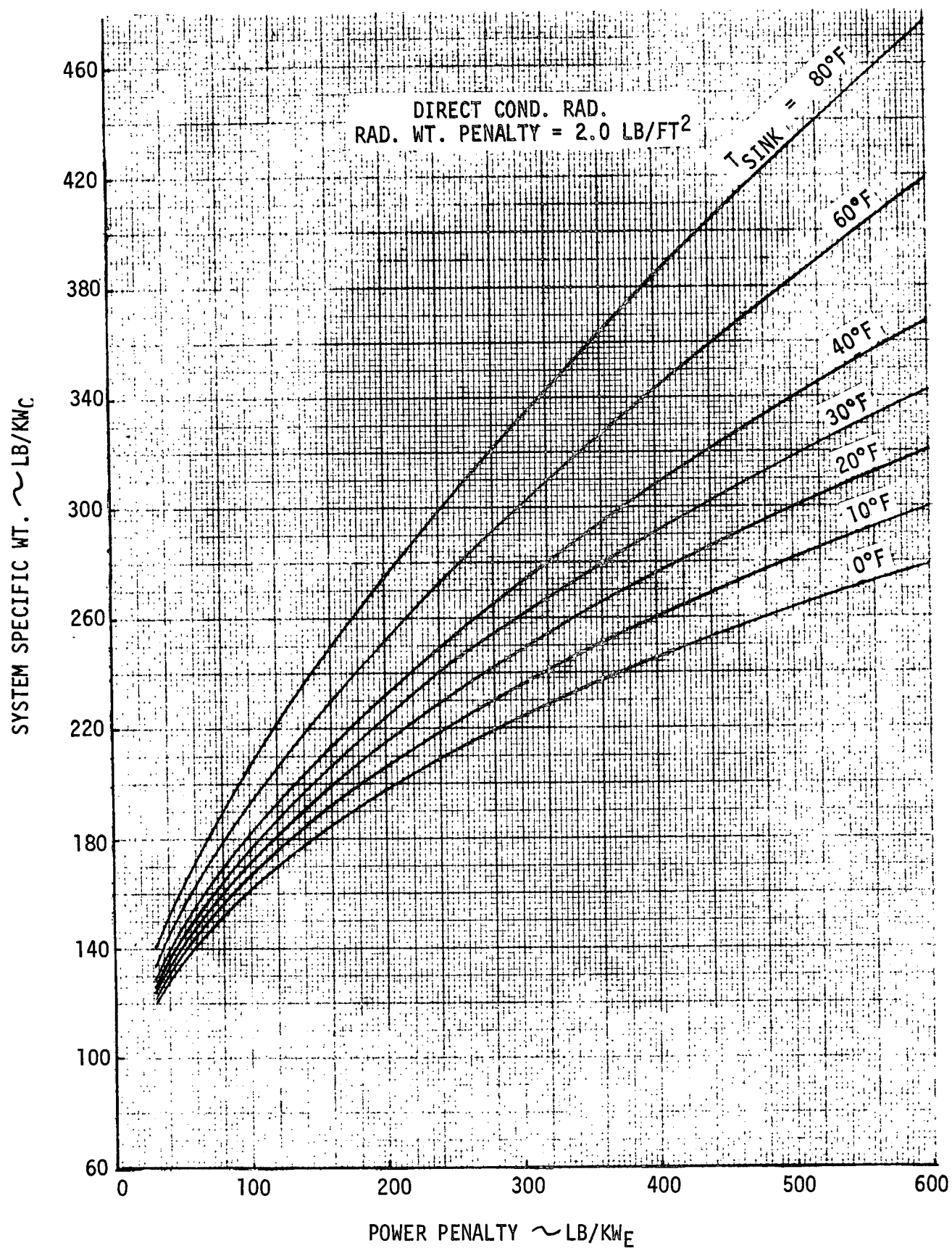


FIGURE 16 VAPOR COMPRESSION ORBITAL HEAT REJECTION SYSTEM WEIGHTS

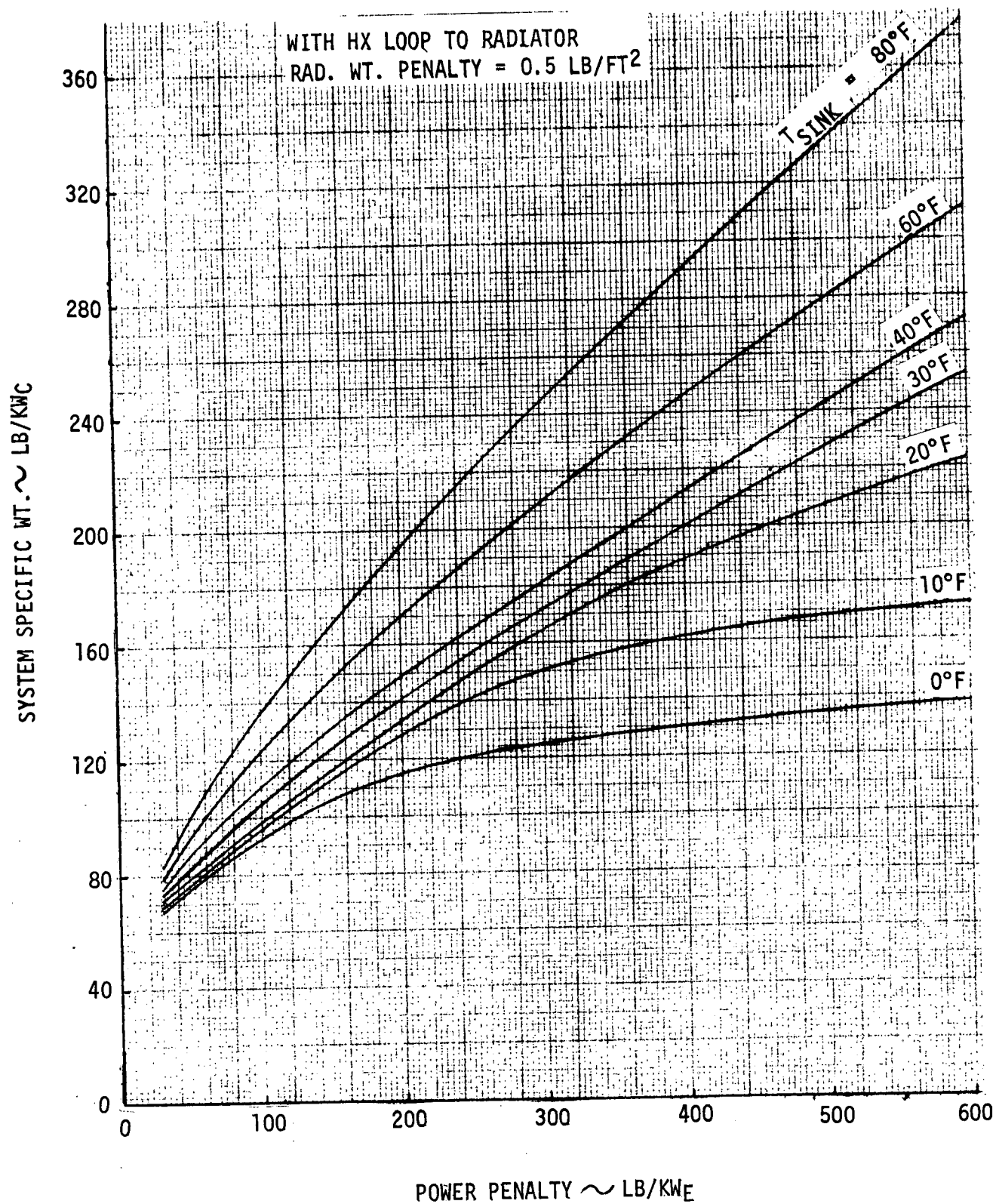


FIGURE 17 VAPOR COMPRESSION ORBITAL HEAT REJECTION SYSTEM WEIGHTS

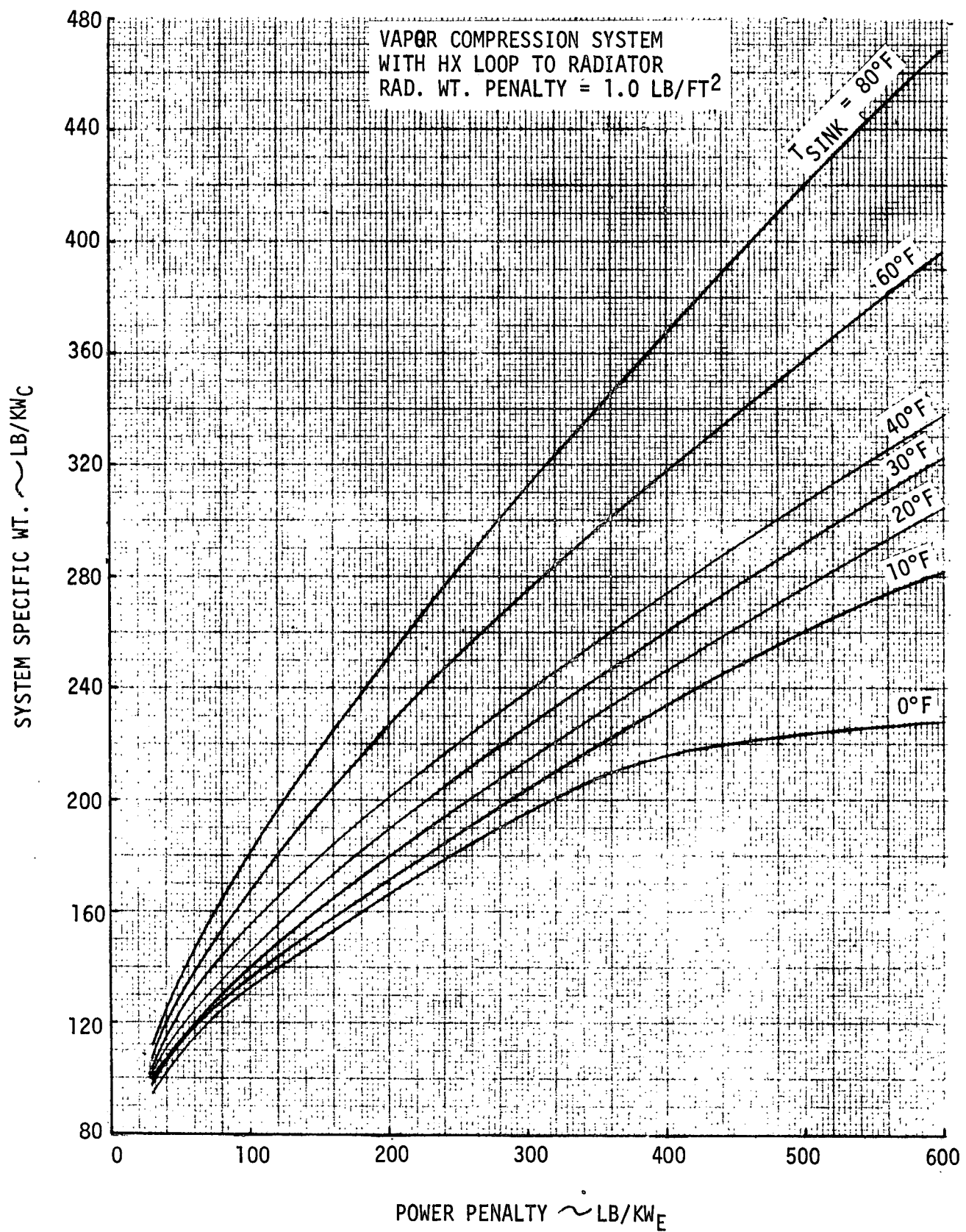


FIGURE 18 VAPOR COMPRESSION ORBITAL HEAT REJECTION SYSTEM WEIGHTS

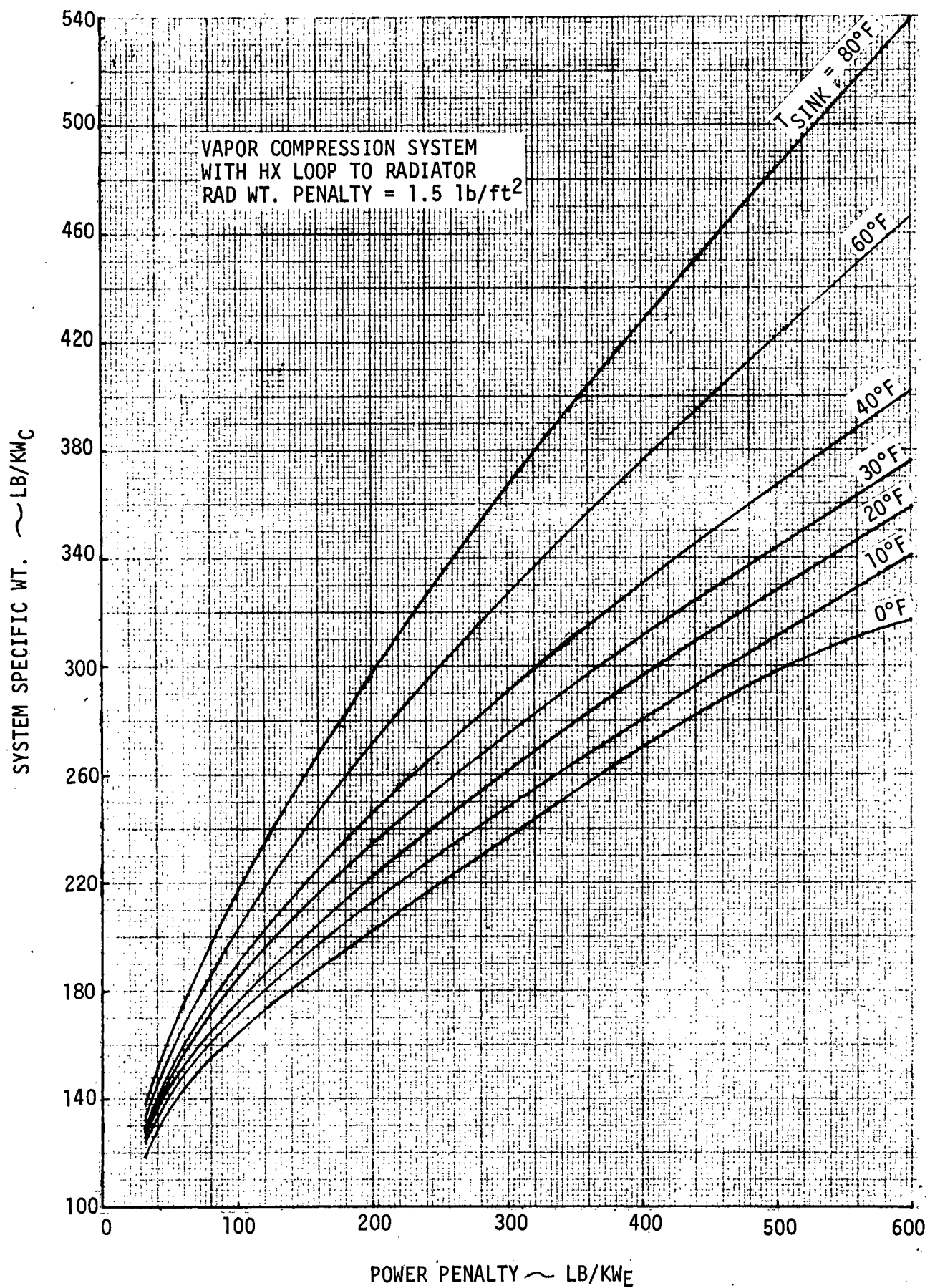


FIGURE 19 VAPOR COMPRESSION ORBITAL HEAT REJECTION SYSTEM WEIGHTS

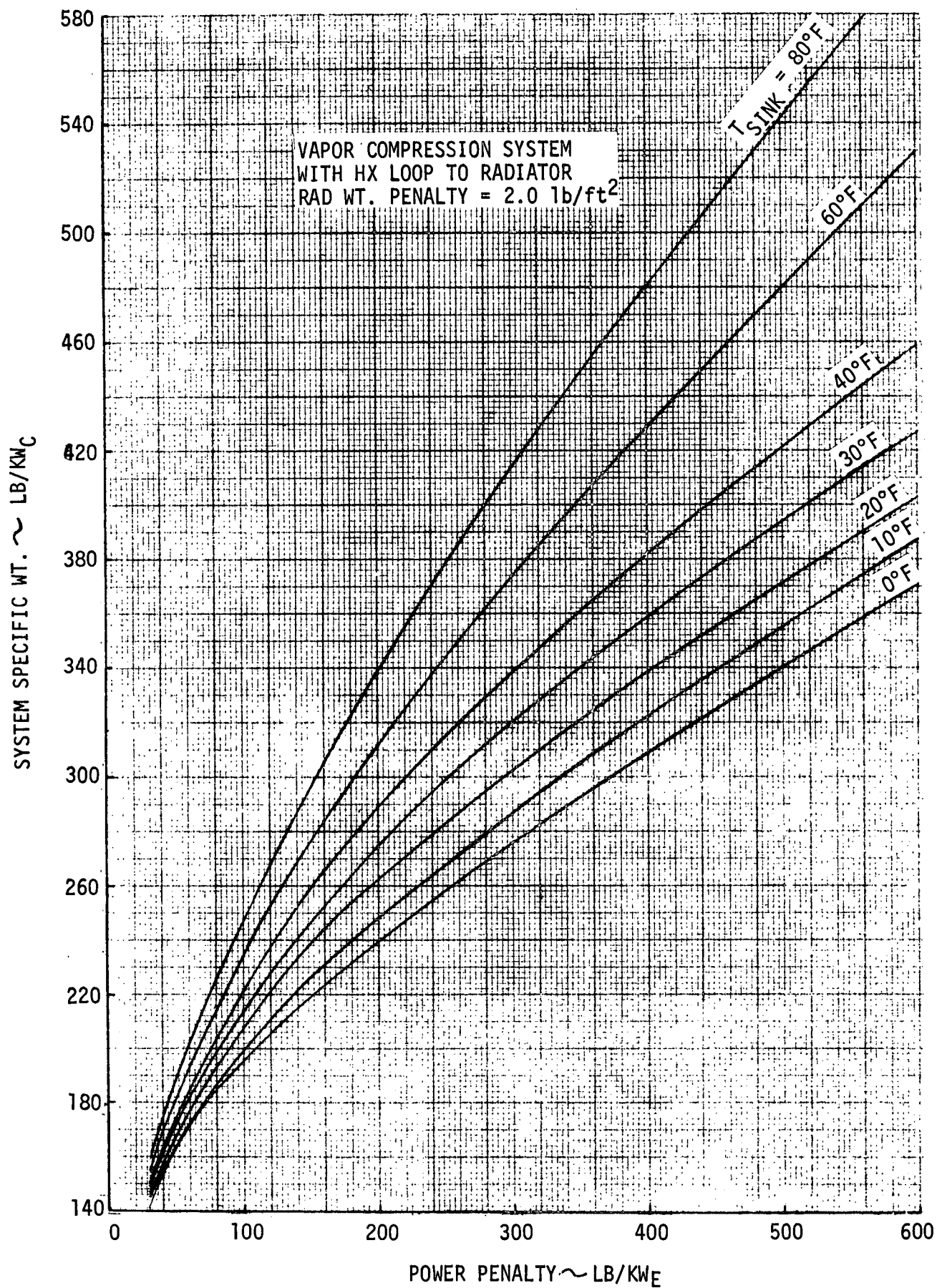


FIGURE 20 VAPOR COMPRESSION ORBITAL HEAT REJECTION SYSTEM WEIGHTS

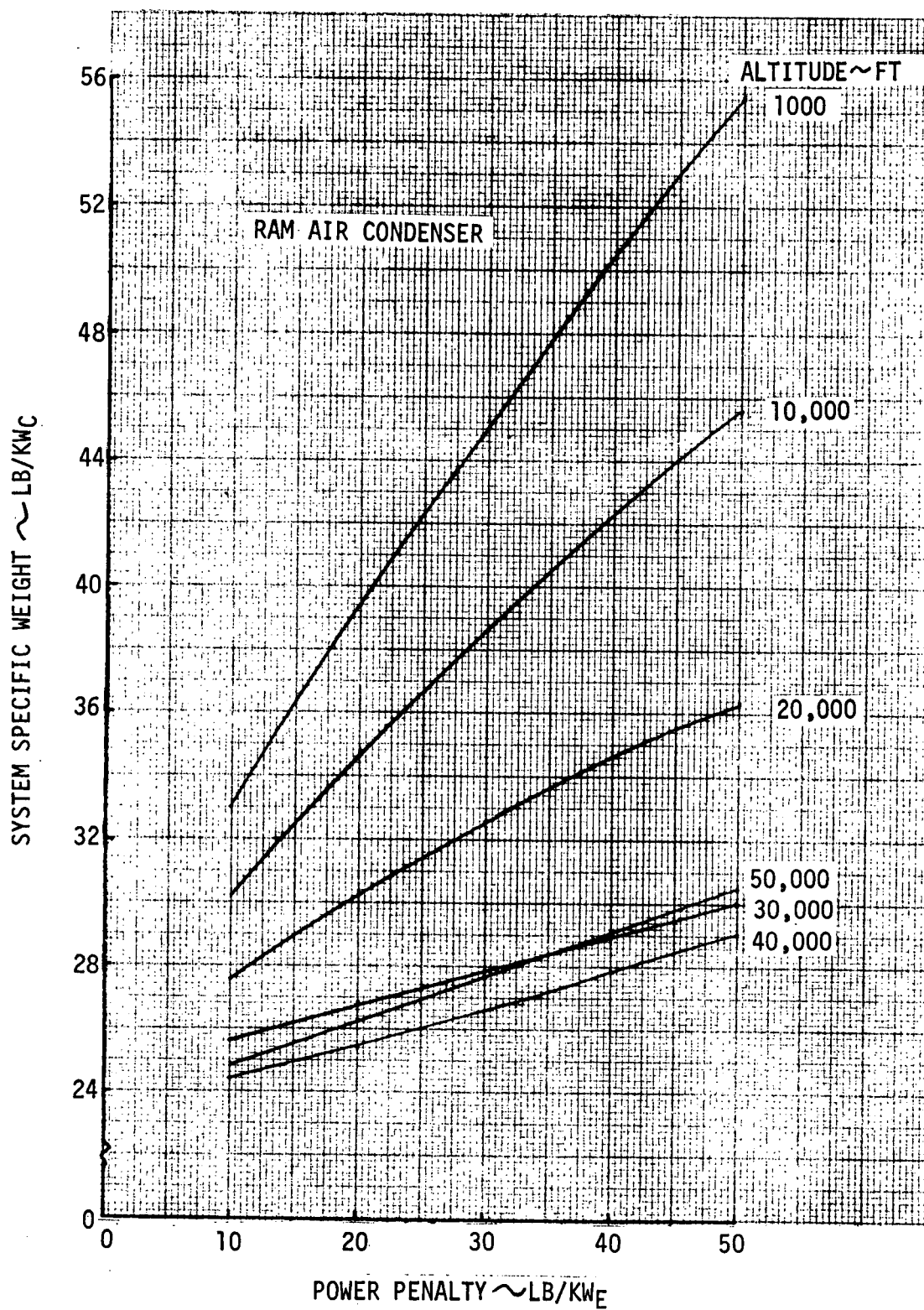


FIGURE 21 VAPOR COMPRESSION ATMOSPHERIC FLIGHT HEAT REJECTION SYSTEM WEIGHTS

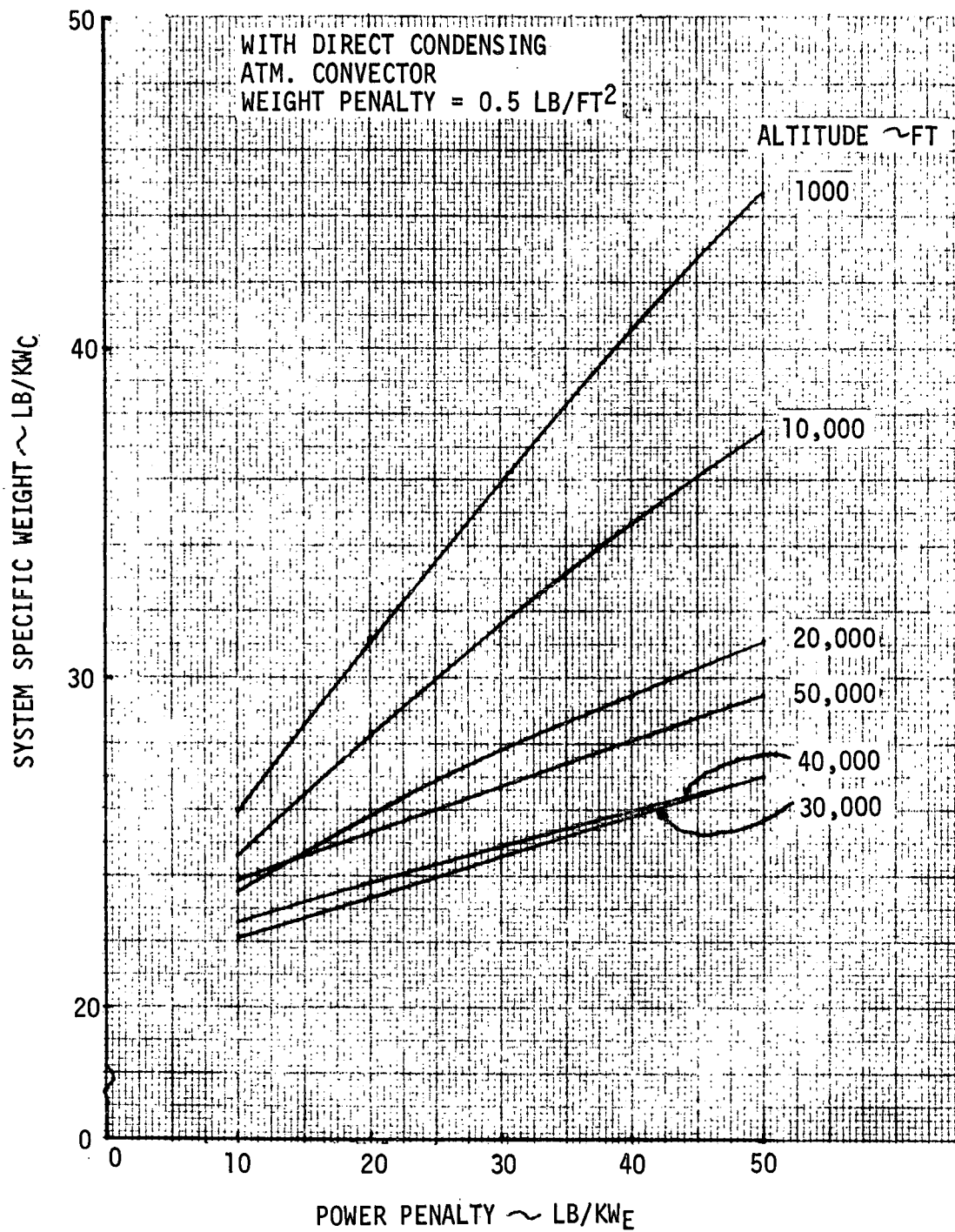


FIGURE 22 VAPOR COMPRESSION ATMOSPHERIC FLIGHT HEAT REJECTION SYSTEM WEIGHTS

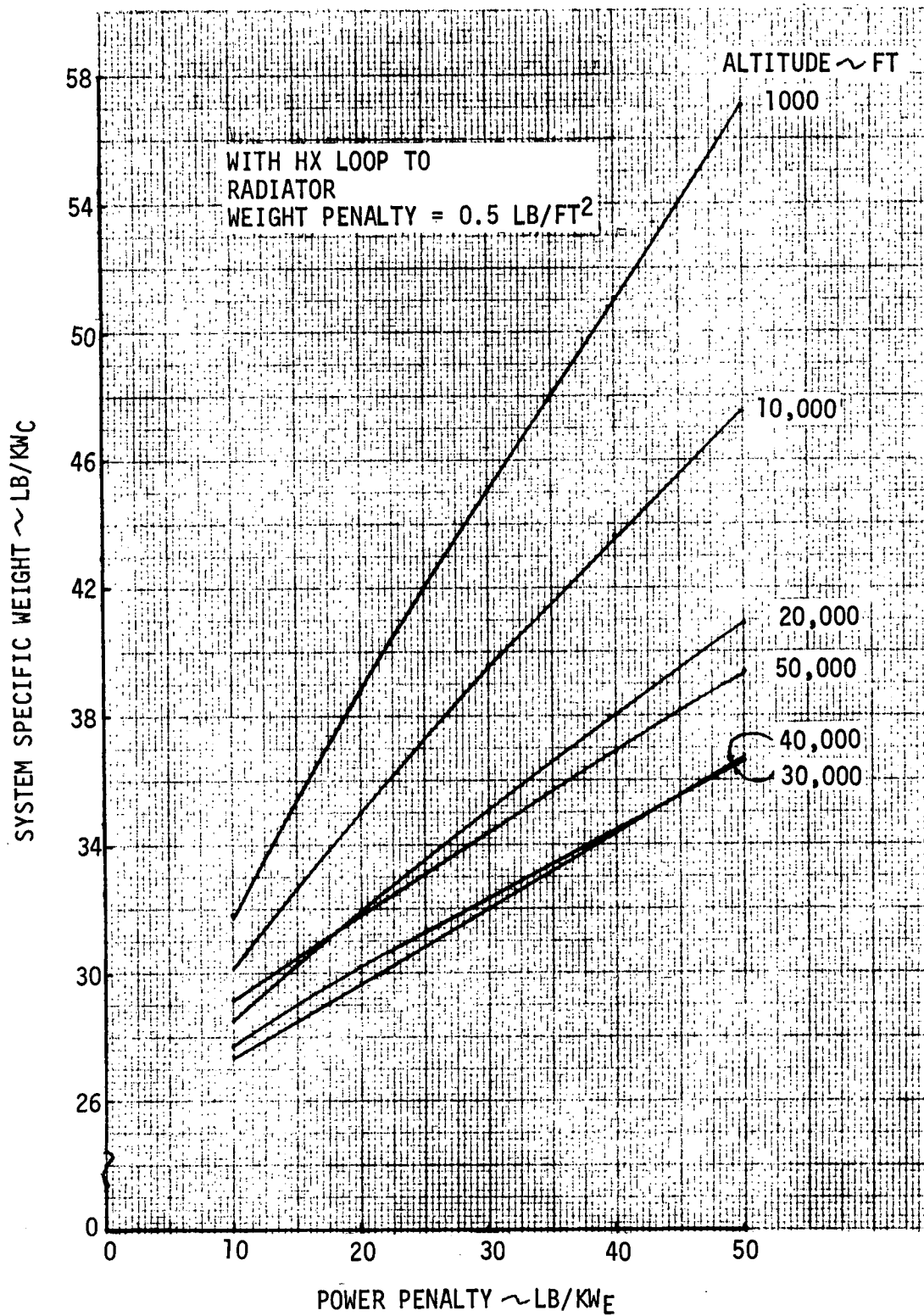


FIGURE 23 VAPOR COMPRESSION ATMOSPHERIC FLIGHT HEAT REJECTION SYSTEM WEIGHTS

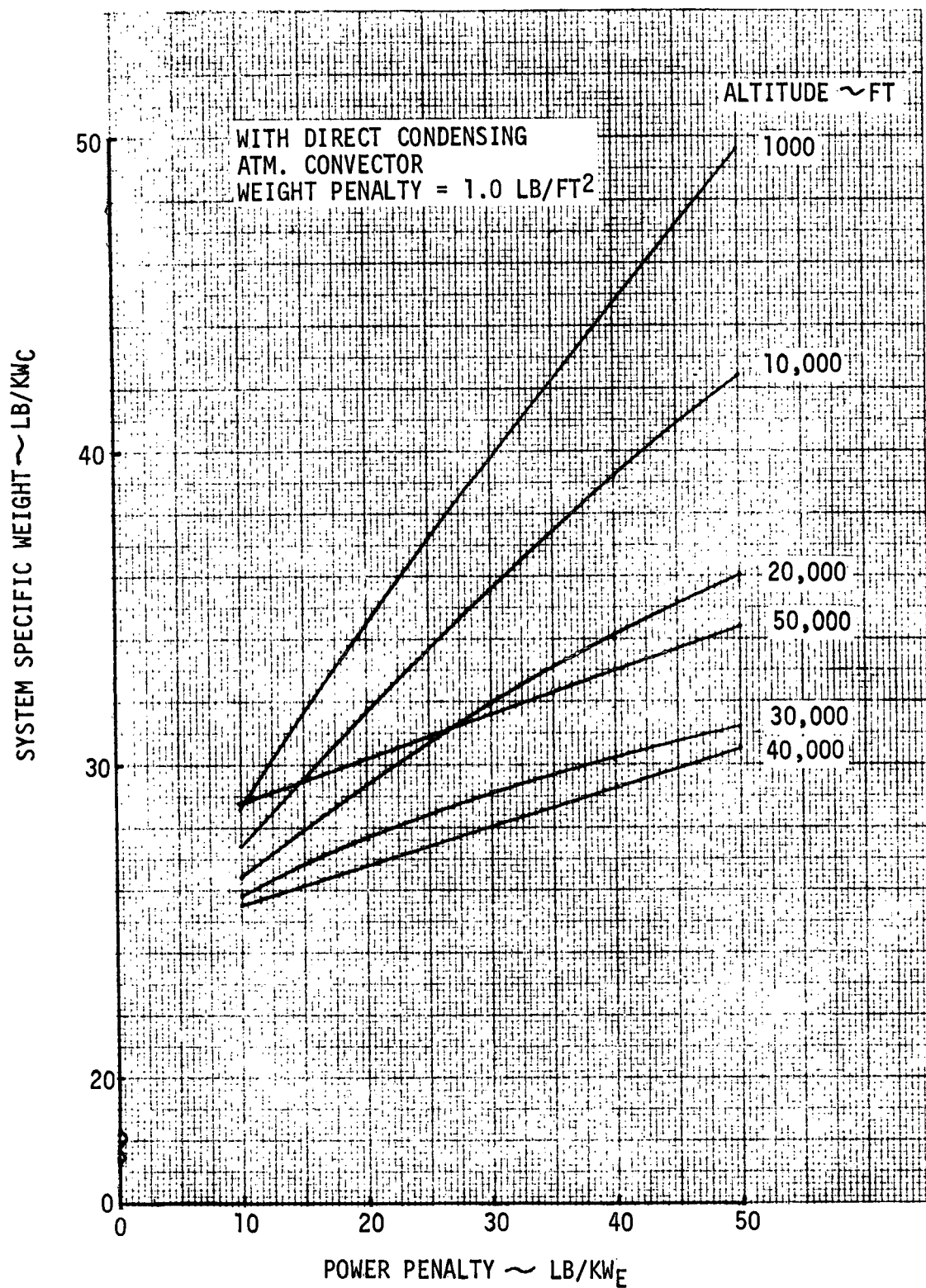


FIGURE 24 VAPOR COMPRESSION ATMOSPHERIC FLIGHT HEAT REJECTION SYSTEM WEIGHTS

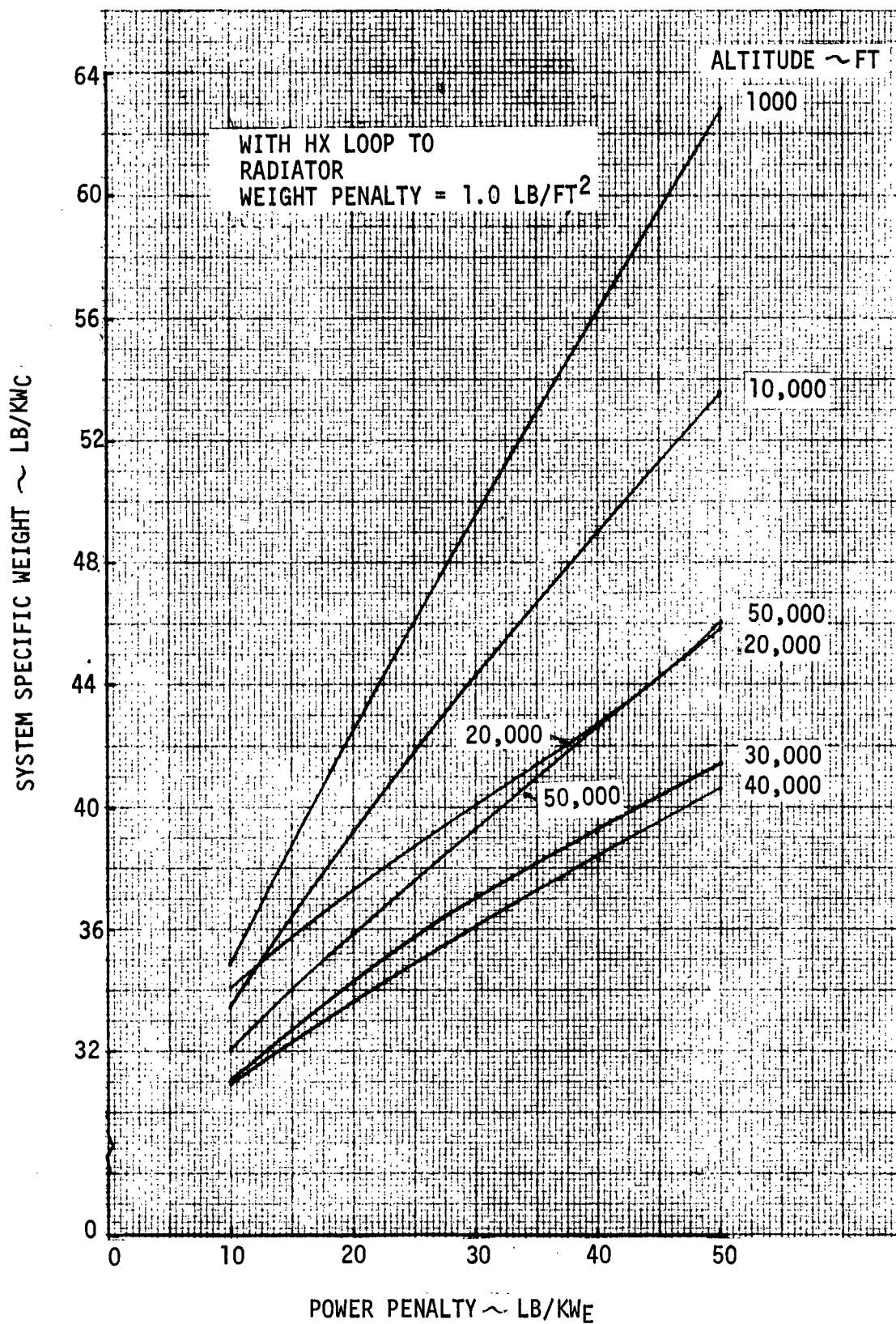


FIGURE 25 VAPOR COMPRESSION ATMOSPHERIC HEAT REJECTION SYSTEM WEIGHTS

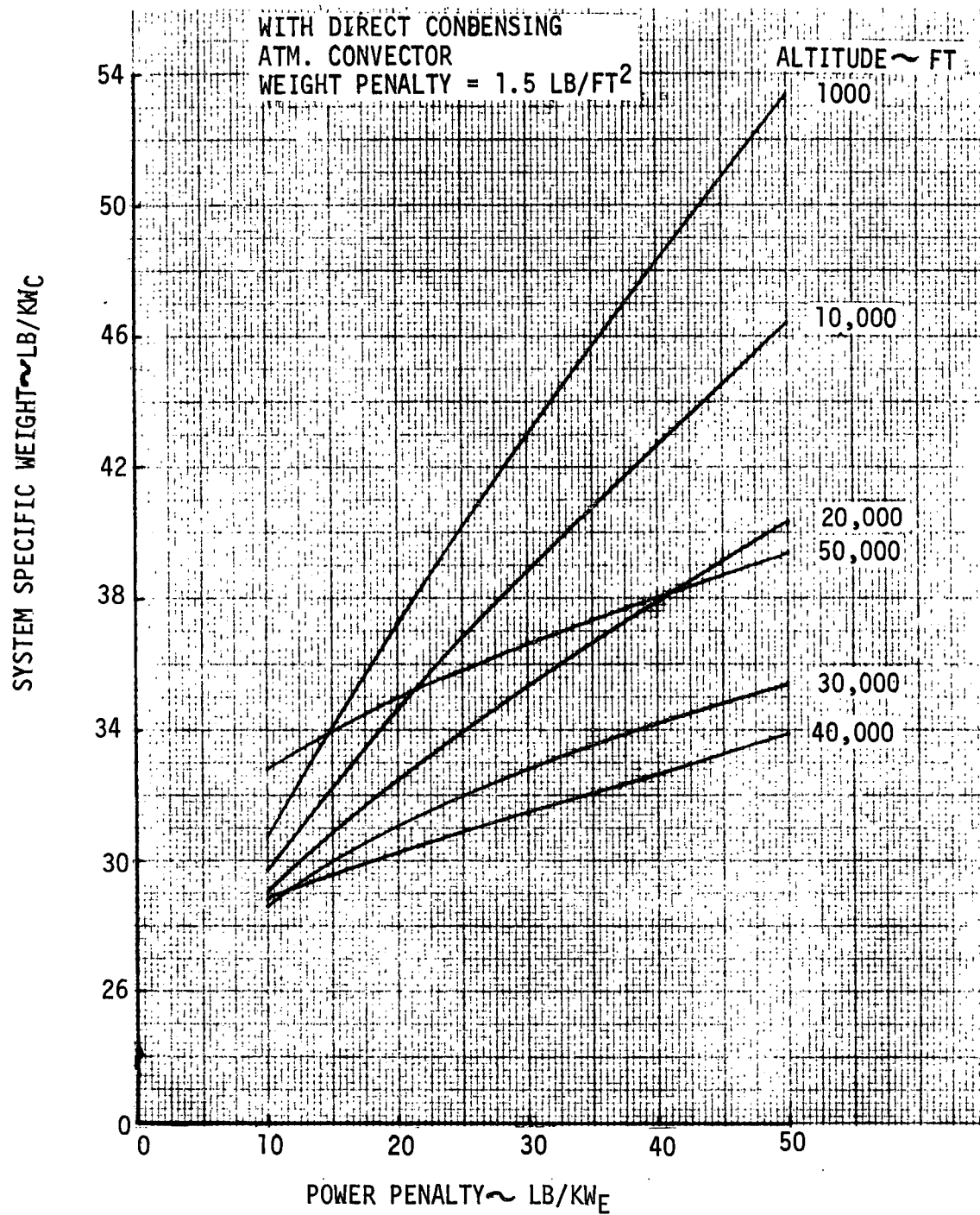


FIGURE 26 VAPOR COMPRESSION ATMOSPHERIC FLIGHT HEAT REJECTION SYSTEM WEIGHTS

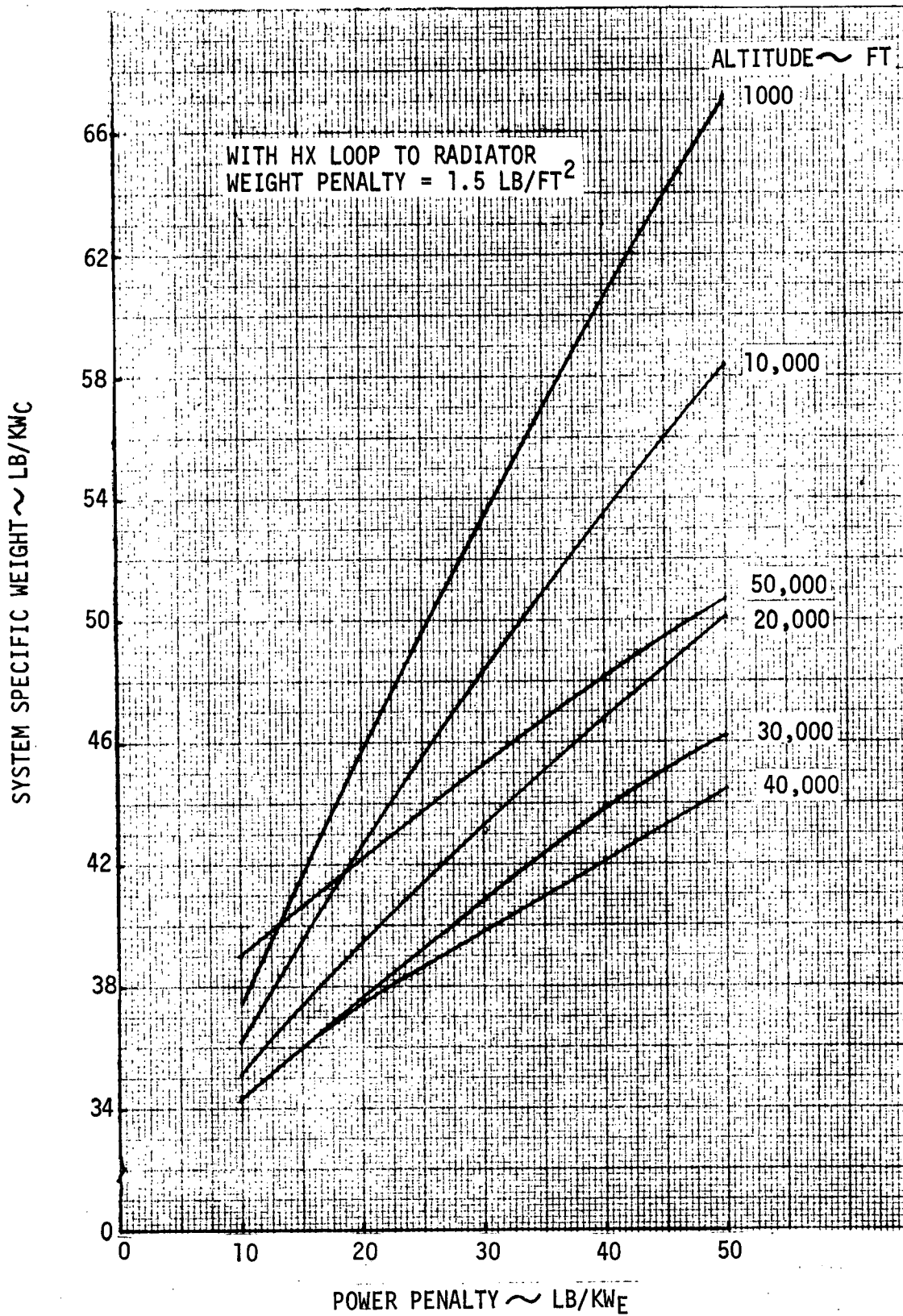


FIGURE 27 VAPOR COMPRESSION ATMOSPHERIC FLIGHT HEAT REJECTION SYSTEM WEIGHTS

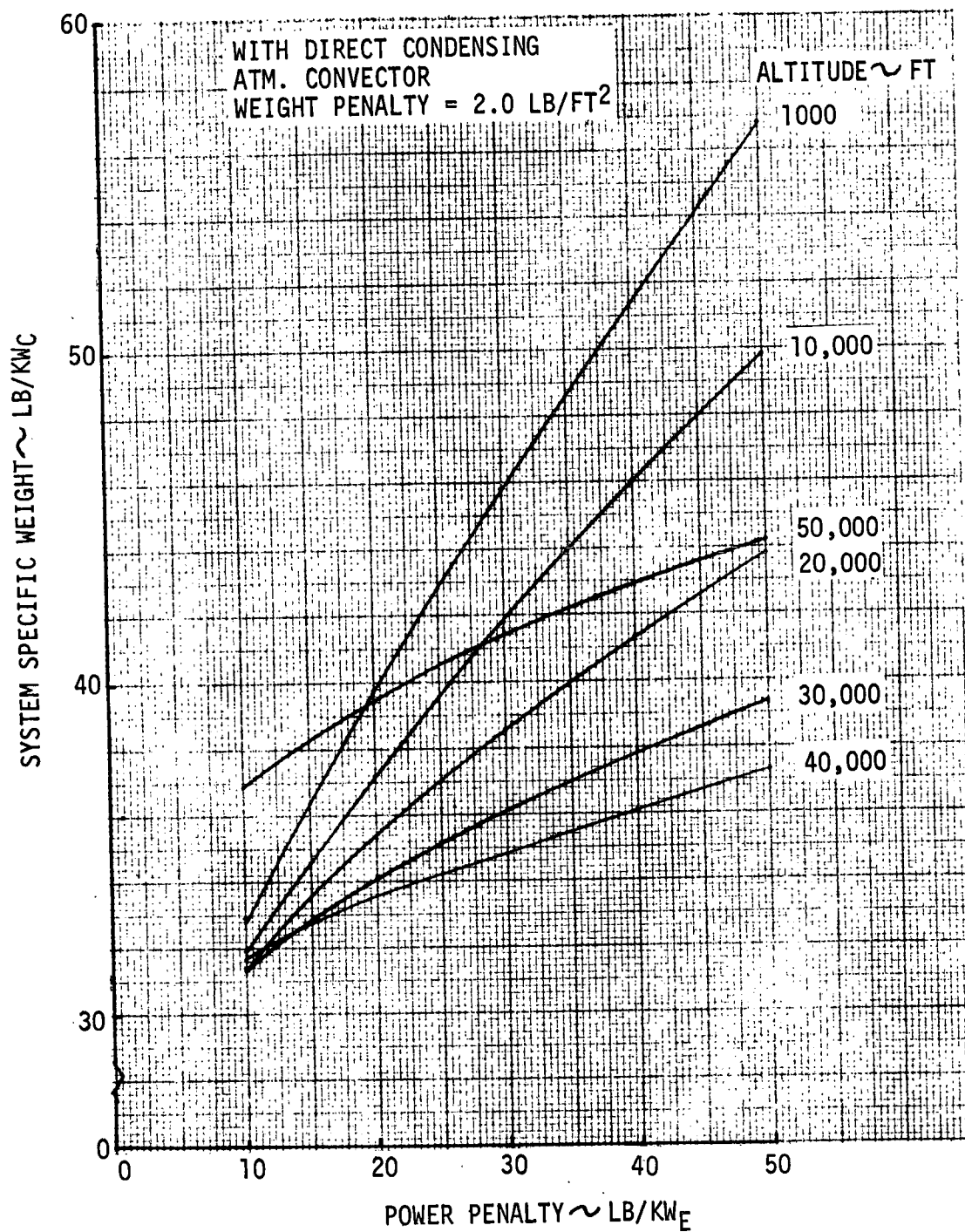


FIGURE 28 VAPOR COMPRESSION ATMOSPHERIC FLIGHT HEAT REJECTION SYSTEM WEIGHTS

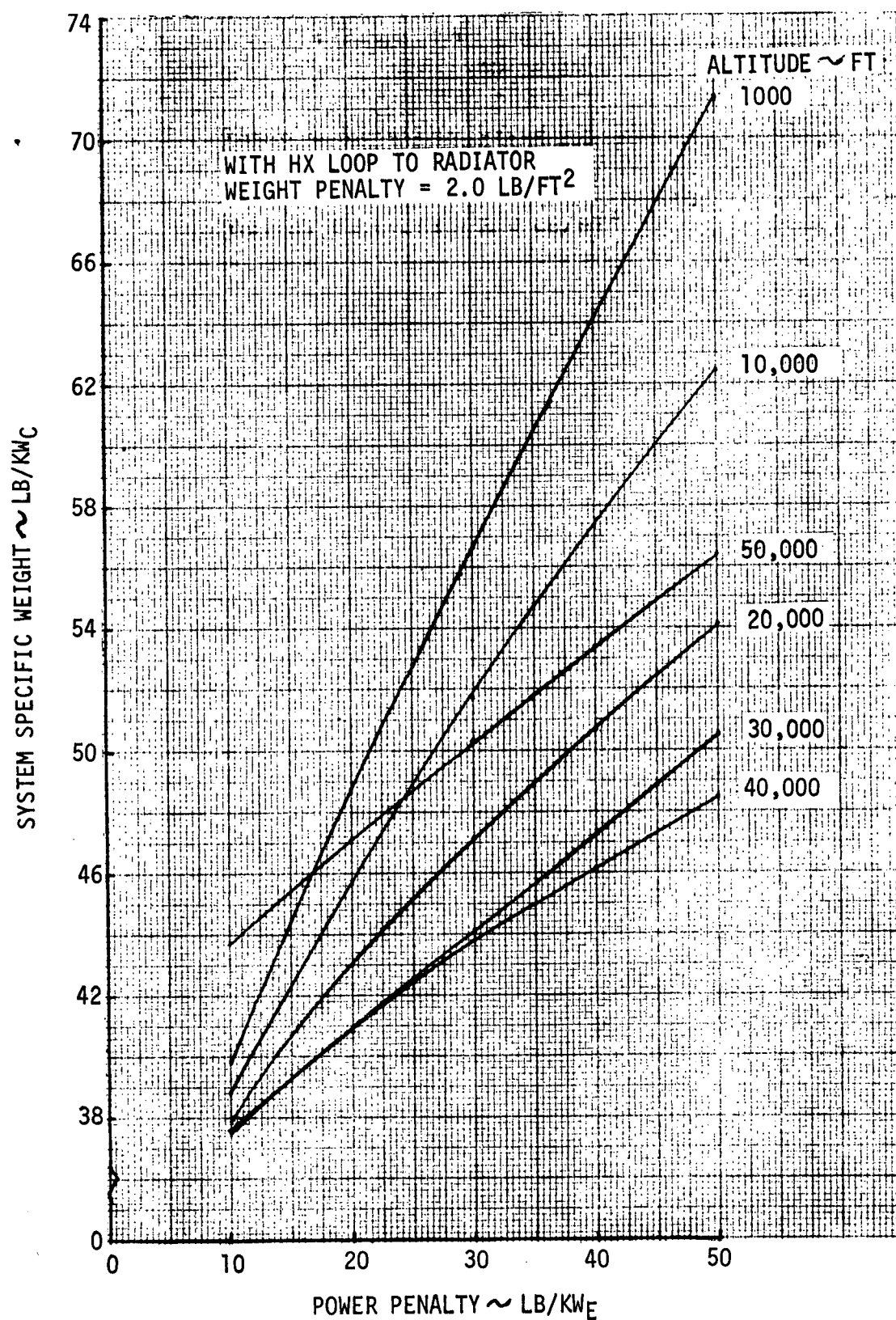


FIGURE 29 VAPOR COMPRESSION ATMOSPHERIC FLIGHT HEAT REJECTION SYSTEM WEIGHTS

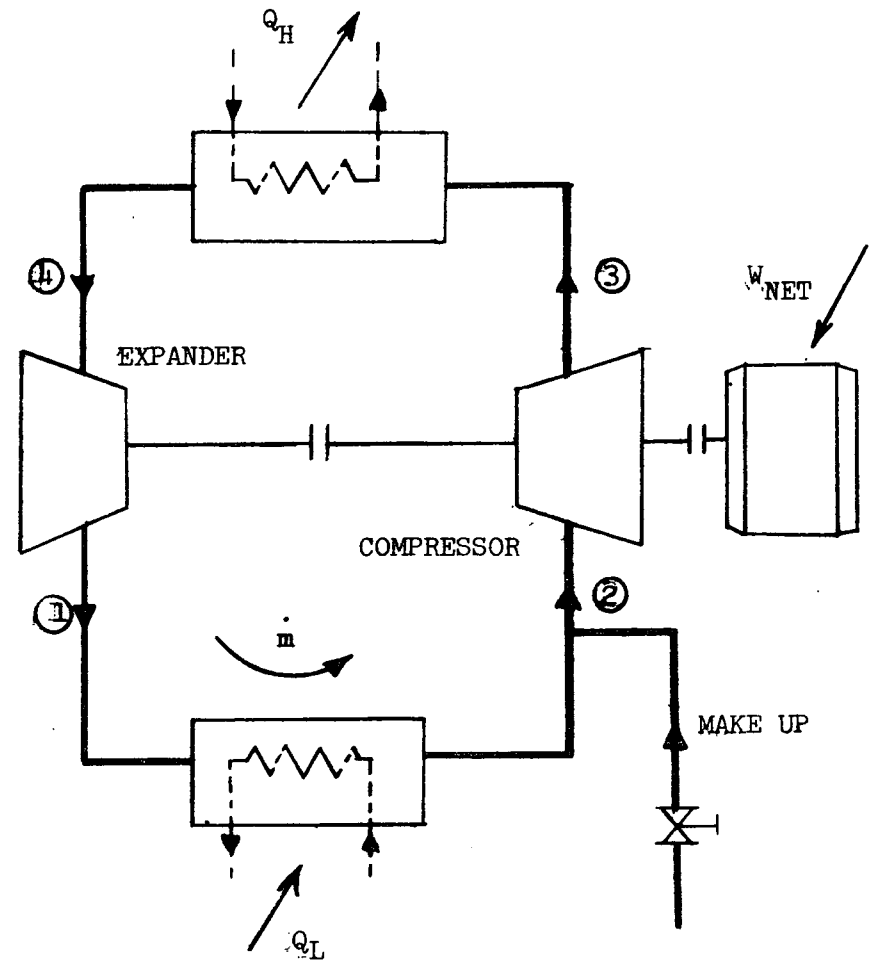
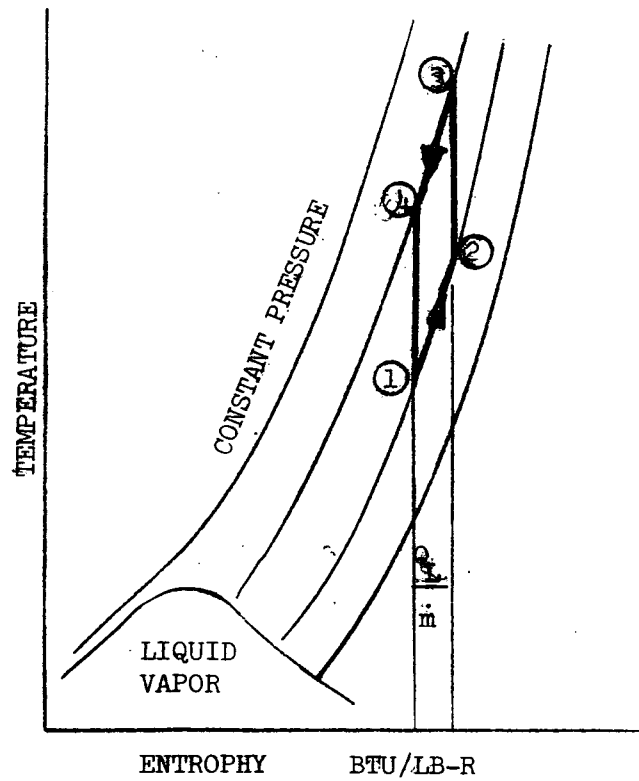


FIGURE 30

AN IDEAL CLOSED GAS CYCLE FOR REFRIGERATION

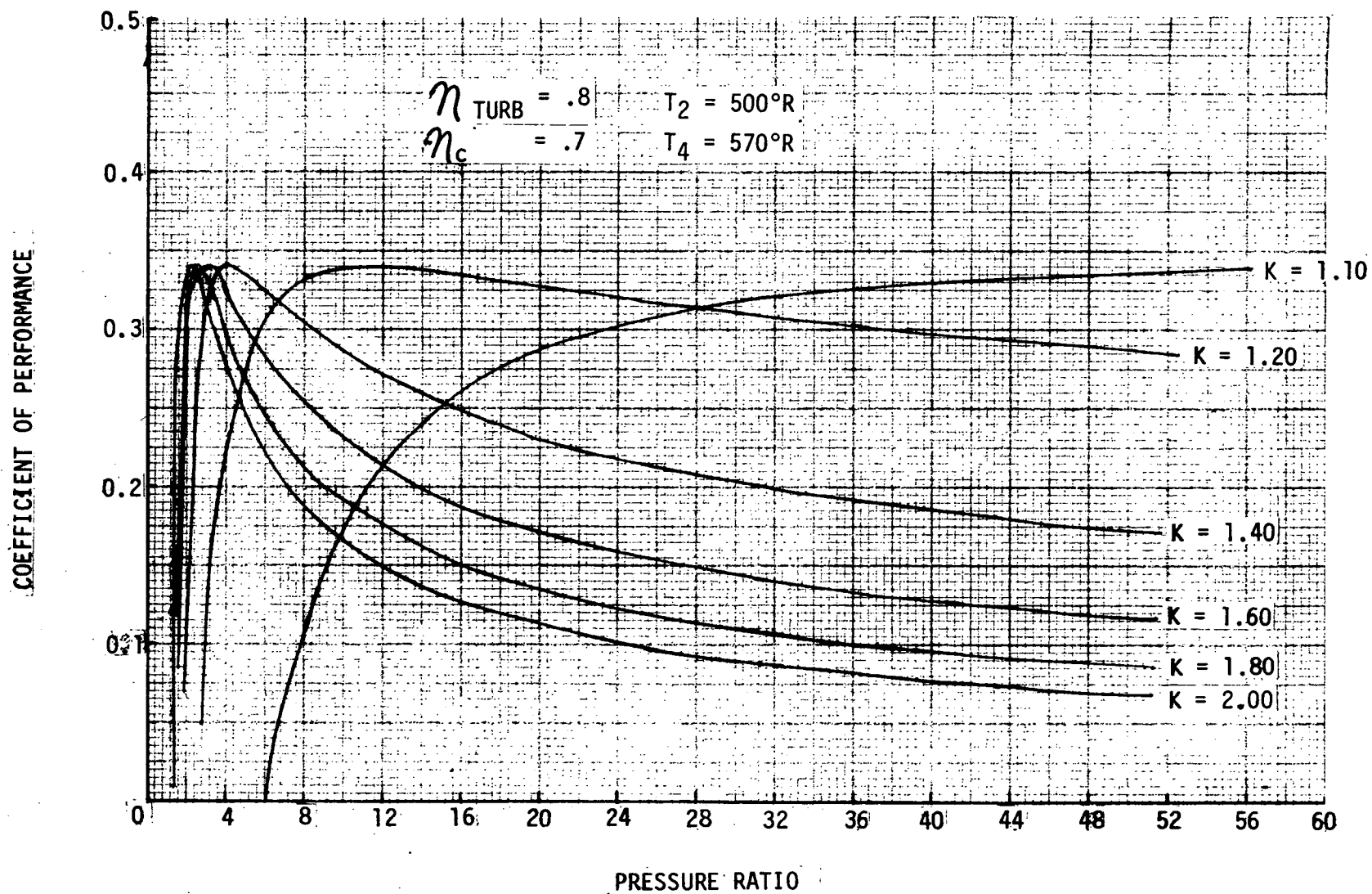


FIGURE 31 EFFECT OF RATIO OF SPECIFIC HEATS ON GAS CYCLE PERFORMANCE

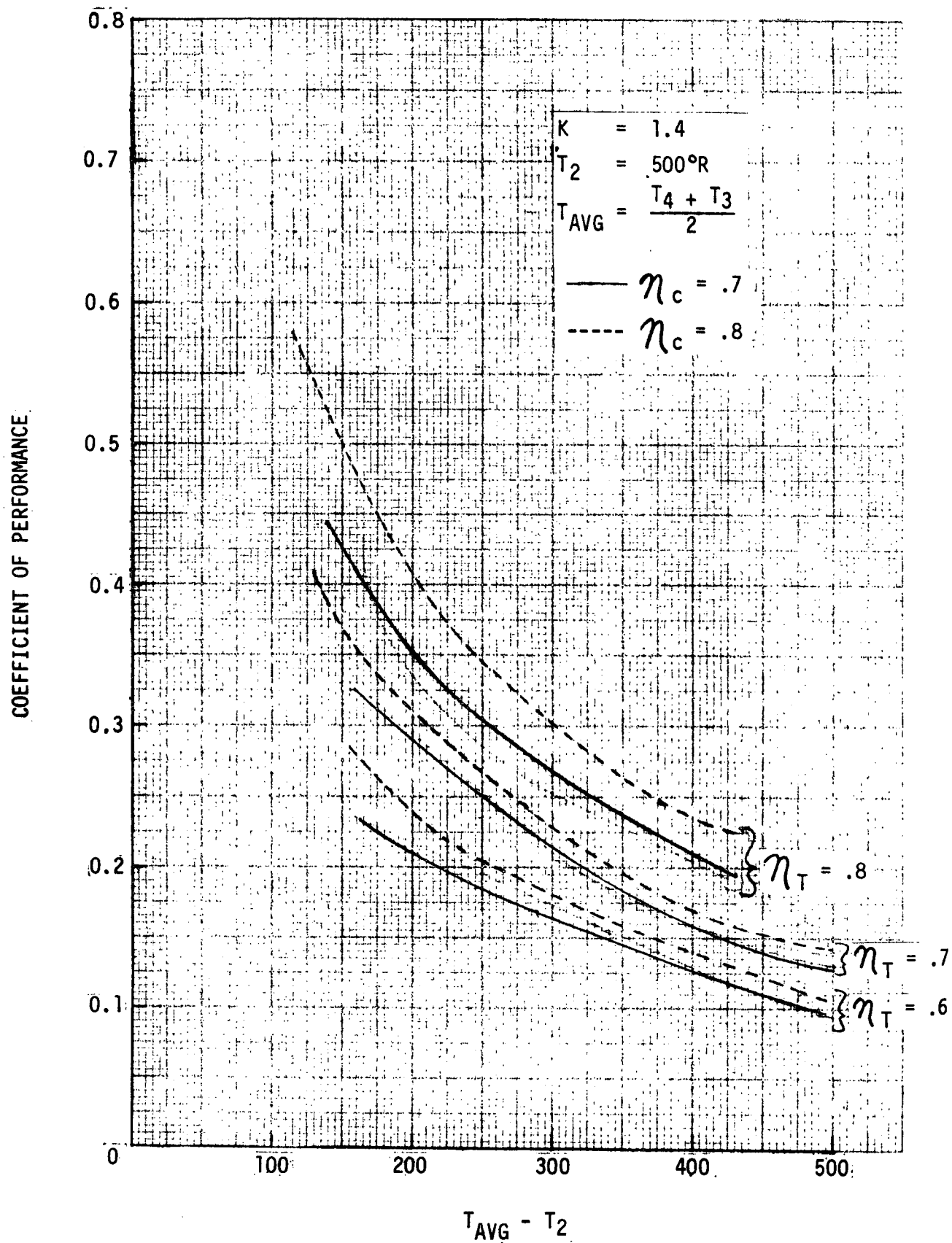
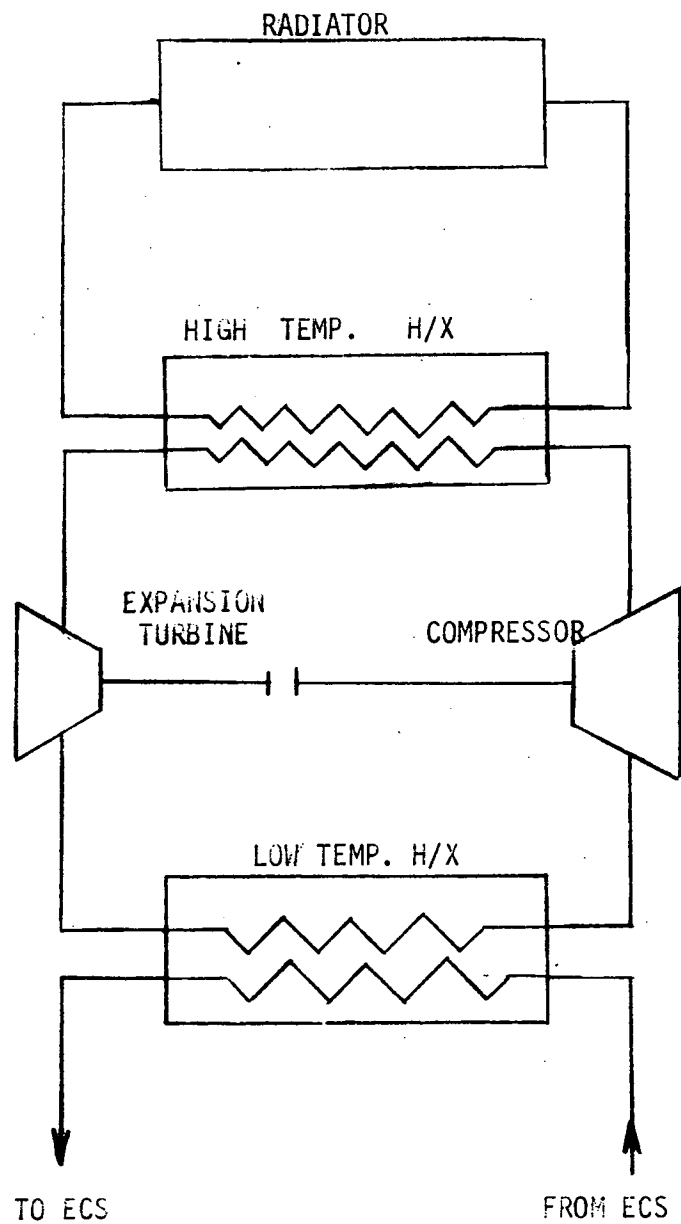
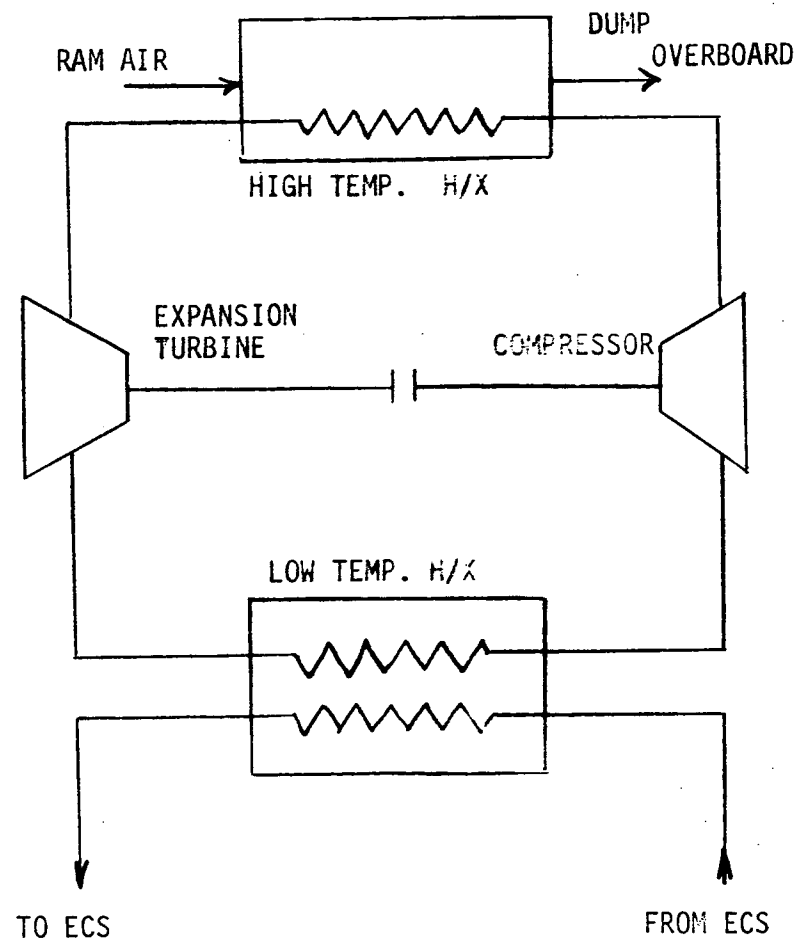


FIGURE 32 GAS CYCLE SYSTEM PERFORMANCE



(a)



(b)

FIGURE 33

ORBITER GAS CYCLE SCHEMATICS

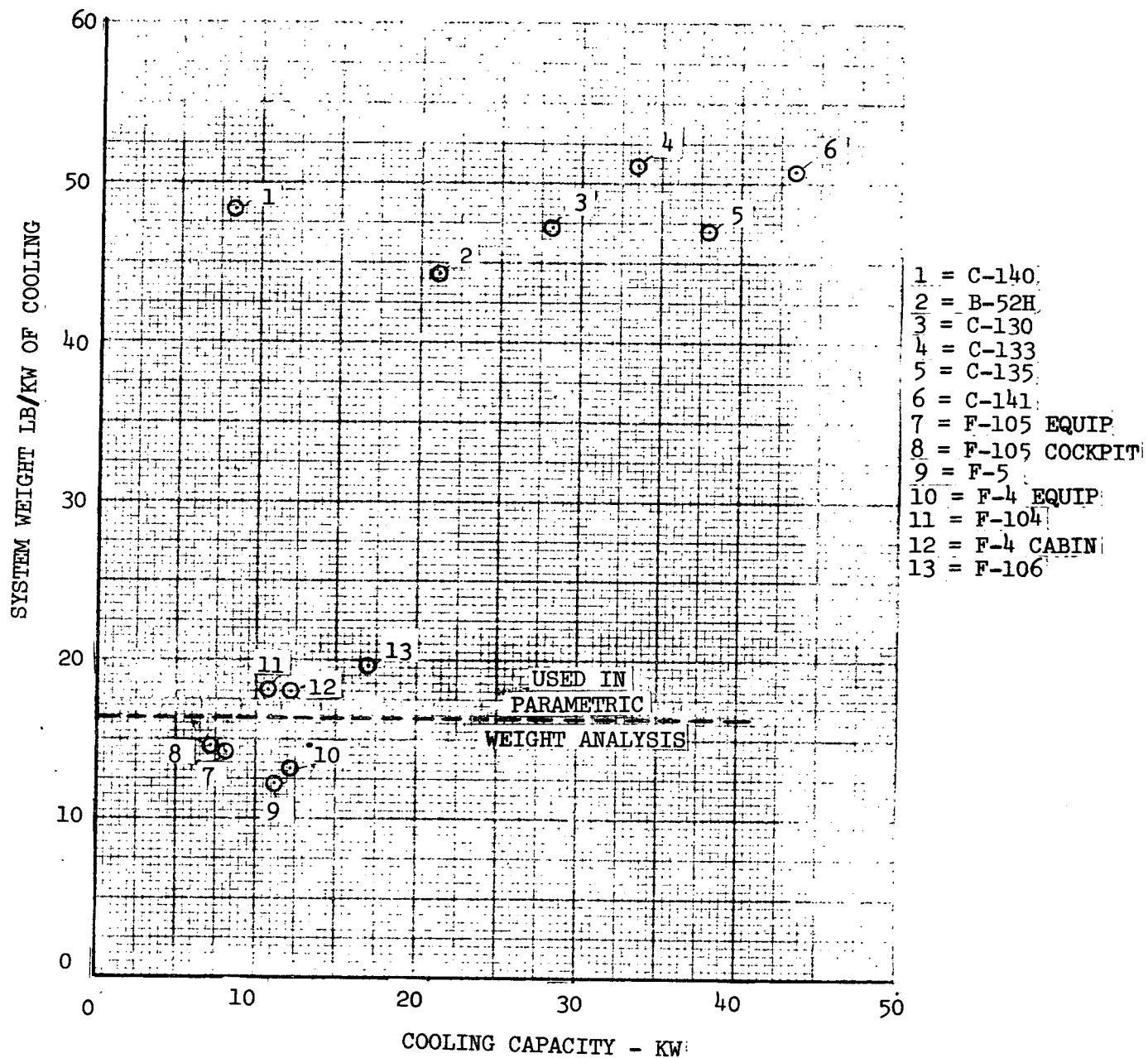


FIGURE 34 OPERATIONAL AIRCRAFT AIRCYCLE SYSTEM WEIGHTS

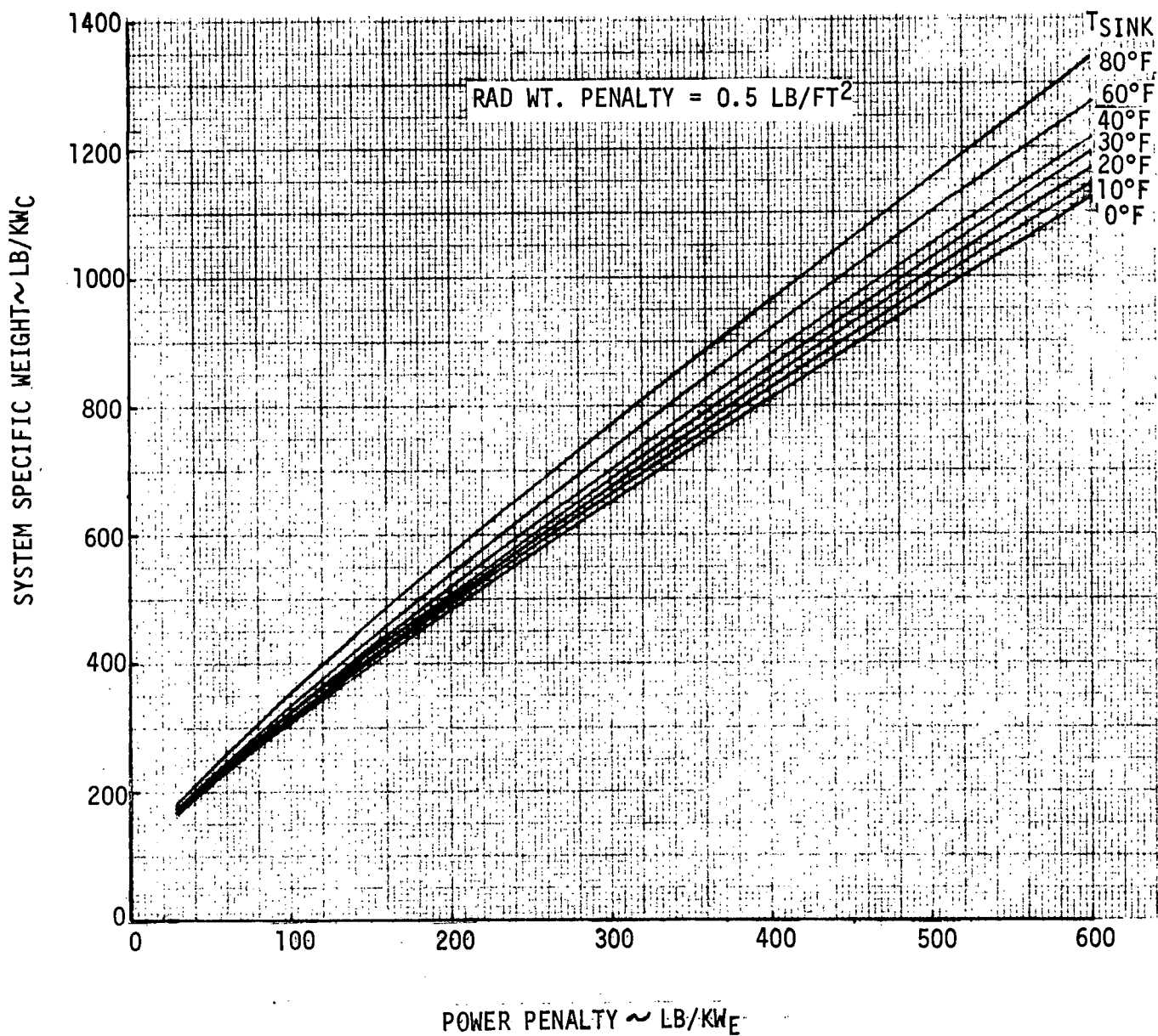


FIGURE 35 GAS CYCLE ORBITAL HEAT REJECTION SYSTEM WEIGHT

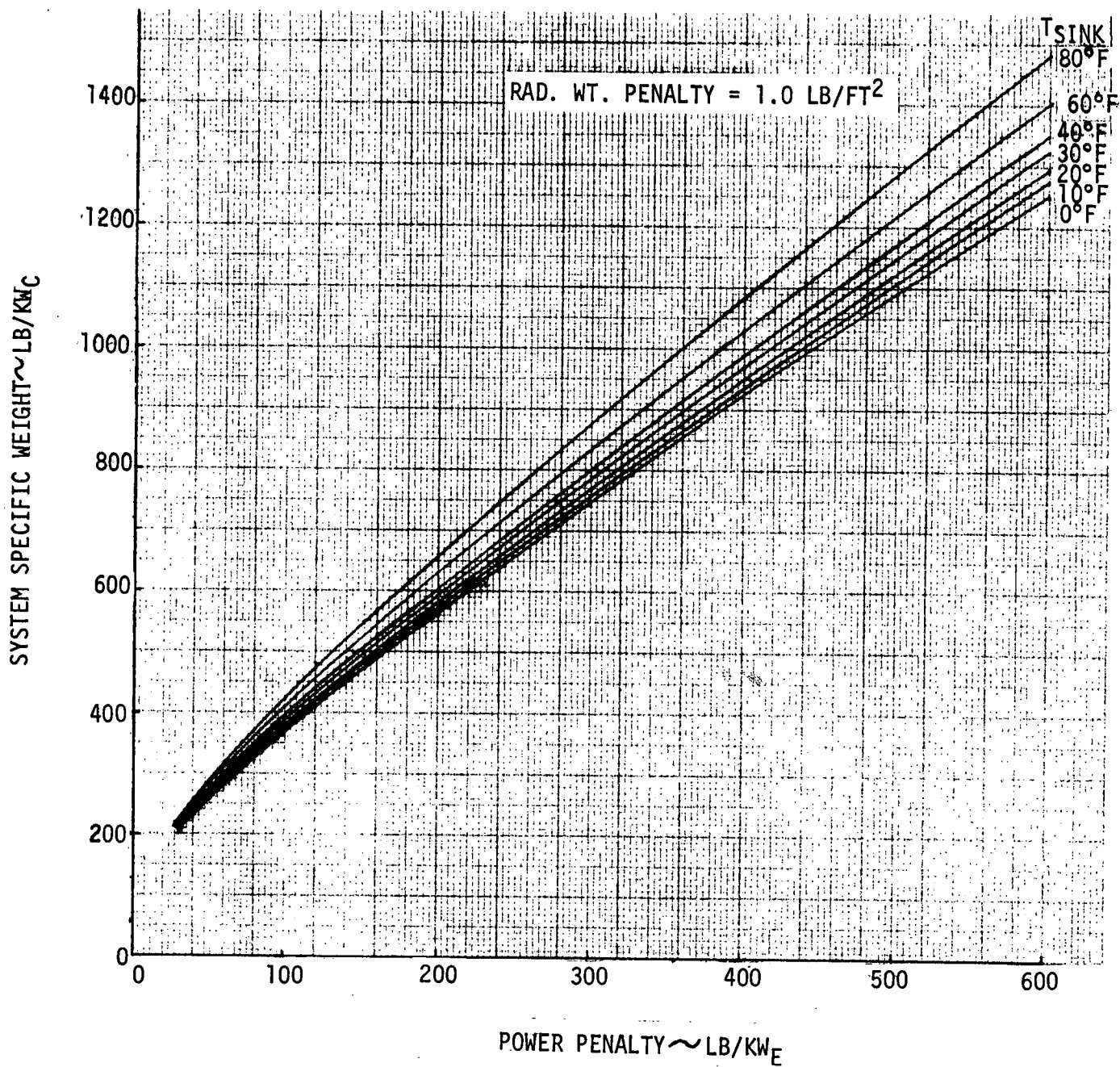


FIGURE 36 GAS CYCLE ORBITAL HEAT REJECTION SYSTEM WEIGHTS

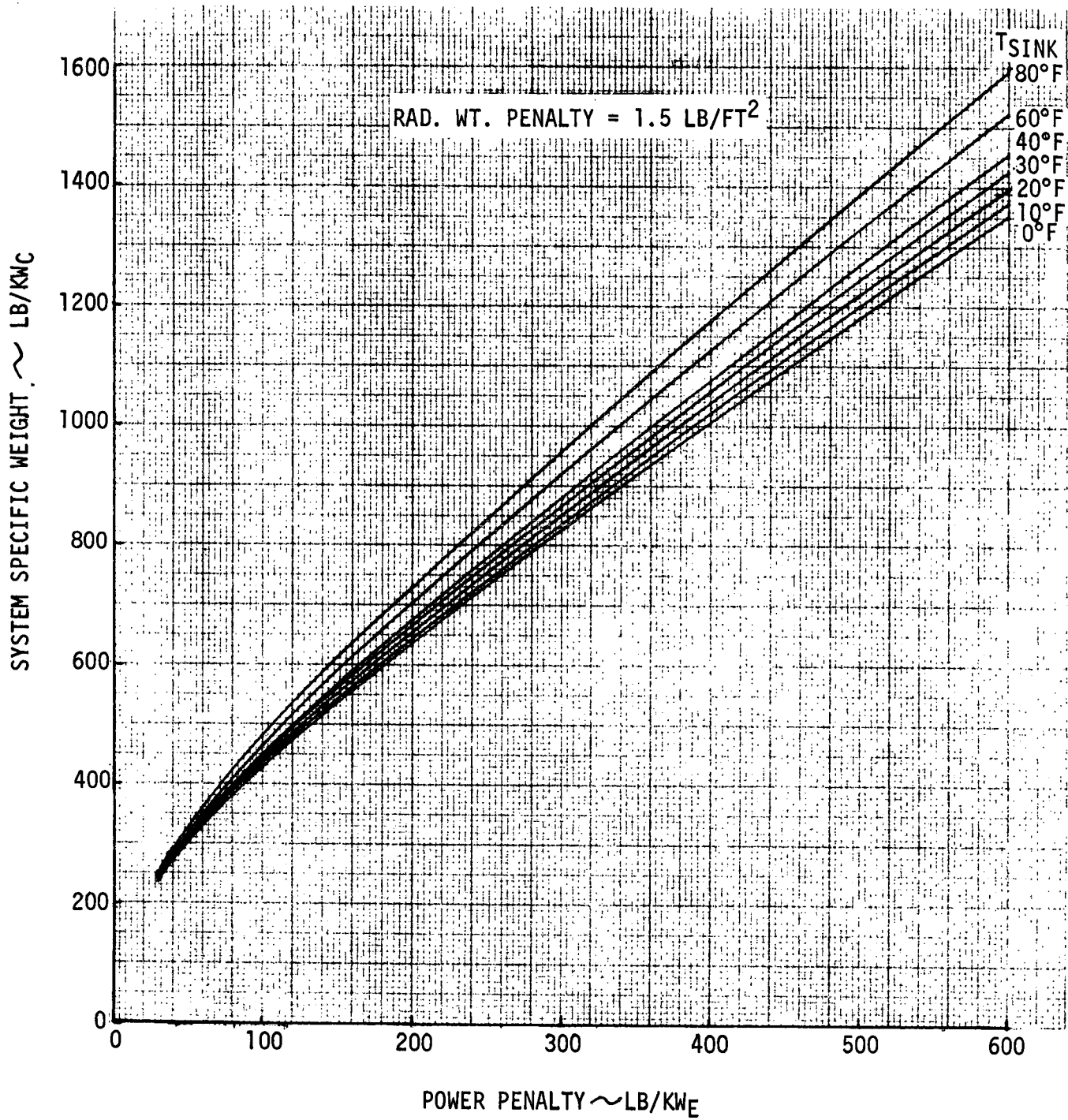


FIGURE 37 GAS CYCLE ORBITAL HEAT REJECTION SYSTEM WEIGHTS

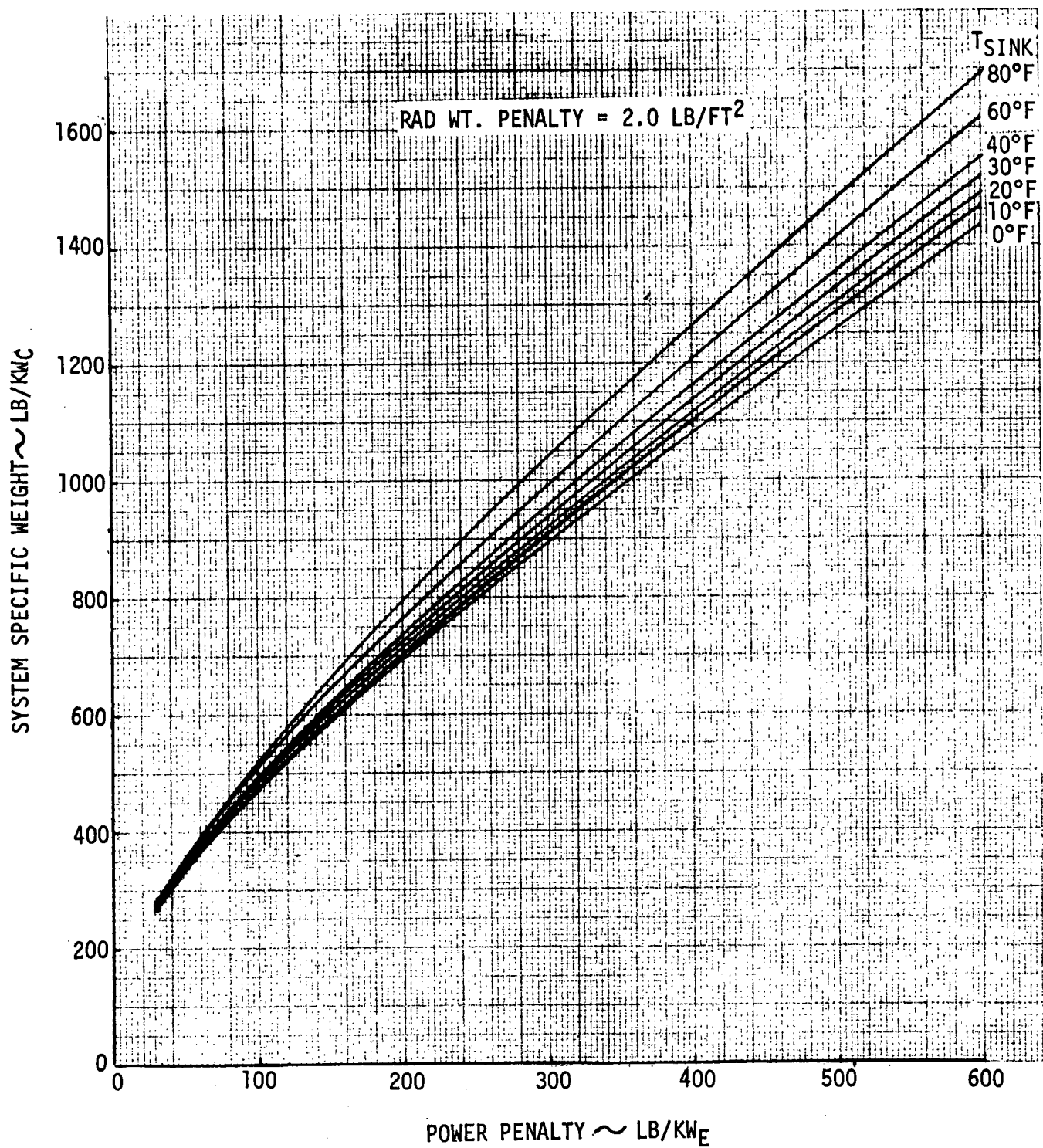


FIGURE 38 GAS CYCLE ORBITAL HEAT REJECTION SYSTEM WEIGHTS

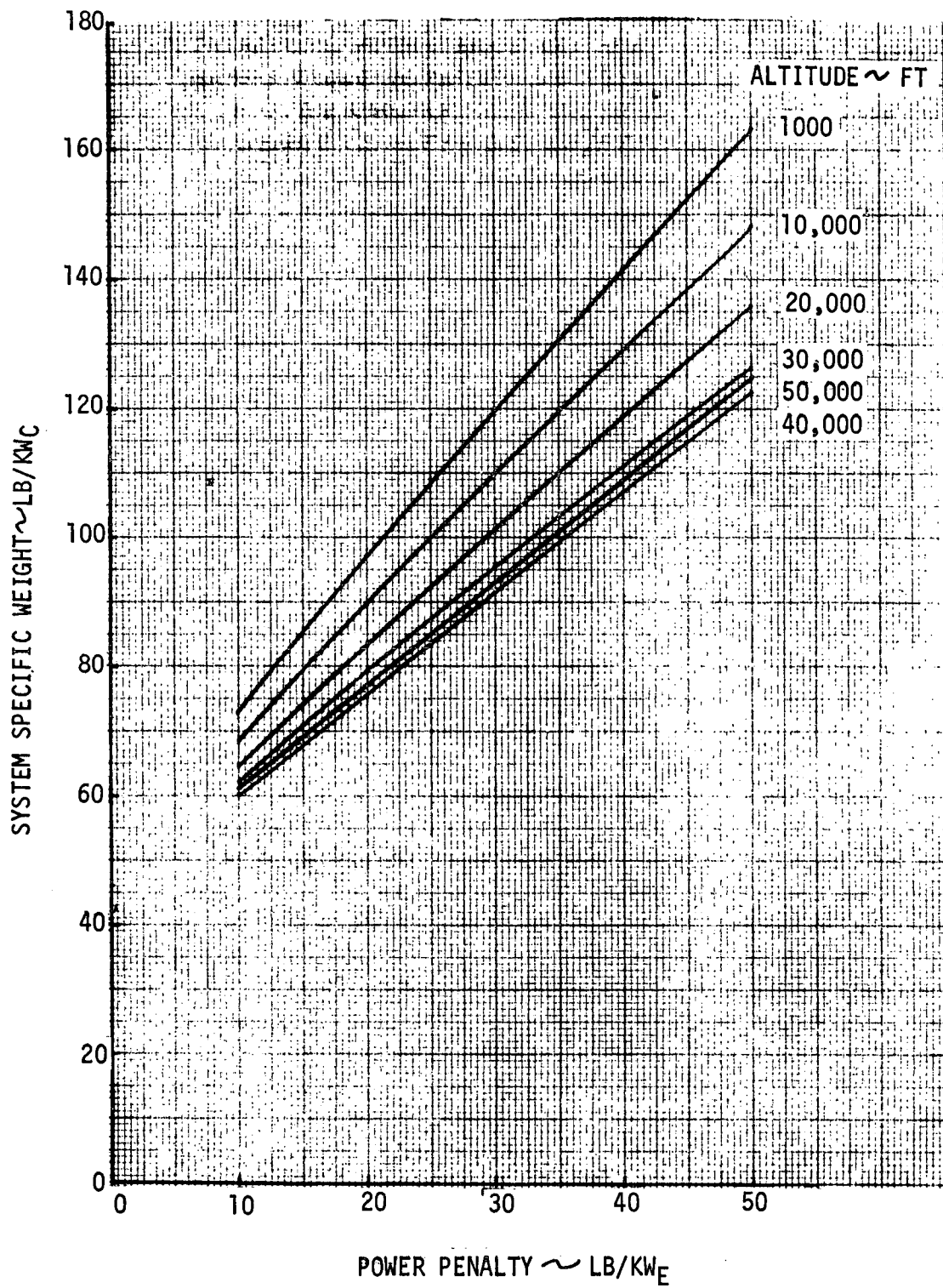
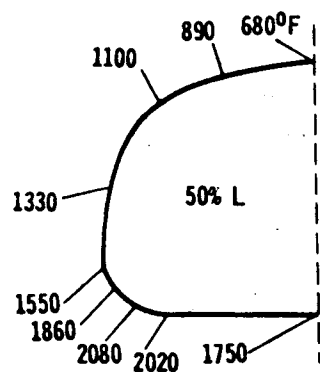
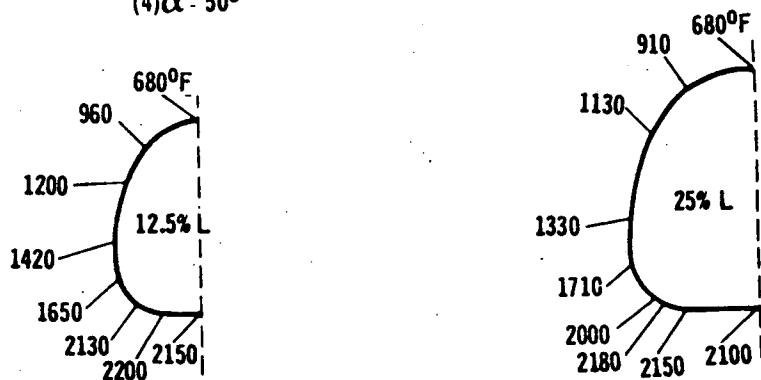


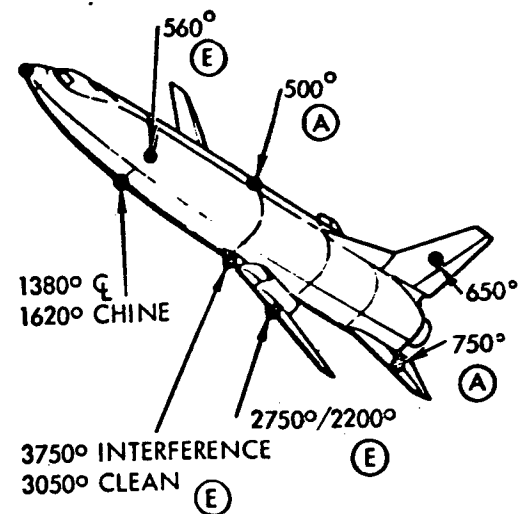
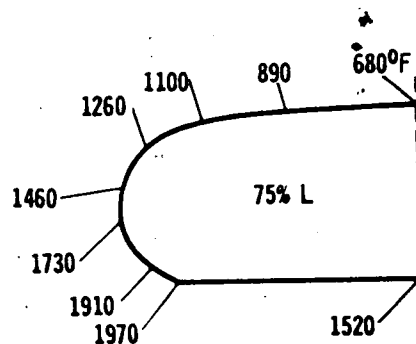
FIGURE 39 GAS CYCLE ATMOSPHERIC FLIGHT HEAT REJECTION SYSTEM WEIGHTS

C

NOTE:
 (1) RADIATION EQUILIBRIUM TEMPERATURES (E .85)
 (2) LAMINAR HEATING
 (3) NO UNCERTAINTY FACTOR
 (4) $\alpha = 50^\circ$



HIGH CROSS RANGE
 (Ref. 14)



LOCATION	CRITICAL FLIGHT CONDITIONS	RADIATION EQUILIBRIUM TEMPERATURE (°F)	
		BOOSTER	ORBITER
FUSELAGE			
NOSE	ENTRY	1275	1860
LOWER SURFACE 20%	ENTRY	1380	1420
LOWER SURFACE 80%	ENTRY	1220	1450
CHINE	ENTRY	1530	1620
SIDE	ENTRY	540	560
UPPER SURFACE	ASCENT	500	500
WING			
L.E. (NO INTERFERENCE)	ENTRY	2200	3000
LOWER SURFACE 20%	ENTRY	1400	1700
UPPER SURFACE 20%	ASCENT	650	700
HORIZONTAL SURFACE			
L.E.	ENTRY	2020	3450
LOWER SURFACE	ENTRY	1390	1500
UPPER SURFACE	ASCENT	600-650	700
VERTICAL SURFACE			
L.E.	ASCENT	1730	2320
SIDE	ASCENT	600-650	650

LOW CROSS RANGE
 (Ref. 13)

FIGURE 40 SHUTTLE BOOST/REENTRY TEMPERATURES

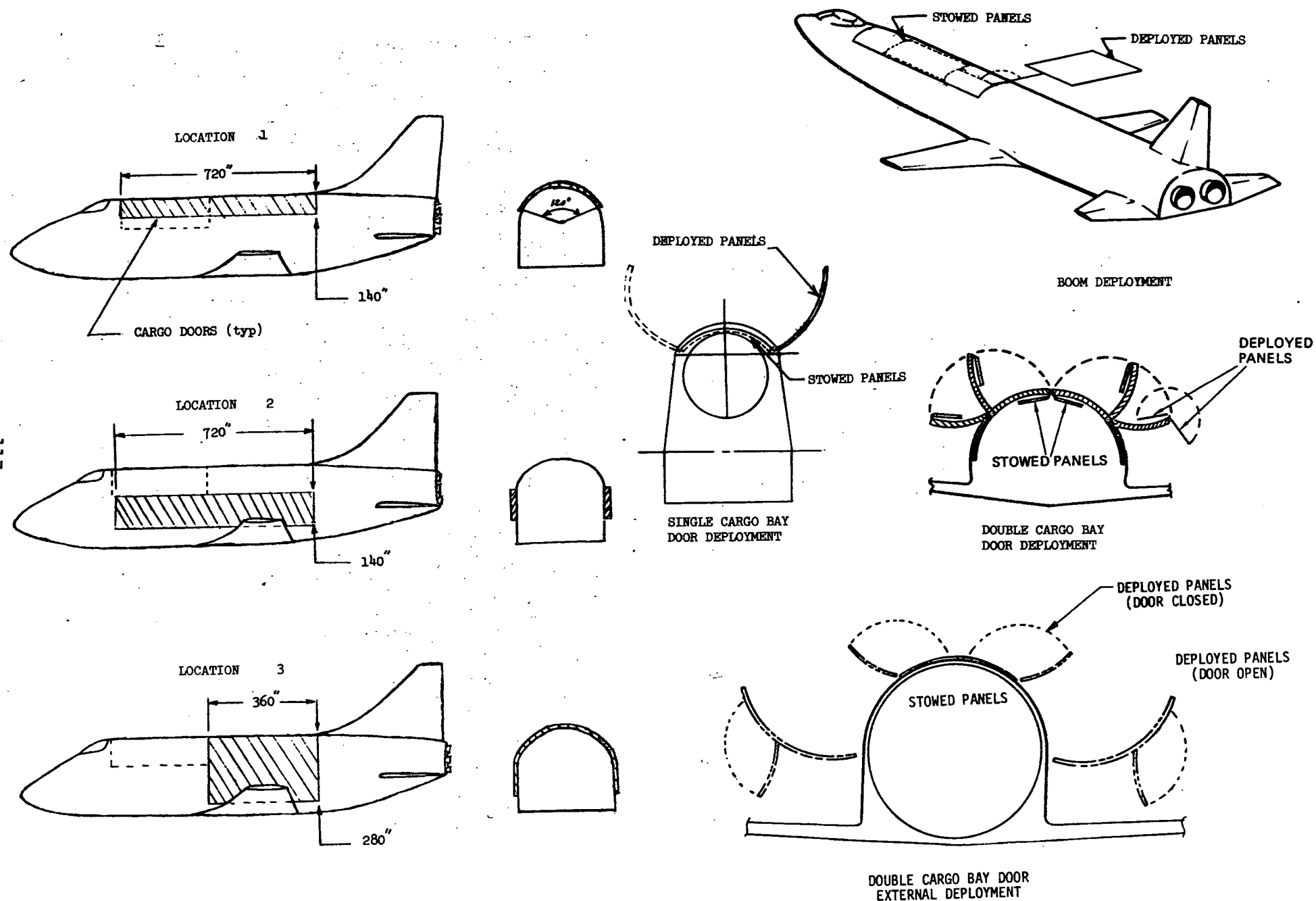


FIGURE 41 ORBITER RADIATOR CONCEPTS

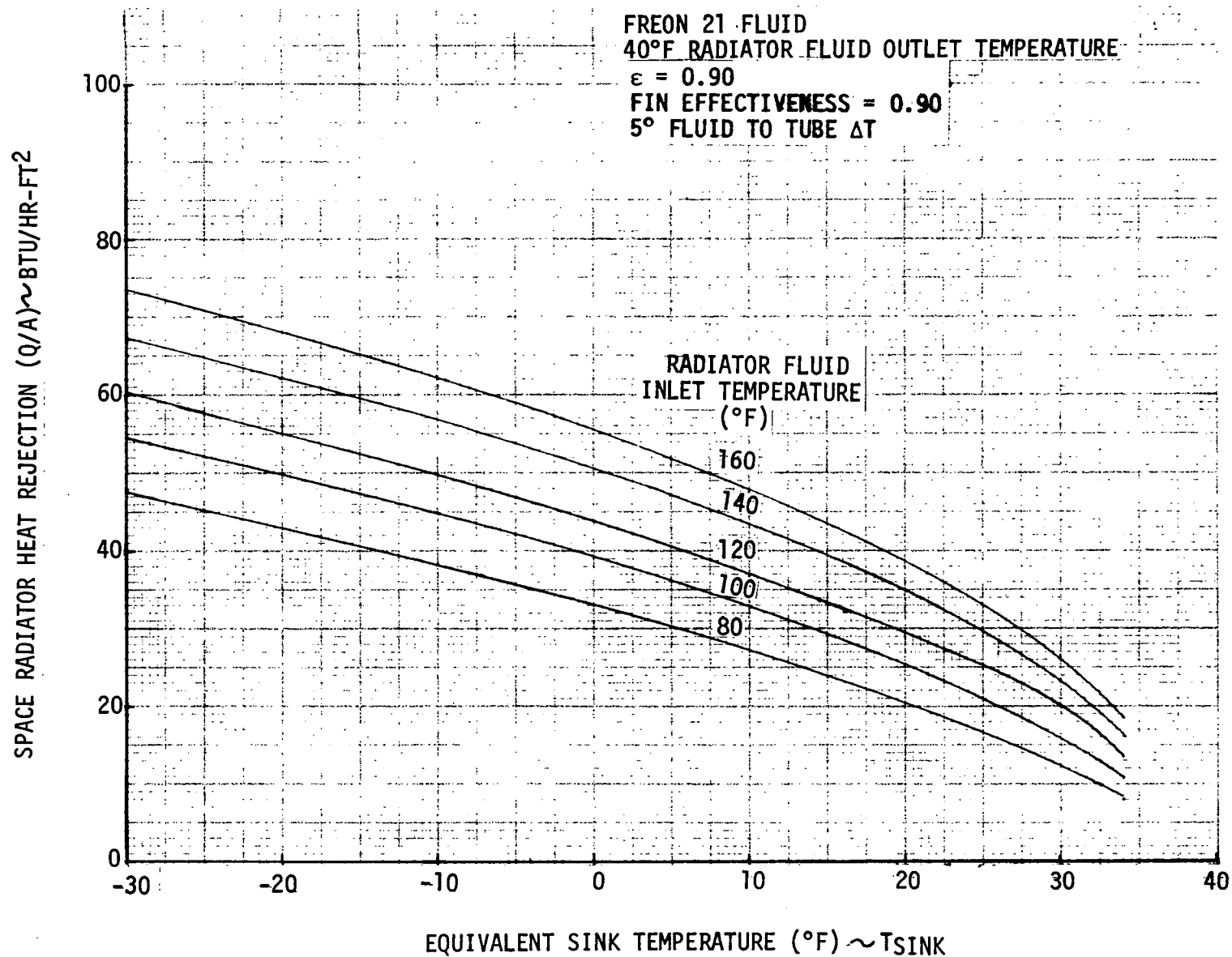


FIGURE 42 SPACE RADIATOR HEAT REJECTION

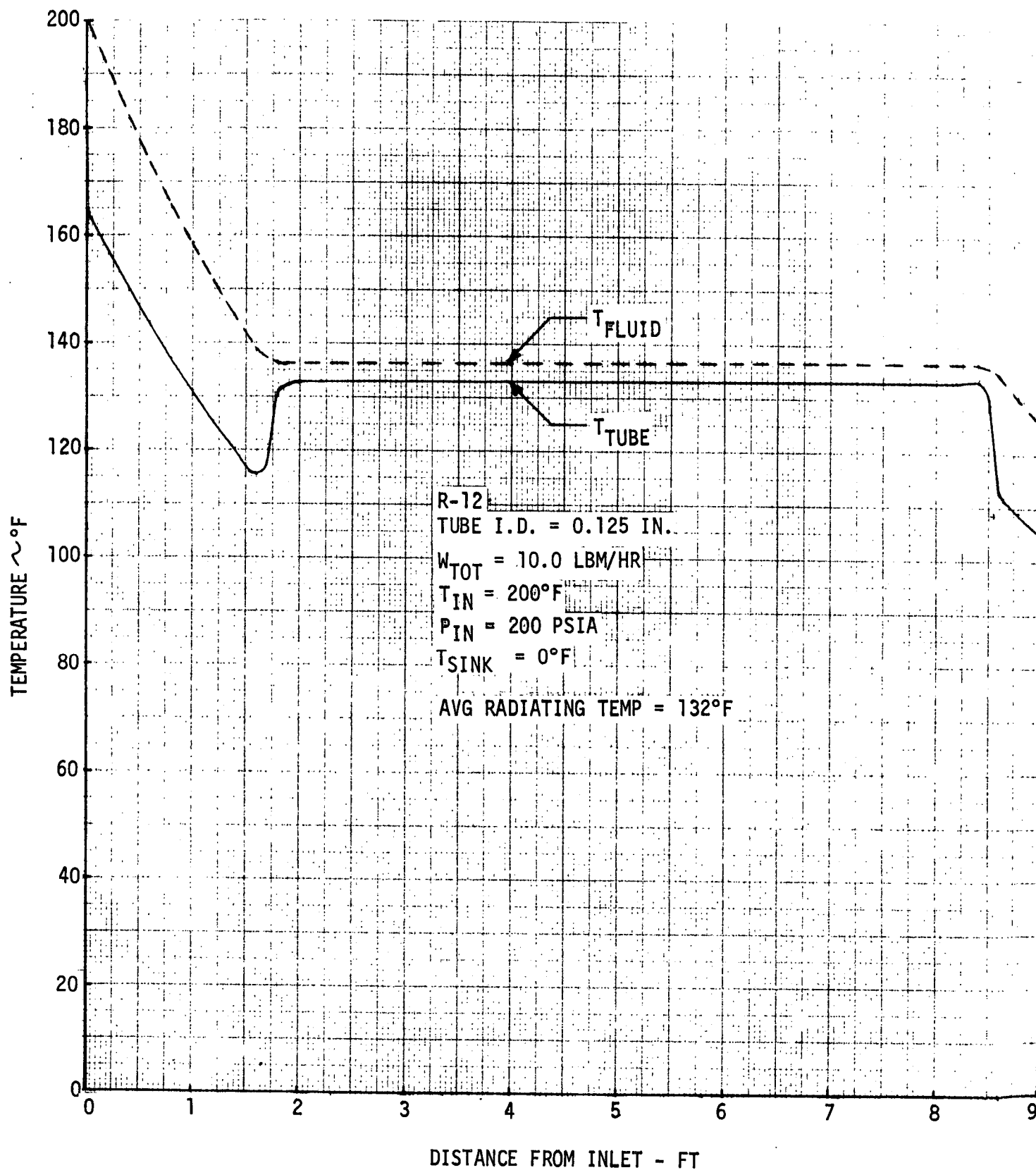


FIGURE 43 CONDENSING RADIATOR TEMPERATURE PROFILE

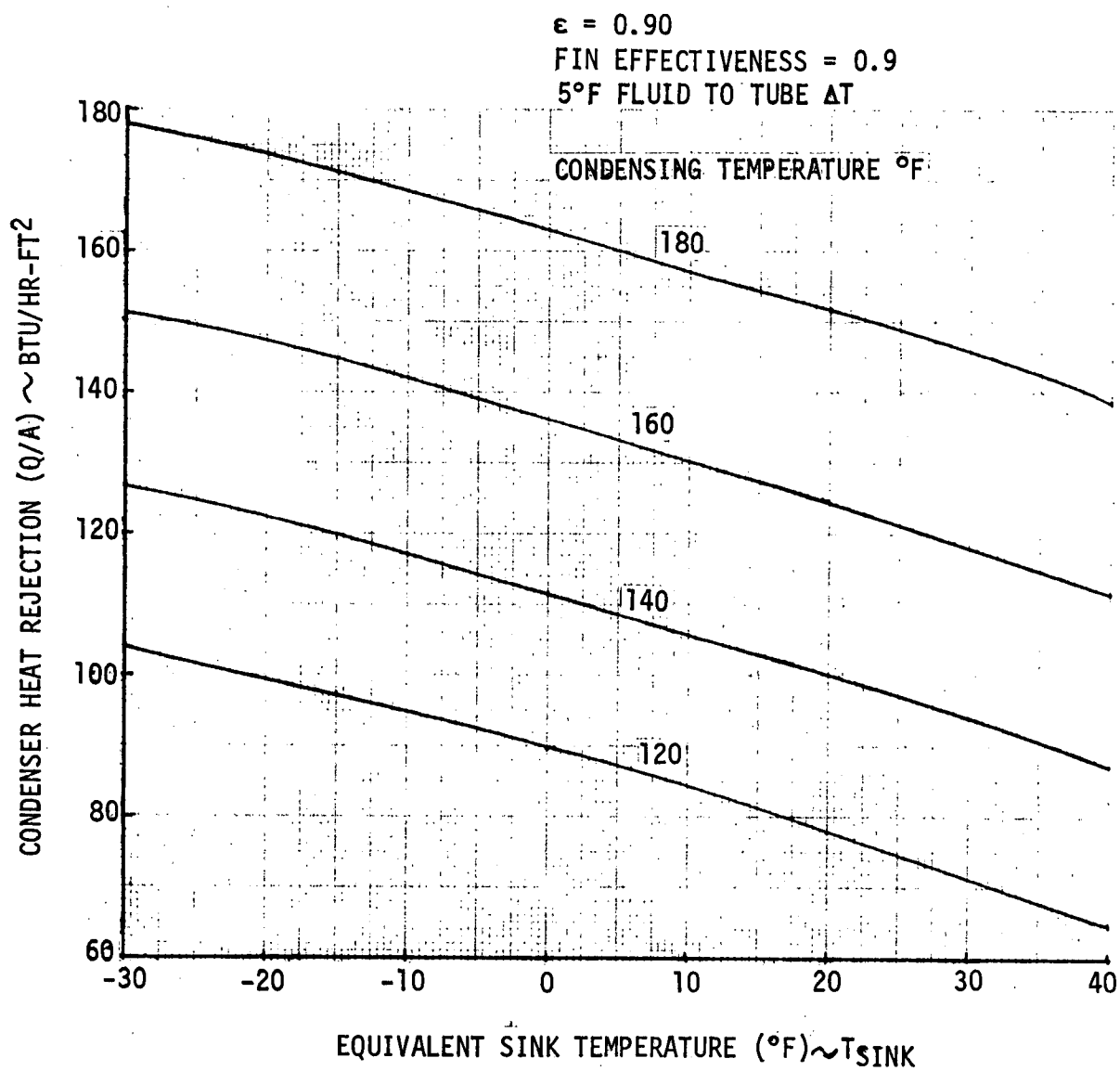
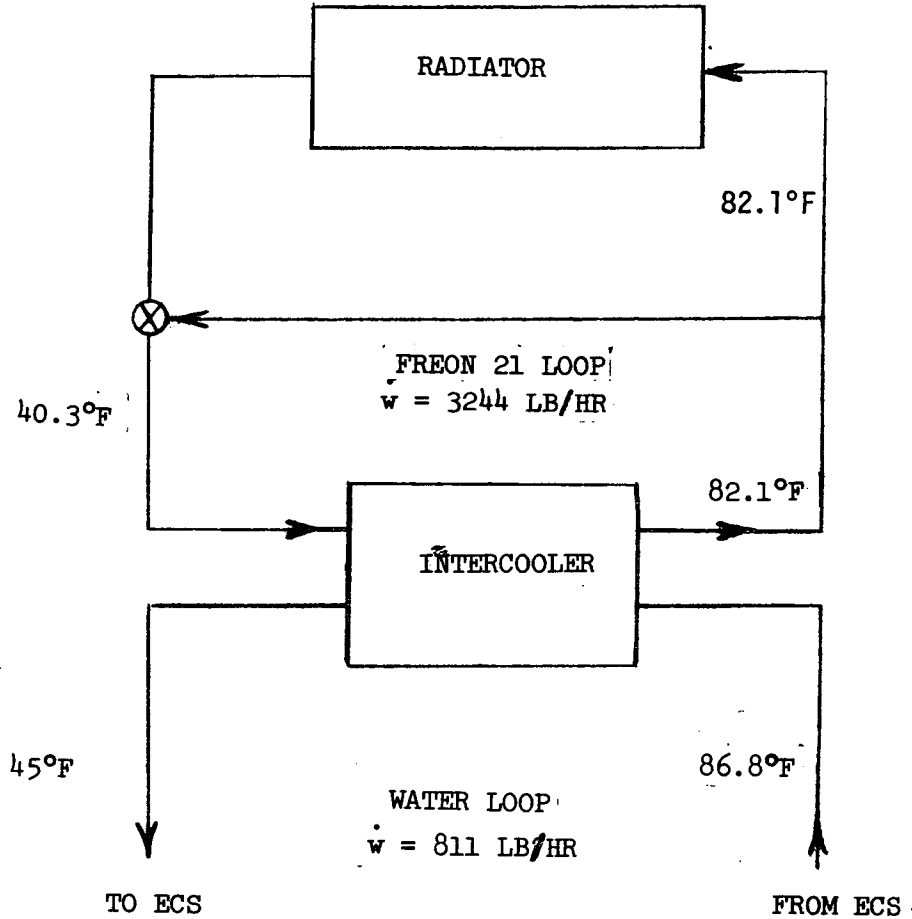


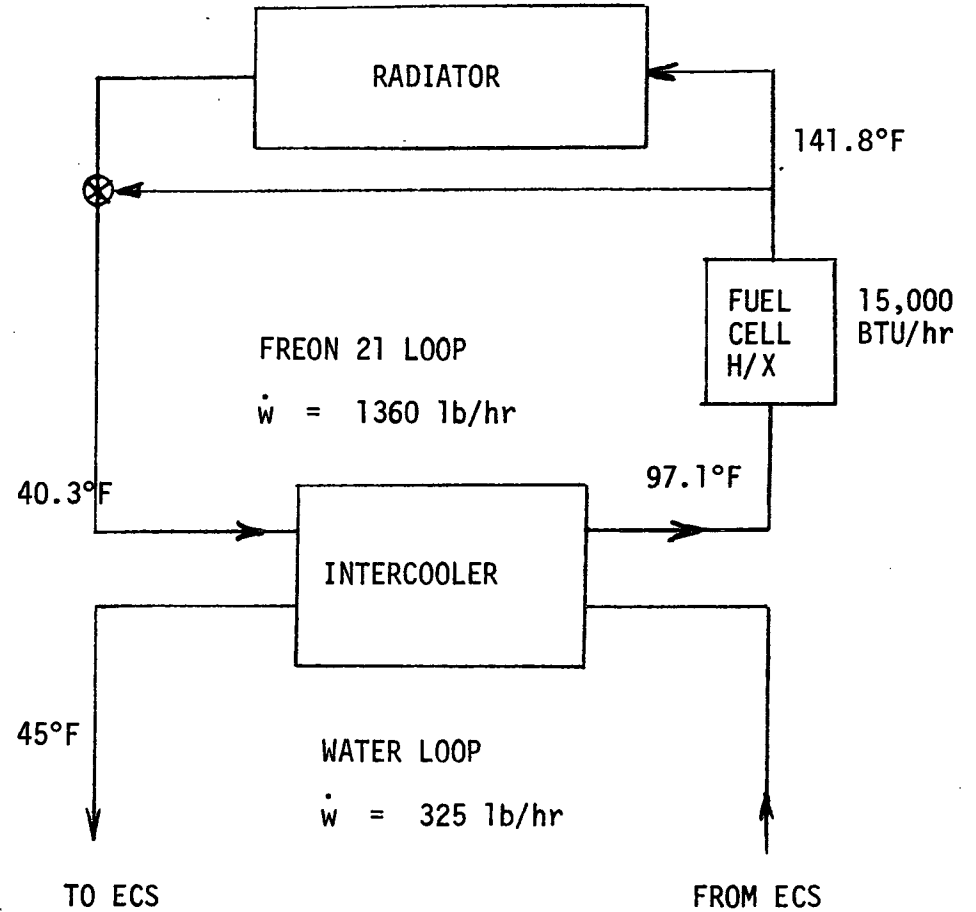
FIGURE 44 CONDENSER HEAT REJECTION

CONCEPT 1



ECS HEAT LOAD = 34,000 BTU/HR

CONCEPT 2



ECS HEAT LOAD = 19,000 BTU/hr

FIGURE 45 TRANSIENT RADIATOR ANALYSIS STEADY STATE DESIGN CONDITIONS

Shadow Q/A based on Shadow T_{SINK} (from Appendix B)
and $T_{OUT} = 40.3^{\circ}F$

Sunlite Q/A based on Sunlite T_{SINK} (from Appendix B)
and $T_{OUT} = T_{PEAK}$

$$(Q/A)_{AVG} = \frac{360(Q/A)_{SHADOW} - 90[(Q/A)_{SHADOW} - (Q/A)_{SUNLITE}]}{360}$$

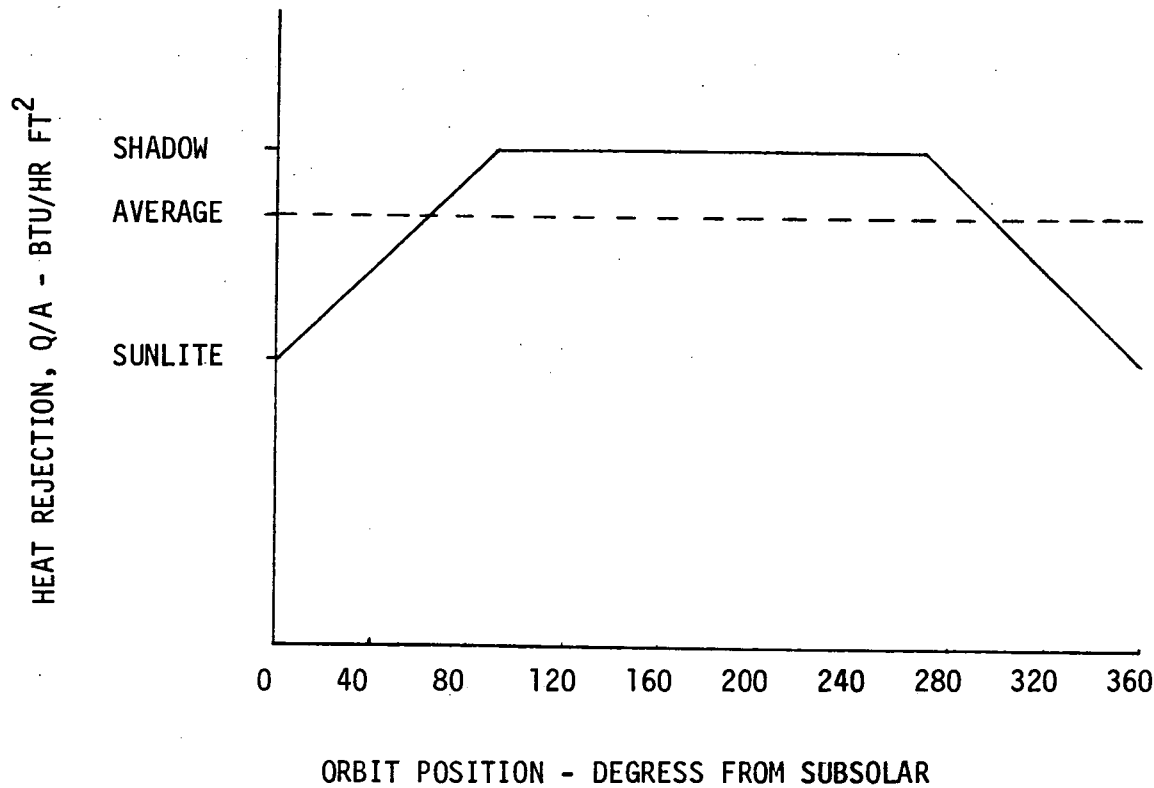


FIGURE 46. DETERMINATION OF AVERAGE Q/A

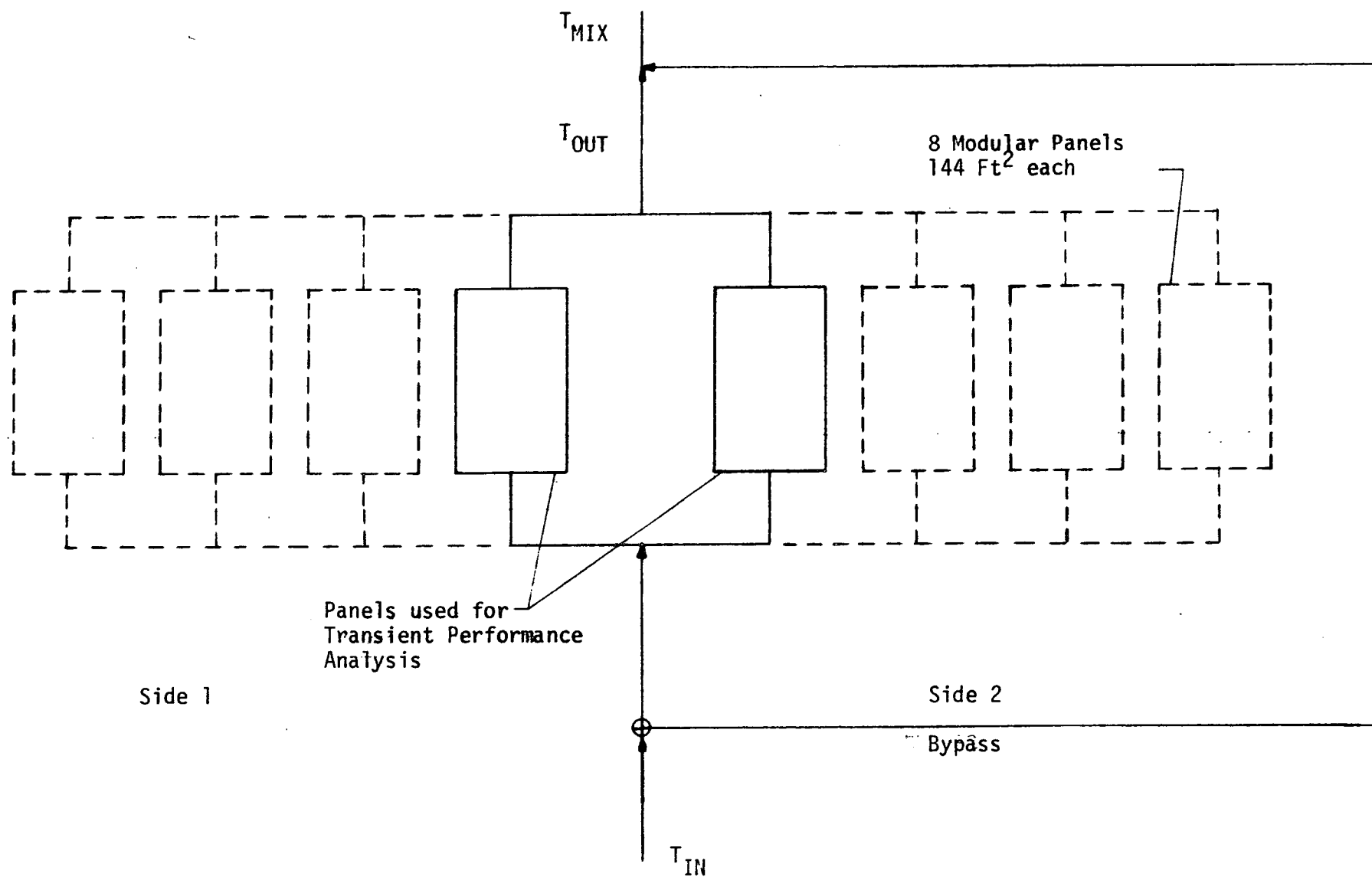


FIGURE 47.1 RADIATOR SYSTEM SCHEMATIC FOR TRANSIENT PERFORMANCE ANALYSIS

Earth Oriented
 Sun Inclination Angle = 0°
 (1) 1-BYPASS TEMP. 2-BEFORE MIXING 3-MIXED OUTLET

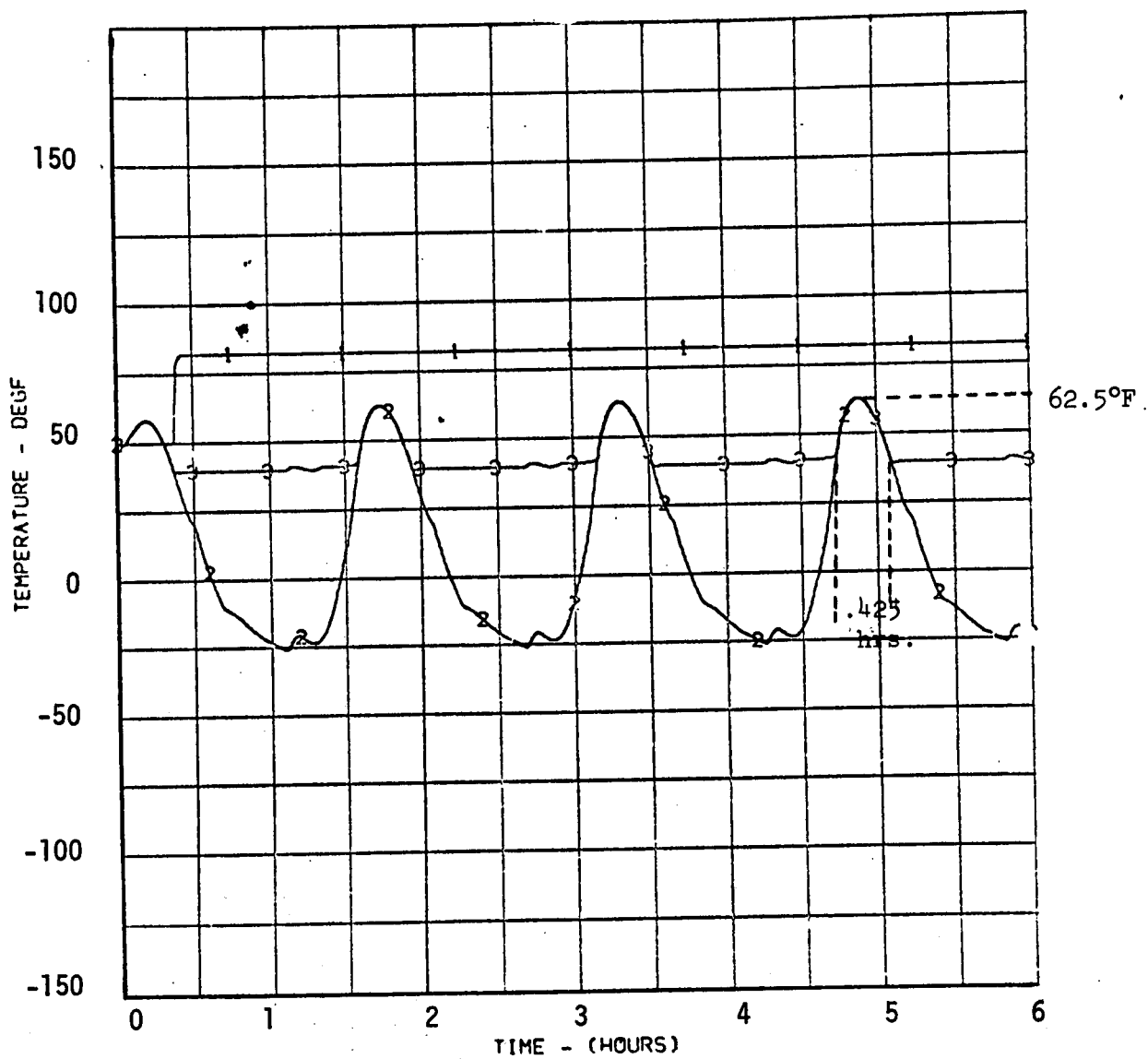


FIGURE 48 TRANSIENT PERFORMANCE OF ORBITER RADIATOR

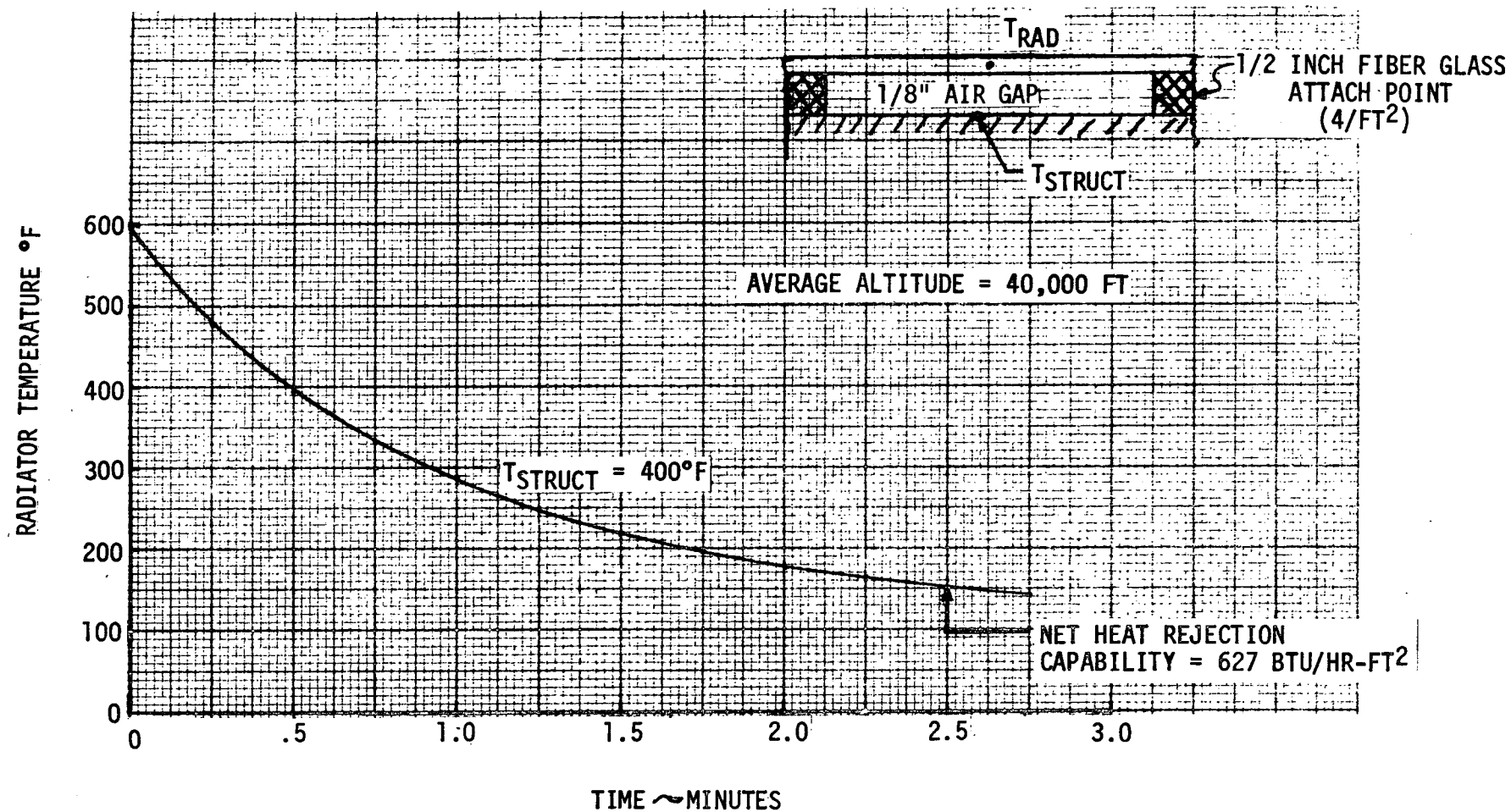


FIGURE 49 RADIATOR COOLDOWN TRANSIENT AFTER REENTRY

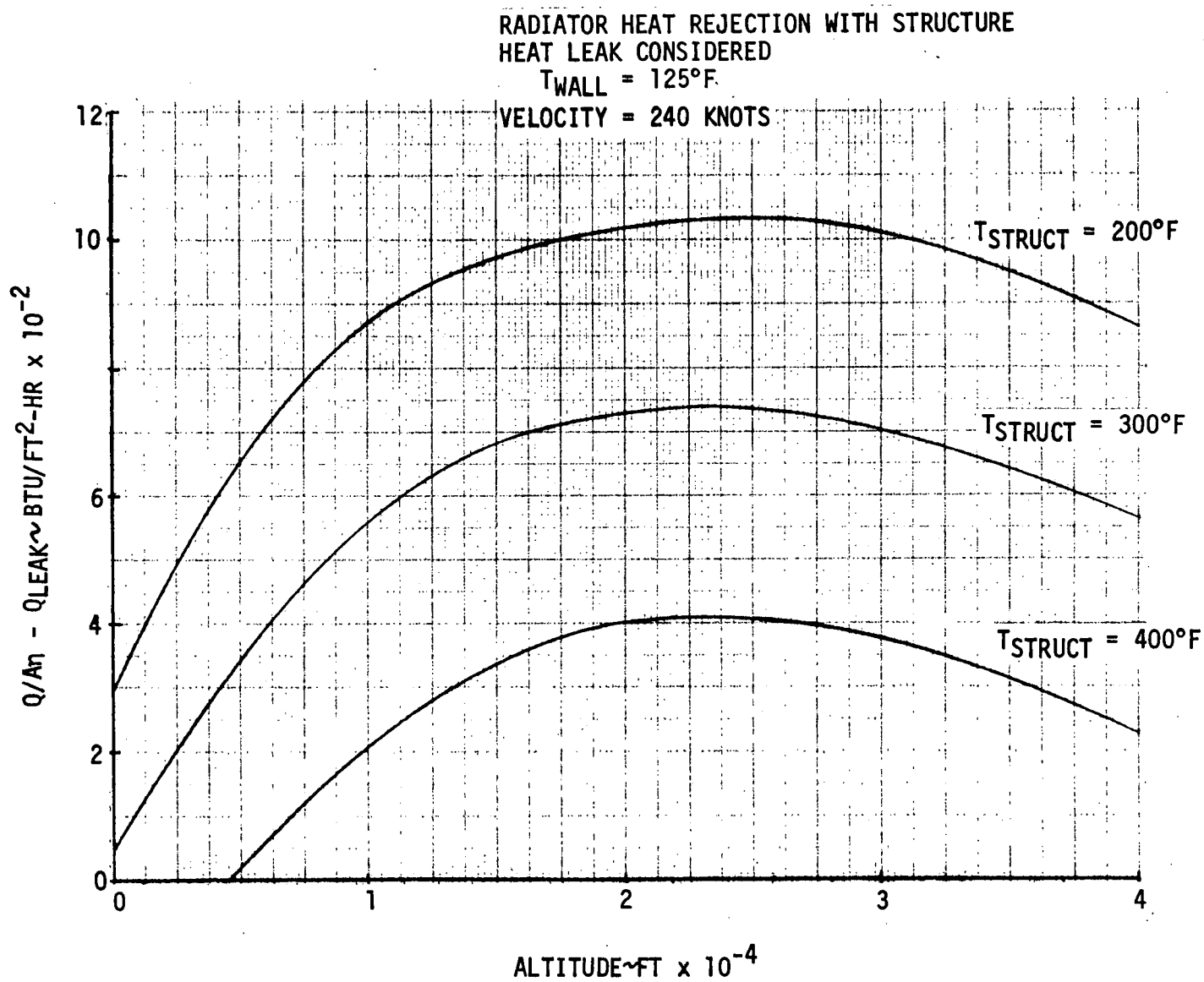


FIGURE 50 INTEGRAL RADIATOR ATMOSPHERIC FLIGHT HEAT REJECTION

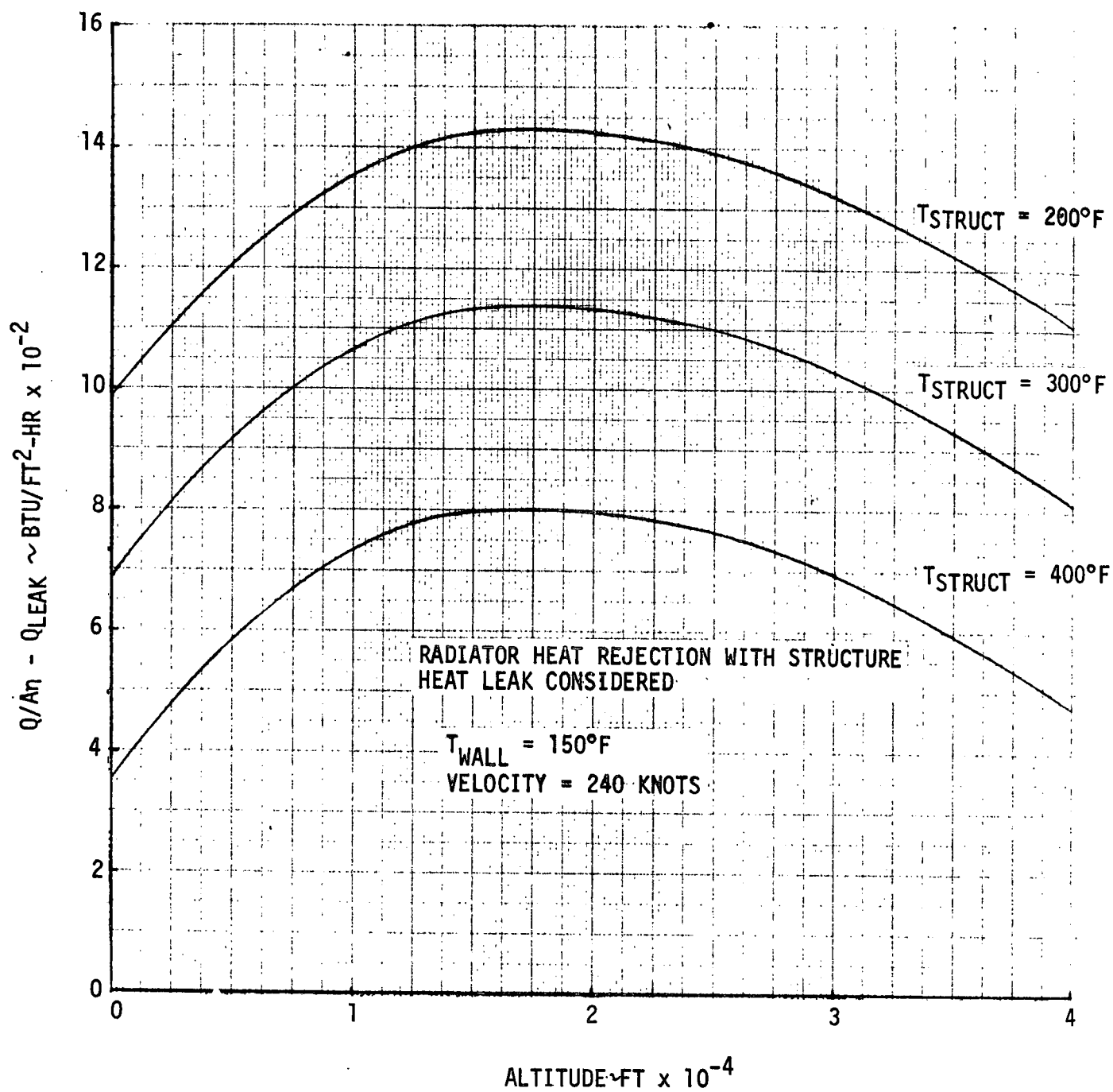


FIGURE 51 INTEGRAL RADIATOR ATMOSPHERIC FLIGHT HEAT REJECTION

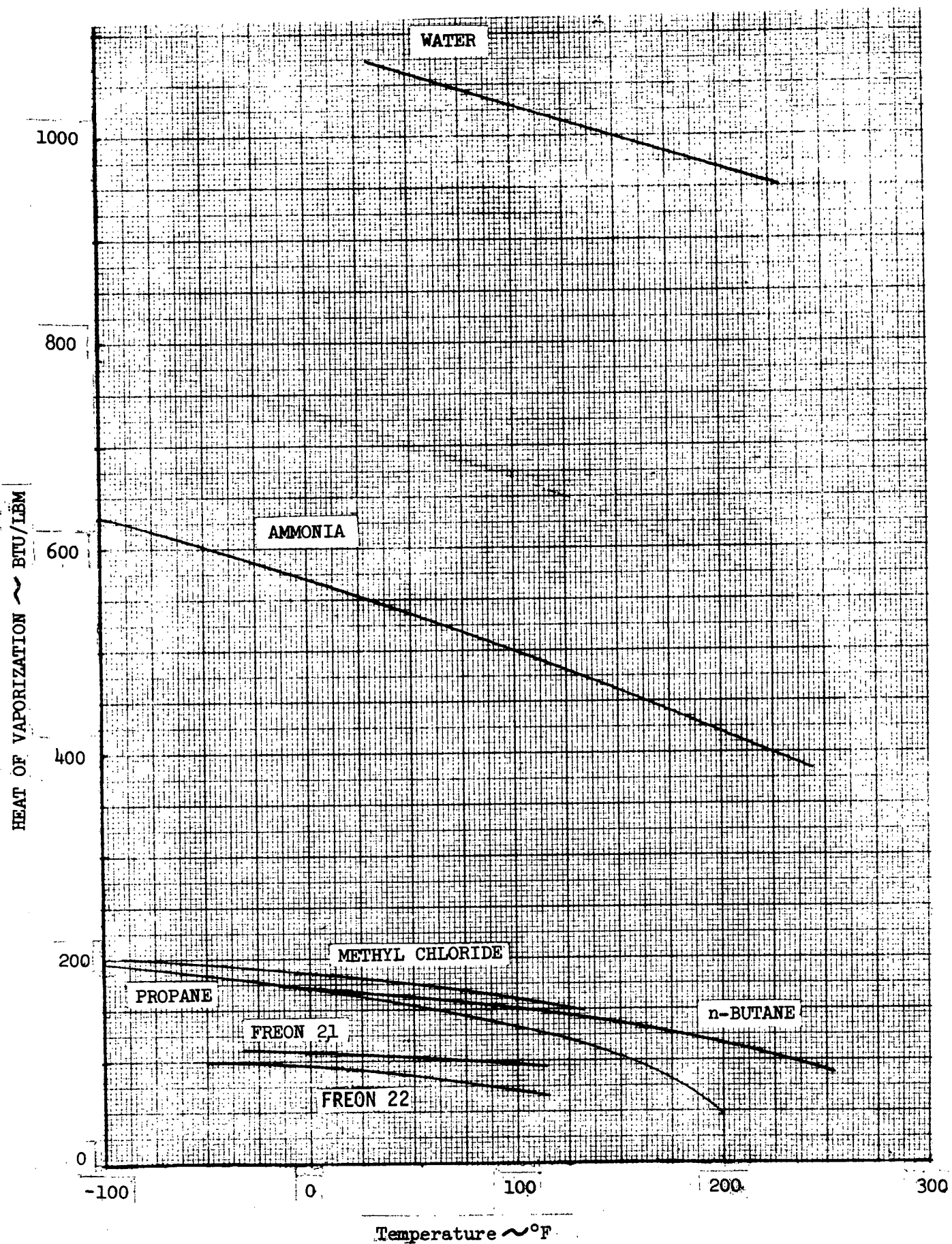


FIGURE 52
EXPENDABLE FLUIDS LATENT HEAT

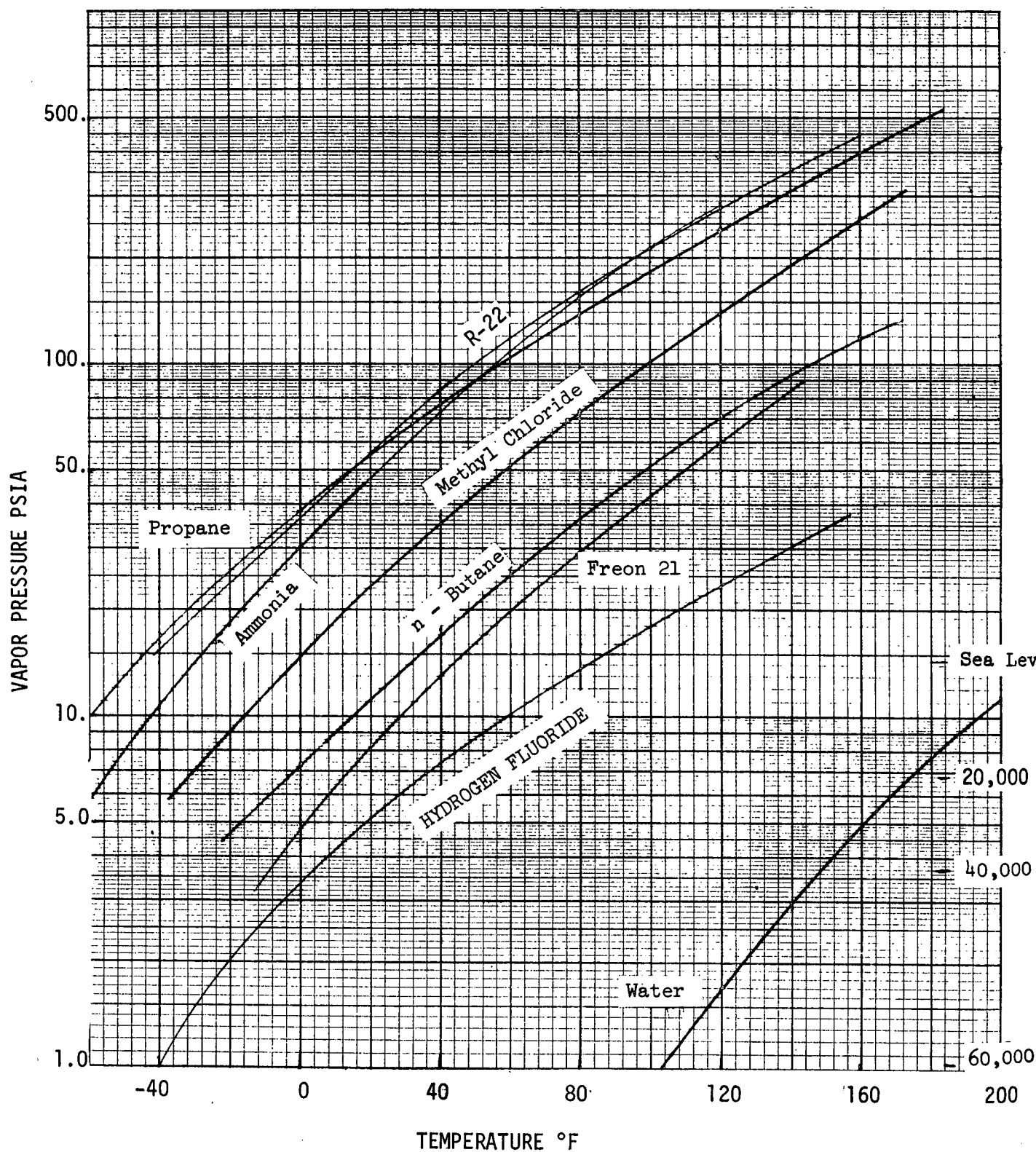


FIGURE 53 VAPOR PRESSURE OF EXPENDABLE FLUIDS

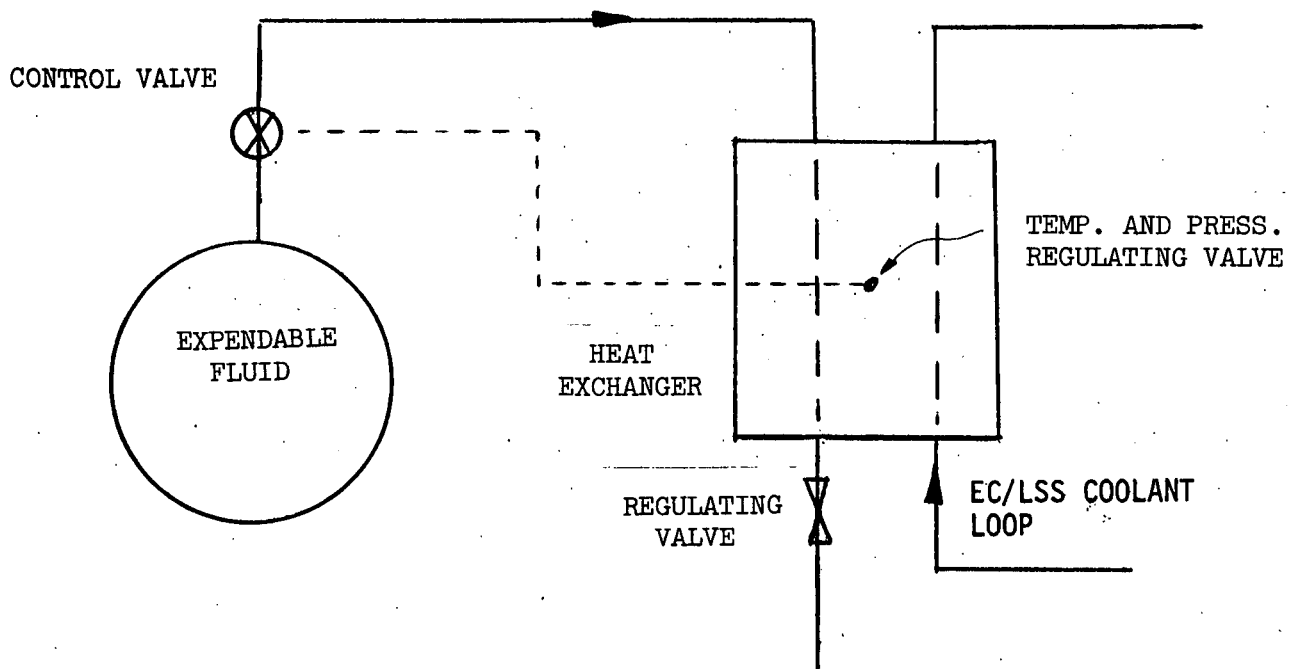


Figure 54 Schematic of the Direct Expendable System

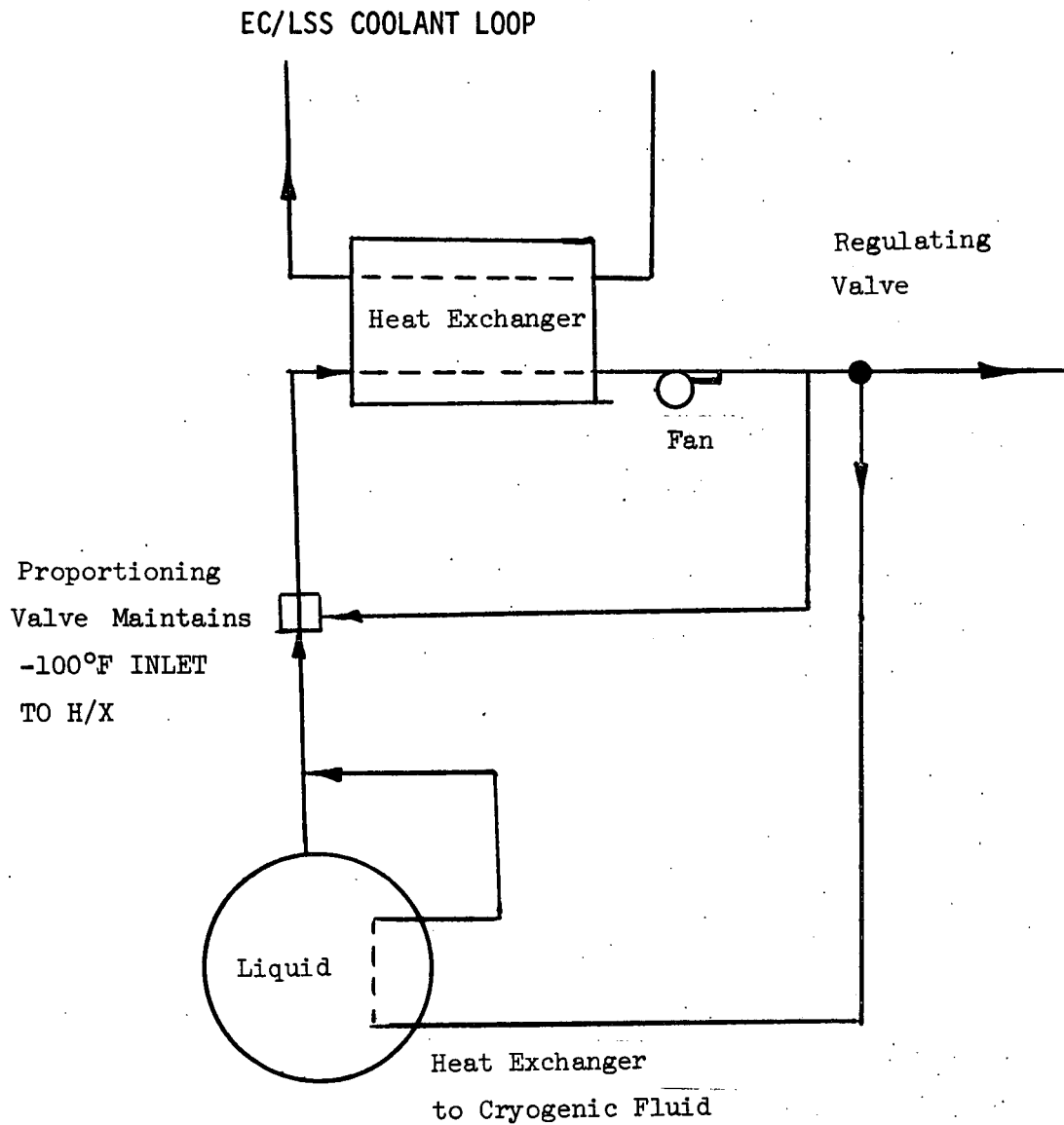


Figure 55 Schematic of the Baseline Cryogenic Coolant System

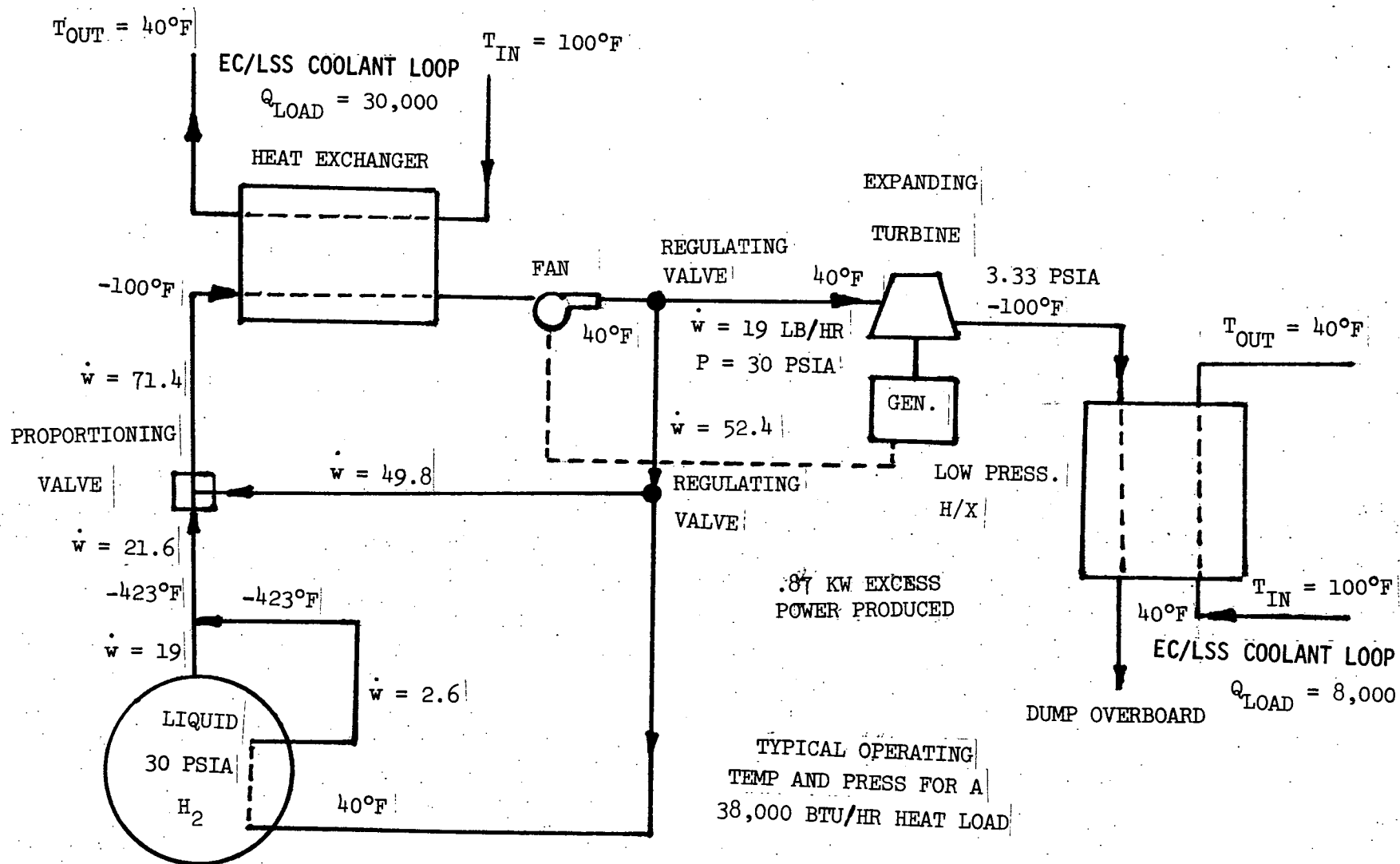


FIGURE 56 SCHEMATIC OF THE CRYOGENIC HYDROGEN SYSTEM WITH EXPANSION TURBINE

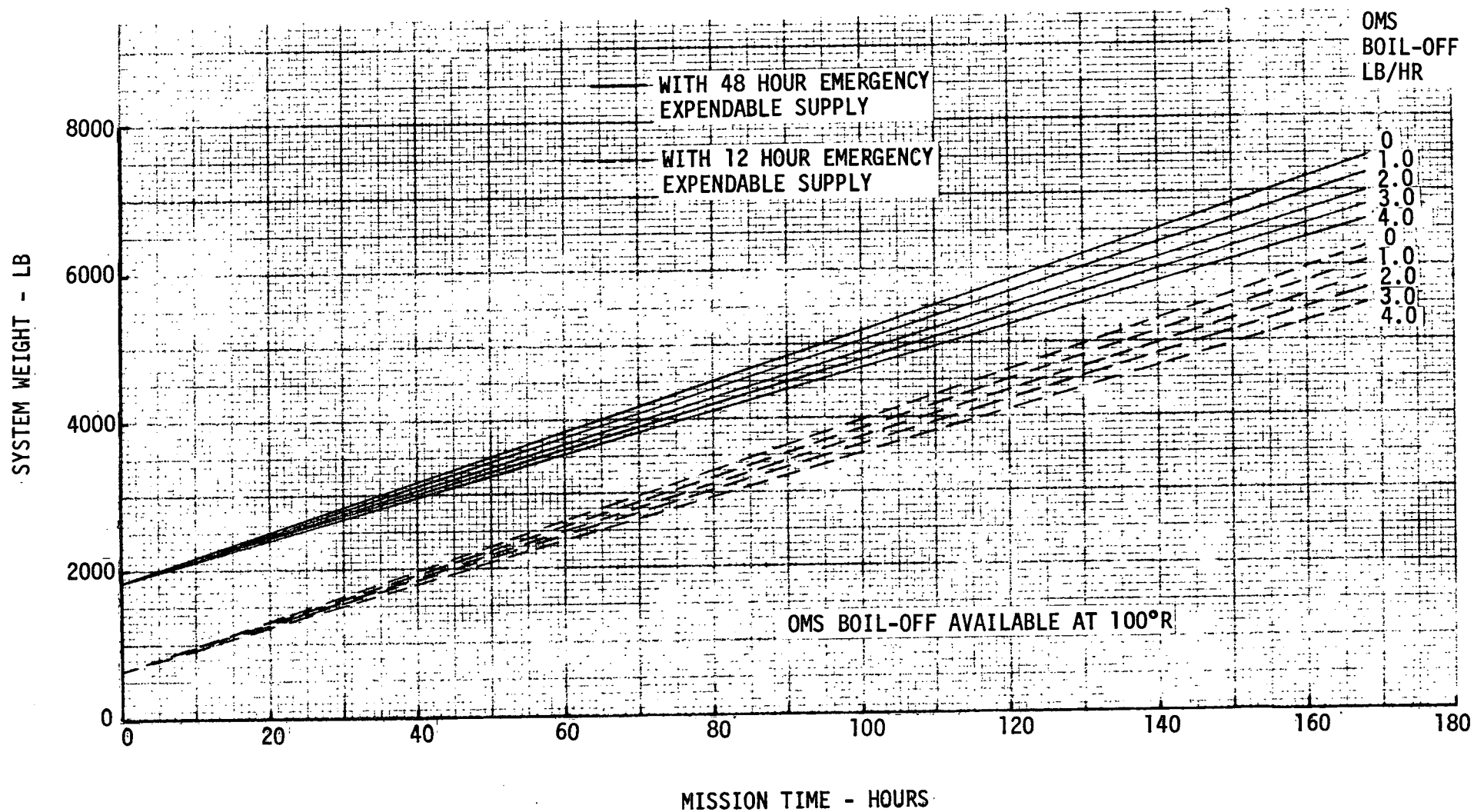


FIGURE 57 EXPENDABLE CRYOGENIC H₂ SYSTEM WEIGHT FOR A 10 KW HEAT LOAD

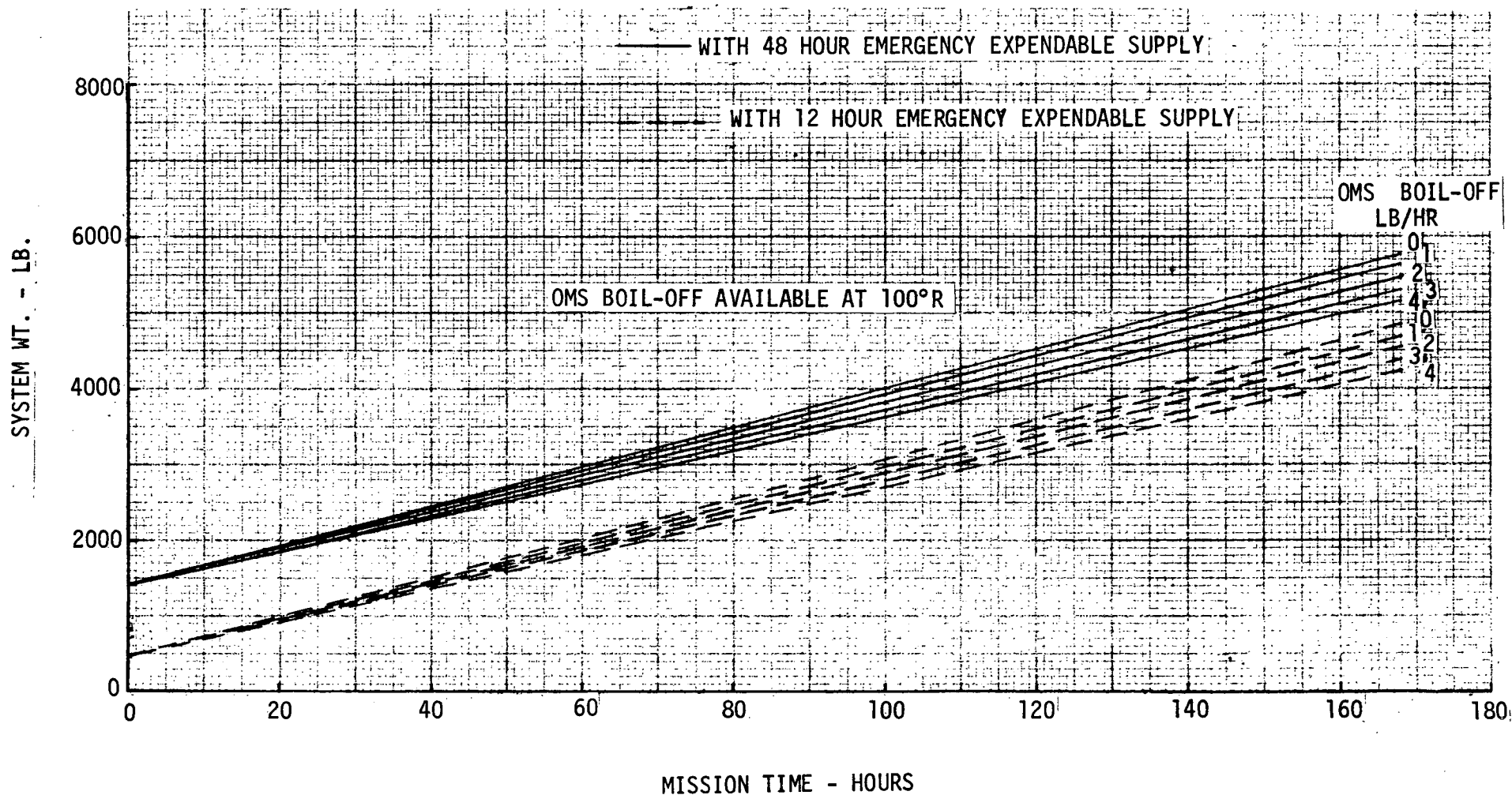


FIGURE 58 EXPENDABLE CRYOGENIC H₂ & GAS CYCLE SYSTEM WEIGHT FOR A 10 KW HEAT LOAD

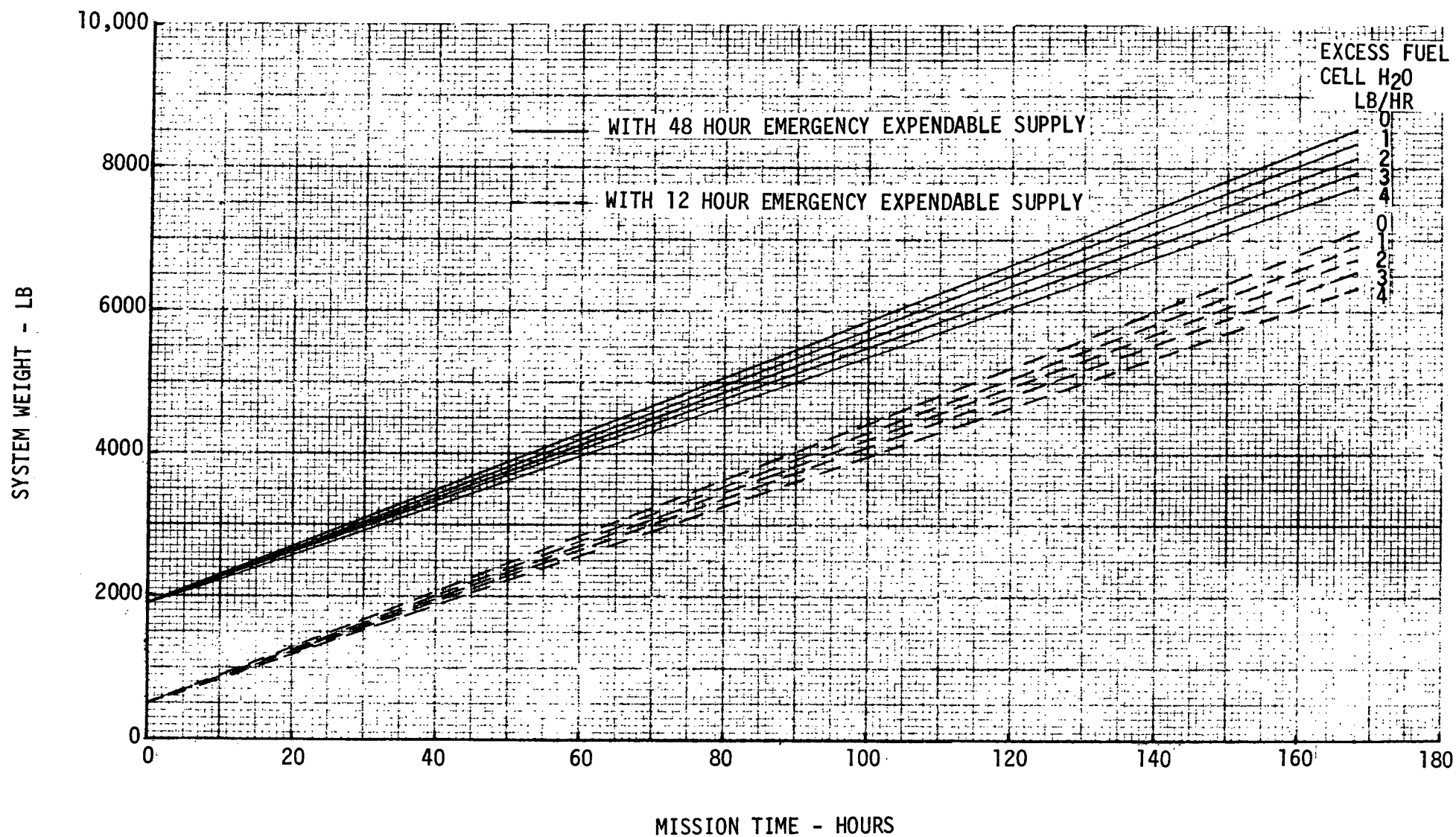


FIGURE 59 EXPENDABLE WATER SYSTEM WEIGHT FOR A 10 KW HEAT LOAD

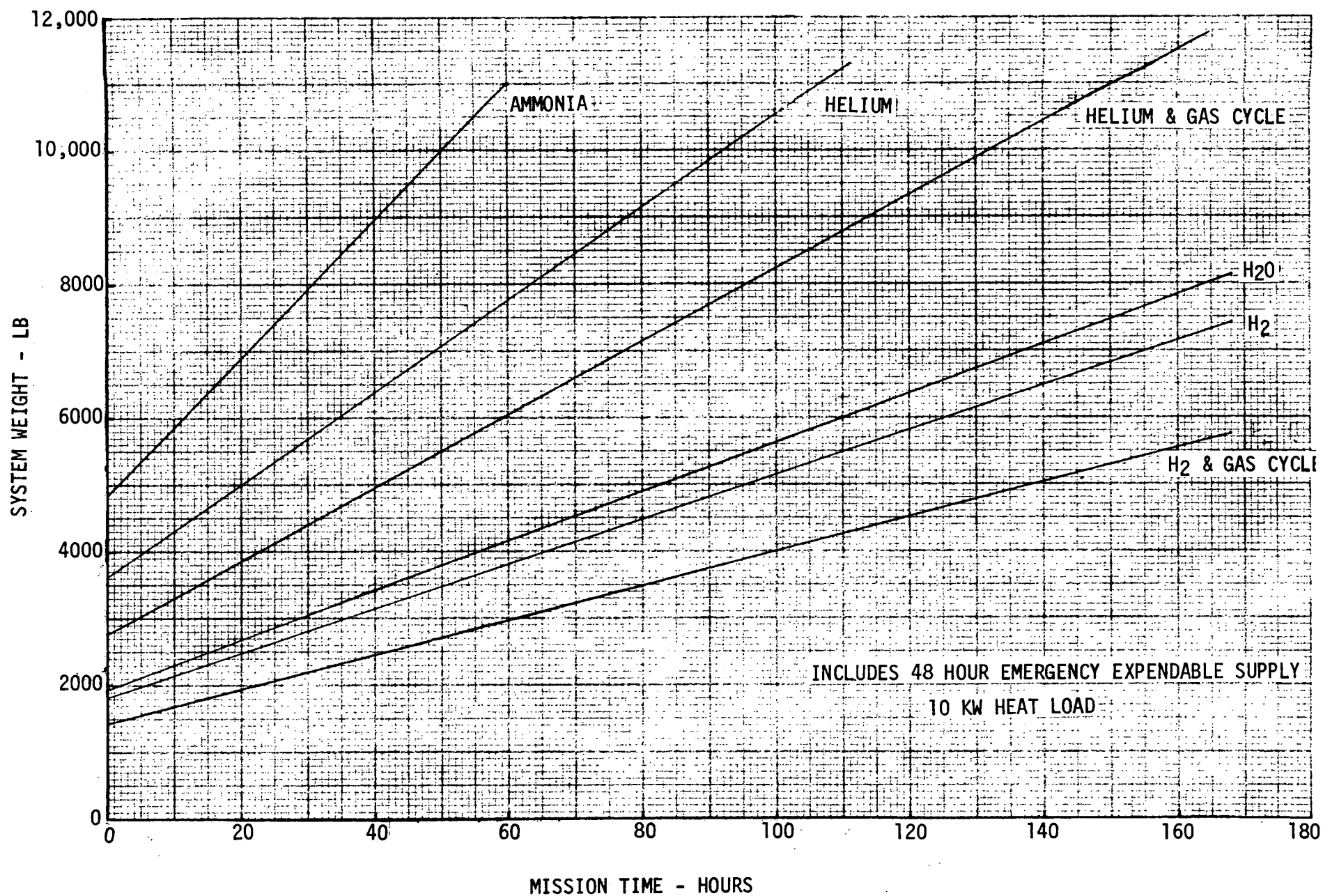


FIGURE 60 COMPARISON OF ORBITAL EXPENDABLE COOLING SYSTEMS

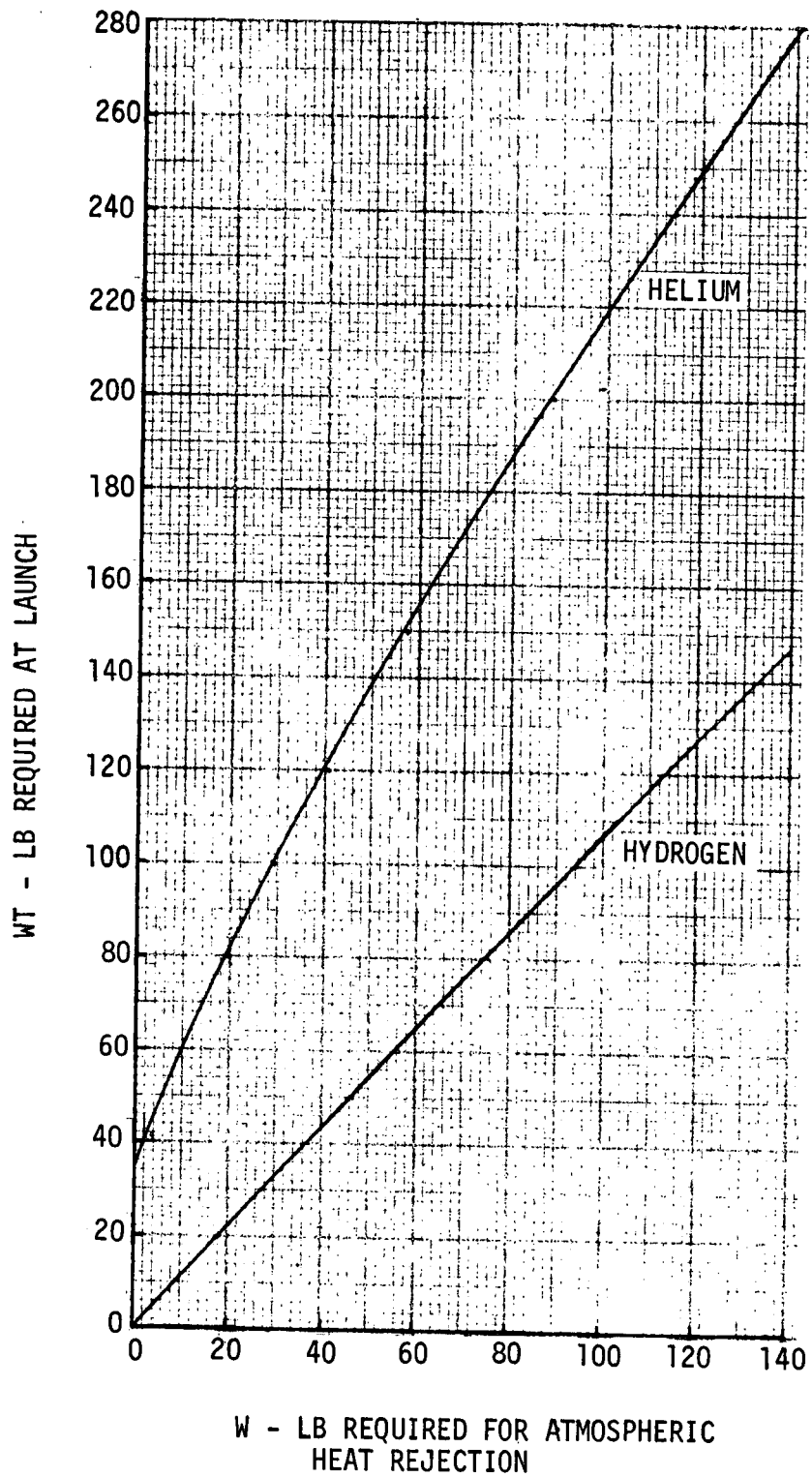


FIGURE 61 SUBORBIT HEAT REJECTION SYSTEM ORBITAL BOIL-OFF PENALTY

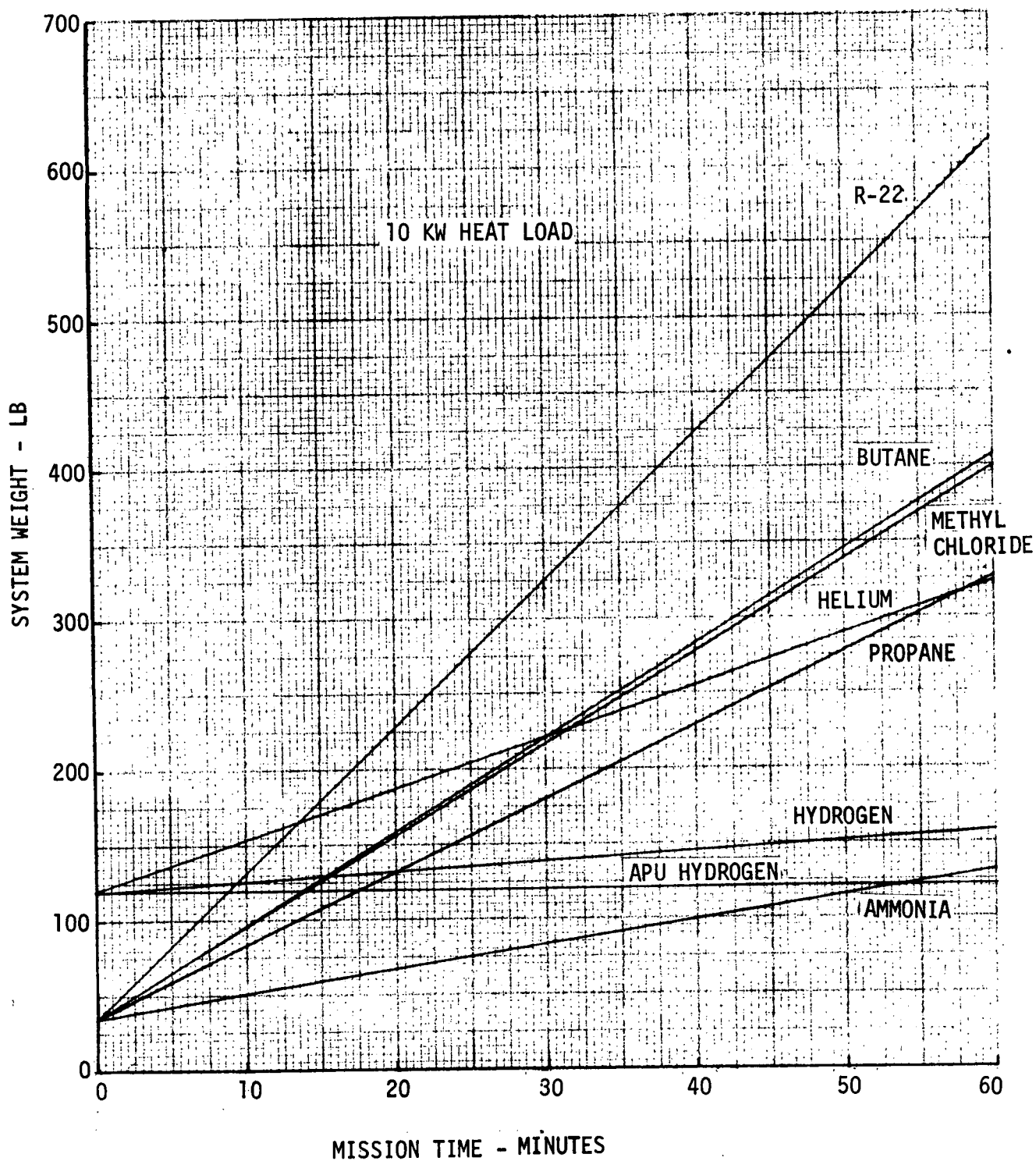


FIGURE 62 ATMOSPHERIC FLIGHT EXPENDABLE FLUID HEAT REJECTION SYSTEM WEIGHTS

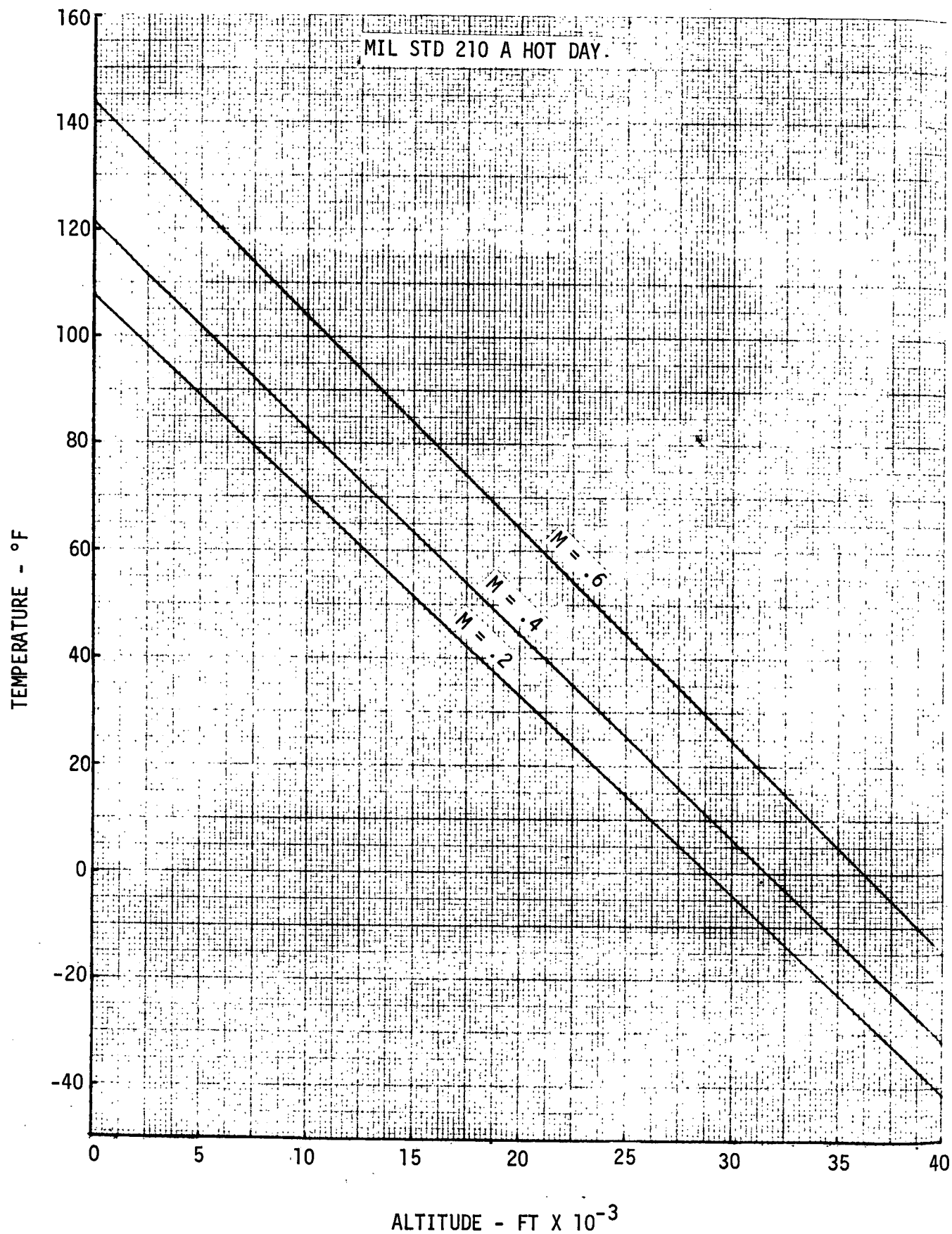


FIGURE 63 RAM AIR TEMPERATURE

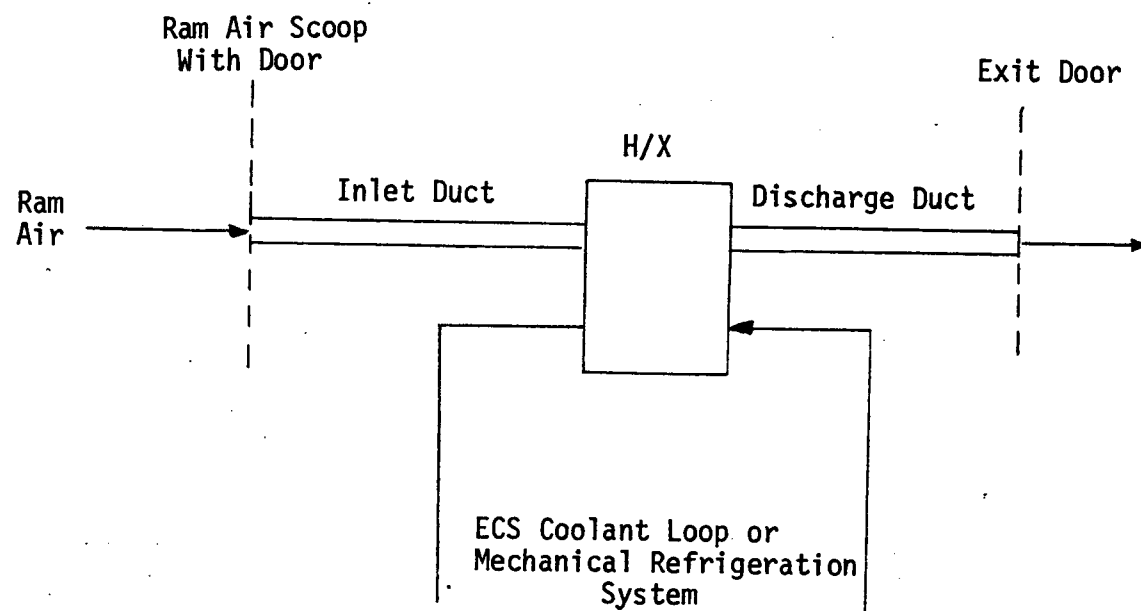


FIGURE 64 RAM AIR SYSTEM SCHEMATIC

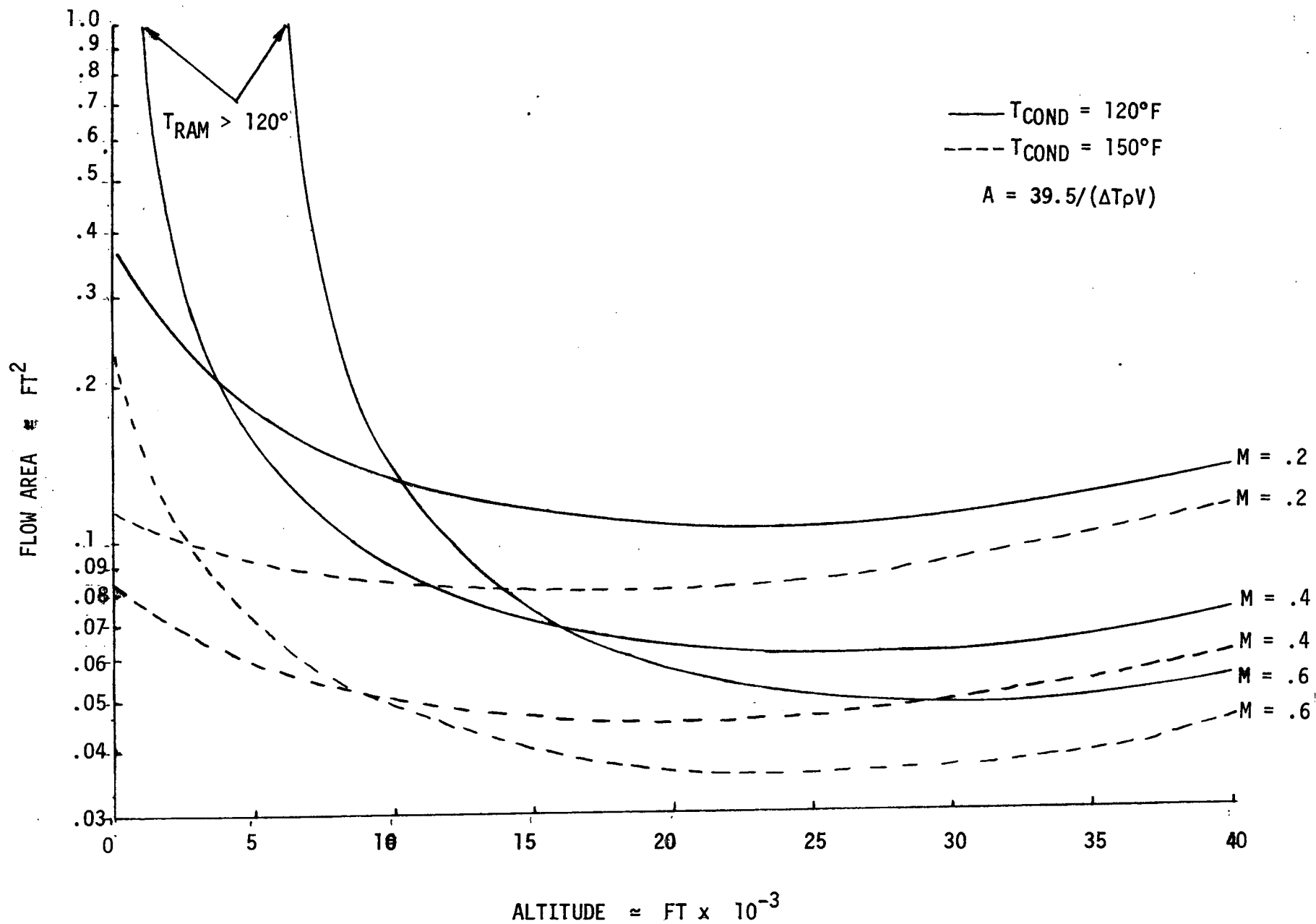


FIGURE 65 RAM AIR INLET REQUIREMENTS

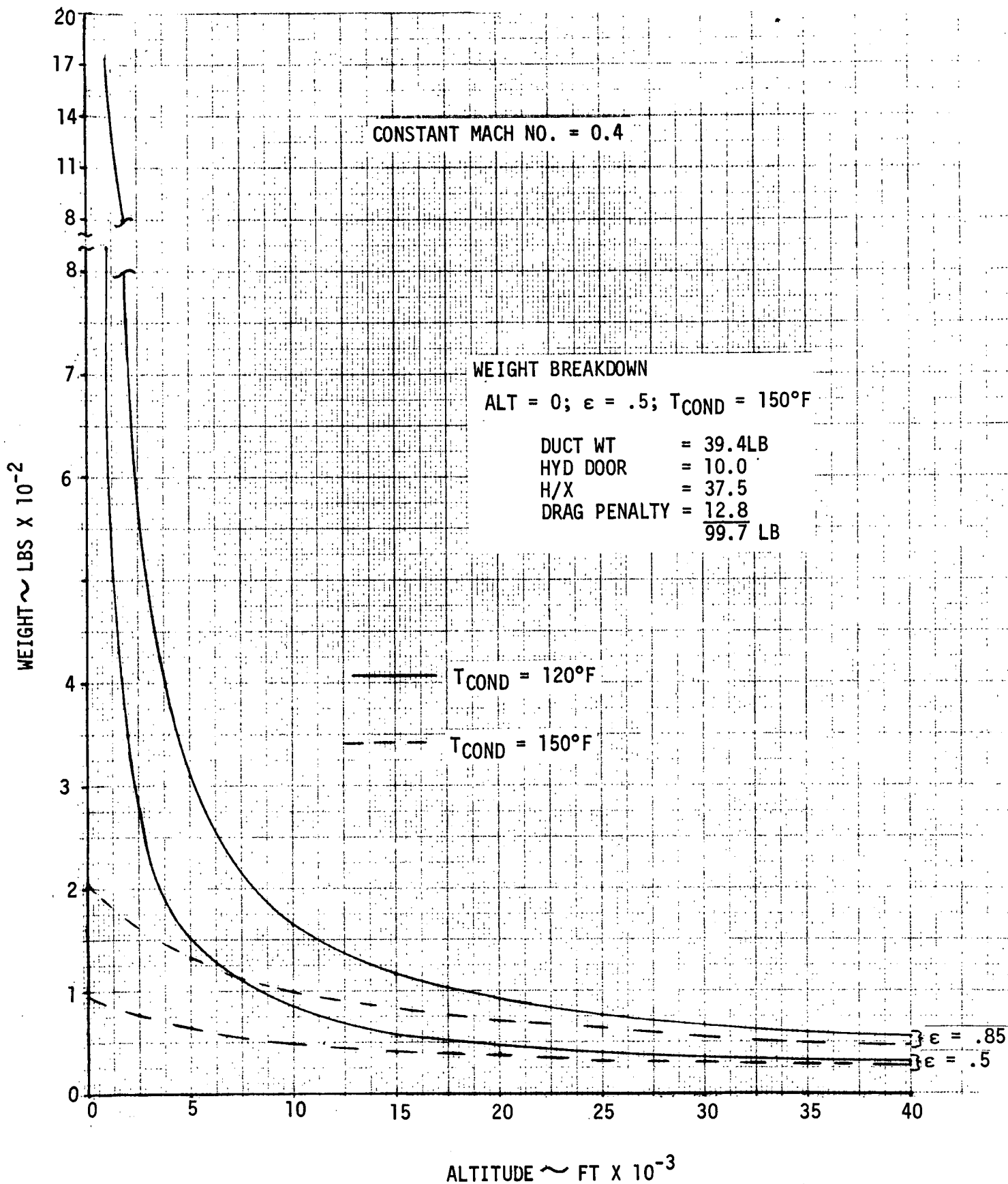


FIGURE 66 RAM AIR SYSTEM WEIGHTS FOR A 10 KW HEAT LOAD

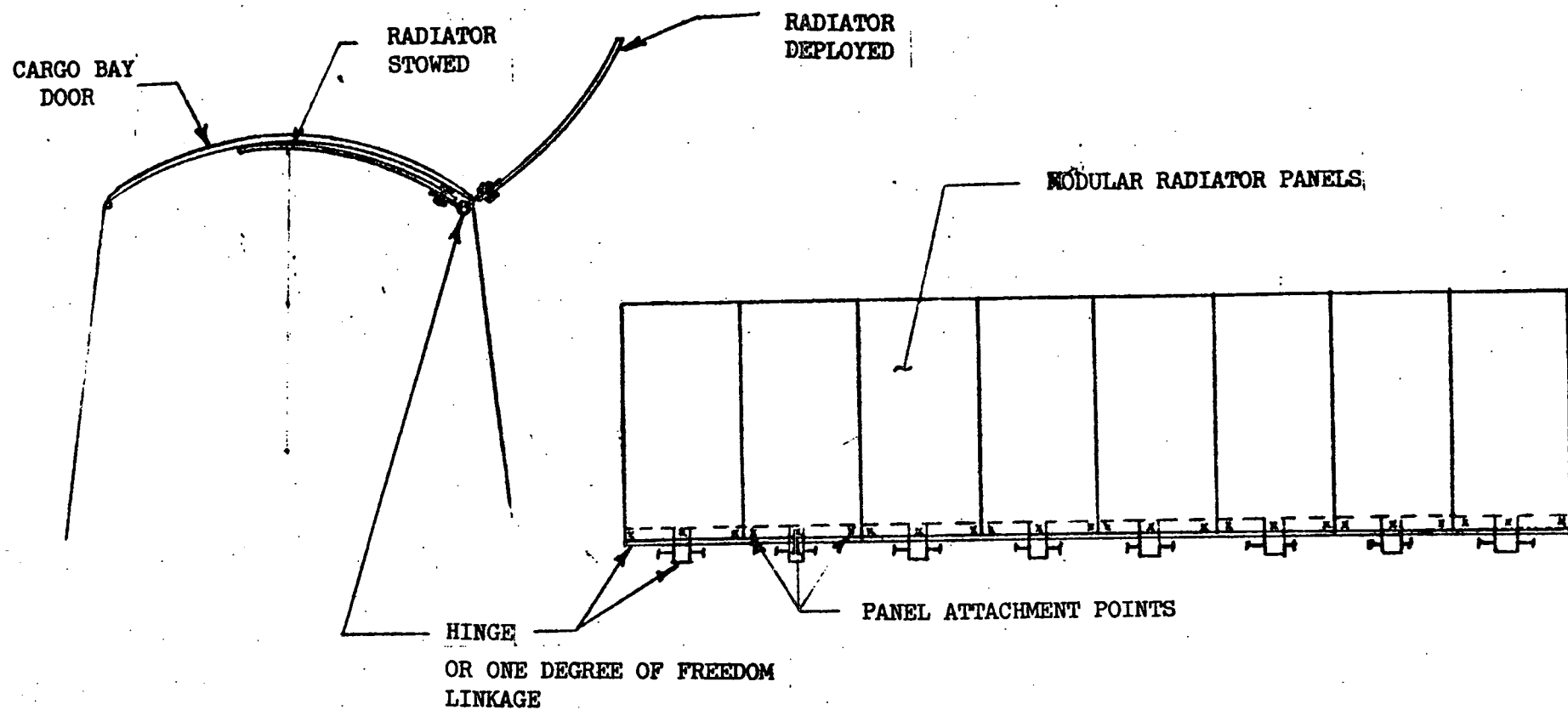


FIGURE 67 SINGLE DOOR DEPLOYED RADIATOR

NOTE:.

ONE SYSTEM
SHOWN,
SIMILAR
ARRANGEMENT
FOR REDUNDANT
SYSTEM

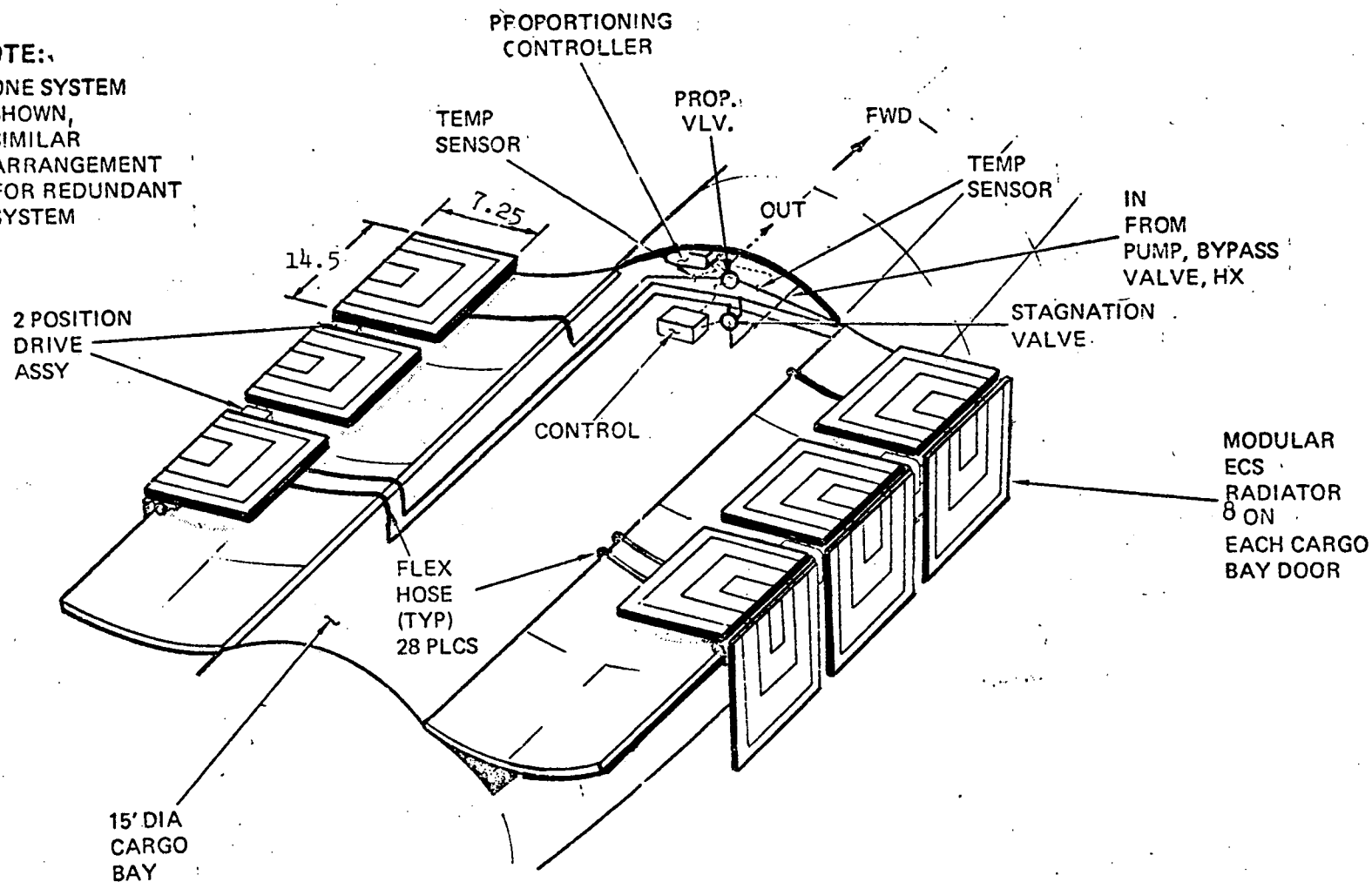


FIGURE 68 DOUBLE DOOR DEPLOYED RADIATOR

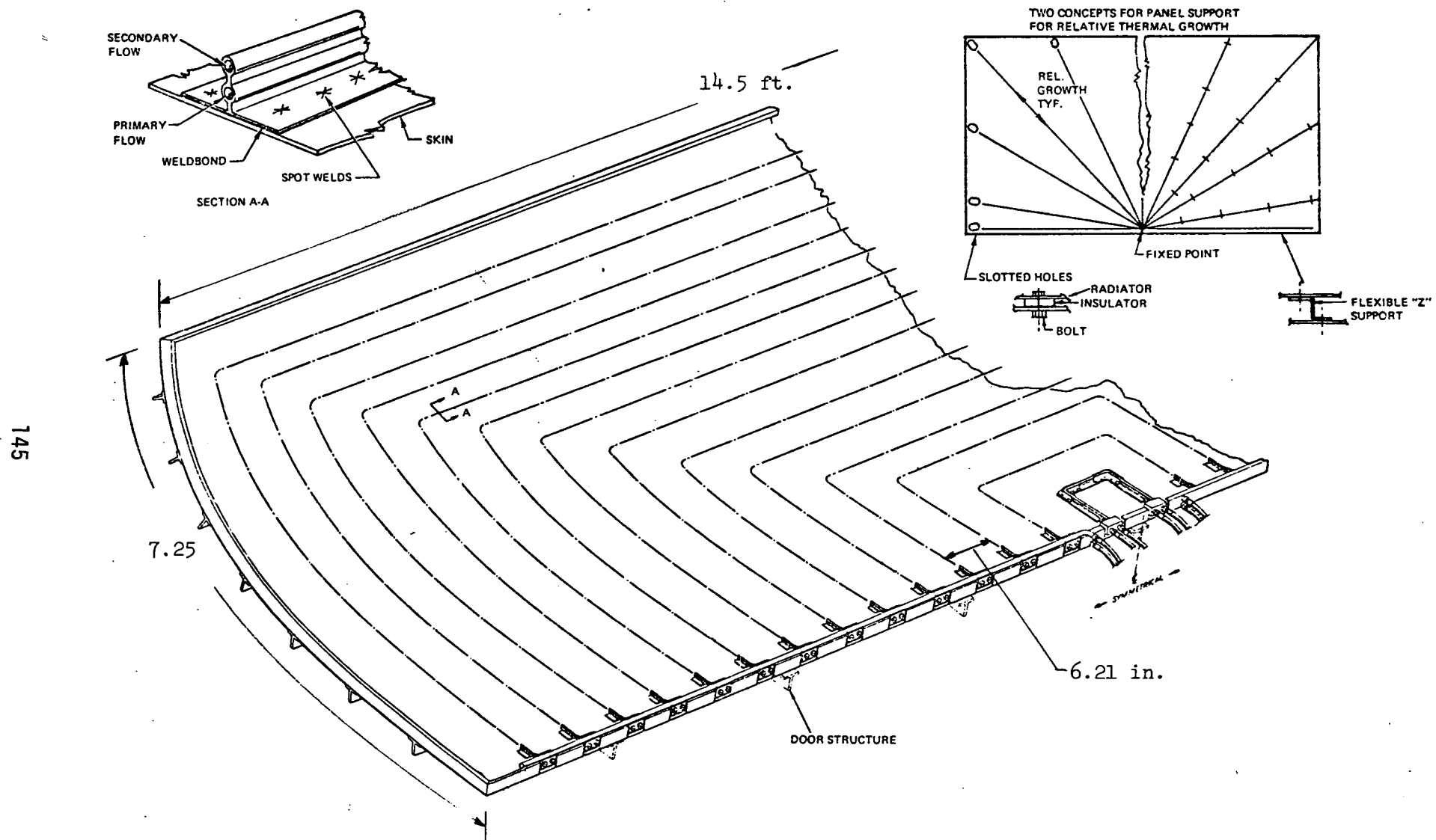


FIGURE 69 MODULAR DEPLOYED PANEL DESIGN

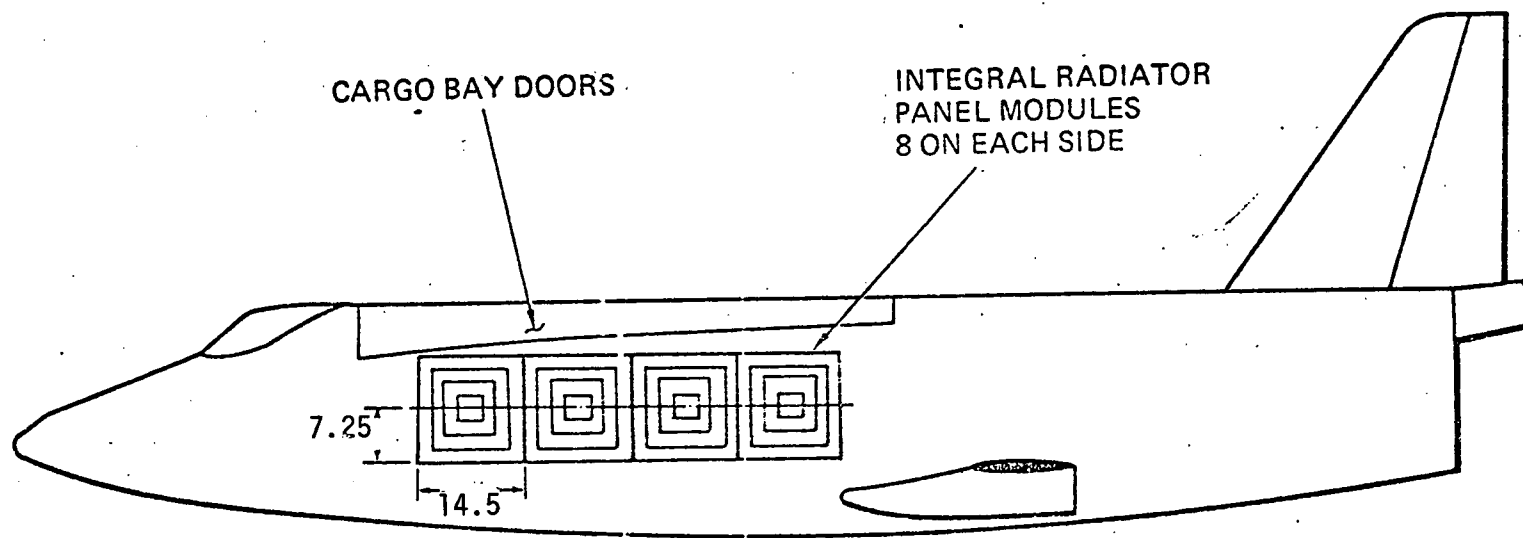


FIGURE 70 INTEGRAL RADIATOR PANEL INSTALLATION

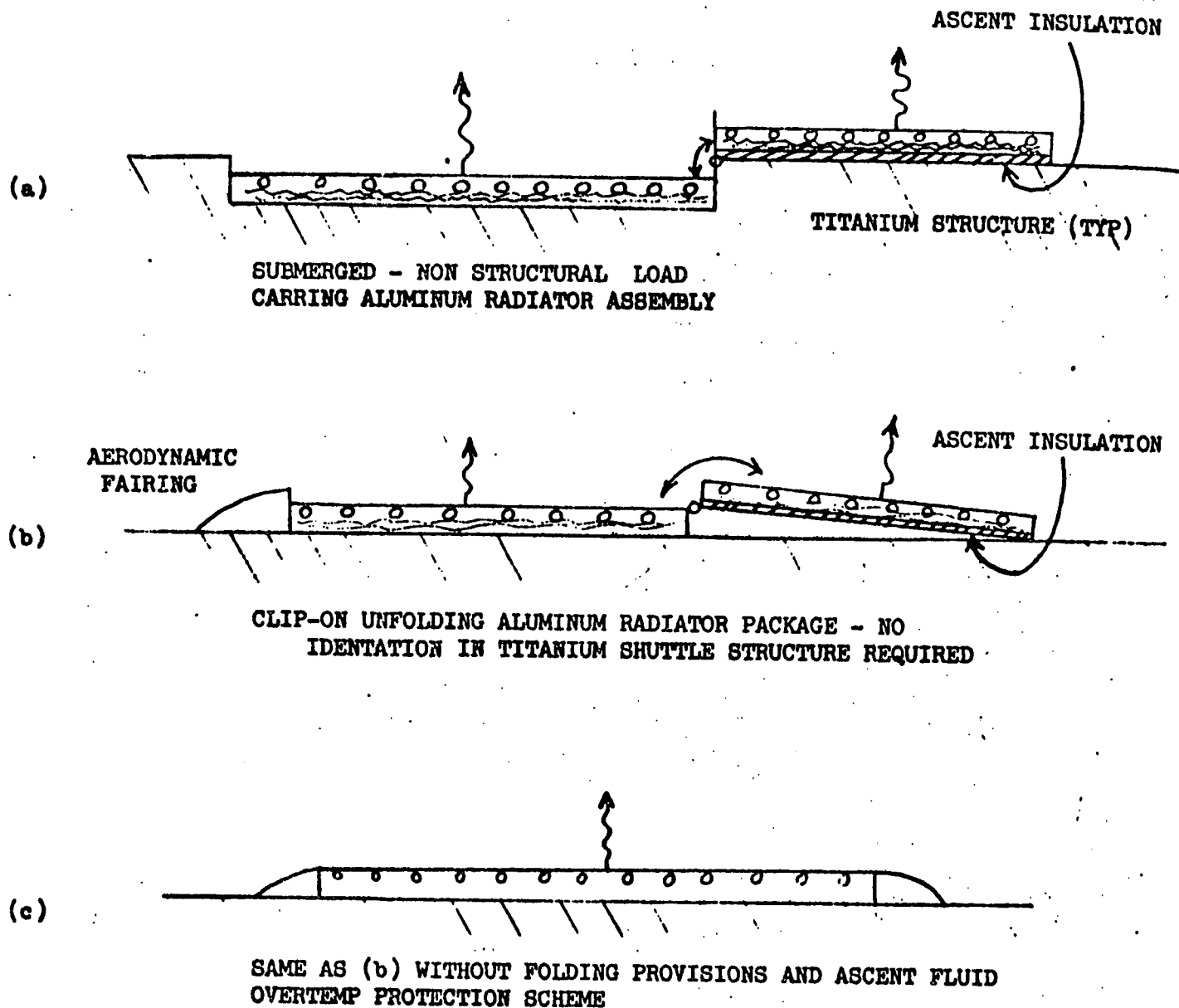


FIGURE .71, RADIATOR PANEL MOUNTING CONFIGURATIONS

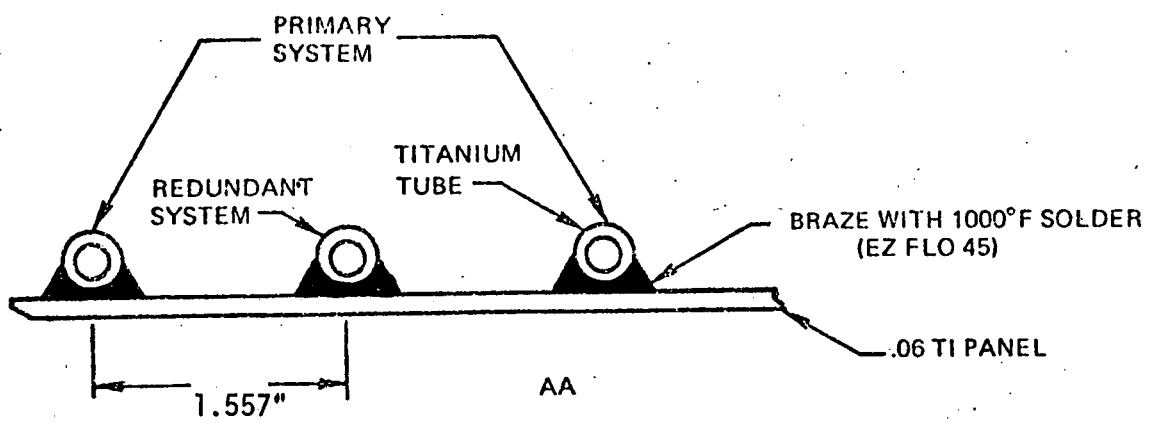
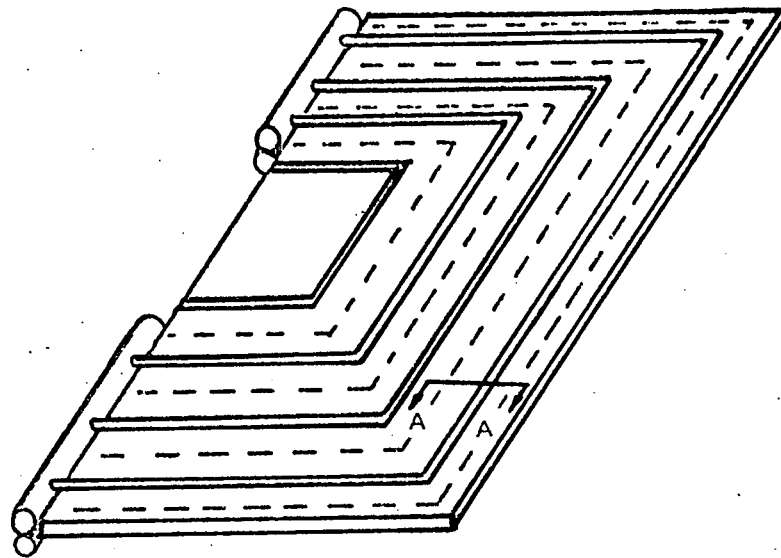


FIGURE 72 INTEGRAL PANEL DESIGN

TOTAL FUEL CELL TERMINAL OUTPUT
PHASE AVERAGE POWER - KILOWATTS

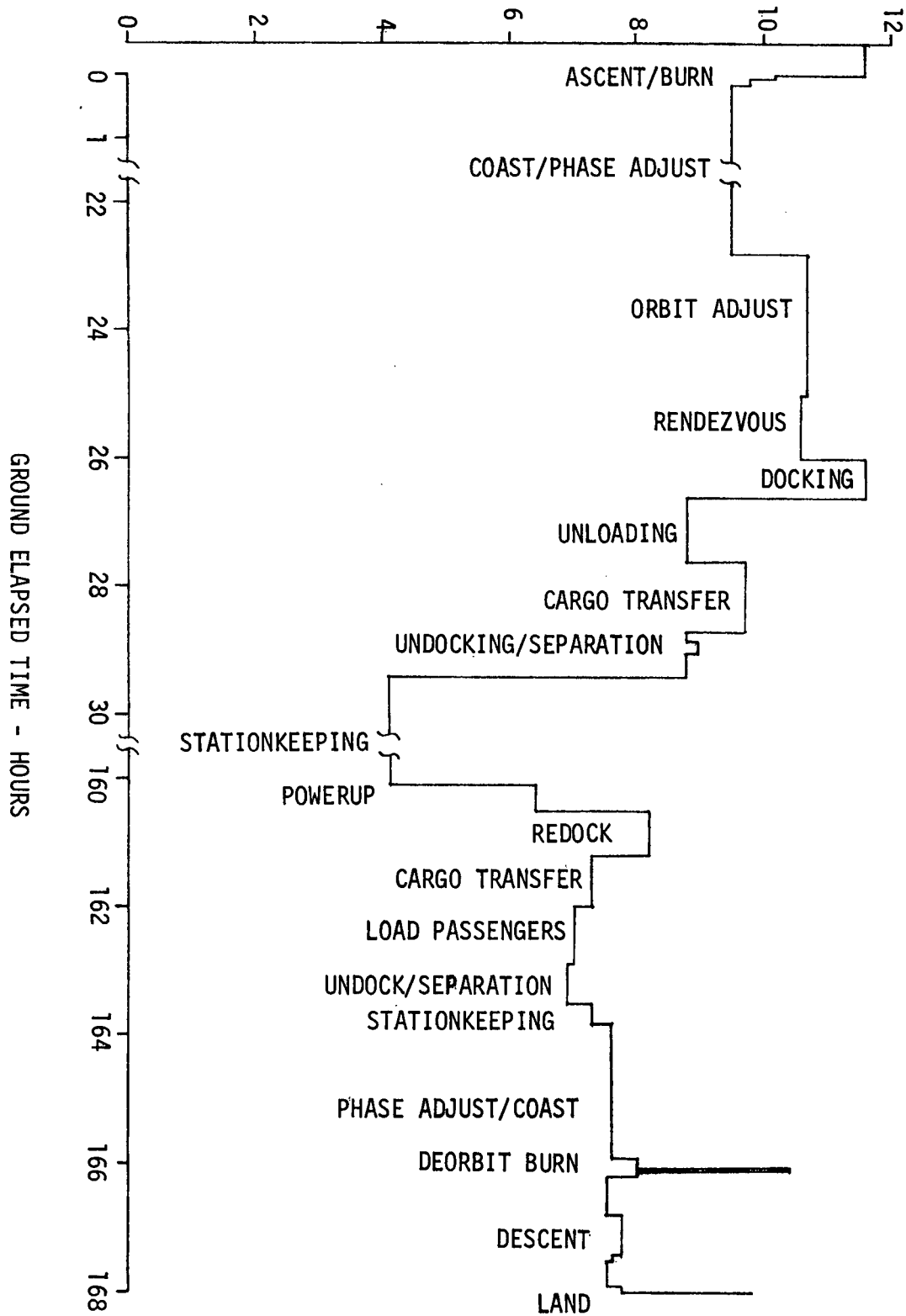
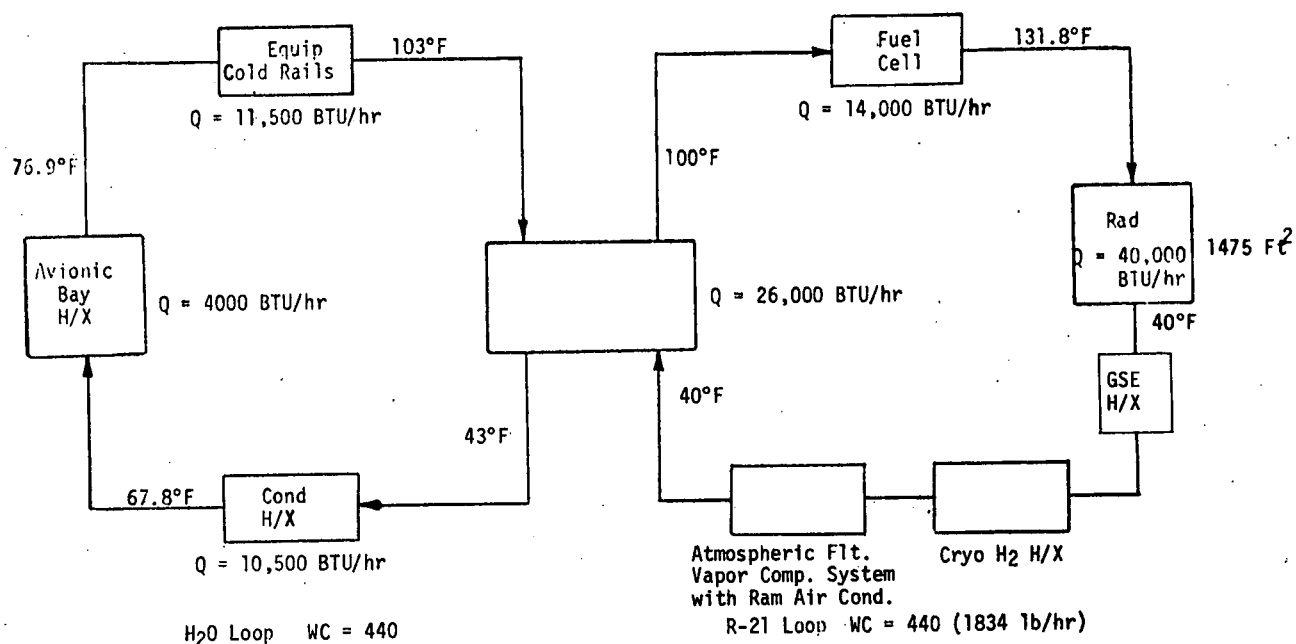


FIGURE 73 TYPICAL ORBITER POWER PROFILE

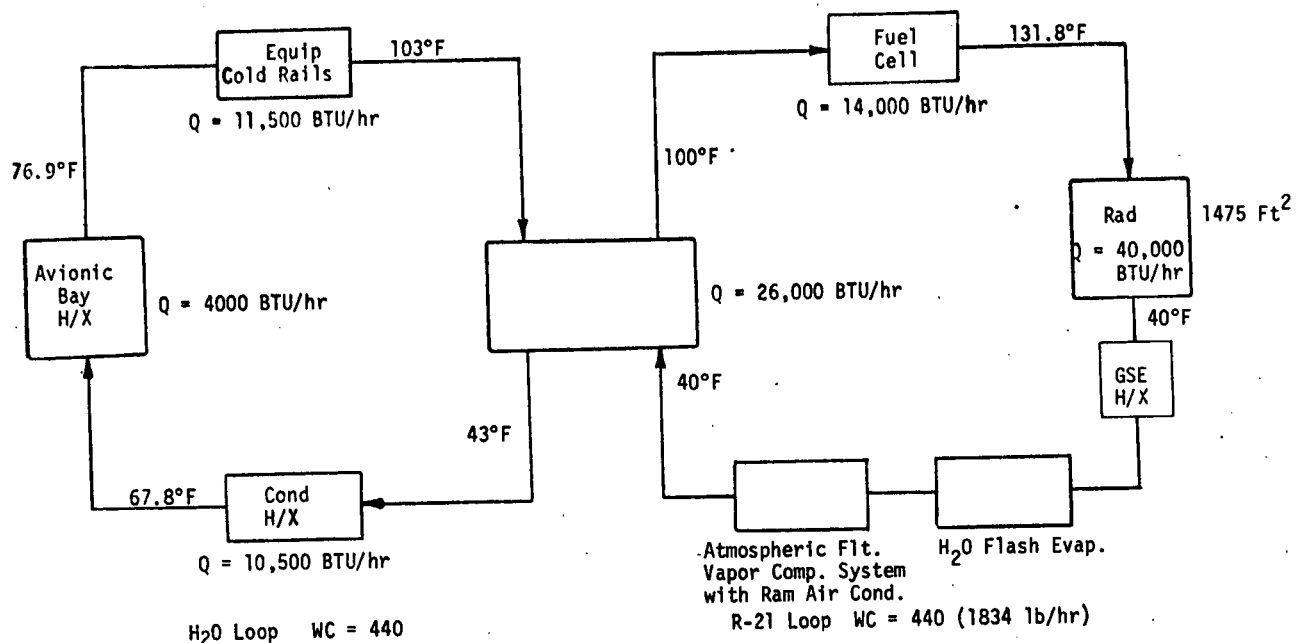


Note: Conditions shown are for powered up orbit phase.

BASELINE SYSTEM

MISSION PHASE	DURATION HRS	HEAT LOAD		HEAT REJECTION SYSTEM	WEIGHT LB
		BTU/HR	KW		
Pre-Launch	2.0	44,000	12.89	GSE Heat Exchanger	20
Launch					
Ascent	0.15	32,000	9.37	Heat Capacity	-
Pre Rad	0.85	40,000	11.72	Expendable H ₂	33
Abort	48.0	40,000	11.72	Expendable H ₂	2125
Orbit					
Power Up	24.0	40,000	11.72	Space Radiator (1475 ft ²)	727
Power Down	141.0	20,000	5.86	Space Radiator	-
Reentry					
DeOrbit	1.12	34,000	9.96	Expendable H ₂	37
Transition	0.13	34,000	9.96	Heat Capacity	-
Flyback	0.5	45,000	13.18	Vapor Compression System with ram air cond.	623
Postlanding	1.0	45,000	13.18	Vapor Compression System with forced air cond.	91
					<u>3656</u>

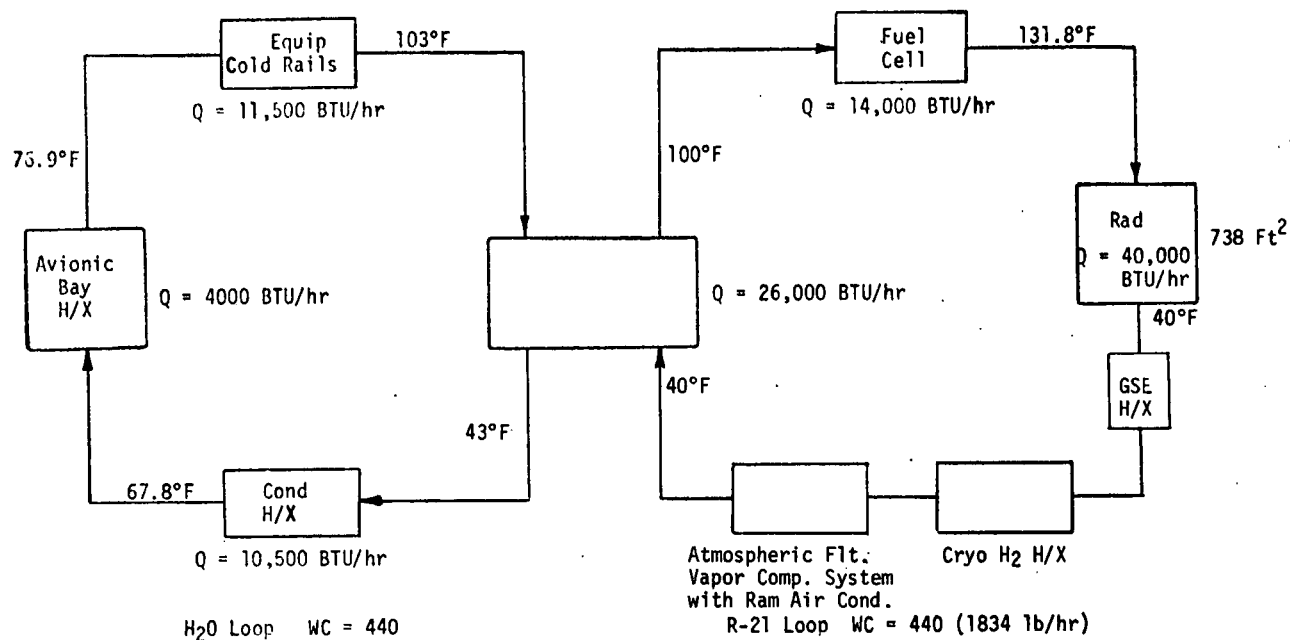
FIGURE 74 BASE LINE EC/LSS HEAT REJECTION SYSTEM



CONFIGURATION 1

MISSION PHASE	DURATION HRS	HEAT LOAD		HEAT REJECTION SYSTEM	WEIGHT LB
		BTU/HR	KW		
Pre-Launch	2.0	44,000	12.89	GSE Heat Exchanger	20
Launch					
Ascent	0.15	32,000	9.37	Heat Capacity	-
Pre Rad	0.85	40,000	11.72	Expendable H ₂ O	39
Abort	48.0	40,000	11.72	Expendable H ₂ O	2260
Orbit					
Power Up	24.0	40,000	11.72	Space Radiator (1475 ft ²)	727
Power Down	141.0	20,000	5.86	Space Radiator	-
Reentry					
DeOrbit	1.12	34,000	9.96	Excess Fuel Cell H ₂ O	-
Transition	0.13	34,000	9.96	Heat Capacity	-
Flyback	0.5	45,000	13.18	Vapor Compression System	623
Postlanding	1.0	45,000	13.18	Vapor Compression System	91
					3760

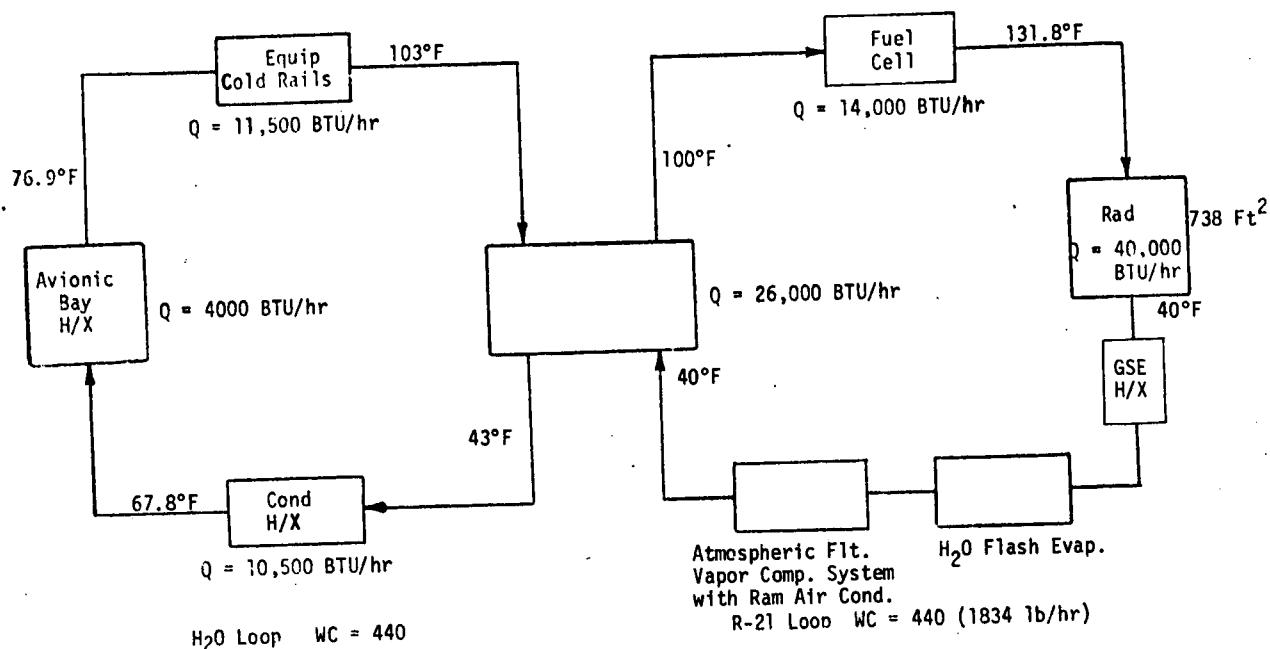
FIGURE 75 EC/LSS HEAT REJECTION SYSTEM - CONFIGURATION 1



CONFIGURATION 2

MISSION PHASE	DURATION HRS	HEAT LOAD		HEAT REJECTION SYSTEM	WEIGHT LB
		BTU/HR	KW		
Pre-Launch	2.0	44,000	12.89	GSE Heat Exchanger	20
Launch					
Ascent	0.15	32,000	9.37	Heat Capacity	-
Pre Rad	0.85	40,000	11.72	Expendable H ₂	33
Abort	48.00	40,000	11.72	Expendable H ₂	2125
Orbit					
Power Up	24.0	40,000	11.72	Space Rad. & Expendable H ₂	469
Power Down	141.0	20,000	5.86	Space Radiator (738 ft ²)	372
Reentry					
DeOrbit	1.12	34,000	9.96	Expendable H ₂	37
Transition	0.13	34,000	9.96	Heat Capacity	-
Flyback	0.5	45,000	13.18	Vapor Compression System	623
Postlanding	1.0	45,000	13.18	Vapor Compression System	91
					<u>3770</u>

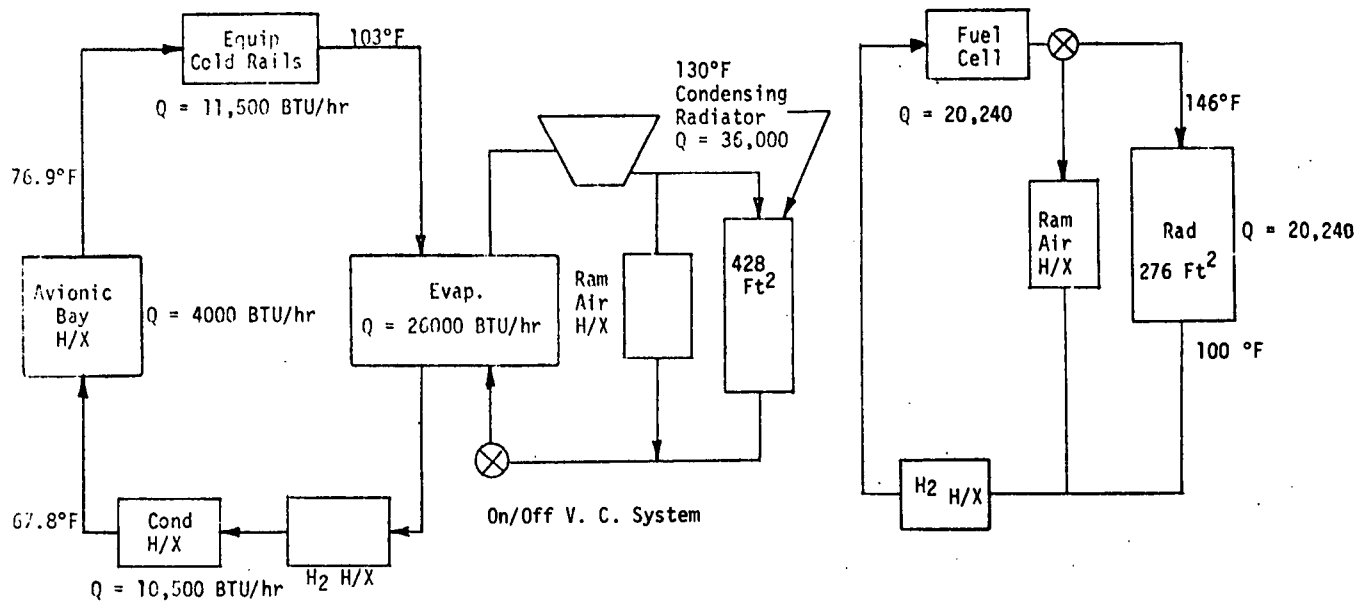
FIGURE 76 EC/LSS HEAT REJECTION SYSTEM - CONFIGURATION 2



CONFIGURATION 3

MISSION PHASE	DURATION HRS	HEAT LOAD		HEAT REJECTION SYSTEM	WEIGHT LB
		BTU/HR	KW		
Pre-Launch	2.0	44,000	12.89	GSE Heat Exchanger	20
Launch					
Ascent	0.15	32,000	9.37	Heat Capacity	-
Pre Rad	0.85	40,000	11.72	Expendable H ₂ O	39
Abort	48.0	40,000	11.72	Expendable H ₂ O	2260
Orbit					
Power Up	24.0	40,000	11.72	Expendable H ₂ O & Space Radiator	552
Power Down	141.0	20,000	5.86	Space Radiator (738 ft ²)	372
Reentry					
DeOrbit	1.12	34,000	9.96	Excess Fuel Cell H ₂ O	-
Transition	0.13	34,000	9.96	Heat Capacity	-
Flyback	0.5	45,000	13.18	Vapor Compression System	623
Postlanding	1.0	45,000	13.18	Vapor Compression System	91
					<u>3957</u>

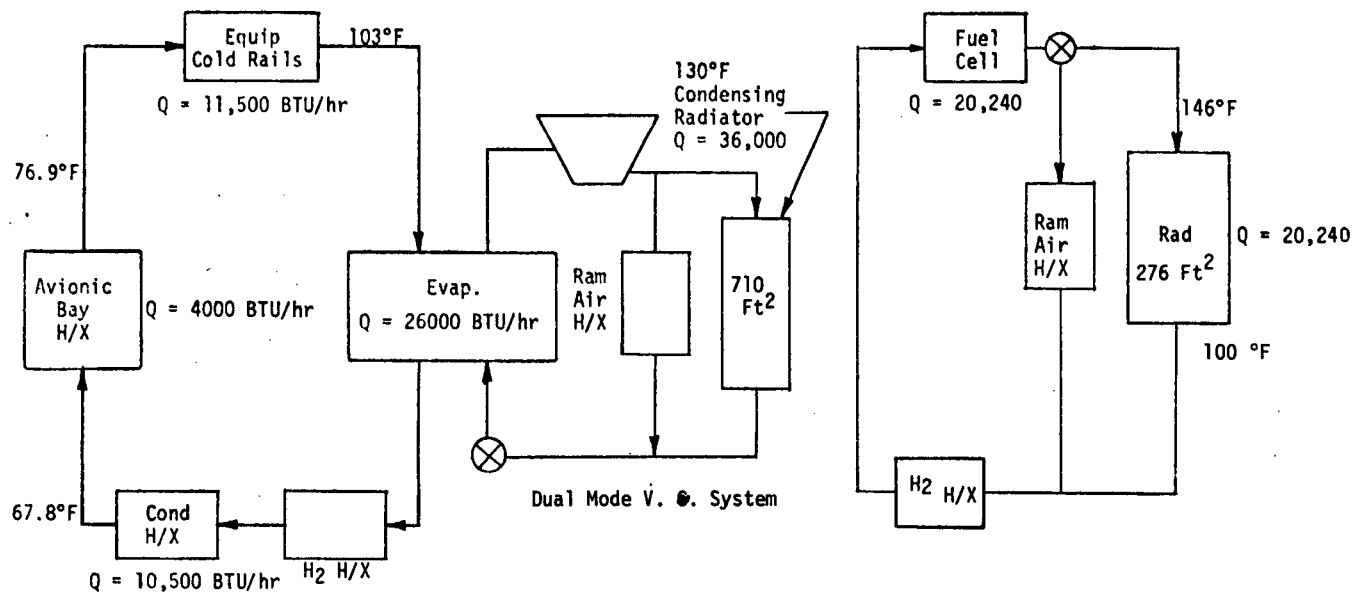
FIGURE 77 EC/LSS HEAT REJECTION SYSTEM - CONFIGURATION 3



CONFIGURATION 4

MISSION PHASE	DURATION HRS	HEAT LOAD		HEAT REJECTION SYSTEM	WEIGHT LB
		BTU/HR	KW		
Pre-Launch	2.0	44,000	12.89	GSE Electrical Power	-
Launch					
Ascent	0.15	32,000	9.37	Heat Capacity	-
Pre Rad	0.85	40,000	11.72	Expendable H ₂	33
Abort	48.0	40,000	11.72	Expendable H ₂	2125
Orbit					
Power Up	24.0	40,000	11.72	V.C. system with on/off control separate F.C. radiator	865 - 1937
Power Down	141.0	20,000	5.86		
Reentry					
DeOrbit	1.12	34,000	9.96	Expendable H ₂	37
Transition	0.13	34,000	9.96	Heat Capacity	-
Flyback	0.5	45,000	13.18	V.C. system with ram air cond. & ram air fuel cell cooling	196
Postlanding	1.0	45,000	13.18	V.C. system with forced air condenser & fuel cell cooling	45
					3301 - 4373

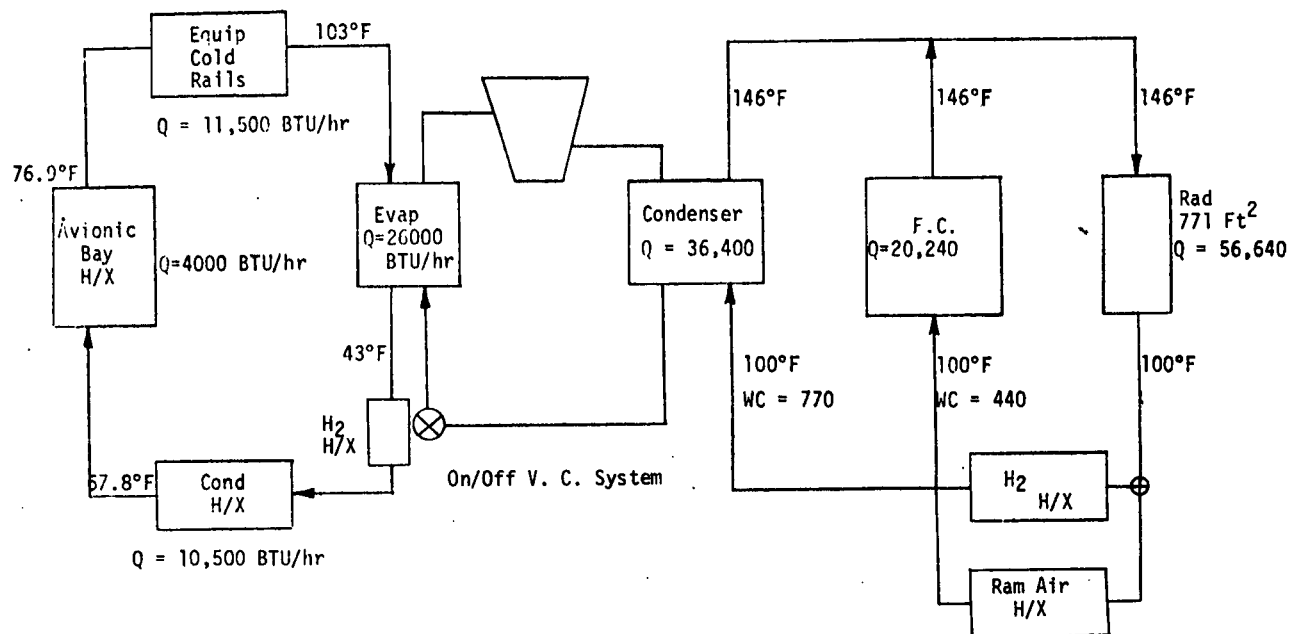
FIGURE 78 EC/LSS HEAT REJECTION SYSTEM - CONFIGURATION 4



CONFIGURATION 5

MISSION PHASE	DURATION HRS	HEAT LOAD		HEAT REJECTION SYSTEM	WEIGHT LB
		BTU/HR	KW		
Pre-Launch	2.0	44,000	12.89	GSE Electrical Power	-
Launch					
Ascent	0.15	32,000	9.37	Heat Capacity	-
Pre Rad	0.85	40,000	11.72	Expendable H ₂	33
Abort	48.0	40,000	11.72	Expendable H ₂	2125
Orbit					
Power Up	24.0	40,000	11.72	Dual mode V.C. system separate F.C. radiator	744 - 1723
Power Down	141.0	20,000	5.86		
Reentry					
DeOrbit	1.12	34,000	9.96	Expendable H ₂	37
Transition	0.13	34,000	9.96	Heat Capacity	-
Flyback	0.5	45,000	13.18	V.C. system with ram air cond. & ram air F.C. cooling	196
Postlanding	1.0	45,000	13.18	V.C. system with forced air cond. and F.C. cooling	45
					3180 - 4159

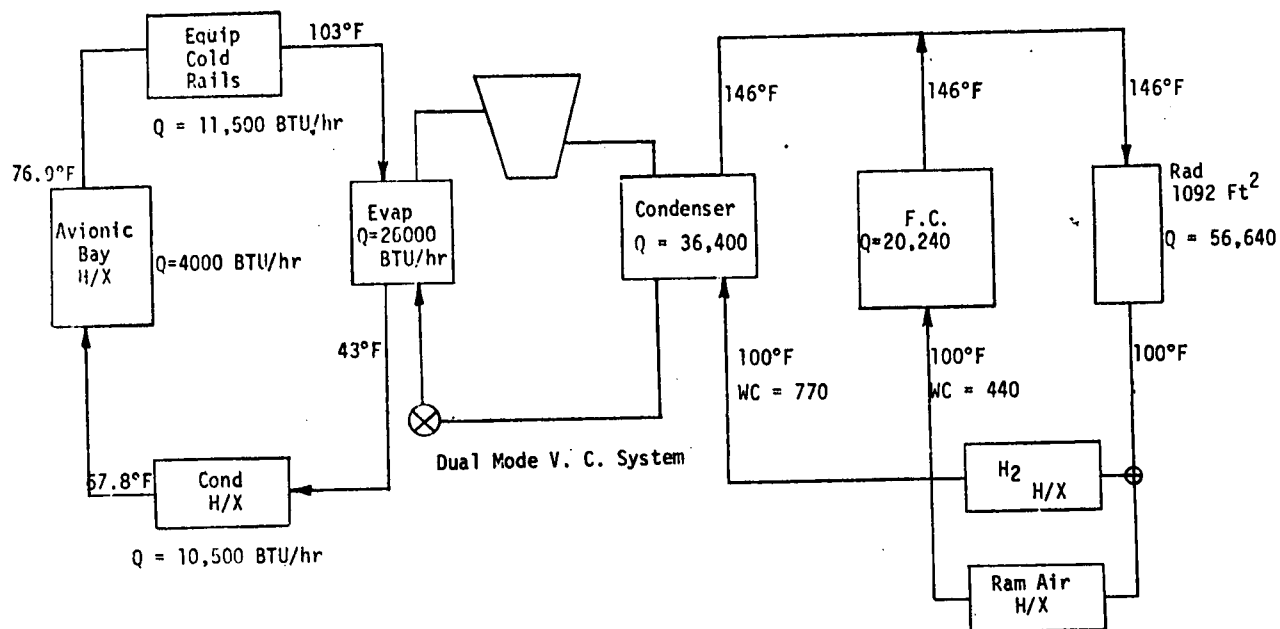
FIGURE 79 EC/LSS HEAT REJECTION SYSTEM - CONFIGURATION 5



CONFIGURATION 6

MISSION PHASE	DURATION HRS	HEAT LOAD		HEAT REJECTION SYSTEM	WEIGHT LB
		BTU/HR	KW		
Pre-Launch	2.0	44,000	12.89	GSE Electrical Power	-
Launch					
Ascent	0.15	32,000	9.37	Heat Capacity	-
Pre Rad	0.85	40,000	11.72	Expendable H ₂	33
Abort	48.0	40,000	11.72	Expendable H ₂	2125
Orbit					
Power Up	24.0	40,000	11.72	V.C. system with on/off control	897 - 1979
Power Down	141.0	20,000	5.86		
Reentry					
DeOrbit	1.12	34,000	9.96	Expendable H ₂	37
Transition	0.13	34,000	9.96	Heat Capacity	-
Flyback	0.5	45,000	13.18	V.C. system with ram air cooling	196
Postlanding	1.0	45,000	13.18	V.C. system with forced air cooling	45
					3333 - 4415

FIGURE 80 EC/LSS HEAT REJECTION SYSTEM - CONFIGURATION 6

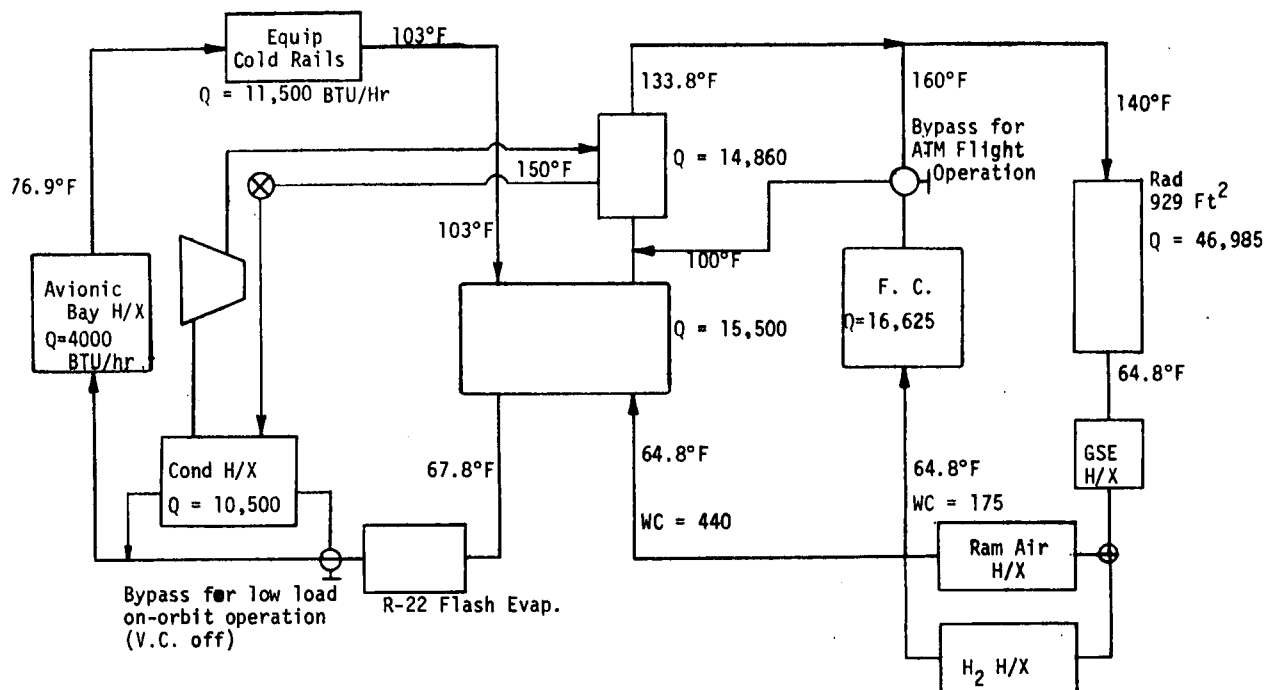


CONFIGURATION 7

MISSION PHASE	DURATION HRS	HEAT LOAD		HEAT REJECTION SYSTEM	WEIGHT LB
		BTU/HR	KW		
Pre-Launch	2.0	44,000	12.89	GSE electrical supply	-
Launch					
Ascent	0.15	32,000	9.37	Heat Capacity	-
Pre Rad	0.85	40,000	11.72	Expendable H ₂	33
Abort	48.0	40,000	11.72	Expendable H ₂	2125
Orbit					
Power Up	24.0	40,000	11.72	Dual mode V.C. system	794 - 1773
Power Down	141.0	20,000	5.86		
Reentry					
DeOrbit	1.12	34,000	9.96	Expendable H ₂	37
Transition	0.13	34,000	9.96	Heat Capacity	-
Flyback	0.5	45,000	13.18	V.C. system with ram air cooling	196
Postlanding	1.0	45,000	13.18	V.C. system with forced air cooling	45
					3230-4209

FIGURE 81 EC/LSS HEAT REJECTION SYSTEM - CONFIGURATION 7

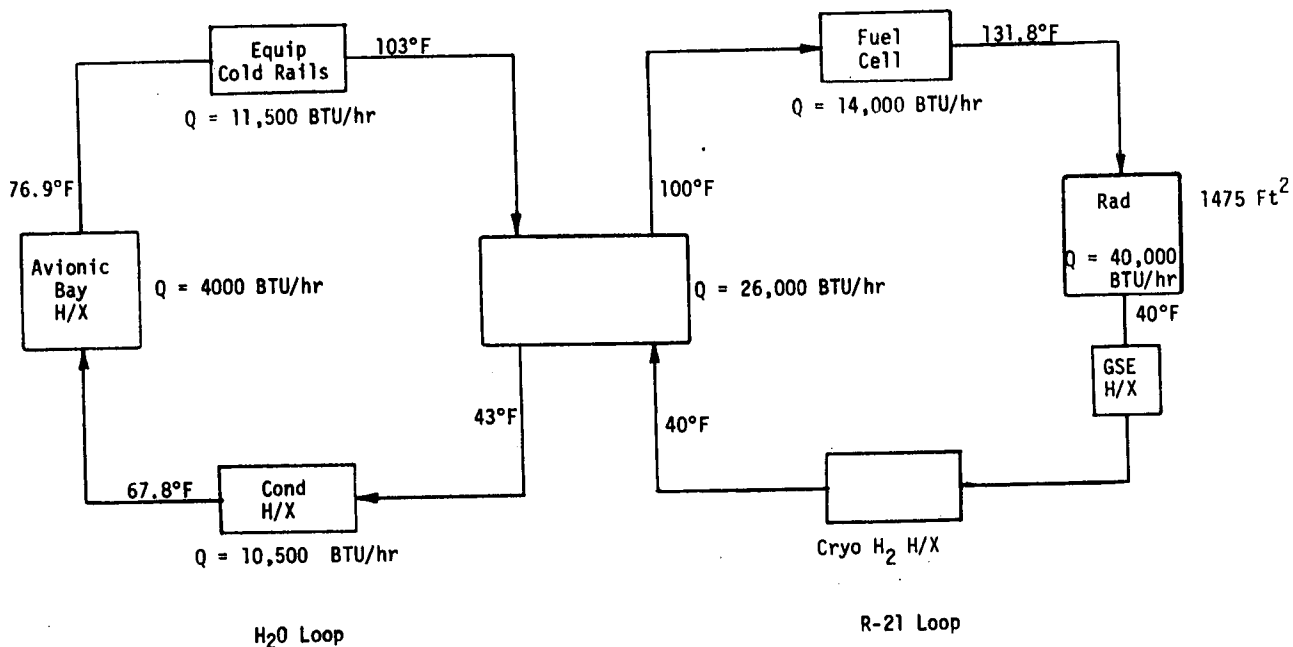
F



CONFIGURATION 8

MISSION PHASE	DURATION HRS	HEAT LOAD		HEAT REJECTION SYSTEM	WEIGHT LB
		BTU/HR	KW		
Pre-Launch	2.0	44,000	12.89	GSE heat exchanger	20
Launch					
Ascent	0.15	32,000	9.37	Heat Capacity	-
Pre Rad	0.85	40,000	11.72	Expendable H ₂	33
Abort	48.0	40,000	11.72	Expendable H ₂	2125
Orbit					
Power Up	24.0	40,000	11.72	Partial load V.C. system & rad.	257 - 973
Power Down	141.0	20,000	5.86	Space rad.	-
Reentry					
DeOrbit	1.12	34,000	9.96	Expendable H ₂	37
Transition	0.13	34,000	9.96	Heat Capacity	-
Flyback	0.5	45,000	13.18	Ram air cooled F.C. & cabin V.C. system cond. Expendable R-22	261
Postlanding	1.0	45,000	13.18	Forced air cooled F.C. & cabin V.C. syst. cond. Expendable R-22	292
					3025-3741

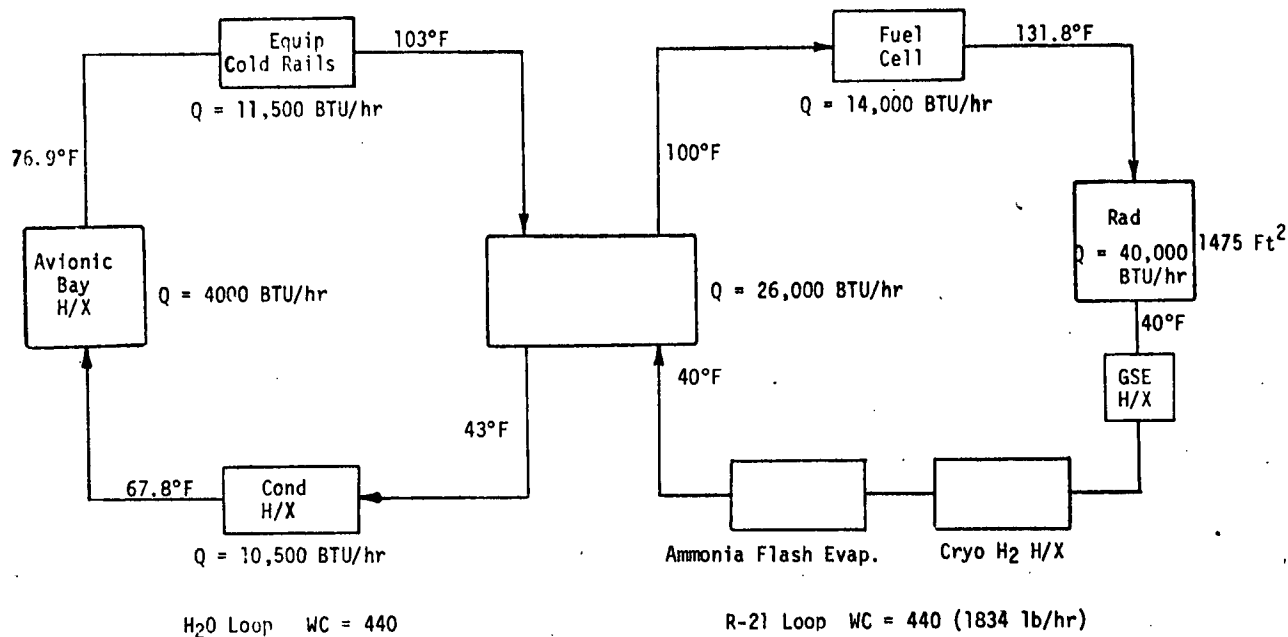
FIGURE 82 EC/LSS HEAT REJECTION SYSTEM - CONFIGURATION 8



CONFIGURATION 9

MISSION PHASE	DURATION HRS	HEAT LOAD		HEAT REJECTION SYSTEM	WEIGHT LB
		BTU/HR	KW		
Pre-Launch	2.0	44,000	12.89	GSE Heat exchanger	20
Launch					
Ascent	0.15	32,000	9.37	Heat Capacity	-
Pre Rad	0.85	40,000	11.72	Expendable H ₂	33
Abort	48.0	40,000	11.72	Expendable H ₂	2125
Orbit					
Power Up	24.0	40,000	11.72	Space Radiator	727
Power Down	141.0	20,000	5.86	Space Radiator	-
Reentry					
DeOrbit	1.12	34,000	9.96	Expendable H ₂	37
Transition	0.13	34,000	9.96	Heat Capacity	-
Flyback	0.5	45,000	13.18	Expendable H ₂	23
Postlanding	1.0	45,000	13.18	Expendable H ₂	46
					<u>3011</u>

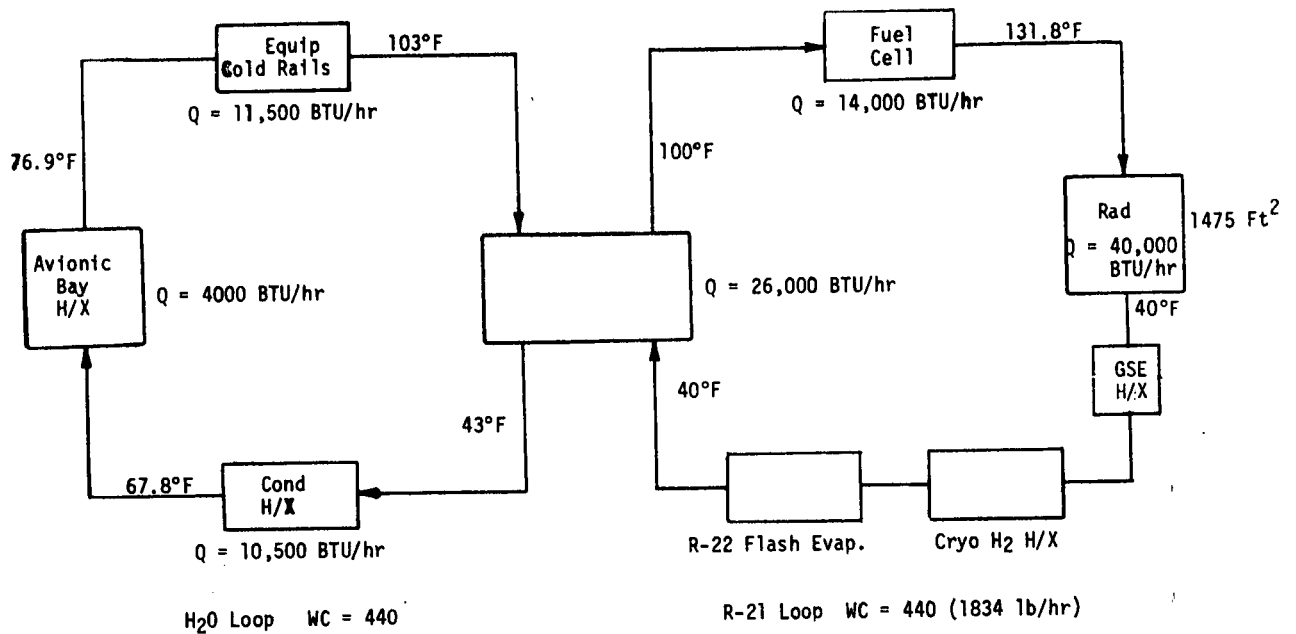
FIGURE 83 EC/LSS HEAT REJECTION SYSTEM - CONFIGURATION 9



CONFIGURATION 10

MISSION PHASE	DURATION HRS	HEAT LOAD		HEAT REJECTION SYSTEM	WEIGHT LB
		BTU/HR	KW		
Pre-Launch	2.0	44,000	12.89	GSE heat exchanger	20
Launch					
Ascent	0.15	32,000	9.37	Heat Capacity	-
Pre Rad	0.85	40,000	11.72	Expendable H ₂	33
Abort	48.0	40,000	11.72	Expendable H ₂	2125
Orbit					
Power Up	24.0	40,000	11.72	Space radiator	727
Power Down	141.0	20,000	5.86	Space radiator	-
Reentry					
DeOrbit	1.12	34,000	9.96	Expendable H ₂	37
Transition	0.13	34,000	9.96	Heat capacity	-
Flyback	0.5	45,000	13.18	Expendable ammonia	112
Postlanding	1.0	45,000	13.18	Expendable ammonia	134
					<u>3188</u>

FIGURE 84 EC/LSS HEAT REJECTION SYSTEM - CONFIGURATION 10



CONFIGURATION 11

MISSION PHASE	DURATION HRS	HEAT LOAD		HEAT REJECTION SYSTEM	WEIGHT LB
		BTU/HR	KW		
Pre-Launch	2.0	44,000	12.89	GSE Heat Exchanger	20
Launch					
Ascent	0.15	32,000	9.37	Heat Capacity	-
Pre Rad	0.85	40,000	11.72	Expendable H ₂	33
Abort	48.0	40,000	11.72	Expendable H ₂	2125
Orbit					
Power Up	24.0	40,000	11.72	Space Radiator (1475 ft ²)	727
Power Down	141.0	20,000	5.86	Space Radiator	-
Reentry					
DeOrbit	1.12	34,000	9.96	Expendable H ₂	37
Transition	0.13	34,000	9.96	Heat Capacity	-
Flyback	0.5	45,000	13.18	Expendable R-22	430
Postlanding	1.0	45,000	13.18	Expendable R-22	770
					<u>4142</u>

FIGURE 85 EC/LSS HEAT REJECTION SYSTEM - CONFIGURATION 11

APPENDIX A

REFRIGERATION SYSTEMS PLOTTING AND LINEARIZED

ANALYSIS TECHNIQUE (RSPLAT)

PARAMETRIC WEIGHT ANALYSES

Computer Program Description

The RSPLAT computer routine is designed to provide a means for comparing specific types of refrigeration systems on a total system weight basis. The weight estimates which are calculated by this routine are functions of seven quantities which can be defined to characterize any probable shuttle application:

- TEVAP, heat absorption temperature (°F)
- TSINK, radiation sink temperature (°F)
- EPP, electrical power weight penalty (lb/KW_{elec})
- RADP, radiator/atmospheric convector area weight penalty (lb/ft²)
- WRAM, ram air penalty (lb/KW)
- ALT, altitude, (ft.)
- M, Mach number

The output of this routine is a set of computer plotted curves. Total system weight (including assigned penalties) is computed and plotted as a function of radiator (heat rejection) temperature (TRAD). The optimum heat rejection temperature for the specified conditions is then determined from the minimum weight point for each system analyzed. The total system weight (WT) calculated for each system at any particular set of environment conditions is the sum of four terms. These include the weight quantities contributed by the electrical power penalty (EPPT), the radiator weight penalty (RPT), the fixed weight quantity (FWT), and the ram air penalty (WRAM).

$$WT = EPPT + RPT + FWT + WRAM \text{ (LB/KW)} \quad (A-1)$$

Each of these terms is computed using the parameters that describe the system. The electrical power term is found by:

$$EPPT = EPP \left(\frac{1}{COP} \right) \text{ (lb/KW)} \quad (A-2)$$

The radiator penalty is given by:

$$RPT = \left(1 + \frac{1.6}{COP} \right) \left(\frac{FRAP}{QREJ} \right) \text{ (lb/KW)} \quad (A-3)$$

where heat rejected through the radiator per unit area is:

$$Q_{REJ} = .0000401 \left[\left(\frac{TRAD + 460^4}{100} \right) - \left(\frac{TSINK + 460^4}{100} \right) \right] \quad (A-4)$$

$$+ .000293 (HTC) [TRAD - TAMB] (KW/ft^2)$$

The first term in equation A-4 is the amount of heat rejected by radiation and is applicable to both orbital and atmospheric environments. The second term is the amount of heat rejected by convection and is only applicable to the flyback phase. TSINK is input for the earth orbit analyses and is computed by the routine for the atmospheric flight analyses for the input altitude. The radiator/convactor was assumed to be located over a 120° circular arc looking directly at the sun. Radiation sink temperatures were calculated at zero altitude and for orbit conditions. It was assumed that the orbit sink temperatures applied for altitudes greater than 50,000 ft. and a linear interpolation was used for altitudes between zero and 50,000 ft.

TAMB in equation A-4 is the ambient air temperature. This value is determined by the routine as a function of altitude for MIL-STD-210A hot or cold day or the U.S. Standard Atmosphere. A hot day atmosphere was specified for the parametric weight analysis.

An empirical expression derived from Reference A-1 is used to compute the heat transfer coefficient for the atmospheric convactor:

$$HTC = \frac{(3.03 + 44.9 M) (1.25 - .0005 TRAD) (1.04 - .00023 VEL)}{38.3^{(ALT \times 10^{-5})}} \quad (A-5)$$

(BTU/hr-ft²°F)

The evaluation of the ram air penalty is made on the basis of no jet engines during the atmospheric flyback. A widely used method of determining the ram air penalty for aircraft is to determine the additional weight of fuel required for the propulsion system to overcome the drag induced by the ram air system. Since the orbiter will not have a propulsion system during the atmospheric flyback, the following method was used: It was assumed that the vehicle design lift to drag (L/D) ratio would have to be maintained and could not be changed by the EC/LSS heat rejection system. Therefore, the ram air penalty was taken as the weight of additional lifting

surfaces required to maintain the same L/D ratio. The drag is computed from the momentum change of the ram air by

$$D = \frac{\dot{w}_a}{g_c} (V_1 - V_2) \quad (A-6)$$

where:

- \dot{w}_a = the required ram air flow, lb/hr
- V_1 = free stream velocity, ft/hr
- V_2 = Exit velocity (assumed to be 1/6 of free stream), ft/hr
- g_c = gravitational constant, lbm-hr²/lbf ft.

The ram air flow requirements are determined by

$$\dot{w}_a = \frac{Q_{\text{cond}}}{C_p(T_{\text{out}} - T_{\text{amb}})} \quad (A-7)$$

where:

- Q_{cond} = condenser heat load, BTU/hr
 - C_p = air specific heat, BTU/lb°F
 - T_{amb} = $T_{\text{AMB}} (1 + .2M^2)$
- and T_{out} is computed from

$$T_{\text{out}} = T_{\text{amb}} - \epsilon (T_{\text{amb}} - T_{\text{cond}}) \quad (A-8)$$

where ϵ is the heat exchanger effectiveness

Reference A-2 reports that during subsonic flight, 90% of the low cross range (stubby wing) shuttle lift is provided by the wing. All of the additional required lift was assumed to be provided by additional wing area. For this analysis a constant L/D of 6.0, a wing loading of 90 lb/ft² and a wing weight of 8.5 lb/ft² was used. From the known drag, and above parameters, the weight of the additional wing can be determined.

The ram air condenser weight was computed by the method presented in Reference A-3 and previously discussed in the section describing the vapor compression system component weight determination. Redundant heat exchangers are included. The ram air duct weights were determined by computing the

required flow area, based on the ambient density and flow rate. The duct length was assumed to be 10 feet and a circular cross section with an aluminum gage thickness of .1 inch was used. A weight penalty of 1.0 lb/KW is used for the hydraulic actuated doors to open the ram air system after reentry.

The resulting expression for the ram air penalty is

$$\begin{aligned} \text{WRAM} = & 32.7 \left[\frac{1 + \frac{1.6}{\text{COP}}}{(\rho) (\text{VEL}) (\text{TRD} - \text{TAMB}) \epsilon} \right]^{.5} + \frac{.0579 (1 + \frac{1.6}{\text{COP}}) (\text{VEL})}{(\text{TRD} - \text{TAMB}) \epsilon} \\ & + \frac{66.4}{(1 - \epsilon)} \left[\frac{1 + \frac{1.6}{\text{COP}}}{\text{TRD} - \text{TAMB}} \right]^{.882} \end{aligned} \quad (\text{A-9})$$

where ρ is the air density in lb/ft^3 , a function of the input altitude, and VEL is the velocity in ft/sec, computed from the input Mach number and altitude.

Analysis

The system characteristics (operating COP and fixed weight) were input to the routine and parametric analyses conducted to determine the optimum system operating temperatures and weight. The specific parameters considered are given in Table A-1. Additional parameters have been considered, but are not presented here due to the large number of curves. The results of all parameters considered are summarized in the main body of this report. The parameters presented herein should cover the range of values expected for the Orbiter.

The system operating COP is input to the routine as a function of the difference between the heat rejection temperature and the heat absorption temperature (TRAD-TEVAP). This data is taken from Paragraphs 3.1.3 and 3.2.3 of the main body of this report. The fixed weight for each of the candidate systems is established in Paragraphs 3.1.4 and 3.2.4 and includes the Orbiter required component redundancy.

In computing the system weight the routine begins at a radiator temperature equal to the evaporator or sink temperature, whichever is larger, and calculates weight totals at fixed increments of radiator temperature until an input maximum temperature value (TMAX) is exceeded. Each point for a system curve is then plotted. Because this routine computes and plots total system weights as a function of heat rejection temperature, lowest system weight for

TABLE A-1

PARAMETERS USED IN REFRIGERATION SYSTEM PARAMETRIC ANALYSIS

ORBITAL PHASE			FLY BACK PHASE		
$T_{\text{sink}} - ^\circ\text{F}$	Power Penalty lb/kw_e	Rad Penalty lb/ft^2	Altitude $\text{ft} \times 10^{-3}$	Power Penalty lb/kw_e	Rad Penalty lb/ft^2
0	100.	.5	1	10	0
20	200.	.75	10	20	.5
40	300.	1.0	20	30	.75
60	400.		30	40	1.0
	500.		40		
	600.				

any application corresponds to an optimum heat rejection temperature. For individual systems, this minimum point occurs at different temperature values depending on the radiator penalty, electrical power penalty and the radiation sink temperature or altitude. The plot comparison then defines not only the lightest weight system, but the optimum design heat rejection temperature for the particular operating conditions.

Results

Figures A-1 through A-51 present the results of the parametric weight analysis. Use of this data involves establishing the design conditions (radiation sink temperature, power penalty and radiator weight penalty, for the orbit phase, for example) and entering the appropriate plot to determine which of the candidate systems is the lightest weight and the optimum operating temperatures. A linear interpolation can be used if the design conditions do not correspond to the exact parameters considered. Extrapolation of the results beyond the range of parameters is not recommended.

APPENDIX A REFERENCES

- A-1 Harms, R. J., "A Manual For Determining Aerodynamic Heating of High Speed Aircraft, Volume I", Bell Aircraft Corp. Report No. 7006-3352-001, June 1959.
- A-2 North American Rockwell Space Division, "Study of Integral Launch and Reentry Vehicle System Final Report, Volume III Technical Report - Second Phase Environment and Performance", SD-69-573-3, MSC00192, December 1969.
- A-3 Blutt, J. R. and Sadek, S. E., "A Gravity Independent Vapor Absorption Refrigerator", NASA CR-836, July 1967.

FIGURE A-1

- 0 VAPOR COMPRESSION SYSTEM WITH DIRECT CONDENSING RADIATOR
- 1 VAPOR COMPRESSION SYSTEM WITH HX LOOP TO RADIATOR
- 2 GAS CYCLE SYSTEM WITH HX LOOP TO RADIATOR

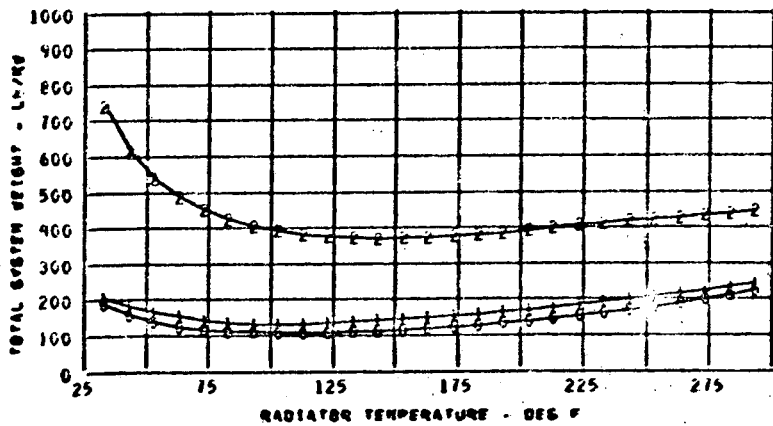
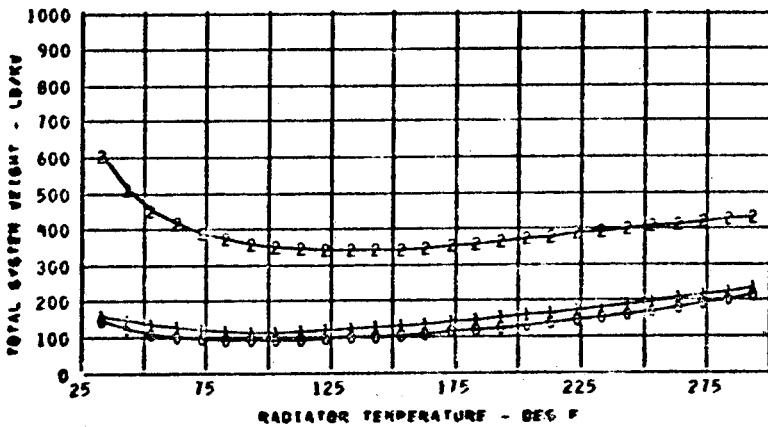
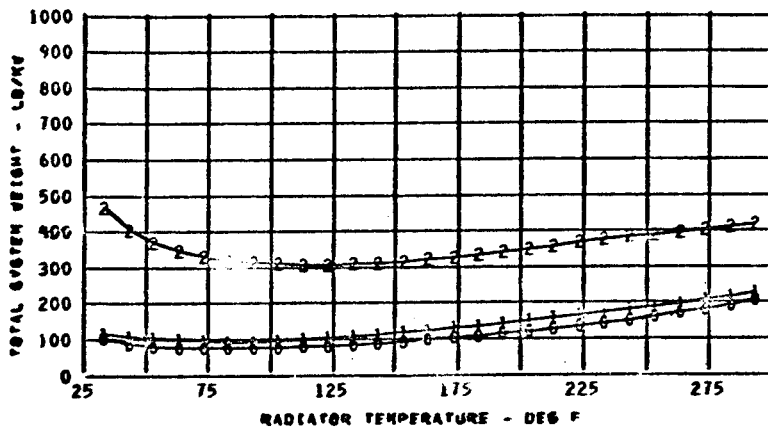
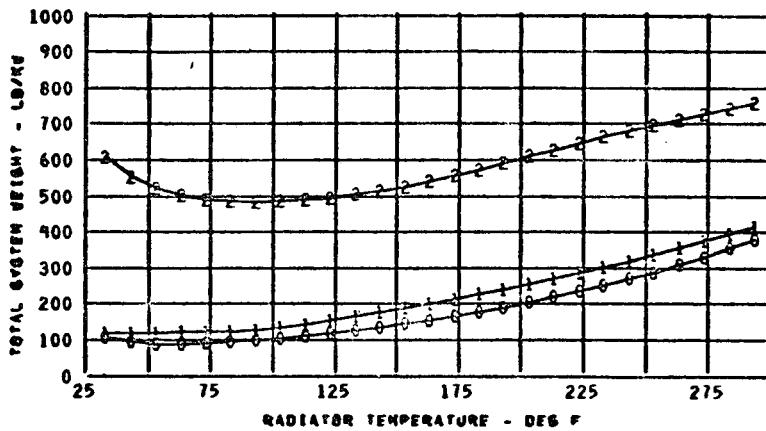
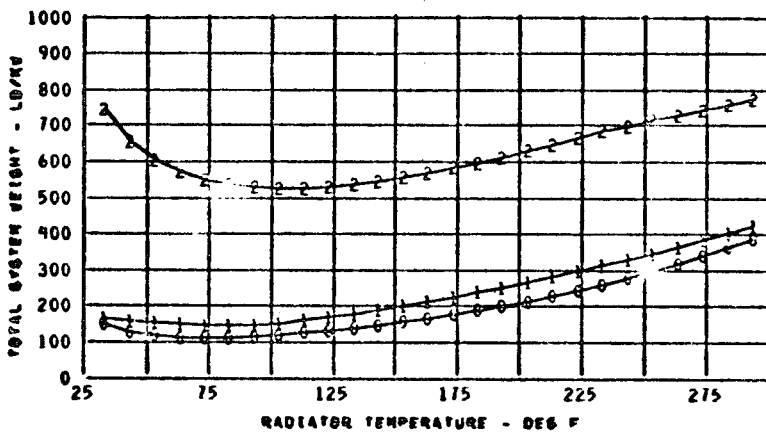


FIGURE A-2

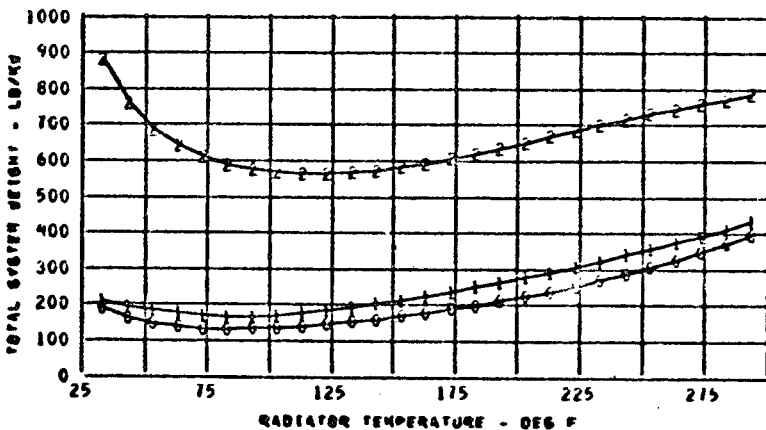
- 0 VAPOR COMPRESSION SYSTEM WITH DIRECT CONDENSING RADIATOR
- 1 VAPOR COMPRESSION SYSTEM WITH HX LOOP TO RADIATOR
- 2 GAS CYCLE SYSTEM WITH HX LOOP TO RADIATOR



TEVAP = 34.0 F
 TSINK = 0.0 F
 EPP = 200.0 LB/KW
 RADP = .50 LB/FT²



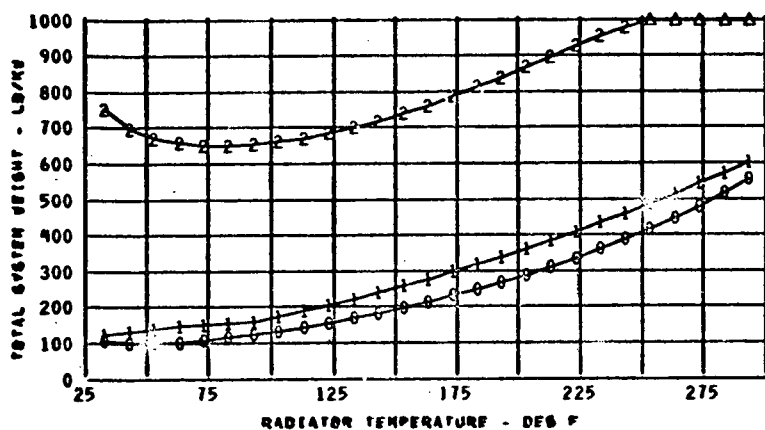
TEVAP = 34.0 F
 TSINK = 0.0 F
 EPP = 200.0 LB/KW
 RADP = .75 LB/FT²



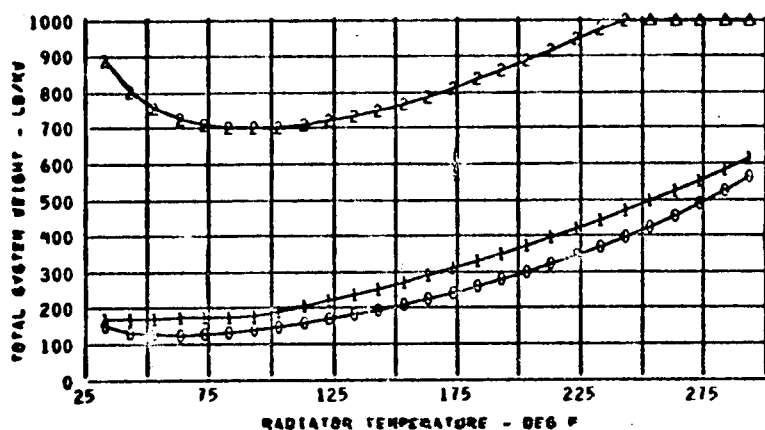
TEVAP = 34.0 F
 TSINK = 0.0 F
 EPP = 200.0 LB/KW
 RADP = 1.0 LB/FT²

FIGURE A-3

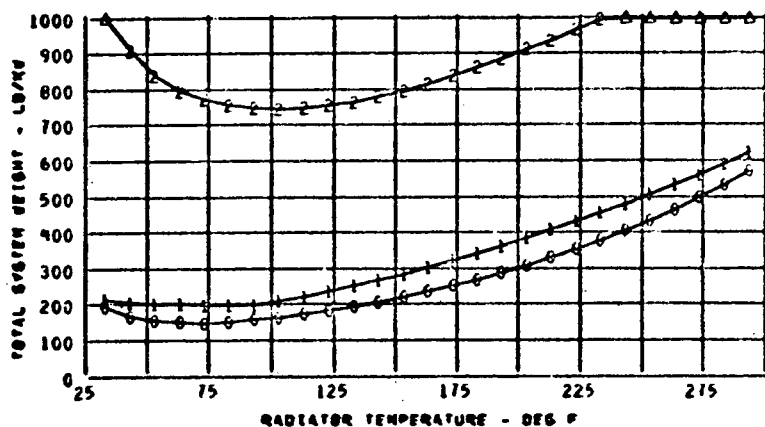
- 0 VAPOR COMPRESSION SYSTEM WITH DIRECT CONDENSING RADIATOR
- 1 VAPOR COMPRESSION SYSTEM WITH HX LOOP TO RADIATOR
- 2 GAS CYCLE SYSTEM WITH HX LOOP TO RADIATOR



TEVAP = 34.0 F
 TSINK = 0.0 F
 EPP = 300.0LB/KW
 RADP = .50LB/FT²



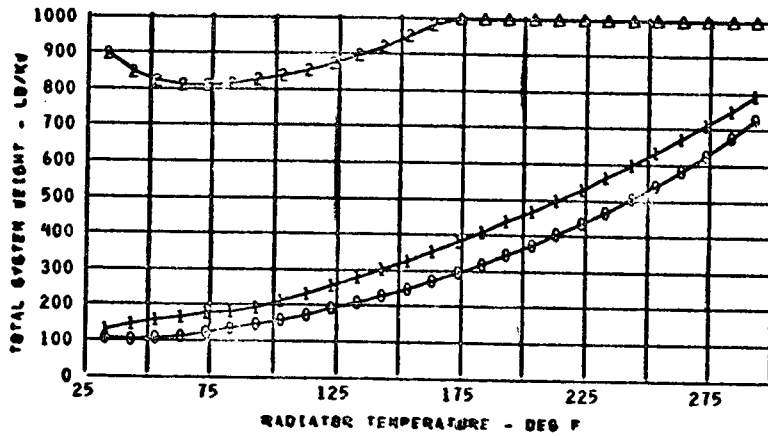
TEVAP = 34.0 F
 TSINK = 0.0 F
 EPP = 300.0LB/KW
 RADP = .75LB/FT²



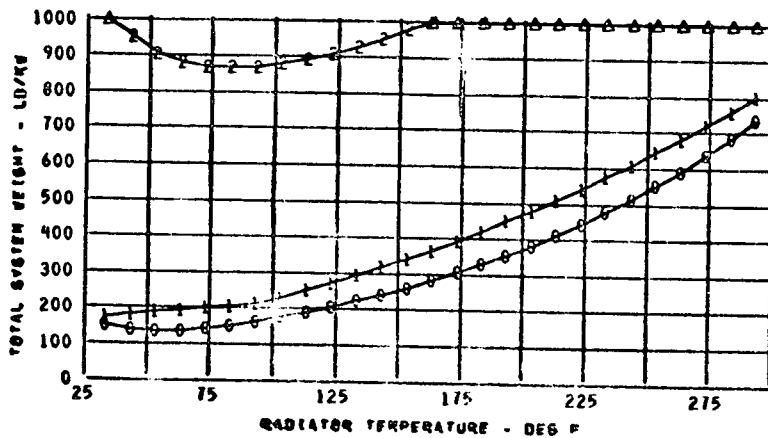
TEVAP = 34.0 F
 TSINK = 0.0 F
 EPP = 300.0LB/KW
 RADP = 1.0LB/FT²

FIGURE A-4

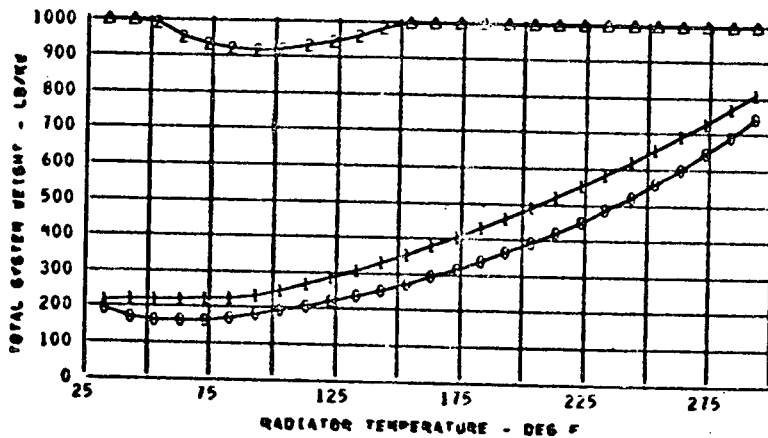
- 0 VAPOR COMPRESSION SYSTEM WITH DIRECT CONDENSING RADIATOR
- 1 VAPOR COMPRESSION SYSTEM WITH HX LOOP TO RADIATOR
- 2 GAS CYCLE SYSTEM WITH HX LOOP TO RADIATOR



TEVAP = 34.0 F
 TSINK = 0.0 F
 EPP = 400.0LB/KW
 RADP = .50LB/FT²



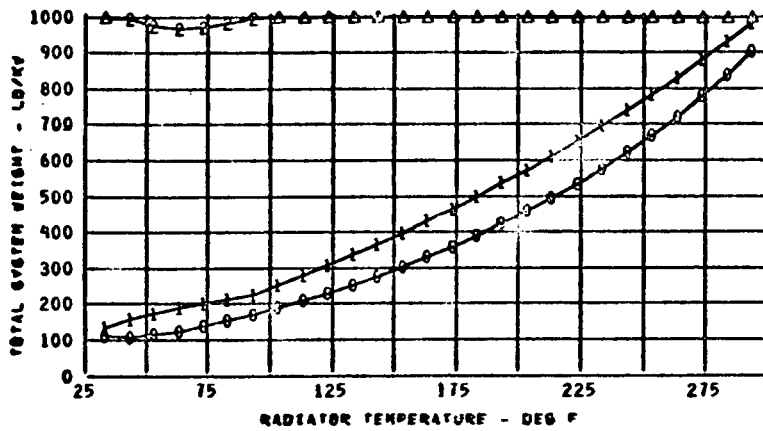
TEVAP = 34.0 F
 TSINK = 0.0 F
 EPP = 400.0LB/KW
 RADP = .75LB/FT²



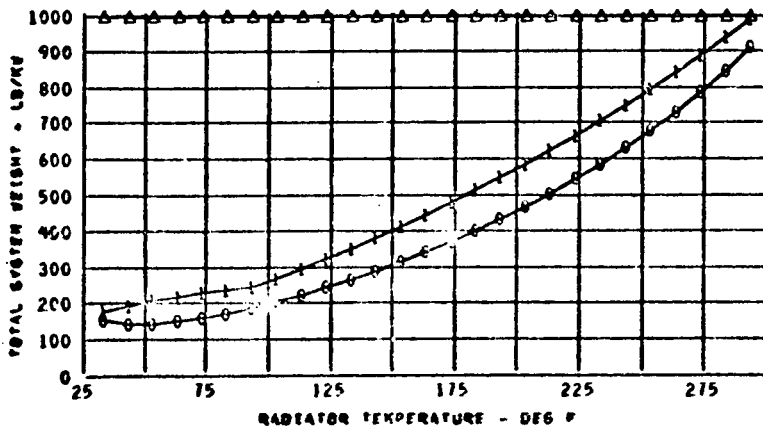
TEVAP = 34.0 F
 TSINK = 0.0 F
 EPP = 400.0LB/KW
 RADP = 1.0LB/FT²

FIGURE A-5

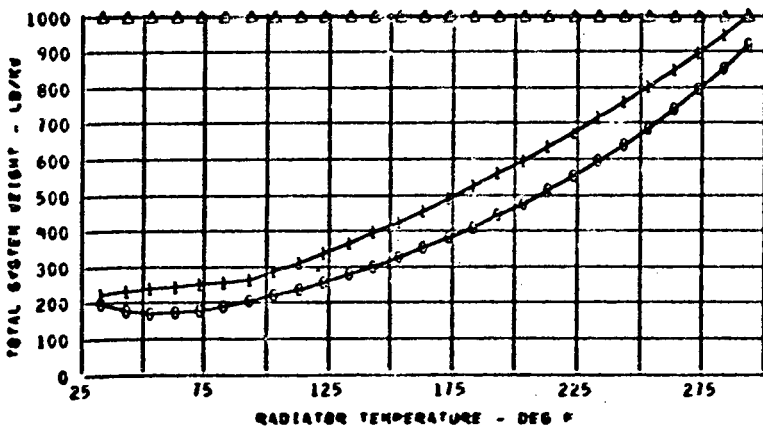
- 0 VAPOR COMPRESSION SYSTEM WITH DIRECT CONDENSING RADIATOR
- 1 VAPOR COMPRESSION SYSTEM WITH HX LOOP TO RADIATOR
- 2 GAS CYCLE SYSTEM WITH HX LOOP TO RADIATOR



TEVAP = 34.0 F
 TSINK = 0.0 F
 EPP = 500.0 LB/KW
 RADP = .50 LB/FT²



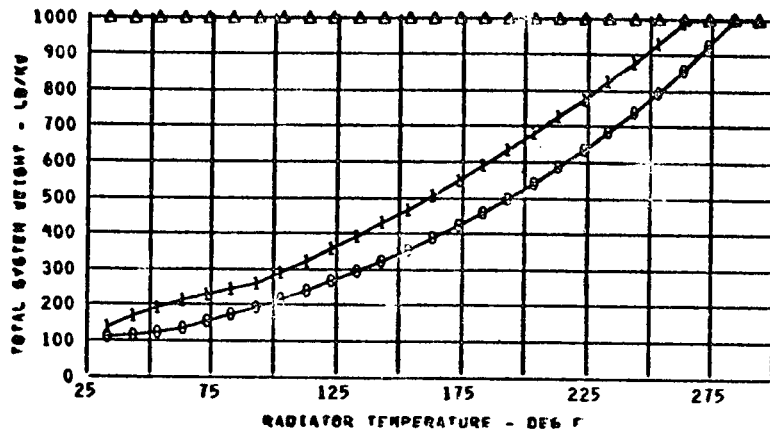
TEVAP = 34.0 F
 TSINK = 0.0 F
 EPP = 500.0 LB/KW
 RADP = .75 LB/FT²



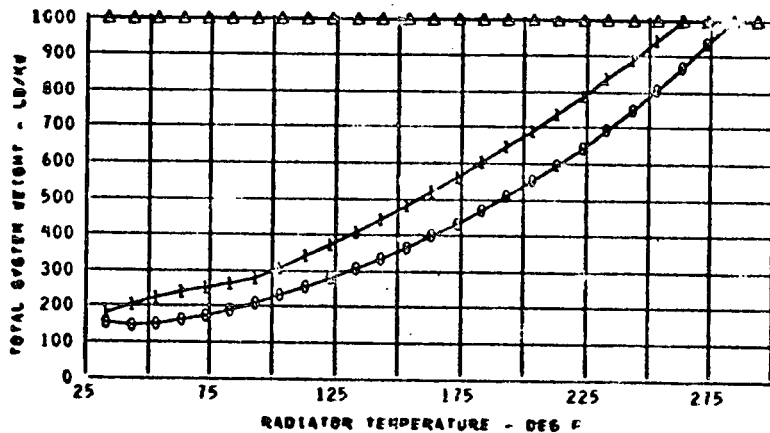
TEVAP = 34.0 F
 TSINK = 0.0 F
 EPP = 500.0 LB/KW
 RADP = 1.0 LB/FT²

FIGURE A-6

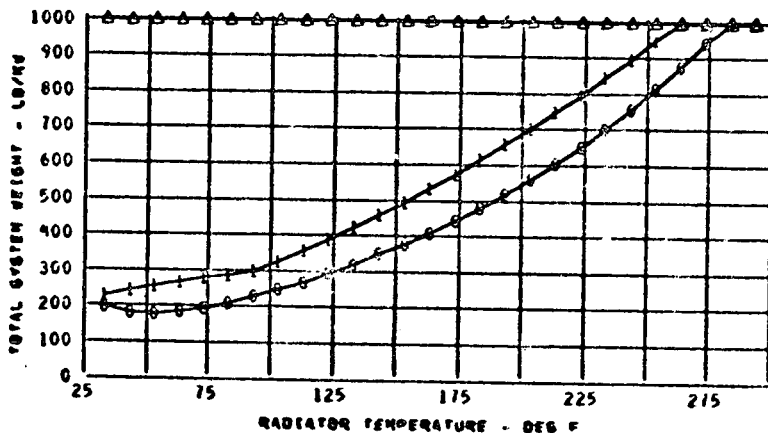
- 0 VAPOR COMPRESSION SYSTEM WITH DIRECT CONDENSING RADIATOR
- 1 VAPOR COMPRESSION SYSTEM WITH HX LOOP TO RADIATOR
- 2 GAS CYCLE SYSTEM WITH HX LOOP TO RADIATOR



TEVAP = 34.0 F
 TSINK = 0.0 F
 EPP = 600.0 LB/KW
 RADP = .50 LB/FT²



TEVAP = 34.0 F
 TSINK = 0.0 F
 EPP = 600.0 LB/KW
 RADP = .75 LB/FT²



TEVAP = 34.0 F
 TSINK = 0.0 F
 EPP = 600.0 LB/KW
 RADP = 1.0 LB/FT²

FIGURE A-7

- 0 VAPOR COMPRESSION SYSTEM WITH DIRECT CONDENSING RADIATOR
- 1 VAPOR COMPRESSION SYSTEM WITH HX LOOP TO RADIATOR
- 2 GAS CYCLE SYSTEM WITH HX LOOP TO RADIATOR

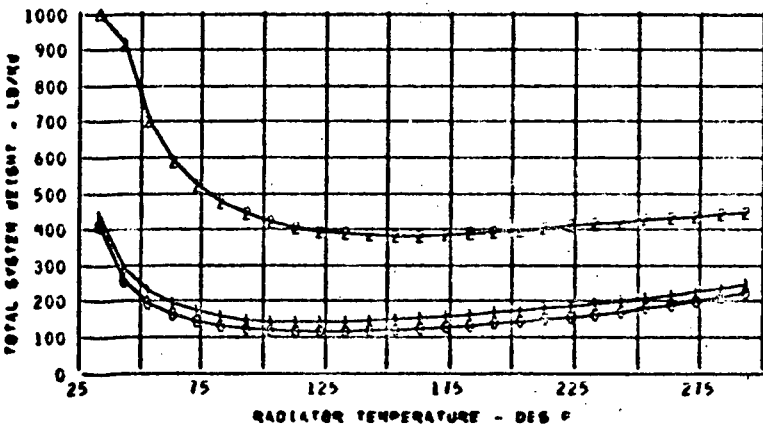
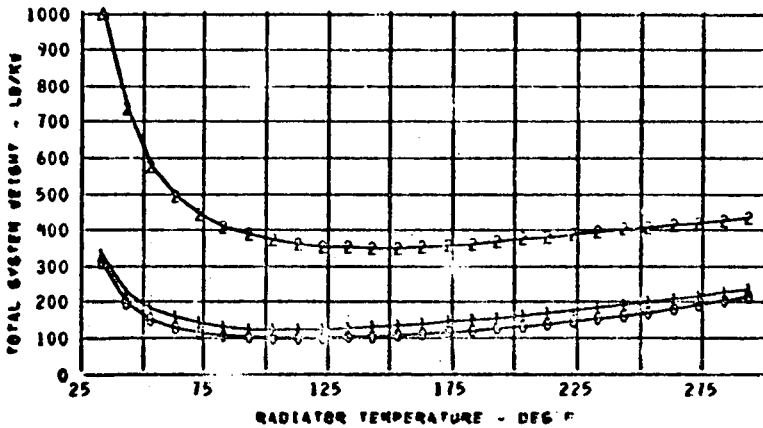
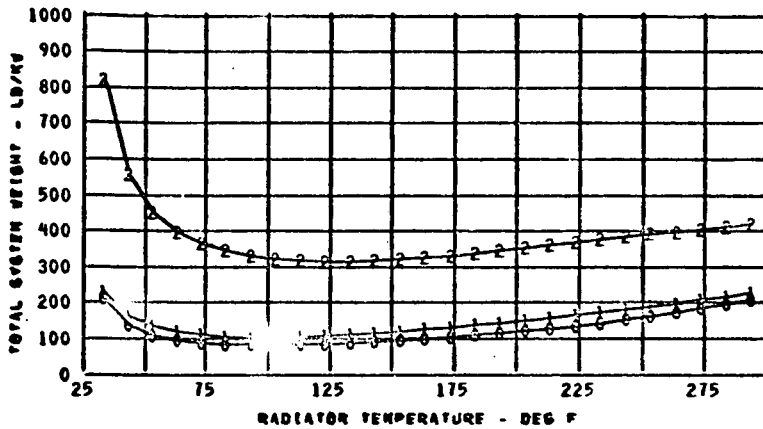
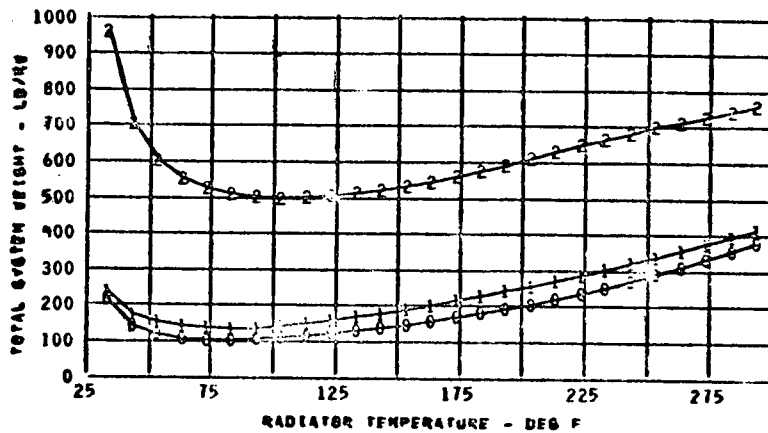
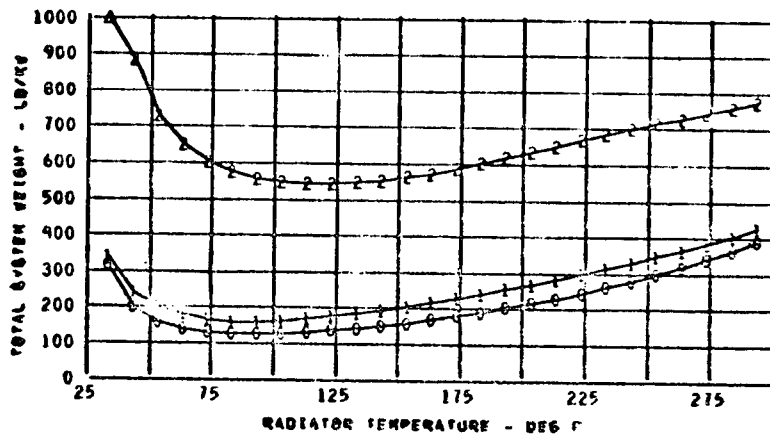


FIGURE A-8

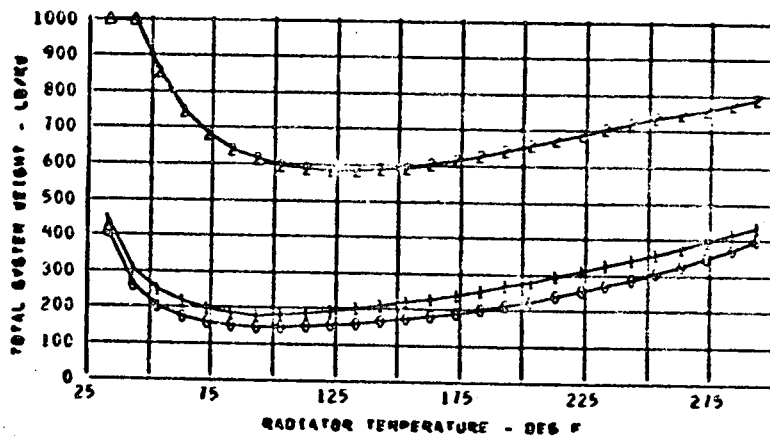
- 0 VAPOR COMPRESSION SYSTEM WITH DIRECT CONDENSING RADIATOR
- 1 VAPOR COMPRESSION SYSTEM WITH HX LOOP TO RADIATOR
- 2 GAS CYCLE SYSTEM WITH HX LOOP TO RADIATOR



TEVAP = 34.0 F
 TSINK = 20.0 F
 EPP = 200.0 LB/KW
 RADP = .50 LB/FT²



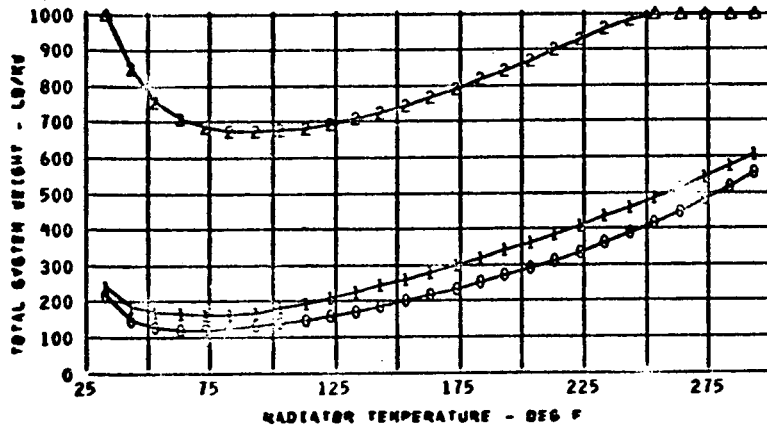
TEVAP = 34.0 F
 TSINK = 20.0 F
 EPP = 200.0 LB/KW
 RADP = .75 LB/FT²



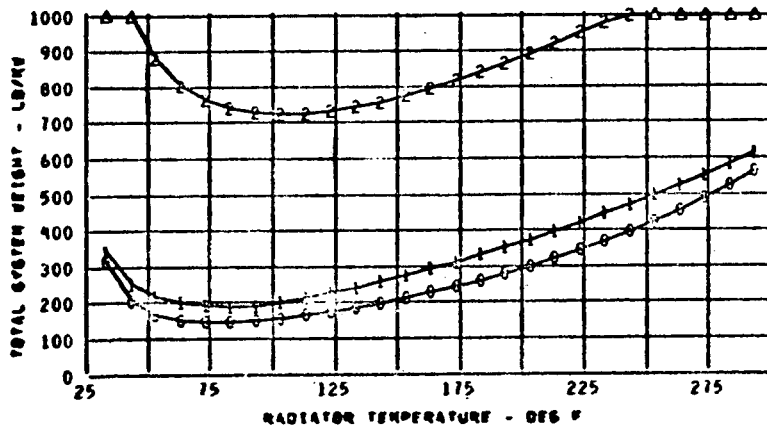
TEVAP = 34.0 F
 TSINK = 20.0 F
 EPP = 200.0 LB/KW
 RADP = 1.0 LB/FT²

FIGURE A-9

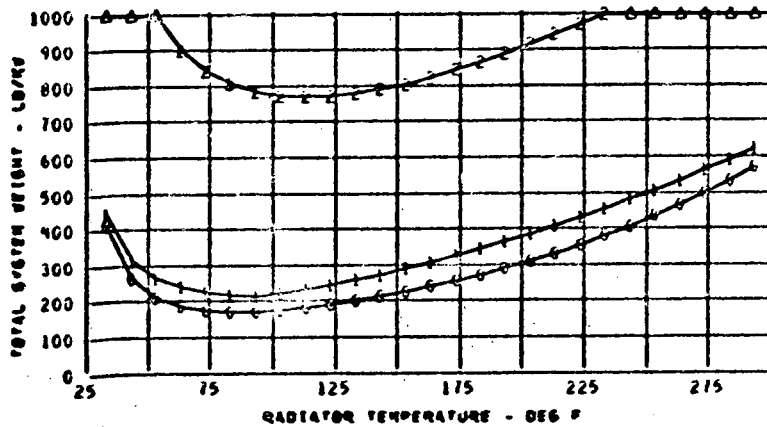
- 0 VAPOR COMPRESSION SYSTEM WITH DIRECT CONDENSING RADIATOR
- 1 VAPOR COMPRESSION SYSTEM WITH HX LOOP TO RADIATOR
- 2 GAS CYCLE SYSTEM WITH HX LOOP TO RADIATOR



TEVAP = 34.0 F
 TSINK = 20.0 F
 EPP = 300.0 LB/KW
 RADP = .50 LB/FT²



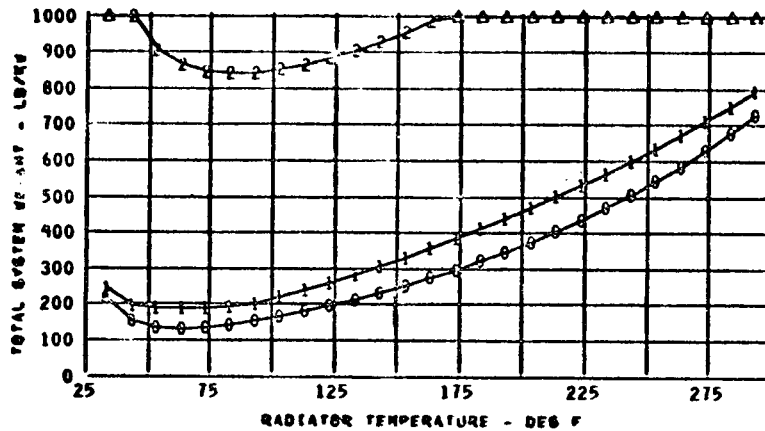
TEVAP = 34.0 F
 TSINK = 20.0 F
 EPP = 300.0 LB/KW
 RADP = .75 LB/FT²



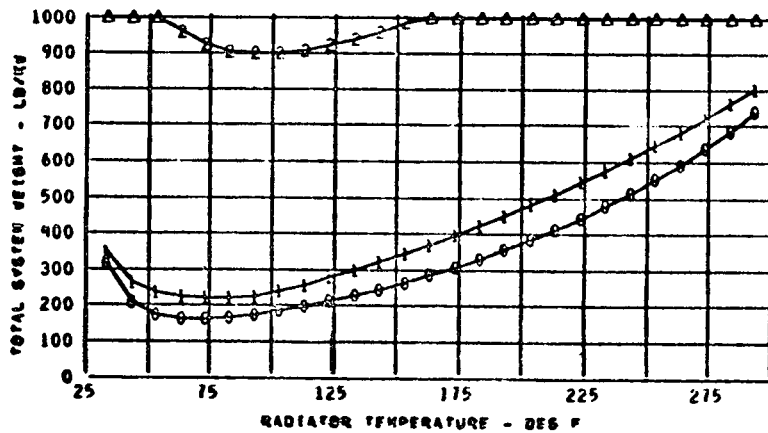
TEVAP = 34.0 F
 TSINK = 20.0 F
 EPP = 300.0 LB/KW
 RADP = 1.0 LB/FT²

FIGURE A-10

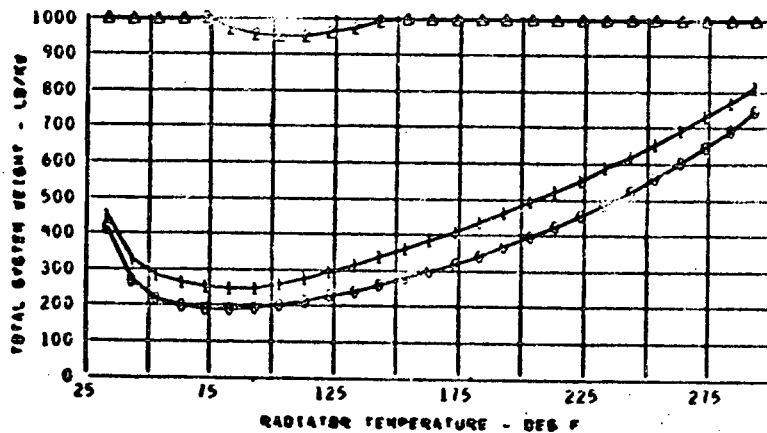
- 0 VAPOR COMPRESSION SYSTEM WITH DIRECT CONDENSING RADIATOR
- 1 VAPOR COMPRESSION SYSTEM WITH HX LOOP TO RADIATOR
- 2 GAS CYCLE SYSTEM WITH HX LOOP TO RADIATOR



TEVAP = 34.0 F
 TSINK = 20.0 F
 EPP = 400.0 LB/KW
 RADP = .50 LB/FT²



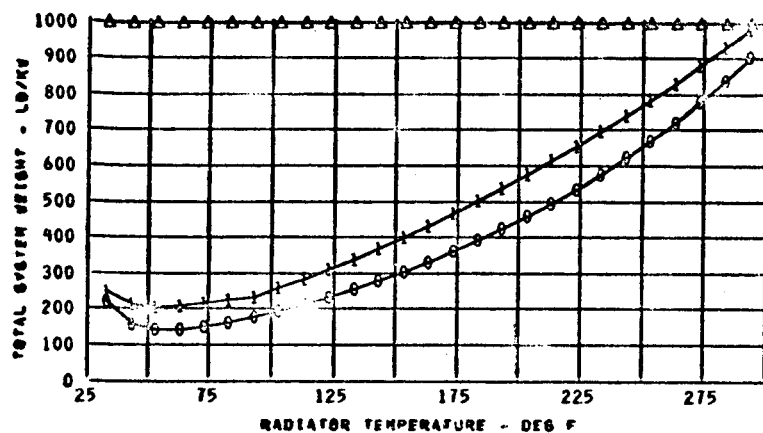
TEVAP = 34.0 F
 TSINK = 20.0 F
 EPP = 400.0 LB/KW
 RADP = .75 LB/FT²



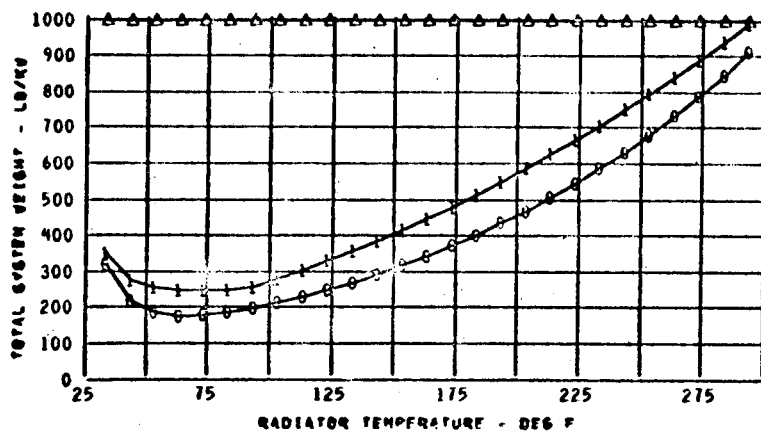
TEVAP = 34.0 F
 TSINK = 20.0 F
 EPP = 400.0 LB/KW
 RADP = 1.0 LB/FT²

FIGURE A-11

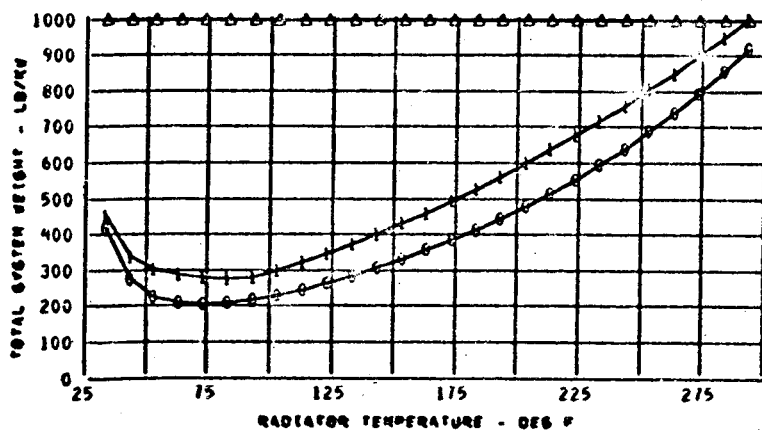
- 0 VAPOR COMPRESSION SYSTEM WITH DIRECT CONDENSING RADIATOR
- 1 VAPOR COMPRESSION SYSTEM WITH HX LOOP TO RADIATOR
- 2 GAS CYCLE SYSTEM WITH HX LOOP TO RADIATOR



TEVAP = 34.0 F
 TSINK = 20.0 F
 EPP = 500.0LB/KW
 RADP = .50LB/FT²



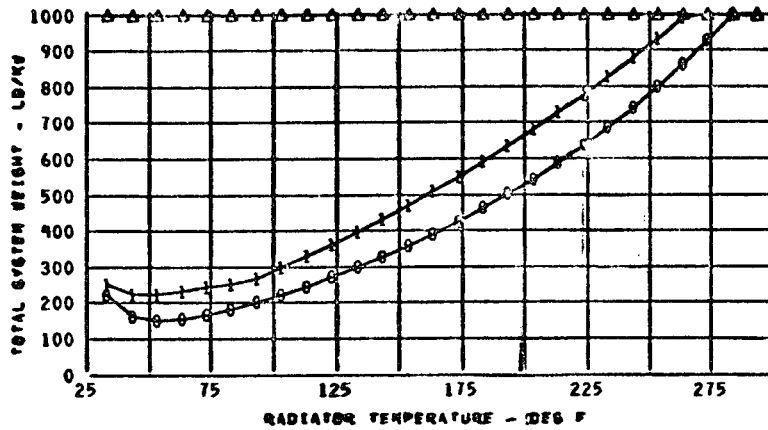
TEVAP = 34.0 F
 TSINK = 20.0 F
 EPP = 500.0LB/KW
 RADP = .75LB/FT²



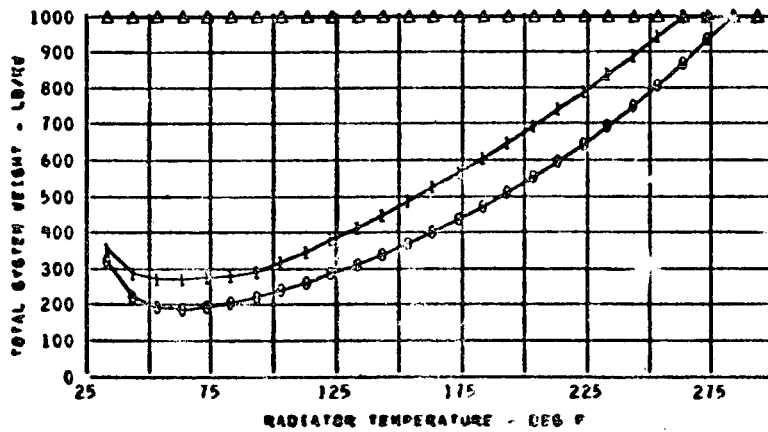
TEVAP = 34.0 F
 TSINK = 20.0 F
 EPP = 500.0LB/KW
 RADP = 1.0LB/FT²

FIGURE A-12

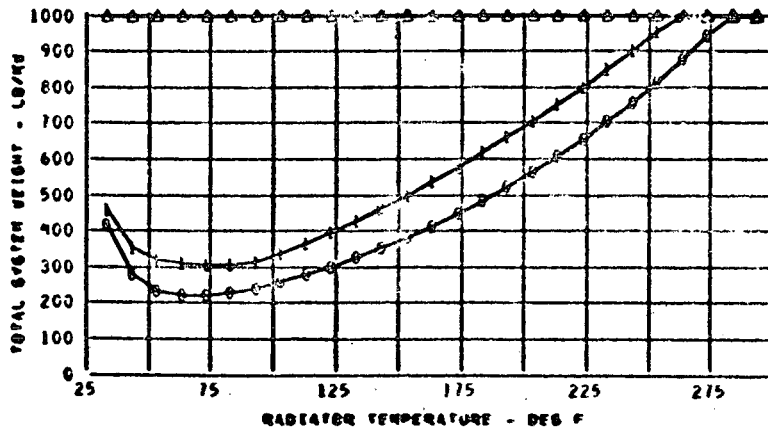
- 0 VAPOR COMPRESSION SYSTEM WITH DIRECT CONDENSING RADIATOR
- 1 VAPOR COMPRESSION SYSTEM WITH HX LOOP TO RADIATOR
- 2 GAS CYCLE SYSTEM WITH HX LOOP TO RADIATOR



TEVAP = 34.0 F
 TSINK = 20.0 F
 EPP = 600.0 LB/KW
 RADP = .50 LB/FT²



TEVAP = 34.0 F
 TSINK = 20.0 F
 EPP = 600.0 LB/KW
 RADP = .75 LB/FT²



TEVAP = 34.0 F
 TSINK = 20.0 F
 EPP = 600.0 LB/KW
 RADP = 1.0 LB/FT²

FIGURE A-13

- 0 VAPOR COMPRESSION SYSTEM WITH DIRECT CONDENSING RADIATOR
- 1 VAPOR COMPRESSION SYSTEM WITH HX LOOP TO RADIATOR
- 2 GAS CYCLE SYSTEM WITH HX LOOP TO RADIATOR

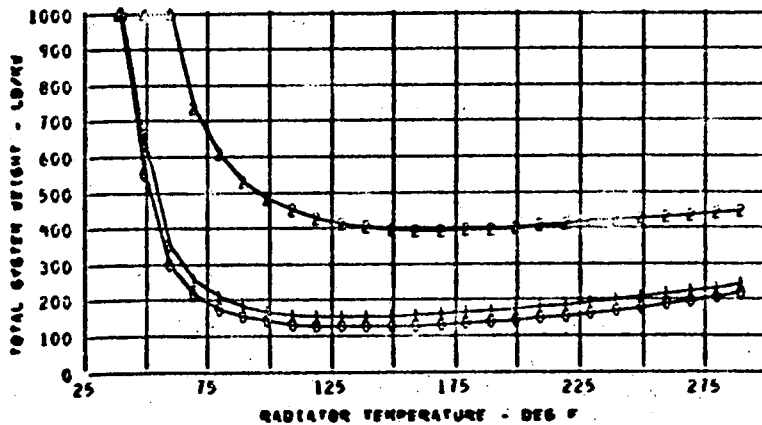
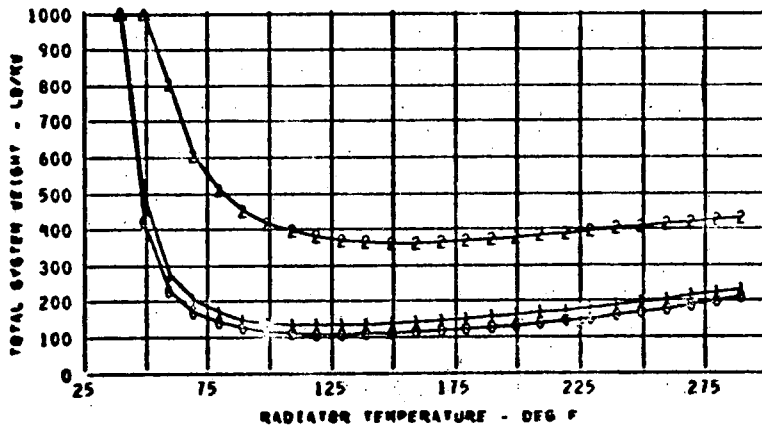
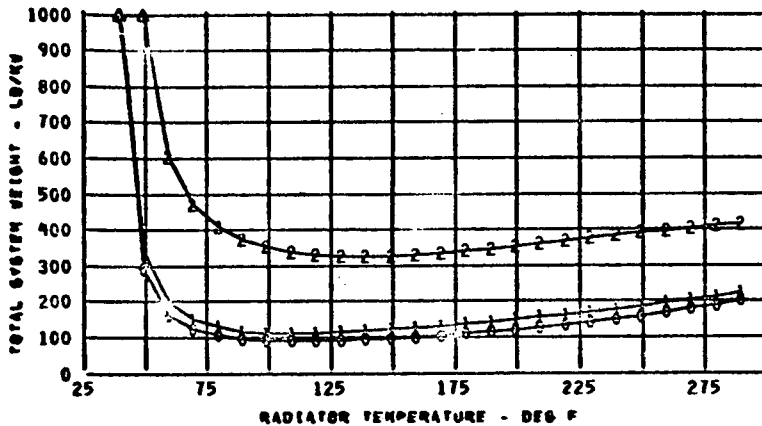
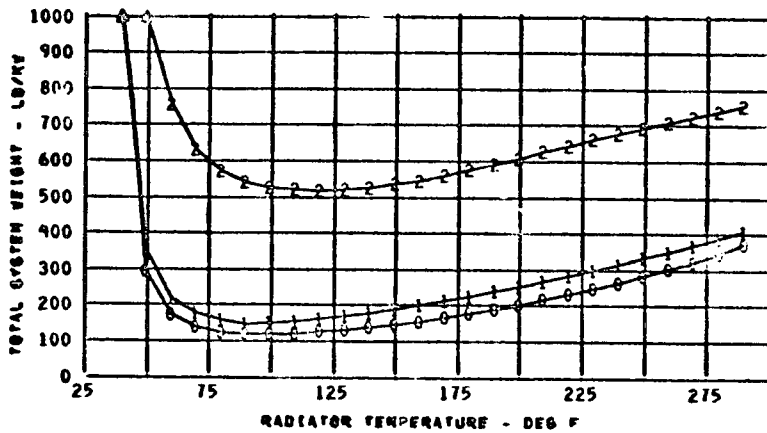
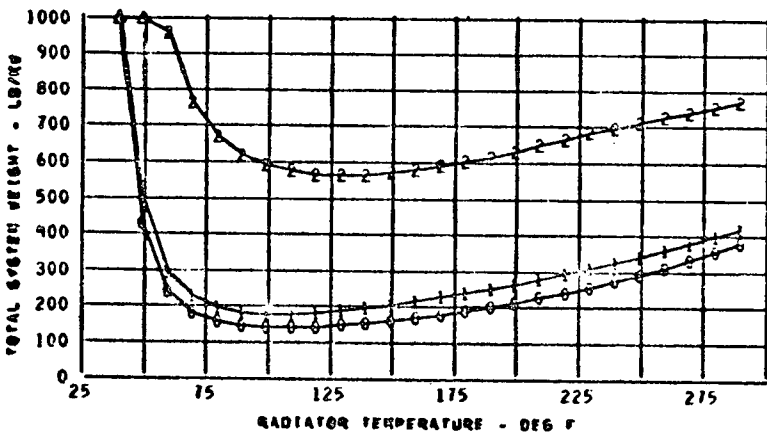


FIGURE A-14

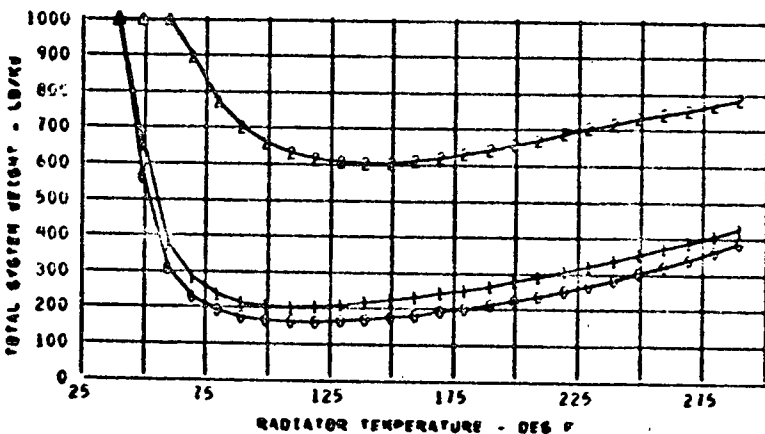
- 0 VAPOR COMPRESSION SYSTEM WITH DIRECT CONDENSING RADIATOR
- 1 VAPOR COMPRESSION SYSTEM WITH HX LOOP TO RADIATOR
- 2 GAS CYCLE SYSTEM WITH HX LOOP TO RADIATOR



TEVAP = 34.0 F
 TSINK = 40.0 F
 EPP = 200.0LB/KW
 RADP = .50LB/FT²



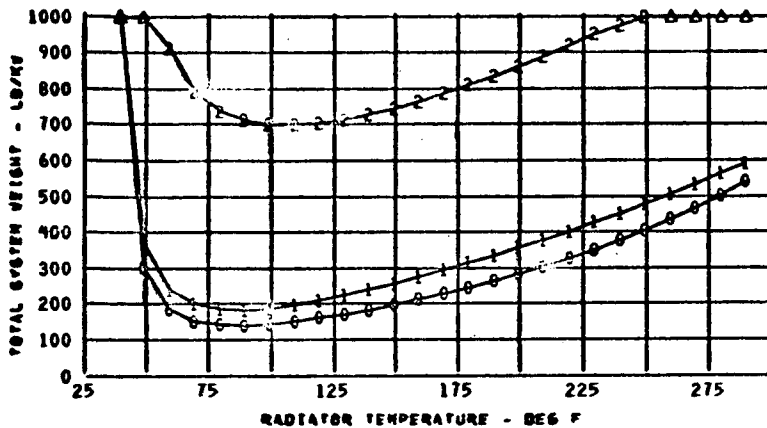
TEVAP = 34.0 F
 TSINK = 40.0 F
 EPP = 200.0LB/KW
 RADP = .75LB/FT²



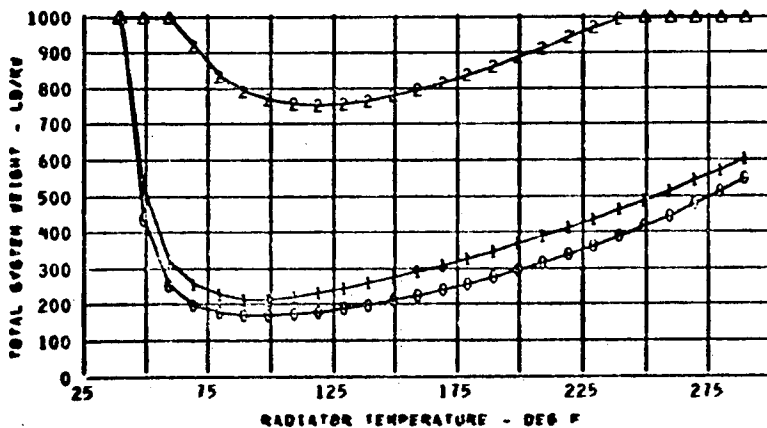
TEVAP = 34.0 F
 TSINK = 40.0 F
 EPP = 200.0LB/KW
 RADP = 1.0LB/FT²

FIGURE A-15

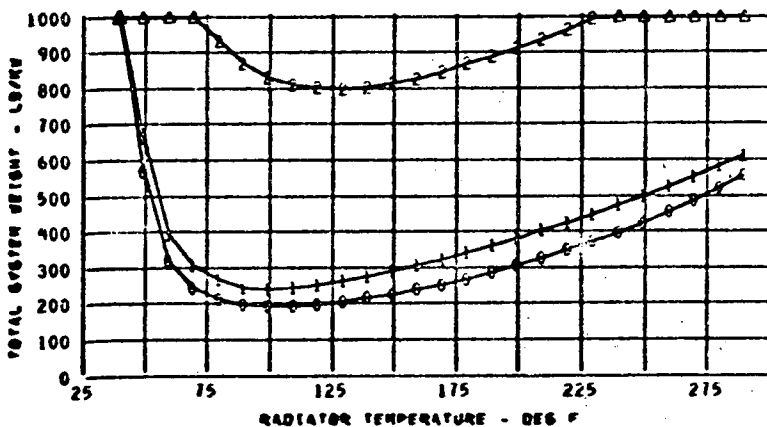
- 0 VAPOR COMPRESSION SYSTEM WITH DIRECT CONDENSING RADIATOR
- 1 VAPOR COMPRESSION SYSTEM WITH HX LOOP TO RADIATOR
- 2 GAS CYCLE SYSTEM WITH HX LOOP TO RADIATOR



TEVAP = 34.0 F
 TSINK = 40.0 F
 EPP = 300.0LB/KW
 RADP = .50LB/FT²



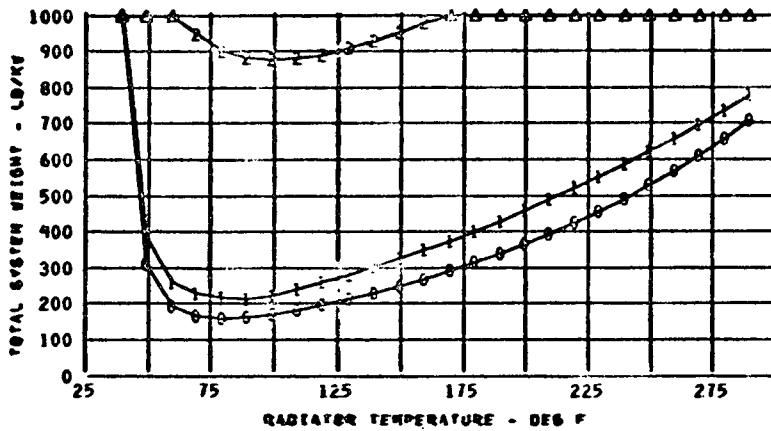
TEVAP = 34.0 F
 TSINK = 40.0 F
 EPP = 300.0LB/KW
 RADP = .75LB/FT²



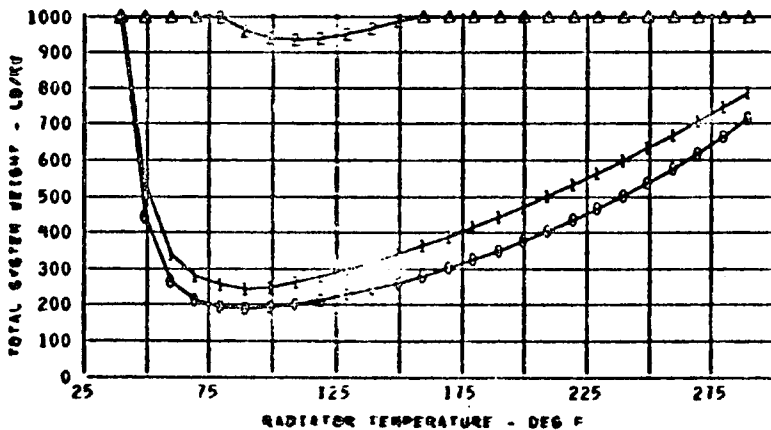
TEVAP = 34.0 F
 TSINK = 40.0 F
 EPP = 300.0LB/KW
 RADP = 1.0LB/FT²

FIGURE A-16

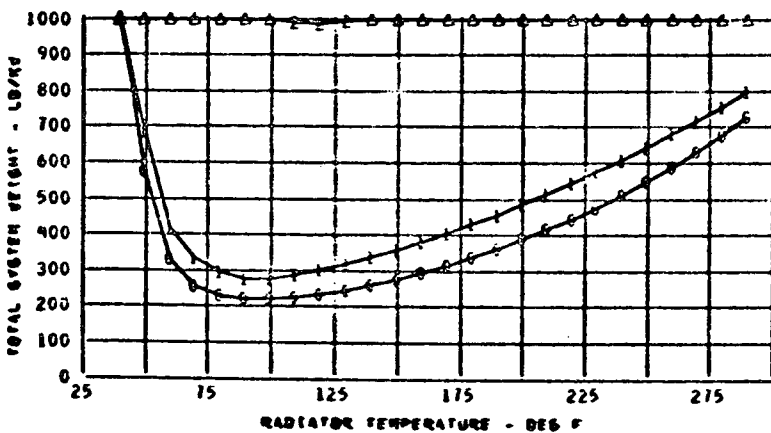
- 0 VAPOR COMPRESSION SYSTEM WITH DIRECT CONDENSING RADIATOR
- 1 VAPOR COMPRESSION SYSTEM WITH HX LOOP TO RADIATOR
- 2 GAS CYCLE SYSTEM WITH HX LOOP TO RADIATOR



TEVAP = 34.0 F
 TSINK = 40.0 F
 EPP = 400.0 LB/KW
 RADP = .50 LB/FT²



TEVAP = 34.0 F
 TSINK = 40.0 F
 EPP = 400.0 LB/KW
 RADP = .75 LB/FT²

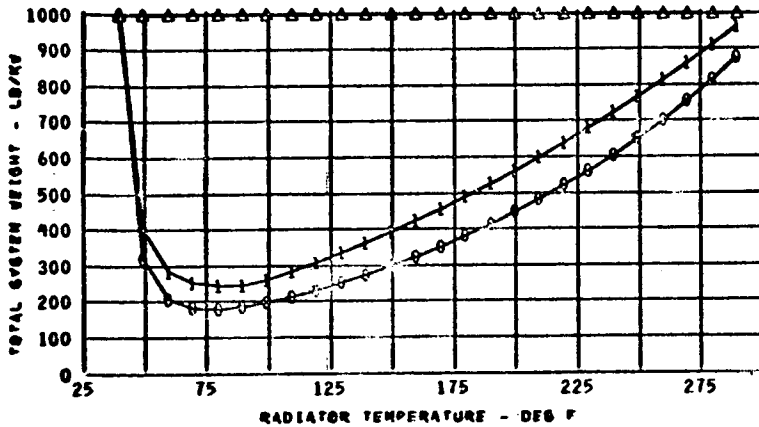


TEVAP = 34.0 F
 TSINK = 40.0 F
 EPP = 400.0 LB/KW
 RADP = 1.0 LB/FT²

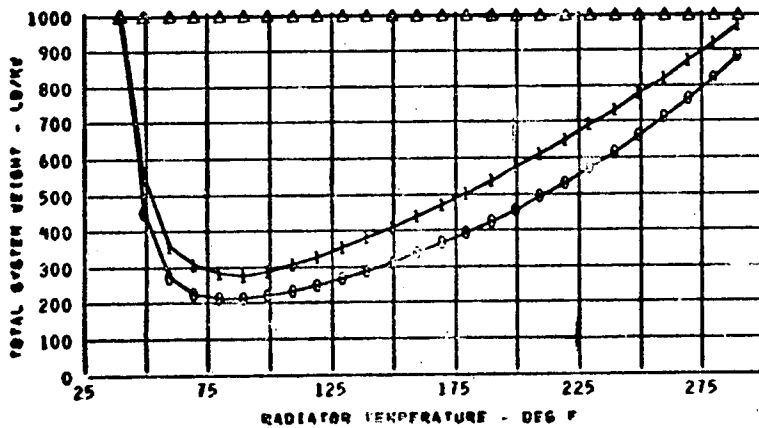
3

FIGURE A-17

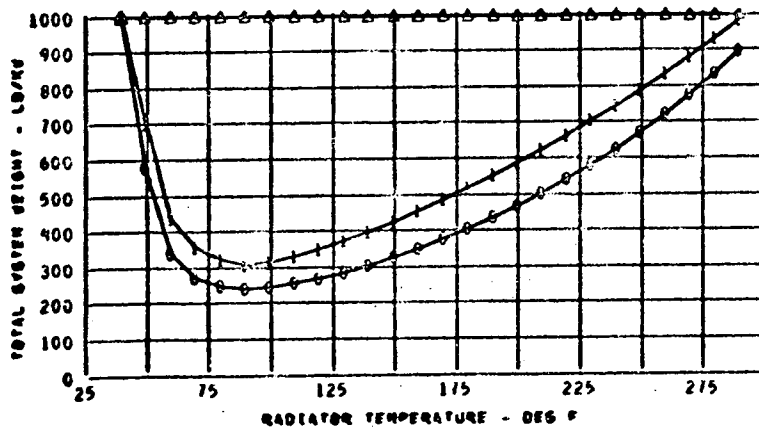
- 0 VAPOR COMPRESSION SYSTEM WITH DIRECT CONDENSING RADIATOR
- 1 VAPOR COMPRESSION SYSTEM WITH HX LOOP TO RADIATOR
- 2 GAS CYCLE SYSTEM WITH HX LOOP TO RADIATOR



TEVAP = 34.0 F
 TSINK = 40.0 F
 EPP = 500.0 LB/KW
 RADP = .50 LB/FT²



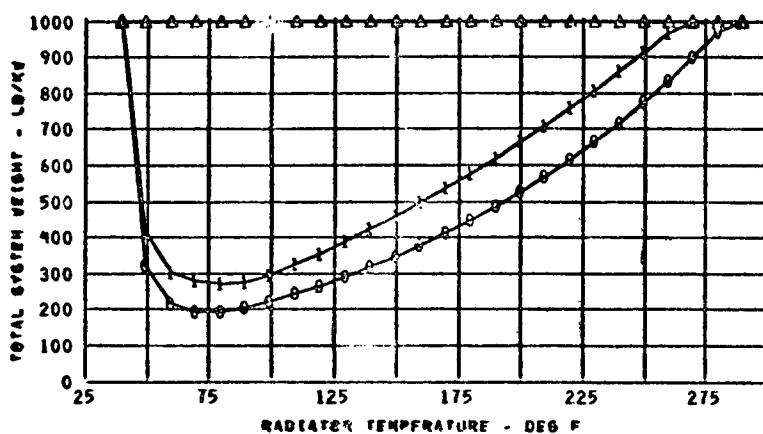
TEVAP = 34.0 F
 TSINK = 40.0 F
 EPP = 500.0 LB/KW
 RADP = .75 LB/FT²



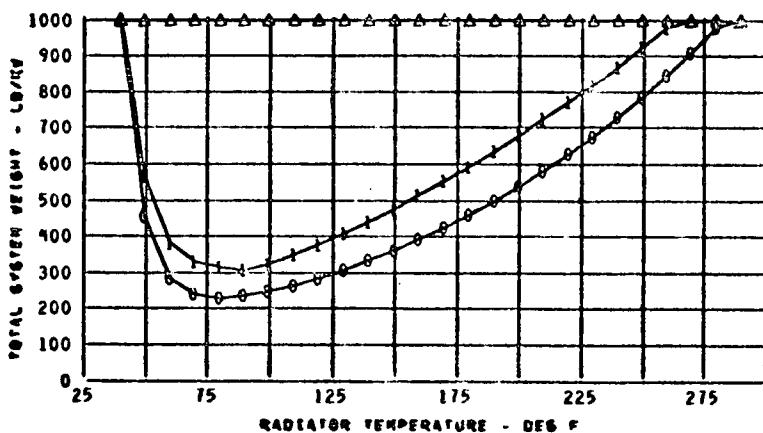
TEVAP = 34.0 F
 TSINK = 40.0 F
 EPP = 500.0 LB/KW
 RADP = 1.0 LB/FT²

FIGURE A-18

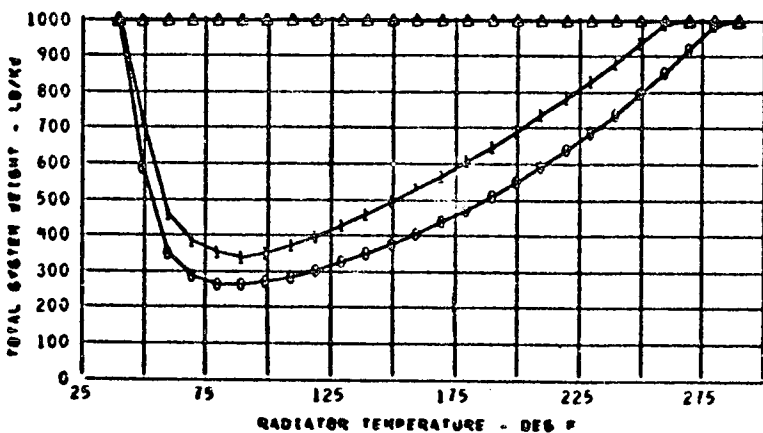
- 0 VAPOR COMPRESSION SYSTEM WITH DIRECT CONDENSING RADIATOR
- 1 VAPOR COMPRESSION SYSTEM WITH HX LOOP TO RADIATOR
- 2 GAS CYCLE SYSTEM WITH HX LOOP TO RADIATOR



TEVAP = 34.0 F
 TSINK = 40.0 F
 EPP = 600.0 LB/KW
 RADP = .50 LB/FT²



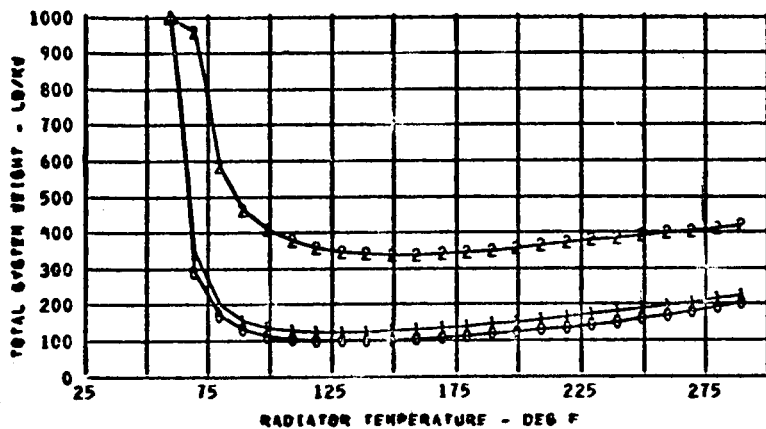
TEVAP = 34.0 F
 TSINK = 40.0 F
 EPP = 600.0 LB/KW
 RADP = .75 LB/FT²



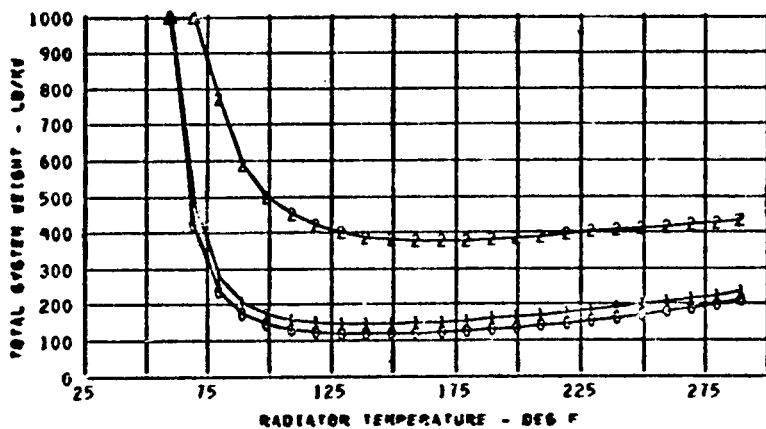
TEVAP = 34.0 F
 TSINK = 40.0 F
 EPP = 600.0 LB/KW
 RADP = 1.0 LB/FT²

FIGURE A-19

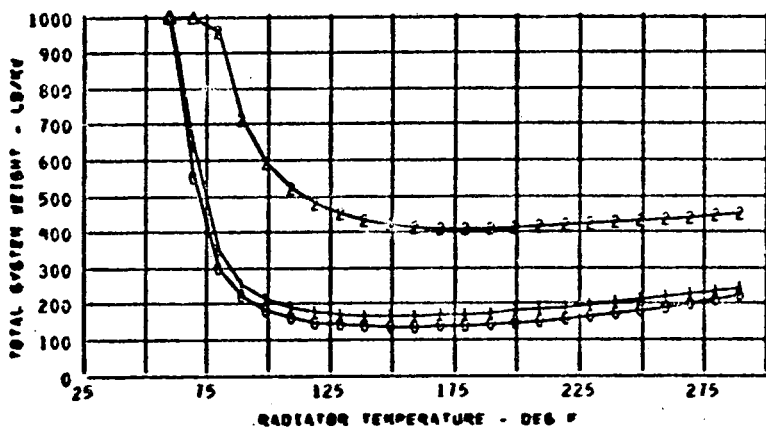
- 0 VAPOR COMPRESSION SYSTEM WITH DIRECT CONDENSING RADIATOR
- 1 VAPOR COMPRESSION SYSTEM WITH HX LOOP TO RADIATOR
- 2 GAS CYCLE SYSTEM WITH HX LOOP TO RADIATOR



TEVAP = 34.0 F
 TSINK = 60.0 F
 EPP = 100.0LB/KW
 RADP = .50LB/FT²



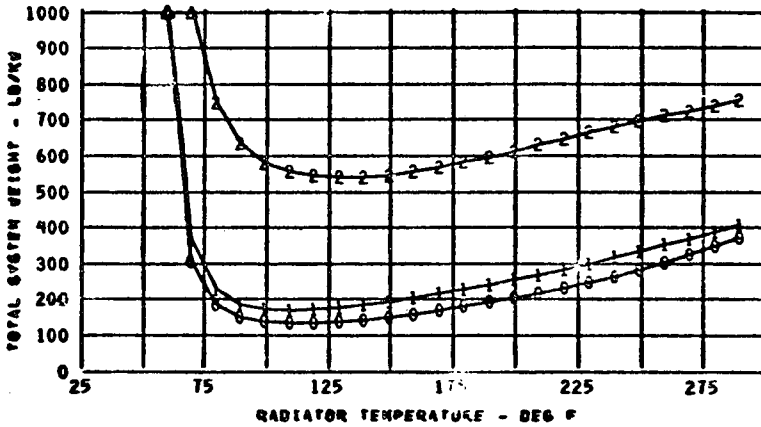
TEVAP = 34.0 F
 TSINK = 60.0 F
 EPP = 100.0LB/KW
 RADP = .75LB/FT²



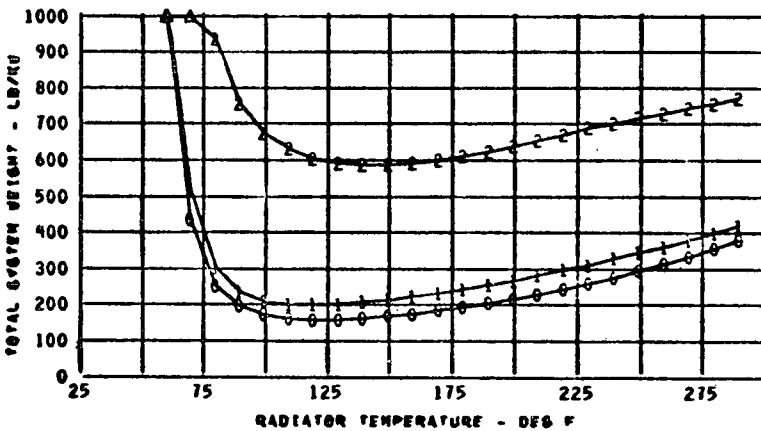
TEVAP = 34.0 F
 TSINK = 60.0 F
 EPP = 100.0LB/KW
 RADP = 1.0LB/FT²

FIGURE A-20

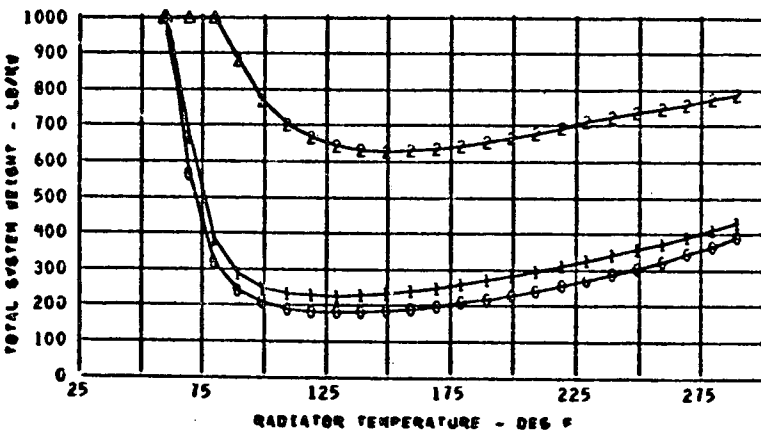
- 0 VAPOR COMPRESSION SYSTEM WITH DIRECT CONDENSING RADIATOR
- 1 VAPOR COMPRESSION SYSTEM WITH HX LOOP TO RADIATOR
- 2 GAS CYCLE SYSTEM WITH HX LOOP TO RADIATOR



TEVAP = 34.0 F
 TSINK = 60.0 F
 EPP = 200.0 LB/KW
 RADP = .50 LB/FT²



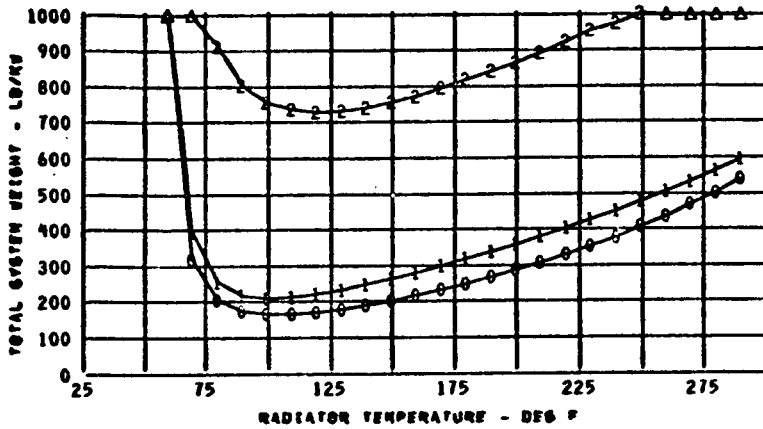
TEVAP = 34.0 F
 TSINK = 60.0 F
 EPP = 200.0 LB/KW
 RADP = .75 LB/FT²



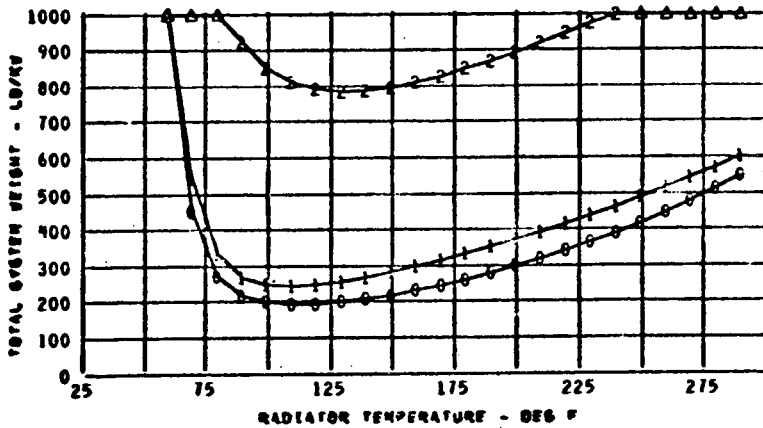
TEVAP = 34.0 F
 TSINK = 60.0 F
 EPP = 200.0 LB/KW
 RADP = 1.0 LB/FT²

FIGURE A-21

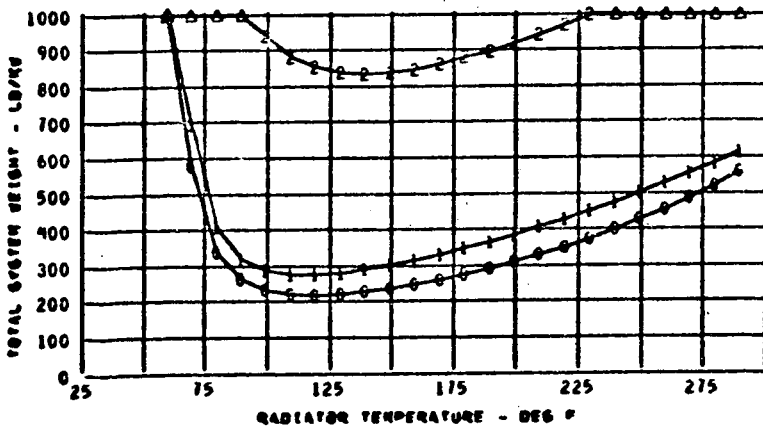
- 0 VAPOR COMPRESSION SYSTEM WITH DIRECT CONDENSING RADIATOR
- 1 VAPOR COMPRESSION SYSTEM WITH HX LOOP TO RADIATOR
- 2 GAS CYCLE SYSTEM WITH HX LOOP TO RADIATOR



TEVAP = 34.0 F
 TSINK = 60.0 F
 EPP = 300.0 LB/KW
 RADP = .50 LB/FT²



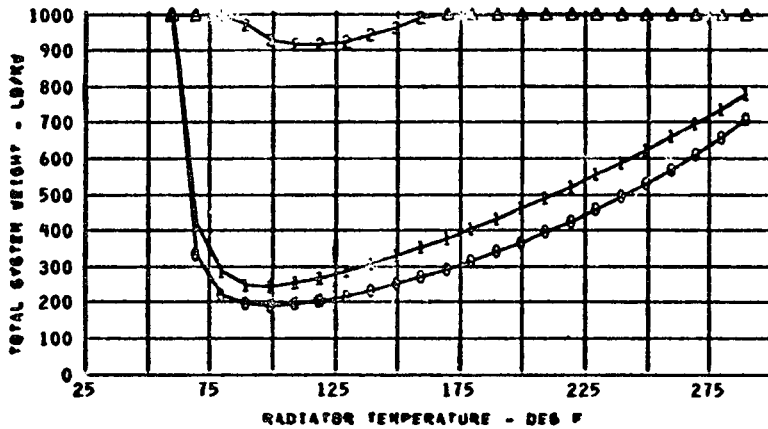
TEVAP = 34.0 F
 TSINK = 60.0 F
 EPP = 300.0 LB/KW
 RADP = .75 LB/FT²



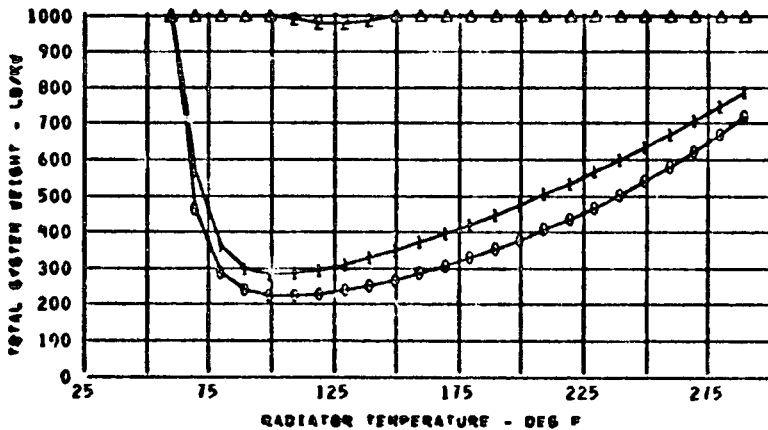
TEVAP = 34.0 F
 TSINK = 60.0 F
 EPP = 300.0 LB/KW
 RADP = 1.0 LB/FT²

FIGURE A-22

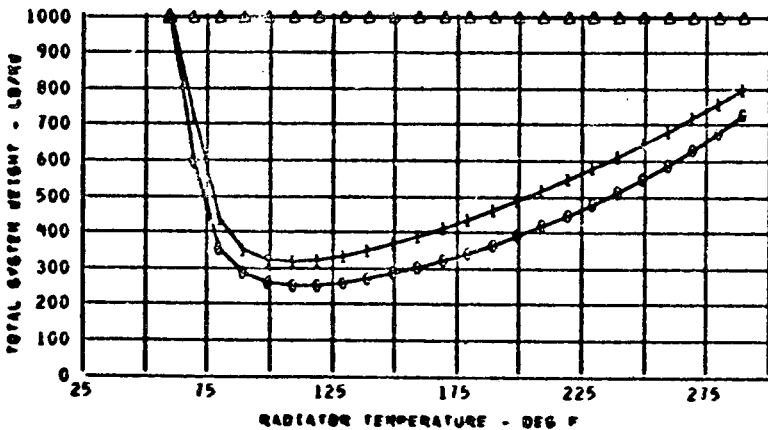
- 0 VAPOR COMPRESSION SYSTEM WITH DIRECT CONDENSING RADIATOR
- 1 VAPOR COMPRESSION SYSTEM WITH HX LOOP TO RADIATOR
- 2 GAS CYCLE SYSTEM WITH HX LOOP TO RADIATOR



TEVAP = 34.0 F
 TSINK = 60.0 F
 EPP = 400.0LB/KW
 RADP = .50LB/FT²



TEVAP = 34.0 F
 TSINK = 60.0 F
 EPP = 400.0LB/KW
 RADP = .75LB/FT²



TEVAP = 34.0 F
 TSINK = 60.0 F
 EPP = 400.0LB/KW
 RADP = 1.0LB/FT²

FIGURE A-23

- 0 VAPOR COMPRESSION SYSTEM WITH DIRECT CONDENSING RADIATOR
- 1 VAPOR COMPRESSION SYSTEM WITH HX LOOP TO RADIATOR
- 2 GAS CYCLE SYSTEM WITH HX LOOP TO RADIATOR

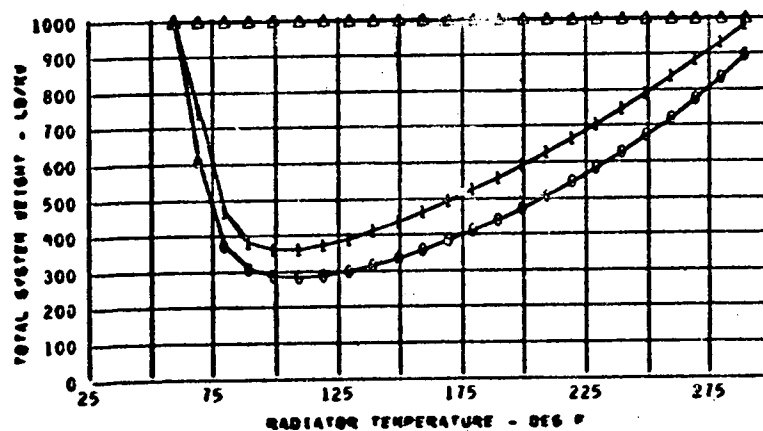
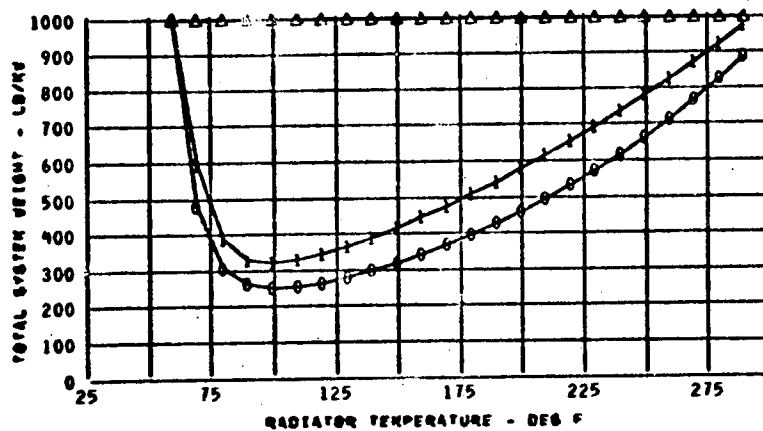
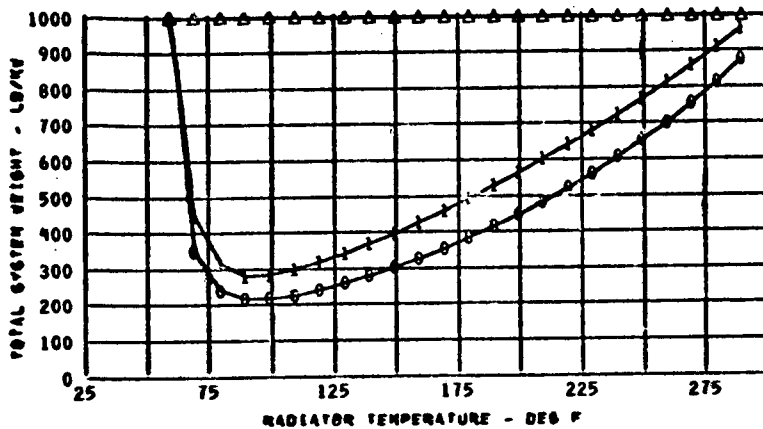
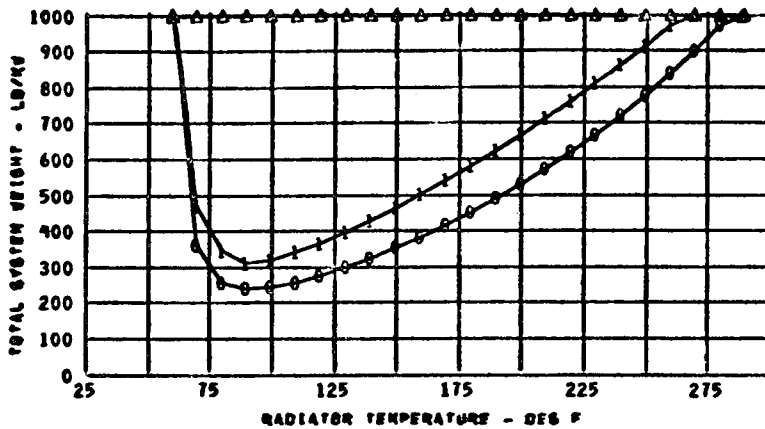
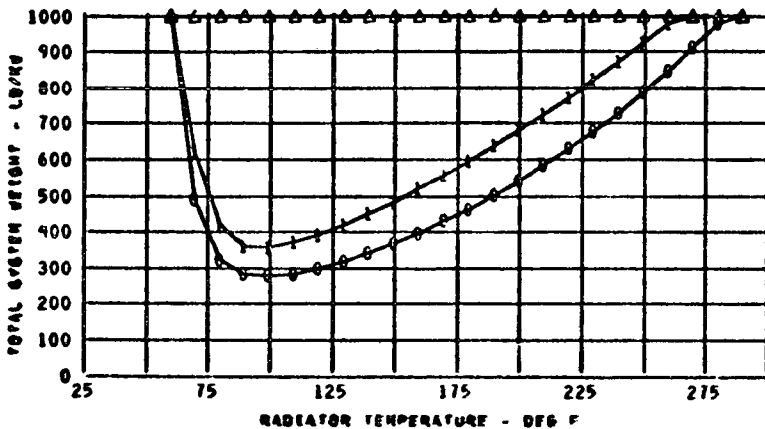


FIGURE A-24

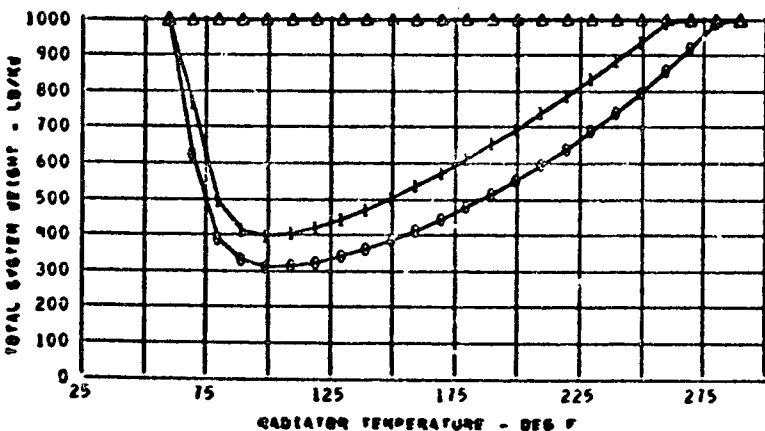
- 0 VAPOR COMPRESSION SYSTEM WITH DIRECT CONDENSING RADIATOR
- 1 VAPOR COMPRESSION SYSTEM WITH HX LOOP TO RADIATOR
- 2 GAS CYCLE SYSTEM WITH HX LOOP TO RADIATOR



TEVAP = 34.0 F
 TSINK = 60.0 F
 EPP = 600.0 LB/KW
 RADP = .50 LB/FT²



TEVAP = 34.0 F
 TSINK = 60.0 F
 EPP = 600.0 LB/KW
 RADP = .75 LB/FT²



TEVAP = 34.0 F
 TSINK = 60.0 F
 EPP = 600.0 LB/KW
 RADP = 1.0 LB/FT²

FIGURE A-25

- 0 VAPOR COMP WITH DIRECT COND ATM CONVECTOR
- 1 VAPOR COMP WITH HX LOOP TO ATM CONVECTOR
- 2 GAS CYCLE WITH RAM AIR COOLING
- 3 VAPOR COMP WITH RAM AIR COOLING

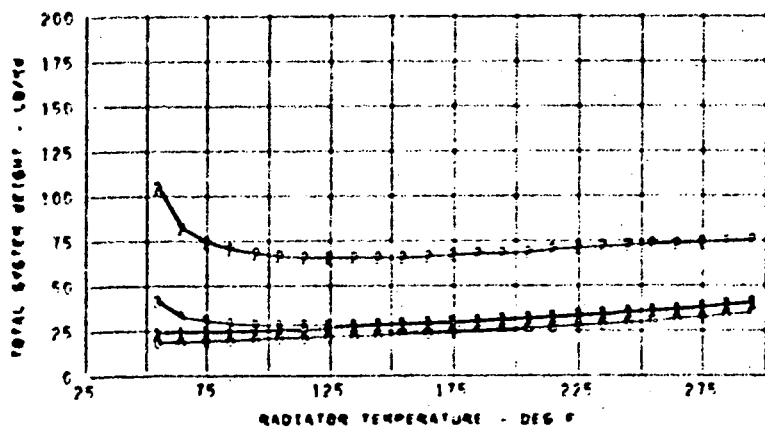
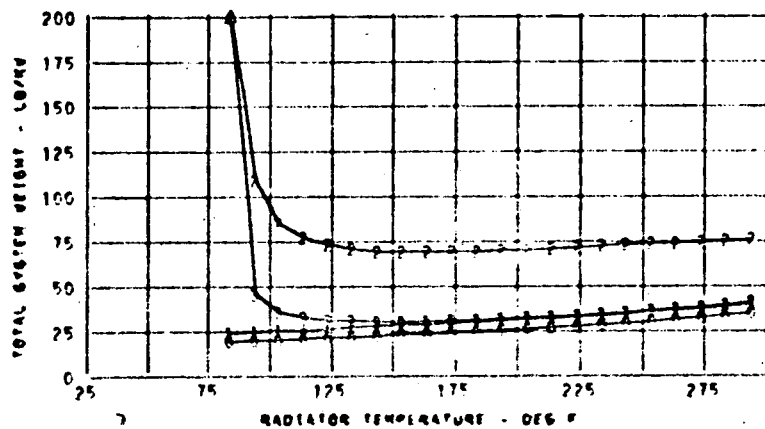
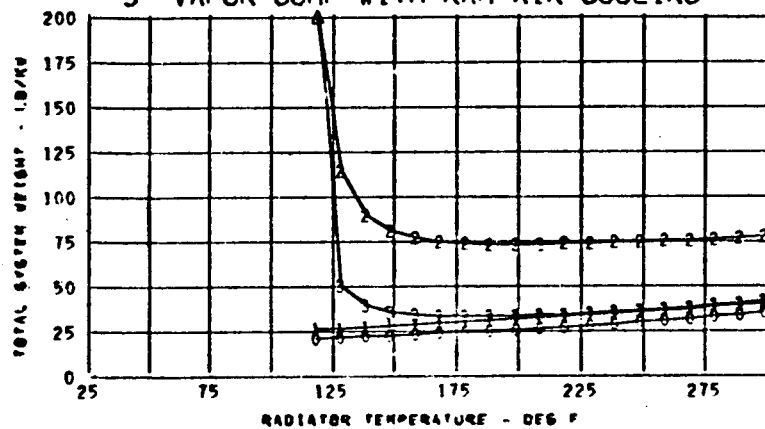
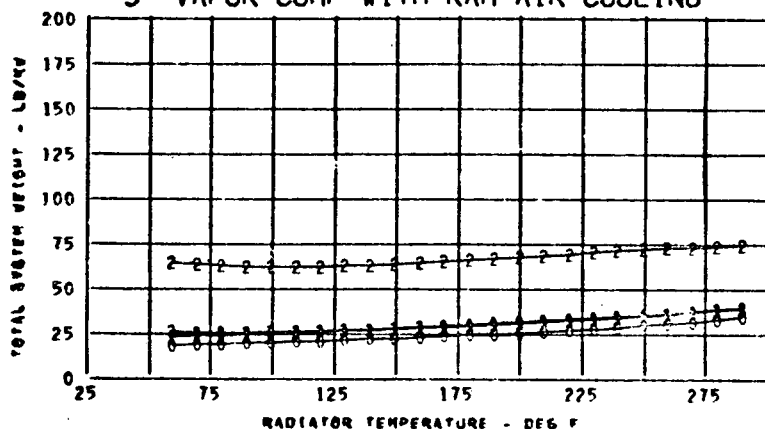
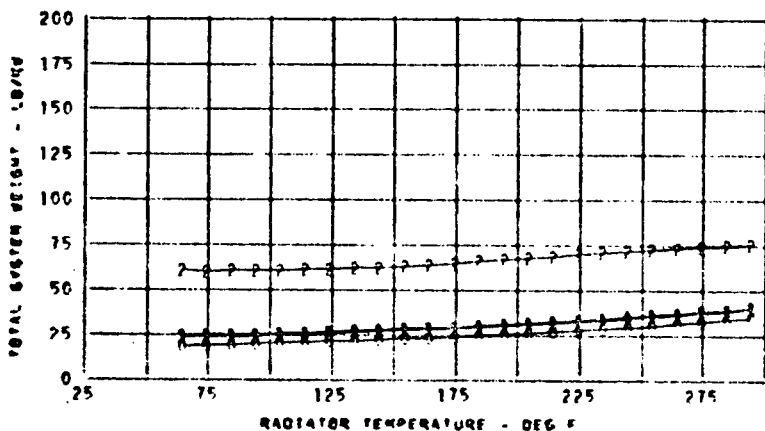


FIGURE A-26

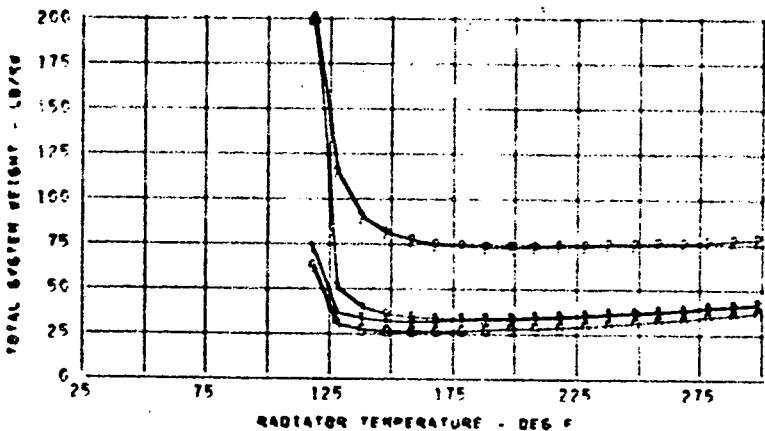
- 0 VAPOR COMP WITH DIRECT COND ATM CONVECTOR
- 1 VAPOR COMP WITH HX LOOP TO ATM CONVECTOR
- 2 GAS CYCLE WITH RAM AIR COOLING
- 3 VAPOR COMP WITH RAM AIR COOLING



ALT = 30000.0 FT
 TEVAP = 34.0 F
 TSINK = 60.4 F
 EPP = 10.0LB/KW
 RADP = 0.0LB/FT²



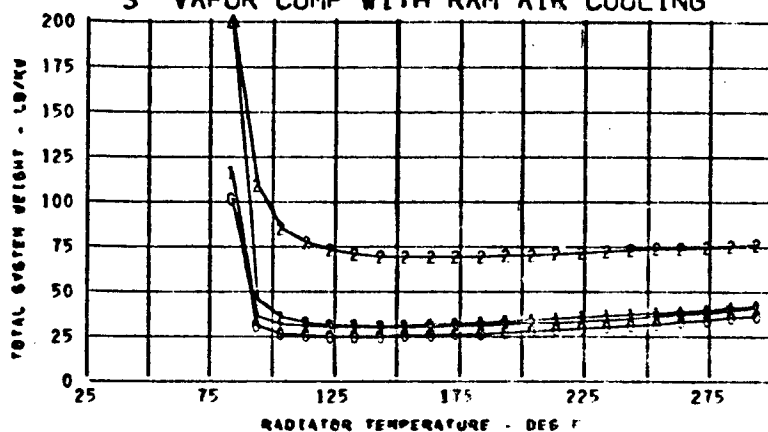
ALT = 40000.0 FT
 TEVAP = 34.0 F
 TSINK = 65.2 F
 EPP = 10.0LB/KW
 RADP = 0.0LB/FT²



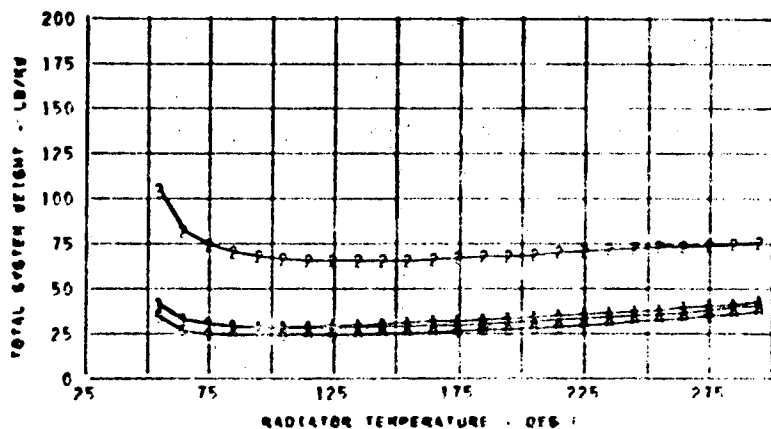
ALT = 1000.0 FT
 TEVAP = 34.0 F
 TSINK = 46.4 F
 EPP = 10.0LB/KW
 RADP = .50LB/FT²

FIGURE A-27

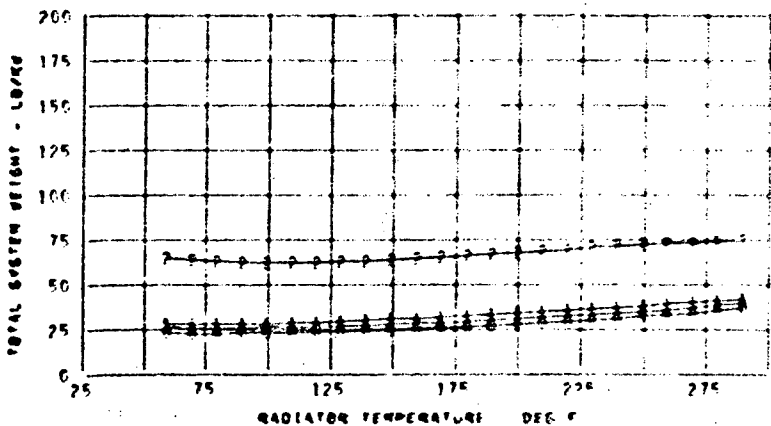
- 0 VAPOR COMP WITH DIRECT COND ATM CONVECTOR
- 1 VAPOR COMP WITH HX LOOP TO ATM CONVECTOR
- 2 GAS CYCLE WITH RAM AIR COOLING
- 3 VAPOR COMP WITH RAM AIR COOLING



ALT = 10000.0 FT
 TEVAP = 34.0 F
 TSINK = 50.8 F
 EPP = 10.0 LB/KW
 RADP = .50 LB/FT²



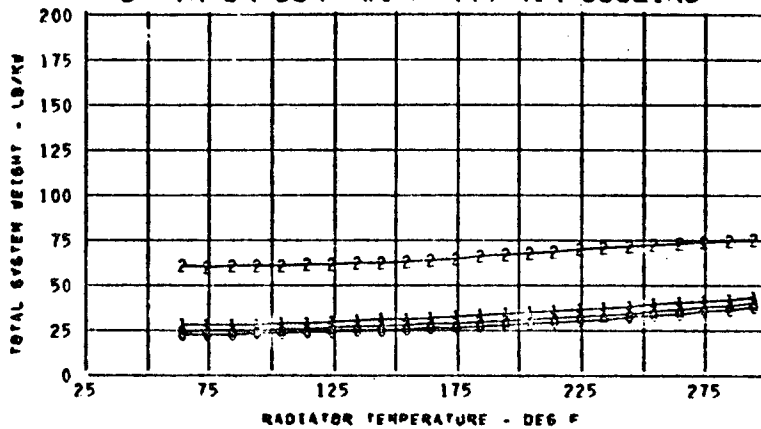
ALT = 20000.0 FT
 TEVAP = 34.0 F
 TSINK = 55.6 F
 EPP = 10.0 LB/KW
 RADP = .50 LB/FT²



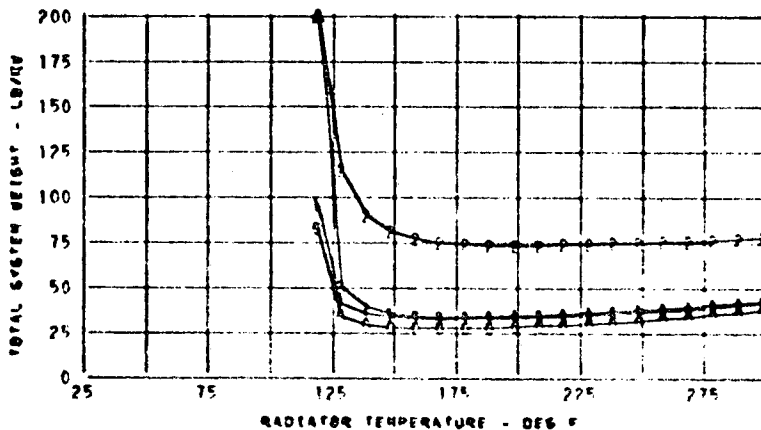
ALT = 30000.0 FT
 TEVAP = 34.0 F
 TSINK = 60.4 F
 EPP = 10.0 LB/KW
 RADP = .50 LB/FT²

FIGURE A-28

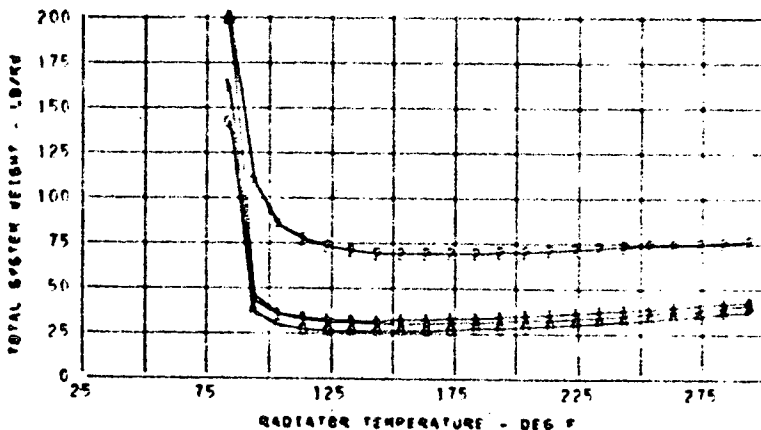
- 0 VAPOR COMP WITH DIRECT COND ATM CONVECTOR
- 1 VAPOR COMP WITH HX LOOP TO ATM CONVECTOR
- 2 GAS CYCLE WITH RAM AIR COOLING
- 3 VAPOR COMP WITH RAM AIR COOLING



ALT = 40000.0 FT
 TEVAP = 34.0 F
 TSINK = 65.2 F
 EPP = 10.0 LB/KW
 RADP = .50 LB/FT²



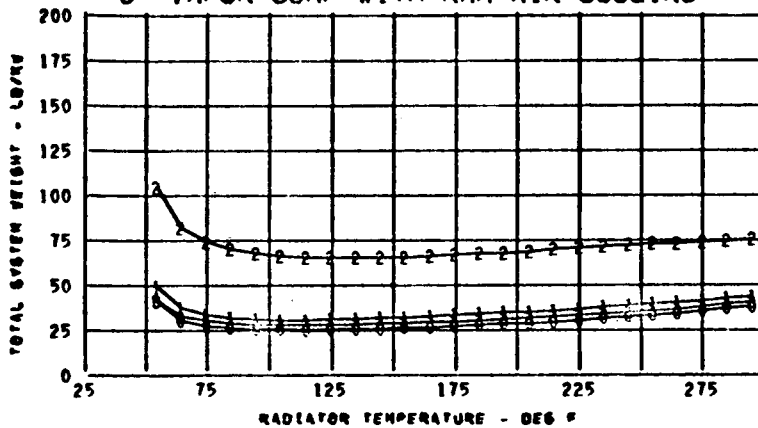
ALT = 1000.0 FT
 TEVAP = 34.0 F
 TSINK = 46.4 F
 EPP = 10.0 LB/KW
 RADP = .75 LB/FT²



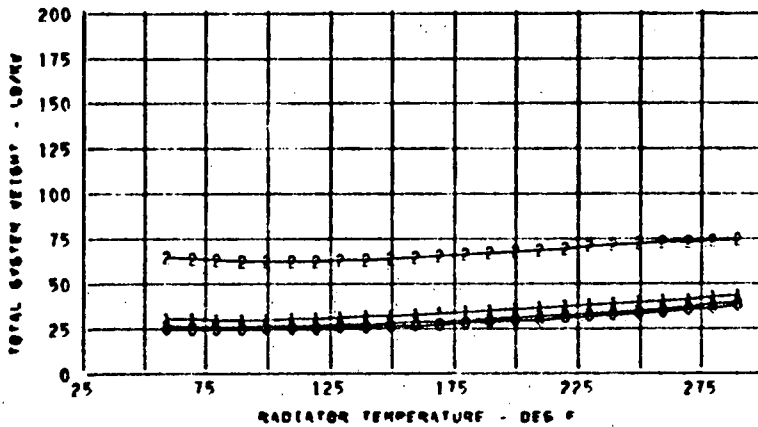
ALT = 10000.0 FT
 TEVAP = 34.0 F
 TSINK = 50.8 F
 EPP = 10.0 LB/KW
 RADP = .75 LB/FT²

FIGURE A-29

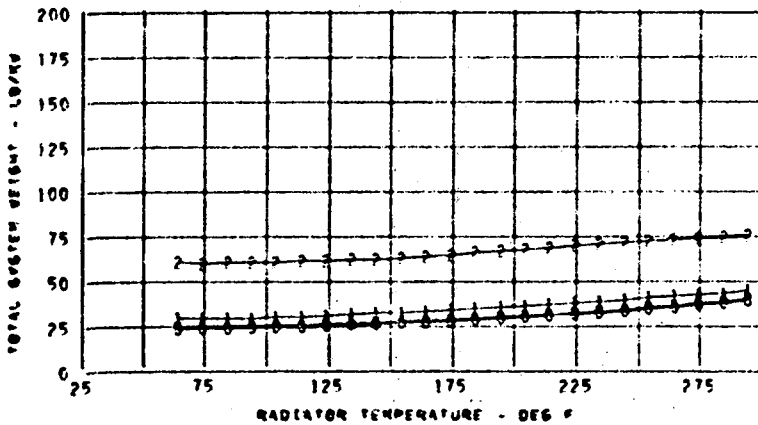
- 0 VAPOR COMP WITH DIRECT COND ATM CONVECTOR
- 1 VAPOR COMP WITH HX LOOP TO ATM CONVECTOR
- 2 GAS CYCLE WITH RAM AIR COOLING
- 3 VAPOR COMP WITH RAM AIR COOLING



ALT = 20000.0 FT
 TEVAP = 34.0 F
 TSINK = 55.6 F
 EPP = 10.0LB/KW
 RADP = .75LB/FT²



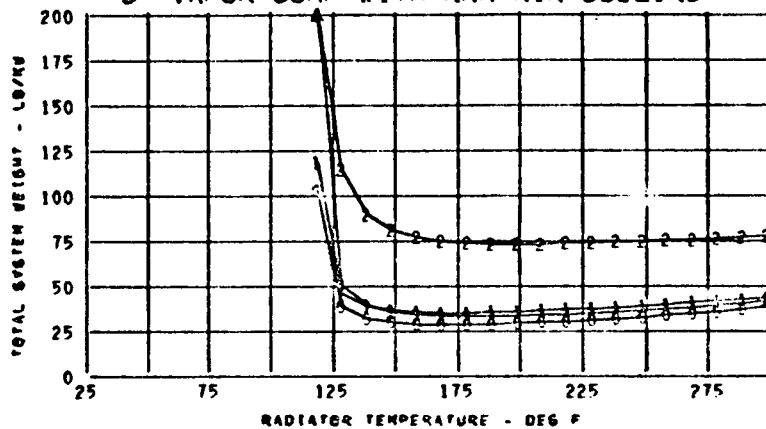
ALT = 30000.0 FT
 TEVAP = 34.0 F
 TSINK = 60.4 F
 EPP = 10.0LB/KW
 RADP = .75LB/FT²



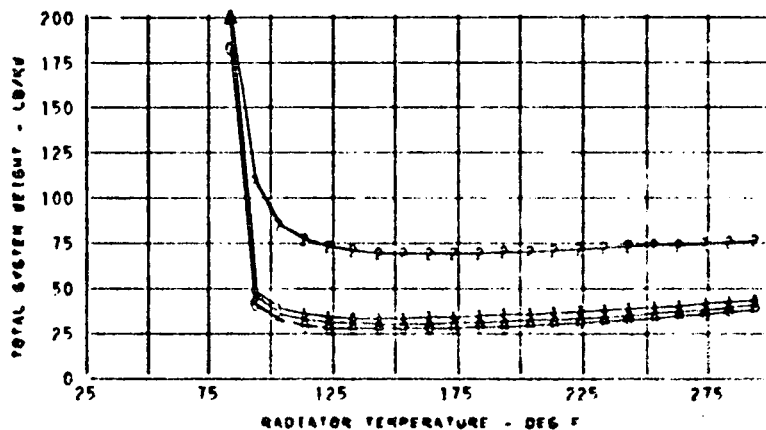
ALT = 40000.0 FT
 TEVAP = 34.0 F
 TSINK = 65.2 F
 EPP = 10.0LB/KW
 RADP = .75LB/FT²

FIGURE A-30

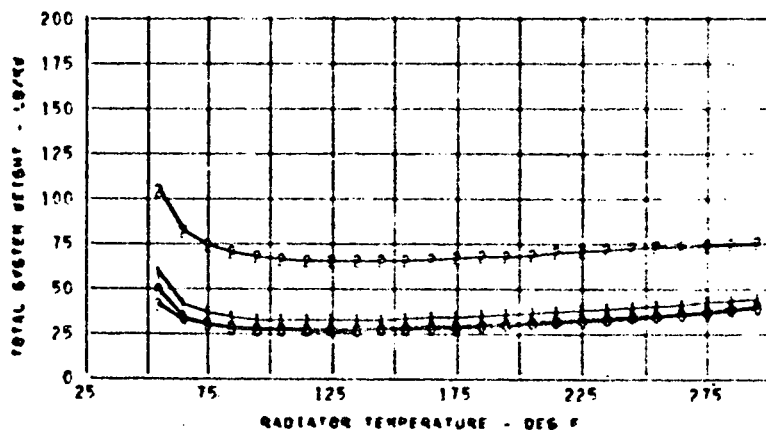
- 0 VAPOR COMP WITH DIRECT COND ATM CONVECTOR
- 1 VAPOR COMP WITH HX LOOP TO ATM CONVECTOR
- 2 GAS CYCLE WITH RAM AIR COOLING
- 3 VAPOR COMP WITH RAM AIR COOLING



ALT = 1000.0 FT
 TEVAP = 34.0 F
 TSINK = 46.4 F
 EPP = 10.0 LB/KW
 RADP = 1.0 LB/FT²



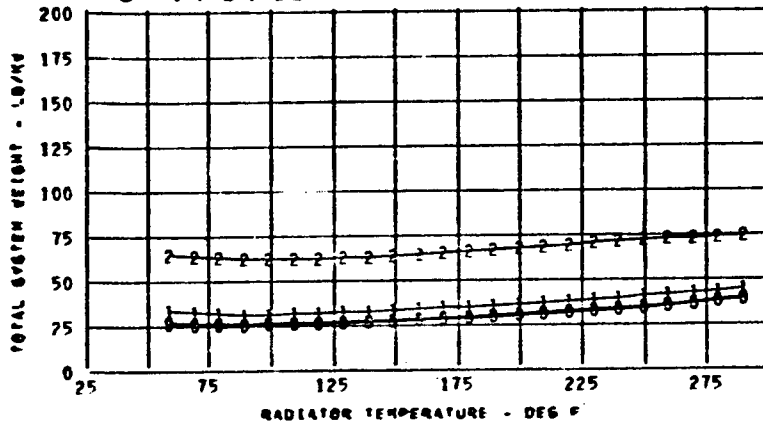
ALT = 10000.0 FT
 TEVAP = 34.0 F
 TSINK = 50.8 F
 EPP = 10.0 LB/KW
 RADP = 1.0 LB/FT²



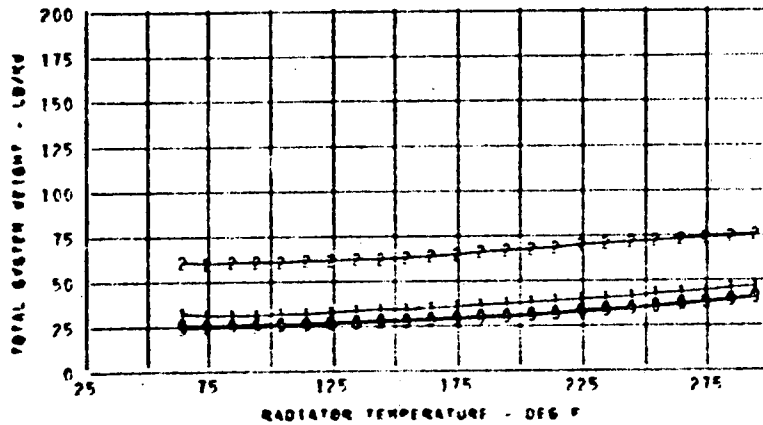
ALT = 20000.0 FT
 TEVAP = 34.0 F
 TSINK = 55.6 F
 EPP = 10.0 LB/KW
 RADP = 1.0 LB/FT²

FIGURE A-31

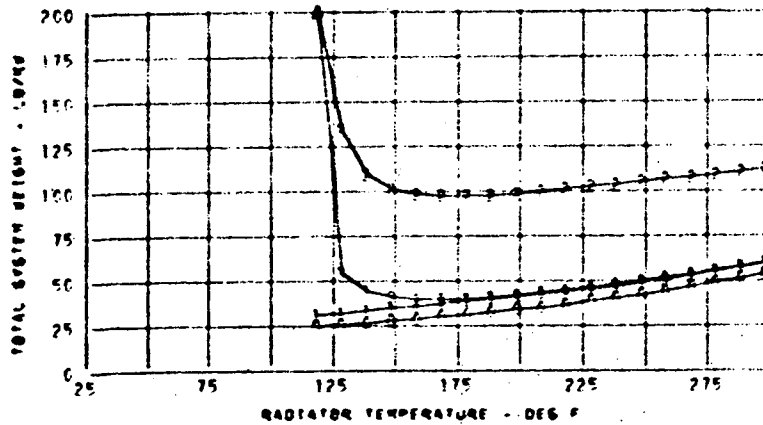
- 0 VAPOR COMP WITH DIRECT COND ATM CONVECTOR
- 1 VAPOR COMP WITH HX LOOP TO ATM CONVECTOR
- 2 GAS CYCLE WITH RAM AIR COOLING
- 3 VAPOR COMP WITH RAM AIR COOLING



ALT = 30000.0 FT
 TEVAP = 34.0 F
 TSINK = 60.4 F
 EPP = 10.0 LB/KW
 RADP = 1.0 LB/FT²



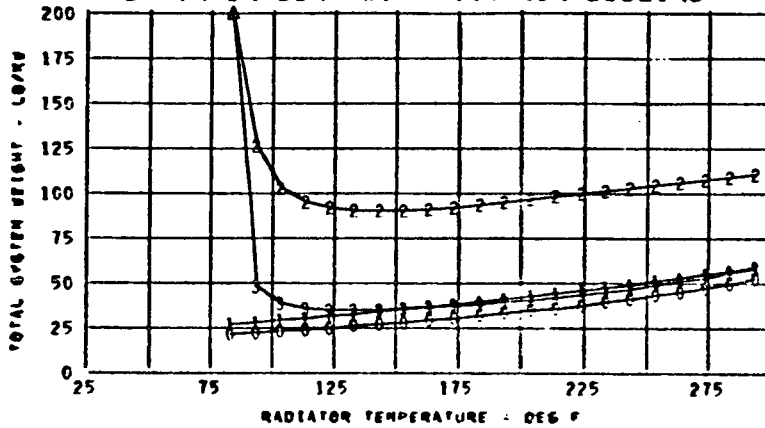
ALT = 40000.0 FT
 TEVAP = 34.0 F
 TSINK = 65.2 F
 ERP = 10.0 LB/KW
 RADP = 1.0 LB/FT²



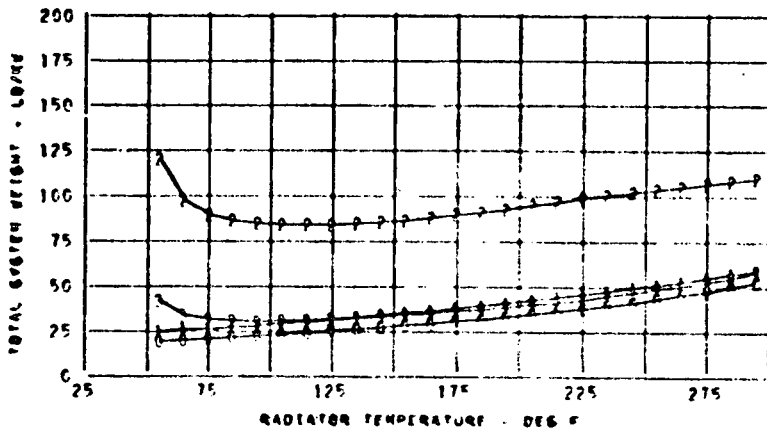
ALT = 10000.0 FT
 TEVAP = 34.0 F
 TSINK = 46.4 F
 EPP = 20.0 LB/KW
 RADP = 0.0 LB/FT²

FIGURE A-32

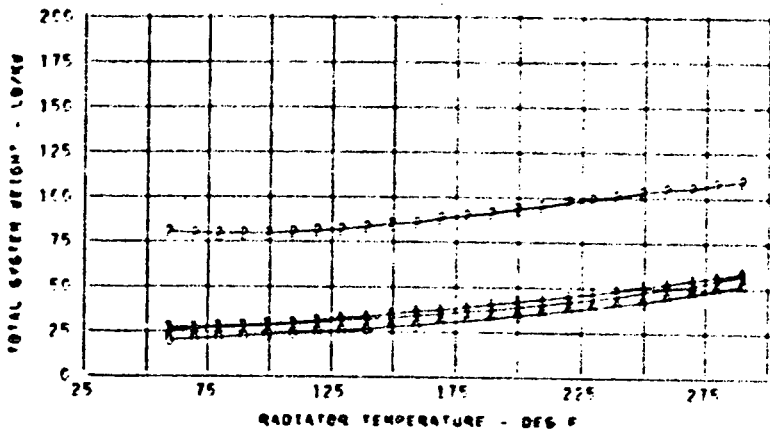
- 0 VAPOR COMP WITH DIRECT COND ATM CONVECTOR
- 1 VAPOR COMP WITH HX LOOP TO ATM CONVECTOR
- 2 GAS CYCLE WITH RAM AIR COOLING
- 3 VAPOR COMP WITH RAM AIR COOLING



ALT = 10000.0 FT
 TEVAP = 34.0 F
 TSINK = 50.8 F
 EPP = 20.0 LB/KW
 RADP = 0.0 LB/FT²



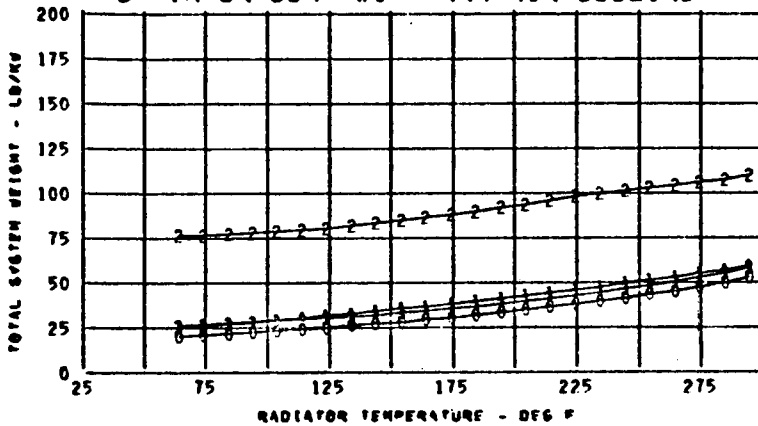
ALT = 20000.0 FT
 TEVAP = 34.0 F
 TSINK = 55.6 F
 EPP = 20.0 LB/KW
 RADP = 0.0 LB/FT²



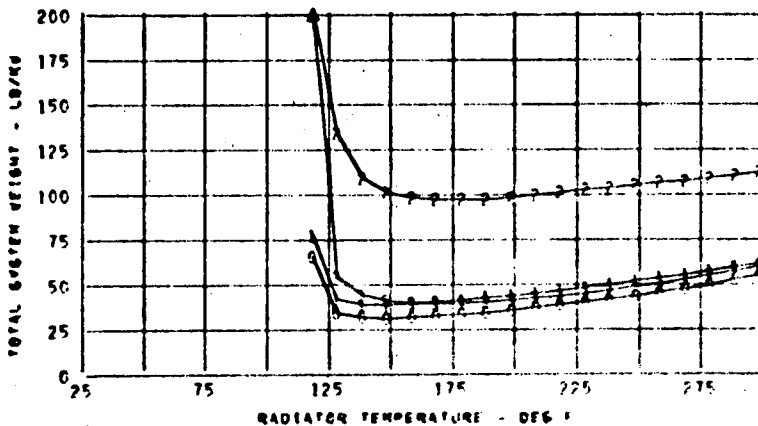
ALT = 30000.0 FT
 TEVAP = 34.0 F
 TSINK = 60.4 F
 EPP = 20.0 LB/KW
 RADP = 0.0 LB/FT²

FIGURE A-33

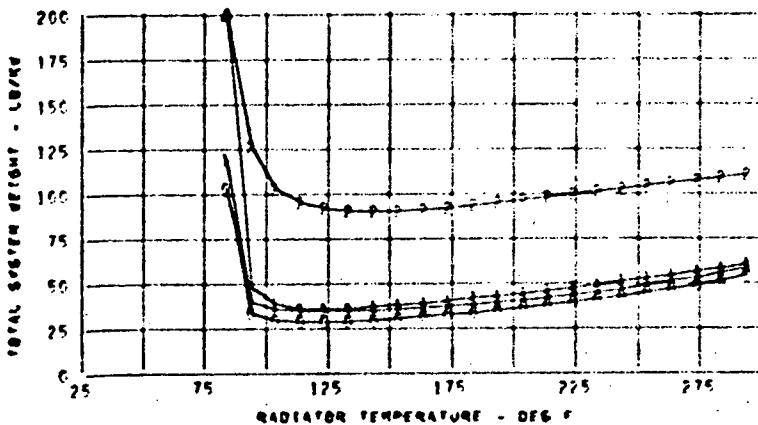
- 0 VAPOR COMP WITH DIRECT COND ATM CONVECTOR
- 1 VAPOR COMP WITH HX LOOP TO ATM CONVECTOR
- 2 GAS CYCLE WITH RAM AIR COOLING
- 3 VAPOR COMP WITH RAM AIR COOLING



ALT = 40000.0 FT
 TEVAP = 34.0 F
 TSINK = 65.2 F
 EPP = 20.0 LB/KW
 RADP = 0.0 LB/FT²



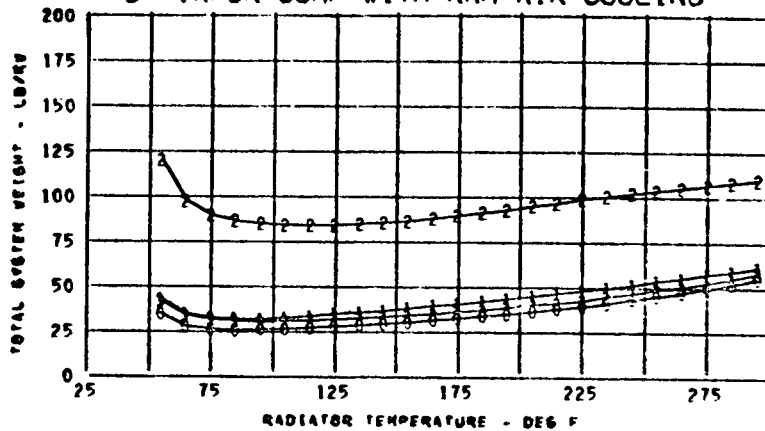
ALT = 1000.0 FT
 TEVAP = 34.0 F
 TSINK = 46.4 F
 EPP = 20.0 LB/KW
 RADP = .50 LB/FT²



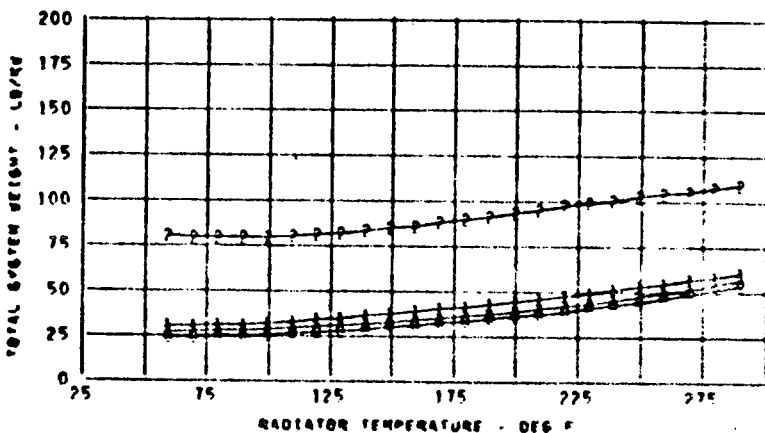
ALT = 10000.0 FT
 TEVAP = 34.0 F
 TSINK = 50.8 F
 EPP = 20.0 LB/KW
 RADP = .50 LB/FT²

FIGURE A-34

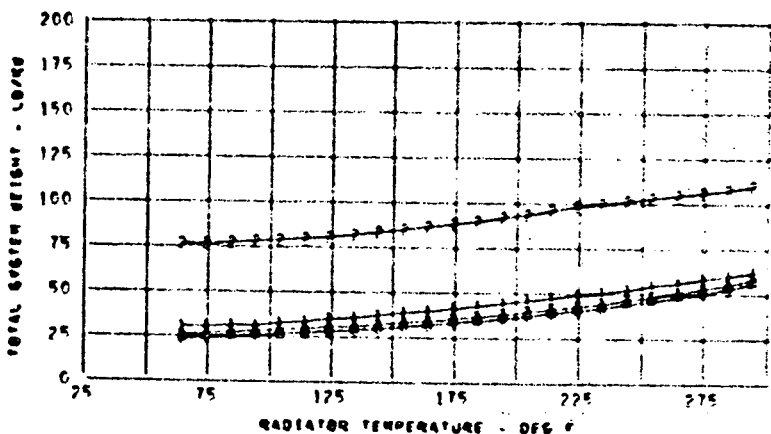
- 0 VAPOR COMP WITH DIRECT COND ATM CONVECTOR
- 1 VAPOR COMP WITH HX LOOP TO ATM CONVECTOR
- 2 GAS CYCLE WITH RAM AIR COOLING
- 3 VAPOR COMP WITH RAM AIR COOLING



ALT = 20000.0 FT
 TEVAP = 34.0 F
 TSINK = 55.6 F
 EPP = 20.0LB/KW
 RADP = .50LB/FT²



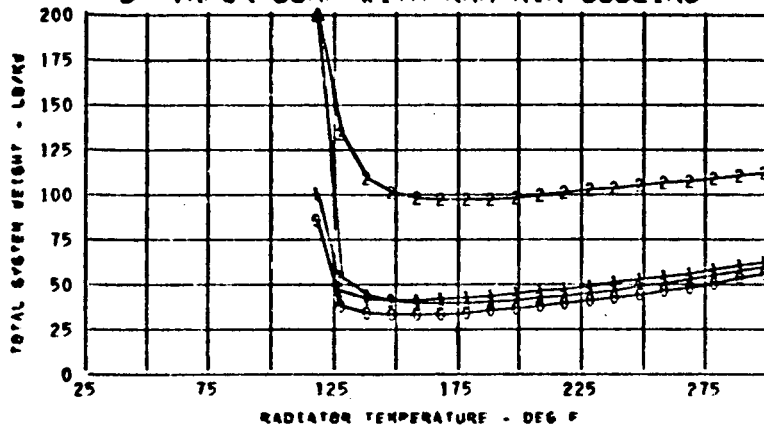
ALT = 30000.0 FT
 TEVAP = 34.0 F
 TSINK = 60.4 F
 EPP = 20.0LB/KW
 RADP = .50LB/FT²



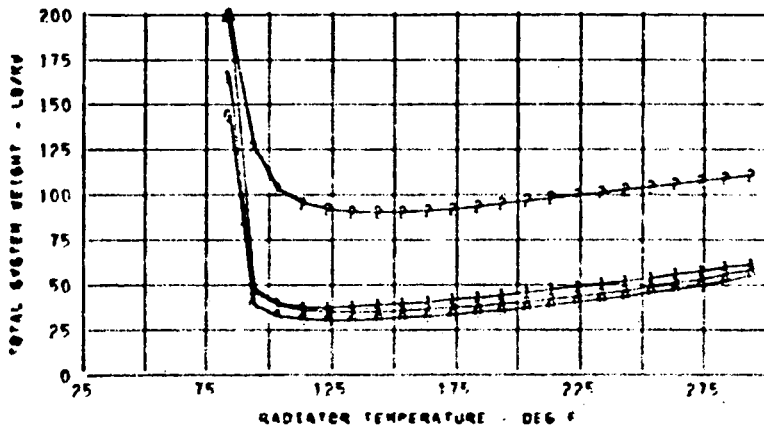
ALT = 40000.0 FT
 TEVAP = 34.0 F
 TSINK = 65.2 F
 EPP = 20.0LB/KW
 RADP = .50LB/FT²

FIGURE A-35

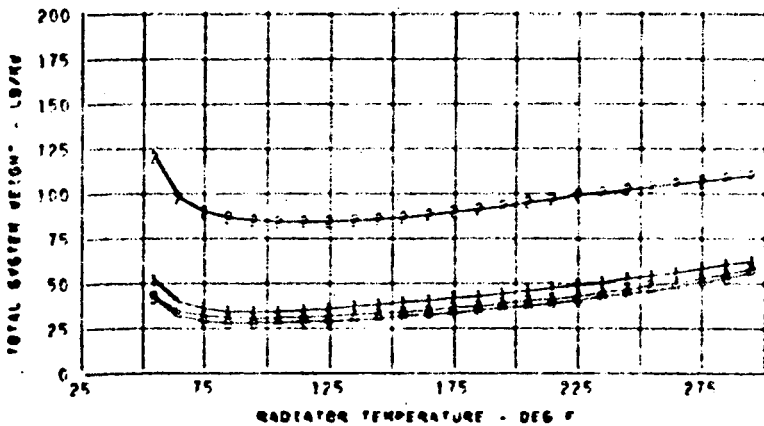
- 0 VAPOR COMP WITH DIRECT COND ATM CONVECTOR
- 1 VAPOR COMP WITH HX LOOP TO ATM CONVECTOR
- 2 GAS CYCLE WITH RAM AIR COOLING
- 3 VAPOR COMP WITH RAM AIR COOLING



ALT = 1000.0 FT
 TEVAP = 34.0 F
 TSINK = 46.4 F
 EPP = 20.0 LB/KW
 RADP = .75 LB/FT²



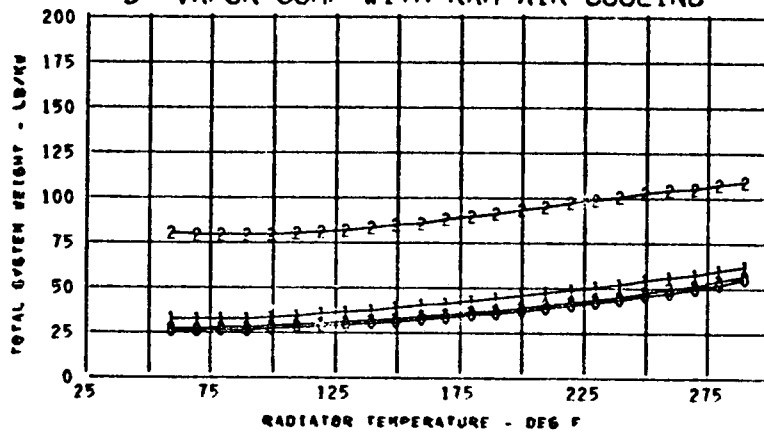
ALT = 10000.0 FT
 TEVAP = 34.0 F
 TSINK = 50.8 F
 EPP = 20.0 LB/KW
 RADP = .75 LB/FT²



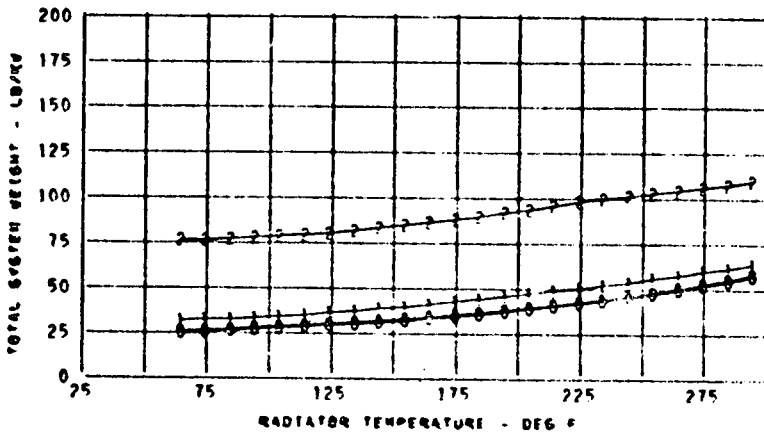
ALT = 20000.0 FT
 TEVAP = 34.0 F
 TSINK = 55.6 F
 EPP = 20.0 LB/KW
 RADP = .75 LB/FT²

FIGURE A-36

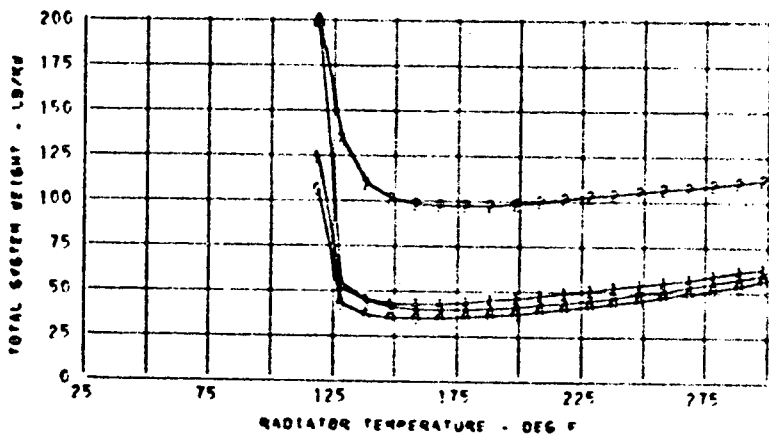
- 0 VAPOR COMP WITH DIRECT COND ATM CONVECTOR
- 1 VAPOR COMP WITH HX LOOP TO ATM CONVECTOR
- 2 GAS CYCLE WITH RAM AIR COOLING
- 3 VAPOR COMP WITH RAM AIR COOLING



ALT = 30000.0 FT
 TEVAP = 34.0 F
 TSINK = 60.4 F
 EPP = 20.0 LB/KW
 RADP = .75 LB/FT²



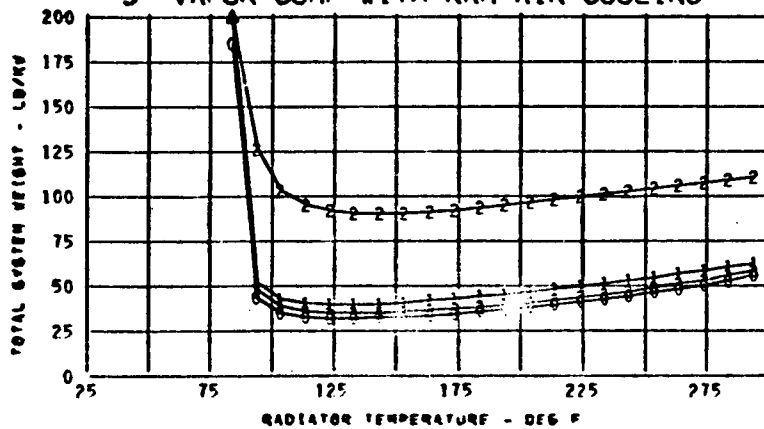
ALT = 40000.0 FT
 TEVAP = 34.0 F
 TSINK = 65.2 F
 EPP = 20.0 LB/KW
 RADP = .75 LB/FT²



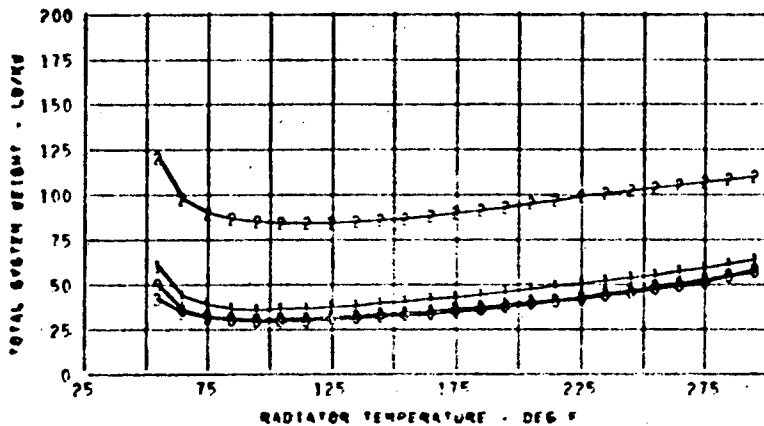
ALT = 1000.0 FT
 TEVAP = 34.0 F
 TSINK = 46.4 F
 EPP = 20.0 LB/KW
 RADP = 1.0 LB/FT²

FIGURE A-37

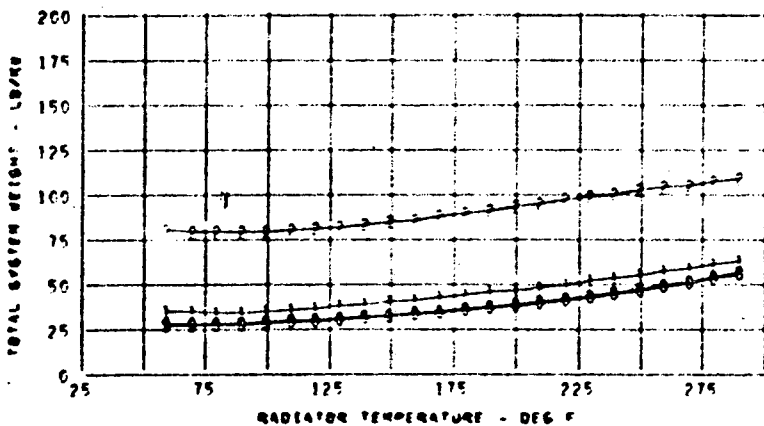
- 0 VAPOR COMP WITH DIRECT COND ATM CONVECTOR
- 1 VAPOR COMP WITH HX LOOP TO ATM CONVECTOR
- 2 GAS CYCLE WITH RAM AIR COOLING
- 3 VAPOR COMP WITH RAM AIR COOLING



ALT = 10000.0 FT
 TEVAP = 34.0 F
 TSINK = 50.8 F
 EPP = 20.0 LB/KW
 RADP = 1.0 LB/FT²



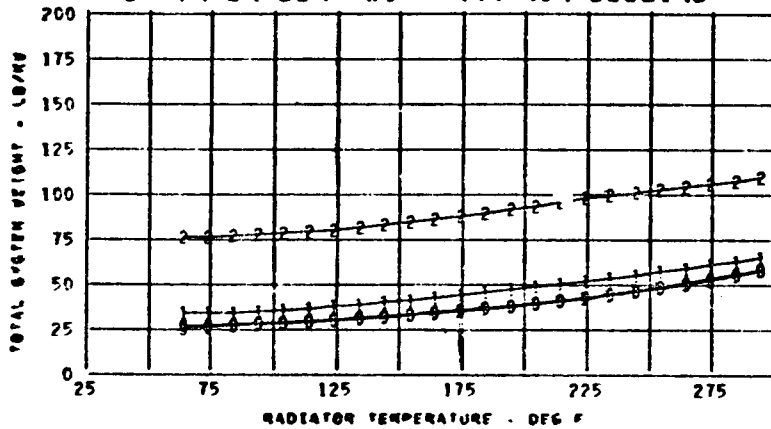
ALT = 20000.0 FT
 TEVAP = 34.0 F
 TSINK = 55.6 F
 EPP = 20.0 LB/KW
 RADP = 1.0 LB/FT²



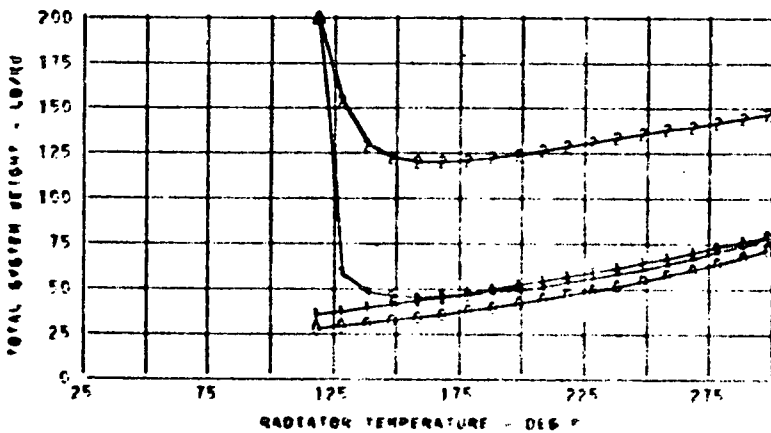
ALT = 30000.0 FT
 TEVAP = 34.0 F
 TSINK = 60.4 F
 EPP = 20.0 LB/KW
 RADP = 1.0 LB/FT²

FIGURE A-38

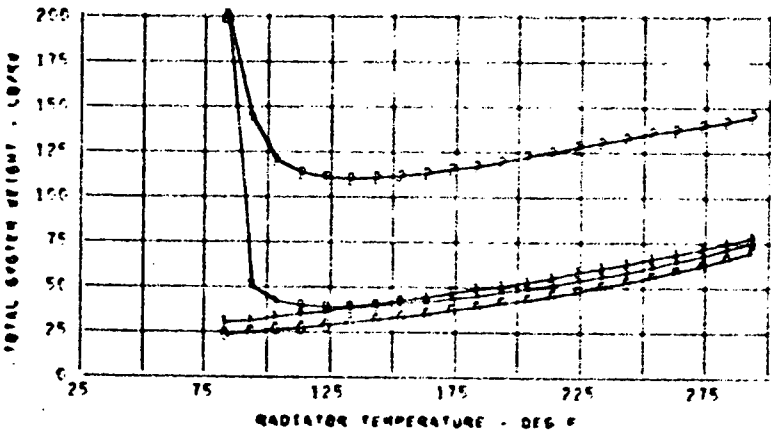
- 0 VAPOR COMP WITH DIRECT COND ATM CONVECTOR
- 1 VAPOR COMP WITH HX LOOP TO ATM CONVECTOR
- 2 GAS CYCLE WITH RAM AIR COOLING
- 3 VAPOR COMP WITH RAM AIR COOLING



ALT = 40000.0 FT
 TEVAP = 34.0 F
 TSINK = 65.2 F
 EPP = 20.0 LB/KW
 RADP = 1.0 LB/FT²



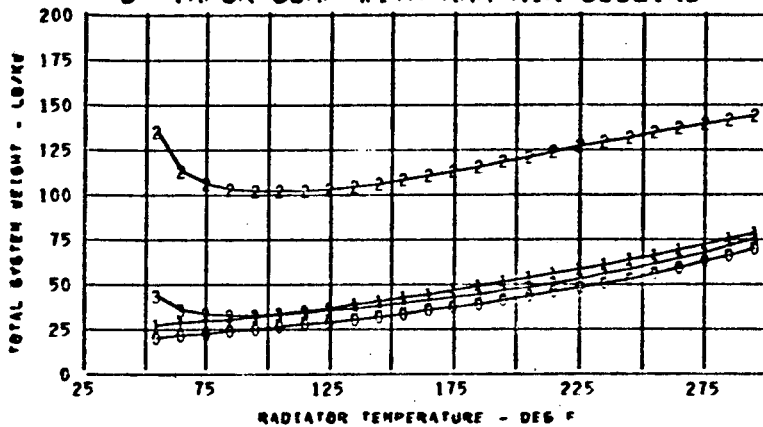
ALT = 10000.0 FT
 TEVAP = 34.0 F
 TSINK = 46.4 F
 EPP = 30.0 LB/KW
 RADP = 0.0 LB/FT²



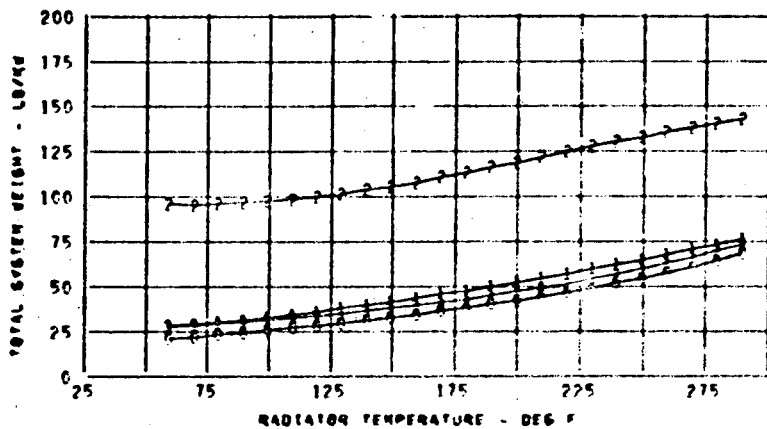
ALT = 10000.0 FT
 TEVAP = 34.0 F
 TSINK = 50.8 F
 EPP = 30.0 LB/KW
 RADP = 0.0 LB/FT²

FIGURE A-39

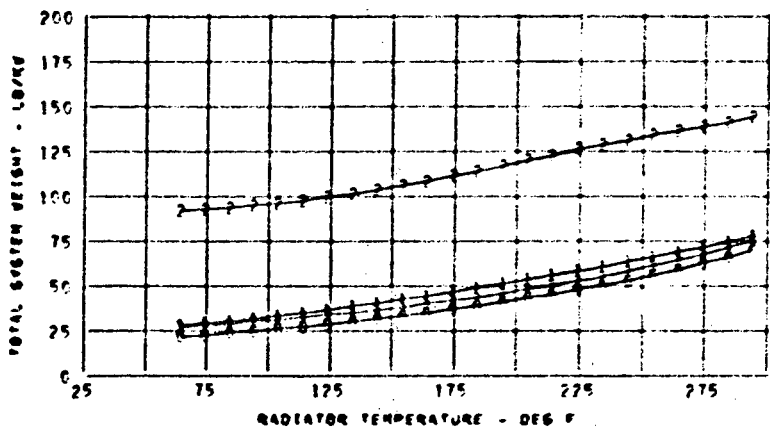
- 0 VAPOR COMP WITH DIRECT COND ATM CONVECTOR
- 1 VAPOR COMP WITH HX LOOP TO ATM CONVECTOR
- 2 GAS CYCLE WITH RAM AIR COOLING
- 3 VAPOR COMP WITH RAM AIR COOLING



ALT = 20000.0 FT
 TEVAP = 34.0 F
 TSINK = 55.6 F
 EPP = 30.0 LB/KW
 RADP = 0.0 LB/FT²



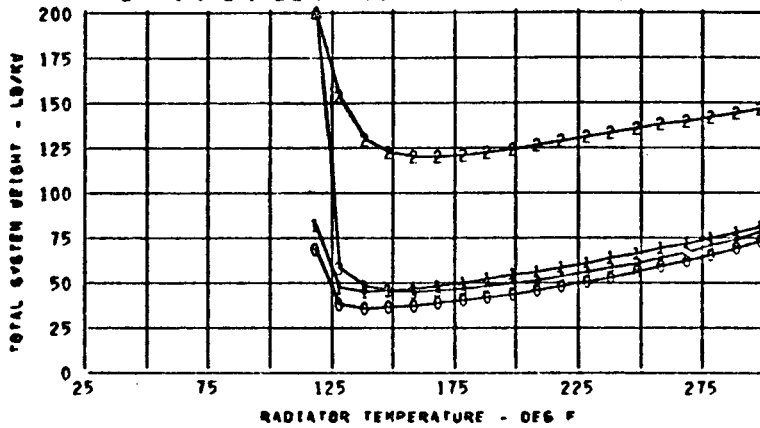
ALT = 30000.0 FT
 TEVAP = 34.0 F
 TSINK = 60.4 F
 EPP = 30.0 LB/KW
 RADP = 0.0 LB/FT²



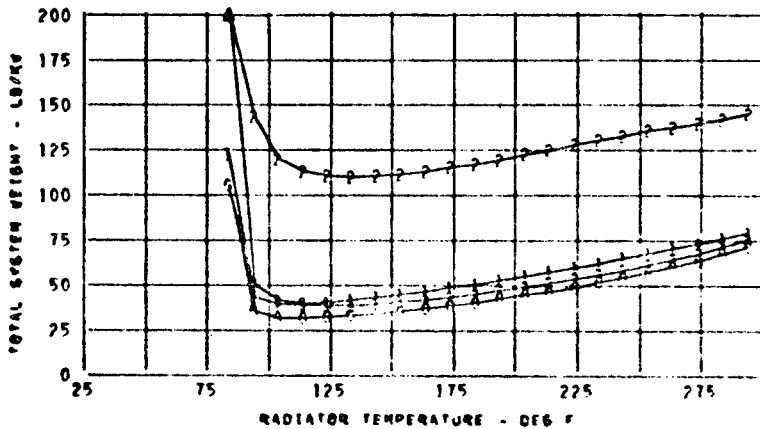
ALT = 40000.0 FT
 TEVAP = 34.0 F
 TSINK = 65.2 F
 EPP = 30.0 LB/KW
 RADP = 0.0 LB/FT²

FIGURE A-40

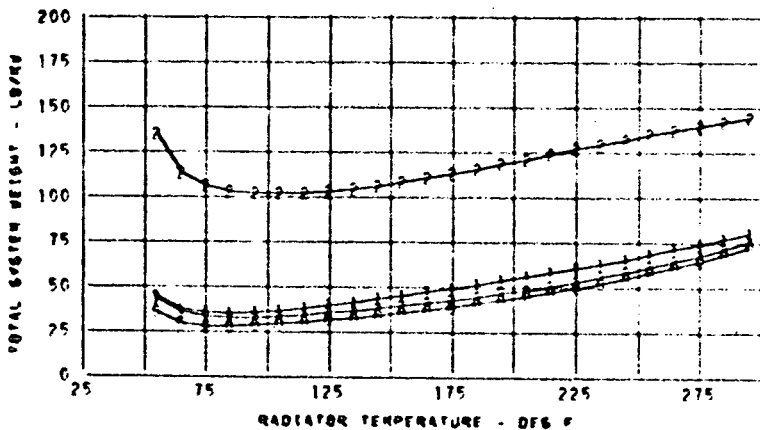
- 0 VAPOR COMP WITH DIRECT COND ATM CONVECTOR
- 1 VAPOR COMP WITH HX LOOP TO ATM CONVECTOR
- 2 GAS CYCLE WITH RAM AIR COOLING
- 3 VAPOR COMP WITH RAM AIR COOLING



ALT = 1000.0 FT
 TEVAP = 34.0 F
 TSINK = 46.4 F
 EPP = 30.0 LB/KW
 RADP = .50 LB/FT²



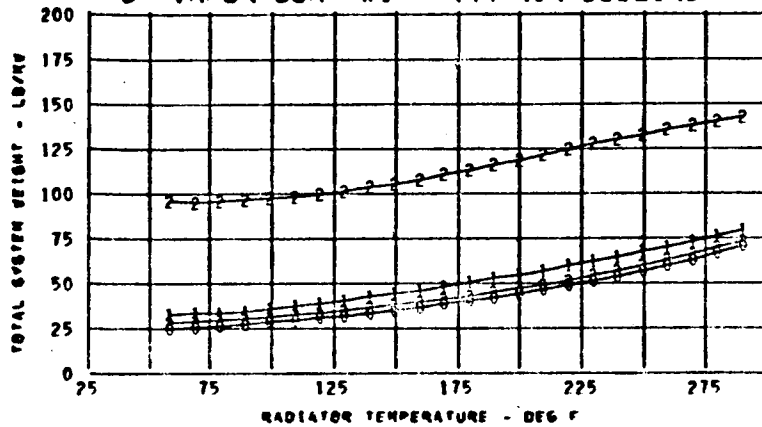
ALT = 10000.0 FT
 TEVAP = 34.0 F
 TSINK = 50.8 F
 EPP = 30.0 LB/KW
 RADP = .50 LB/FT²



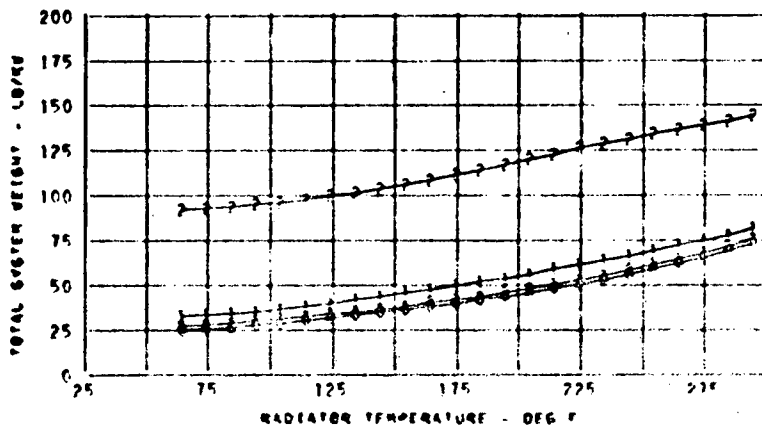
ALT = 20000.0 FT
 TEVAP = 34.0 F
 TSINK = 55.6 F
 EPP = 30.0 LB/KW
 RADP = .50 LB/FT²

FIGURE A-41

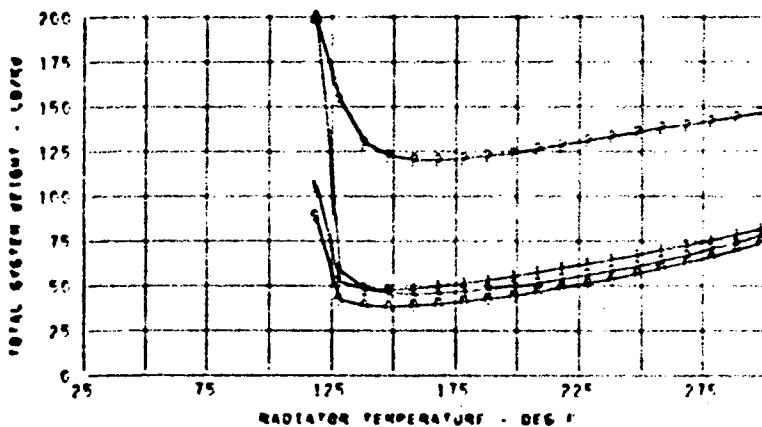
- 0 VAPOR COMP WITH DIRECT COND ATM CONVECTOR
- 1 VAPOR COMP WITH HX LOOP TO ATM CONVECTOR
- 2 GAS CYCLE WITH RAM AIR COOLING
- 3 VAPOR COMP WITH RAM AIR COOLING



ALT = 30000.0 FT
 TEVAP = 34.0 F
 TSINK = 60.4 F
 EPP = 30.0 LB/KW
 RADP = .50 LB/FT²



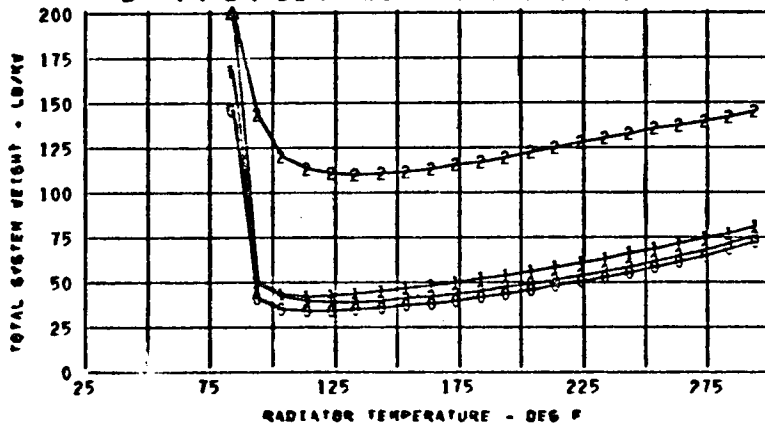
ALT = 40000.0 FT
 TEVAP = 34.0 F
 TSINK = 65.2 F
 EPP = 30.0 LB/KW
 RADP = .50 LB/FT²



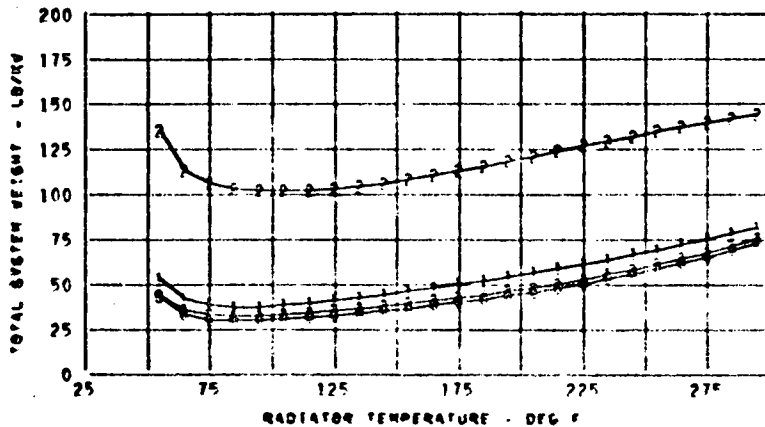
ALT = 1000.0 FT
 TEVAP = 34.0 F
 TSINK = 46.4 F
 EPP = 30.0 LB/KW
 RADP = .75 LB/FT²

FIGURE A-42

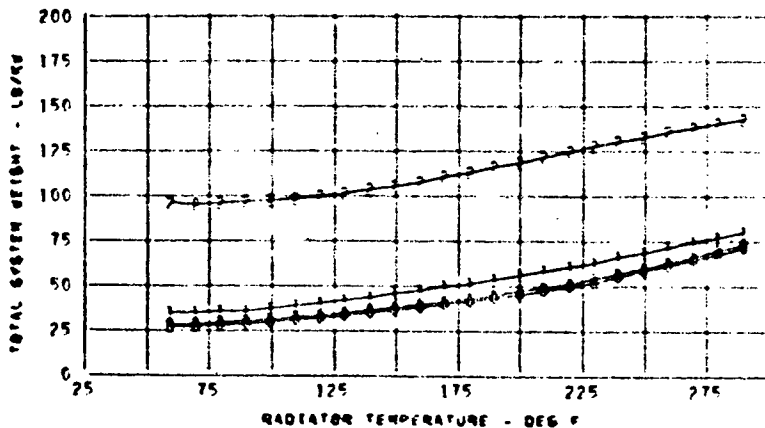
- 0 VAPOR COMP WITH DIRECT COND ATM CONVECTOR
- 1 VAPOR COMP WITH HX LOOP TO ATM CONVECTOR
- 2 GAS CYCLE WITH RAM AIR COOLING
- 3 VAPOR COMP WITH RAM AIR COOLING



ALT = 10000.0 FT
 TEVAP = 34.0 F
 TSINK = 50.8 F
 EPP = 30.0 LB/KW
 RADP = .75 LB/FT²



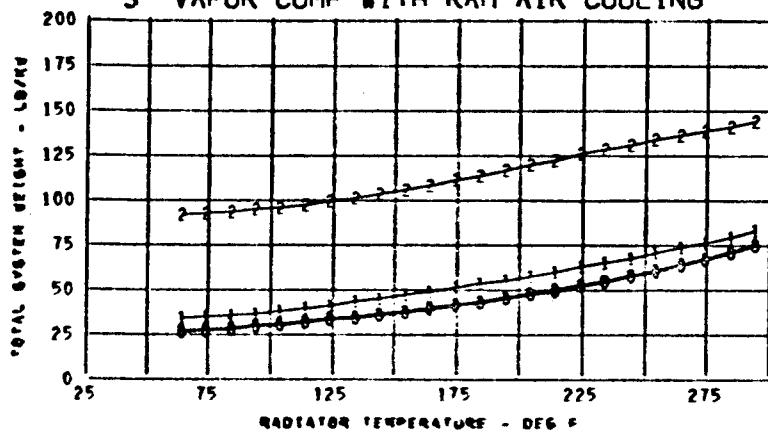
ALT = 20000.0 FT
 TEVAP = 34.0 F
 TSINK = 55.6 F
 EPP = 30.0 LB/KW
 RADP = .75 LB/FT²



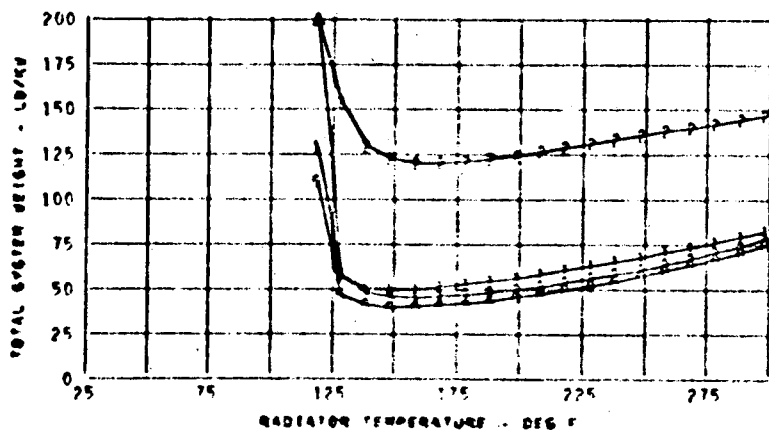
ALT = 30000.0 FT
 TEVAP = 34.0 F
 TSINK = 60.4 F
 EPP = 30.0 LB/KW
 RADP = .75 LB/FT²

FIGURE A-43

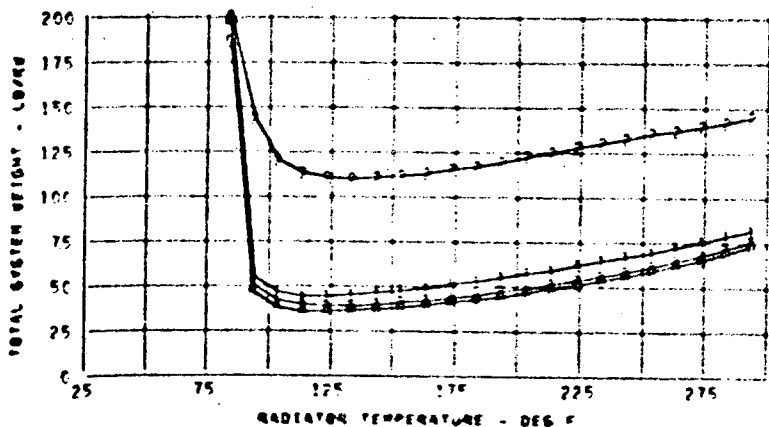
- 0 VAPOR COMP WITH DIRECT COND ATM CONVECTOR
- 1 VAPOR COMP WITH HX LOOP TO ATM CONVECTOR
- 2 GAS CYCLE WITH RAM AIR COOLING
- 3 VAPOR COMP WITH RAM AIR COOLING



ALT = 40000.0 FT
 TEVAP = 34.0 F
 TSINK = 65.2 F
 EPP = 30.0LB/KW
 RADP = .75LB/FT²



ALT = 1000.0 FT
 TEVAP = 34.0 F
 TSINK = 46.4 F
 EPP = 30.0LB/KW
 RADP = 1.0LB/FT²

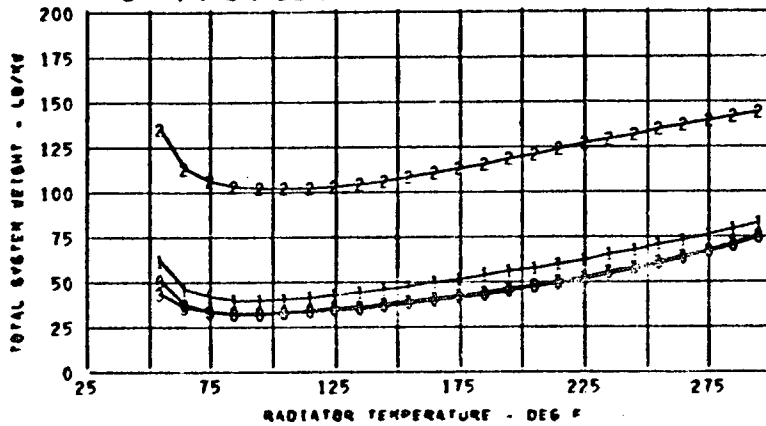


ALT = 10000.0 FT
 TEVAP = 34.0 F
 TSINK = 50.8 F
 EPP = 30.0LB/KW
 RADP = 1.0LB/FT²

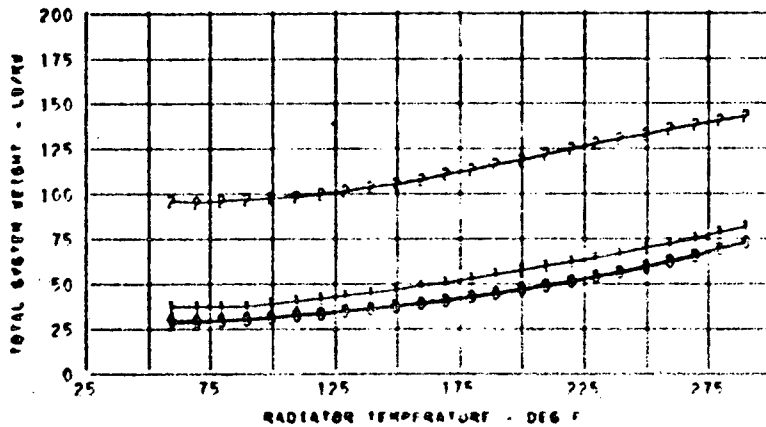
C

FIGURE A-44

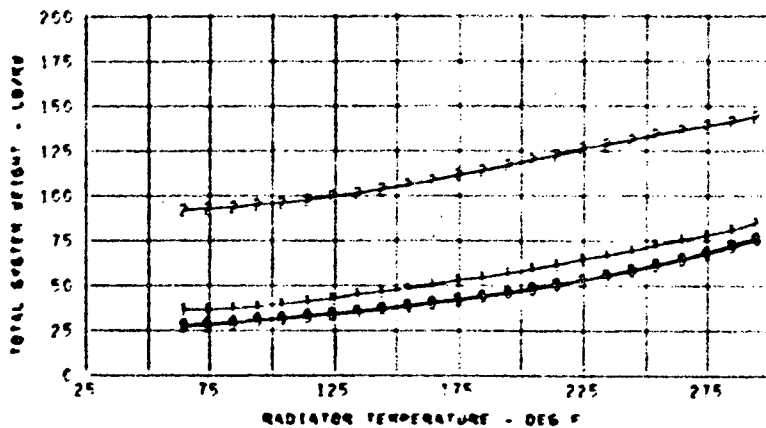
- 0 VAPOR COMP WITH DIRECT COND ATM CONVECTOR
- 1 VAPOR COMP WITH HX LOOP TO ATM CONVECTOR
- 2 GAS CYCLE WITH RAM AIR COOLING
- 3 VAPOR COMP WITH RAM AIR COOLING



ALT = 20000.0 FT
 TEVAP = 34.0 F
 TSINK = 55.6 F
 EPP = 30.0 LB/KW
 RADP = 1.0 LB/FT²



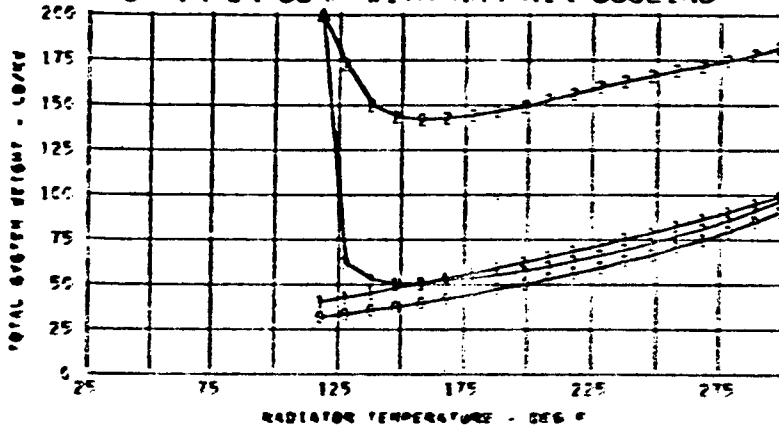
ALT = 30000.0 FT
 TEVAP = 34.0 F
 TSINK = 60.4 F
 EPP = 30.0 LB/KW
 RADP = 1.0 LB/FT²



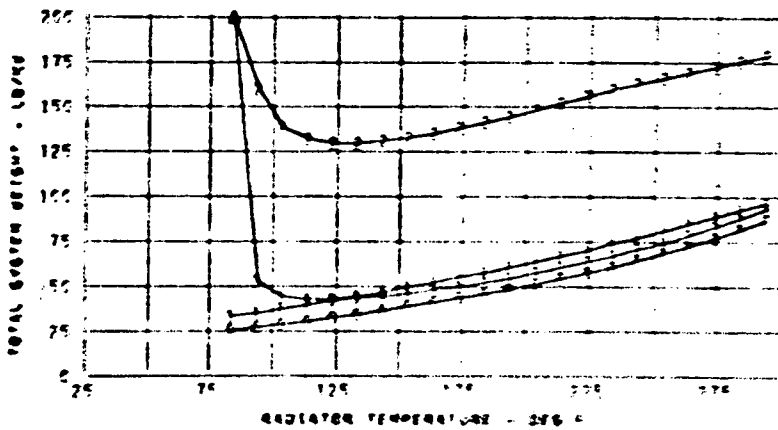
ALT = 40000.0 FT
 TEVAP = 34.0 F
 TSINK = 65.2 F
 EPP = 30.0 LB/KW
 RADP = 1.0 LB/FT²

FIGURE A-45

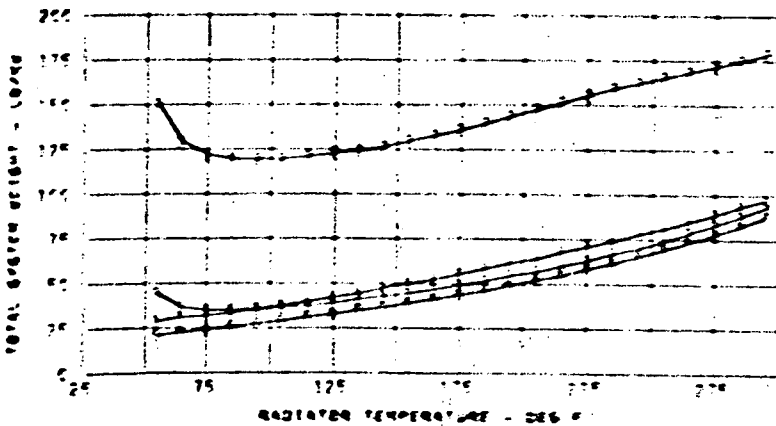
- 0 VAPOR COMP WITH DIRECT COND ATM CONVECTOR
- 1 VAPOR COMP WITH HX LOOP TO ATM CONVECTOR
- 2 GAS CYCLE WITH RAM AIR COOLING
- 3 VAPOR COMP WITH RAM AIR COOLING



ALT = 1000.0 FT
 TEVAP = 34.0 F
 TSINK = 46.4 F
 EPP = 40.0 LB/KW
 RADP = 0.0 LB/FT²



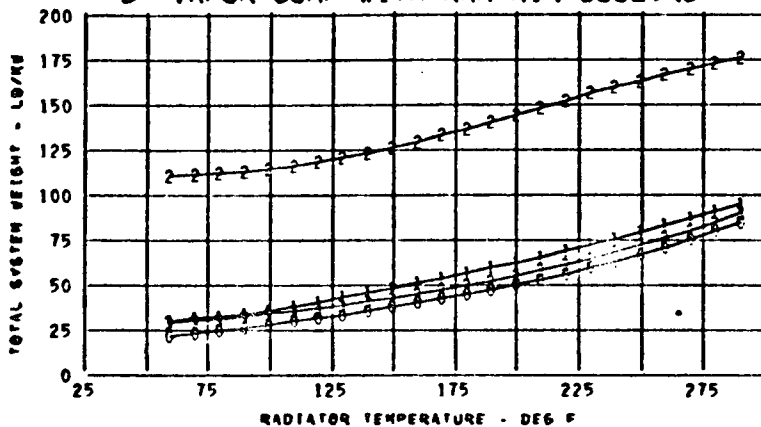
ALT = 10000.0 FT
 TEVAP = 34.0 F
 TSINK = 50.8 F
 EPP = 40.0 LB/KW
 RADP = 0.0 LB/FT²



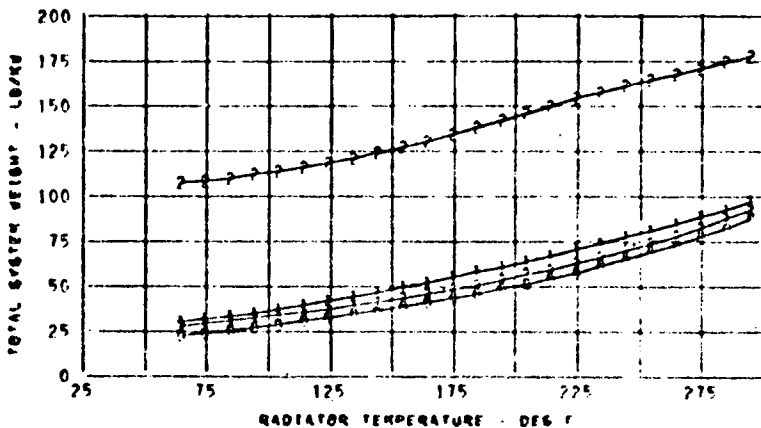
ALT = 20000.0 FT
 TEVAP = 34.0 F
 TSINK = 55.6 F
 EPP = 40.0 LB/KW
 RADP = 0.0 LB/FT²

FIGURE A-46

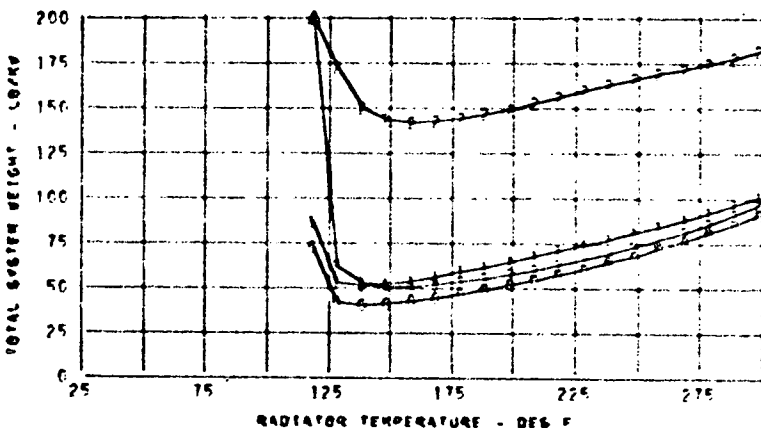
- 0 VAPOR COMP WITH DIRECT COND ATM CONVECTOR
- 1 VAPOR COMP WITH HX LOOP TO ATM CONVECTOR
- 2 GAS CYCLE WITH RAM AIR COOLING
- 3 VAPOR COMP WITH RAM AIR COOLING



ALT = 30000.0 FT
 TEVAP = 34.0 F
 TSINK = 60.4 F
 EPP = 40.0 LB/KW
 RADP = 0.0 LB/FT²



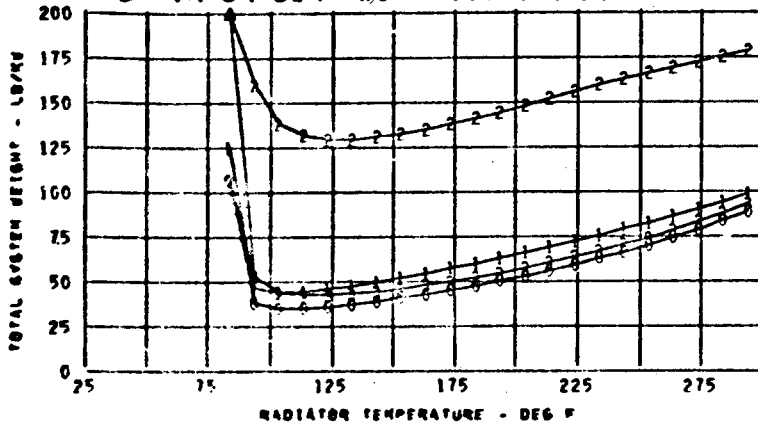
ALT = 40000.0 FT
 TEVAP = 34.0 F
 TSINK = 65.2 F
 EPP = 40.0 LB/KW
 RADP = 0.0 LB/FT²



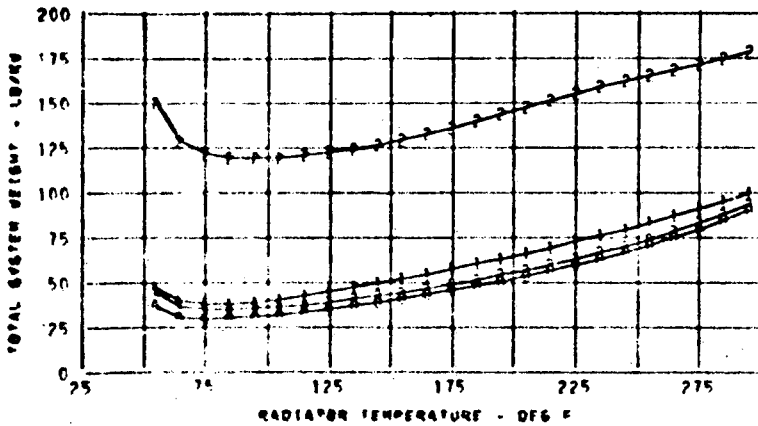
ALT = 1000.0 FT
 TEVAP = 34.0 F
 TSINK = 46.4 F
 EPP = 40.0 LB/KW
 RADP = .50 LB/FT²

FIGURE A-47

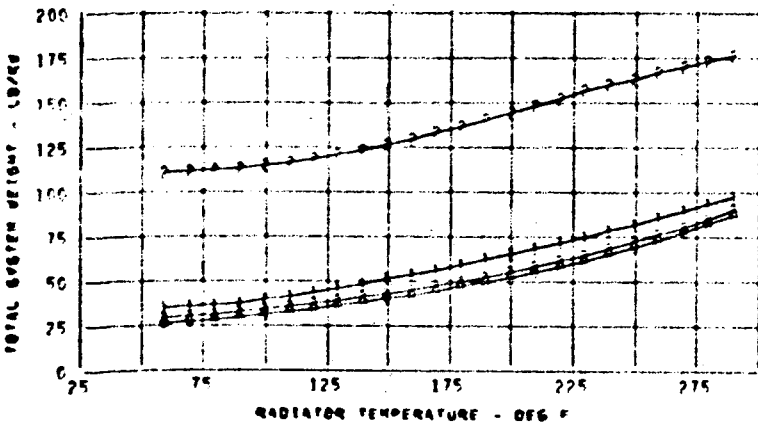
- 0 VAPOR COMP WITH DIRECT COND ATM CONVECTOR
- 1 VAPOR COMP WITH HX LOOP TO ATM CONVECTOR
- 2 GAS CYCLE WITH RAM AIR COOLING
- 3 VAPOR COMP WITH RAM AIR COOLING



ALT = 10000.0 FT
 TEVAP = 34.0 F
 TSINK = 50.8 F
 EPP = 40.0 LB/KW
 RADP = .50 LB/FT²



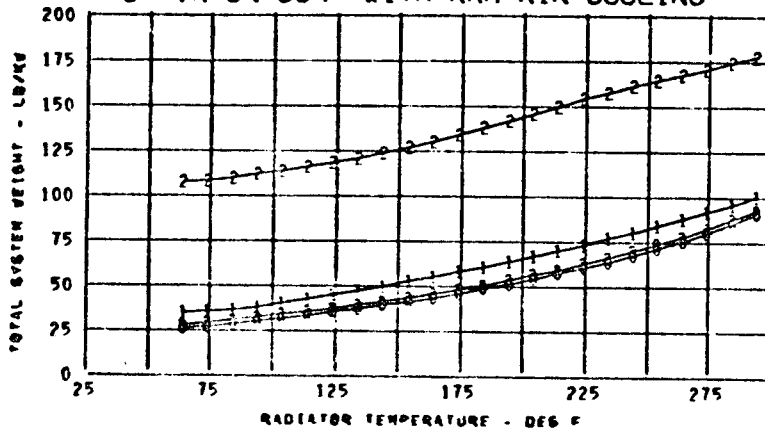
ALT = 20000.0 FT
 TEVAP = 34.0 F
 TSINK = 55.6 F
 EPP = 40.0 LB/KW
 RADP = .50 LB/FT²



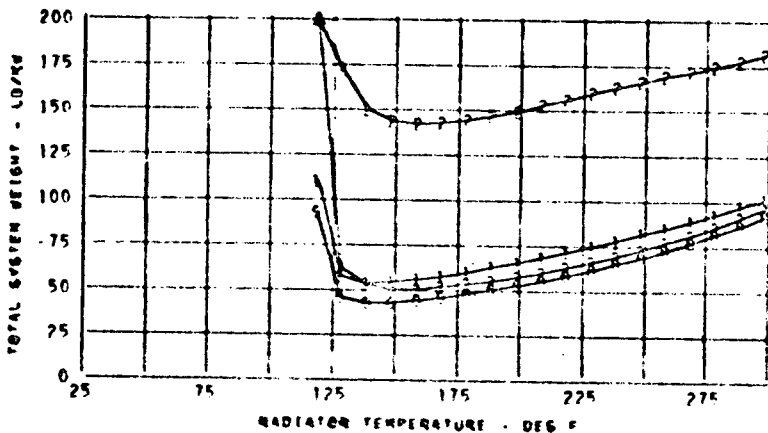
ALT = 30000.0 FT
 TEVAP = 34.0 F
 TSINK = 60.4 F
 EPP = 40.0 LB/KW
 RADP = .50 LB/FT²

FIGURE A-48

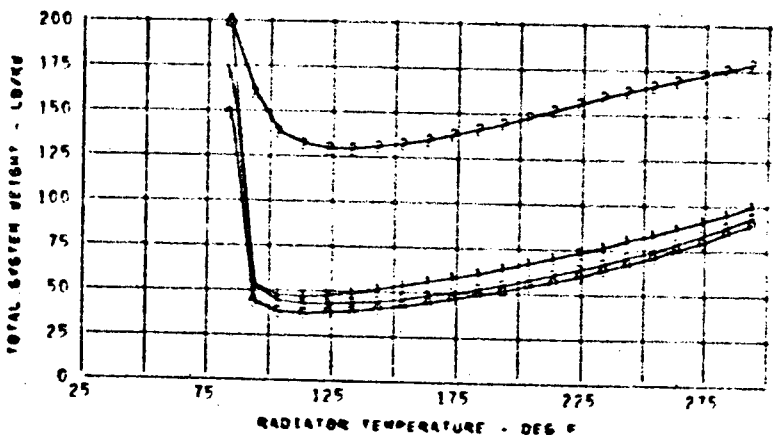
- 0 VAPOR COMP WITH DIRECT COND ATM CONVECTOR
- 1 VAPOR COMP WITH HX LOOP TO ATM CONVECTOR
- 2 GAS CYCLE WITH RAM AIR COOLING
- 3 VAPOR COMP WITH RAM AIR COOLING



ALT = 40000.0 FT
 TEVAP = 34.0 F
 TSINK = 65.2 F
 EPP = 40.0 LB/KW
 RADP = .50 LB/FT²



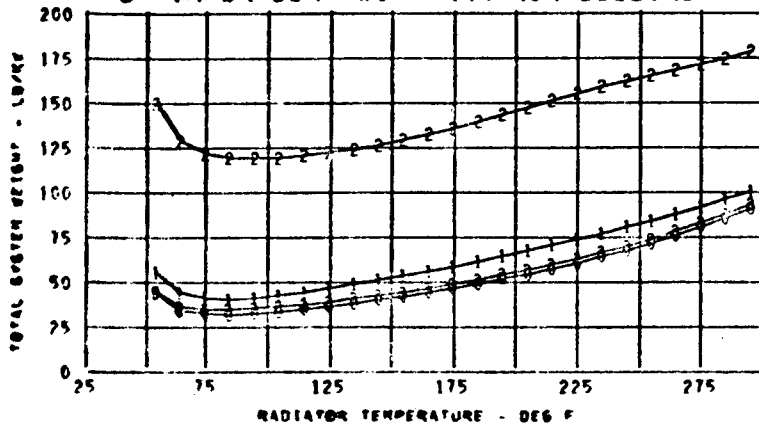
ALT = 10000.0 FT
 TEVAP = 34.0 F
 TSINK = 46.4 F
 EPP = 40.0 LB/KW
 RADP = .75 LB/FT²



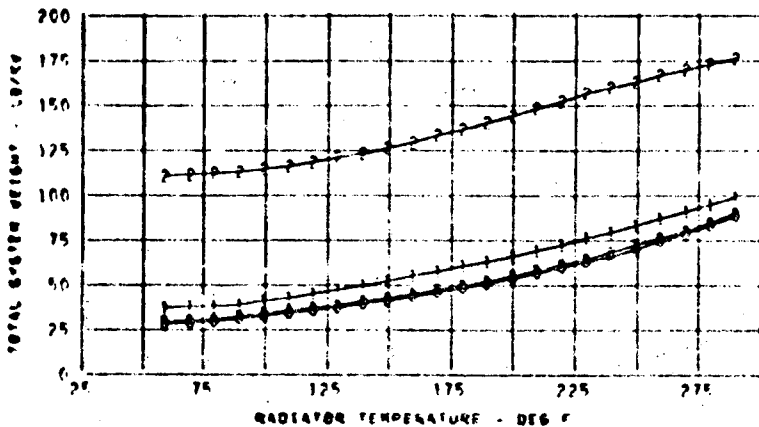
ALT = 10000.0 FT
 TEVAP = 34.0 F
 TSINK = 50.8 F
 EPP = 40.0 LB/KW
 RADP = .75 LB/FT²

FIGURE A-49

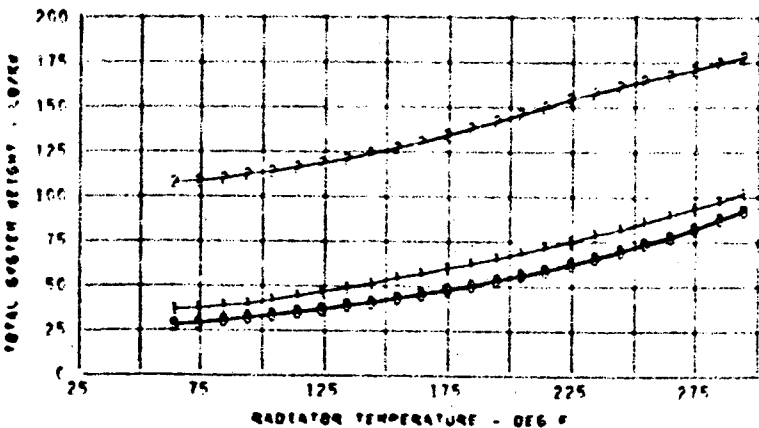
- 0 VAPOR COMP WITH DIRECT COND ATM CONVECTOR
- 1 VAPOR COMP WITH HX LOOP TO ATM CONVECTOR
- 2 GAS CYCLE WITH RAM AIR COOLING
- 3 VAPOR COMP WITH RAM AIR COOLING



ALT = 20000.0 FT
 TEVAP = 34.0 F
 TSINK = 55.6 F
 EPP = 40.0 LB/KW
 RADP = .75 LB/FT²



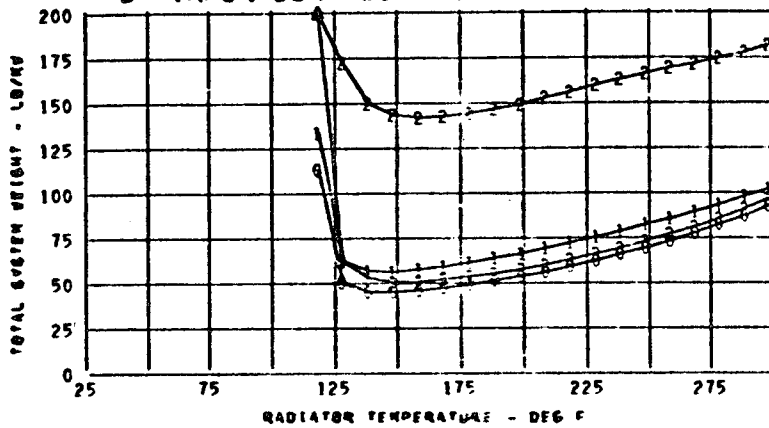
ALT = 30000.0 FT
 TEVAP = 34.0 F
 TSINK = 60.4 F
 EPP = 40.0 LB/KW
 RADP = .75 LB/FT²



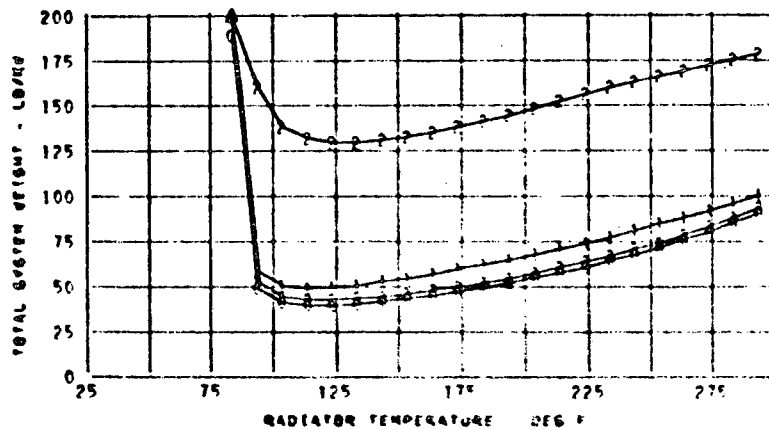
ALT = 40000.0 FT
 TEVAP = 34.0 F
 TSINK = 65.2 F
 EPP = 40.0 LB/KW
 RADP = .75 LB/FT²

FIGURE A-50

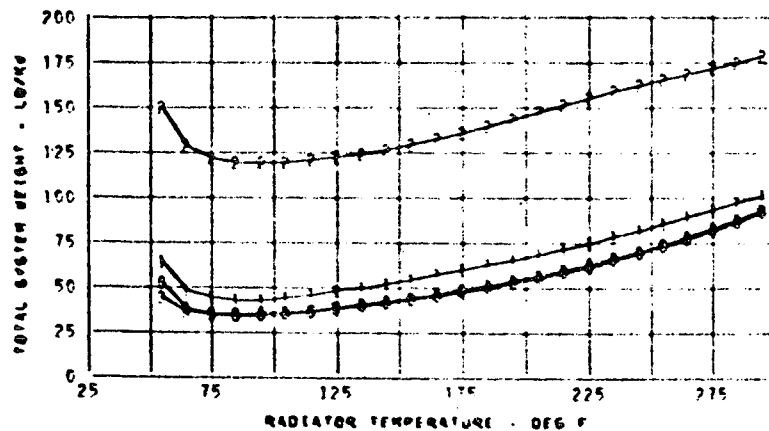
- 0 VAPOR COMP WITH DIRECT COND ATM CONVECTOR
- 1 VAPOR COMP WITH HX LOOP TO ATM CONVECTOR
- 2 GAS CYCLE WITH RAM AIR COOLING
- 3 VAPOR COMP WITH RAM AIR COOLING



ALT = 1000.0 FT
 TEVAP = 34.0 F
 TSINK = 46.4 F
 EPP = 40.0 LB/KW
 RADP = 1.0 LB/FT²



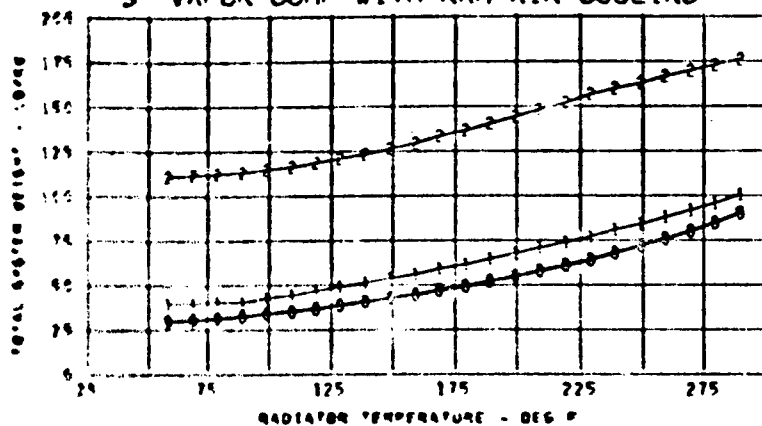
ALT = 10000.0 FT
 TEVAP = 34.0 F
 TSINK = 50.8 F
 EPP = 40.0 LB/KW
 RADP = 1.0 LB/FT²



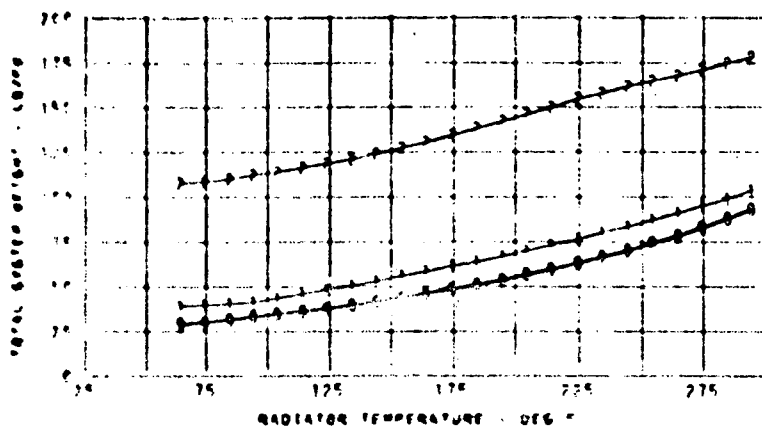
ALT = 20000.0 FT
 TEVAP = 34.0 F
 TSINK = 55.6 F
 EPP = 40.0 LB/KW
 RADP = 1.0 LB/FT²

Figure A-51

- 0 VAPOR COMP WITH DIRECT COND ATM CONVECTOR
- 1 VAPOR COMP WITH HX LOOP TO ATM CONVECTOR
- 2 GAS CYCLE WITH RAM AIR COOLING
- 3 VAPOR COMP WITH RAM AIR COOLING



ALT = 30000.0 FT
 TEVAP = 34.0 F
 TSINK = 60.4 F
 EPP = 40.0 LB/KW
 RADP = 1.0 LB/FT²



ALT = 40000.0 FT
 TEVAP = 34.0 F
 TSINK = 65.2 F
 EPP = 40.0 LB/KW
 RADP = 1.0 LB/FT²

APPENDIX B

DETERMINATION OF ORBITER SPACE RADIATOR

STEADY STATE DESIGN ENVIRONMENTS

This Appendix presents the results of a comprehensive analysis to determine the maximum effective environment to use in the steady state method of analysis of the Orbiter space radiators. Transient earth orbit adiabatic surface temperatures of an 0.04 inch aluminum plate were obtained for various attitudes and orientations. The maximum adiabatic surface temperatures are then used as the effective radiation sink temperature for the steady state radiator analysis.

Cyclical repeating temperatures were obtained for flat plates, with surface coating properties of $\alpha = .3$ and $\epsilon = .9$, located at 15° increments around the periphery of a cylinder in earth orbit. The Midwest Research Institute (MRI) (Reference B1) computer routine was used for this analysis. The adiabatic surface temperatures provide an estimate of the thermal lag of the radiator and the use of the maximum temperature or maximum combination of several temperatures in orbit as the effective radiation sink temperature in the steady state method of analysis will provide a more realistic radiator design.

To determine average environments for several different radiator configurations MRI is run with four different nodal breakdowns. Each type is a series of nodes located around the perimeter of a circle created by the intersection of a plane with the sphere. The nodes are 15 degrees apart and are numbered from 1 to 24.

Nodes located as such give the environments seen by a cylinder in a particular orbit. The four breakdowns result from the different ways a cylinder may be oriented in orbit. The cylinder may have one node constantly facing the earth, this is designated as a planet oriented vehicle, or the cylinder may have one node constantly facing the sun, a solar oriented vehicle. In each of these orientations the cylinder may have its longitudinal, X-axis, or its transverse, Y-axis, perpendicular to either the orbit plane or the plane of the ecliptic. Hence, for a planet oriented vehicle the designation X-POP signifies that a vehicle, such as in Figure B-1, has its longitudinal or X-axis perpendicular to the orbit plane. Y-POP is similar. For a planet oriented vehicle in both X-POP and Y-POP orientation, the X and Y axes are perpendicular to the orbit plane regardless of the orbit inclination as seen in Figure B-1.

However, for the solar oriented vehicle X-POP signifies the longitudinal axis is perpendicular to the orbit plane only when the vehicle is in an orbit inclination of 0 degrees. For orbit inclinations greater than 0 degrees, X-POP signifies the longitudinal axis is perpendicular to the plane of the ecliptic with the subsolar point on the equator. Y-POP is similar. See Figure B-1. Node locations for both planet and solar orientation are given in Figure B-2. Figures B-3 through B-66 present plotted data for each node in both planet, solar, X-POP, and Y-POP orientations for various orbit inclinations.

Effective radiation environments for use with the steady state method of analysis for the candidate radiator configurations presented in Figure B-67 have been determined from the temperature plots (Figures B-3 through B-66). Each of the plots were surveyed to determine the position in orbit which gives the maximum combination of sink temperatures for each radiator configuration. Integral location 2, the single door deployed and the boom deployed panels all have the same sink temperature. Table B-1 presents a summary of the maximum sink temperatures for each radiator configuration and the conditions for which it occurs. Table B-2 shows the sink temperatures calculated for each radiator configuration and orbit inclination and attitude. The radiator design conditions depend on whether peaking above the radiator control point is allowed for short periods of time and whether a proportioning valve is used.

For low inclination orbits with alternate hot and cold environments, the radiator outlet may be allowed to peak for short periods of time at values above the desired outlet control point. For orbit inclinations above 68.5° (270 N.M. circular orbit) the shadow time is zero and the radiator control point must always be maintained. Therefore, although a higher design sink temperature results from a low inclination orbit, this is not necessarily the radiator design point since higher radiator temperatures may be allowed for this condition.

The use of a proportioning valve in the system also influences the radiator design conditions. The condition of maximum total absorbed heat will not be the design condition if a proportioning valve is used and the

TABLE B-1

SUMMARY OF RADIATOR STEADY-STATE
DESIGN SINK TEMPERATURES

<u>CONFIGURATION</u>	<u>T_{SINK} - °F</u>	<u>ORBIT AND CONDITIONS</u>
Integral Location 1, External Double Door (door closed)	63	90° inclination, solar oriented, No peaking above control point
Integral Location 2, Single Door, Boom De- ployed and External Double Door (Door Open)	26	68.5° inclination, solar oriented, No peaking above control point, No proportioning valve
	40	0° inclination, planet oriented, Peaking above control point, with proportioning valve
Integral Location 3	24-29	Sun Oriented: 32°, 68.5° & 90° Planet Oriented: 90° & 0° Peaking above control point allowed only for inclinations less than 68.5°. No proportion- ing valve.
Double Door Deployed	34	68.5° inclination, solar oriented No peaking above control point, no proportioning valve

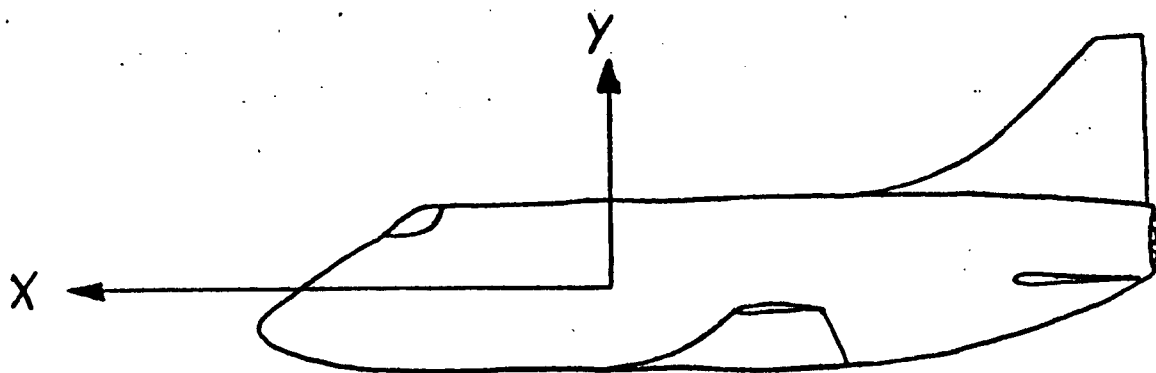
TABLE B-2 RADIATOR STEADY STATE DESIGN SINK TEMPERATURES

ORBIT INCLINATION (DEGREES)	PLANET ORIENTED			SOLAR ORIENTED		
	RADIATOR LOCATION	VEHICLE ATTITUDE (@ SUB-SOLAR POINT)	T _{SINK} (°R)	RADIATOR LOCATION	VEHICLE ATTITUDE (@ SUB-SOLAR POINT)	T _{SINK} (°R)
0°	2	Y-POP, Side-To-Plnt	500	2	Y-POP, Side-To-Sun	505
	2	Y-POP, Btm-To-Plnt	359			
	3	X-POP, Side-To-Plnt	419			
	3	X-POP, Top-To-Plnt	482			
	3	X-POP, Btm-To-Plnt	454	3	X-POP, Top-To-Sun	460
	3	Y-POP, Top-To-Plnt	428			
	3	Y-POP, Btm-To-Plnt	437			
	4	Y-POP, Btm-to-Plnt	450			
	4	Y-POP, Top-To-Plnt	438			
	4	Y-POP, Side-To-Plnt	444	4	Y-POP, Side-To-Sun	447
32°				4	Y-POP, Btm-To-Sun	411
				4	Y-POP, Top-To-Sun	488
	3	X-POP, Side-To-Plnt	413			
	3	X-POP, Top-To-Plnt	471			
	3	X-POP, Btm-To-Plnt	435	3	X-POP, Top-To-Sun	485
	3	Y-POP, Top-To-Plnt	424			
68.5°	3	Y-POP, Btm-To-Plnt	468	3	Y-POP, Btm-To-Sun	483
				2	X-POP, Top-To-Sun	485
				2	Y-POP, Side-To-Sun	486
90°				3	Y-POP, Top-To-Sun	489
				4	Y-POP, Top-To-Sun	494
	1	Y-POP, Side-To-Plnt	528			
	2	X-POP, Btm-To-Plnt	328			
90°	2	Y-POP, Side-To-Plnt	367	2	Y-POP, Side-To-Sun	483
	2	Y-POP, Top-To-Plnt	485			
	3	X-POP, Top-To-Plnt	385			
	3	X-POP, Btm-To-Plnt	276			
	3	Y-POP, Side-To-Plnt	484			
	3	Y-POP, Top-To-Plnt	480			
				3	Y-POP, Top-To-Sun	483
				4	Y-POP, Top-To-Sun	490

environment of one panel is such that one-half the radiator area can meet the heat rejection requirements.

APPENDIX B REFERENCES

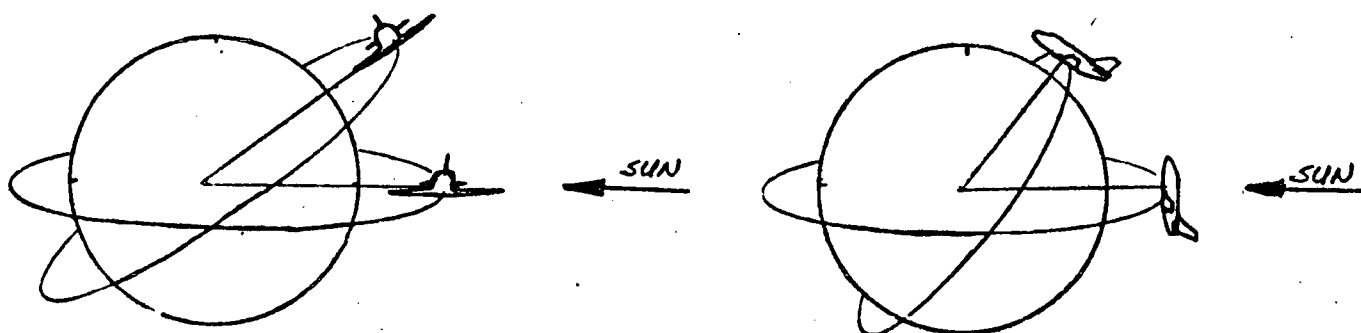
- B-1 Finch, H. L., "Orbiting Satellite Surface Temperature Prediction and Analysis", Midwest Research Institute Project No. 2669-E, Contract No. NAS9-1059, February 1964.



PLANET ORIENTED

Y-POP

X-POP



SOLAR ORIENTED

Y-POP

X-POP

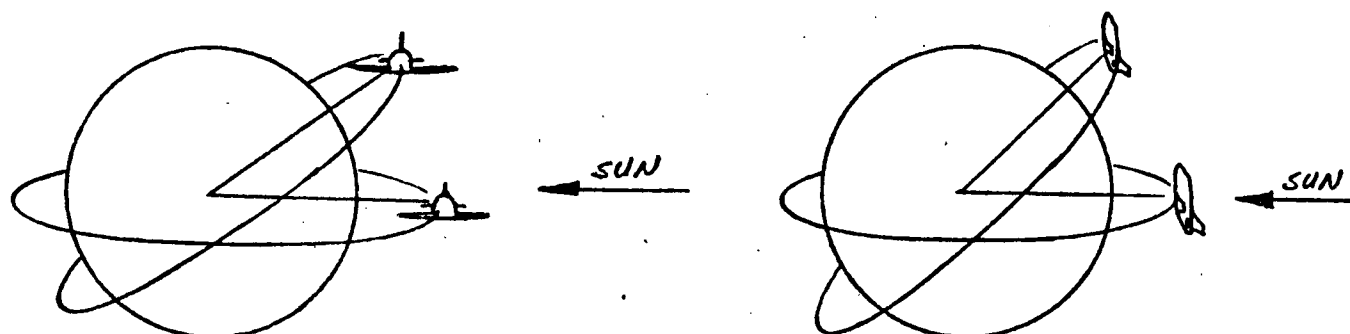
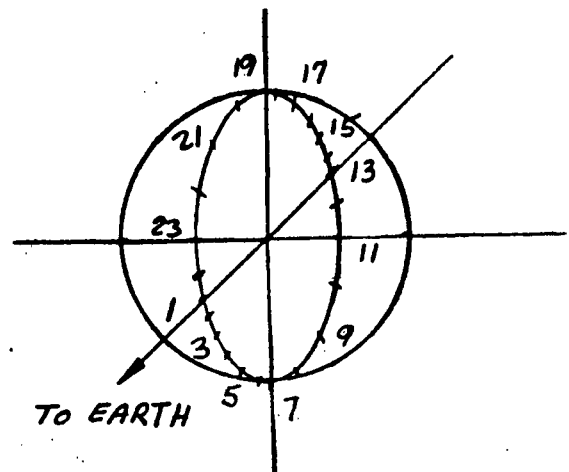
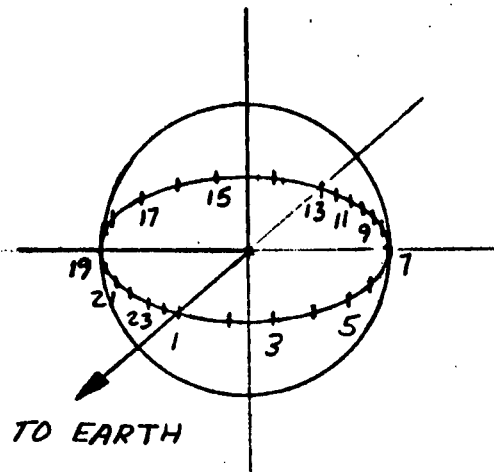


FIGURE B-1 ORBIT DEFINITIONS

PLANET ORIENTED

X-POP

Y-POP



SOLAR ORIENTED

X-POP

Y-POP

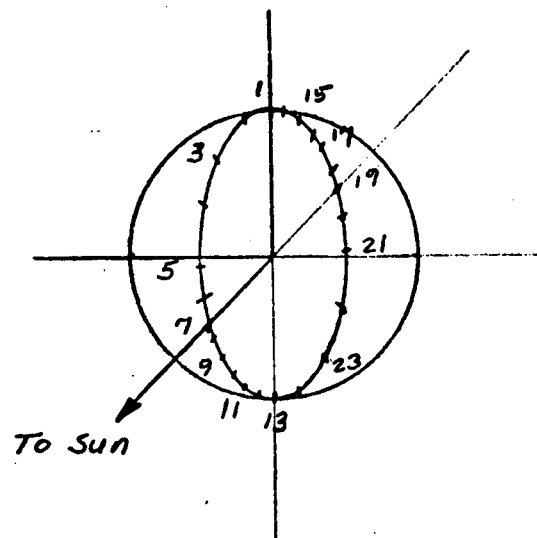
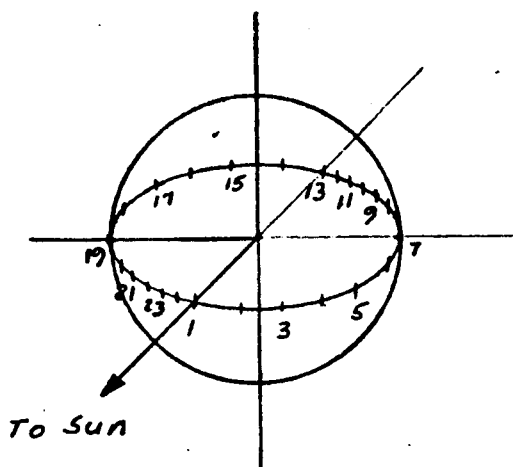
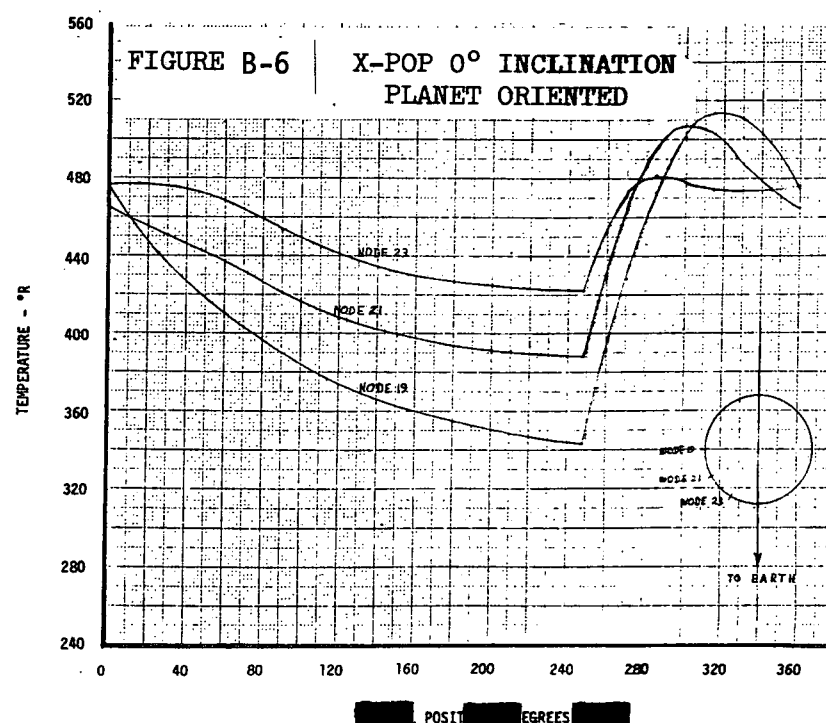
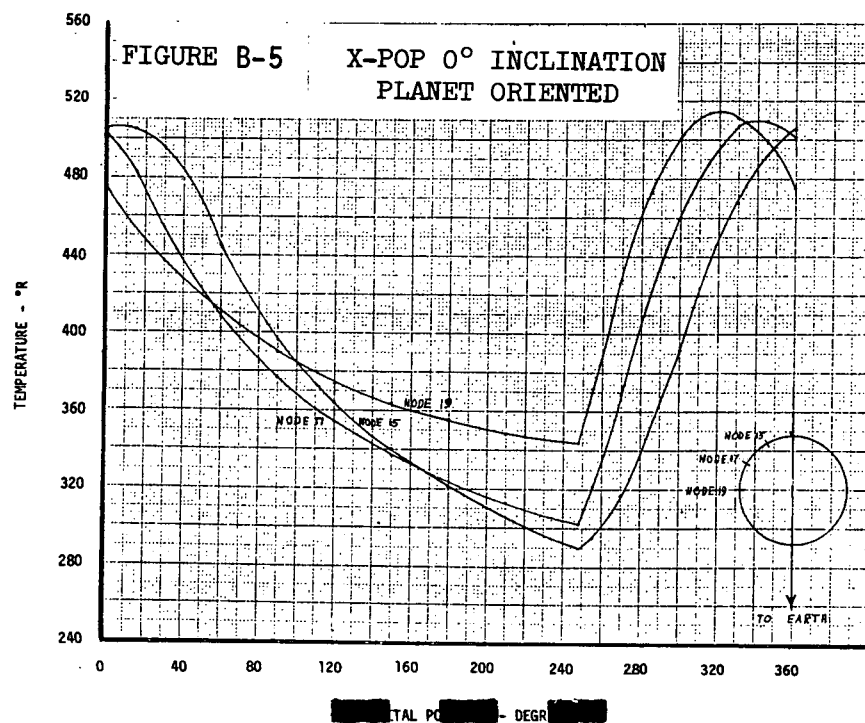
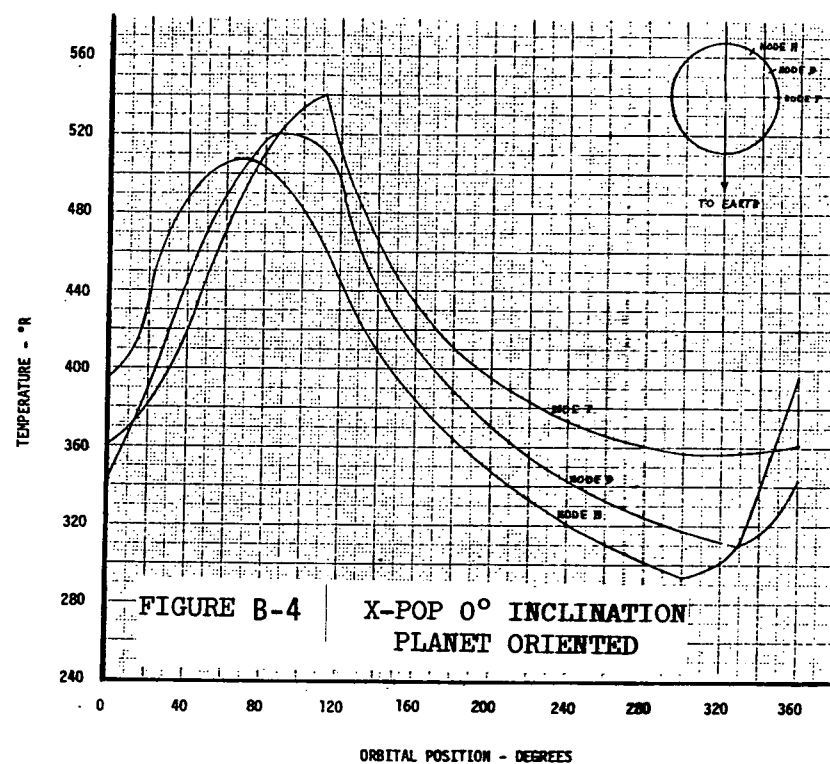
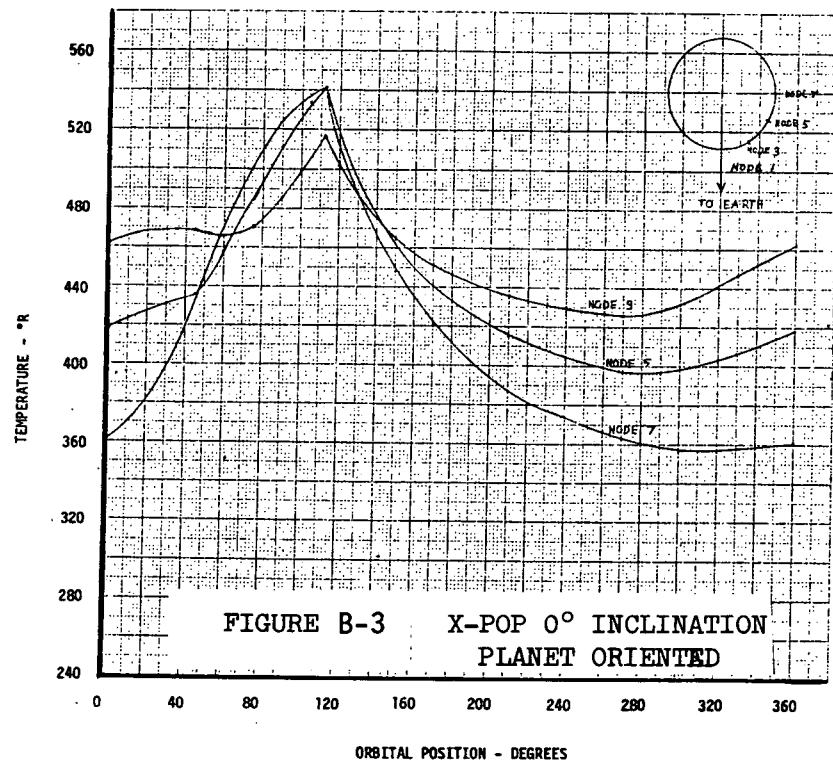
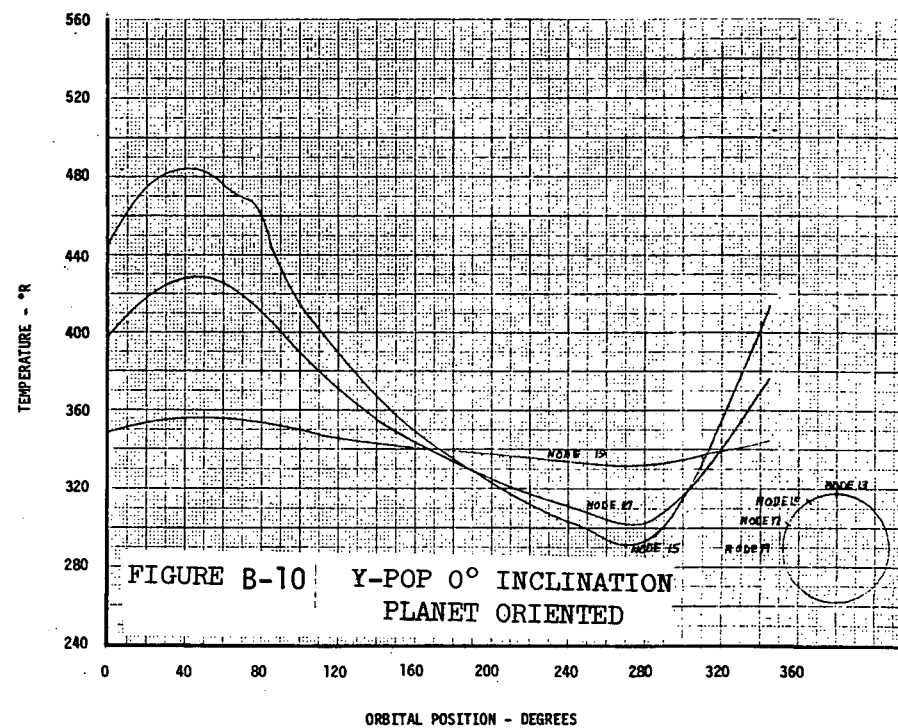
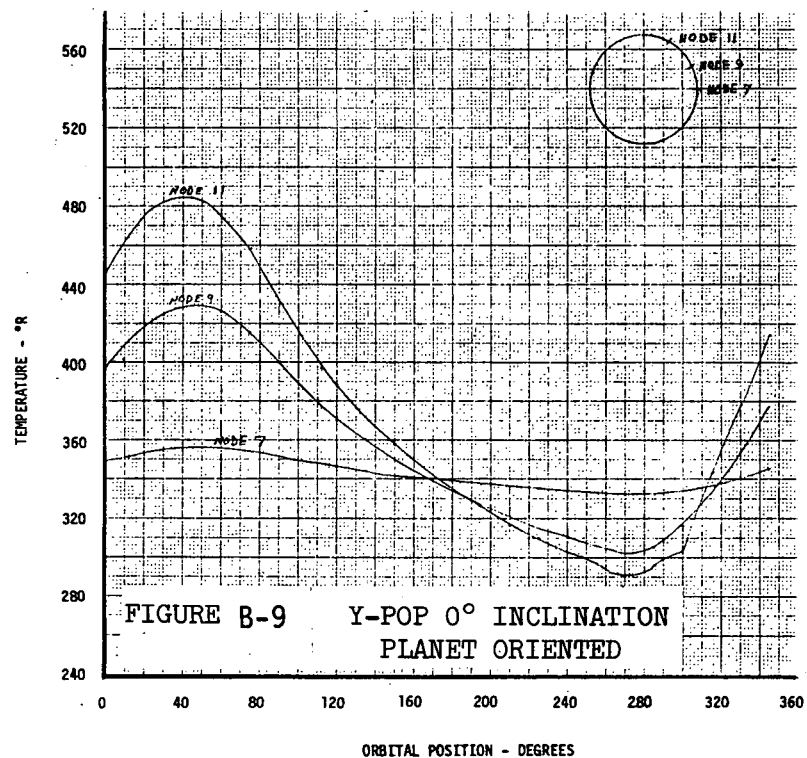
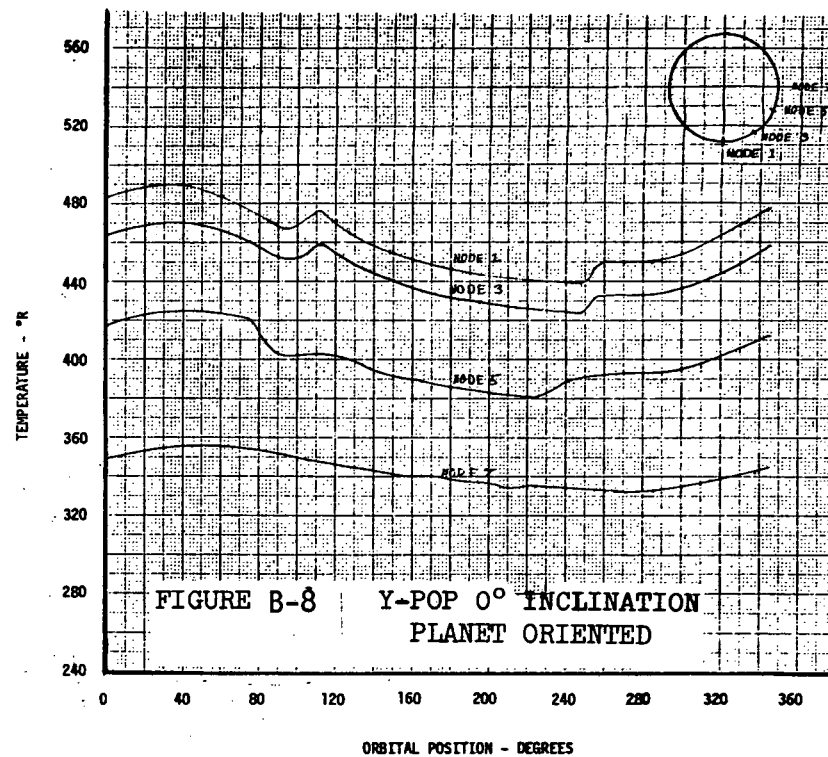
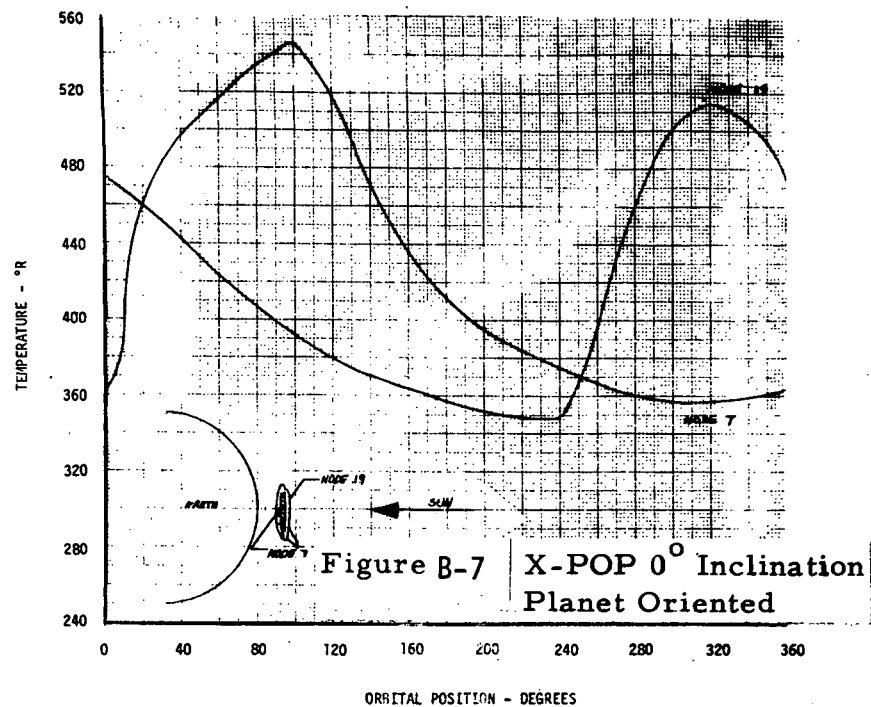
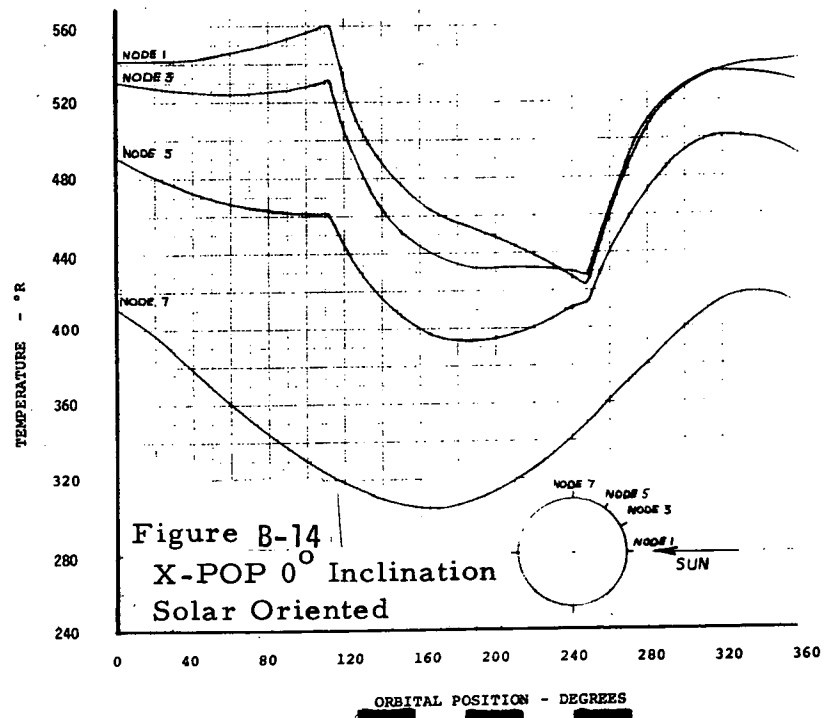
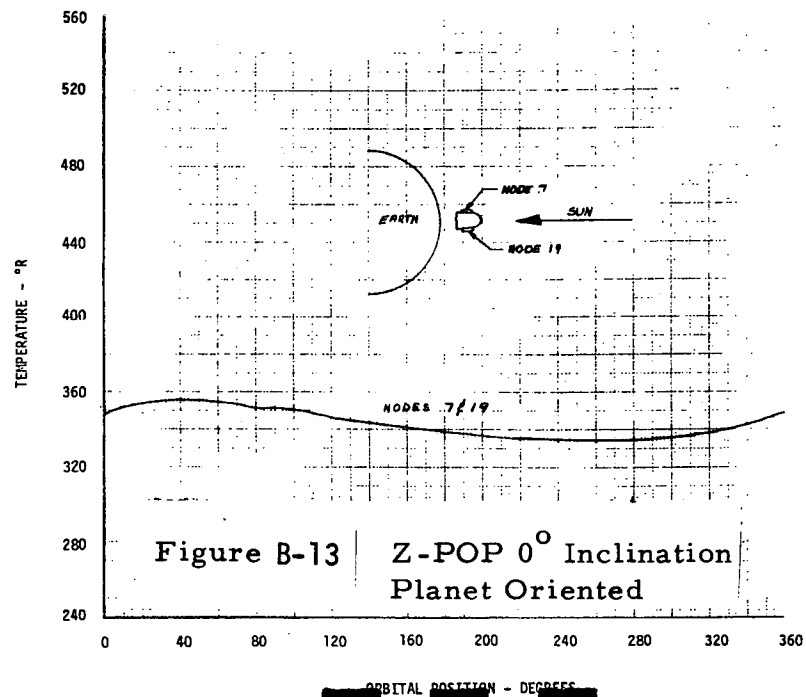
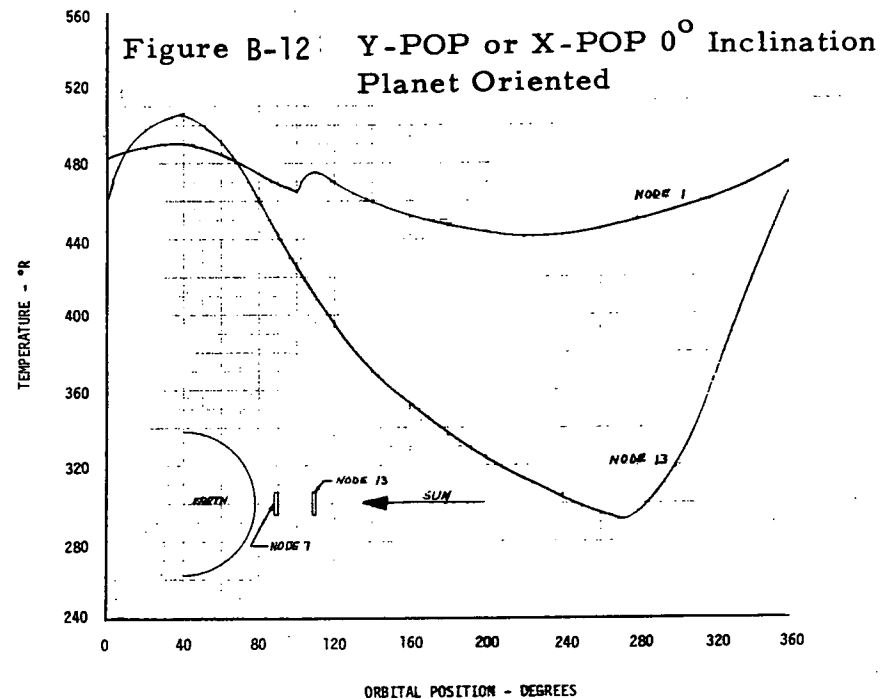
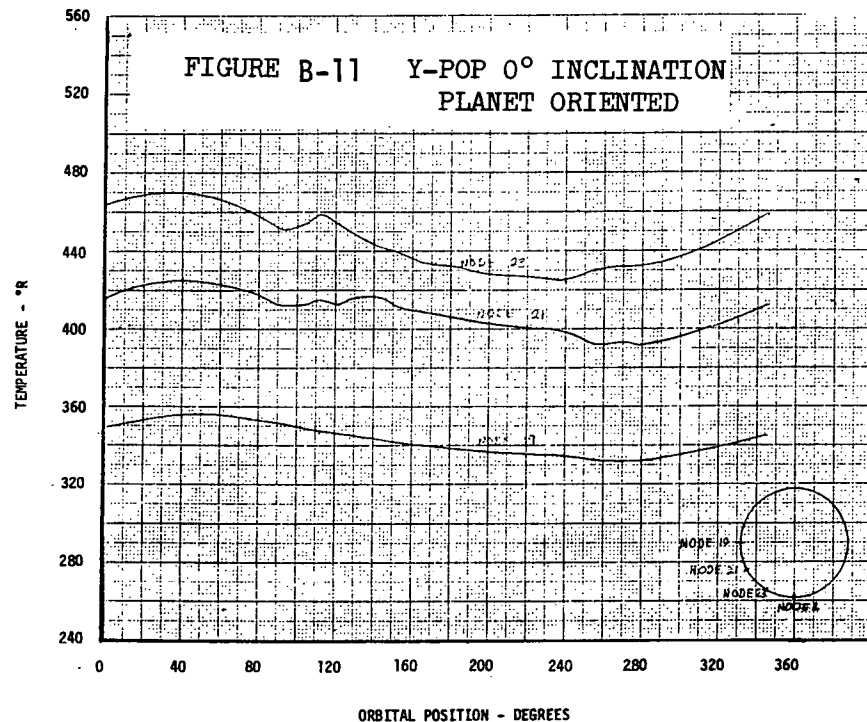
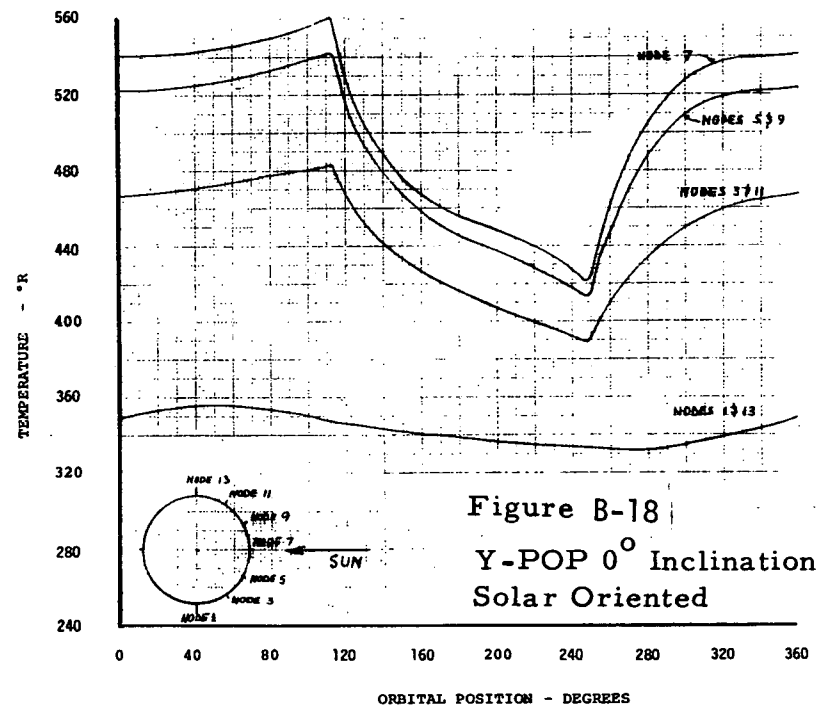
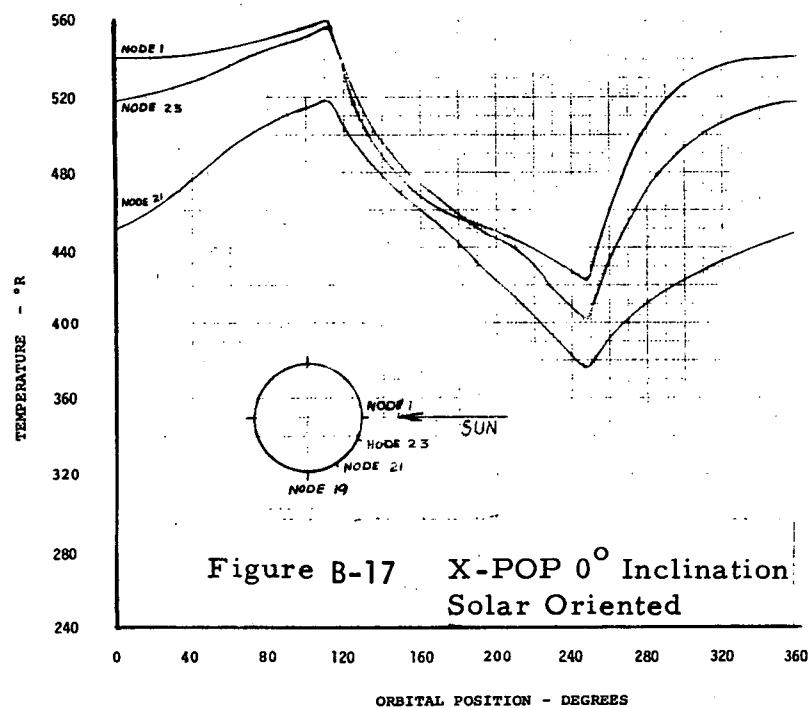
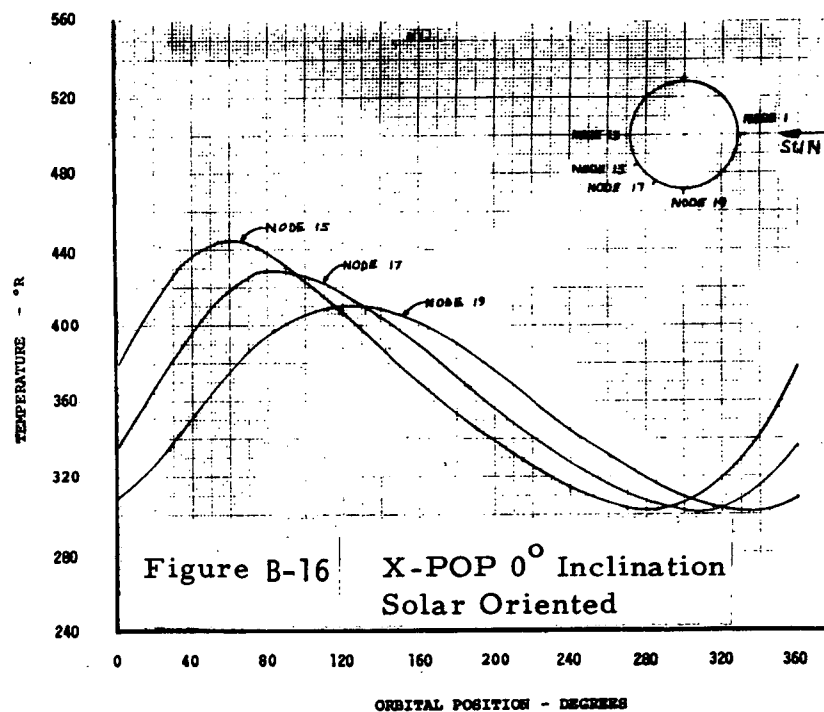
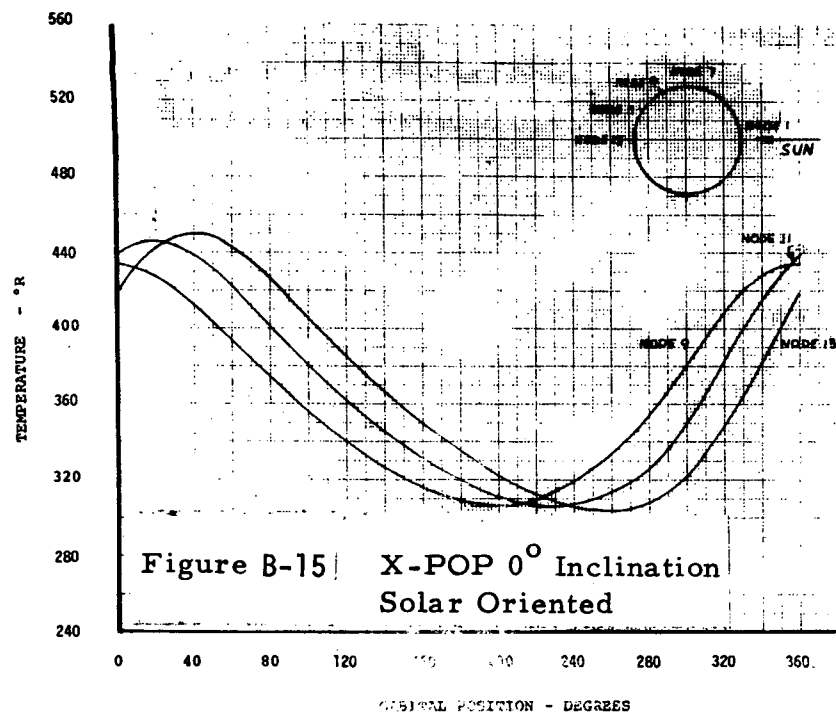


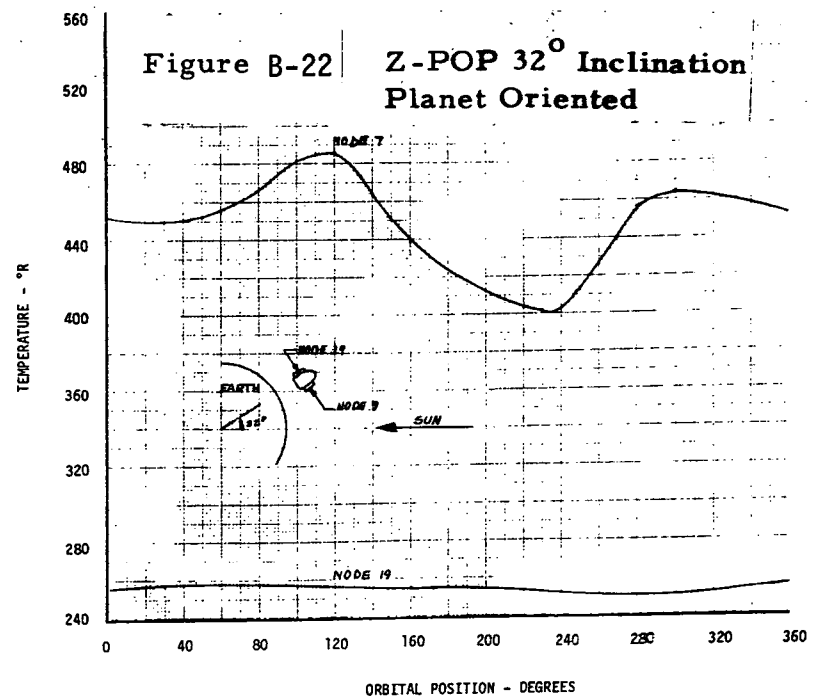
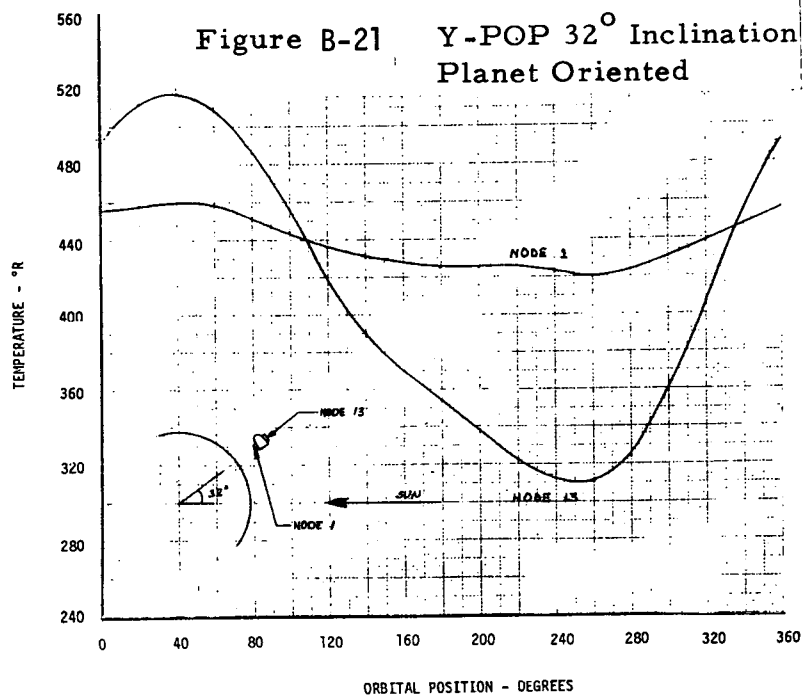
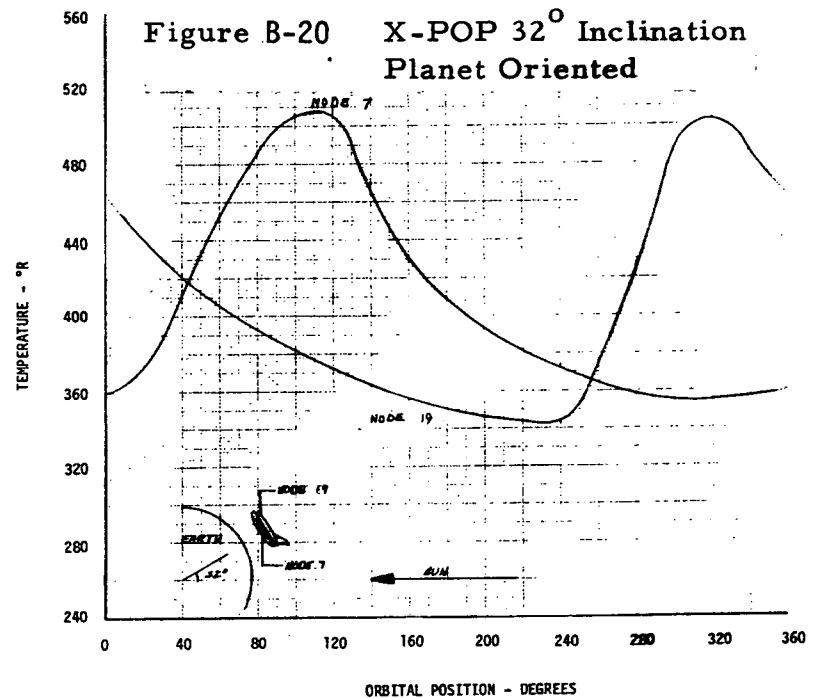
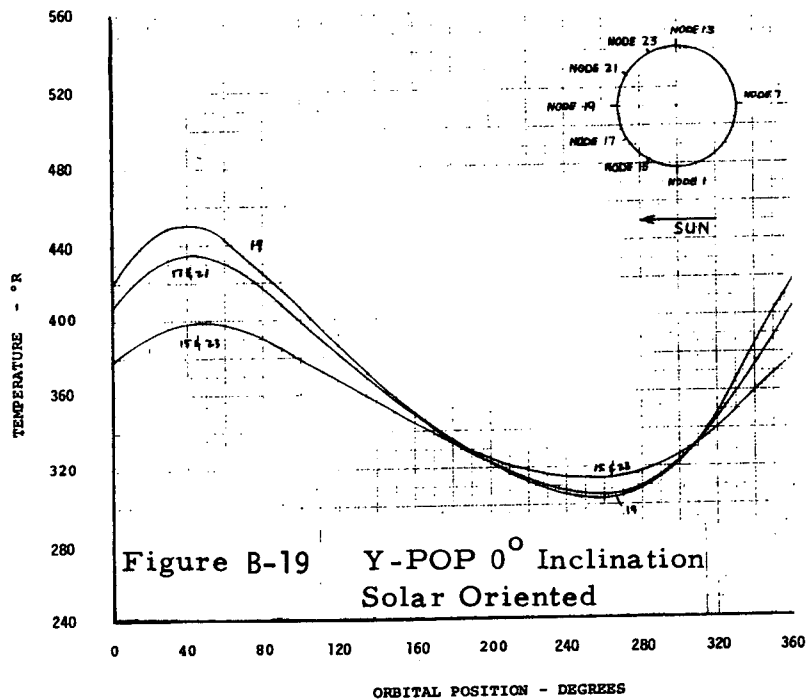
FIGURE B-2 NODE LOCATIONS

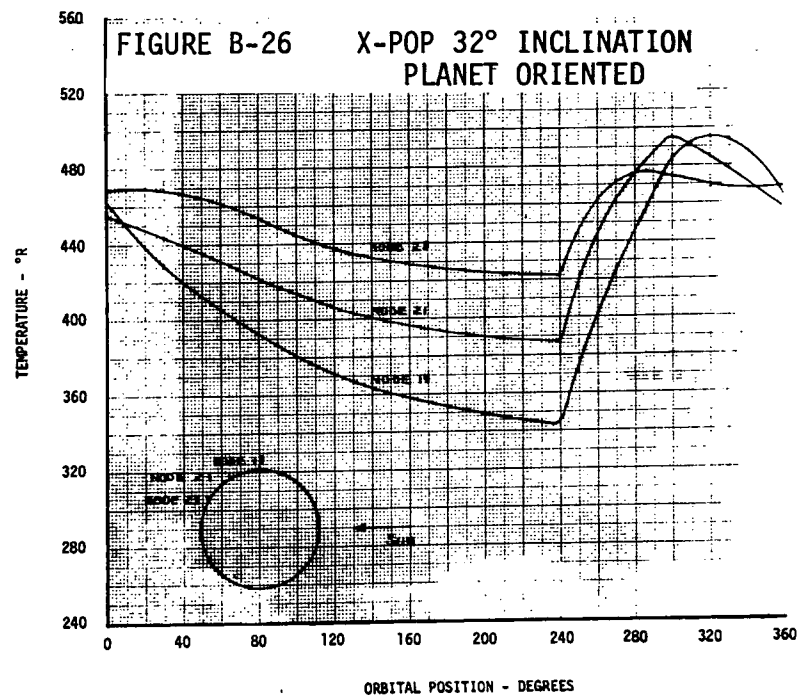
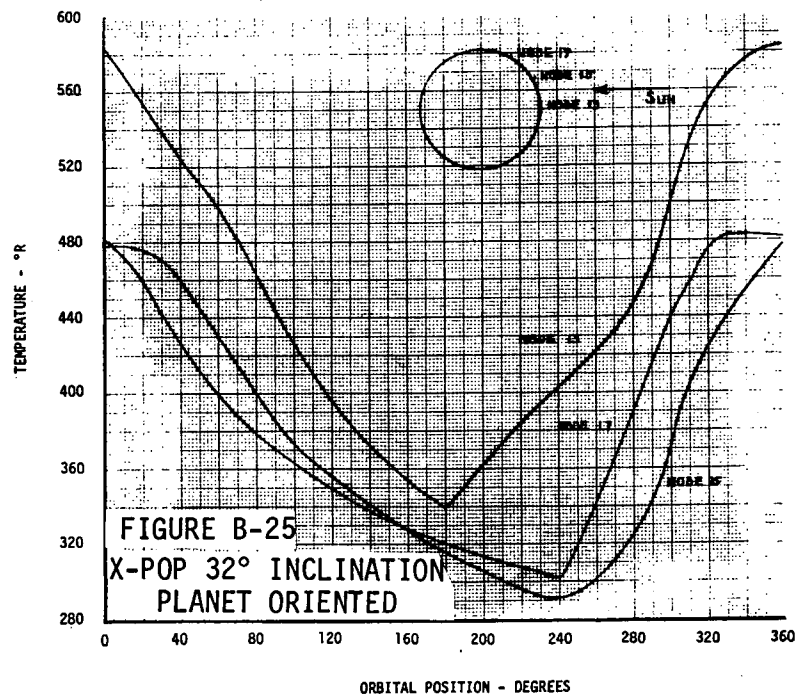
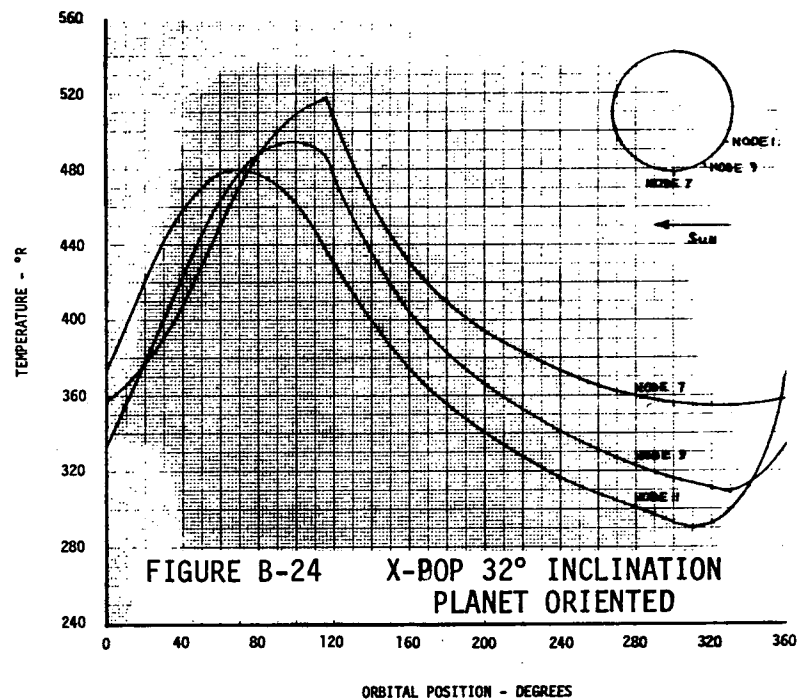
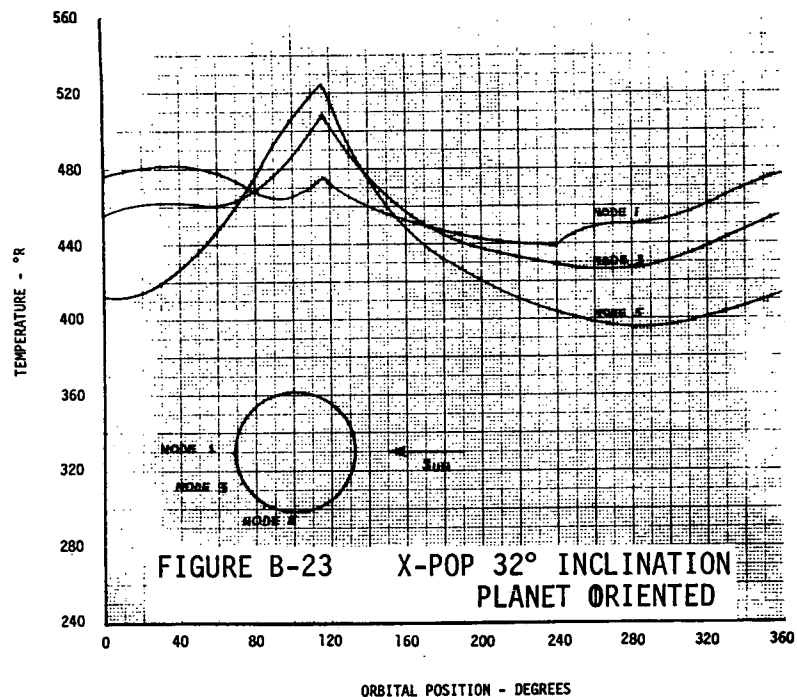


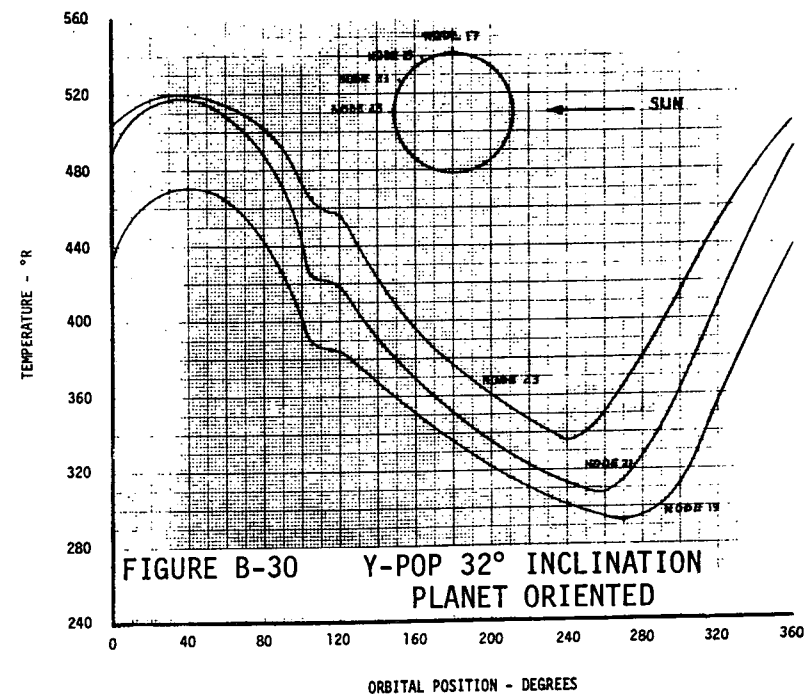
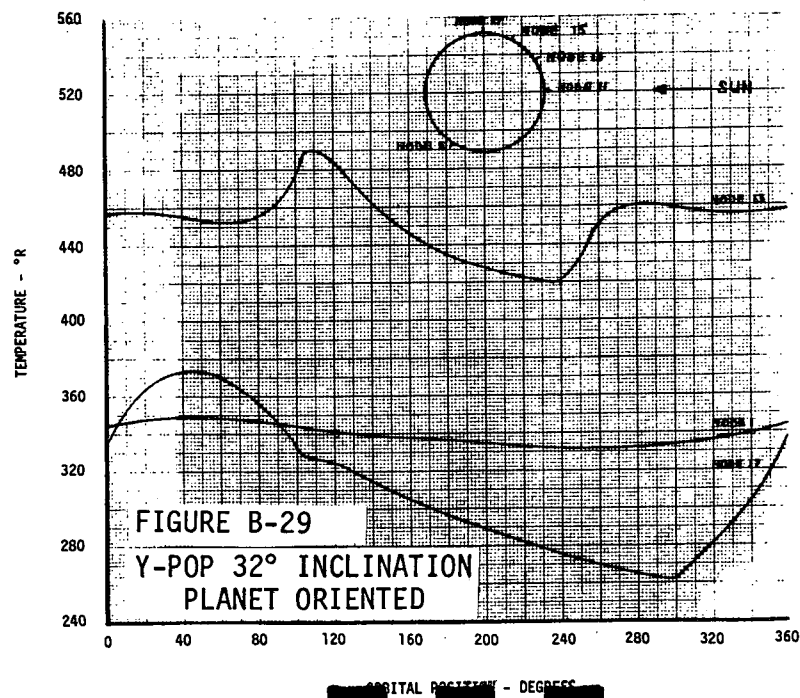
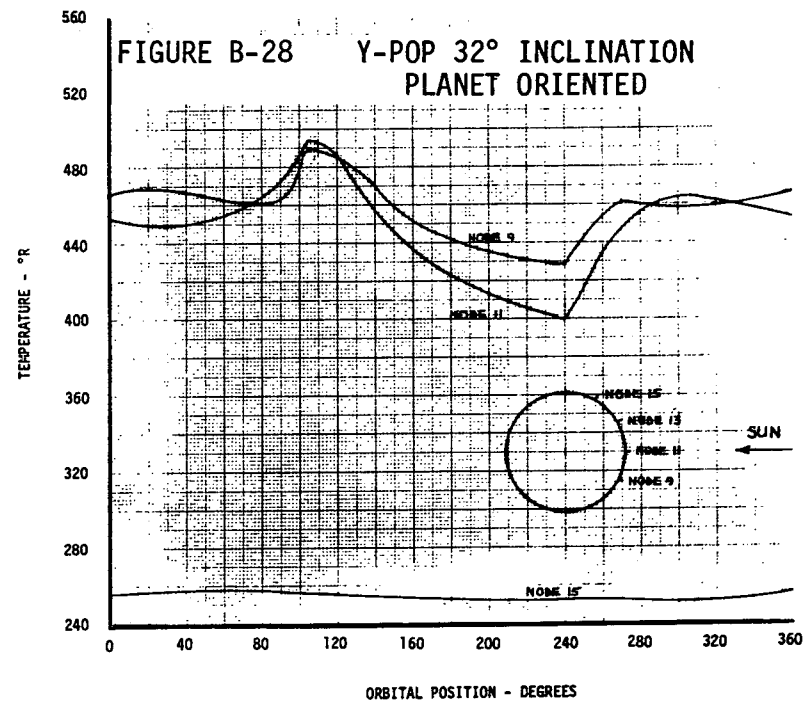
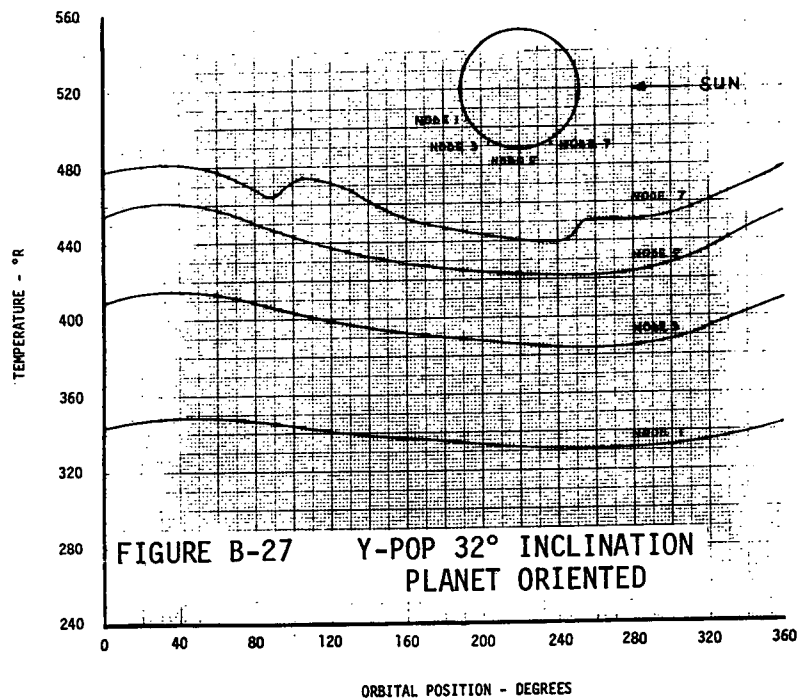


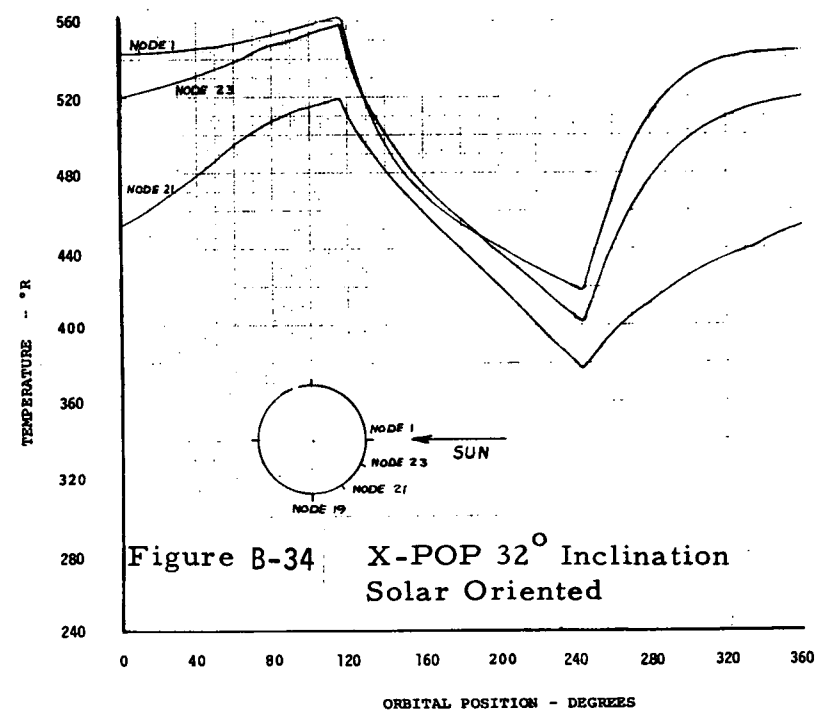
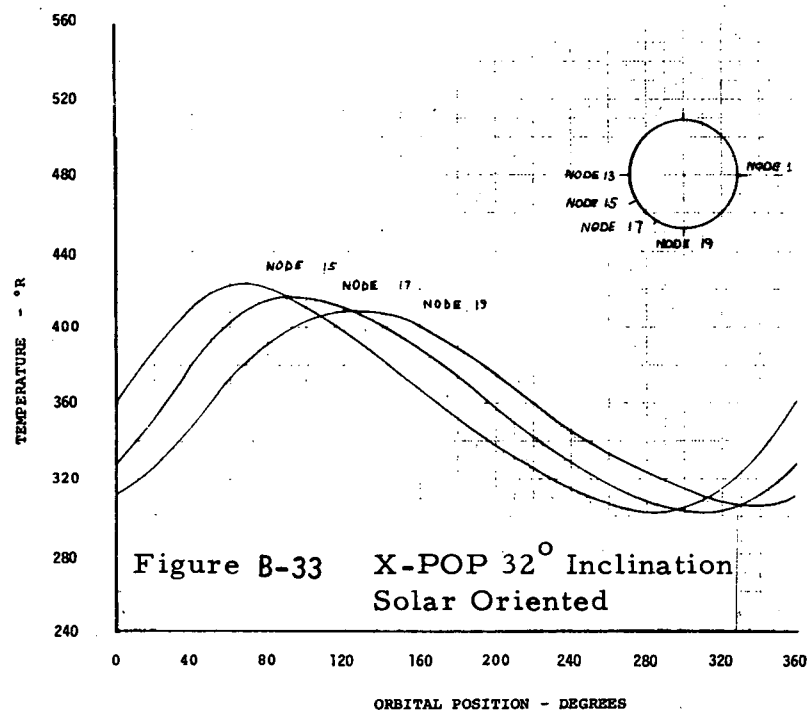
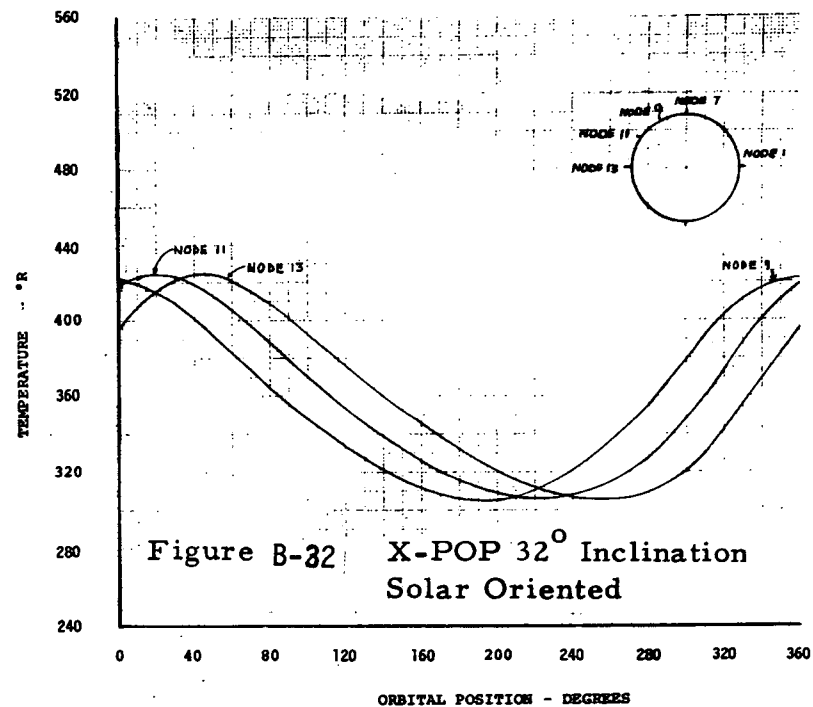
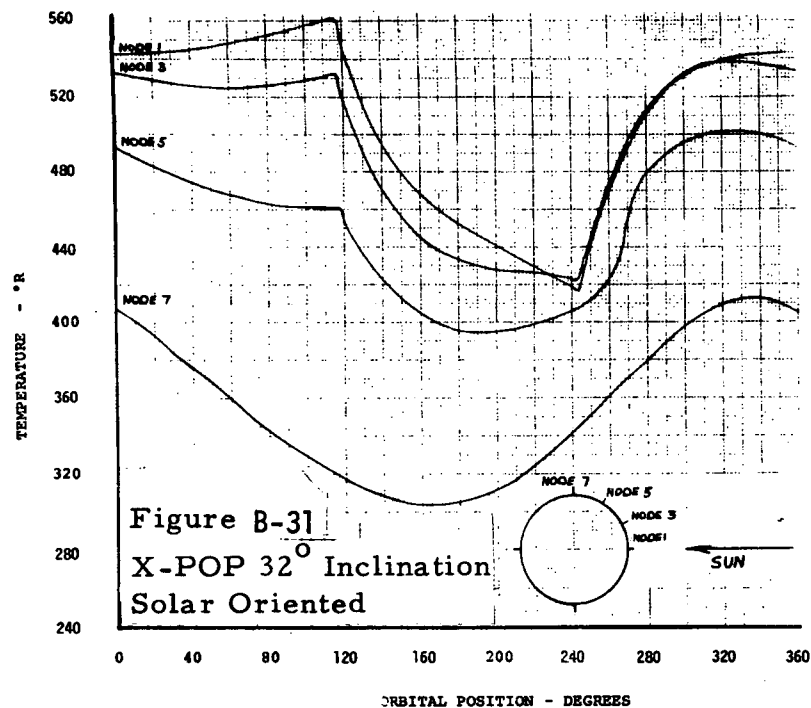


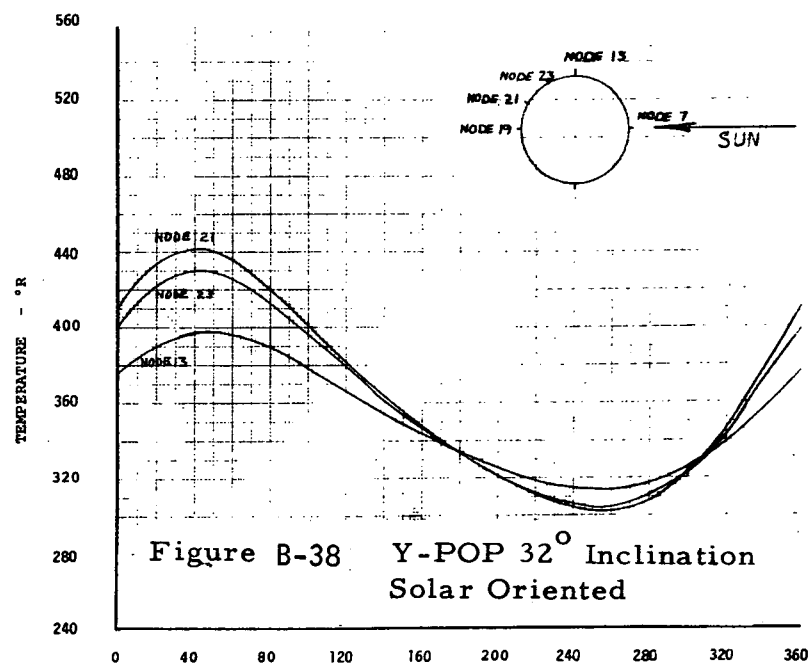
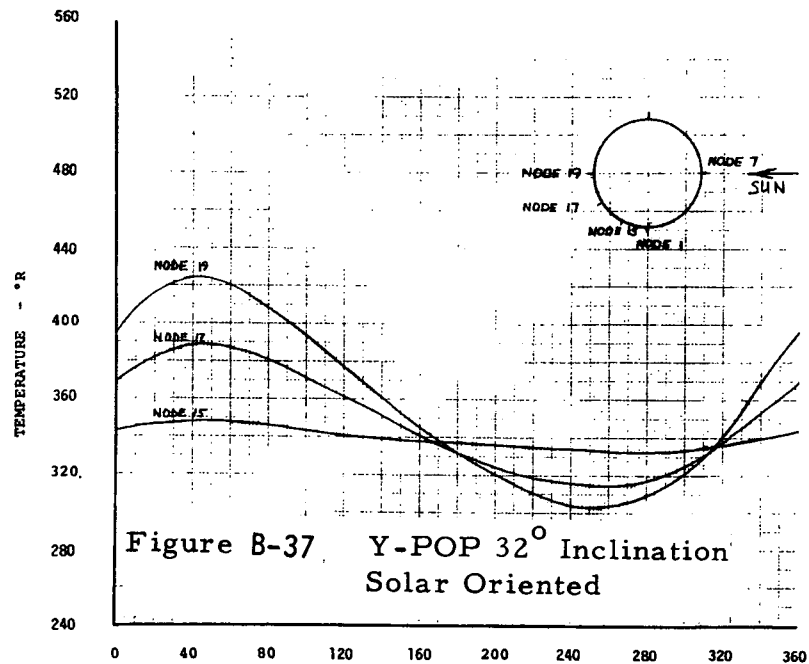
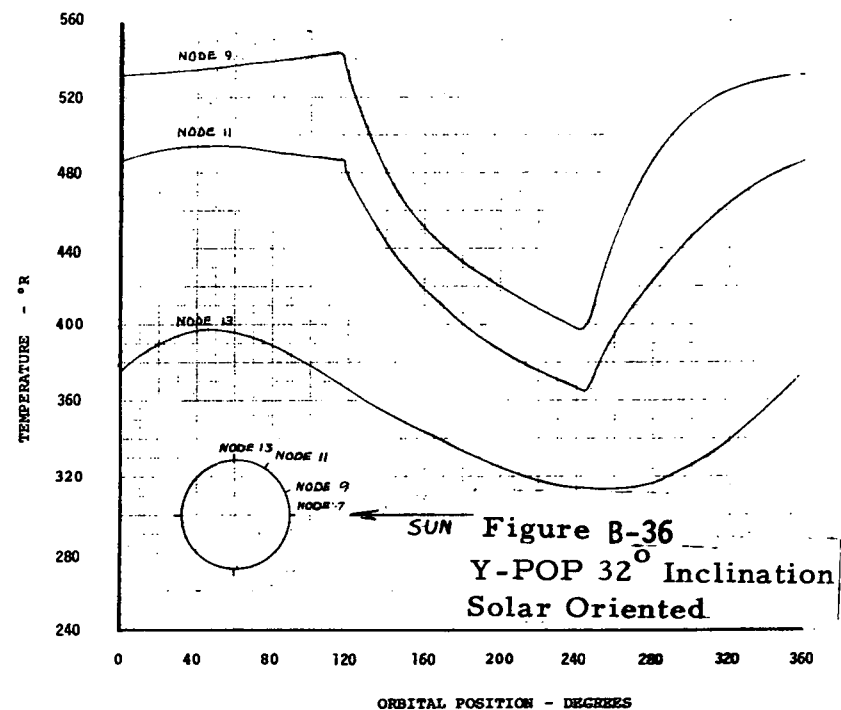
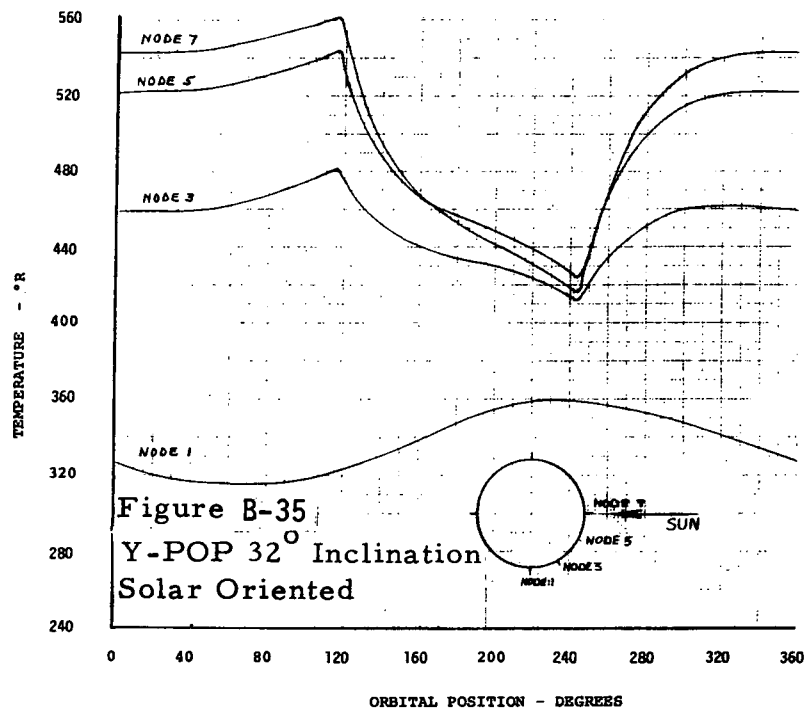


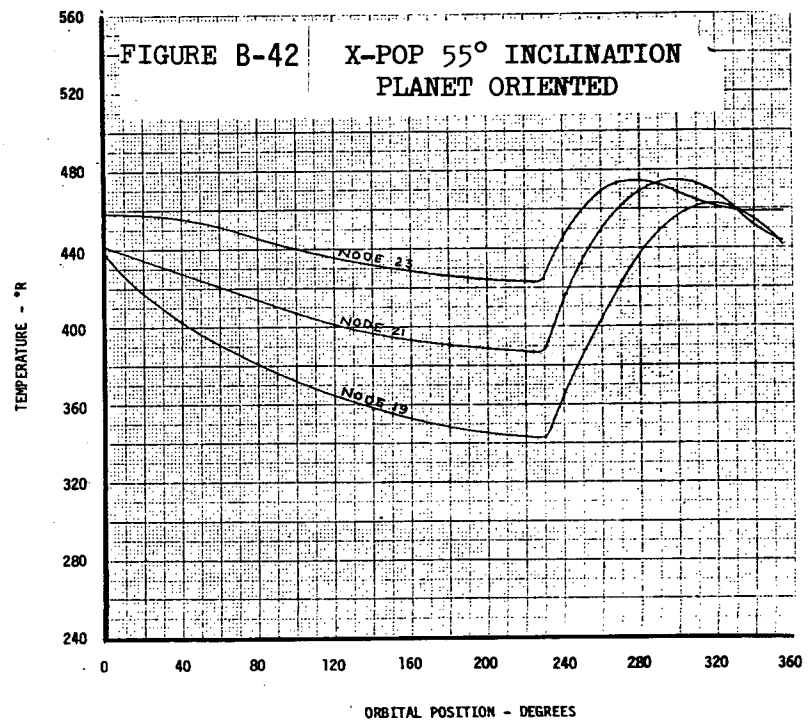
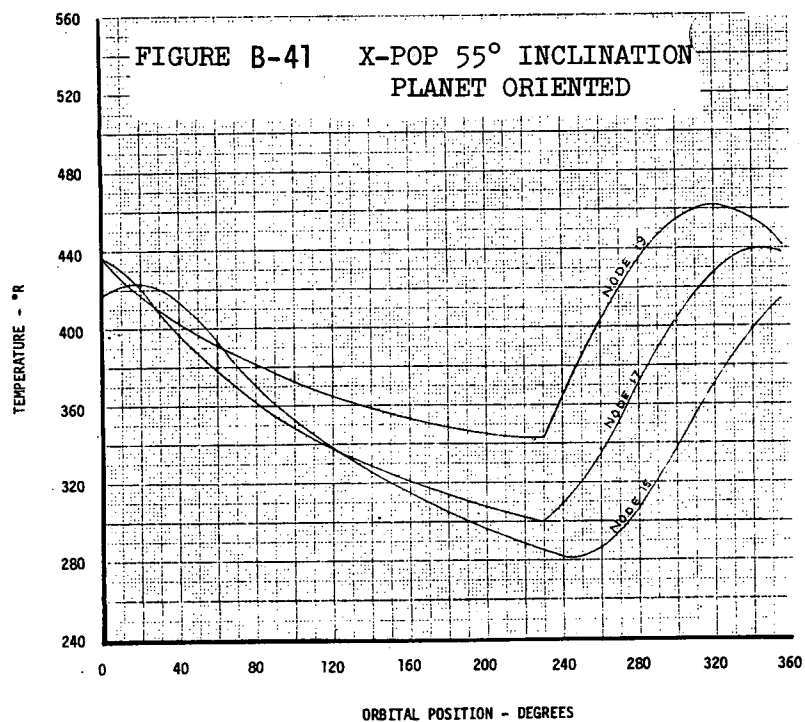
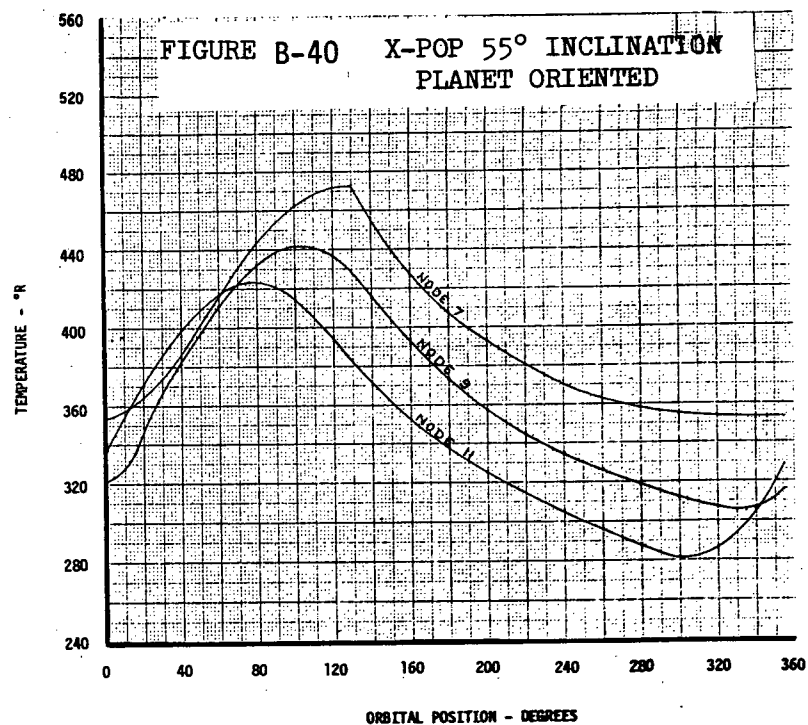
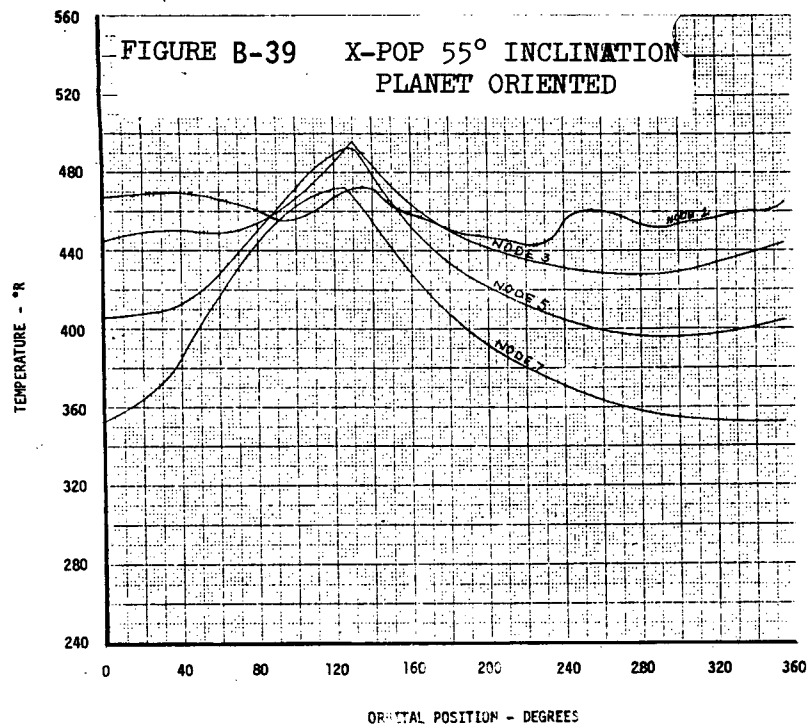


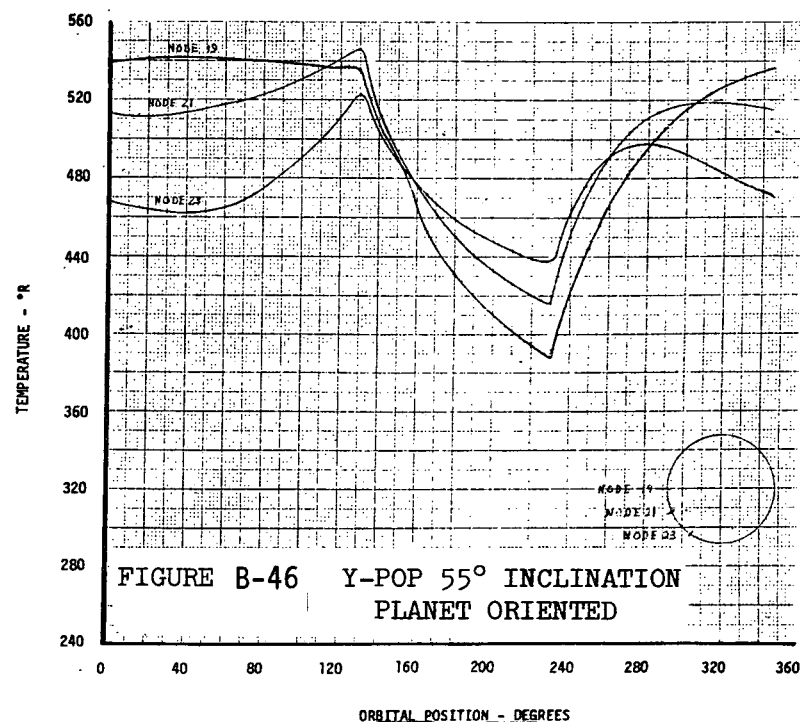
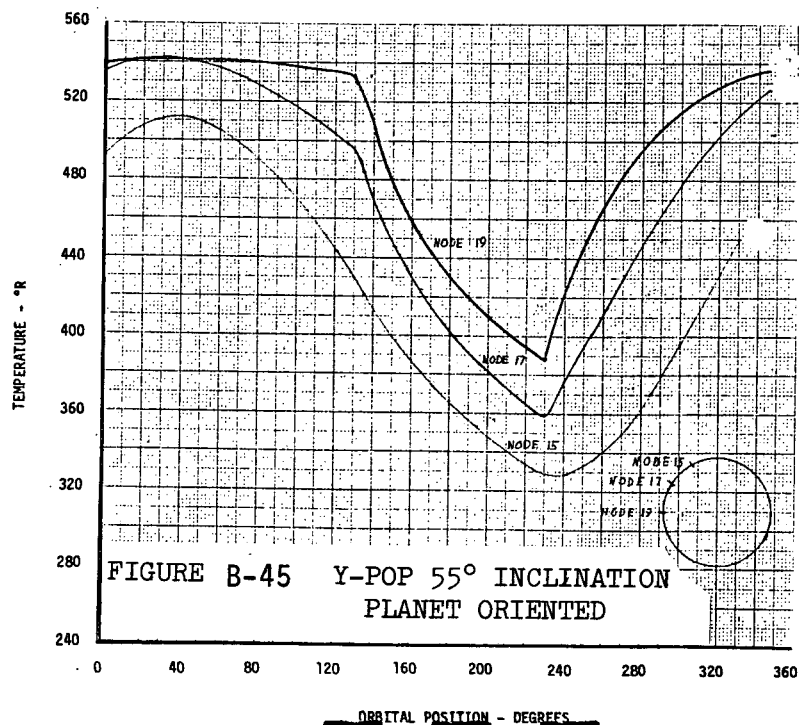
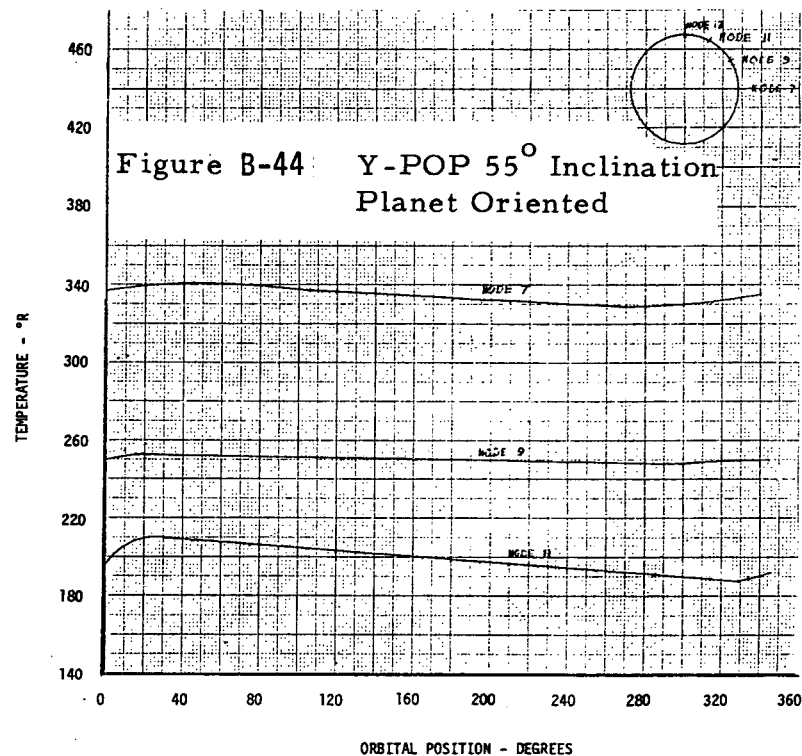
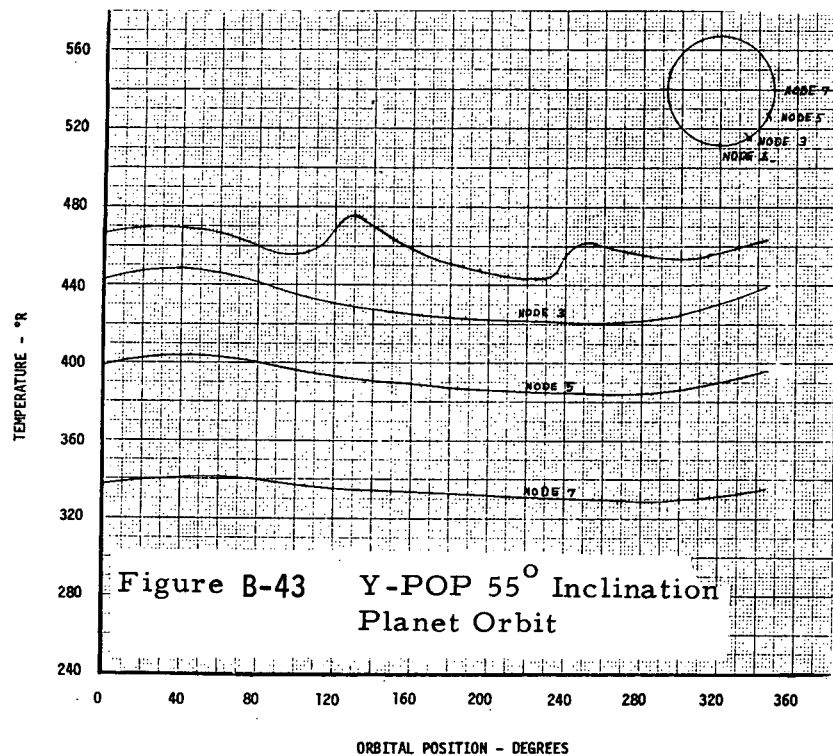


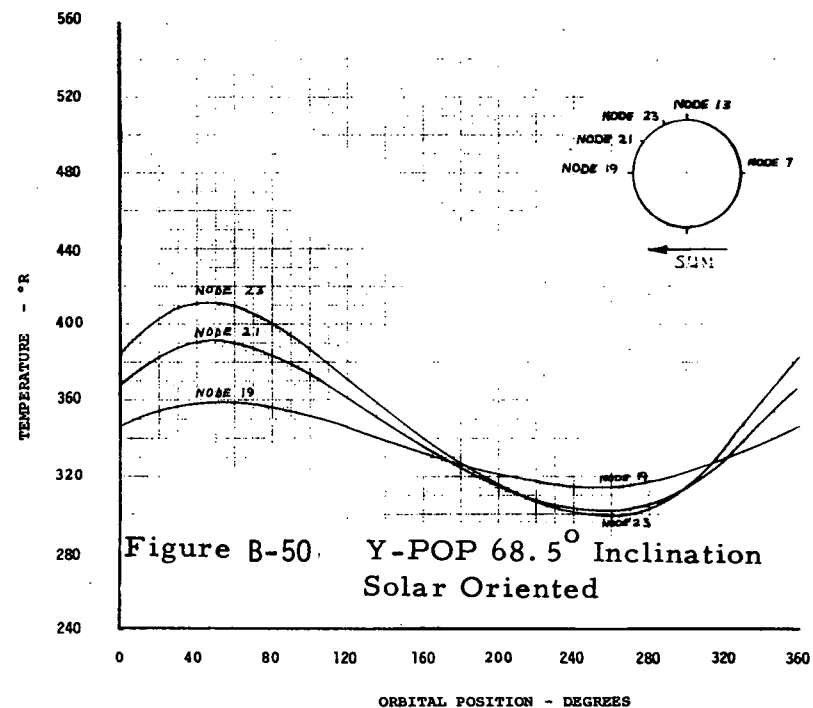
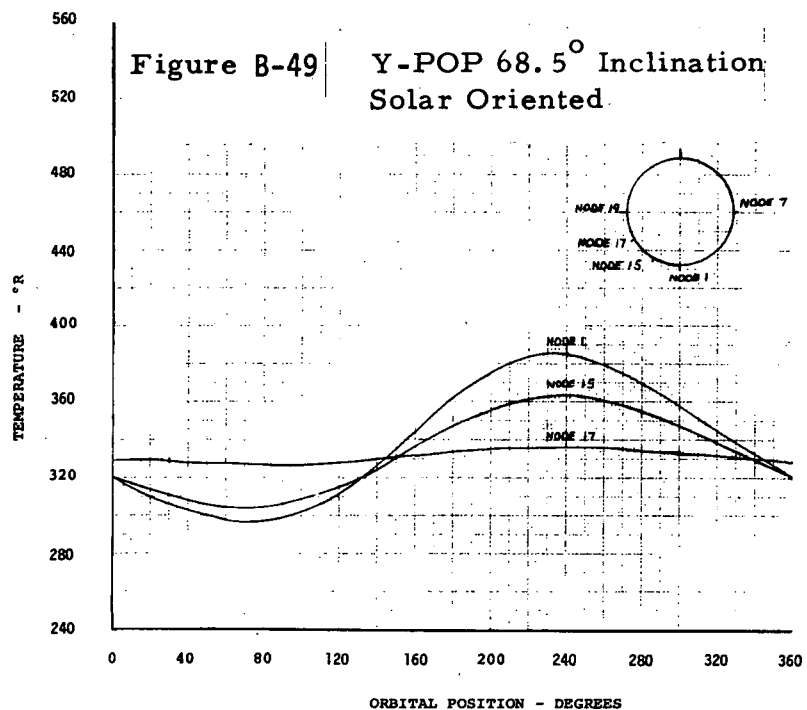
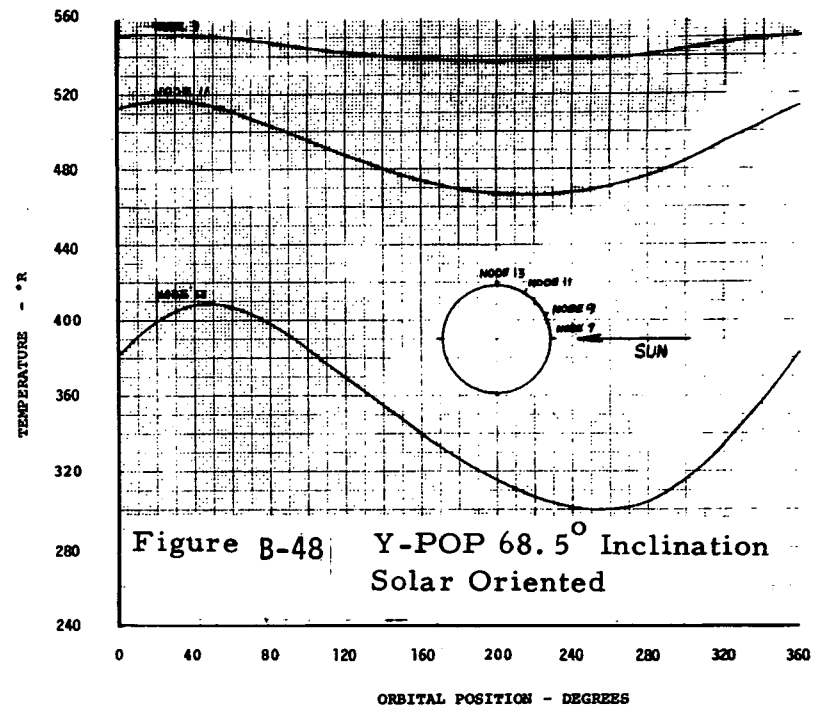
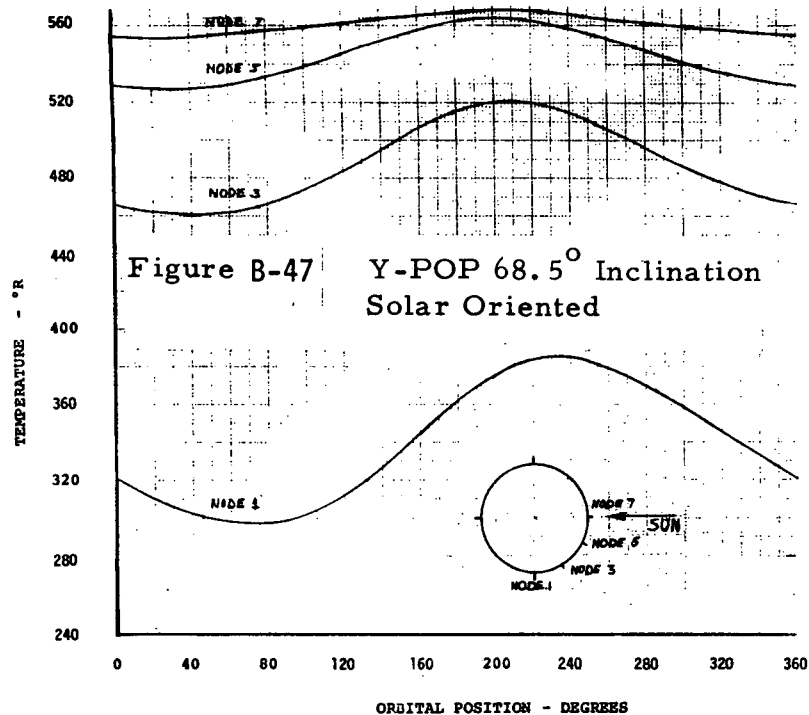


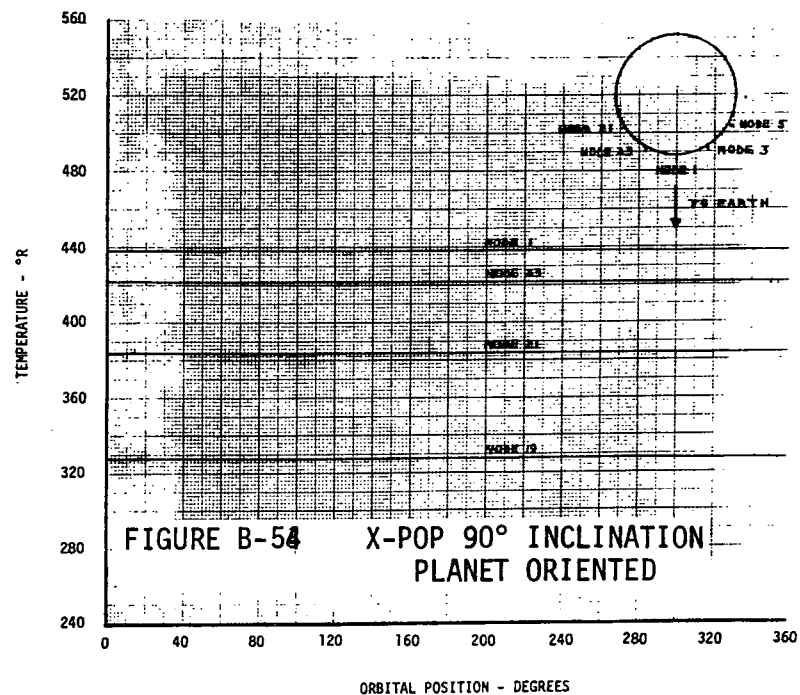
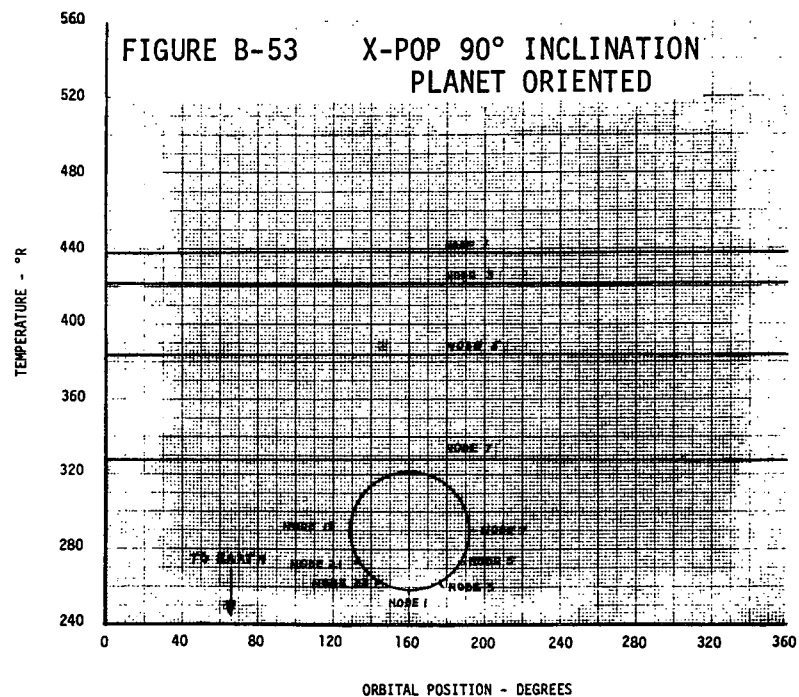
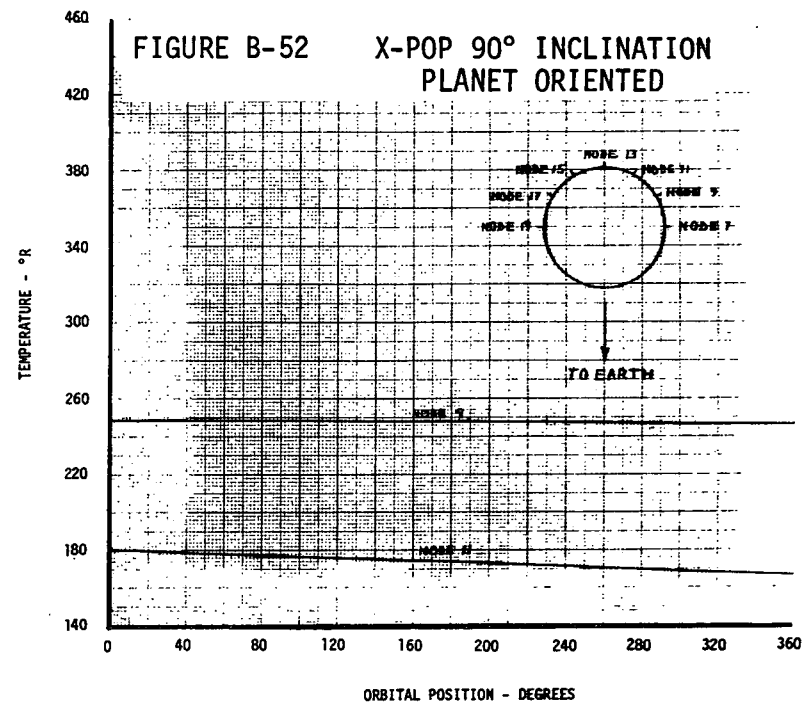
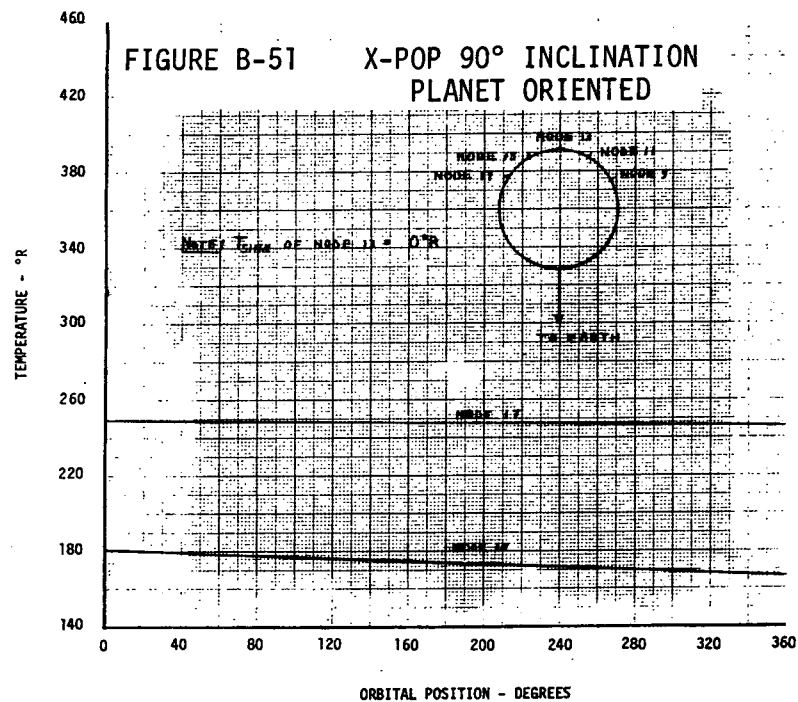


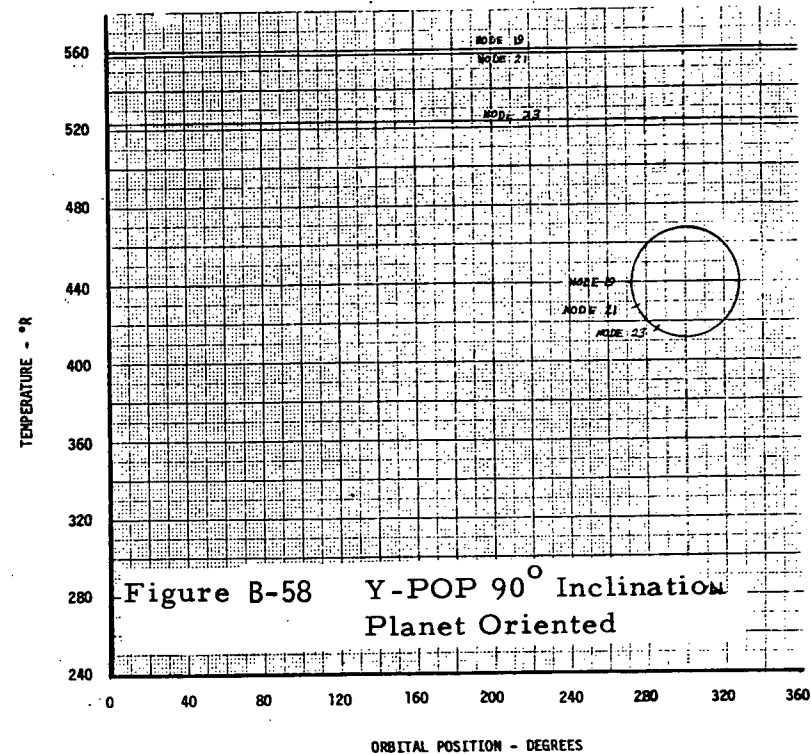
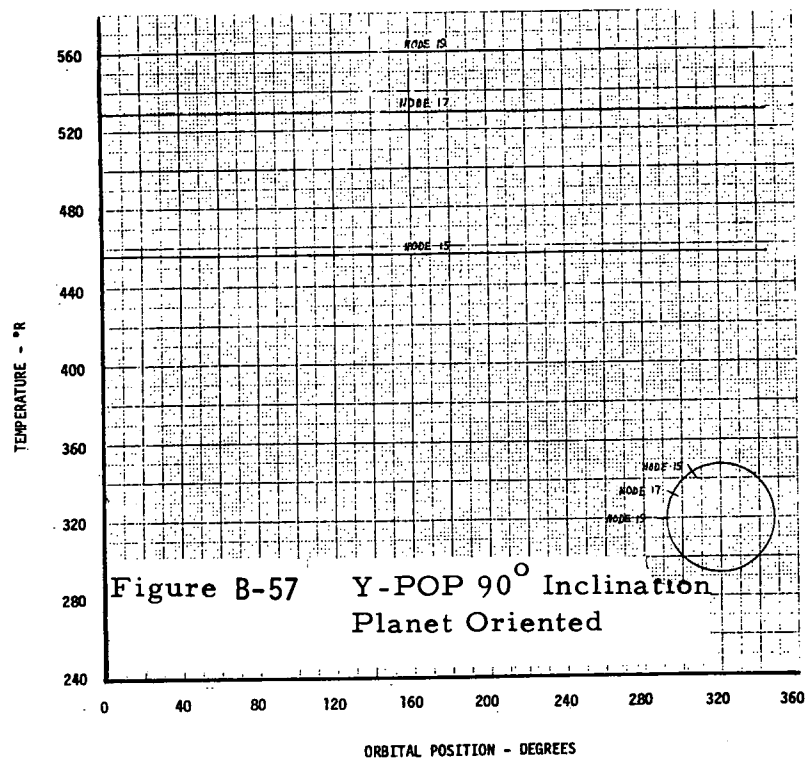
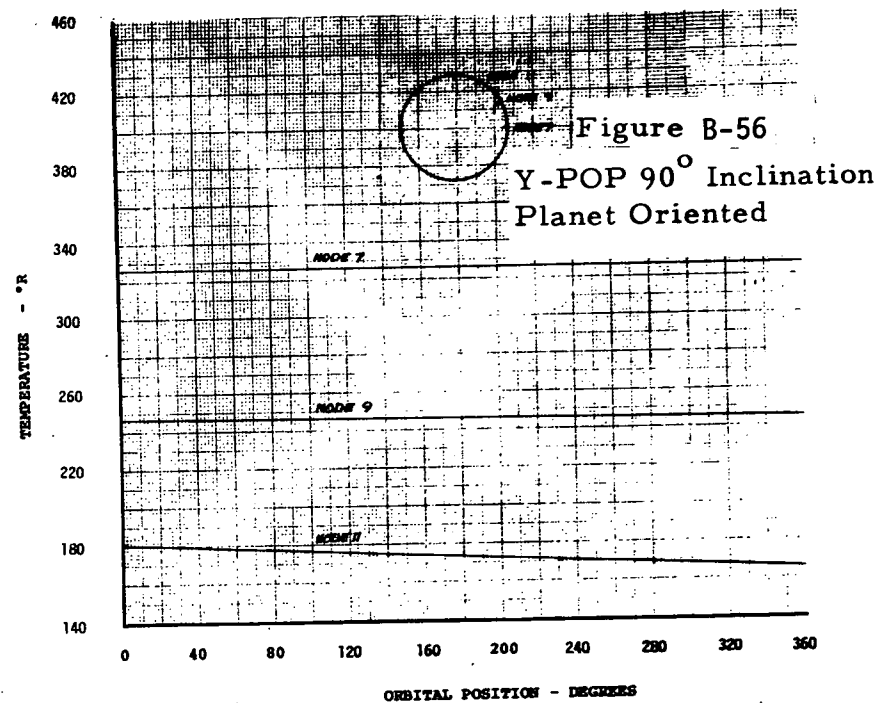
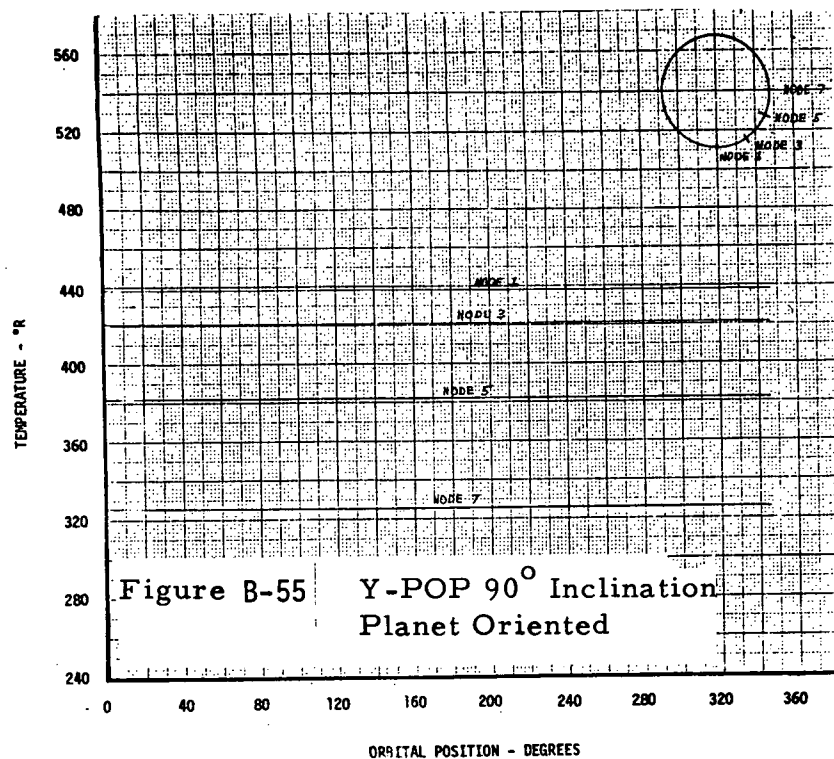


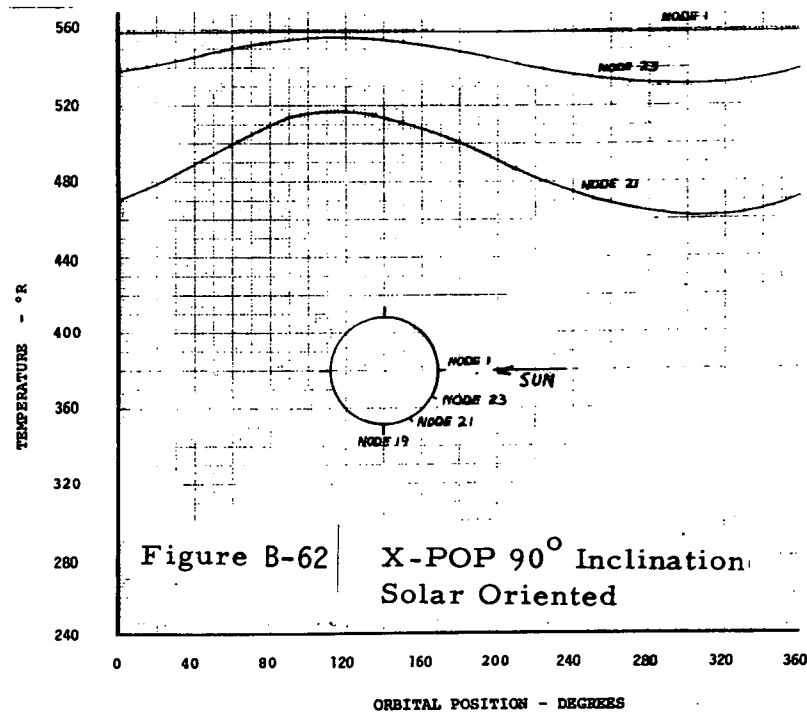
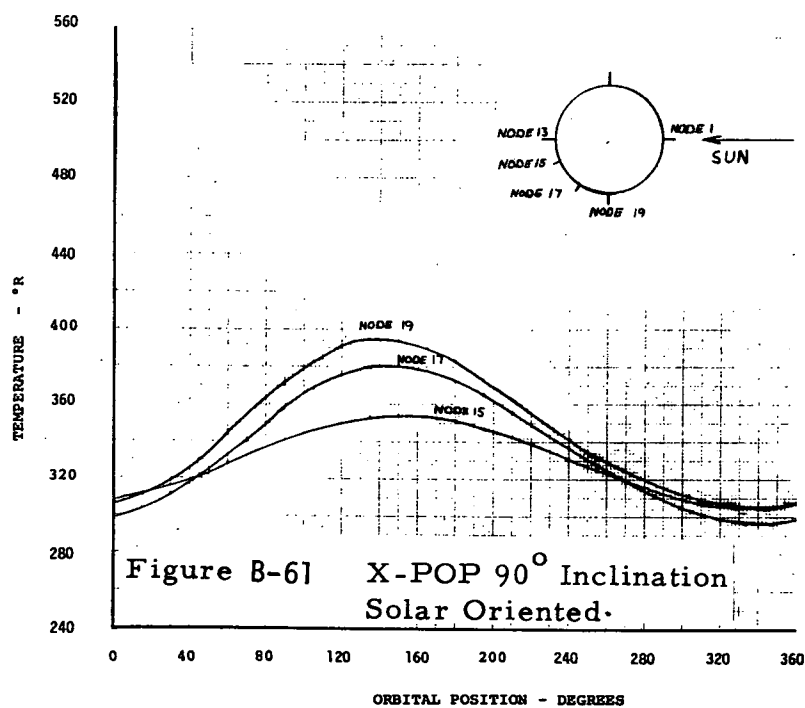
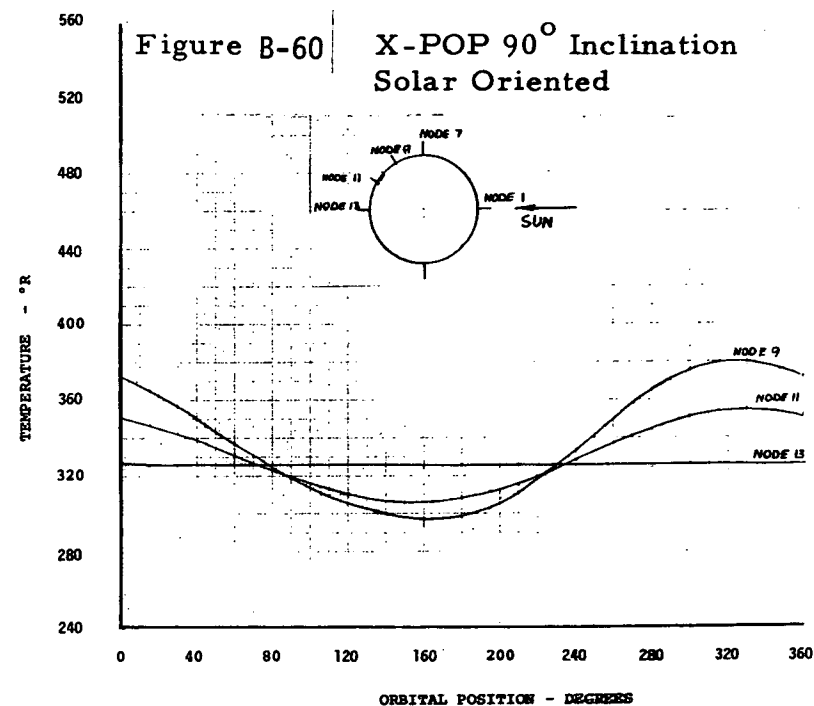
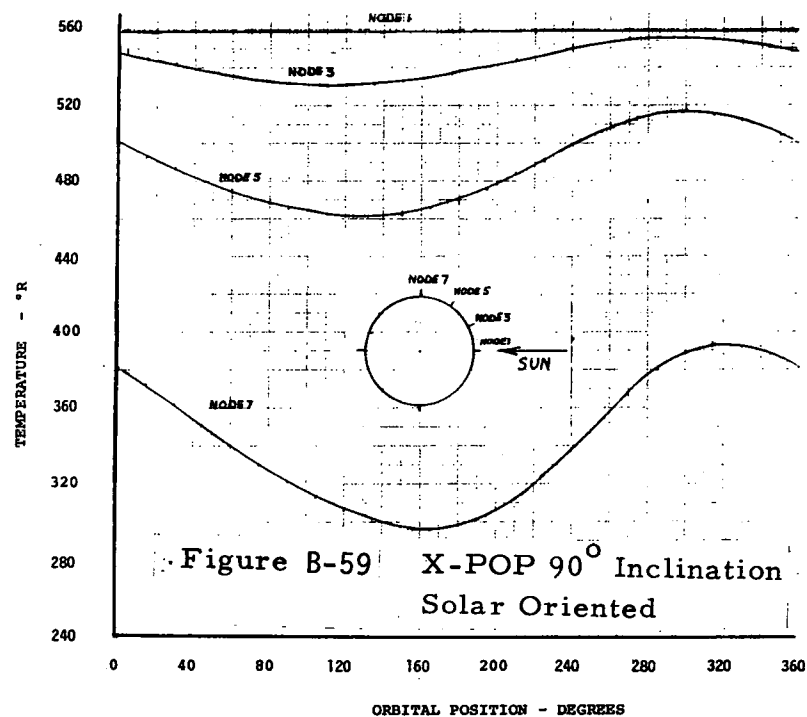


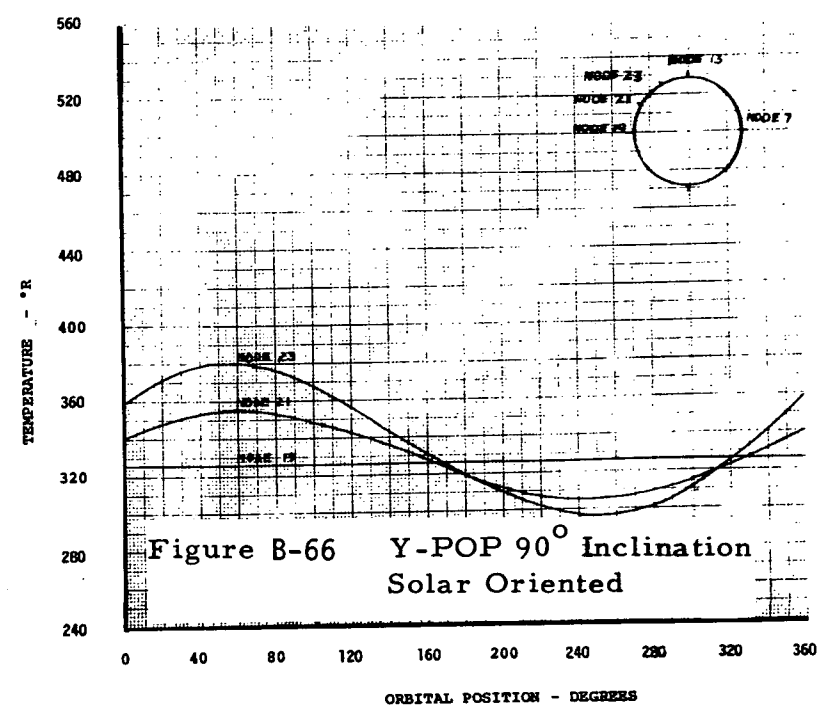
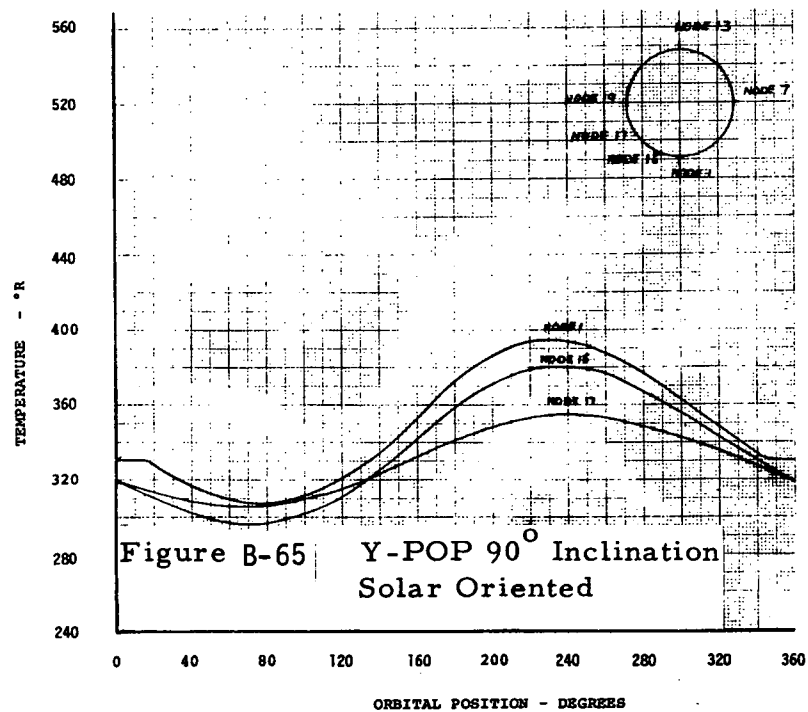
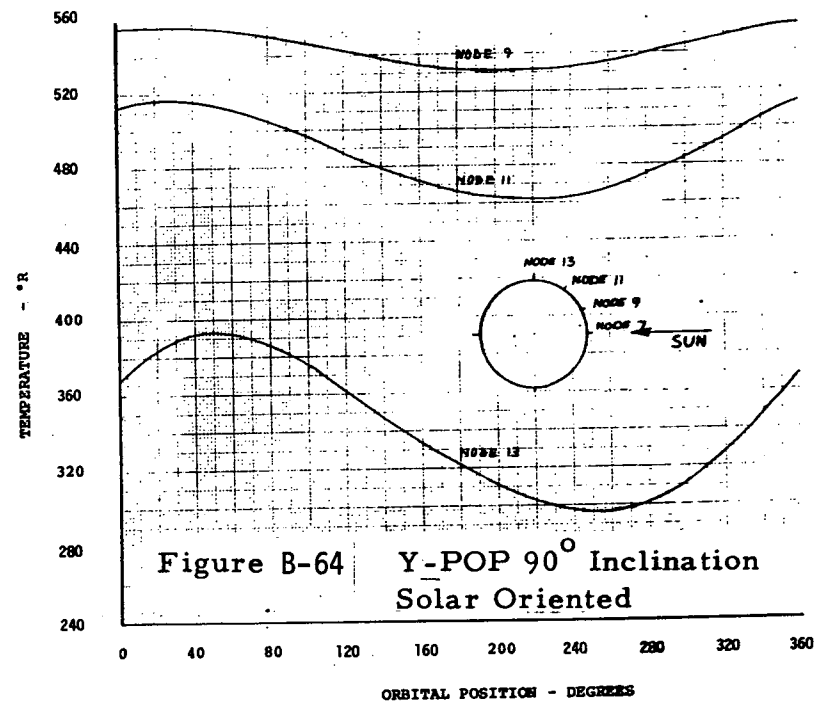
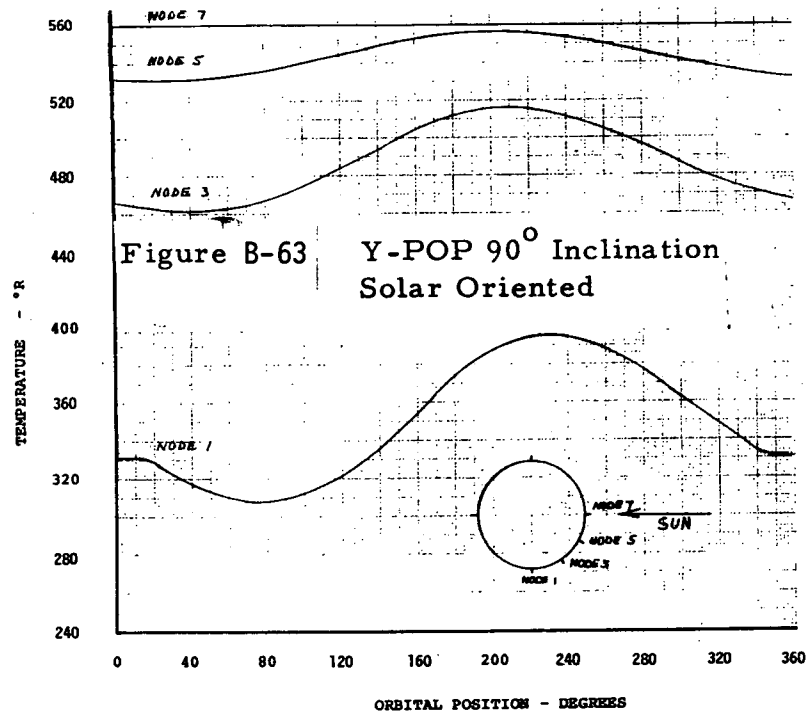




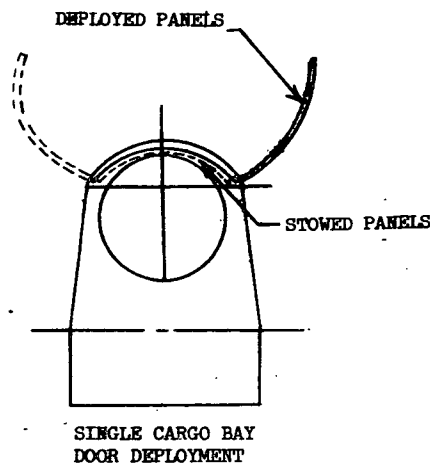
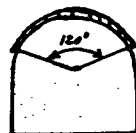
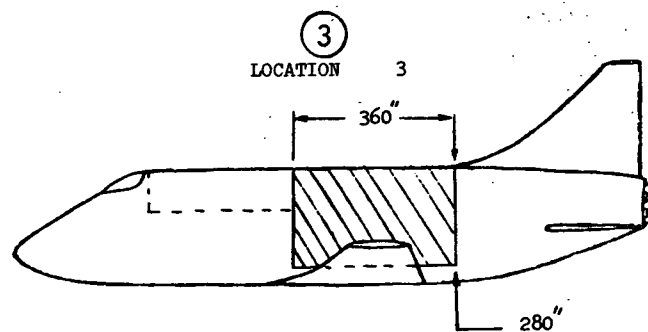
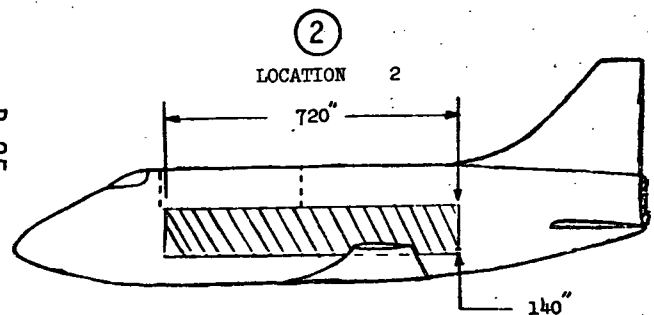
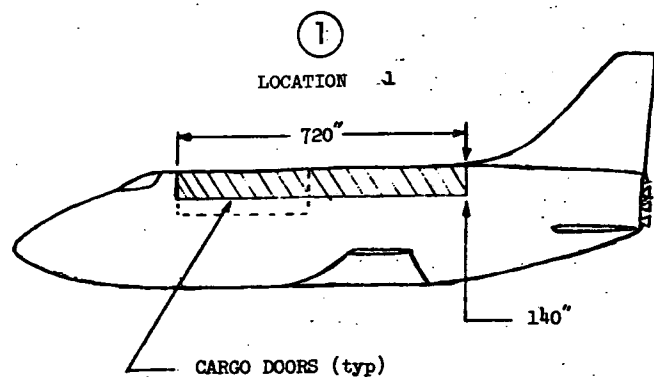




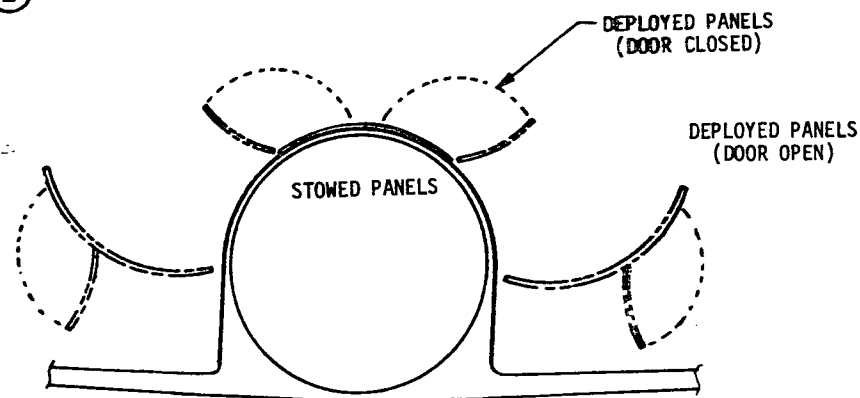
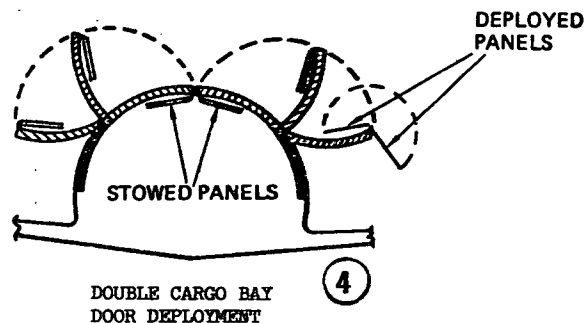




B-25

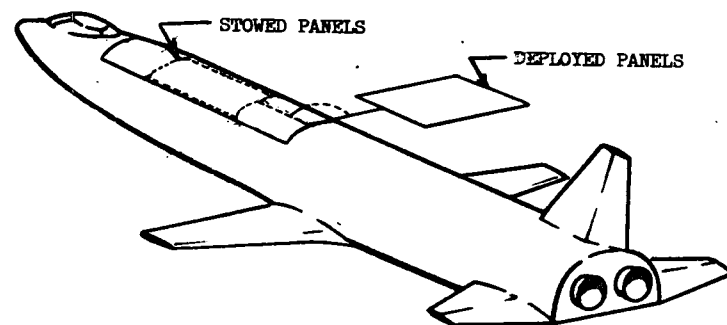


②



DOUBLE CARGO BAY DOOR
EXTERNAL DEPLOYMENT

②



②

FIGURE B-67 ORBITER RADIATOR CONCEPTS

APPENDIX C

SPACE RADIATOR DESIGN

C-1

This Appendix presents results of the Orbiter space radiator design study. Three conventional radiator subsystems have been conceptually defined and evaluated; two deployed subsystems and a skin mounted radiator panel concept. One deployed subsystem consists of the single cargo bay door deployment technique and the other deployed subsystem consists of the double door deployment technique. The alternate concept consists of panels mounted to the vehicle skin which do not interface with vehicle structure. Common to all concepts are the evaluation and design considerations of reliability and replacement, the panel materials, the coolant fluid, the heat load control method and the radiator coatings. These general considerations are discussed in subsequent paragraphs. Based on these considerations, the subsystem configurations were selected and weight estimates made for the deployed and integral panel concepts.

GENERAL RADIATOR SUBSYSTEM DESIGN

Radiator Reusability and Replacement

Due to the reusable nature of the Space Shuttle vehicle and the relatively short (two weeks) refurbishment time, a radiator concept which is essentially reusable with the capability of easy replacement should be baselined. The radiator subsystem should be designed such that, barring some physical damage, the subsystem could be used for several missions with no replacement of components or panels. The components should be packaged such that they can be replaced easily in case of failures. The radiator panels also should be easily replaced in case of damage. A modularized radiator subsystem which is composed of several separate radiator panels flow connected together will meet these requirements. The modular panel size and design of the panel installation will be influenced by reusability and replacement as discussed below. In addition, a discussion of the overall problem of radiator subsystem refurbishment between flights is included.

Reusability/Replacement Effects on Panel Size and Installation Design

Weight and reliability are closely tied to the reusability/replacement requirements when selecting the size of the modular radiator panels. There is a subsystem weight advantage to making the panels as large as possible since smaller panels result in increased manifold weight due to the larger number of manifolds required. Reliability of the system would be decreased by the larger number of connections and components required with smaller panels; however, it is possible that reliability could be enhanced with smaller panels if the radiator subsystem was capable of operation with partial capacity. If the subsystem is designed such that a damaged panel can be shut off and the remainder of the subsystem can continue to operate then reliability is increased with smaller panels since failure of one small panel would leave more of the subsystem operational. For the Orbiter application a redundant fluid system is baselined for reliability, and in this case, the size of the panels may not significantly affect the reliability. Both size and weight of an individual panel are important considerations when sizing the modular panels for easy handling during manufacture, assembly on the vehicle, and in-service maintenance. The panel should be sized such that a minimum of men and equipment are necessary to replace the modular panel thus favoring as small a modular panel as possible.

For the Orbiter application a modular panel size of about 15 feet long and 7.5 feet wide has been baselined as a compromise of the above considerations. The exact size and/or number of the modular panels can be adjusted to obtain the required area for a particular design concept and heat load requirement.

The installation of the modular radiator panels must be such that they can be removed and replaced easily. Such a system requires fluid connections at each panel and structural attachment by means of removable members such as bolts. The fluid connections and structural attachments must be located such that they are easily accessible for removal.

Refurbishment of the Radiator Subsystem

The refurbishment of the radiator subsystem which will be necessary during the life of the Orbiter could consist of : (1) replacement of subsystem components, (2) refurbishment of radiator panel coatings, and (3) replacement of damaged modular panels. Ground testing should indicate failures in subsystem components and, as was discussed previously, these components should be located and designed such that they can be replaced easily. The possibility of degradation over a period of time of the surface coating properties which are critical to the proper operation of the radiator panels necessitates that some provision be made to restore the coatings, preferably without replacing the entire panel. Coating degradation would be expected to be more severe for externally mounted panels than for internally mounted. Experience has shown, however, that routine handling of equipment will eventually degrade radiator coatings. Refurbishment of these coatings could be accomplished by use of coating tapes or by replacing the coating. Various radiator panel coatings are discussed in subsequent paragraphs. The possibility of physical damage to the radiator panels during transport, maintenance or operation requires that provision be made to replace panels selectively. It would also be possible although not desirable to replace panels when necessary because of surface coating degradation; this is considered as a backup mode to the concept of refurbishing the coatings only.

Radiator Panel Materials and Coolant Fluid

Radiator Material

Selection of a material for the radiator panel should be based on system weight, temperature constraints, strength requirements, availability, cost and manufacturing considerations. A comparison of several material candidates is shown in Table C-1. The weight of a radiator system can vary greatly with different materials as is illustrated in Figure C-1 which compares the weights and areas of aluminum and titanium. Since titanium has a higher density and lower thermal conductivity the weight of the radiator is greater. Aluminum has proven to be a good material for radiator application since it has low density, high thermal conductivity, high strength at low temperatures; it is a common material and has good manufacturing characteristics. As long as the temperatures the radiator panels will experience in flight are low (less than 400°F), as is the case for the radiator system which is stowed in the cargo bay, aluminum panels will be quite satisfactory. Aluminum, however, rapidly loses strength at temperatures greater than 400°F as would be experienced with radiator panels located on the external skin of the Orbiter. For external panels a material must be used which retains the strength at the higher temperatures. Several candidate materials for this application have been identified. These are titanium, stainless steel, and composite materials shown

TABLE C-1. COMPARISON OF CANDIDATE PANEL MATERIALS

Material	Weight	Strength	Availability	Manufacturing Characteristics	Thermal Conductivity
1. Aluminum*	Low density	good	good	good	High
2. Titanium	Heavy, high density	good	good	Some problems	Low
3. Stainless Steel	Heavy, high density	good	good	good	Low
4. Composite Material	Low density	good	Developmental	Developmental	High

*Aluminum material loses strength at temperatures greater than 400°F and can not be considered for externally mounted panels.

as materials 2 through 4 on Table C-1. The first two of these, titanium and stainless steel retain strength over the expected temperature range but both have low thermal conductivity and high density. Some fabrication problems may be associated with titanium while stainless steel panels should be relatively easy to fabricate. Analysis indicates that stainless steel radiators would be heavier than titanium. A significant weight savings could be obtained by using a composite material which has low density and high thermal conductivity. These materials retain their strength over the temperature range expected. One of these lighter materials would make the skin mounted configuration integral panels weight competitive with the deployed system.

Radiator Panel, Tube Size, Tube Spacing and Fin Thickness

The size of a radiator tube is a function of the flow rate, the fluid properties, the panel material, and the size of the radiator panel. All of these considerations determine the pressure drop through the panel. As pressure drop is increased, the weight attributable to the radiator system can be expected to increase due to the higher pumping power required. Panel weight will increase with tube diameter due to the increased tube and fluid weight. The correct tube size for a particular application which will minimize the weight is then a balance between these considerations.

There is also an interaction between tube size and tube spacing. Tube spacing can be optimized based on criteria similar to that for tube size with the addition of fin thickness and fin material as parameters. Weight optimization would trade the added weight of additional tubes against the weight of the area saved by the increased fin effectiveness due to closer tube spacing. Thus, the weight of the tube which varies with its size will affect the spacing, and the relationship between fin effectiveness and spacing can affect the tube size for minimum panel weight. If there are additional constraints on the panel such as a maximum allowable pressure drop or panel size these will also affect the tube size and spacing. The tube spacing is a strong function of the panel material. A high density material with a low thermal conductivity is a strong driving force toward small tube spacing whereas low density and high thermal conductivity result in a larger tube spacing.

Fin thickness can also affect the panel tube size and spacing in that it also affects fin effectiveness. As the fin thickness is increased the effectiveness will also increase. In general however the increase in weight due to the increased thickness is greater than that of the area saved by increased fin effectiveness and the thickness of a fin is determined by other considerations such as required stiffness and manufacturing and operational considerations which define a minimum fin thickness.

In a previous study, Reference C-1, radiators were designed using four fluids: RS89-A, MSC-198, FC-75, and F-21. Some results of this study are shown in Table C-2. In that study a maximum pressure drop of 10 psi and a minimum fin thickness of .03 Al were specified. For all of the fluids the minimum fin thickness was used in the design. The tube diameter for all the fluids except F-21 proved to be 0.25 in. I.D.. The F-21 design used 0.125 in. I.D. tubing. Due to the lower viscosity of F-21 this fluid was able to meet

TABLE C-2

OPTIMUM RADIATOR DESIGN CHARACTERISTICS

Max ΔP = 10 psia

Min Fin Thickness = .03"

Material = 6061 T6 Aluminum

FLUID	FIN THICKNESS inches	TUBE DIAMETER inches	TUBE SPACING inches
RS89A	.03	.250	5.3
MCS198	.03	.250	3.5
FC-75	.03	.250	8.2
F-21	.03	.125	4.9

the maximum pressure drop at a lower tube diameter. The tube spacings ranged from 3.5 in. for MCS198 to 8.2 in. for FC-75. These tube spacings are not a result of the fluid alone but resulted from a combination of all the considerations which were discussed previously. In order to design a modular radiator panel one must consider the tube spacing, tube size and fin thickness which results in the maximum heat rejection per unit weight for a radiator which is limited in area to the size of the modular panel. In this manner the overall system weight can be minimized. Studies have shown that panels designed in this manner with F-21 as a coolant and Aluminum as a material resulted in tube spacing from 5 to 7 inches with a .125 inch tube I.D. Studies of titanium panels using F-21 indicated a smaller tube spacing with the 0.125 inch I.D. tube.

Radiator Coolant Fluid

Considerations which are important in coolant fluid selection are: low weight, a viscosity which is stable over a wide temperature range, low freezing temperature, good compatibility, low toxicity, stability of composition, and good thermal properties. A comparison of the areas and weight of radiator subsystems for four fluids is given in Figure C-2. For this case the F-21 fluid indicated an area and weight savings over the other fluids. In addition the F-21 has the lowest freezing point (-211°F) of the fluids considered and can be vented without leaving a residue such as is left by RS89-A fluid after venting. The latter property becomes important in the application to an externally mounted panel configuration. The viscosity of F-21 has low sensitivity to temperature, and has fair compatibility and is not highly toxic. Freon-21 appears to have sufficient advantages over other fluids to warrant its selection for Orbiter radiator application.

Wide Heat Load Range Radiators

The size of a radiator system for a particular application is determined by the maximum heat load and the worst thermal environment. The Orbiter heat loads, however, are not constant and the environments may vary widely since it is to be designed for no attitude constraints. The multiplicity of missions being considered for the Orbiter make it desirable for the radiator system to have the capability to function over as wide a heat load range as practically possible with the capability of returning to high heat load operation rapidly from low heat load conditions.

The minimum heat load capability for the fixed radiator system is determined by the minimum thermal environment, the radiator system control method, the panel tube arrangement, and the minimum allowable temperature of the radiator coolant. A combination of an effective control method with a good panel design and a fluid which has a low freezing temperature is required to obtain a low minimum heat load capability.

Heat load control by stagnation methods has been shown to result in wide heat load range systems. This control method utilizes a technique whereby flow is stopped in all but one of the radiator tubes at low heat loads to reduce radiator heat rejection and thereby prevent fluid freezing

in the flowing tube. This flow stoppage or stagnation can be accomplished either passively by fluid viscosity - temperature characteristics (called selected stagnation) or by closing a valve which stops flow in all but one radiator tube (valve stagnation). The stagnation heat load control has been demonstrated to provide wide heat load range. A selective-stagnation control was used in the Apollo Block II ECS radiator to achieve a 2.5:1 heat load ratio (maximum:minimum heat rejection). It has also been applied (Reference C-2) in a feasibility test panel with a two-dimensional tube pattern (Figure C-3) for the Lunar Module to achieve a 5:1 heat load ratio. Both of these radiator systems used glycol-water as a coolant fluid. The two-dimensional tube pattern when used in conjunction with stagnation control was shown to approximately double the heat load range. In a later test the valve stagnation control concept with a two dimensional tube pattern was employed using Freon 21 as the coolant fluid, and a heat load ratio of 30:1 was obtained. In an extension of this work the concept was modified and demonstrated heat load ratios of up to 200:1.

The low heat load capability of the stagnation systems is limited by the number of tubes in which flow can be recovered within reasonable time periods. A comparison of the heat load recovery times for the Apollo Block II radiator, Lunar Module feasibility panel and Freon 21 panels are shown in Figure C-3. Transition of the Freon 21 test panel from low load to full heat rejection was demonstrated by this concept in from 1.5 to 1.9 hours under a zero incident heat flux environment. The limits of the heat load ratio for the Freon 21 designs studied and tested to date have not been reached. Test results which showed similar recovery transients for single sided and two sided operation indicate that a much larger panel (with greater high load capability) could be successfully operated at a similar low load.

The Freon 21 coolant is a particularly good fluid for use in these wide heat load range concepts because of its low freezing point and temperature-viscosity characteristics. The freezing point of Freon 21 is -211°F which makes low load operation possible. The viscosity of Freon 21 remains low at temperatures approaching its freezing point and thus demonstrates rapid recovery rates in stagnation control radiator systems.

These F-21 radiator designs which have demonstrated wide heat load range are applicable to the Orbiter EC/LSS. These designs have the capability to meet any heat load range requirements which the Orbiter may experience and have demonstrated adequate recovery rates from low to high heat load operation.

Radiator Panel Coatings

The baseline mission of 7 days in orbit under full sunlight conditions at an orbital altitude of 270 nautical miles defines the space radiation environment to be considered for coating degradation. The resulting damaging radiation will be 168 sun-hours of solar-ultraviolet per mission plus auroral electrons* (Reference C-3). Auroral radiation is currently poorly defined,

* The auroral zones are chiefly between 60° and 70° geomagnetic latitude in each hemisphere and range from 70 to 500 miles in height. Since the earth's magnetic axis is inclined about 11.5° relative to the rotational axis, the nominal 55° orbit inclination for the Orbiter will place it within the auroral region.

The optical solar reflector is a second surface mirror, consisting of a fused silica tile, about 1-inch square and 0.006-inch thick, with an evaporated silver film on the underside. A second film, inconel, is added behind the silver for durability.

Coatings are fabricated by attaching the tiles to the substrate using an appropriate adhesive (usually silicone rubber), double-backed tape, or, possibly, a mechanical fastener. The tiles are spaced about 0.005 to 0.010 inch apart to account for thermal expansion (1% to 2% of the total area is crack area). The substrate can be any material; successful application to aluminum and magnesium panels about 0.020-inch thick has been obtained and proven in several boost-vibration environments. Thermal cycling over the temperature range of -300°F to 300°F is reported (Reference C-5) to be acceptable. A maximum temperature limit of 710°F is reported for the existing adhesive system, although the basic tile/metal film system would be useful to at least 1340°F if a suitable adhesive were developed (Reference C-4). The coatings are cleanable and easily repairable.

Potential problem areas with the OSR are adherence of the tiles under the extremely long duration thermal cycling/vacuum conditions, difficulty of application to surfaces with a radius of curvature under 10 feet, and difficulty of application in area of weld seams or warps (entrapment of air in the bond can cause subsequent breakage of mirrors by expansion). It is also reported (Reference C-7) that the OSR is degraded "very badly" by exhaust contaminants.

Cost is a major disadvantage, with the tiles pricing at \$7 - \$10 each for small quantities, and about \$3 each for very large quantities (on the order of 25,000). Manufacturing costs of the assembly also run high. Weight is approximately 1-1/2 to 2 times that of paint coatings.

Flexible Optical Solar Reflector. - A much less expensive, more practical, version of second surface mirror coatings is being developed for applications that do not require quite the low solar absorptance or stability of the OSR's (Reference C-4). This coating, the FOSR, consists of an organic film, about 0.005 inch thick, with evaporated aluminum on the underside. It is useful from cryogenic temperatures up to about 750°F. Its solar absorptance is 0.16 and its emittance is 0.82. Tests to date have shown an increase in solar absorptance of about 0.03 after 4000 equivalent sun hours (ESH) ultra-violet exposure, and no effects due to low energy proton exposure. It is planned that the FOSR will eventually be available in tape form, about 1-foot wide. It offers very significant reductions in cost compared to the OSR, and should be cleanable, repairable, and offer minimum problems in attachment and mechanical integrity. However, the FOSR is in a lesser stage of development than the OSR, and more extensive basic testing is required.

In the same family of coatings as the FOSR are the teflon films which are silvered or aluminized. A one-mil thick aluminized teflon film was flown on Mariner V, and experienced a solar absorptance increase of about 0.04 after 5000 equivalent sun hours (Reference C-8). Its initial properties

were a solar absorptance of 0.15 - 0.21 and an emittance of 0.53. A silver-teflon coating, two-mils thick, has been selected for the Small Astronomy Satellite (Reference C-9). Its initial properties are a solar absorptance of 0.059 and an emittance of 0.675. Laboratory tests of a half-mil thick specimen showed no degradation after 1000 ESH ultraviolet exposure combined with 100 MRADS of X-radiation. Additional tests on flexible films (Reference C-10) indicate good stability of both a vinyl silicone and teflon when applied to aluminum foil to form a tape. Tests on the vinyl silicone showed that the initial solar absorptance degraded from 0.16 to 0.18 upon exposure to 1720 ESH ultraviolet combined with 100 MRADS of X-radiation. For ultraviolet only, no degradation occurred for a 3800 ESH exposure. The vinyl silicone emittance varied from 0.15 to 0.90 depending on film thickness. Solar absorptance of a 5-mil thick teflon film applied to aluminum did not change from the initial value of 0.21 upon exposure to 1150 ESH combined with 115 MRADS of X-radiation. The emittance of the 5-mil teflon is about 0.9. Thermal stability tests showed a capability of about 400°F for the best adhesive evaluated.

Organic White Paints. - Silicone paints pigmented with inorganic oxides are of some interest because their degradation is partially reversible upon re-exposure to air (Reference C-3). The IITRI S-13G formulation, pigmented with a treated zinc oxide, exhibits about the best stability. Its initial properties are a solar absorptance of 0.23 and an emittance of 0.88 (Reference C-11). After about 200 ESH exposure on the OSO-III flight its solar absorptance increased by 0.01, and after 1580 ESH it increased by about 0.065. These paints are fairly easy to repair and clean, and will withstand about 650°F heating (Reference C-3). Their degradation due to exhaust plume contaminants is listed as "fairly bad" (Reference C-7).

Inorganic White Paints. - To date, no white paints have offered really good long term stability in combined radiation environments. The zinc/oxide potassium silicate formulation (current Apollo radiator coating) has been found, however, to possess exceptional stability when exposed to vacuum and ultraviolet. The IITRI Z-93 formulation of this coating tested on OSO-III in a near-earth orbit, had an initial solar absorptance of 0.17 and degraded by only 0.005 after 1580 ESH (Reference C-10). Its emittance is about 0.9. Stability up to 24,000 ESH in near-earth orbit flight is reported in Reference C-7 with a degradation of only 0.02. Earth-based in situ vacuum and ultraviolet tests (Reference C-12) showed a solar absorptance increase of 0.04 during the first 500 ESH, followed by an essentially constant (slight decrease) solar absorptance until conclusion of the test at 10,000 ESH. Reference C-13 reports pre-flight absorptance measurements for the Apollo 14 ECS radiator of 0.226 and states that previous flight experience indicates the in-flight absorptance will be 20% higher due to boost and staging, ultraviolet and vacuum degradation. An in-flight solar absorptance of 0.272 is recommended. Reference C-14 reports that the Z-93 has poor cleanability and resistance to plume contamination. Reference C-3 reports the Z-93 maximum temperature capability as greater than 700°F.

The most promising inorganic paint for combined radiation environments and very low solar absorptance appears to be a synthetic zirconia-silica/potassium silicate formulation (Reference C-15). This coating is not considered to be fully optimized yet (Reference C-5). Its solar absorptance

is 0.07 and its emittance is 0.85. Degradation studies have shown an increase of 0.04 in solar absorptance due to 500 equivalent sun hours of ultraviolet exposure, and an increase of 0.02 due to proton irradiation. Under long term exposure, the solar absorptance would be expected to stabilize-out at a value less than the zinc oxide pigmented paint. This coating has been successfully tested to a 900°F thermal environment when applied to a titanium substrate (Reference C-15). Work on optimizing this class of coatings is continuing (Reference C-16). Because of its porosity, the cleanability, maintainability, and contamination resistance would be expected to be no better than the Z-93. The Z-93, and probably also the zirconia silica/potassium silicate, can be applied with moderate ease and repaired in the field.

Flame Spray Coatings. - Flame sprayed aluminum oxide, Rockide A, is of interest because of its high temperature capability of greater than 1000°F (Reference C-3) limited mainly by the substrate. It has an emittance of about 0.75 and a solar absorptance of about 0.27, both somewhat dependent on the application process. Little data is available on its space stability, although it flew successfully on Explorer I. However, data on aluminum oxide powders indicates fairly strong degradation (Reference C-17), while controlled aluminum oxide films applied by an anodizing or evaporation process show good inflight stability (Reference C-18). It is expected that a high-purity flame-spray aluminum oxide coating would offer the potential for fairly good stability, and since aluminum oxide tends to degrade to a suboxide, reentry would likely tend to restore the initial properties. Other flame-spray ceramics, such as zircon or zirconia, are also possible candidates. In all cases, however, the flame spray process leads to a porous coating which can be easily contaminated and is hard to clean. Applicability and repairability are expected to be moderately good.

Procelain Enamel. - A white porcelain enamel was flown on the S-16 orbiting solar observatory, and showed an increase in solar absorptance of less than 10% for 1000 ESH (Reference C-18). Initial values were a solar absorptance of 0.26 and an emittance of 0.75. Although temperature limits are not given for this particular enamel, porcelain enamels are generally capable of higher temperatures than paints, depending on the particular formulation, some much over 1000°F. Their major advantages are durability and cleanability, and, because of their lack of porosity, probably good contamination resistance. Original application is relatively difficult, requiring firing at 1000°F and higher.

Developmental Coatings

Coatings using new high temperature polymers under development (Reference C-19) offer the potential for use as a binder with inorganic pigments for use in the 800°F range. Sintered glass coatings have been fabricated at VMSC with a solar absorptance of 0.18 and an emittance of 0.92 at 700°F. These coatings offer potentially a very stable solar absorptance and a temperature capability limited primarily by the substrate. They have a porosity similar to the inorganic paints.

Conclusions and Recommendations

For the deployed panel concept, existing information indicates that the current Z-93 inorganic paint used on the Apollo or the FSOR tape are both excellent candidates. From practical considerations, the FSOR is most desirable, but it needs more testing for repeated long-term use. Another good candidate is the S-13G, if it recovers its solar absorptance repeatedly upon reentry. If it does, it is probably preferable over the Z-93 from a practical viewpoint. For any of these a careful evaluation of reaction control motor contamination effects while deployed, and contamination effects due to out-gassing from other components while stowed, must be made.

For the skin mounted panel concept, the FSOR tapes are again leading candidates for easily replaceable coatings. However, there is an excellent possibility that the coatings will not need to be replaced between missions. It is likely that the Z-93 or a similar paint can withstand the 800°F reentry environment, and can be used if contamination effects from the hot exterior areas or RCS motors are not too serious. Testing will be required here. Porcelain enamels are quite attractive from a handling/cleaning viewpoint, and tests should be conducted to determine if any existing enamels offer suitable environmental stability and/or recovery characteristics in the repeated long-term application. If these candidates are not found to be suitable, the other possibilities discussed should be explored. From existing data, there is no reason to doubt that a satisfactory coating approach for fixed radiators can be implemented.

In keeping with the concept of conservatism used throughout this report, the Orbiter radiator coating properties have been chosen as $\alpha = .30$ and $\epsilon = .90$ for the radiator design. This represents a degraded Z-93 Apollo coating considering the multi-mission requirement of the Orbiter.

Aerodynamic Heating Protection

The Orbiter is exposed to high aerodynamic heating rates during boost and reentry. For boost heating the fluxes in the area of the cargo bay door are given in Table C-3. For reentry heating higher peak fluxes are expected, and the exposure time with high fluxes is two to three times that of ascent heating.

For deployed radiator panels that are stowed inside the cargo bay, aerodynamic heating protection is provided by the cargo bay door. Since temperatures in the cargo bay should not exceed 300°F, the Freon 21 pressure in the panels should not exceed 500 psi. Normal system operating pressure will be 150 to 200 psi so no significant penalty is anticipated for the design of radiator tubing and system interconnecting tubing and valves to withstand 500 psi. Significant penalties may be involved, however, in the design of compact heat exchangers for this higher pressure. If the system weight is increased enough to offset the additional weight, cost, and unreliability of an overpressure protection system, a set of isolation and pressure relief valves could be included. For launch and reentry, radiator isolation valves would close to protect pumps, filter, accumulator, and compact heat exchangers from pressures above

TABLE C-3 LOW CROSS RANGE FIXED WING ORBITER

TIME FROM LIFT-OFF (SEC)	UPPER SIDE ASCENT LAUNCH HEATING COLD WALL HEATING RATE (BTU/FT ² HR ³)	EQUILIBRIUM TEMPERATURE (°F)
0		100
100	510	325
120	1020	470
140	900	440
160	720	390
180	490	310
200	270	205
220	200	160
240	1630	590
260	1400	550
280	1150	500
300	1100	490
320	1150	500
340	1250	520 Alt = 310000 ft. Vel = 19000 ft/sec
600	0	

X/L = .75

ϵ = .8

0° Flow Deflection

" μ " Heating Rates

WD Trajectory

their design pressure. Additional protection for the isolated radiators could be provided by a relief valve which either vents overboard or relieves pressure due to fluid expansion by bleeding fluid around the isolation valve. The accumulator could be designed to accommodate this fluid at normal system pressure.

For skin mounted panels it is expected that overboard venting of the fluid will be required for reentry. Estimates of peak upper surface temperatures for the Orbiter during reentry are in the 700°F to 800°F range and Freon 21 has a pressure on the order of 8000 psi at 740°F. There is also the possibility of Freon 21 decomposition at temperatures above 600°F with possible corrosion resulting from decomposition products. A simple mechanical overpressure relief valve could be used to vent the fluid during reentry, but this would leave residual freon in the hot radiator tubes. The surest method to avoid problems would be to vent the radiator panels to the vacuum of space prior to reentry and to use an over-pressure relief valve as a backup system. This could also serve as a backup relief in case of over-pressurization during ascent.

The ascent heating data of Table C-3 was used with a simplified finite difference analysis to predict the radiator skin temperature transient shown on Figure C-4. It was assumed that the heating rates were independent of skin temperature which is a conservative assumption for cold wall heating rates. Another conservative assumption was that heat is radiated from the panel at the average temperature during each of the time increments listed in Table C-3. The panel heat capacity was assumed to be equal to that of an 0.040 in. thick aluminum plate and the emissivity was assumed to be 0.9. The results show that the maximum temperature of 376°F occurs at the end of the high flux heating profile. This is approximately 200°F less than the radiation equilibrium temperature at that time based on the instantaneous heat flux and corresponds to a fluid pressure of approximately 800 psi.

The system could be designed with radiator isolation valves and fixed expansion relief valves as discussed above and the radiator panels could be designed for 800 psi internal pressure. The backup pressure relief valve needed for reentry would protect the panels in the event that ascent heating were greater than expected or if the fluid expansion relief valve failed. To provide for the possibility that the over-pressure relief valve may be actuated during ascent the system accumulator should be sized with sufficient volume to refill the radiator panels. The isolation valve should be located as close as possible to the radiators to limit the amount of Freon vented overboard during ascent and reentry.

Deployed Radiator Subsystems

Subsystem Description

The radiator panels are stowed in the cargo bay compartment for protection from the severe launch/reentry thermal environments and are deployed for orbital operation.

The single door deployment sequence consists of opening the cargo bay door, deploying the radiators, and closing the door. The deployment

mechanism is a 2 position drive assembly located in the cargo bay (Figure C-5) which rotates the panels to the deployed position. In the event of mechanical failure, manual operation of the radiator deployment mechanism could be performed by an EV astronaut.

The panel area which can be deployed by this method is limited by the size of the cargo bay doors; the maximum area available is approximately 1800 ft² (15' x 60', with radiation from both sides of the panel).

The double door deployment technique requires that the cargo bay doors remain open while the radiators are operating. In order to reduce the thermal environment the panels are stowed in a double fold configuration and folded down over the edge of the door (see Figure C-6) when deployed. This requires that the door open only to the 180° position as shown on Figure C-6. A 2 position drive assembly located on the cargo bay door rotates the panels to the required position. As in the case of the single door deployment, an EV astronaut could manually deploy the radiators in the event of a failure.

The maximum area available with the double door deployed technique is 1800 ft². The deployed area is obtained by using the inside of the cargo doors and one side of the fold down panel.

Heat load control is accomplished for the deployed subsystems by utilizing a bypass-stagnation concept with the two-dimensional tube pattern on the panel. This control technique allows a much wider heat load range than is currently anticipated thus permitting operation under adverse contingency conditions. If more detailed vehicle integration studies show that Freon 21 radiator control range requirements can be satisfied with simple bypass control, then the stagnation valve, flow restrictors, and two dimensional tube pattern can be eliminated with a corresponding improvement in cost and reliability.

Vehicle/Radiator Interface

The radiator subsystem interfaces with the Orbiter at three locations; (1) the structural attachment points of the panels to the vehicle and deployment mechanism, (2) the fluid connections from the panels to the remainder of the radiator system, and (3) location and mounting of the radiator subsystem components (pumps, valves, fluid reservoir).

For the single door deployment configuration the structural attachments must be such that the cargo doors may be closed after deployment, (Refer to Figure C-5). The deployment requirements necessitates that the vehicle/radiator attachments in use when the panels are deployed allow approximately a 120° maximum rotation in a single direction. This can be accomplished through use of a single hinge or several one degree of freedom linkages. These attachments are illustrated in the sketch of Figure C-5. If movement of the panel must be other than pure rotation due to problems of deploying the panels from the cargo bay, additional linkage bars could be used to provide the required movement. This would result in additional complexity and reduced reliability. The structural attachments for the radiator in the stowed position

must be adequate to withstand the launch loads. In order to utilize the cargo door structure, latches would have to be configured for panel attachments to the door which would disconnect prior to opening of the cargo door and deployment of the radiator panels. Such a mechanism would be added at the expense of increased complexity and decreased reliability. The alternative to this type of structural attachment would be to design the panels with sufficient stiffness to withstand the launch loads without such attachments. This would result in much heavier radiator panels but would remove the complexity of the latches.

Since the single door and double door deployment mechanisms rotate in one direction only, flex lines should be used to provide for fluid transfer across the hinge joint. Such a system would have the advantage of simplicity and higher reliability over configurations with fluid swivels which have potential leakage problems. The single door concept requires a minimum of 6 flex lines for the primary and redundant systems and the double door concept requires a minimum of 24. Additional flex lines may be required if the cargo bay doors are opened in segments. For each system there will be at least one main coolant line, one line carrying flow to the prime tubes for low heat load operation and one outlet line returning the flow to the pump and heat exchanger assemblies.

In order to insure proper operation of the radiator subsystem while in the deployed position it will be necessary to provide for thermal isolation of the panels. The area of contact at the attachment to the hinge or swivel linkage will require conduction insulation. A thermal analysis considering the Orbiter temperatures while in orbit will be necessary to determine the required insulation to make these heat leaks negligible. In addition, insulation of the flex lines may be necessary to insure fluid in the main coolant line will not freeze at low load when flow in this line is stagnated.

The structural and fluid attachments for the radiator subsystem must be designed for contingency operation in possible failure modes. For example if the latches on a structural attachment to the cargo door should fail to operate some method of disconnecting these must be provided. If the deployment mechanism should fail to operate either in the closed or open position a provision must be made to allow continuation of the mission. For some of the failure modes the possibility of using pyrotechnic devices to jettison the panels may prove feasible. Additional methods such as back up manual systems are also a possibility. Further study of possible redundant systems and contingency operation modes will be necessary to define these requirements in detail. Another area for future development of the vehicle/radiator interface will be the two position deployment mechanism and associated power, weight, volume and reliability requirements.

The integration and location of the pumps, valves and controls servicing the radiator subsystem should not have appreciable effect on the operation of the subsystem. Location of these components could be such that the fluid lines connecting them with the radiator panels would tend to dampen the transient response of the system to perturbations in heat loads and environments. This could be an advantage in sizing the radiator system in that the system can be designed for lower effective environments. The length

of these fluid lines will also affect the power requirements, however, with proper sizing of the lines this should not be a large factor.

Panel Design

The single and double door deployed radiator panels are sized for an assumed heat load of 30,000 BTU/hr and a radiator inlet temperature of 140°F and an outlet of 40°F. From the data presented in the main body of this report it is determined that the single and double door design sink temperatures are 26°F and 34°F respectively, and the required radiator area is:

Single Door Deployed - 1051 ft²

Double Door Deployed - 1665

A modular panel size of 14.5 x 7.25 ft has been selected for both concepts. Therefore, 5 modular panels radiating from both sides are required for the single door concept and 16 modular panels radiating from one side only are required for the double door concept.

Figure C-7 shows the basic panel construction of dual tube flanged extrusions welded to a thin sheet in a two dimensional tube pattern. The panel shown is door mounted; however, the fold down and single door panels have the same basic design. Structural stiffness is provided by the over/under tube arrangement on 6.21 inch centers and a frame around the edges. Additional structural support of the single door deployed panels is provided by two diagonal hat sections. Two concepts for panel mounting to accommodate differential thermal expansion between the panel and the door are also illustrated in Figure C-7. Each utilizes fixed hard mounting at the center of the panel and expansion accommodation mounts at other locations at appropriate. The exact panel thickness will require a detailed structural analysis of the panels. It is anticipated that a fin thickness of approximately 0.030 inch will be required for the single door deployed panel and the fold down portion of the double door deployed panel. The panel attached to the inside of the door is expected to be approximately 0.016 inch thick. Table C-4 summarizes the two deployed panel designs.

Weight estimates of the deployed panel concept are presented in Tables C-5 and C-6.

Skin Mounted Concept

Subsystem Description

The design concepts selected for skin mounted panels are shown in Figures C-8 and C-9. Three concepts for mounting radiator panels to the vehicle skin have been generated and consist of: unfolding (butterfly) panels which are imbedded in the vehicle skin (Figure C-9a), clip-on folding panels (Figure C-9b), and the clip-on non folding panels (Figure C-9c). Panels which are

TABLE C-4
DEPLOYED RADIATOR DESIGN SUMMARY

	SINGLE DOOR	DOUBLE DOOR
Design Sink Temp - °F	26	34
Required Area - ft ²	1051	1665
Modular Panel Size	14.5 x 7.25	14.5 x 7.25
Tube Spacing - in.	6.21	6.21
Fin Thickness - in.	.030	.030(fold down panel) .016(door mounted)
Number of Panels	5	16
Total Area Available - ft ²	1051	1682

TABLE C-5
SINGLE DOOR DEPLOYED RADIATOR WEIGHT ESTIMATE

Radiator Panels (0.030 inch skin) - 5 @ 80 lb each	400
Deployment Mechanism	35
Temperature Controller - 2 @ 8 lb each	16
Isolation Valve	1.5
Check Valve	0.5
Stagnation Valve - 2 @ 4 lb each	8
Bypass Valve - 2 @ 4 lb each	8
Flex Hose	<u>2</u>
Dry Weight	471.0
R-21 - 6.6 lb/panel	<u>33.0</u>
Total Weight	504.0 lb
Weight Density	0.48 lb/ft ²

TABLE C-6

DOUBLE DOOR DEPLOYED RADIATOR WEIGHT ESTIMATE

Radiator Panels - 8 (.030 in skin) @ 80 lb each	640
8 (.016 in skin) @ 56 lb each	448
Deployment Mechanism	40
Temperature Controller - 2 @ 8 lb each	16
Isolation Valves - 4 @ 1.5 lb each	6
Check Valves - 4 @ .5 lb each	2
Stagnation/Proportioning Valve - 2 @ 4 lb each	8
Bypass Valve - 2 @ 4 lb each	8
Flex Hose	<u>8</u>
Dry Weight	1176
R-21 - 6.6 lb/panel	<u>105.6</u>
Total Weight	1311.6
Weight Density	0.79 lb/ft ²

imbedded into the vehicle skin impact the structural design of the vehicle and are, therefore, not as desirable as the clip-on panels. The non-folding clip-on panels require no deployment/folding either after launch or prior to reentry operations and are baselined for the design and weight analyses conducted herein.

The component and subsystem design are very similar to the deployed concept except for the details of radiator panels design and the addition of an overboard dump valve to vent the radiator fluid overboard for reentry. The critical design constraint for this system is the combined structural loads and high temperatures imposed on the system during ascent and reentry. For maximum design flexibility and highest design confidence a modular titanium panel attached to the Orbiter skin is selected. The basic Orbiter skin could be used as the fin material if structural design integration permits. For concept comparisons it is assumed, however, that the addition of tubes, fluid, and multiple fluid connections would make this integrated design unfeasible even though it could provide weight savings.

Vehicle/Radiator Interface

The interface between the vehicle and radiator subsystem for the skin mounted panel concept occurs in four general areas as compared to three for the deployed system. The four areas of interface are: (1) the structural attachment points of the panels to the vehicle, (2) integration of the externally mounted panels with the vehicle skin, (3) the fluid connection of the panels with the remainder of the radiator subsystem, and (4) integration of the radiator subsystem components into the Orbiter.

The previous discussion of item 4 (the integration of the subsystem components) of the deployed systems also applies to the skin mounted panel concept since a similar subsystem component arrangement is used in both concepts.

The structural attachments and fluid connections for the skin mounted panels, in contrast to the deployed concept, require no provisions for the movement of the panels and are subsequently less complex. A sketch of the installation of this concept is shown in Figure C-10. Due to the external location of the panels, the structural attachments must be designed such that the panels can withstand the launch and aerodynamic loads during ascent and the aerodynamic loads and reentry environment during descent. In addition refurbishment requirements necessitate that these panels be replaceable. The external loads during launch and reentry on the skin mounted panels will probably require more structural attachments than were necessary for the concept which is protected by the cargo bay door during these mission phases. The structural interface design should also consider that external location of the panels makes them more susceptible to damage and therefore more frequent replacement may be required. As was the case for the deployed concept, proper operation of the radiator panels requires that the heat leak from the panels to the Orbiter be minimized. Since the vehicle skin in this area will be titanium, a low conductivity metal, the conduction heat leak may not be severe, however, radiation insulation may be required between the panels and the vehicle skin. As was pointed out for the deployed insulation requirements

further definition of skin temperatures and more detailed design of the attachment will be required before the insulation requirements can be fixed.

For this externally mounted concept consideration must be given to integrating the panels with the vehicle skin line. It is not desirable from a replacement standpoint to have the radiator panels serve as a part of the structural skin of the Orbiter, however, if the panels did replace the portion of the vehicle skin at their location a significant weight savings could be obtained since only tube, fluid, and manifold weight could be attributed to the radiator subsystem. The major portion of the weight of a radiator panel is that of the fins. Assuming for this concept that the fins would be made of .06 in. titanium a weight savings of about 1300 lbs. could be obtained through replacing structural skin with radiator panels. Using a modular panel approach with easy replacement capability, the externally mounted panels must be integrated with the skin line. Two methods of accomplishing this would be to install a fairing around the edges of the panels to smooth the skin line or to recess the vehicle skin line at the panel location to accommodate the radiators. The thickest portion of the radiator panels will be the fluid manifolds which will require 7/8 to 1 in. I.D. tubing. The panels themselves will be only .06 in. thick fins with .125 in. I.D. tubing. Some thickness of insulation between the panels and skin will also be present. If provisions could be made to locate the manifolds below the skin line the fairing of the remainder of the panels would not be a severe problem. Addition of fairings around the panel edge would increase the subsystem weight somewhat. Orbiter design considerations and impact on the aerodynamics characteristics would define the detailed panel skin line interface.

There is no flexibility requirement for the fluid lines connecting the panels with the remainder of the radiator system since the panels are fixed in position. Since the radiator subsystem components will be located in the inside of the vehicle and the panels mounted on the outside, provision must be made for a fluid path across the vehicle skin. In addition since there will be panels located on both sides of the Orbiter more connecting lines may be required than for the baseline deployed system.

Panel Design

The design sink temperature for the skin mounted panels is the same as the single door deployed concept (26°F). Therefore the same area is required assuming that a high effectiveness radiator can be obtained. From thermal design consideration titanium is a very poor choice of materials for a radiator fin because of its low thermal conductivity. The radiator design for titanium panels will require thicker panels and additional fluid and tubes in order to maintain high radiating fin effectiveness. This will result in higher radiator panel weights than for the deployed subsystems. The computer analyses conducted in Reference C-1 indicated that in order to obtain a high radiator effectiveness, a 0.06 inch titanium fin with approximately 3.0 inch tube spacing is required. Figure C-11 shows the basic panel construction of 0.125 in. I.D. diameter tubes brazed to the titanium fin at 3.1 inch intervals.

The secondary system tubes are located between the primary tubes. The over/under tube arrangement used for the deployed panels is not used to minimize the radiator stand-off from the Orbiter skin. Sixteen modular panels (8 on each side) each 14.5 x 7.25 ft. are required to give a total area of 1051 ft². A weight estimate of the skin mounted panel is presented in Table C-7.

Radiator Penalty Summary

Radiator weight penalties have been determined for four different radiator design concepts as follows:

<u>CONCEPT</u>	<u>WEIGHT PENALTY</u>
Single Door Deployed	0.48 lb/ft ²
Double Door Deployed	0.79
Skin Mounted - Clip On	2.20
Skin Mounted - Integral	0.84

Final selection of a radiator design will require detailed studies of the thermal performance, operational procedures, structural performance and vehicle integration. Based on the preliminary design analyses conducted herein the single door deployed system will be the lightest weight.

TABLE C-7

SKIN MOUNTED RADIATOR WEIGHT ESTIMATE

Radiator Panels - 10 @ 222 lb each	2220
Temperature Controller - 2 @ 8 lb each	16
Isolation Valve - 2 @ 1.5 lb each	3
Check Valve - 2 @ 0.5 lb each	1
Stagnation/Proportioning Valve - 2 @ 4 lb each	8
Bypass Valve - 2 @ 4 lb each	8
Pressure Relief Valve 4 @ 4 lb each	<u>16</u>
Dry Weight	2272
R-21 - 6.6 lb/panel	<u>66</u>
Total Weight	2338
Weight Density	2.2 lb/ft ²

Note: If Orbiter skin is used for fin material a weight savings of 1450 lb is realized. The resulting weight density would be 0.835 lb/ft².

APPENDIX C REFERENCES

- C-1 Gaddis, J. L., "Report On Preliminary Study of Crew and Equipment Thermal Control Systems For The Space Shuttle", Vought Missiles and Space Division Report No. 00.1323, 19 July 1970.
- C-2 Rogers, R. R. and Gayer, M. D., "Thermal Vacuum Test of Freon 21 and Ethylene-Glycol Radiator Panels", Vought Missiles and Space Co. Test Information Release No. 353-TIR-0004, 3 November 1969.
- C-3 Ruttenhouse, J. B. and Singletary, J. B., "Space Materials Handbook, Third Edition", USAF Technical Report AFML-TR-68-205, July 1968.
- C-4 Marshall, K. N., and Breuch, R. A., "Optical Solar Reflector: A Highly Stable, Low α/ϵ Spacecraft Thermal Control Surface", J. Spacecraft, Volume 5, No. 9, September 1968 (pp 1051-1056)
- C-5 Greenberg, S. A., Personal Communication, Lockheed Missiles and Space Company, November 1969.
- C-6 Fisher, Carl, Personal Communication, Aerojet Corp., November 1969.
- C-7 Russell, D. J. and Savage, R. T., "Status Report - Thermal Control Coating Evaluation Study", Boeing Letter 5-2940-1-HOU-961 (CSD), March 30, 1970.
- C-8 Carroll, W. F., "Mariner V Temperature Control Reference Design, Test and Performance", AIAA Paper 68-791, 3rd Thermophysics Conference, June 1968.
- C-9 Brenza, Peter, Personal Communication, John Hopkins Applied Physics Laboratory, March 1969.
- C-10 Linder, B., "Series Emittance Thermal Control Coatings", Proceedings of the Joint AF-NASA Thermal Control Working Group, Aug. 16, 17, 1967 AFML-TR-68-198, August 1969, pp 602-629.
- C-11 Millard, J. P., "Results From the Thermal Control Coatings Experiment on OSO-III", AIAA Paper No. 68-794, AIAA 3rd Thermophysics Conference, June 24-26, 1968.
- C-12 Cunningham, G. R., et.al., "Emissivity Coatings For Low Temperature Space Radiators", NASA CR-1420, September 1969.
- C-13 Belshaw, G. W., "Apollo 14 ECS Radiator Solar Absorptance", General Electric Apollo System Department, Technical Information Release, TIR-728-S-1015(S), 26 January 1971.

APPENDIX C REFERENCES (CONTD)

- C-14 Williamson, F. D., Smith, F. M., and Stanley, V. J., "Utilization of Inorganic Thermal Control Coating", Proceedings of the Joint AF-NASA Thermal Control Working Group, Aug. 16, 17, 1967, AFML-TR-68-198, August 1968. (pp 583-601).
- C-15 Bailin, L. J., "Production of High Purity Thermal Control Coatings", USAF Technical Report ARML-TR-68-70, April 1968.
- C-16 Bailin, L. J., and Sibert, M. E., "New Development in Refractory Pigments for White Thermal Control Coatings", Proceedings of Thermodynamics and Thermophysics of Space Flight, March 23-25, 1970, pp 191-209.
- C-17 Plunkett, J. D., "NASA Contributions to the Technology of Inorganic Coatings", NASA SP-5014, 1964.
- C-18 Boebel, C. P., "Preliminary Data: OV1-10 Thermal Control Coating Experiment", Proceedings of the Joint AF-NASA Thermal Control Working Group, Aug. 16-17, 1967, AFML-TR-68-198, Aug. 1968, pp. 656-695.
- C-19 Schmitt, G. F., "Experimental High Temperature Polymers for Protective Coatings", AFML-TR-67-174, Pt. II, March 1969.

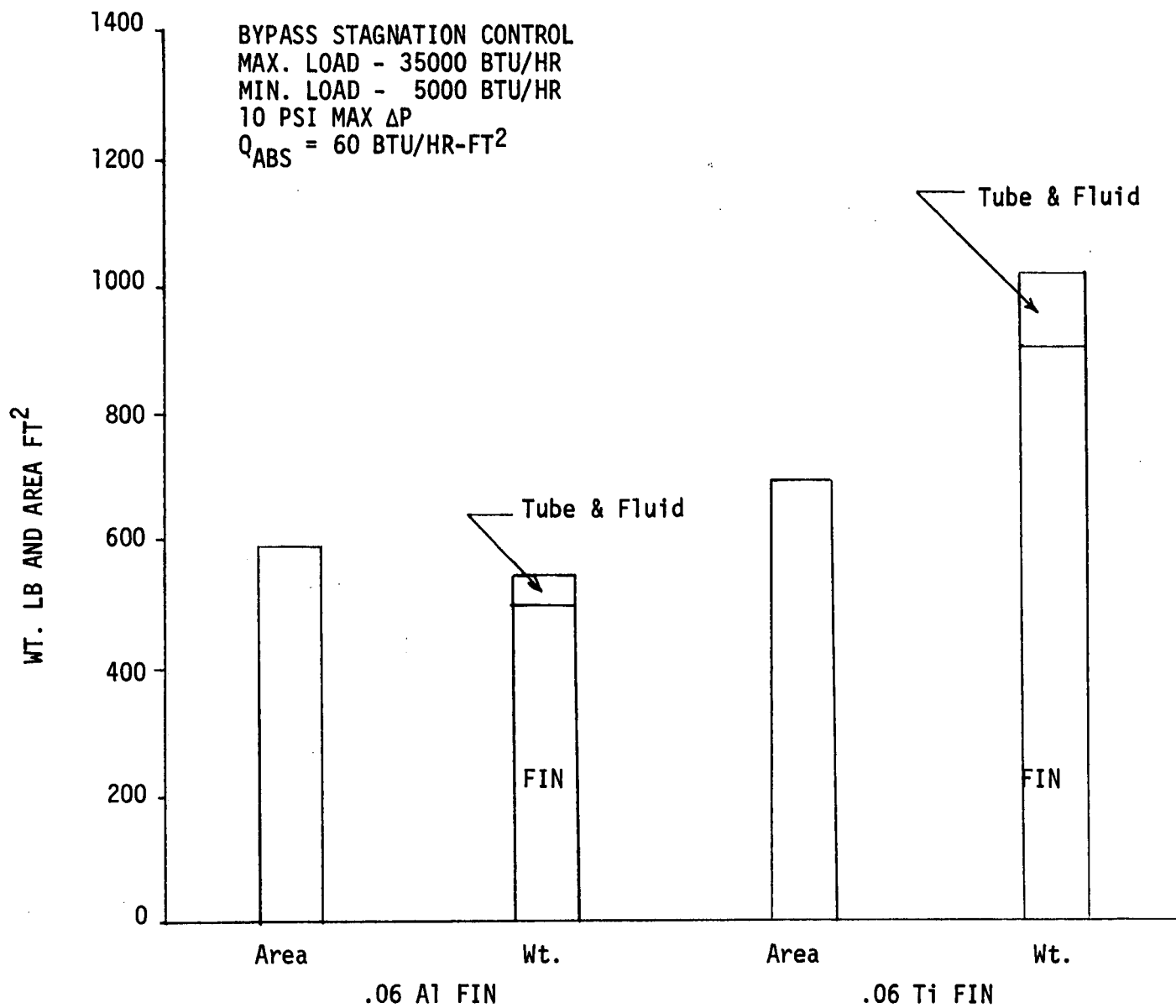


FIGURE C-1 RADIATOR FIN MATERIAL COMPARISON WITH R-21 FLUID

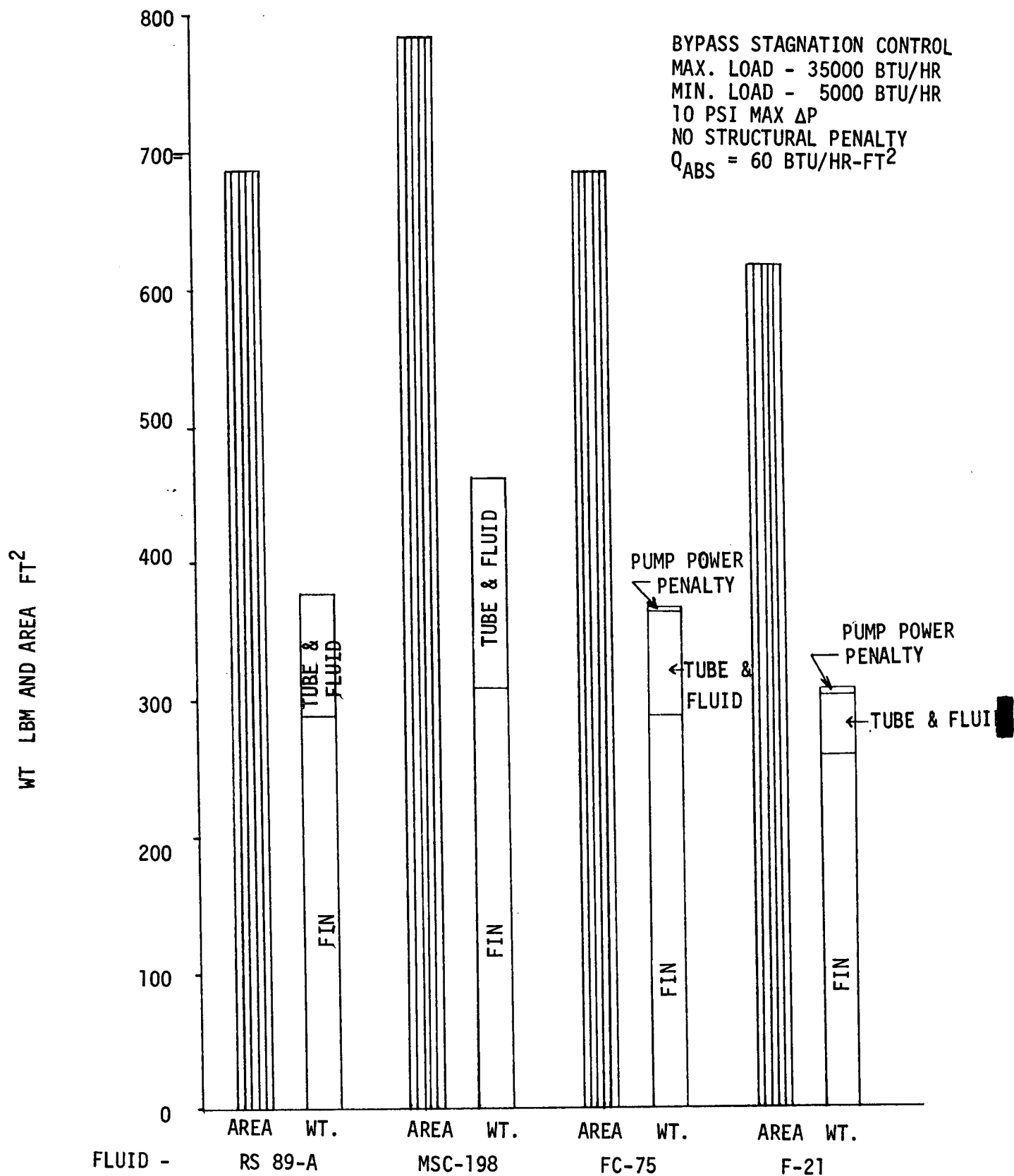


FIGURE C-2 RADIATOR FLUID COMPARISON WITH 0.030 IN ALUMINUM FIN

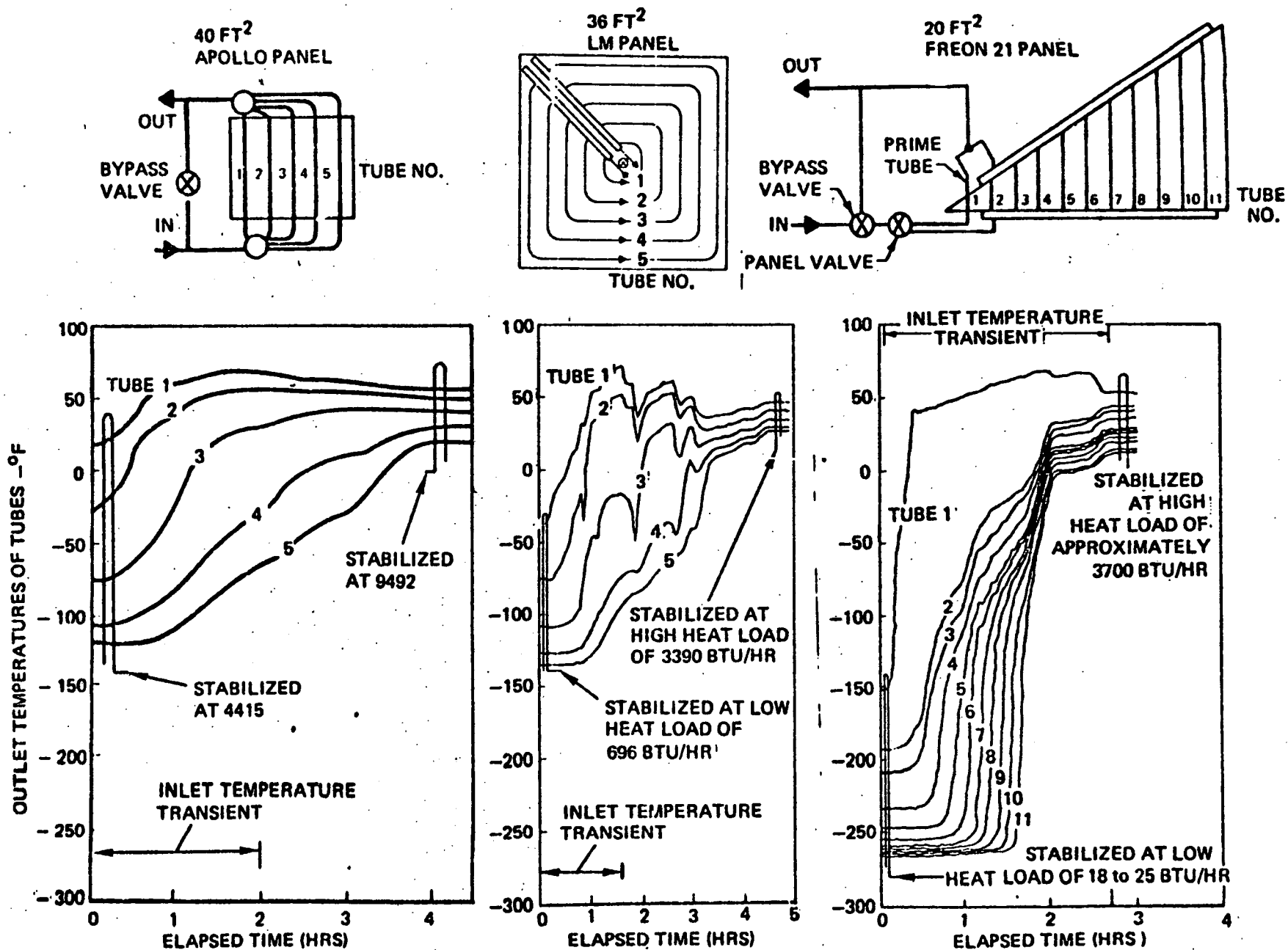


FIGURE C-3 COMPARISON OF RADIATOR SYSTEM HEAT LOAD RECOVERY CHARACTERISTICS

C-30

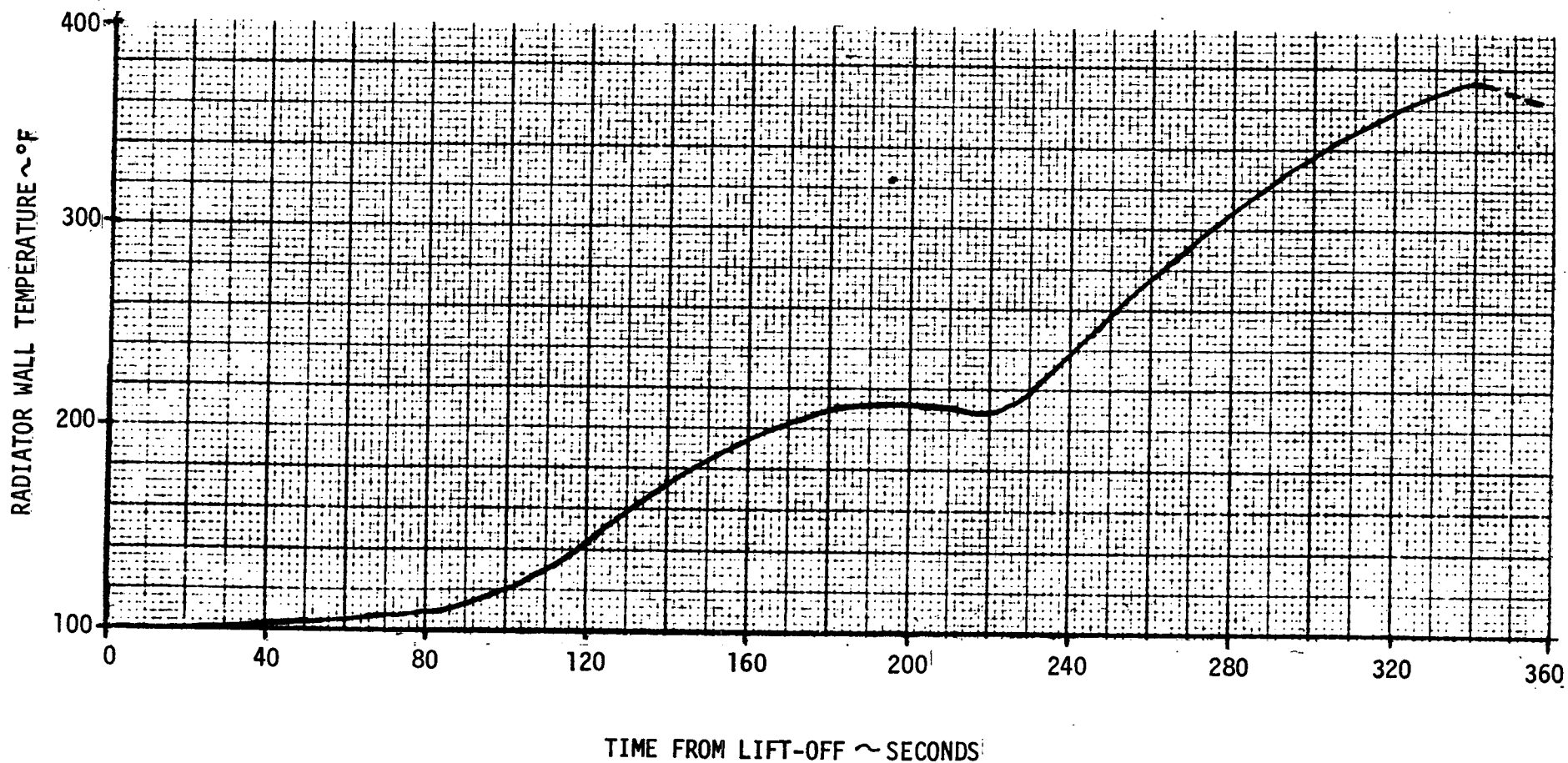


FIGURE C-4 RADIATOR WALL TEMPERATURE - BOOST TRAJECTORY - LOW CROSS RANGE ORBITER

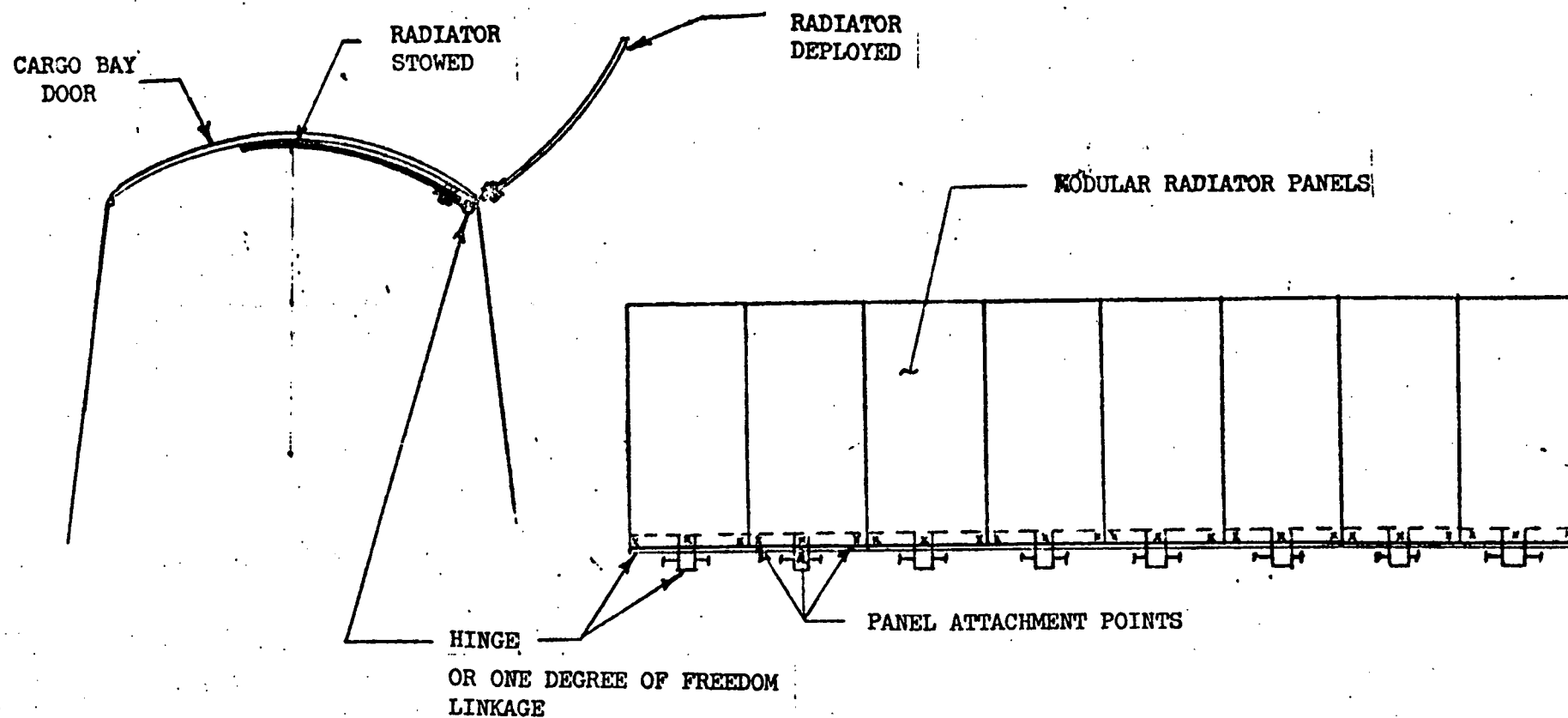


FIGURE C-5 SINGLE DOOR DEPLOYED RADIATOR

NOTE:

ONE SYSTEM
SHOWN,
SIMILAR
ARRANGEMENT
FOR REDUNDANT
SYSTEM

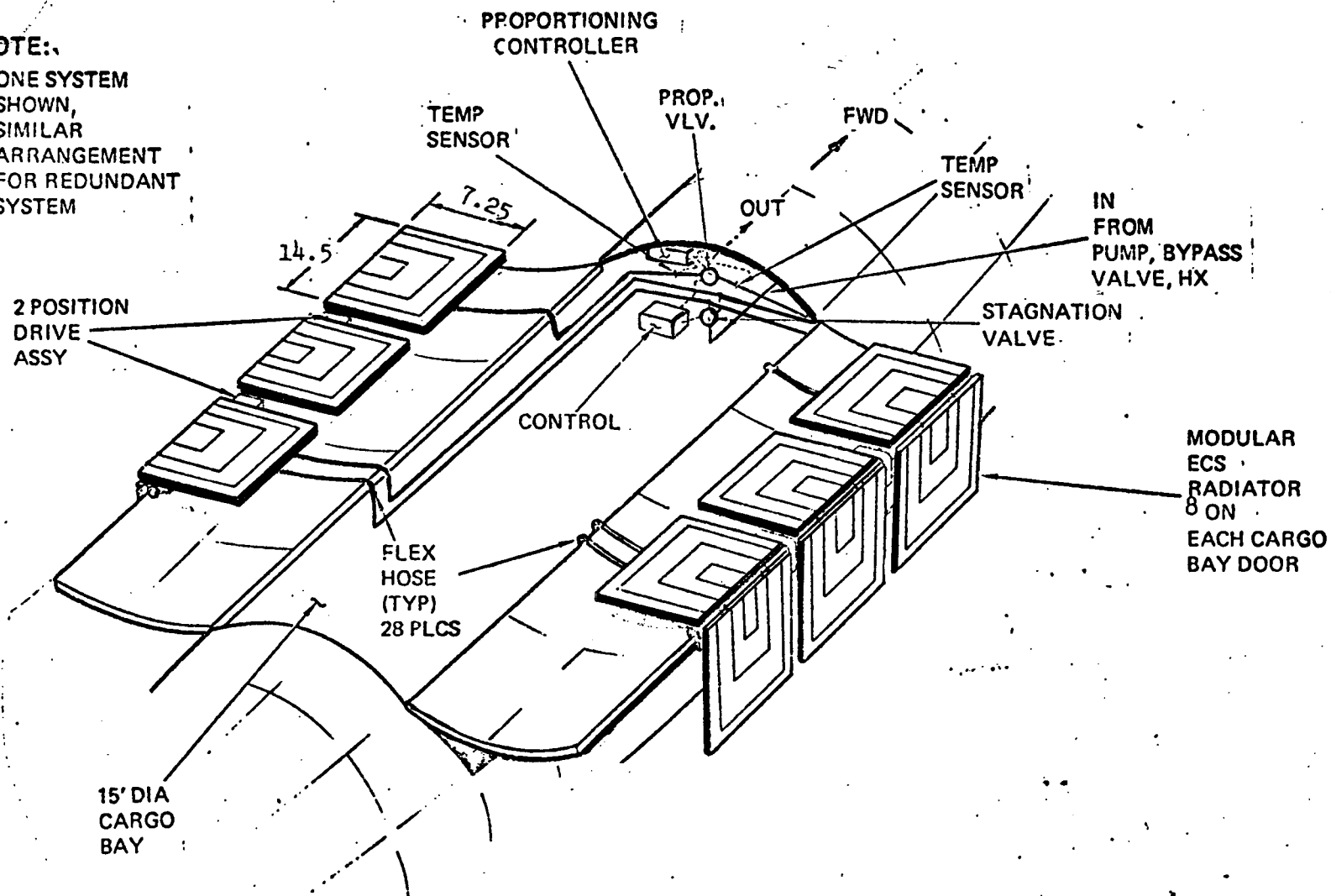
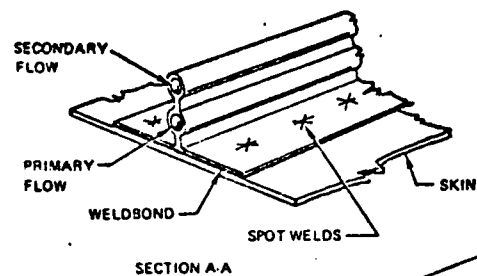
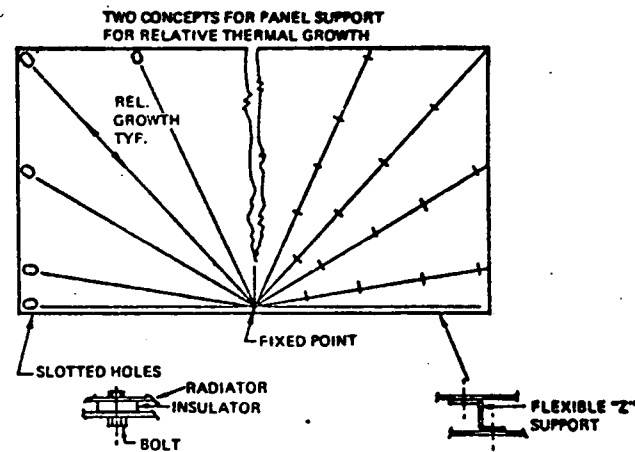


FIGURE C-6 DOUBLE DOOR DEPLOYED RADIATOR



14.5 ft.



7.25

6.21 in.

DOOR STRUCTURE

FIGURE C-7 MODULAR DEPLOYED PANEL DESIGN

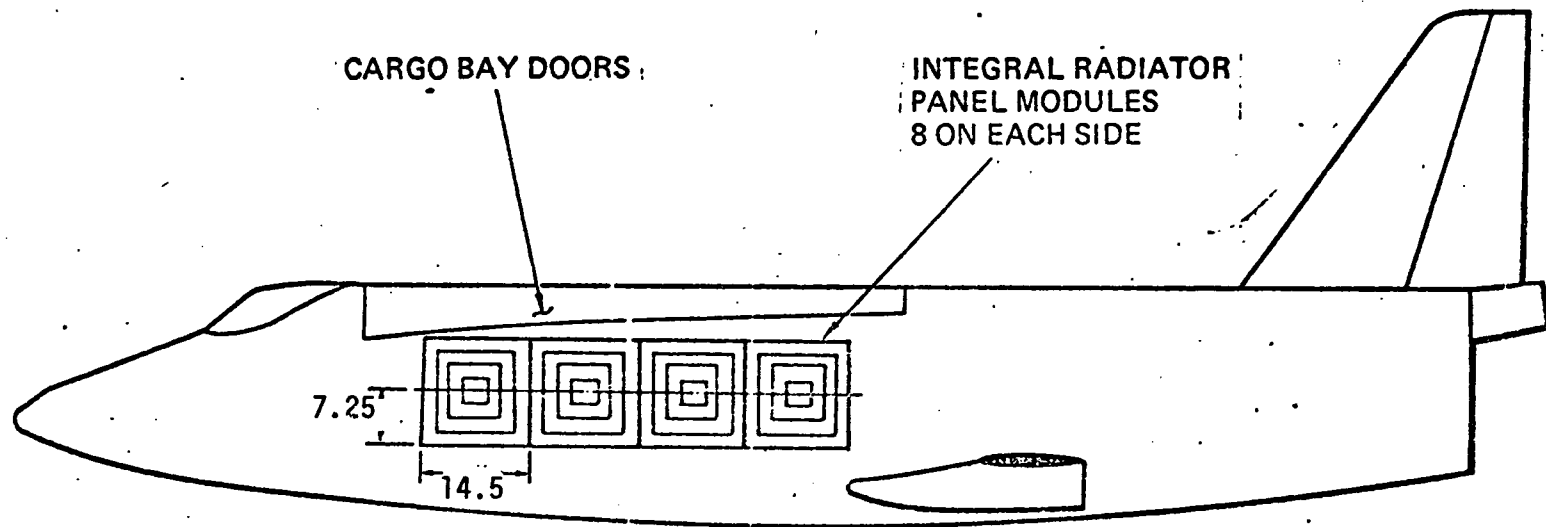


FIGURE C-8 INTEGRAL RADIATOR PANEL INSTALLATION

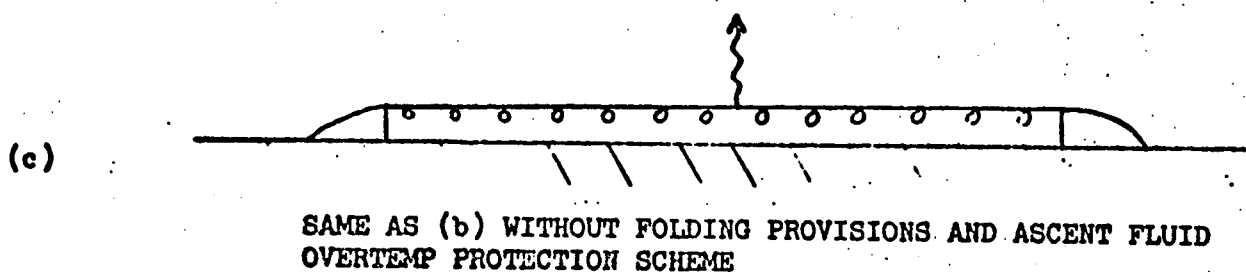
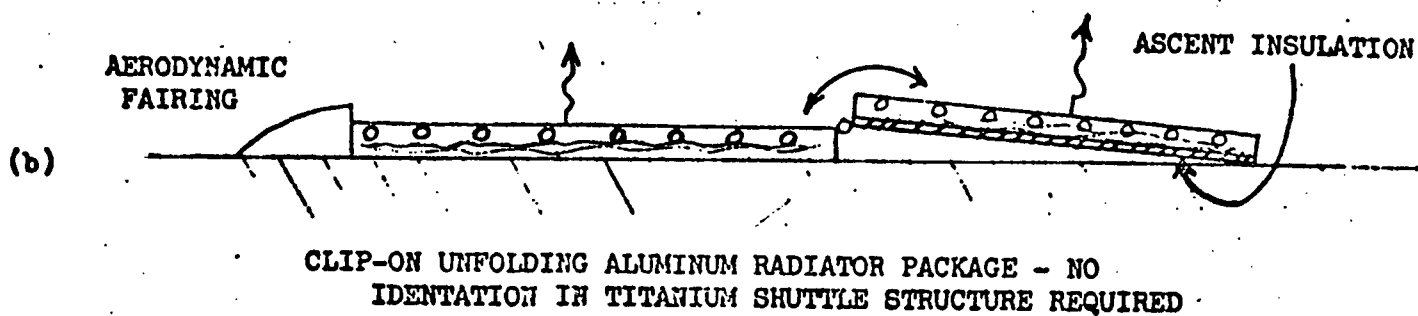
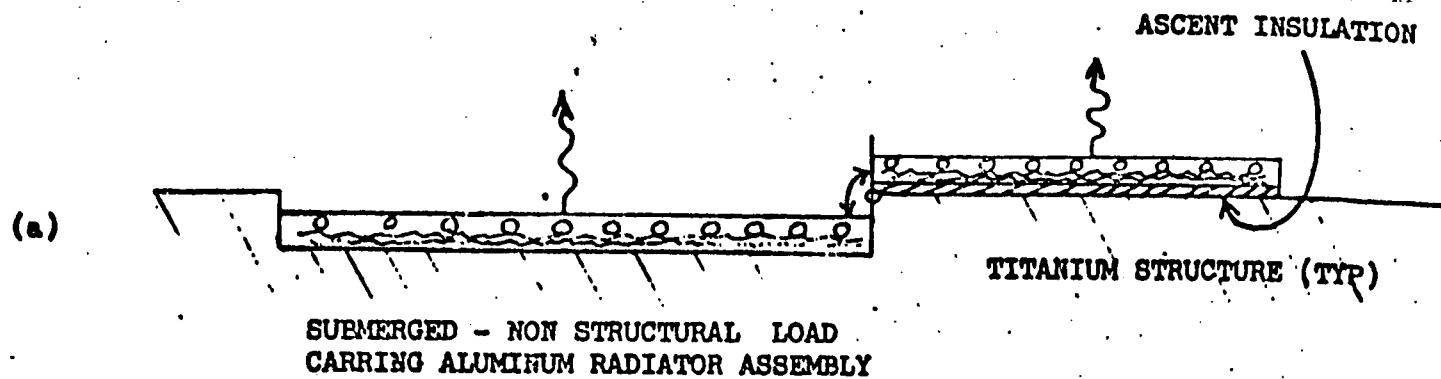


FIGURE C-9 RADIATOR PANEL MOUNTING CONFIGURATIONS

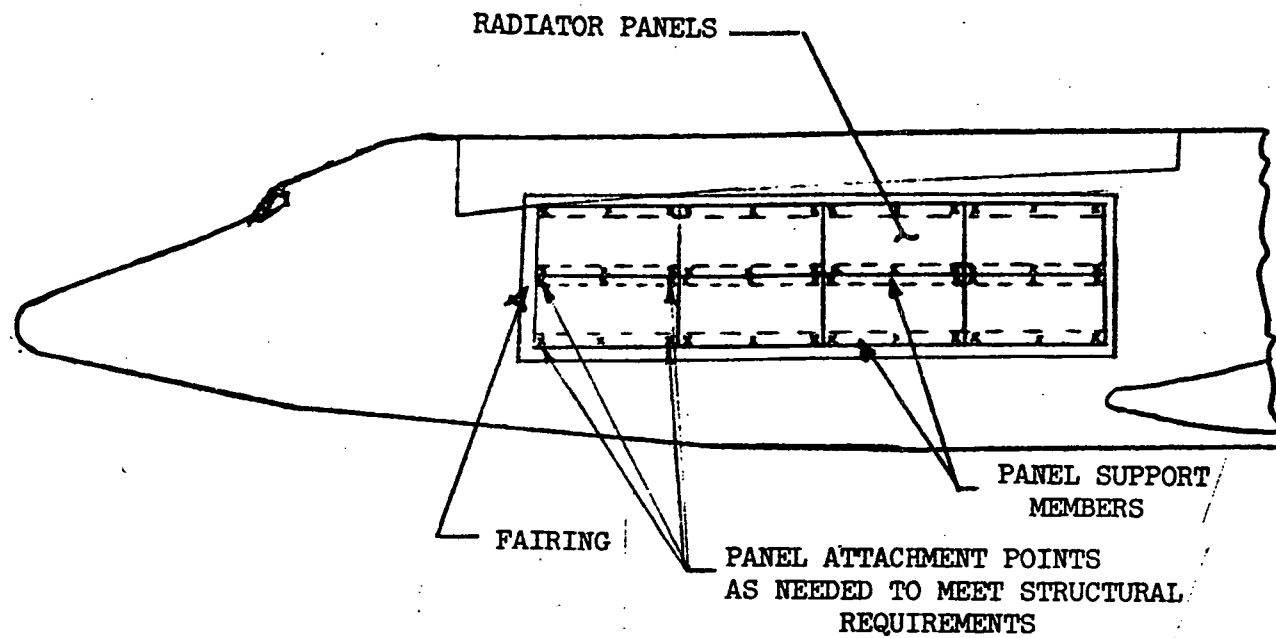


FIGURE C-10 RADIATOR INTEGRATION WITH VEHICLE

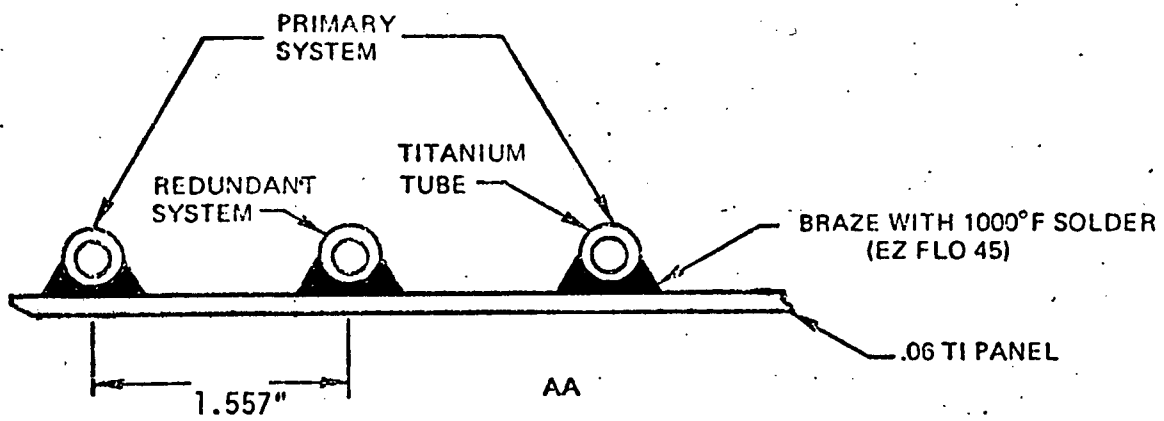
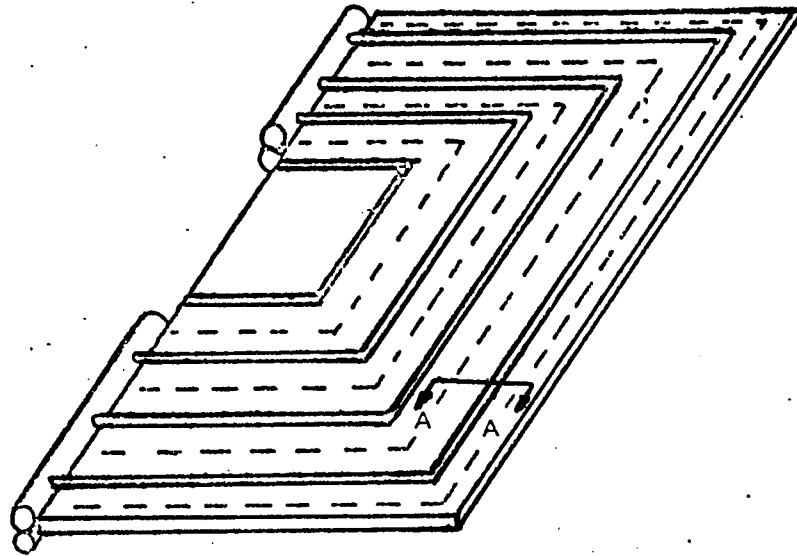


FIGURE C-11 INTEGRAL PANEL DESIGN